Modular Calabi-Yau Manifolds, Attractor Points, and Flux Vacua



Pyry Kuusela

Green Templeton College

University of Oxford

A thesis submitted for the degree of

Doctor of Philosophy

Trinity 2022

Acknowledgements

I would like to thank my supervisors Philip Candelas and Xenia de la Ossa for introducing me to the fascinating subject of relations between number theory, geometry, and physics, and encouraging me to follow my interests in this vast field. This thesis would not have been possible without their advice, support and valuable insights into physics and mathematics.

I would also like to thank my friend and collaborator Joseph McGovern for countless hours of interesting conversation, which originated many of the results presented in this thesis.

I am grateful to the DPhil students and postdocs in the mathematical physics group for fostering a friendly and welcoming environment, for many interesting and entertaining discussions, and many memorable moments. I am lucky to be able to count many of them among my friends.

This research was supported by the Osk. Huttunen Foundation and the Jenny and Antti Wihuri Foundation. I am also grateful to the Björkqvist-rahasto and the Emil Aaltonen Foundation for providing assistance with additional expenses.

Abstract

The overarching theme of this thesis is the relation of physics — specifically string theory compactifications — to Calabi-Yau modularity, which is a phenomenon where it is possible to associate a modular form to a Calabi-Yau manifold. The coefficients of this modular form can be related to the number of points on the manifold defined over finite fields.

We begin by studying the geometry of a five-parameter family of Calabi-Yau manifolds first studied in connection with modularity by Hulek and Verrill, focusing on aspects related to mirror symmetry. These Hulek-Verrill manifolds have an S_6 symmetry group, which makes the seemingly daunting task of finding periods and computing instanton numbers and monodromies significantly easier.

Using the geometric results, we investigate the modular properties of these manifolds. Extending the existing computational methods to cover multiparameter families, we are able to compute the zeta function on various one-parameter subfamilies of Hulek-Verrill manifolds. We observe that along the locus of S_5 symmetric manifolds, the zeta function numerator factorises, revealing that this locus consists of weight-two modular manifolds. This is related to existence of supersymmetric flux vacua in type IIB string theory compactified on these manifolds. We introduce a method of constructing families of such modular supersymmetric flux vacua by utilising the $\mathbb{Z}_2$ symmetry of the compactification manifold. As expected by modularity conjectures, the zeta function of the manifold can be related, in numerous examples we study, to elliptic, Hilbert, or Bianchi modular forms, depending on the number field the manifold is defined over.

It is an interesting question whether these modular forms and their coefficients have a natural geometric of physical interpretation. We take steps towards answering this question by developing an iterative procedure for solving attractor equations in one-parameter compactifications. In some important special cases we find closed-form series solutions, which can be used to compute the entropy of associated black holes in terms of Gromov-Witten invariants of the compactification manifold. The entropy formula takes on a form very reminiscent of modular form asymptotics and can be shown to satisfy some properties expected of the asymptotic form of a modular form counting black hole microstates.

Statement of Originality

Except where otherwise stated, the work presented in thesis is a product of the following collaborations to which the author contributed substantially:

[1] **"Attractors with Large Complex Structure for One-Parameter Families of Calabi-Yau Manifolds"** by Philip Candelas, Pyry Kuusela, and Joseph McGovern, *JHEP 11 (2021) 032*

[2] **"Mirror Symmetry for Five-Parameter Hulek-Verrill Manifolds"** by Philip Candelas, Xenia de la Ossa, Pyry Kuusela, and Joseph McGovern, *(arXiv:2111.02440)*

[3] **"Zeta Functions from Picard-Fuchs Equations for Multiparameter Manifolds"** by Philip Candelas, Xenia de la Ossa, Pyry Kuusela, and Joseph McGovern, *(To Appear)*

[4] **"Supersymmetric Flux Vacua and their Modularity on $\mathbb{Z}_2$ Symmetric Manifolds"** by Philip Candelas, Xenia de la Ossa, Pyry Kuusela, and Joseph McGovern, *(To Appear)*

Contents

I Introduction and Background **1**

1 Introduction **2**

1.1 Introduction 2

1.2 Outline 5

1.2.1 Conventions 6

2 Geometry and Mirror Symmetry **7**

2.1 Calabi-Yau manifolds and their moduli spaces 7

2.1.1 Complex structure moduli space 8

2.1.2 Complexified Kähler moduli space 10

2.2 Mirror map 11

2.2.1 Integral basis 11

2.2.2 Frobenius basis 12

2.2.3 Relating the integral and the Frobenius basis 15

2.3 Toric geometry and Calabi-Yau manifolds 16

2.3.1 Basics of toric geometry 16

2.3.2 Batyrev's construction 21

2.3.3 The method of Batyrev and Borisov 22

3 Calabi-Yau Modularity and Physics **24**

3.1 One-dimensional example: elliptic curves 24

3.2 Modularity 26

3.3 Modular forms 28

3.3.1 Elliptic modular forms 28

3.3.2 Hilbert modular forms 29

3.4 Zeta function 31

3.5 Modularity from attractor points and flux vacua 33

3.5.1 Calabi-Yau compactifications 33

3.5.2 Attractor mechanism 34

3.5.3 Flux compactifications 38

3.5.4 Relation to modularity 42

II Five-parameter Hulek-Verrill Manifolds and their Mirrors 43

4 Introduction 44

4.1 Introduction . . . 44

4.2 Outline . . . 45

5 Toric Geometry and Mirror Symmetry 50

5.1 The polytopes corresponding to singular varieties . . . 51

5.1.1 Five-dimensional description . . . 51

5.1.2 Four-dimensional description of $\widehat{\Delta}$ . . . 52

5.1.3 The dual polytope $\widehat{\Delta}^*$ . . . 54

5.2 The polytopes corresponding to small resolutions . . . 55

5.2.1 The small polytopes Δ_1 and Δ_2 . . . 55

5.2.2 The small polytopes ∇_1 and ∇_2 . . . 55

5.3 The Hulek-Verrill manifolds and their mirrors . . . 57

5.3.1 The singular Hulek-Verrill manifold $\widehat{\mathrm{HV}}$ . . . 58

5.3.2 The singular mirror Hulek-Verrill manifold $\widehat{\mathrm{H}\Lambda}$ . . . 58

5.3.3 The Hulek-Verrill manifold HV . . . 60

5.3.4 The mirror Hulek-Verrill manifold HΛ . . . 61

6 The Mirror Map and Moduli Space 64

6.1 Periods . . . 64

6.1.1 Moduli space . . . 65

6.1.2 The fundamental period . . . 65

6.1.3 The ordinary differential equation obeyed by the fundamental period . . . 67

6.1.4 The partial Picard-Fuchs system . . . 68

6.1.5 The Frobenius method . . . 68

6.1.6 Separation of variables . . . 69

6.1.7 Determining closed form expressions for all periods . . . 70

6.1.8 The Frobenius elements as cohomology . . . 74

6.1.9 The periods near large complex structure points . . . 74

6.2 Mirror map and instanton numbers . . . 76

6.2.1 Yukawa couplings and instanton numbers . . . 78

6.2.2 Genus-1 instanton numbers . . . 79

6.2.3 Relations between the instanton numbers . . . 81

6.2.4 Duality webs . . . 83

6.2.5 Recovering the results on quotient manifolds . . . 91

6.3 Monodromies . . . 92

6.3.1 Monodromies around the large complex structure points E_i . . . 93

6.3.2 Monodromies around the loci D_I . . . 93

6.3.3 Monodromy around infinity, E_0 . . . 97
6.3.4 Recovering monodromies for the quotient manifolds . . . 97

7 Counting Curves on the Mirror Hulek-Verrill Manifold 99
7.1 Blow-down and elliptic fibration . . . 100
7.2 Complete intersection curves on $(\mathbb{P}^1)^5$ . . . 104
7.3 Lines . . . 105
7.3.1 Horizontal lines . . . 106
7.3.2 Vertical lines . . . 107
7.4 Quadrics . . . 108
7.5 Cubics . . . 110
7.6 Summary . . . 111

III Supersymmetric Flux Vacua on Hulek-Verrill Manifolds 112

8 Introduction 113
8.1 Introduction . . . 113
8.2 Outline . . . 114
8.2.1 Conventions . . . 116

9 Zeta Function 117
9.1 Frobenius map . . . 117
9.1.1 Basis of the vector bundle $\mathcal{H}$ . . . 118
9.1.2 The differential equation satisfied by the Frobenius map . . . 119
9.1.3 Inversion of $\mathrm{E}(\varphi)$ . . . 121
9.1.4 The form of $\mathrm{U}(\varphi)$ . . . 122
9.2 Constraints from the Weyl conjectures . . . 122
9.3 Examples . . . 124
9.3.1 Two-parameter example: the mirror octic . . . 124
9.3.2 Five-parameter example: the Hulek-Verrill manifold . . . 127

10 Supersymmetric Flux Vacua on Hulek-Verrill Manifolds 133
10.1 The supersymmetric flux vacuum equations . . . 133
10.2 Solutions from $\mathbb{Z}_2$ symmetry . . . 134
10.2.1 The Hulek-Verrill manifold . . . 135
10.3 Flux vacuum modularity . . . 136
10.3.1 The S_5 symmetric family $\varphi^i = \varphi$ . . . 136
10.3.2 Rational points and elliptic modular forms . . . 137
10.3.3 Real quadratic points and Hilbert modular forms . . . 141
10.3.4 Imaginary quadratic fields and Bianchi modular forms . . . 142
10.3.5 Base changes, from Hilbert and Bianchi to elliptic modular forms . . . 144

IV Towards Microscopic Interpretation: Attractors with Large Complex Structure 145

11 Introduction 146

11.1 Preamble . . . 146
11.2 Outline . . . 149
11.3 Notation . . . 150

12 Solving the Attractor Equations: a General Overview 153

12.1 The large complex structure region . . . 153
12.2 Particular brane systems . . . 154
12.3 General comments concerning the alignment equations . . . 155
12.4 Setting up the iteration . . . 156
12.5 Partitions . . . 158
12.5.1 Basic definitions and notation . . . 158
12.5.2 Operations on partitions . . . 158
12.5.3 Series expansions . . . 160

13 Brane Systems 163

13.1 The D4-D2-D0 system . . . 163
13.1.1 The orthogonality equation . . . 163
13.1.2 The alignment equations . . . 166
13.2 The D6-D2-D0 system . . . 170
13.2.1 The orthogonality equation . . . 170
13.2.2 The alignment equations . . . 172

14 Solutions 175

14.1 The D6-D2-D0 alignment equations . . . 175
14.2 The D4-D2-D0 orthogonality equation . . . 178
14.3 Entropy at rank-two attractor points . . . 179
14.3.1 An example: a rank-two attractor point on AESZ34 . . . 180
14.4 Solutions with large charge ratios . . . 182
14.4.1 The D4-D2-D0 system . . . 183
14.4.2 The D6-D2-D0 system . . . 184

15 Outlook: Comparison with Microscopic Entropy 186

15.1 The central charge and entropy . . . 187
15.2 Entropy from conformal field theory . . . 188
15.2.1 Microscopic charge vector . . . 188
15.2.2 Entropy from modular form asymptotics . . . 190
15.3 Entropy from supergravity . . . 191
15.4 Open questions . . . 192

Appendices **194**

A Toric Geometry Data **195**

B Series Expressions and Bessel Integrals **200**

C Instanton Numbers of Mirror Hulek-Verrill Manifolds **201**

D Zeta Function Numerators **216**

D.1 The mirror octic 216

D.2 The S_5 symmetric Hulek-Verrill manifolds 221

E Modular Forms Associated to Flux Vacua **229**

E.1 Rational points and elliptic modular forms 229

E.2 Totally real number fields and Hilbert modular forms 243

E.3 Imaginary quadratic number fields and Bianchi modular forms 246

F Monodromy Around Large Complex Structure Points **249**

F.1 D4-D2-D0 system 250

F.2 D6-D2-D0 system 250

G The perturbative equations for the D6 system **251**

G.1 The orthogonality equation 251

G.1.1 The σ-expansion 252

G.2 The alignment equations 253

G.2.1 The σ-expansion 256

H Convergence of Solutions **258**

H.1 Bound for $a_{\mathfrak{p}}$ 260

Bibliography **261**

Part I

Introduction and Background

In this part, we give a concise overview of the research presented in this thesis, giving it some background and context. We also review briefly some of the background material that the following parts extensively draw from. This includes theory of mirror symmetry, some toric geometry, a lightning review of modularity and modular forms, and discussion of the relation of Calabi-Yau modularity to two string theory compactification setups: black holes and attractor mechanism and supersymmetric flux vacua. These short reviews are intended to set the research presented in this thesis into context, but also to allow us to set up conventions and notation that will be used throughout the thesis.

Chapter 1

Introduction

1.1 Introduction

Throughout the history of physics, continuous and discrete descriptions of physical phenomena have had significant tension but also complemented each other. After the advent of quantum mechanics these two have been increasingly seen as opposite sides of the same coin. Despite this, the interaction between mathematics and physics has been dominated by study of geometries over continuous fields such as $\mathbb{C}$ and $\mathbb{R}$. However, in light of quantisation conditions it is natural to consider geometric objects, such as cohomology groups over integers, which have a close connection to varieties defined over the discrete field $\mathbb{Q}$ or finite fields $\mathbb{F}_{p^n}$. Although often overlooked in physics, varieties over these fields have been intensively studied by number theorists, and have some fascinating and beautiful properties. One such property, which forms a central theme of this thesis, is *modularity*, by which we mean a striking correspondence between the number of points on a variety defined over finite fields, and coefficients of modular forms. In this thesis, we study variety of topics related to modularity of Calabi-Yau manifolds, which have deep connections to both physics and number theory.

In physics, Calabi-Yau manifolds appear naturally in compactifications of superstring theories, M-theory, or F-theory. These give an unified description of fundamental interactions as strings moving in 10, 11 or 12 dimensions. We appear to live in a four-dimensional world, so to obtain a theory consistent with this elementary observation, these theories must be compactified on a 6-, 7-, or 8-dimensional manifold. For string theories, a relatively simple, albeit very rich, class of such manifolds is given by Calabi-Yau threefolds, and for F-theory interesting examples are provided by elliptically fibred Calabi-Yau fourfolds.

Compactifying type IIA or IIB string theories on Calabi-Yau threefolds, one obtains four-dimensional, $\mathcal{N}$=2 supersymmetric theories, which reduce in the low-energy limit to $\mathcal{N}$=2 supergravity theories. One of the most interesting properties of string theory is its ability to potentially incorporate gravity into theory of other three fundamental interactions, and thus elucidate the quantum nature of gravity. Black holes provide ideal theoretical 'laboratories' to study this relation of quantum theory and gravity,

due to their strong curvature.

In the four-dimensional $\mathcal{N}$=2 theories, supersymmetry-preserving BPS black hole solutions are governed by the attractor mechanism. The rough idea behind the attractor mechanism is that the continuous moduli of the solution vary when approaching the horizon of the black hole, and take on a fixed value — dependent only on charges and other discrete data — on the horizon. In the context of Calabi-Yau compactifications, the continuous moduli include the geometric moduli of the manifold, and the attractor mechanism can thus be thought of as picking out a particular Calabi-Yau manifold determined by the black hole charges.

A certain class of these attractor points, so-called *rank-two attractor points*, where a single Calabi-Yau manifold supports black holes with two linearly independent integeral charge vectors, have a relation to modularity, meaning that there is a modular form associated to the number of points on the manifold when considered as a variety over finite fields $\mathbb{F}_{p^n}$. This relation can be traced back to the existence of the two independent charge vectors. Similar relation between modular manifolds and physics can be found via supersymmetric flux compactifications, where there exist two linearly independent integeral flux vectors.

The best-understood case of modularity concerns elliptic curves $E(\mathbb{Q})$ defined over $\mathbb{Q}$. These can be described by a single cubic polynomial in two variables, with coefficients in $\mathbb{Z}$. The number $\#E(\mathbb{F}_p)$ of solutions to these polynomials over finite fields $\mathbb{F}_p$ can be counted. The modularity theorems [5–7] imply that the constants a_p, defined by

$$a_p \;=\; \#E(\mathbb{F}_p) - p - 1 \;, \tag{1.1}$$

are coefficients of an elliptic modular form, at least for all but finitely many primes p.

Modularity can be seen as one aspect of the Langlands programme, which is a wide set of conjectures about the relation of number theory, geometry, and representation theory. These conjectures imply that also higher-dimensional Calabi-Yau manifolds have analogous properties. In general, in the case of threefolds X, the role of modular form is instead played by a more general automorphic form. However, in special cases where the middle cohomology $H^3(X, \mathbb{C})$ satisfies certain properties, the automorphic forms are again elliptic modular forms, and the relation between these forms and the arithmetic properties of the manifold becomes more tractable.

Given that the above modularity considerations apply to varieties defined over finite fields, it is perhaps surprising that modularity of Calabi-Yau manifolds has an intricate relation to physics. It was first noticed by Moore [8, 9] that attractor mechanism has a connection to arithmetic properties of the compactification manifolds. For instance, among many other interesting observations, he noted that

if one takes the compactification manifold to be of the form $E \times E \times E$, then the elliptic curves corresponding to attactor points have complex multiplication.

Later, Candelas et al. [10] found examples of rank-two attractor points on one-parameter Calabi-Yau threefolds by studying factorisations of the *zeta function* associated to these manifolds. They presented extensive numerical evidence for interesting relations between the modular forms associated to the manifold and physical quantities related to the black holes connected to the rank-two attractor points. For instance, the area of the black hole can be expressed in terms of *L-functions* related to these modular forms.

A similar story can be told about supersymmetric flux vacua. These were investigated by Kachru, Nally, and Yang, who studied supersymmetric flux vacua on the mirror of the octic Calabi-Yau manifold. In [11, 12], the relation of flux vacua, splitting of Galois representations, and factorisations of the zeta function was explained. In addition, the authors presented an F-theory uplift, where the elliptic fibre can be identified with the elliptic curve corresponding to the elliptic modular form associated to the manifold supporting a supersymmetric flux vacuum. Conjecturally, this correspondence generalises also to Hilbert and Bianchi modular forms associated to field extensions of $\mathbb{Q}$.

The rather mysterious relation of modularity, black holes and flux vacua opens up questions both in physics and mathematics — and novel approaches to answering them. For instance: is there a natural geometric or physical interpretation of the modular forms related to the arithmetic of manifolds corresponding to rank-two attractor points and supersymmetric flux vacua? How do these solutions behave under mirror symmetry?

Unfortunately, the set of presently known examples of rank-two attractor points and supersymmetric flux vacua is rather limited both in number and variety. One of the main results of this thesis is presenting new constructions of supersymmetric flux vacua, and studying their modularity. We also generalise the method of Candelas, de la Ossa, and van Straten [13] for computing zeta functions of multiparameter manifolds, which can be used to identify new rank-two attractor points and modular supersymmetric flux vacua.

For this purpose, we undertake a detailed study of geometry and mirror symmetry of five-parameter Hulek-Verril manifolds, which were first investigated in relation to their modular properties by Hulek and Verrill, who showed that certain manifolds in the five-parameter family can be associated to modular forms. The rank-two attractor points found by Candelas et al. exist on the $\mathbb{Z}_5$ and $\mathbb{Z}_{10}$ quotients of an S_5 symmetric subfamily of the family of Hulek-Verrill manifolds. We show that the full five-parameter family also exhibits not only rank-two attractor points but also families of supersymmetric flux vacua.

We also take steps towards understanding the physical significance of the relation of modular forms and L-functions and physical quantities such as black hole entropy by studying attractor points with large (but finite) complex structure. Developing a novel resummation procedure, we are able to find intriguing formulae expressing the entropy of black holes associated to rank-two attractor points as a function of black hole charges and Gromov-Witten invariants of the compactification manifold, possibly giving a hint of microstate counting. These formulae also imply interesting relations between Gromov-Witten invariants and L-functions associated to rank-two attractor points.

1.2 Outline

The first part of this thesis gives a brief review of Calabi-Yau manifolds, their moduli spaces, and mirror symmetry. This discussion forms the backbone of the work presented in this thesis. In addition a lightning overview of toric geometry is given with an eye on applications to mirror symmetry, which are used to construct some of the manifolds we focus extensively on later parts. We also introduce most of the notation used in the following parts. After this, a brief, physicist-oriented overview of topics related to Calabi-Yau modularity is given. We omit most mathematical details and instead focus on practical aspects and the relation to physics.

For the majority of the thesis, we illustrate and supplement general theory by providing numerous explicit examples. For this purpose, we often use Hulek-Verrill manifolds [14], which have numerous interesting number theoretic properties, such as exhibiting rank-two attractor points and supersymmetric flux vacua [10]. The second part of this thesis, based on [2], sets the stage for the following analysis by studying certain properties these manifolds and their mirrors. We use toric geometry to find the mirror manifold. By using the high degree of symmetry of the five-parameter family of Hulek-Verrill manifolds, we are able to find the periods and their monodromies around the singular loci, and use this information to compute the mirror symmetry prediction for the number of rational and genus-one curves of low degree. It is possible to verify this by direct analysis of the geometry: counting some of these curves is possible as the mirror manifold is an elliptically fibred Calabi-Yau threefold, and we are able to use the techniques of Kodaira to classify the singular fibres, which contain the rational curves of low degree as the irreducible components.

In the next part, containing aspects of upcoming work [3, 4], we present a novel construction of modular supersymmetric flux vacua on manifolds admitting a $\mathbb{Z}_2$ symmetry. To prove the modularity of the manifolds admitting these vacua, we generalise the practical methods of computing the zeta functions of one-parameter Calabi-Yau manifolds presented in [13]. Building on the careful study of the geometry of Hulek-Verrill manifolds, we explore these flux vacua and their modularity on highly symmetric Hulek-Verrill manifolds. These flux vacua have a similar relation to F-theory compactifications as those studied in [11, 12], where it was also conjectured that certain manifolds correspond to Hilbert or

Bianchi modular forms, but due to lack of zeta function data, this could not be ascertained. With the highly symmetric Hulek-Verrill manifolds, we are able to formulate analogous conjectures, for which we can also provide a large amount of evidence.

The last part, based on [1], studies the attractor equations on one-parameter families of Calabi-Yau manifolds with large complex structure. These equations, which can be formulated as the requirement that the central charge of the $\mathcal{N}$=2 supersymmetry algebra takes on a local minimum, determine the near-horizon geometry of black holes in $\mathcal{N}$=2 supergravity. On one-parameter Calabi-Yau manifolds this condition can be written in a more tractable form, as the condition that the three-form corresponding to the charge of the black hole lies in the plane spanned by $H^{(3,0)}$ and $H^{(0,3)}$.

We develop a systematic procedure for solving this condition, including all perturbative and non-perturbative corrections, explicitly: first the attractor equations are formulated in terms of recurrence relations, for which we seek closed-form solutions. It turns out that in many interesting cases these solutions take a surprisingly simple form, giving an explicit series solution for the attractor equations. These can be used to write down a simple series expansion for the entropy of black holes associated to rank-two attractor points. Intriguingly, this expansion has a form that is very reminiscent of the asymptotics of modular forms appearing in microscopic descriptions in some known theories [15–17], and involve Gromov-Witten invariants that have a clear function as counting rational curves on the compactification manifold.

1.2.1 Conventions

In this part, unless otherwise stated, we employ the Einstein summation convention, with the indices $a, b, c, \ldots$ from the beginning of the Latin alphabet taking values $0, \ldots, m$, and the indices $i, j, k, \ldots$ from the middle of the alphabet taking values $1, \ldots, m$, with m being the dimension of the complex structure moduli space of the Calabi-Yau manifold we study.

Chapter 2

Geometry and Mirror Symmetry

2.1 Calabi-Yau manifolds and their moduli spaces

Calabi-Yau manifolds are examples of geometrical objects that find numerous applications in both physics and mathematics. By Calabi-Yau manifold we mean an m-dimensional (compact) complex manifold which is Kähler, with associated Kähler form $\widetilde{J}$, and has a vanishing second Chern class. By Calabi's conjecture [18], proven by Yau [19, 20], such manifolds have a Ricci-flat metric with a Kähler form J in the cohomology class of $\widetilde{J}$.

In this thesis, we mostly concentrate on three-dimensional manifolds with strict SU(3) holonomy. This restriction eliminates some 'trivial' cases, such as $E \times E \times E$ or $\mathrm{K3} \times E$. In the cases with strict SU(3) holonomy, the Calabi-Yau manifolds admit, in addition to the Kähler form J, an up to scaling unique holomorphic three-form $\Omega \in H^3(X)$.

A central object of our study is the moduli space of a family of Calabi-Yau manifolds, by which we mean the parameter space of Ricci flat metrics. Let us briefly review these, closely following the classic treatment of [21].

Consider a variation $g + \delta g$ of the metric, which we demand is Ricci flat

$$R_{mn}(g + \delta g) \;=\; 0 \;.$$

Requiring the gauge condition $\nabla^n \delta g_{mn} = 0$ and linearising gives the *Lichnerowicz equation*

$$\nabla^k \nabla_k \delta g_{mn} + 2R_{m\ n}^{\ p\ q} \delta g_{mn} \;=\; 0 \;.$$

Decomposing the metric variations in the holomorphic and antiholomorphic indices to variations of pure and mixed type allows relating the variations to harmonic forms of type $(1,1)$ and $(2,1)$. To the variations of mixed type, we associate a $(1,1)$-form

$$\mathrm{i}\, \delta g_{\mu\bar{\nu}}\, \mathrm{d}z^{\mu} \wedge \mathrm{d}z^{\bar{\nu}} \;=\; \mathrm{i}\, \delta J \;.$$

As this suggests, we can identify these variations with the variations of the Kähler form. The Lichnerowicz equation is equivalent to requiring that δJ is harmonic. This gives $h^{1,1}$ real variations. String theory suggests that the Kalb-Ramond field $B_{\mu\nu}$, a real harmonic $(1,1)$-form, enters on a similar footing to the metric. In addition, this field turns out to be necessary for mirror symmetry. For this reason, we consider variations of the *complexified Kähler structure* $B + \mathrm{i}J$

$$\delta(B + \mathrm{i}J) \;=\; \delta B_{\mu\bar{\nu}}\, \mathrm{d}z^{\mu} \wedge \mathrm{d}z^{\bar{\nu}} + \mathrm{i}\, \delta g_{\mu\bar{\nu}}\, \mathrm{d}z^{\mu} \wedge \mathrm{d}z^{\bar{\nu}} \;,$$

which gives a $2h^{1,1}$ real variations, or $h^{1,1}$ complex variations.

The variations of mixed type can be related to complex $(2,1)$-forms via

$$\Omega_{\kappa\lambda}{}^{\bar{\nu}} \delta g_{\mu\bar{\nu}}\, \mathrm{d}z^{\kappa} \wedge \mathrm{d}z^{\lambda} \wedge \mathrm{d}z^{\bar{\nu}} \;,$$

which satisfies the Lichnerowicz equation if and only if this form is harmonic. Thus there are $h^{2,1}$ independent complex variations, or equivalently $2h^{2,1}$ real variations.

The moduli space $\mathcal{M}(X)$ of a Calabi-Yau manifold X consists of these variations. A natural metric for this space is given by

$$\mathrm{d}s^2 \;=\; \frac{1}{4\mathrm{Vol}(\mathcal{M}(X))} \int_X g^{km} g^{ln} \left(\delta g_{kl} \delta g_{mn} + \delta B_{kl} \delta B_{mn}\right) \;.$$

Decomposing the indices into holomorphic and antiholomorphic, we find that the pure and mixed variations are not mixed

$$\mathrm{d}s^2 \;=\; \frac{1}{2\mathrm{Vol}(\mathcal{M}(X))} \int_X g^{\kappa\bar{\mu}} g^{\lambda\bar{\nu}} \left(\delta g_{\kappa\lambda} \delta g_{\bar{\mu}\bar{\nu}} + \left(\delta g_{\kappa\bar{\nu}} \delta g_{\lambda\bar{\mu}} + \delta B_{\kappa\bar{\nu}} \delta B_{\lambda\bar{\mu}}\right)\right) \;.$$

Thus the moduli space, at least outside points corresponding to singular manifolds X, decomposes into a product of a *complexified Kähler moduli space* $\mathcal{M}_{\mathbb{C}K}(X)$ and a *complex structure moduli space* $\mathcal{M}_{\mathbb{C}S}(X)$, of complex dimensions $h^{1,1}$ and $h^{2,1}$, respectively

$$\mathcal{M}(X) \;=\; \mathcal{M}_{\mathbb{C}K}(X) \times \mathcal{M}_{\mathbb{C}S}(X) \;. \tag{2.1}$$

These spaces have additional structure of special Kähler manifolds.

2.1.1 Complex structure moduli space

We are particularly interested in the complex structure moduli space, which we take to be parametrised by coordinates $\boldsymbol{\varphi} = (\varphi^1, \ldots, \varphi^m)$. It can be shown that the Kähler potential of $\mathcal{M}_{\mathbb{C}S}$ is given by [21]

$$K \stackrel{\mathrm{def}}{=} -\log\left[\mathrm{i}\int_X \Omega \wedge \overline{\Omega}\right] \;. \tag{2.2}$$

The Kähler transformations $K \mapsto K - \log|\lambda|^2$ correspond to the freedom to locally rescale the holomorphic three-form, $\Omega \to \lambda(\boldsymbol{\varphi})\Omega$ with $\lambda(\boldsymbol{\varphi}) \in \mathbb{C}^*$. Physically, these can be seen as a gauge transformations, so it is useful to introduce the *Kähler covariant derivatives*

$$D_a \;=\; \partial_a + n\, \partial_a K \;,$$

where n is the 'charge' of the object the derivative operates on.

To see that the complex structure moduli space is not only Kähler, but also special Kähler, we need to find a *prepotential* in terms of which the Kähler potential can be written. To do this, choose first a basis A^0, A^i, A_i, A_0 of $H_3(X,\mathbb{Z})$, with the dual basis $\alpha_0, \alpha_i, \alpha^i, \alpha^0$ of $H^3(X,\mathbb{Z})$ satisfying

$$\int_{A^a} \alpha^b \;=\; \int_X \alpha_a \wedge \alpha^b \;=\; -\,\delta_a^b \;, \qquad \int_{A_a} \alpha_b \;=\; \int_X \alpha^a \wedge \alpha_b \;=\; \delta_b^a \;,$$
$$\int_{A^a} \alpha^b \;=\; \int_{A_a} \alpha_b \;=\; 0 \;,$$

Then define the *periods* z^a and $\mathcal{G}_a$ of the holomorphic three-form Ω as its integrals over the cycles A^a and A_a

$$z^a \;=\; \int_{A^a} \Omega \;, \qquad \mathcal{G}_a \;=\; \int_{A_a} \Omega \;.$$

In terms of the periods, Ω can be written as

$$\Omega \;=\; z^a \alpha_a - \mathcal{G}_a \alpha^a \;. \tag{2.3}$$

Choosing $-\alpha^a$ and α_a as a basis of a complex vector space, we can identify Ω with the *period vector* in the *symplectic integral basis*,

$$\Pi \;=\; \begin{pmatrix} \partial_{z^0}\mathcal{G} \\ \partial_{z^i}\mathcal{G} \\ z^0 \\ z^i \end{pmatrix} \;. \tag{2.4}$$

In this basis the inner product

$$(\xi,\omega) \;=\; \int_X \xi \wedge \omega \;, \qquad \xi,\omega \in H^3(X,\mathbb{C})$$

is represented by the symplectic matrix Σ

$$\Sigma \;=\; \begin{pmatrix} 0 & \mathbb{I} \\ -\mathbb{I} & 0 \end{pmatrix} \;,$$

where $\mathbb{I}$ is the $m \times m$ identity matrix.

Recalling the freedom to rescale Ω by a constant, we can view z^a as projective coordinates in the complex structure moduli space. In fact, it can be shown [21, 22] that $\mathcal{G}_a$ are functions of z^a, and can be expressed in terms of a single function $\mathcal{G}(z)$ that is homogeneous of degree 2:

$$\mathcal{G}_a \;=\; \frac{\partial}{\partial z^a}\mathcal{G}(z) \;. \tag{2.5}$$

Substituting the form (2.3) with (2.5) into the integral in (2.2), we see that the Kähler potential can be written in terms of $\mathcal{G}(z)$ as

$$K \;=\; -\log\left[\,\mathrm{i}\left(\overline{z}^a \partial_a \mathcal{G} - z^a \overline{\partial_a \mathcal{G}}\right)\right] \;, \tag{2.6}$$

so we identify $\mathcal{G}(z)$ as the prepotential of the Kähler potential K, verifying the special Kähler nature of the complex structure moduli space. The relation (2.6) is often practical to write using the period vector Π as

$$\mathrm{e}^{-K} \;=\; -\mathrm{i}\Pi^\dagger \Sigma \Pi \ .$$

2.1.2 Complexified Kähler moduli space

It is not difficult to show that the Kähler potential of the complexified Kähler moduli space can be written as

$$K_{\mathbb{C}K} \;=\; \log\left[\frac{4}{3}\int_X J\wedge J\wedge J\right] \ .$$

Introducing a basis e_i of $H^2(X,\mathbb{Z})$ with the dual basis $E^i \in H_2(X,\mathbb{Z})$, we can express this in complex coordinates by first introducing t^i, $i=1,\ldots,s=b^2$, defined as

$$B+iJ \;=\; t^i\,\mathrm{e}_i \ , \qquad t^i \stackrel{\mathrm{def}}{=} \int_{E^i} B+iJ \ .$$

Then the Kähler potential $K_{\mathbb{C}K}$ can be expressed in terms of the triple intersection numbers Y_{ijk}

$$K_{\mathbb{C}K} \;=\; \log\left[\frac{4}{3}\sum_{i,j,k=1}^{s} Y_{ijk}t^it^jt^k\right] \ , \qquad \text{where} \qquad Y_{ijk} \stackrel{\mathrm{def}}{=} \int_X \mathrm{e}_i\wedge\mathrm{e}_j\wedge\mathrm{e}_k \ .$$

By introducing a set of projective coordinates w^a and identifying $t^i = w^i/w^0$, we can write down a prepotential $\mathcal{F}(w)$ for this Kähler potential:

$$\mathcal{F}(w) \;=\; -\frac{1}{6!}\sum_{i,j,k=1}^{s} Y_{ijk}\frac{w^iw^jw^k}{w^0}. \tag{2.7}$$

Then, analogously to the expression (2.6) for $\mathcal{M}_{\mathbb{C}S}$,

$$K_{\mathbb{C}K} \;=\; -\log\left[\mathrm{i}\left(\overline{w}^a\partial_a\mathcal{F} - w^a\overline{\partial_a\mathcal{F}}\right)\right] \ .$$

We are, however, primarily interested in string theories on Calabi-Yau manifolds. In this context it is natural to define a prepotetial which includes quantum and instanton corrections to the prepotential (2.7). Unlike in the case of the complex structure moduli space, here the prepotential is not protected from quantum corrections [23]. The quantum-corrected prepotential can be shown to take the form

$$\mathcal{F}(w^0,\ldots,w^s) = -\frac{1}{3!}\sum_{a,b,c=0}^{m} Y_{abc}\frac{w^aw^bw^c}{w^0} + (w^0)^2\sum_{\boldsymbol{p}\neq\boldsymbol{0}} n_{\mathfrak{p}}\,\mathrm{Li}_3(\boldsymbol{q}^{\boldsymbol{p}}) \ , \qquad q_i \stackrel{\mathrm{def}}{=} \exp(2\pi\mathrm{i}\,t^i) \ . \tag{2.8}$$

Here $\mathfrak{p}$ is an s-component multi-index, $n_{\mathfrak{p}}$ the associated instanton numbers counting the rational curves of multi-degree $\mathfrak{p}$, and it is possible to choose the symplectic integeral basis so that the Y_{abc} are given by topological quantities related to X:

$$\begin{aligned} Y_{ijk} \;&=\; \int_X \mathrm{e}_i\wedge\mathrm{e}_j\wedge\mathrm{e}_k \ , & Y_{ij0} \;&\in\; \left\{0,\frac{1}{2}\right\} \ , \\ Y_{i00} \;&=\; -\frac{1}{12}\int_X c_2(X)\wedge\mathrm{e}_i \ , & Y_{000} \;&= -3\chi(X)\frac{\zeta(3)}{(2\pi\mathrm{i})^3} \ , \end{aligned} \tag{2.9}$$

It is convenient to combine these quantities into the s-component vectors $\boldsymbol{Y}_{ab}$ and the $s \times s$ matrices $\mathbb{Y}_a$, whose components are given by

$$(\boldsymbol{Y}_{ab})_i = Y_{abi} \ , \qquad (\mathbb{Y}_a)_{ij} \ = \ Y_{aij} \ .$$

2.2 Mirror map

The discussion above shows some of the many similarities that the complex structure and the complexified Kähler moduli spaces share. The similarities, together with the remarkable factorisation (2.1) of the Calabi-Yau moduli space are not coincidental - they are consequences of *mirror symmetry*.

Mirror symmetry is a conjectured duality between two Calabi-Yau manifolds, X and its mirror $\widetilde{X}$. (For a detailed review, see for example [24].) Specifically, it it conjectured that for every Calabi-Yau manifold, there exists a *mirror manifold* such that the type IIA string theory compactified on X is dual to the IIB string theory compactified on $\widetilde{X}$. This duality maps the complex structure moduli space $\mathcal{M}_{\mathbb{C}S}(X)$ of X with the complexified Kähler structure moduli space $\mathcal{M}_{\mathbb{C}K}(\widetilde{X})$ of its mirror.

It is possible to define a *mirror map*, which gives explicit mapping of the coordinates z^a on $\mathcal{M}_{\mathbb{C}}(X)$ to the coordinates t^a on $\mathcal{M}_{\mathbb{C}K}(\widetilde{X})$. In this section, we review the construction of the mirror map near *large complex structure points*, also known as *points of maximal unipotent monodromy* (*MUM points*) in the moduli space $\mathcal{M}_{\mathbb{C}}(X)$, which correspond to the large volume singularity in $\mathcal{M}_{\mathbb{C}K}(\widetilde{X})$.

2.2.1 Integral basis

One of the predictions of mirror symmetry is that the lattices $H^3(X,\mathbb{Z})$ and $H^2(\widetilde{X},\mathbb{Z})$ should be identified [25]. One of the consequences of this identification is that there exists an symplectic integral basis where we can make the natural identifications

$$w^a \ = \ z^a \ , \qquad \mathcal{F}(w) \ = \ \mathcal{G}(z) \ . \tag{2.10}$$

Thus, in what follows, we do not normally distinguish the prepotentials $\mathcal{G}$ and $\mathcal{F}$ nor the coordinates z^a and w^a, but instead use coordinates z^a, and denote the prepotential as $\mathcal{F}$ on both the complex structure and the complexified Kähler moduli spaces.

Symplectic transformations

Before requiring that the identifications (2.10) hold, the integral symplectic basis is only defined up to an integral symplectic change of basis. In particular, it is possible to choose a set of bases where the prepotential $\mathcal{G}(z)$ is of the form (2.8), but the coefficients Y_{abc} are no longer related to topological quantities as in (2.9).

Let us focus on the subgroup of symplectic matrices that are of the form

$$S = \begin{pmatrix} 1 & \mathbf{0}^T & C & \boldsymbol{B}^T \\ \mathbf{0} & \mathbb{I} & \boldsymbol{B} & \mathbb{A} \\ 0 & \mathbf{0}^T & 1 & \mathbf{0}^T \\ \mathbf{0} & \mathbb{0} & \mathbf{0} & \mathbb{I} \end{pmatrix},$$

where C and the components of $\boldsymbol{B}$ and $\mathbb{A}$ are integral, and $\mathbb{A}$ is a symmetric matrix. This subgroup is isomorphic to $\mathbb{Z}^{\frac{1}{2}(n^2+3n+2)}$. Acting with S on Π, the vector transforms as $\Pi \to S\Pi$, and is still of the form (2.4) with the prepential given by (2.8). However, the quantities Y_{abc} get shifted under this action by

$$\begin{aligned} Y_{ijk} &\to Y_{ijk} \ , \\ Y_{0ij} &\to Y_{0ij} - (\mathbb{A})_{ij} \ , \\ Y_{00i} &\to Y_{00i} - 2(\boldsymbol{B})_i \ , \\ Y_{000} &\to Y_{000} - 3C \ . \end{aligned} \tag{2.11}$$

Throughout this thesis, we will use a symplectic basis in which the Y_{ijk} take the canonical form (2.9). If one is working with a basis with different set of values for the Y_{abc} then a transformation of the above form will relate the two bases.

2.2.2 Frobenius basis

While the mirror map (2.10) is already very non-trivial and highly intriguing, it has limited immediate applicability as we do not have a natural way of computing the prepotential $\mathcal{G}(z)$ directly in the integral basis. However, there exists an alternative basis, the *Frobenius basis*, where the periods are seen to satisfy differential equations which, together with natural boundary conditions, can be used to explicitly find the periods as functions of the moduli. Then, by finding a transformation taking us from the Frobenius basis to integral basis, which we do in the next subsection 2.2.3, we are able to express the prepotential (2.8) in terms of the solutions to the differential equations. This logic was famously employed by Candelas, de la Ossa, Green, and Parkes to compute the numbers of rational curves on the quintic Calabi-Yau threefold [26].

It is not difficult to see [21] that differentiating the holomorphic three-form with respect to the complex structure moduli gives three-forms that are no longer holomorphic. Rather, by taking enough derivatives the whole of $H^3(X,\mathbb{C})$ can be spanned by the following forms

$$\begin{aligned} \Omega &\in H^{(3,0)}(X,\mathbb{C}) \ , \\ \partial_{\varphi^i}\Omega &\in H^{(3,0)}(X,\mathbb{C}) \oplus H^{(2,1)}(X,\mathbb{C}) \ , \\ \partial_{\varphi^i}\partial_{\varphi^j}\Omega &\in H^{(3,0)}(X,\mathbb{C}) \oplus H^{(2,1)}(X,\mathbb{C}) \oplus H^{(1,2)}(X,\mathbb{C}) \ , \\ \partial_{\varphi^i}\partial_{\varphi^j}\partial_{\varphi^k}\Omega &\in H^{(3,0)}(X,\mathbb{C}) \oplus H^{(2,1)}(X,\mathbb{C}) \oplus H^{(1,2)}(X,\mathbb{C}) \oplus H^{(0,3)}(X,\mathbb{C}) \ . \end{aligned}$$

We can therefore always choose a basis for the $2m+2$-dimensional space $H^3(X,\mathbb{C})$ among these derivatives. Any additional derivatives can then be expressed in terms of the basis, leading to differential equations that Ω satisfies, called the *Picard-Fuchs equations*. These can be used to find Ω in practice.

Picking a basis of $2m+2$ functions among the space of solutions to the Picard-Fuchs equations is equivalent to choosing a particular basis (β_a, β^a) of $H^3(X)$. The holomorphic three-form can be expanded as

$$\Omega \;=\; \sum_{a=0}^{m} \varpi^a \beta_a - \varpi_a \beta^a \ .$$

Equivalently, the three-form Ω can be written as a vector

$$\varpi \;=\; \begin{pmatrix} \varpi^0 \\ \varpi^i \\ \varpi_i \\ \varpi_0 \end{pmatrix} ,$$

We will later fix the basis of solutions by imposing a set of boundary conditions (2.13) on ϖ^a and ϖ_a. Then we refer to this vector as the *period vector* in the *(arithmetic) Frobenius basis.*

Indicial algebra and Frobenius basis

The *indicial algebra* of the Picard-Fuchs equation satisfied by the periods [27, 28] is defined by the relations satisfied by the (co-)homology ring elements ϵ_i, μ^i, and η, viewed as elements of $H^2(\widetilde{X}, \mathbb{Z})$, $H^4(\widetilde{X}, \mathbb{Z})$, and $H^6(\widetilde{X}, \mathbb{Z})$, or their homology duals

$$\epsilon_i \epsilon_j \;=\; \epsilon_j \epsilon_i \ , \qquad \epsilon_i \epsilon_j = Y_{ijk}\, \mu^k \ , \qquad \epsilon_i \epsilon_j \epsilon_k \;=\; Y_{ijk}\, \eta \ , \qquad \epsilon_i \eta \;=\; 0 \tag{2.12}$$

To justify the second term, notice that $\epsilon_i \epsilon_j$ can be viewed as an element of $H^4(\widetilde{X}, \mathbb{Z})$, whose dimension is $b^4(\widetilde{X}) = b^2(\widetilde{X}) = h^{2,1}(X)$, so $\epsilon_i \epsilon_j = c_{ijk} \mu^k$ for some basis μ^k of $H^4(\widetilde{X}, \mathbb{Z})$. The algebra elements μ^j can be most conveniently chosen so that

$$\epsilon_i \mu^j \;=\; \delta_i^j \eta \ ,$$

and in this case, on multiplying this relation by ϵ_k, we see that $c_{ijk} = Y_{ijk}$ from the third relation.

The periods can be extracted as coefficients in the expansion of

$$\varpi(\boldsymbol{\varphi}, \boldsymbol{\epsilon}) \;=\; f(\boldsymbol{\varphi}, \boldsymbol{\epsilon})\, \boldsymbol{\varphi}^{\boldsymbol{\epsilon}} \stackrel{\text{def}}{=} \varpi^0 + \varpi^i \epsilon_i + \varpi_i \mu^i + \varpi_0 \eta \ ,$$

where

$$f(\boldsymbol{\varphi}, \boldsymbol{\epsilon}) \;=\; \sum_{\boldsymbol{p}} A_{\boldsymbol{p}}(\boldsymbol{\epsilon})\, \varphi^{\boldsymbol{p}}$$

is a series in $\boldsymbol{\varphi}$ with rational coefficients.

We define the "inverse triple intersection numbers" $\widehat{Y}^{ijk}$ as a set of constants that satisfy the relation

$$Y_{ijk} \widehat{Y}^{ijs} \;=\; \delta_k^s \ .$$

This does not define the quantities $\widehat{Y}^{ijk}$ uniquely. Rather, one can shift $\widehat{Y}^{ijk}$ by any A^{ijk} which is 'orthogonal' to the triple intersection numbers, that is

$$Y_{ijk}A^{ijk} \;=\; 0 \ .$$

This freedom can always be used to make $\widehat{Y}^{ijk}$ symmetric in the first two indices, which fixes the anti-symmetric part $A^{[ij]k}$. Otherwise we leave A^{ijk} unspecified in general, and choose these conveniently on a case-by-case basis. Any ambiguities resulting from this will not affect the following discussion, and we will always specify the choice we have made in particular examples.

With the help of $\widehat{Y}^{ijk}$, the elements μ^k can be expressed as

$$\mu^k \;=\; \widehat{Y}^{ijk}\epsilon_i\epsilon_j \ ,$$

Returning to $\varpi(\boldsymbol{\varphi},\boldsymbol{\epsilon})$, using the indicial algebra that the ϵ_i satisfy, we can expand it as a series

$$\begin{aligned}\varpi(\boldsymbol{\varphi},\boldsymbol{\epsilon}) \;=\; & f + (\partial^i f + f\ell^i)\epsilon_i + \frac{1}{2!}\left(\partial^i\partial^j f + 2\partial^i f\ell^j + f\ell^i\ell^j\right)Y_{ijk}\mu^k \\ & + \frac{1}{3!}\left(\partial^i\partial^j\partial^k f + 3\partial^i\partial^j f\ell^k + 3\partial^i f\ell^j\ell^k + f\ell^i\ell^j\ell^k\right)Y_{ijk}\eta \ ,\end{aligned}$$

where we use the shorthand $\ell^i = \log\varphi^i$, and the derivatives are with respect to ϵ_i. Thus we can identify the period vector in the *arithmetic Frobenius basis* as

$$\varpi \;=\; \begin{pmatrix} f \\ f^i + f\ell^i \\ \frac{1}{2!}Y_{ijk}\left(f^{jk} + 2f^j\ell^k + f\ell^j\ell^k\right) \\ \frac{1}{3!}Y_{ijk}\left(f^{ijk} + 3f^{ij}\ell^k + 3f^i\ell^j\ell^k + f\ell^i\ell^j\ell^k\right) \end{pmatrix} \ , \tag{2.13}$$

where we have denoted $\partial^i f = f^i$, $\partial^{ij} f = f^{ij}$, and $\partial^{ijk} f = f^{ijk}$.

The periods have a monodromy around the loci φ^i. Using the series expansions, the monodromy $\varphi^i \to \mathrm{e}^{2\pi\mathrm{i}}\varphi^i$, $\varphi^j \to \varphi^j$ for $j \neq i$ can be written as

$$\varpi \to \mathrm{e}^{2\pi\mathrm{i}\epsilon_i}\varpi = \mathrm{M}_i^{\varpi}\varpi \ .$$

This allows identification of the indicial algebra elements ϵ_i in terms of the monodromy matrices as

$$\epsilon_i \;=\; \frac{1}{2\pi\mathrm{i}}\log\mathrm{M}_i^{\varpi} \ ,$$

and the monodromy matrices M_i^{ϖ} can be easily found by considering the form (2.13) of the period vector:

$$\mathrm{M}_i^{\varpi} \;=\; \begin{pmatrix} 1 & \mathbf{0}^T & \mathbf{0}^T & 0 \\ 2\pi\mathrm{i}\boldsymbol{\delta}_i & \mathbb{I} & 0 & \mathbf{0} \\ \frac{(2\pi\mathrm{i})^2}{2!}\boldsymbol{Y}_{ii} & 2\pi\mathrm{i}\,\mathbb{Y}_i & \mathbb{I} & \mathbf{0} \\ \frac{(2\pi\mathrm{i})^3}{3!}Y_{iii} & \frac{(2\pi\mathrm{i})^2}{2!}\boldsymbol{Y}_{ii}^T & 2\pi\mathrm{i}\boldsymbol{\delta}_i^T & 1 \end{pmatrix} .$$

This identification also gives an explicit representation for the indicial algebra elements as

$$\epsilon_i \;=\; \begin{pmatrix} 0 & \mathbf{0}^T & \mathbf{0}^T & 0 \\ \boldsymbol{\delta}_i & 0 & 0 & \mathbf{0} \\ \mathbf{0} & \mathbb{Y}_i & 0 & \mathbf{0} \\ 0 & \mathbf{0}^T & \boldsymbol{\delta}_i^T & 0 \end{pmatrix} \;, \qquad \mu^i \;=\; \begin{pmatrix} 0 & \mathbf{0}^T & \mathbf{0}^T & 0 \\ \mathbf{0} & 0 & 0 & \mathbf{0} \\ \boldsymbol{\delta}_i & 0 & 0 & \mathbf{0} \\ 0 & \boldsymbol{\delta}_i^T & \mathbf{0}^T & 0 \end{pmatrix} \;, \qquad \eta \;=\; \begin{pmatrix} 0 & \mathbf{0}^T & \mathbf{0}^T & 0 \\ \mathbf{0} & 0 & 0 & \mathbf{0} \\ \mathbf{0} & 0 & 0 & \mathbf{0} \\ 1 & \mathbf{0}^T & \mathbf{0}^T & 0 \end{pmatrix} \;.$$

2.2.3 Relating the integral and the Frobenius basis

We can find a change of basis from the Frobenius basis to the integral symplectic basis by comparing the asymptotics and monodromies of the vectors Π and ϖ. To make this identification, we must ensure that the monodromy around

$$\varphi^i \to e^{2\pi \mathrm{i}} \varphi^i \;, \qquad \varphi^j \to \varphi^j \quad \text{for } j \neq i$$

corresponds to

$$t^i \to t^i + 1 \;, \qquad t^j \to t^j \quad \text{for } i \neq j.$$

This requires the identification

$$z^0 \;=\; \varpi^0 \;, \qquad z^i \;=\; \frac{1}{2\pi \mathrm{i}} \varpi^i \;,$$

which gives the *mirror map* that identifies points in the complex structure moduli space with the points in the complexified Kähler structure moduli space:

$$t^i \;=\; \frac{1}{2\pi \mathrm{i}} \frac{\varpi^i}{\varpi^0} \;=\; \frac{1}{2\pi \mathrm{i}} \log \varphi^i + \mathcal{O}(\boldsymbol{\varphi}) \;. \tag{2.14}$$

Expressing the period vector (2.4) in terms of the affine coordinates t^i, the asymptotic form of Π in the limit $t^i \to \infty$ for $i = 1, \dots, m$, neglecting the exponentially suppressed instanton corrections, is given by

$$\Pi \sim z^0 \begin{pmatrix} \frac{1}{6} Y_{ijk} t^i t^j t^k - \frac{1}{2} \boldsymbol{Y}_{00} \cdot \boldsymbol{t} - \frac{1}{3} Y_{000} \\ -\frac{1}{2} \boldsymbol{t}^T \mathbb{Y}_i \boldsymbol{t} - \boldsymbol{Y}_{i0} \cdot \boldsymbol{t} - \frac{1}{2} Y_{i00} \\ 1 \\ \boldsymbol{t} \end{pmatrix} \;.$$

This can be compared with the asymptotics of the vector in the Frobenius basis in the corresponding limit $\varphi \to 0$

$$\varpi \;=\; \begin{pmatrix} \varpi^0 \\ \varpi^i \\ \varpi_i \\ \varpi_0 \end{pmatrix} \sim \begin{pmatrix} 1 \\ \boldsymbol{\ell}^i \\ \frac{1}{2!} \boldsymbol{\ell}^T \mathbb{Y}_i \boldsymbol{\ell} \\ \frac{1}{3!} Y_{ijk} \ell^i \ell^j \ell^k \end{pmatrix} \sim \begin{pmatrix} 1 \\ 2\pi \mathrm{i} \boldsymbol{t}^i \\ \frac{(2\pi \mathrm{i})^2}{2!} \boldsymbol{t}^T \mathbb{Y}_i \boldsymbol{t} \\ \frac{(2\pi \mathrm{i})^3}{3!} Y_{ijk} t^i t^j t^k \end{pmatrix} ,$$

where the last asymptotic form follows from expressing the periods appearing in ϖ in terms of the coordinates t^i using the mirror map (2.14). Comparing these asymptotic forms uniquely fixes the

change-of-basis matrix ρ,

$$\rho \;=\; \begin{pmatrix} -\frac{1}{3}Y_{000} & -\frac{1}{2}\boldsymbol{Y}_{00}^T & \mathbf{0}^T & 1 \\ -\frac{1}{2}\boldsymbol{Y}_{00} & -\mathbb{Y}_0 & -\mathbb{I} & \mathbf{0} \\ 1 & \mathbf{0}^T & \mathbf{0}^T & 0 \\ \mathbf{0} & \mathbb{I} & 0 & \mathbf{0} \end{pmatrix} .$$

In writing this, we have separated the diagonal matrix ν, which affects the normalisation of the periods, giving the transformation between the period vectors ϖ and $\widehat{\varpi}$ in what were termed in [13] the *arithmetic Frobenius basis* and the *complex Frobenius basis*.

$$\widehat{\varpi} \;=\; \nu^{-1}\varpi \; . \tag{2.15}$$

The relation between the vectors in the Frobenius and integral bases is given by

$$\Pi \;=\; \rho\nu^{-1}\varpi \; , \qquad \text{with} \qquad \nu = \mathrm{diag}\left(1, 2\pi\mathrm{i}\,\mathbf{1}, (2\pi\mathrm{i})^2\,\mathbf{1}, (2\pi\mathrm{i})^3\right) \; . \tag{2.16}$$

The action of the monodromy on the period vector Π can be read directly from the expression (2.4), and is given by

$$\mathrm{M}_i^{\Pi} \;=\; \begin{pmatrix} 1 & -\boldsymbol{\delta}_i^T & \frac{1}{6}Y_{iii} - Y_{00i} & \frac{1}{2}\boldsymbol{Y}_{ii}^T - \boldsymbol{Y}_{0i}^T \\ \mathbf{0} & \mathbb{I} & -\frac{1}{2}\boldsymbol{Y}_{ii} - \boldsymbol{Y}_{i0} & -\mathbb{Y}_i \\ 0 & \mathbf{0}^T & 1 & \mathbf{0}^T \\ \mathbf{0} & \mathbb{0} & \boldsymbol{\delta}_i & \mathbb{I} \end{pmatrix} . \tag{2.17}$$

2.3 Toric geometry and Calabi-Yau manifolds

The techniques of toric geometry allow not only constructing a wide variety of families of Calabi-Yau manifolds, some of which we will encounter in the following chapters, but also give a procedure for constructing mirrors of these manifolds. Here we review very briefly some central ideas and results in toric geometry, which will later see extensive use in the study of the geometry and mirror symmetry of a family of Calabi-Yau manifolds with interesting modular properties.

2.3.1 Basics of toric geometry

We give a lightning review of some central concepts of toric geometry, concentrating mainly on those pertaining to mirror symmetry. Due to the vast scope of the topic, we will inevitably have to skip over many subtleties and details for which we refer the reader to the monographs [29, 30]. For physicist-oriented reviews in the spirit of the present discussion see [31, 32].

Toric varieties $\mathbb{P}$ are algebraic varieties which have an alegbraic torus $\mathbb{T}^d \stackrel{\text{def}}{=} (\mathbb{C}^*)^d$ as an open dense subset, and admits a natural action $\mathbb{T}^d \times \mathbb{P} \to \mathbb{P}$ of the torus on $\mathbb{P}$, induced from the action of $\mathbb{T}^d$ on itself:

$$\mathbb{T}^d \times \mathbb{T}^d \to \mathbb{T}^d \; : \; ((z_1, \ldots, z_d), (z'_1, \ldots, z'_d)) \mapsto (z_1 z'_1, \ldots, z_d z'_d) \; .$$

The toric varieties have a natural description in terms of global coordinates as a quotient space

$$\mathbb{P}_\Delta \;=\; \frac{\mathbb{C}^n \setminus Z_\Delta}{(\mathbb{C}^*)^{n-d} \times \Gamma} \;, \tag{2.18}$$

where Z_Δ is a point set, and Γ is an abelian discrete group.

An alternative description can be obtained in terms of local affine patches, with appropriate gluing conditions. In both descriptions, the data defining the toric variety can be encoded by lattice-geometric objects, *cones*, *fans*, and *polytopes*.

Cones, fans, and polytopes

Let N be a rank-r lattice, $N \simeq \mathbb{Z}^r$, and $M = \mathrm{Hom}(N, \mathbb{R}) \simeq \mathbb{Z}^r$ it dual lattice, with the associated pairing $\langle *, * \rangle$. Let $N_\mathbb{R}$ and $M_\mathbb{R}$ be the real vector spaces $N_\mathbb{R} \stackrel{\text{def}}{=} N \otimes \mathbb{R} \simeq \mathbb{R}^r$ and $M_\mathbb{R} \stackrel{\text{def}}{=} M \otimes \mathbb{R}$. A *strongly convex rational polyhedral cone* (which we will refer to simply as a *cone*) is a subspace $\sigma \subset N_\mathbb{R}$ such that

1. **Polyhedrality**: σ is bounded by a finite number of hyperplanes in $N_\mathbb{R}$.
2. **Rationality**: the edges of σ are spanned by a finite number of lattice vectors.
3. **Strong convexity**: σ does not contain a complete line in $N_\mathbb{R}$.

These imply that any strongly convex rational polyhedral cone can be written as

$$\sigma \;=\; \left\{ \sum_{i=1}^{k} a_i v_i \;\middle|\; v_i \in N \;,\;\; a_i \geq 0 \right\} \;,$$

where the lattice vectors v_i must in addition be such that the convexity condition $\sigma \cap -\sigma = \{0\}$ is satisfied. We denote the cone σ generated by vectors $v_1, \ldots, v_k$ by $\sigma = \langle v_1, \ldots, v_k \rangle$. This should not be confused with the inner product, and it should be clear from context which is meant. A *dual cone* σ^* of a cone σ is defined as

$$\sigma^* \;=\; \{ m \in M_\mathbb{R} | \langle m, s \rangle \geq 0 \text{ for all } s \in \sigma \} \;.$$

It is easy to check that the dual of a cone is also a cone, and that this duality is involutive $(\sigma^*)^* = \sigma$. A *face* τ of a cone σ is defined as the intersection of the cone σ with a *supporting hyperplane* H_u associated to a lattice point $u \in M$. A hyperplane H_u associated to $u \in M$ is defined as

$$H_u \;=\; \left\{ n \in N_\mathbb{R} \;\middle|\; \langle u, n \rangle = 0 \right\} \;,$$

and it is called an supporting hyperplane of σ if σ is contained in the half-space

$$H_m^+ \;=\; \left\{ n \in N_\mathbb{R} \;\middle|\; \langle u, n \rangle \geq 0 \right\} \;.$$

We denote $\tau \prec \sigma$ if τ is a face of σ. Every face of σ is also a (lower-dimensional) cone, and an intersection if two faces of σ is again a face of σ.

A *fan* Σ is a collection of cones, such that

1. A face of a cone in Σ is also a cone in Σ.
2. The intersection of two cones in Σ is a face of each cone, and a cone in Σ.

A fan is called

1. *complete* if the union of the cones in Σ is equal to $N_{\mathbb{R}}$.
2. *smooth* if the minimal generators of every cone form a subset of a lattice basis of N.

Polytopes are multidimensional generalisations of three-dimensional polyhedra. We are interested in *convex integral polytopes* Δ (which we simply call polytopes), which are subsets of $N_{\mathbb{R}}$ satisfying the following conditions

1. **Convexity**: Δ is bounded by a finite number of hyperplanes.
2. **Integrality**: the vertices of Δ are contained in the lattice N.

Further, a polytope containing the origin 0 as an internal point is *reflexive* if its dual Δ^*, defined by

$$\Delta^* \;=\; \{m \in M_{\mathbb{R}} | \langle m, s\rangle \geq -1 \text{ for all } s \in \Delta\}$$

is again integral. The duality is involutive, $(\Delta^*)^* = \Delta$, so the dual of a reflexive polytope is again reflexive. To a reflexive polytope, we can associate a fan $\Sigma(\Delta)$ whose cones $\sigma(\Theta)$ are supported by the faces $\Theta \prec \Delta$

$$\sigma(\Theta) \;=\; \{\lambda f \,|\, f \in \Theta \;,\quad \lambda \in \mathbb{R}_+\} \;.$$

Fans and toric varieties

To a cone σ, we can associate a commutative semigroup

$$S_\sigma \;=\; \sigma^* \cap M \;,$$

to which we associate an algebra $\mathbb{C}[S_\sigma]$ and an affine variety

$$U_\sigma \;=\; \mathrm{Spec}\,[\mathbb{C}[S_\sigma]] \;.$$

If $\tau \prec \sigma$, then $\sigma^* \prec \tau^*$, which implies that S_σ is a sub-semigroup of S_τ, and that $\mathbb{C}[S_\sigma]$ is a subalgebra of $\mathbb{C}[S_\tau]$, and we have an inclusion $U_\tau \hookrightarrow U_\sigma$ of affine varieties. In fact, U_τ is an open subset of U_σ.

We can use these inclusions to define a set of transition functions from one patch to another. Indeed, consider a fan Σ and two cones $\sigma_1, \sigma_2 \in \Sigma$. The intersection $\tau = \sigma_1 \cap \sigma_2$ is a face of both σ_1 and σ_2. Thus we have inclusions

$$U_{\sigma_1} \hookleftarrow U_\tau \hookrightarrow U_{\sigma_2} \ ,$$

which can be used to identify the coordinates on a common open subset of U_{σ_1} and U_{σ_2}, giving coordinate transformations from the patch U_{σ_1} to U_{σ_2}. The patches U_{σ_i} corresponding to cones in Σ, together with the transition functions, define the toric variety $\mathbb{P}_\Sigma$ associated to the fan Σ. If the fan is associated to a reflexive polytope Δ, we denote the toric variety by $\mathbb{P}_\Delta$.

As an example, consider a simple fan in $N = \mathbb{Z}^2$ with top-dimensional cones $\sigma_1 = \langle \boldsymbol{e}_1, \boldsymbol{e}_2 \rangle$, $\sigma_2 = \langle \boldsymbol{e}_1, -\boldsymbol{e}_1 - \boldsymbol{e}_2 \rangle$, and $\sigma_3 = \langle \boldsymbol{e}_2, -\boldsymbol{e}_1 - \boldsymbol{e}_2 \rangle$. The dual cones are given by $\sigma_1^* = \langle \boldsymbol{e}_1, \boldsymbol{e}_2 \rangle$, $\sigma_2^* = \langle -\boldsymbol{e}_2, \boldsymbol{e}_1 - \boldsymbol{e}_2 \rangle$. and $\sigma_3^* = \langle -\boldsymbol{e}_1, -\boldsymbol{e}_1 + \boldsymbol{e}_2 \rangle$, with the corresponding semigroups generated by the generators of the cones.

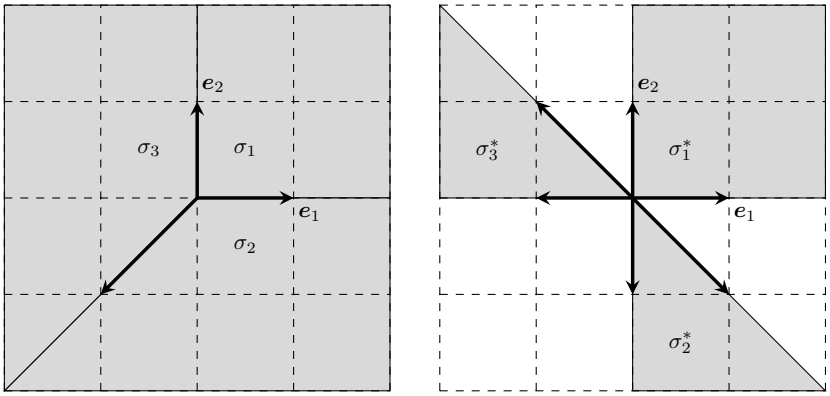


Figure 2.1: *A fan Σ corresponding to $\mathbb{P}^2$, and the dual cones σ_1^*, σ_2^*, and σ_3^*.*

These semigroups are free, so the corresponding group algebras are all isomorphic to the algebra of two-variable polynomials over complex numbers, $\mathbb{C}[x, y]$. To distinguish between different algebras, we denote these by $\mathbb{C}[x_1, y_1]$, $\mathbb{C}[x_2, y_2]$, and $\mathbb{C}[x_3, y_3]$. All of the cones contain the zero-dimensional cone at the origin as their common intersection. To this cone, we associate the semigroup generated by $\boldsymbol{e}_1, -\boldsymbol{e}_1, \boldsymbol{e}_2$, and $-\boldsymbol{e}_2$. This semigroup is not free, but rather has the dependencies among the generators $\boldsymbol{e}_1 + (-\boldsymbol{e}_1) = 0$ and $\boldsymbol{e}_2 + (-\boldsymbol{e}_2) = 0$. Therefore the corresponding algebra is

$$\frac{\mathbb{C}[x, y, z, w]}{\langle xz - 1, yw - 1 \rangle} \simeq \mathbb{C}[x, x^{-1}, y, y^{-1}] \ .$$

This is nothing but the coordinate ring of the algebraic torus, Spec $\left[\mathbb{C}[x, x^{-1}, y, y^{-1}]\right] = \mathbb{T}^2$. This torus is a common open subset of the patches U_{σ_1}, U_{σ_2}, and U_{σ_3}. Indeed, it is straightforward to find the corresponding inclusions of algebras. For example, we have that $\mathbb{C}[x_1, y_1] \hookrightarrow \mathbb{C}[x, x^{-1}, y, y^{-1}]$, with the identifications

$$x_1 = x \ , \qquad y_1 \ = \ y \ .$$

Making similar identifications with other algebras, we can write the three algebras corresponding to the patches U_{σ_i} as

$$\mathbb{C}[x,y], \qquad \mathbb{C}[y^{-1},xy^{-1}], \qquad \mathbb{C}[x^{-1},x^{-1}y] \ .$$

Finally, in this case we can further recognise these as corresponding to the affine patches of the complex projective space $\mathbb{P}^2$ with projective coordinates $[x,y,z]$.

Many of the properties of the toric variety $\mathbb{P}_\Sigma$ are encoded in the corresponding fan. For instance

1. $\mathbb{P}_\Sigma$ is compact if and only if Σ is complete.
2. $\mathbb{P}_\Sigma$ is smooth if and only if Σ is smooth.

Cox coordinates and quotient spaces

A complementary way of studying toric varieties is to use the construction of the toric variety as a quotient variety (2.18), analogous to how projective spaces are constructed. To each generator $v_i \in N$ of a ray (a one-dimensional cone) in the fan $\Sigma(\Delta)$, we associate a corresponding *Cox coordinate* z_{v_i}, which we also often denote by z_i. These parameterise the space $\mathbb{C}^n$. The set of scaling relations $(\mathbb{C}^*)^{n-d}$ by which we quotient by is found by identifying the set of relations between the ray generators $v_i \in N$. To be precise, defining a matrix

$$\mathrm{M} = (v_1, \ldots, v_n) \ , \tag{2.19}$$

the set of scaling relations can be identified with the nullspace Null(M). A vector $u \in \mathrm{Null(M)}$ with components $(u^1, \ldots, u^n)$ corresponds to the scaling relation

$$\mathbb{C}^* \times \mathbb{C}^n \to \mathbb{C}^n \ : \ (z_1, \ldots, z_n) \mapsto (\lambda^{u^1} z_1, \ldots, \lambda^{u^n} z_n) \ . \tag{2.20}$$

The point set Z_Δ is given by the following construction: for every subset I of the rays $I \subset \{v_1, \ldots, v_n\}$ such that there does not exist a cone in $\Sigma(\Delta)$ containing every $v_i \in I$, we associate a subvariety of $\mathbb{C}^n$ given by $V_I = \{(z_{v_1}, \ldots, z_{v_n}) \in \mathbb{C}^n \mid z_{v_i} = 0 \text{ for all } v_i \in I\}$. The point set Z_Δ is given by the union of these varieties.

Finally, the discrete group Γ is given by N/N', where N' is the sublattice of N generated by the ray generators $v_1, \ldots, v_n$.

Let us re-examine the example from the previous section in this language. There are three ray generators $v_1 = \boldsymbol{e}_1$, $v_2 = \boldsymbol{e}_2$, and $v_3 = -\boldsymbol{e}_1 - \boldsymbol{e}_2$, so we begin with the space $\mathbb{C}^3$. There is one relation among the generators, $v_1 + v_2 + v_3 = 0$, which corresponds to a scaling relation

$$\mathbb{C}^* \times \mathbb{C}^3 \to \mathbb{C}^3 \ : \ (z_1, z_2, z_3) \mapsto (\lambda z_1, \lambda z_2, \lambda z_3) \ .$$

The only set of generators that is not contained in a cone in the fan is $\{v_1, v_2, v_3\}$, which implies that $Z_\Delta = \{0\}$. The discrete subgroup Γ is trivial, as the ray generators generate the full lattice $N = \mathbb{Z}_2$. Thus the toric variety is given by

$$\mathbb{P}_\Delta \;=\; \frac{\mathbb{C}^3 \setminus \{0\}}{\mathbb{C}^*} \simeq \mathbb{P}^2 \;,$$

which agrees with the more involved analysis in the previous section.

2.3.2 Batyrev's construction

While the Calabi-Yau manifolds that are also toric are necessarily non-compact or *local*, compact Calabi-Yau manifolds can be obtained as subvarieties of toric varieties. A construction of such Calabi-Yau varieties, due to Batyrev [33], can also be used to find their mirror manifolds.

Let Δ be a reflexive polytope, with a dual polytope Δ^*. To the polytope Δ with integral points $s_i = (s_i^1, \ldots, s_i^r)$, we can associate a family Laurent polynomials $P \in \mathbb{C}[X_1^{\pm 1}, \ldots, X_r^{\pm 1}]$

$$P \;=\; \sum_{i=1}^{n} a_i X^{s_i} \;, \qquad \text{where } X^{s_i} \stackrel{\text{def}}{=} X_1^{s_i^1} \ldots X_r^{s_i^r} \;.$$

Interpreting the coordinates X_j as those of the algebraic torus $\mathbb{T}^r$, the vanishing locus of such a polynomial defines an affine hypersurface $V'(P) \stackrel{\text{def}}{=} \{(X_1, \ldots X_r) \in \mathbb{T}^n \,|\, P^i(X_1, \ldots, X_r) = 0\} \subset \mathbb{T}^r$. This has a closure $\widehat{V}(P) \subset \widehat{\mathbb{P}}_{\Delta^*}$, with $\widehat{\mathbb{P}}_{\Delta^*}$ the toric variety associated to Δ^*. In general the ambient toric variety $\widehat{\mathbb{P}}_{\Delta^*}$ need not be smooth, and so the closure $\widehat{V}(P)$ may inherit some singularities of $\widehat{\mathbb{P}}_{\Delta^*}$.

The ambient variety $\widehat{\mathbb{P}}_{\Delta^*}$ associated a reflexive polytope with exactly one integral internal point admits at least one *maximal projective crepant partial* (*MPCP*) desingularisation $\mathbb{P}_{\Delta^*}$ (for definitions, see [33]), associated to a *maximal projective* triangulation of the polytope Δ^*. We again have a closure $\mathcal{F}(\Delta) \stackrel{\text{def}}{=} V(P) \subset \mathbb{P}_{\Delta^*}$, defining the MPCP desingularisation of the hypersurface $\widehat{V}(P)$. The hypersurface $\mathcal{F}(\Delta)$ can be shown to be a Calabi-Yau variety with at most canonical singularities.

Batyrev identified the natural involutive map of polytopes $\Delta \mapsto \Delta^*$ given by the duality of reflexive polytopes with the mirror duality mapping the Calabi-Yau variety $\mathcal{F}(\Delta)$ to its dual $\mathcal{F}(\Delta^*)$. A strong suggestion of correctness of this identification is provided by the Hodge numbers of these varieties, for which Batyrev found the following formula:

$$\begin{aligned} h^{12}(\mathcal{F}(\Delta)) \;&=\; \text{pts}(\Delta^*) - \sum_{\text{codim}\,\Theta^*=1} \text{int}(\Theta^*) \quad + \sum_{\text{codim}\,\Theta=2} \text{int}(\Theta^*)\,\text{int}(\Theta) - 5 \;, \\ h^{11}(\mathcal{F}(\Delta)) \;&=\; \text{pts}(\Delta) \;- \sum_{\text{codim}\,\Theta=1} \text{int}(\Theta) \quad + \sum_{\text{codim}\,\Theta=2} \text{int}(\Theta^*)\,\text{int}(\Theta) - 5 \;, \end{aligned}$$

where $\text{pts}(\Theta)$ and $\text{int}(\Theta)$ denote the number of lattice points and interior lattice points of Θ. Θ and Θ^* are faces of Δ and Δ^*, respectively.

These formulae are manifestly compatible with mirror symmetry, as can be easily seen by noting that by definition of the duality of relexive polyhedra, the d-dimensional faces of Δ are in one-to-one correspondence with the $r-d-1$-dimensinal faces of Δ^*.

2.3.3 The method of Batyrev and Borisov

Batyrev's construction applies only for toric Calabi-Yau varieties defined be a single Laurent polynomial. However, there is a generalisation to varieties defined by multiple polynomials due to Batyrev and Borisov [33–35]. We briefly review this approach[1].

Given a variety defined as a vanishing locus of the set of n Laurent polynomials $\{P^i\}_{i=1}^n$, one can study the intersection of affine hypersurfaces $V'(P^i) \stackrel{\text{def}}{=} \{P^i = 0\} \subset \mathbb{T}$. If the polytopes $\{\Delta_i\}_{i=1}^n$ corresponding to the polynomials P^i form a nef-partition of a reflexive polytope Δ, we can define an ambient space $\widehat{\mathbb{P}}_{\Delta^*} \supset \mathbb{T}$ corresponding to the fan associated to Δ^*. The toric variety $\widehat{\mathbb{P}}_{\Delta^*}$ has a desingularisation $\mathbb{P}_{\Delta^*}$, corresponding to a maximal projective triangulation of Δ^*. The surfaces $V'(P^i)$ have closures $\widehat{V}(P^i) \subset \widehat{\mathbb{P}}_{\Delta^*}$ and $V(P^i) \subset \mathbb{P}_{\Delta^*}$, and we can define the closures of the intersections $\widehat{\mathcal{M}} = \widehat{V}(P^1) \cap \ldots \cap \widehat{V}(P^n)$ and $\mathcal{M} = V(P^1) \cap \ldots \cap V(P^n)$. It can be shown [34] that if $\widehat{\mathcal{M}}$ is non-empty and irreducible, and also $\dim \mathcal{M} \geq 3$, then $\mathcal{M}$ defined in this way is a smooth manifold.

To find the mirror variety of the smooth manifold constructed in this way, we note that by the definition of a nef-partition

$$\Delta \;=\; \mathrm{Mink}\big(\{\Delta_i\}_{i=1}^n\big)\ ,$$

where Mink denotes the Minkowski sum. In addition, we can define the convex hull of the union of the polytopes Δ_i:

$$\nabla^* \;\stackrel{\text{def}}{=}\; \mathrm{Conv}\big(\{\Delta_i\}_{i=1}^n\big).$$

One can show [34] that the polytope ∇^* so defined is also a reflexive polytope. In particular, it has a well-defined dual polytope ∇. This, and the dual polytope Δ^* of Δ, can be shown to be expressible in terms of n smaller polytopes $\{\nabla_i\}_{i=1}^n$:

$$\nabla \;=\; \mathrm{Mink}\big(\{\nabla_i\}_{i=1}^n\big)\ , \qquad \Delta^* \;=\; \mathrm{Conv}\big(\{\nabla_i\}_{i=1}^n\big)\ ,$$

where the sum is again a Minkowski sum, and $\{\nabla_i\}_{i=1}^n$ gives a nef-partition of ∇. Now we can define the mirror manifold of $\widehat{\mathcal{M}}$ as follows: first we use the polytopes ∇_i to define a set of polynomials $\{Q^i\}_{i=1}^n$ and a desingularisation $\mathbb{P}_{\nabla^*}$ corresponding to a maximal projective triangulation of ∇^*. Then the mirror manifold $\mathcal{W}$ of $\mathcal{M}$ can be expressed as the closure $V(Q^1) \cap \cdots \cap V(Q^n)$ of the variety

[1] To keep the notation consistent throughout the thesis, we adopt here notation that is slightly different from that of [34]. For example, their $\mathbb{P}_\Delta$ corresponds to our $\widehat{\mathbb{P}}_{\Delta^*}$.

$\{Q^1 = \cdots = Q^n = 0\} \subset \mathbb{T}$. Due to the way $\mathcal{W}$ is constructed, it follows that it is smooth and irreducible if and only if $\mathcal{M}$ is [34].

There is an algorithm for computing the Hodge numbers of varieties defined in this way [36, 37]. In the case of complete intersection varieties, it is more complicated than Batyrev's original formulae for the Hodge numbers [33]. We will not review the details here, and simply note that some computer algebra packages, such as PALP [38], provide an implementation of the algorithm.

Chapter 3

Calabi-Yau Modularity and Physics

3.1 One-dimensional example: elliptic curves

To introduce the concept of modularity, let us give an example of the simplest case, that of elliptic curves. Elliptic curves are one-dimensional Calabi-Yau manifolds, which can be expressed as a subset of $\mathbb{P}^2$ of points satisfying a cubic polynomial

$$\sum_{\substack{i+j+k=3 \\ i,j,k>0}} a_{ijk} x^i y^j z^k \;=\; 0 \;.$$

When this polynomial is defined over $\mathbb{Q}$, i.e. the coefficients $a_{ijk} \in \mathbb{Q}$, by rescaling the equation, we can take $a_{ijk} \in \mathbb{Z}$. Going to an affine patch, every such elliptic curve can be also written in the Weierstrass form

$$y^2 + a_1 xy + a_3 y \;=\; x^3 + a_2 x^2 + a_4 x + a_6 \;,$$

with $a_i \in \mathbb{Z}$. Since there is a natural projection $\mathbb{Z} \to \mathbb{F}_{p^n}$, this equation can also be seen as defining a variety $E(\mathbb{F}_{p^n})$ over finite fields $\mathbb{F}_{p^n}$. By $E(\mathbb{F}_{p^n})$ we mean the set of points $x \in \mathbb{F}_{p^n}$ satisfying the above equation, taking into account precisely one point 'at infinity', that does not lie on this affine patch. It is in principle straightforward to count the number of points on $E(\mathbb{F}_{p^n})$. Denoting this quantity $\#_p(E)$, it is consequence of modularity theorem [5–7] that the quantities a_p defined by

$$a_p = p + 1 - \#_p(E) \;.$$

are Fourier coefficients of a modular form.

To formulate this correspondence more carefully, we need to consider the *zeta function* of the elliptic curve. It is defined as a generating function for the point counts $\#_{p^n}(E)$:

$$\zeta_p(T) \;=\; \exp\left(\sum_{n=1}^{\infty} \frac{\#_{p^n}(E) T^n}{n} \right) \;.$$

The *Weil conjectures* [39] (which have been proven, see §3.4) can be used to show that this zeta function takes the form

$$\zeta_p(T) \;=\; \frac{1 - a_p T + pT^2}{(1-T)(1-pT)} \;.$$

Associated to these zeta functions, one can define a *Hasse-Weil L-function*

$$L(E,s) \;=\; \prod_{p \text{ good}} \frac{1}{1 - a_p p^{-s} + p^{1-2s}} \prod_{p \text{ bad}} \frac{1}{1 \pm p^{-s}}.$$

Here the first product runs over the *primes of good reduction* p for which the variety $E(\mathbb{F}_p)$ is smooth, and the second product is over *primes of bad reduction* p for which $E(\mathbb{F}_p)$ has a singularity. The sign in the second product is chosen based on whether E has a *split* or *non-split multiplicative reduction* at p (for explanation of these terms, see for example [40]). The primes of bad reduction can also be used to define an invariant called *conductor*, which is divisible precisely by the primes of bad reduction, although they may appear with multiplicity, again related to whether the reduction is split or non-split multiplicative.

It is also possible to associate an *Hecke L-function* to an modular form. Consider a cusp form f of a congruence subgroup $\Gamma_0(N)$ with Fourier expansion

$$f(\tau) \;=\; \sum_{n=1}^{\infty} a_n q^n \;.$$

Then we define the associated L-function as

$$L(f,s) \;=\; \sum_{n=1}^{\infty} \frac{a_n}{n^s}.$$

If f is an Hecke eigenform, then we can write this in a suggestive form as

$$L(f,s) \;=\; \prod_{p \nmid N} \frac{1}{1 - a_p p^{-s} + p^{1-2s}} \prod_{p \mid N} \frac{1}{1 - a_p p^{-s}}.$$

The modularity theorem states that, for any elliptic curve E defined over $\mathbb{Q}$, there exists an Hecke eigenform f of level N, divisible only by the bad primes of E, and weight 2 such that

$$L(E,s) \;=\; L(f,s).$$

For example, consider a simple elliptic curve

$$y^2 \;=\; x^3 + x^2 + 1 \;,$$

Consider solutions over $\mathbb{F}_p \simeq \mathbb{Z}/p\mathbb{Z}$. The primes of bad reduction are $p = 2, 31$ [41], and the conductor of this curve is given by $N = 2^3 \cdot 31 = 248$. We can count the number solutions over $\mathbb{F}_p$, $\#_p(E)$, and use them to tabulate the values of a_p for the first ten primes in table 3.1.

p	1	2	3	5	7	11	13	17	19	23	29
a_p	1	0	-2	1	-3	-2	-2	-6	1	-6	4

Table 3.1: *The coefficients a_p computed from the number of points on elliptic curves defined over finite fields $\mathbb{F}_p$ for the first ten primes.*

In accordance with the modularity theorem, there is a modular form for $\Gamma_0(248)$ of weight 2 with *The L-functions and modular forms database* LMFDB [41] label **248.2.a.a**, whose Fourier expansion is given by

$$f(q) = q - 2q^3 + q^5 - 3q^7 + q^9 - 2q^{11} - 2q^{13} - 2q^{15} - 6q^{17} + q^{19} + 6q^{21} - 6q^{23} - 4q^{25} + 4q^{27} + 4q^{29} + \dots ,$$

and the agreement of the Fourier coefficients with the point counts persists to higher orders, as can be easily verified.

3.2 Modularity

Modularity of Calabi-Yau manifolds can be seen as an aspect of the Langlands program, which is a highly-influential and far-reaching set of conjectures on the relation of number theory, geometry and representation theory (for an introductory exposition, see for example [42]. For a physicist-oriented review, see [43]). We give a very brief overview of the aspects relevant to Calabi-Yau modularity, focusing on the case of two-dimensional representations, which will be most relevant for the rest of this thesis. This overview is meant to provide some intuition behind the connection of zeta function and modular forms, and makes no attempt at rigour.

A special case of the correspondence can be stated [43] as a relation between two-dimensional representations of the *absolute Galois group* $\mathrm{Gal}(\bar{\mathbb{Q}}/\mathbb{Q})$ and modular forms. Further, this correspondence should relate the eigenvalues of an element of the representation associated to the Frobenius map (see (3.8)), and the Hecke eigenvalues of the modular forms (see (3.5)). Thus the correspondence is

$$\begin{aligned} \text{2-dimensional representations of } \mathrm{Gal}(\bar{\mathbb{Q}}/\mathbb{Q}) \quad &\longleftrightarrow \quad \text{Modular forms,} \\ \text{Frobenius eigenvalues} \quad &\longleftrightarrow \quad \text{Hecke eigenvalues.} \end{aligned} \tag{3.1}$$

The Galois representations arise naturally in theory of manifolds $X(\mathbb{F}_p)$ defined over finite fields. The absolute Galois group acts on so-called étale cohomology $H^3_{\text{ét}}(X, \mathbb{Q}_\ell)$, which is a vector space with coefficients in the field of ℓ-adic numbers, and can be thought of as an analogue of the usual de Rham cohomology. It can be shown that there is a natural action of $\mathrm{Gal}(\bar{\mathbb{Q}}/\mathbb{Q})$ on $H^3_{\text{ét}}(X, \mathbb{Q}_\ell)$, defining a representation ρ of the absolute Galois group.

If the third cohomology group is two-dimensional, as is the case with elliptic curves, it then follows that there should be a correspondence between the Frobenius eigenvalues and the Hecke eigenvalues of an modular form. This is nothing but the correspondence we saw in the previous section. However,

stated in this form, it is clear that the correspondence should not be limited to elliptic curves. Indeed, it has been shown, for example, that *rigid* Calabi-Yau threefolds, for which the third cohomology group is two-dimensional, are modular [44].

However, the third cohomology group $H^3_{\text{ét}}(X, \mathbb{Q}_\ell)$ need not be two-dimensional in order for the corresponding manifold to be modular. It can happen that the representation of $\text{Gal}(\bar{\mathbb{Q}}/\mathbb{Q})$ is reducible, and one of the irreducible pieces is two-dimensional. This is the origin of modularity for Calabi-Yau manifolds that we study: we look for Calabi-Yau threefolds whose Hodge structure splits, by which we mean that there exist two subspaces $V, V' \subset H^3(X, \mathbb{Q})$ with definite Hodge type, such that the third de Rham cohomology group can be written as a direct sum

$$H^3(X, \mathbb{Q}) \;=\; V \oplus V' \;. \tag{3.2}$$

It can then be shown that the étale cohomology has a similar split, and the representation of the absolute Galois group reduces. This process, which we briefly review, has been explained in detail in [12].

Let $X(\mathbb{K})$ be a Calabi-Yau manifold defined over a number field $\mathbb{K}$. It can be shown that if there is a split of type (3.2), then there exists a number field $\mathbb{E} \supseteq \mathbb{K}$, such that the étale cohomology of $X(\mathbb{E})$ splits

$$H^3_{\text{ét}}(X(\mathbb{E}), \mathbb{Q}_\ell) \;=\; U \oplus U' \;,$$

where U and U' have the same dimensions and Hodge types as V and V', respectively. This in turn leads to reduction of the representation ρ of the absolute Galois group:

$$\rho(X) \;=\; \rho(U) \oplus \rho(U') \;. \tag{3.3}$$

Modularity is best-understood for varieties defined over $\mathbb{Q}$. In this case the two-dimensional subspaces with the Hodge type $(2,1) + (1,2)$ correspond to weight-two modular forms, whereas the spaces with Hodge type $(3,0) + (0,3)$ correspond to weight-four modular forms [12]. However, the modular forms associated to representations over field extensions of $\mathbb{Q}$ are more complicated. In [12], it was conjectured, in the spirit of the Langlands correspondence, that when the extension field $\mathbb{E}$ is a real quadratic field, the corresponding modular forms are Hilbert modular forms, instead of 'ordinary' elliptic modular form. In part III, where we investigate supersymmetric flux vacua, we are indeed able to find significant evidence for this conjecture.

In the rest of this chapter, we review some relevant properties of the objects appearing on the two sides of this correspondence — modular forms and zeta functions — after which we explain how modular Calabi-Yau manifolds are related to interesting physical solutions: black holes associated to rank-two attractor points, and supersymmetric flux vacua.

3.3 Modular forms

3.3.1 Elliptic modular forms

Elliptic, or "ordinary", modular forms are simplest examples of automorphic forms we will encounter in this thesis. We recall their definition and some important properties mainly following [45].

Elliptic modular forms are holomorphic functions on the upper half plane

$$\mathbb{H} \;=\; \{z \in \mathbb{C} \,|\, \mathrm{Im}\, z > 0\}$$

which have prescribed transformation properties under the action of the Möbius transformations

$$z \mapsto \gamma z \;\stackrel{\text{def}}{=}\; \frac{az+b}{cz+d}\;, \qquad \gamma \;=\; \begin{pmatrix} a & b \\ c & d \end{pmatrix} \in \mathrm{SL}(2,\mathbb{Z})\;.$$

Mere generally, we can take $\gamma \in \Gamma \subset \mathrm{SL}(2,\mathbb{R})$ for some discrete subgroup Γ. Some useful subgroup we will encounter later in this thesis are *principal congruence subgroups* $\Gamma(N)$ and *Hecke congruence subgroups* $\Gamma_0(N)$, which are defined as

$$\begin{aligned}
\Gamma(N) \;&=\; \left\{ \begin{pmatrix} a & b \\ c & d \end{pmatrix} \in \mathrm{SL}(2,\mathbb{Z}) \;\middle|\; b, c \equiv 0 \bmod N \right\}\;, \\
\Gamma_0(N) \;&=\; \left\{ \begin{pmatrix} a & b \\ c & d \end{pmatrix} \in \mathrm{SL}(2,\mathbb{Z}) \;\middle|\; c \equiv 0 \bmod N \right\}\;, \\
\Gamma_1(N) \;&=\; \left\{ \begin{pmatrix} a & b \\ c & d \end{pmatrix} \in \mathrm{SL}(2,\mathbb{Z}) \;\middle|\; c \equiv 0 \bmod N \quad a, d \equiv 1 \bmod N \right\}\;.
\end{aligned}$$

The integer N is called the *level* of the subgroup.

Under a transformation $\gamma \in \Gamma$, a (*holomorphic*) *modular form* f (for group Γ) of *weight* k transforms as

$$f(\gamma z) \;=\; (cz+d)^k f(z)\;, \qquad \gamma = \begin{pmatrix} a & b \\ c & d \end{pmatrix} \in \Gamma. \tag{3.4}$$

In addition, it is required that $f(x+\mathrm{i}y)$ is bounded as $y \to \infty$.

For all groups Γ, such as $\Gamma_0(N)$, that contain the element

$$T \;=\; \begin{pmatrix} 1 & 1 \\ 0 & 1 \end{pmatrix}$$

corresponding to the transformation $\tau \mapsto \tau + 1$, the transformation law (3.4) implies that f is periodic in τ, and thus has a Fourier expansion

$$f(\tau) \;=\; \sum_{n=0}^{\infty} a_n\, q^n\;, \qquad q \;=\; e^{2\pi \mathrm{i} \tau}\;.$$

We call f a *cusp form* if the Fourier coefficient a_0 is vanishing. The terminology "cusp form" is related to the fact that such modular forms vanish at the cusps of Γ in the moduli space.

We denote the space of modular forms for group Γ of weight k by $M_k(\Gamma)$, and the weight-k cusp forms for the same group by $S_k(\Gamma)$. Due to their transformation properties, modular forms are highly constrained, and importantly the spaces $M_k(\mathrm{SL}(2,\mathbb{Z}))$ and $M_k(\Gamma_0(N))$, and thus also $S_k(\mathrm{SL}(2,\mathbb{Z}))$ and $S_k(\Gamma_0(N))$ are finite-dimensional.

Hecke operators

If n and N are integers such that $\gcd(n, N) = 1$, it is possible to define a set of *Hecke operators* T_n acting on the spaces $M_k(\Gamma_0(N))$ as

$$T_n f(\tau) \;=\; n^{k-1} \sum_{\gamma \in \Gamma_0(N) \backslash \mathcal{M}_n(N)} (c\tau + d)^{-k} f(\gamma\tau) \;, \qquad \text{where } \gamma \;=\; \begin{pmatrix} a & b \\ c & d \end{pmatrix}, \tag{3.5}$$

and $\mathcal{M}_n(N)$ is the subset of $\Gamma_0(N)$ of matrices with determinant n. By expanding f as a Fourier series, and using a suitable set of representatives for $\mathcal{M}_n(N)$, it can be shown that these act on the Fourier coefficients as

$$a_i \mapsto \sum_{r | \gcd(n,i)} r^{k-1} a_{in/r^2} \;.$$

From this we also see that any two Hecke operators commute with each other, which allows us to find an basis for $M_k(\Gamma_0(N))$ which a simultaneous eigenbasis of all Hecke operators. A simultaneous eigenvector of all Hecke operators is called a *Hecke eigenform*. We say such a form is *normalised* if $a_1 = 1$.

Note that for $N = 1$, $\gcd(n, N) = 1$ for all n, and thus a normalised Hecke eigenform is completely determined by its Hecke eigenvalues. If $N \neq 1$ this is no longer true, but it is possible to define a space of modular forms, called *newforms*, for which this property holds.

Let M be an integer $M \mid N$. Then for every $d \mid N/M$ and $g \in M_k(M)$, the function f defined by $f(\tau) = g(d\tau)$ is a cusp form of weight k and level N, $f \in S_k(\Gamma_0(N))$. These modular forms are said to be *oldforms*. The orthogonal complement of the space of oldforms in $S_k(\Gamma_0(N))$ under the Petersson inner product (see for example [46] for definition) is the space of *newforms*, so we have a decomposition

$$S_k(\Gamma_0(N)) \;=\; S_k^{\text{old}}(\Gamma_0(N)) \oplus S_k^{\text{new}}(\Gamma_0(N)) \;.$$

A modular form in $S_k^{\text{new}}(\Gamma_0(N))$ is called a *newform* if it is also a normalised Hecke eigenform. Newforms form a basis of $S_k^{\text{new}}(\Gamma_0(N))$.

3.3.2 Hilbert modular forms

Another important class of modular forms consists of Hilbert modular forms. These are modular forms associated to totally real number fields, such as real quadratic fields, which we consider here for simplicity, although generalisation to other totally real number fields is obvious. We review some of the properties of real quadratic fields and Hilbert modular forms, following [46].

Real quadratic fields and embeddings

Real quadratic fields F are field extensions of $\mathbb{Q}$ of the form $\mathbb{Q}(\sqrt{D})$, where D is a square-free integer. The ring of integers is given by

$$\mathcal{O}_F \;=\; \begin{cases} \mathbb{Z}\left(\frac{1+\sqrt{D}}{2}\right) \;, & \text{if } D \equiv 1 \mod 4 \;, \\ \mathbb{Z}(\sqrt{D}) \;, & \text{if } D \equiv 2,3 \mod 4 \;, \end{cases}$$

The analogues of the groups $\mathrm{GL}(2,\mathbb{Q})$ and $\mathrm{GL}(2,\mathbb{Z})$ are $\mathrm{GL}(2,F)$ and $\mathrm{GL}(2,\mathcal{O}_F)$. These can be embedded into $\mathrm{GL}(2,\mathbb{R})\times\mathrm{GL}(2,\mathbb{R})$ using the two inequivalent embeddings of F into $\mathbb{R}$. To be explicit, choose an embedding of F into $\mathbb{R}$ so that we can write every $a \in F$ as $a_1 + \sqrt{D}a_2$, $a_1, a_2 \in \mathbb{Q}$. This has a conjugate which is precisely the image of a in the second embedding. Let us denote this by $\bar{a} = a_1 - \sqrt{D}a_2$. Then an element of γ of $\mathrm{GL}(2,F)$ is embedded into $\mathrm{GL}(2,\mathbb{R}) \times \mathrm{GL}(2,\mathbb{R})$ by

$$\gamma \;=\; \begin{pmatrix} a & b \\ c & d \end{pmatrix} \mapsto \left[\begin{pmatrix} a_1+\sqrt{D}a_2 & b_1+\sqrt{D}b_2 \\ c_1+\sqrt{D}c_2 & d_1+\sqrt{D}d_2 \end{pmatrix}, \begin{pmatrix} a_1-\sqrt{D}a_2 & b_1-\sqrt{D}b_2 \\ c_1-\sqrt{D}c_2 & d_1-\sqrt{D}d_2 \end{pmatrix} \right] \in \mathrm{GL}(2,\mathbb{R}) \times \mathrm{GL}(2,\mathbb{R}) \;.$$

Thus $\mathrm{SL}(2,F)$ has a natural action on the upper half space $\mathbb{H}^2 = \mathbb{H} \times \mathbb{H}$, on which it acts by

$$(z_1, z_2) \mapsto \left(\frac{az_1 + b}{cz_1 + d}, \frac{\bar{a}z_1 + \bar{b}}{\bar{c}z_1 + \bar{d}} \right) \;.$$

Hilbert modular forms

Let $\mathfrak{n}$ be a nonzero ideal of $\mathcal{O}_F$, and let $\Gamma_0(\mathfrak{n}) \subset \mathrm{GL}(2,F)$ be a subgroup *commensurable* with $\mathrm{GL}(2,\mathcal{O}_F)$ (i.e. $\Gamma_0(\mathfrak{n}) \cap \mathrm{SL}(2,\mathcal{O}_F)$ has a finite index in both $\Gamma_0(\mathfrak{n})$ and $\mathrm{SL}(2,\mathcal{O}_F)$), defined by

$$\Gamma_0(\mathfrak{n}) \stackrel{\text{def}}{=} \left\{ \gamma = \begin{pmatrix} a & b \\ c & d \end{pmatrix} \in \mathrm{GL}(2,\mathcal{O}_F) \middle| c \in \mathfrak{n} \;, \text{ and } \det\gamma \text{ totally positive} \right\} .$$

A meromorphic function $f : \mathbb{H}^2 \to \mathbb{C}$ is a *Hilbert modular form* of weight $k = (k_1, k_2) \in \mathbb{Z}^2$ for Γ if it satisfies the transformation law

$$f(\gamma z) \;=\; (cz_1 + d)^{k_1} (\bar{c}z_2 + \bar{d})^{k_2} f(z) \tag{3.6}$$

for all $\gamma \in \Gamma$. In particular

$$\begin{pmatrix} 1 & \mu \\ 0 & 1 \end{pmatrix} \in \Gamma_0(\mathfrak{n})$$

for all $\mu \in \mathcal{O}_F$ and for all integral ideals $\mathfrak{n}$. Applying the transformation law (3.6), it follows that

$$f(z + \mu) \;=\; f(z)$$

for all $\mu \in \mathcal{O}_F$. Hence, f has a Fourier expansion of the form

$$f \;=\; \sum_{\nu \in \mathfrak{d}^{-1}} a_\nu \exp\left(2\pi \mathrm{i}\,\mathrm{Tr}\,(\nu z)\right) \;,$$

where Tr is the field trace and $\mathfrak{d}^{-1}$ denotes the inverse different defined by

$$\mathfrak{d}^{-1} \stackrel{\text{def}}{=} \left\{ x \in F \middle| \,\mathrm{Tr}\,(xy) \in \mathbb{Z} \text{ for all } y \in \mathcal{O}_F \right\} .$$

The coefficients in the Fourier expansion can be associated to integral ideals $\mathfrak{m}$ of F:

$$a_{\mathfrak{m}} \stackrel{\text{def}}{=} a_u \ ,$$

where u is a totally positive element satisfying $(u) = \mathfrak{m}\mathfrak{d}^{-1}$.

3.4 Zeta function

Under the Langlands correspondence discussed in §3.2 modular forms correspond to zeta functions, which are generating functions for the number of points on an algebraic variety defined over finite fields, that is the number of solutions of the defining equations, over finite fields $\mathbb{F}_{p^n}$.

We consider mainly m-parameter families of Calabi-Yau manifolds $X_{\boldsymbol{\varphi}}$ defined over rational numbers, parametrised by $\boldsymbol{\varphi} = (\varphi_1, \ldots, \varphi_m)$. That is, we require that the polynomials defining the manifold, at least locally, have coefficients in $\mathbb{Q}$, or equivalently in $\mathbb{Z}$, with compatible transition functions. Given the natural projections $\mathbb{Z} \to \mathbb{F}_{p^n}$, we can think of these equations also as defining a family of manifolds over these finite fields. To avoid any confusion, where needed, we will denote the manifold $X_{\boldsymbol{\varphi}}$ defined over field $\mathbb{K}$ by $X_{\boldsymbol{\varphi}}(\mathbb{K})$.

Denoting the number of points on a manifold $X_{\boldsymbol{\varphi}}(\mathbb{F}_{p^n})$ by $\#_{p^n}(\boldsymbol{\varphi})$, we define

$$\zeta_p(\boldsymbol{\varphi}; T) \ = \ \exp\left(\sum_{n=1}^{\infty} \frac{\#_{p^n}(\boldsymbol{\varphi}) T^n}{n}\right).$$

The Weil conjectures, originally stated by Weil [39], and later proven by Dwork [47], Grothendiek [48], and Deligne [49, 50], can be stated as:

1. **Rationality**: $\zeta_p(X, T)$ is a rational function of T of the form

   $$\zeta(X, T) \ = \ \frac{R_1(X,T) R_3(X,T) \ldots R_{2d-1}(X,T)}{R_0(X,T) R_2(X,T) \ldots R_{2d}(X,T)},$$

   where $R_i(X, T)$ is a polynomial in T with integer coefficients, and whose degree in given by the Betti number b_i.

2. **Functional equation**: $\zeta(X, T)$ satisfies

   $$\zeta\left(X, p^{-d} T^{-1}\right) \ = \ \pm p^{\frac{d}{2}\chi} T^{\chi} \zeta(X, T) \ , \tag{3.7}$$

   where χ is the Euler characteristic of X.

3. **Riemann hypothesis**: The polynomials $R_i(X, T)$ factorise over $\mathbb{C}$ as

   $$R_i(X, T) \ = \ \prod_{j=1}^{b_j} (1 - \lambda_{ij}(X) T) \ ,$$

   where the $\lambda_{ij}(X)$ are algebraic integers of absolute value $p^{i/2}$.

The m-parameter Calabi-Yau threefolds have Hodge diamonds given by

$$h^{p,q} \;=\; \begin{array}{ccccccc} & & & 1 & & & \\ & & 0 & & 0 & & \\ & 0 & & h^{1,1} & & 0 & \\ 1 & & m & & m & & 1 \\ & 0 & & h^{1,1} & & 0 & \\ & & 0 & & 0 & & \\ & & & 1 & & & \end{array} \;.$$

In this case, the form of the zeta function simplifies greatly, being determined by the degree-$(2m+2)$ polynomial $R(X,T) = R_3(X,T)$

$$\zeta(X,T) = \frac{R(X,T)}{(1-T)(1-pT)^{h^{11}}(1-p^2T)^{h^{11}}(1-p^3T)}.$$

As reviewed in detail in [13] (see also [51] for a physics-oriented exposition, or [52] for a physicist-friendly mathematical treatment), this polynomial can be computed explicitly using the periods of the Calabi-Yau manifold. Roughly speaking, the reason for the relation to the periods is due to the fact that the polynomial $R(T,X)$ can be related to the *Frobenius map* acting on the third cohomology.

Denote by Frob_p the Frobenius map

$$\mathbb{K}^k \to \mathbb{K}^k \;:\; \boldsymbol{x} = (x_1,\ldots,x_k) \mapsto (x_1^p,\ldots,x_k^p) \;=\; \boldsymbol{x}^p \;.$$

As a consequence of Fermat's little theorem, Frob_p fixes the elements of $\mathbb{F}_p^k \subset \mathbb{K}^k$. Analogously, we define the Frobenius maps Frob_{p^n}

$$\text{Frob}_{p^n} \;:\; \boldsymbol{x} \mapsto \boldsymbol{x}^{p^n} \;, \tag{3.8}$$

which fix the elements of $\mathbb{F}_{p^n} \subset \mathbb{K}$. Importantly, this action maps the points on a manifold $X(\mathbb{F}_{p^n})$ to other points on the manifold. To see this, consider a manifold locally defined as a locus $P(\boldsymbol{x}) = 0$, with P having coefficients in $\mathbb{F}_{p^n}$. Then, as the Frobenius map fixes the elements of $\mathbb{F}_{p^n}$, we have that $\text{Frob}_{p^n}(\boldsymbol{x}) = \boldsymbol{x}^{p^n}$ also satisfies the polynomial P

$$P\left(\boldsymbol{x}^{p^n}\right) \;=\; P(\boldsymbol{x})^{p^n} \;=\; 0 \;.$$

As explained in [13], it is possible to define corresponding Frobenius maps Fr_{p^n}, which act on certain p-adic cohomology groups $H^n(X_{\boldsymbol{\varphi}})$:

$$\text{Fr}_{p^n} : H^n(X_{\boldsymbol{\varphi}}) \to H^n(X_{\boldsymbol{\varphi}}) \;. \tag{3.9}$$

Using the Lefschetz fixed point theorem, it is then possible to count the number of points on manifolds $X_{\boldsymbol{a}}(\mathbb{F}_{p^n})$ using traces of this map,

$$\#_{p^n}(\boldsymbol{\varphi}) \;=\; \sum_{k=0}^{6}(-1)^k \text{Tr}\left(\text{Fr}_{p^n}\big|H^k(X_{\boldsymbol{\varphi}})\right) \;.$$

Furthermore, the characteristic polynomial of the inverse Frobenius maps can be associated to the polynomial $R(T)$:

$$R(T) \;=\; \text{Det}\left(\mathbb{I} - T\,\text{Fr}_p^{-1}\big|H^3(X_{\boldsymbol{\varphi}})\right) \;. \tag{3.10}$$

Factorisations

The reduction of the Galois representation (3.3) can be seen in the structure of the Zeta function, as the Frobenius map can be associated to an element of the Galois representation [43]. When the representation ρ reduces, the matrices F and U, representing the actions of Fr_p and Fr_p^{-1} on $H^3(X_{\boldsymbol{\varphi}})$, expressed in a suitable basis, are block diagonal. This immediately implies that the characteristic polynomial $R(T)$ will factorise over integers to a product of the characteristic polynomials of the blocks, corresponding to the irreducible representations.

Based on the Langlands correspondence, we expect that when the representation has a two-dimensional irreducible subrepresentation so that the polynomial $R(T)$ has a quadratic factor $R_2(T) \mid R(T)$, the coefficients of $R_2(T)$, only one of which is not fixed by the functional equation, should correspond to Hecke eigenvalues of a modular form. This is the central property that we are interested in investigating with regards to modularity: we search for string theory compactifications where the zeta function of the compactification manifold factorises in this manner, find the associated modular forms, and try to make connections between the physical properties of the string theory solution and the attributes of the modular form.

3.5 Modularity from attractor points and flux vacua

We have seen above that the modularity of Calabi-Yau threefolds can be traced back to the properties of their middle cohomologies. In fact, the zeta function denominator has a quadratic factor if there exists a suitable two-dimensional subspace $\Lambda \subset H^3(X)$. Existence of these these subspaces can be shown to be equivalent to existence of certain physical solutions in type IIA or IIB string theories compactified on the Calabi-Yau manifold X, specifically black holes and supersymmetric flux vacua. We review these in the following sections, and briefly discuss their relation to Calabi-Yau modularity.

3.5.1 Calabi-Yau compactifications

A large family of four-dimensional $\mathcal{N} = 2$ supergravity theories can be obtained by compactifying IIA or IIB supergravity theories on Calabi-Yau threefolds. As discussed in §2.2, mirror symmetry relates the IIA and IIB compactifications, so we freely switch between the two. In this section, we will look at things from the IIB point-of-view.

The massless field content of type IIB string theory consists of the even-form Ramond-Ramond fields C_0, C_2, C_4 with field strengths $F_i = \mathrm{d}C_{i-1}$; the Kalb-Ramond two-form field B_2 with field strength $H_3 = \mathrm{d}B_2$; the metric g; and the dilaton ϕ. In addition to this field content, the theory can contain even-dimensional (localised) D-branes, that is D1-, D3-, D5-, D7-, and D9-branes, which couple to the gauge field potentials electrically or magnetically.

The axion C_0 and dilaton ϕ are packaged into a single complex scalar field, the axiodilaton τ:

$$\tau \;=\; C_0 + \mathrm{i}\mathrm{e}^{-\phi} \;. \tag{3.11}$$

The field strengths $H_3 = \mathrm{d}B_2$ and $F_3 = \mathrm{d}C_2$ are also for convenience combined into the complex field strength

$$G_3 \;=\; F_3 - \tau H_3 \;. \tag{3.12}$$

Compactifying the ten-dimensional theory on a Calabi-Yau threefold X, one obtains a four-dimensional $\mathcal{N} = 2$ theory with $h^{1,2}$ vector multiplets, $h^{1,1} + 1$ hypermultiplets, and one gravity multiplet (for a review, see for example [53]). The scalar fields in the vector and hyper multiplets can be seen to parametrise the geometry of the internal Calabi-Yau manifold. Specifically, the scalars in the vector multiplets can be identified with the complex structure moduli space coordinates, while the scalars in the hypermultiplets, apart from one so-called universal hypermultiplet, parametrise the complexified Kähler structure moduli space.

3.5.2 Attractor mechanism

The authors of [54, 55] studied a four-dimensional $\mathcal{N} = 2$ supergravity theory coupled to $\mathcal{N} = 2$ vector multiplets, which can be conveniently formulated in terms of special geometry [56]. (For a textbook introduction to the attractor mechanism, see for example [53, 57].) It was noticed that, for the supersymmetric black hole solutions in these theories, the special geometry moduli have to satisfy a pair of relatively simple differential equations. These equations can be interpreted as requiring that the central charge of the supergravity theory has a critical point at the horizon of the black hole.

If a black hole solution in $\mathcal{N} = 2$ supergravity is spherically symmetric and static, we can write the line element

$$\mathrm{d}s^2 \;=\; e^{2U(r)}\mathrm{d}t^2 - e^{-2U(r)}(\mathrm{d}r^2 + r^2\mathrm{d}\Omega^2) \;,$$

where the radial coordinate r is zero on the horizon. A key quantity is the central charge $\mathcal{Z}$ of the supersymmetry algebra, which is related to the mass and entropy of the black hole.

$$\mathcal{Z}(Q) \;=\; \frac{Q^T\,\Sigma\,\Pi}{\sqrt{-\mathrm{i}\Pi^\dagger\,\Sigma\,\Pi}} \;. \tag{3.13}$$

The dynamics of the $\mathcal{N} = 2$ vector multiplet scalars z^a, which can be viewed as coordinates on the moduli space $\mathcal{M}_{\mathbb{C}}$, and the function U can be written in terms of a new coordinate $\rho = 1/r$, so that, for 1/2-BPS solutions, they are governed by a pair of differential equations

$$\frac{dU(\rho)}{d\rho} \;=\; -e^{U(\rho)}|\mathcal{Z}| \;, \qquad \frac{dz^a(\rho)}{d\rho} \;=\; -2e^{U(\rho)}g^{a\bar{b}}\partial_{\bar{b}}|\mathcal{Z}| \;, \tag{3.14}$$

where $g_{a\bar{b}}$ is the special geometry metric on the moduli space $\mathcal{M}_{\mathbb{C}S}$. These equations describe flows of scalar field values from $\rho = 0$ at spatial infinity to $\rho = \infty$ at the black hole horizon. The terminology

"attractor mechanism" owes to the fact that the values of z^a are fixed at the black hole horizon at $r = 0$ ($\rho = \infty$) by the black hole charges, and so are independent of the values they take at $r = \infty$ ($\rho = 0$), at least for sufficiently small variations of the boundary values.

The second equation in (3.14) can be used to find a gradient flow equation:

$$\frac{d|\mathcal{Z}|}{d\rho} \;=\; -4e^{U(\rho)} g^{a\bar{b}} \partial_a |\mathcal{Z}| \partial_{\bar{b}} |\mathcal{Z}| \;.$$

since the metric $g_{a\bar{b}}$ is positive definite, this reveals that the end points of attractor flows are critical values of $|\mathcal{Z}|$. This also shows that $|\mathcal{Z}|$ decreases along attractor flows.

It was pointed out early on by Strominger [58] that at an attractor point where the central charge is not vanishing, the period vector Π of the Calabi-Yau manifold satisfies a relation that we shall refer to as the *alignment equations*

$$\mathrm{Im}\,[C\Pi] \;=\; Q \;, \tag{3.15}$$

where Q is the charge vector of the corresponding black hole, and the constant C can be written as a function of the central charge $\mathcal{Z}$, and the Kähler potential (2.2):

$$C \;=\; 2\mathrm{e}^{-K/2}\overline{\mathcal{Z}} \;.$$

The equation (3.15) can be thought of as determining the relation between the charges and the prepotential (2.8). We utilise this in part IV to solve for the prepotential.

If, on the other hand, the central charge vanishes, then the corresponding relation is

$$Q^T \,\Sigma\, \Pi \;=\; 0 \;, \tag{3.16}$$

which we will refer to as the *orthogonality equation*. This determines the prepotential in such a case.

The alignment equations

It is convenient to write $C = a + \mathrm{i}b$ and express the alignment equation (3.15) in the form

$$a\,\mathrm{Im}\,\Pi + b\,\mathrm{Re}\,\Pi \;=\; Q \;. \tag{3.17}$$

This equation can also be understood in terms of cohomology, and amounts to the condition that

$$\Gamma \in \left(H^{(3,0)}(X,\mathbb{C}) \oplus H^{(0,3)}(X,\mathbb{C}) \right) \cap H^3(X,\mathbb{Z}) \;.$$

We can think of the period vector Π as defining a two-plane over the reals, spanned by $\mathrm{Re}\,\Pi$ and $\mathrm{Im}\,\Pi$. This two-plane varies as we move in the moduli space giving a family of two-planes in $\mathbb{R}^{2+2m}$, parametrised by the moduli space coordinate t.

In order to satisfy the alignment equations, the plane

$$V = \mathrm{Span}(\mathrm{Re}\,\Pi, \mathrm{Im}\,\Pi)$$

must contain a non-zero point of the charge lattice $H^3(X,\mathbb{Z}) \simeq \mathbb{Z}^{2+2m}$, and so a lattice line consisting of integer multiples of smallest such point. If the intersection is a lattice line, the attractor is said to be of rank one. Exceptionally, the plane V will intersect the charge lattice in two linearly independent points, and so in a lattice plane. Then the attractor point is said to be of *rank two*. If this is so, the alignment equations are satisfied for two linearly independent vectors Q.

The orthogonality equation

In addition to the attractor points solving the alignment equations, there are attractor points where the central charge vanishes, since these points are necessarily local minima of the nonnegative quantity $|\mathcal{Z}(Q)|$. In this case

$$\Gamma \in \left(H^{(2,1)}(X,\mathbb{C}) \oplus H^{(1,2)}(X,\mathbb{C})\right) \cap H^3(X,\mathbb{Z}).$$

There is again an interpretation of this equation in terms of planes and lattices. The charge vector Γ lies in the plane $V^\perp$ that is orthogonal to V under the symplectic inner product, corresponding to Σ. For there to be an attractor point, the plane $V^\perp$ must also intersect the charge lattice $H^3(X,\mathbb{Z})$, and this intersection can also be of rank one, or exceptionally, of a higher rank $\leq 2m$.

In the case of one-parameter models with $m = 1$, solutions to the alignment equations and the orthogonality equation are related. The fact that V is to some extent rational with respect to the charge lattice has consequences for the rationality of the orthogonal plane $V^\perp$. In particular, if V intersects the lattice in a lattice plane, then $V^\perp$ does so also. To see this, note that in this case $V = \mathrm{Span}(Q_1, Q_2)$ for some independent lattice vectors Q_1 and Q_2. Then the space $V^\perp$ that is orthogonal to V under the symplectic inner product, can also be taken to be spanned by two lattice vectors $V = \mathrm{Span}(Q_3, Q_4)$. The alignment equations at rank-two attractor points can be then written as

$$\mathrm{Span}(\mathrm{Re}\,\Pi, \mathrm{Im}\,\Pi) \;=\; \mathrm{Span}(Q_1, Q_2) \;\;=\; \mathrm{Span}(Q_3, Q_4)^\perp \;.$$

Likewise, the orthogonality equation can be written as

$$\mathrm{Span}(\mathrm{Re}\,\Pi, \mathrm{Im}\,\Pi) \;=\; \mathrm{Span}(Q_1, Q_2)^\perp = \;\mathrm{Span}(Q_3, Q_4) \quad .$$

Thus alignment equations can be, in this case, written as an orthogonality equation and vice versa.

We wish to be clear about an issue of terminology. The term "attractor point" is often used to refer exclusively to massive black holes, and so to solutions to the alignment equations, ignoring possible solutions to the orthogonality equation. In the following, we will understand an attractor point to be a point that is either a solution to the alignment equations or a solution to the orthogonality equation. By a rank-two attractor point, we will continue to mean that there are two independent solutions to the alignment equations, and hence that V intersects the charge lattice in a plane.

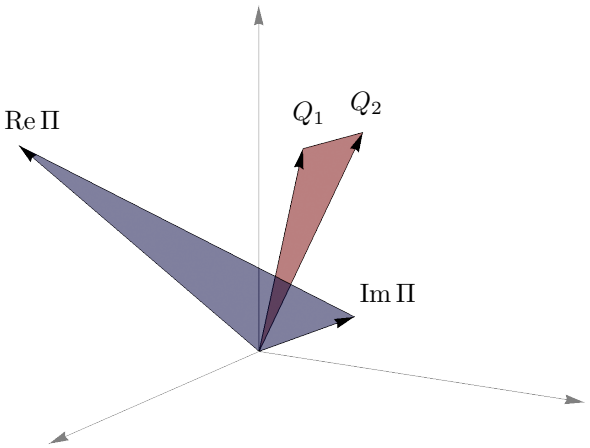


Figure 3.1: *A schematic figure of the $H^3(X,\mathbb{R})$. Here we show the real and imaginary parts of Π as vectors in this space, along with the charge vectors Q_1, Q_2. As the moduli space coordinate t varies, the vectors $Re\,\Pi$ and $Im\,\Pi$, as well as the vectors orthogonal to these, move. When we have a solution to the alignment equations, at least one of the vectors Q_1 and Q_2 will align with the plane generated by $Re\,\Pi$ and $Im\,\Pi$.*

Interpretation

The solutions to the alignment and orthogonality equations can be given very different physical interpretations, owing to their relation to the BPS state existence conjecture and the nature of the corresponding attractor flows. The BPS state existence conjecture [8, 9, 59–61] asserts that, in the full quantum theory of gravity, the existence of a BPS state corresponding to the black hole with a certain charge vector is determined by the nature of the attractor point where the flow ends. If we leave aside the possibility of a limiting cycle, there are three different types of flows:

1. The attractor flow ends at a point where $|\mathcal{Z}| \neq 0$.
2. The attractor flow ends at a point where $|\mathcal{Z}| = 0$, and the point is a regular point on the moduli space of the Calabi-Yau manifold.
3. The attractor flow ends at a point where $|\mathcal{Z}| = 0$, and the point is a singular point on the moduli space of the Calabi-Yau manifold.

The BPS state existence conjecture asserts that a BPS state always exists in the first case, and never in the second case, while in the third case a BPS state may or may not exist, and this question cannot be determined from the attractor flow data alone [8, 9]. Thus the conjecture asserts that the solutions to the alignment equations should have an associated BPS state in the full theory, while the solutions to the orthogonality equation do not correspond to such states.

3.5.3 Flux compactifications

Even though the BPS state existence conjecture asserts that solutions to the orthogonality equation do not correspond to BPS black hole states in the full theory of quantum gravity, this does not mean that the solutions are not physically significant. Indeed, the solutions to the orthogonality equations correspond to supersymmetric flux vacua in flux compactifications of IIB string theory [11, 12] (see also the section 4 of [10]). It has also been suggested [10] that, at least at rank-two attractor points, the existence of solutions to the orthogonality equation may indicate supersymmetry enhancement.

Flux compactifications refer to a class of string theory compactifications with non-trivial background values for the $(p+1)$-form field strengths. When compactifying in the presence of fluxes, the four-dimensional action includes a non-zero potential term which couples the vector multiplet scalars to the axiodilaton τ and the background fluxes F_3, H_3. This potential is constructed from a superpotential [62] which has the form

$$W \stackrel{\text{def}}{=} \int_X G_3 \wedge \Omega \;=\; \int_X (F_3 - \tau H_3) \wedge \Omega \;. \tag{3.18}$$

It can be shown [63] that in order to obtain non-trivial supersymmetric solutions to the equations of motion, the field strenghts must satisfy

$$\int_X H_3 \wedge F_3 > 0 \;.$$

This can be satisfied by choosing constant values for the fields F_3 and H_3. Decomposing the fluxes $H_3, F_3 \in H^3(X, \mathbb{C})$ in a basis, which we choose to be the integral symplectic basis,

$$H_3 \;=\; (2\pi)^2\alpha' \left(h^a\alpha_a - h_a\beta^a\right), \quad F_3 \;=\; (2\pi)^2\alpha' \left(f^a\alpha_a - f_a\beta^a\right) \;, \quad \text{with} \quad h_a, h^a, f_a, f^a \in \mathbb{Z} \;.$$

We collect these components into vectors F and H

$$F \;=\; (f^0, f^1, \ldots, f^{h^{1,2}}, f_0, f_1, \ldots, f_{h^{1,2}})^T \;, \qquad H \;=\; (h^0, h^1, \ldots, h^{h^{1,2}}, h_0, h_1, \ldots, h_{h^{1,2}})^T \;. \tag{3.19}$$

The superpotential can be written in terms of these vectors and the period vector Π as

$$W \;=\; (F - \tau H)^T \Sigma\, \Pi \;.$$

In F-theory compactifications there is also a tadpole cancellation condition

$$\frac{1}{2\kappa_{10}^2 T_3} \int_X H_3 \wedge F_3 + Q^{D3} \;=\; \frac{\chi\,(X_4)}{24} \;,$$

where X_4 is the Calabi-Yau fourfold on which the F-theory is compactified. Since we are free to add localised D3-branes, this imposes the following condition on the fluxes:

$$F^T \Sigma H \leq \frac{\chi\,(X_4)}{24} \;.$$

Supersymmetric vacuum equations

The potential that the fluxes give rise to in the four-dimensional action is (for a review, see for example [64])

$$V \stackrel{\text{def}}{=} \mathrm{e}^{\mathcal{K}} \left(\sum_{a,b} G^{a,\bar{b}} D_a W \overline{D_b W} - 3|W|^2 \right) \ . \tag{3.20}$$

The sums over a and b run over all scalar fields: the axiodilaton τ, the complex structure moduli z_i, and the Kähler structure moduli ρ_k. G is the metric on the total moduli space $\mathcal{M}$ of the theory

$$\mathcal{M} \ = \ \mathbb{H} \times \mathcal{M}_{\mathbb{C}S} \times \mathcal{M}_{\mathbb{C}K}$$

Here $\mathbb{H}$ is the upper half plane in which τ is valued while the two other factors, $\mathcal{M}_{\mathbb{C}S}$ and $\mathcal{M}_{\mathbb{C}K}$ are the complex structure and complexified Kähler moduli spaces of X, respectively. This total moduli space is a Kähler manifold with the Kähler potential

$$\mathcal{K} \ = \ -\log\left[-\mathrm{i}\,(\tau - \bar{\tau})\right] + K_{\mathbb{C}S} + K_{\mathbb{C}K} \ ,$$

and D_a are the Kähler covariant derivatives on this space.

The potential (3.20) satisfies the "no-scale" relation of [65, 66] leading to a cancellation between the derivatives with respect to the Kähler moduli, $D_{\rho_k} W$, and the rightmost term $-3|W|^2$, so that [67]

$$V \ = \ \mathrm{e}^{\mathcal{K}} \left(|D_\tau W|^2 + \sum_{i,j=1}^{h^{1,2}} g^{i\bar{j}}\, (D_{z_i} W)\, \overline{(D_{z_j} W)} \right) \ .$$

In a vacuum configuration, the potential V must vanish, in addition to which the superpotential W vanishes in supersymmetric configurations. The potential V is clearly positive semidefinite, and thus the equations defining a supersymmetric flux vacuum, requiring that both W and V vanish, read:

$$W \ = \ 0 \ , \qquad D_\tau W \ = \ 0 \ , \qquad D_{z_i} W \ = \ 0 \ .$$

Since we demand that $W = 0$, the Kähler connection terms $K_i W$ must also vanish, and the covariant derivatives of W with respect to the moduli simplify to partial derivatives. The above equations thereby reduce to

$$W \ = \ 0 \ , \qquad \partial_\tau W \ = \ 0 \ , \qquad \partial_{z_i} W \ = \ 0 \ . \tag{3.21}$$

Given vacuum expectation values for field strengths F_3 and H_3, these equations can be solved for the complex structure moduli z_i as well as the value of the axiodilaton field. The Kähler moduli are unconstrained, although this ceases to be true when instanton corrections to the action are incorporated [67].

F-theory uplift

It is known that the IIB theory possesses an $\mathrm{SL}(2,\mathbb{Z})$ symmetry that acts on τ and G_3 by

$$\tau \mapsto \frac{a\tau+b}{c\tau+d}\ , \qquad G_3 \mapsto \frac{G_3}{c\tau+d}\ , \qquad \begin{pmatrix} a & b \\ c & d \end{pmatrix} \in \mathrm{SL}(2,\mathbb{Z})\ . \tag{3.22}$$

F-theory [68] (for a review, see for example [69]) geometrises the axiodilaton, giving it an interpretation as the complex structure parameter of an elliptic fibre of an elliptically fibred Calabi-Yau fourfold. The moduli space of elliptic curves can be taken to be the upper half plane, where two distinct points correspond to complex-isomorphic elliptic curves if and only if they are related by a Möbius transformation

$$\tau \mapsto \frac{a\tau+b}{c\tau+d}\ , \qquad \begin{pmatrix} a & b \\ c & d \end{pmatrix} \in \mathrm{SL}(2,\mathbb{Z})\ .$$

An unique characterisation of the complex isomorphism classes of elliptic curves is provided by the j-invariant

$$j(\tau) \ = \ 1728\,\frac{60^3 E_4^3(\tau)}{\Delta(\tau)} \ = \ \mathrm{e}^{-2\pi\mathrm{i}\tau} + 744 + 196884\,\mathrm{e}^{2\pi\mathrm{i}\tau} + 21493760\,\mathrm{e}^{4\pi\mathrm{i}\tau} + \ldots$$

which is a modular function, and takes the same values on Möbius transformation orbits of τ. Any elliptic curves with the same j-invariant are isomorphic as complex varieties. However, this property does not hold over subfields of $\mathbb{C}$. For instance, the curves

$$y^2 \ = \ x^3 + 2x\ , \qquad y^2 \ = \ x^3 - 2x$$

both have j-invariant 1728. Indeed, one can obtain the latter from the former by the twist $(x,y) \mapsto (-x,\mathrm{i}y)$. Despite this, they are not isomorphic over $\mathbb{Q}$ as there is no *rational* morphism that will take one between the above pair of curves. We say that the two curves have different *rational structures*. As there is a morphism over $\mathbb{C}$ that accomplishes this, the two curves are said to be *twists* of one another.

While the j-invariant is too coarse to differentiate curves with different rational structures, the zeta function does depend on the rational structure. It is an interesting question to ask whether physics 'knows' about the rational structure. In [12], evidence was presented that a class of flux compactifications on the mirror octic Calabi-Yau manifolds, whose zeta function was computed in [70], are related to F-theory solutions with an elliptic fibre that can in fact be identified with the elliptic curve prescribed by the zeta function, at least up to a rational isomorphism, which cannot be uniquely fixed by F-theory considerations alone.

Following [12, 63, 71] we can find an F-theory solution corresponding to a supersymmetric flux vacuum in type IIB theory compactified on a Calabi-Yau manifold X. The F-theory solutions are compactifications on an elliptically fibred Calabi-Yau manifold X_4 with the manifold X being a double cover of the base of this fibration. Taking the weak coupling orbifold limit retrieves the IIB theory on X with

a pair of D7-branes coincident with an O7 plane [71], and with the axiodilaton corresponding to the elliptic fibre.

The compactification manifold X_4 can be identified by using a "top-down" approach starting with the most general elliptic fibration, finding the restrictions imposed by requiring that supersymmetry is preserved, and fixing the fibre by comparing to the IIB data. Let X_4 be a generic elliptically fibred manifold with base B. The most generic elliptic fibre over B can be written in Weierstrass form as

$$y^2 \;=\; x^3 + f(u)x + g(u) \;, \tag{3.23}$$

where u are the coordinates on the base B. When compactifying F-theory on the fourfold X_4, the complex structure parameter τ of this elliptic curve is identified with the axiodilaton. For this reason, in the following we make no distinction between the two.

The points in the moduli space satisfying $\Delta = 4f^3 + 27g^2 = 0$, where the elliptic curve degenerates, can be identified with the locations of D7-branes. For this reason, it is convenient [71] to reparametrise the pair of functions f, g in terms of functions η and h such that

$$f(u) \;=\; C\eta(u) - 3h(u)^2 \;, \qquad g(u) \;=\; h(u)\left[C\eta(u) - 2h(u)^2\right] + C^2\chi \;.$$

In this parametrisation the limit $C \to 0$ corresponds to the weak coupling limit in which the locus where the elliptic fibre degenerates is given by $\eta(u) = \pm\sqrt{-12h(u)\chi}$. This can be interpreted as the location of a pair of D7-branes which fill the spacetime and intersect the base on this four-dimensional locus. Similarly, the locus $h(u) = 0$ gives the intersection of spacetime-filling O7-planes with the base.

Since we are looking for supersymmetric solutions, in the weak coupling limit $C \to 0$, the solutions must reduce to a supersymmetric IIB configuration. To obtain a maximally supersymmetric background in this limit, we require that the O7-planes and D7-branes coincide. It will turn out that, for the models we study, such solutions can be found among those studied in [63] where $\chi = 0$, so that the O7 and D7 loci are respectively $h = 0$ and $\eta = 0$, and furthermore $\eta = h^2$ so that these loci coincide.

With these choices made, the fibre (3.23) becomes

$$y^2 \;=\; x^3 + h(u)^2(C-3)x + h(u)^3(C-2) \;. \tag{3.24}$$

Away from the singular locus $h = 0$ this can be simplified by a fibrewise rescaling of the coordinates

$$y \to h^{3/2}(u)y,\; x \to h(u)x \;.$$

In these coordinates the fibre reads

$$y^2 \;=\; x^3 + (C-3)x + (C-2) \;. \tag{3.25}$$

The constant C is fixed by matching the complex structure modulus of this fibre to the IIB axiodilaton profile.

3.5.4 Relation to modularity

The connection between modularity and physics is based on the observation [10, 12] that existence of physical solutions, such as attractor points and supersymmetric flux vacua imply, due to quantisation conditions, existence of a two-dimensional subspace Λ of the integral middle cohomology. In the case of alignment equations and attractor points with non-vanishing central charge, this subspace is spanned by the two charge forms

$$\Gamma_1,\ \Gamma_2 \in \Big(H^{(3,0)}(X,\mathbb{C}) \oplus H^{(0,3)}(X,\mathbb{C})\Big) \cap H^3(X,\mathbb{Z})$$

associated to the attractor point, and the subspace

$$\Lambda\ =\ \mathrm{Span}(\Gamma_1,\Gamma_2) \subset H^3(X,\mathbb{Z})$$

has a pure Hodge structure of type $(3,0)+(0,3)$. As in §3.2, existence of a subspace of this type implies that the Galois representation ρ has an irreducible two-dimensional subrepresentation. Furthermore, it can be shown [12] that such a representation corresponds to a weight-four modular form. We say that the corresponding manifold is *weight-four modular*.

Similarly, in the case of the orthogonality equations and supersymmetric flux vacua, the subspace Λ is generated by the flux vectors H and F, and has a pure Hodge structure of type $(2,1)+(1,2)$. In this case the two-dimensional irreducible subrepresentation corresponds to a weight-two modular form, and the manifold is said to be *weight-two modular*.

Part II

Five-parameter Hulek-Verrill Manifolds and their Mirrors

We study the mirrors of the five-parameter Calabi-Yau threefolds first studied by Hulek and Verrill in the context of observed modular behaviour of the zeta functions for Calabi-Yau manifolds. Toric geometry allows for a simple explicit construction of these mirrors, which turn out to be familiar manifolds. These are elliptically fibred in multiple ways. By studying the singular fibres, we are able to identify the rational curves of low degree on the mirror manifolds. This verifies the mirror symmetry prediction obtained by studying the mirror map near large complex structure points.

We undertake also an extensive study of the periods of the Hulek-Verrill manifolds and their monodromies. On the mirror, we compute the instanton numbers of genus zero and one, which are labelled by 5 indices, as $h^{1,1} = 5$. There is an obvious permutation symmetry on these indices, but in addition there is a surprising repetition of values. We trace this back to an S_6 symmetry made manifest by certain constructions of the complex structure moduli space of the Hulek-Verrill manifold. Among other consequences, we see in this way that the moduli space has six large complex structure limits. It is the freedom to expand the prepotential about any one of these points that leads to this symmetry in the instanton numbers. The group orbits under this symmetry have a 'web' structure, and with certain qualifications the instanton numbers are only nonzero if they belong to what we term 'positive webs'. This structure has consequences for instanton numbers at all genera.

Chapter 4

Introduction

4.1 Introduction

In this part, we study mirror symmetry for a family of Calabi-Yau manifolds associated to the root lattice A_4, a family first investigated in relation to the modularity of its zeta-function by Hulek and Verrill [14]. *Singular Hulek-Verrill varieties* comprise a five-parameter family, parametrised by $\phi = (\varphi^0, \varphi^1, \varphi^2, \varphi^3, \varphi^4, \varphi^5)$ and denoted[1] $\widehat{\mathrm{HV}}_\phi$. They are embedded in the projective torus $\mathbb{T}^4 = \mathbb{P}^4 \setminus \{X_1 \cdots X_5 = 0\}$ as the vanishing loci of

$$(X_1 + X_2 + X_3 + X_4 + X_5)\left(\frac{\varphi^1}{X_1} + \frac{\varphi^2}{X_2} + \frac{\varphi^3}{X_3} + \frac{\varphi^4}{X_4} + \frac{\varphi^5}{X_5}\right) \;=\; \varphi^0 \;. \tag{4.1}$$

These varieties admit toric compactifications, which we will review briefly in chapter 5. Of particular interest are small projective resolutions HV of $\widehat{\mathrm{HV}}$, which have smooth projective Calabi-Yau models with five complex structure parameters [14]. We concentrate mostly on analysing these, and call them simply *Hulek-Verrill manifolds*.

These manifolds have received attention in the physics literature, since the periods of these manifolds (and their analogues in each dimension) are related to the banana Feynman graphs [72]. The particular manifolds $\mathrm{HV}_{(1,1,1,1,1,1/\varphi)}$ and their quotients exhibit, for certain values of φ, rank-two attractor points with interesting number theoretic properties. These attractor varieties were identified in [10]. In addition, we will shown in part III that Hulek-Verrill manifolds admit large families of supersymmetric flux vacua, with equally intriguing properties.

The mirror-symmetric counterpart to the work of [10] involves a IIA setup. In part IV, nonperturbative solutions are given to the attractor equations which involve instanton numbers, or Gromov-Witten invariants, giving a hint of microstate counting. This motivates us to study the geometry of the mirror Hulek-Verrill manifold focusing especially on aspects related to counting microstates of D4-D2-D0 brane systems on the manifold.

Some of the material appearing in this part has been studied from an alternative point-of-view in [72].

[1] We often do not display the parameter ϕ explicitly.

4.2 Outline

Toric geometry of mirror Hulek-Verrill manifolds

In chapter 5, we briefly review the toric construction of the singular Hulek-Verrill manifolds $\widehat{\mathrm{HV}}$ as first discussed in [14]. Then we proceed to find a toric description of its small resolution. These are given as toric compactifications of intersections of two polynomials

$$P^1(\mathbf{X}) \;=\; \sum_{\mu=0}^{5} X_\mu \;, \qquad P^2(\mathbf{X};\phi) \;=\; \sum_{\mu=0}^{5} \frac{\varphi^\mu}{X_\mu} \tag{4.2}$$

on a torus $\mathbb{T}^5$. We denote these manifolds by $\mathrm{HV}_{(\varphi^0,\ldots,\varphi^5)}$, or more compactly by HV. We use the method of Batyrev and Borisov [34, 35] to find the toric description of the mirror Hulek-Verrill manifolds HΛ. Somewhat surprisingly, these mirror manifolds turn out to be familiar spaces [73, 74], given by the complete intersection

$$\begin{matrix}\mathbb{P}^1\\ \mathbb{P}^1\\ \mathbb{P}^1\\ \mathbb{P}^1\\ \mathbb{P}^1\end{matrix}\begin{bmatrix}1 & 1\\ 1 & 1\\ 1 & 1\\ 1 & 1\\ 1 & 1\end{bmatrix} .$$

Parenthetically, we note that this manifold is itself a remarkable split of the tetraquadric,

$$\begin{matrix}\mathbb{P}^1\\ \mathbb{P}^1\\ \mathbb{P}^1\\ \mathbb{P}^1\end{matrix}\begin{bmatrix}2\\ 2\\ 2\\ 2\end{bmatrix} .$$

In the complex structure moduli space of Hulek-Verrill manifolds, there exist subfamilies that admit a $\mathbb{Z}_5 \times \mathbb{Z}_2 \times \mathbb{Z}_2$ symmetry, or a subgroup thereof. The symmetry has a simple description: denoting the coordinates in each of these projective spaces by $Y_{i,0}$ and $Y_{i,1}$, the symmetries act for all i as

$$S \,:\, Y_{i,a} \mapsto Y_{i+1,a} \;, \qquad U \,:\, Y_{i,a} \mapsto (-1)^a Y_{i,a} \;, \qquad V \,:\, Y_{i,0} \leftrightarrow Y_{i,1} \;.$$

Periods of the five-parameter family

Chapter 6 deals with the periods of HV, which describe the variation of the Hodge structure as a function of moduli space coordinates. We study the five-parameter family (5.2). The overall scaling of coordinates φ^μ does not affect the vanishing locus, and thus we can identify the moduli space[2] with $\mathbb{P}^5$.

Often it is necessary to work on an affine patch, for which we most often choose $\varphi^0 = 1$. Results obtained in this patch apply in any patch $\varphi^i = 1$, with Latin indices running from 1 to 5, after making a suitable permutation of indices.

We begin investigating the periods by recalling a series expansion of the fundamental period [75, 76],

$$\varpi^{(0);0}(\varphi) \;=\; \sum_{n=0}^{\infty} \sum_{|\boldsymbol{p}|=n} \binom{n}{\boldsymbol{p}}^2 \boldsymbol{\varphi}^{\boldsymbol{p}} \;, \tag{4.3}$$

[2]Note that two distinct points in $\mathbb{P}^5$ can correspond to biholomorphic manifolds. There exists a 'fundamental domain' in $\mathbb{P}^5$, where the points are in one-to-one correspondence with distinct biholomorphism classes.

where $\boldsymbol{p} = (p_1, \ldots, p_5)$ is a five-component multi-index, $|\boldsymbol{p}|$ is the sum $p_1 + \cdots + p_5$, and

$$\binom{n}{\boldsymbol{p}} \;=\; \frac{n!}{p_1!p_2!p_3!p_4!p_5!}$$

is the multinomial coefficient. By $\boldsymbol{x}^{\boldsymbol{p}}$ we mean the product $x_1^{p_1}x_2^{p_2}x_3^{p_3}x_4^{p_4}x_5^{p_5}$. The superscript (0) in $\varpi^{(0);0}$ refers to the coordinate patch $\varphi^0 = 1$.

On seeking the differential equations obeyed by this period, we are led to the system

$$\mathcal{L}_i\varpi^{(0);0}(\boldsymbol{\varphi}) \;\stackrel{\text{def}}{=}\; \left(\frac{1}{\varphi^0}\,(\Theta+1)^2 - \frac{1}{\varphi^i}\theta_i^2\right)\varpi^{(0);0}(\boldsymbol{\varphi}) \;=\; 0\;, \quad \text{with} \quad \theta_i \;=\; \varphi^i\frac{\partial}{\partial\varphi^i}\;, \quad \Theta \;=\; \sum_{i=1}^{5}\theta_i\;.$$

These constitute a partial Picard-Fuchs system, giving 32 solutions among which we find the 12 periods[3]. These are the components of the period vector

$$\varpi^{(0)} \;=\; (\varpi^{(0);0}, \varpi^{(0);i}, \varpi^{(0)}_j, \varpi^{(0)}_0)^T\;, \qquad i,j \;=\; 1,\ldots,5\;.$$

By a simple separation-of-variables argument, it can be shown that integrals of Bessel functions of the following form furnish a basis of solutions:

$$\frac{\varphi^0}{\mathrm{i}\pi}\int_0^\infty \mathrm{d}z\, z\, B_0\left(\sqrt{\varphi^0}z\right)\prod_{i=1}^{5}B_i\left(\sqrt{\varphi^i}z\right)\;, \tag{4.4}$$

where $B_i(\zeta)$ is either $K_0(\zeta)$ or $\mathrm{i}\pi I_0(\zeta)$. Naïvely there are $2^6 = 64$ integrals of this type. However, at a generic point in the moduli space there are exactly 32 such integrals that converge. The analytic continuation of each integral outside of its domain of convergence can be written as a linear combination of integrals of the general form (4.4) that converge in the new region.

Despite lacking the explicit form of the general Picard-Fuchs system, we can fix the 12 periods among the 32 solutions of the partial system by imposing boundary conditions. These are found by matching the asymptotics of the solutions to the asymptotics near the large complex structure point predicted by mirror symmetry. We also give explicit series expansions for these periods near the large complex structure point.

Mirror map and large complex structure

The large complex structure points are located at the loci where all but one of the coordinates φ^μ vanish. Near the large complex structure point with $\varphi^0 \neq 0$, the period vector in the integral basis can be written in terms of the prepotential $\mathcal{F}$ as

$$\Pi^{(0)} \;=\; \begin{pmatrix}\Pi^{(0)}_0\\ \Pi^{(0)}_i\\ \Pi^{(0);0}\\ \Pi^{(0);i}\end{pmatrix} \;=\; \begin{pmatrix}\frac{\partial}{\partial z^0}\mathcal{F}\\ \frac{\partial}{\partial z^i}\mathcal{F}\\ z^0\\ z^i\end{pmatrix}\;, \quad \mathcal{F}(z^0,\ldots,z^5) = -\frac{1}{3!}\sum_{a,b,c=0}^{5}Y_{abc}\frac{z^az^bz^c}{z^0} + (z^0)^2\sum_{\boldsymbol{p}\neq\boldsymbol{0}}n_{\boldsymbol{p}}\,\mathrm{Li}_3(q^{\boldsymbol{p}})\;.$$

[3] 12 is the dimension of the third cohomology of HV.

The relation between the integral basis period vector $\Pi^{(0)}$ and the period vector $\varpi^{(0)}$ is given by (2.16), so we can compute the instanton numbers by studying the Yukawa couplings y_{ijk}. These are given by the formula

$$y_{ijk} \;=\; -(\Pi^{(0)})^T \Sigma\, \partial_{ijk} \Pi^{(0)} \ ,$$

but also have the following expansions in terms of the instanton numbers:

$$y_{ijk} \;=\; Y_{ijk} + \sum_{n=1}^{\infty} \sum_{|\boldsymbol{p}|=n} \frac{p_i\, p_j\, p_k\, n_{\boldsymbol{p}}\, \boldsymbol{q}^{\boldsymbol{p}}}{1-\boldsymbol{q}^{\boldsymbol{p}}} \ , \qquad \text{where} \qquad q^i \;=\; \mathrm{e}^{2\pi \mathrm{i} t^i} \ .$$

Due to the permutation symmetry of the parameters φ^i, we can express many quantities in terms of the elementary symmetric polynomials. This results in a significantly less complicated series expressions which are far more amenable to computation. While we are still unable to reach the degrees possible in one-parameter computations, we find the genus-0 instanton numbers up to a total degree of 29, first of which we collect in table 6.1. All of these numbers are collected, in terms of webs, in table C.1.

Having computed these numbers to a high order, some patterns become evident, many of which we are able to prove. Owing to the freedom to expand the prepotential about any one of the six large complex structure limits, an S_6 symmetry can be seen within the instanton number. In fact, there is an infinite group $\mathfrak{W} \subset \mathrm{Sp}(12,\mathbb{Z})$ acting on the periods. An S_5 subgroup is immediately manifest, as there is a permutation symmetry in the five Kähler structure moduli of HΛ.

Monodromies

In §6.3, we turn to computing the monodromies around the singular loci $\varphi^0\varphi^1\varphi^2\varphi^3\varphi^4\varphi^5 = 0$ and

$$\mathbb{\Delta} \;\stackrel{\text{def}}{=}\; \prod_{\epsilon_i \in \{\pm 1\}} \left(\sqrt{\varphi^0} + \epsilon_1 \sqrt{\varphi^1} + \epsilon_2 \sqrt{\varphi^2} + \epsilon_3 \sqrt{\varphi^3} + \epsilon_4 \sqrt{\varphi^4} + \epsilon_5 \sqrt{\varphi^5}\right) \;=\; 0 \ .$$

As hinted by the fact that (4.4) is a function of $\sqrt{\varphi^\mu}$, this is most conveniently done by first classifying the singularities in coordinates $\sqrt{\varphi^\mu}$. Then the singular locus $\mathbb{\Delta} = 0$ becomes a reducible union of codimension-1 hyperplanes of the form

$$D_I \;=\; \left\{ (a_0,\ldots,a_5) \in \mathbb{P}^5 \;\middle|\; \sum_{\mu\in I} \sqrt{\varphi^\mu} = \sum_{\nu \in I^c} \sqrt{\varphi^\nu} \right\} \ , \qquad I \subset \{0,\ldots,5\} \ .$$

The monodromies around these loci can be found by numerically integrating the Picard-Fuchs equations on a path circling around these loci. Alternatively, one can find the linear relations between analytically continued Bessel function integrals in different regions, and use this to compute the monodromies. While the former approach is too difficult with arbitrary paths due to the complicated nature of the complete Picard-Fuchs system, we can integrate along various lines on which the Picard-Fuchs operator can be found using the method which will be discussed in §6.1.3. By studying various

different lines and using symmetry, we can use the resulting "reduced" monodromy matrices to piece together the full monodromies.

What makes this computation simpler than it first appears is the fact that the monodromy matrix around a conifold locus should be expressible in terms of a single vector:

$$\mathrm{M}_I \;=\; \mathrm{I}_{12} - \boldsymbol{w}_I(\Sigma \boldsymbol{w}_I)^T \;. \tag{4.5}$$

Here $\boldsymbol{w}_I$ is a 12-component vector that gives the integral basis components of the three-cycle vanishing at the conifold locus. Consequently, the vector $\boldsymbol{w}_I$ should also observe the symmetries relevant to each locus.

Counting curves on the mirror Hulek-Verrill manifold

In chapter 7, we use use elementary geometric methods in tandem with the Kodaira classification of singular elliptic fibres [77, 78] to directly count curves of certain multi-degrees on generic manifolds in the family HΛ.

Counting of these curves is based on the observation that HΛ can be viewed as an elliptic fibration with base $\mathbb{P}^1 \times \mathbb{P}^1$. While the generic fibre is an elliptic curve, it is possible to find the discriminant locus corresponding to base points above which the fibres are singular. According to Kodaira classification, the fibres over nodes of the discriminant locus are unions of two rational curves. By classifying the these fibres, we find all rational curves of degrees ≤ 3, and some of the higher-degree curves.

As the discriminant of the elliptic fibration is relatively simple for tetraquadrics, it is often beneficial to consider the singular manifolds $\widehat{\mathrm{H}\Lambda}_i$ obtained by blowing down 24 lines along the i'th copy of $\mathbb{P}^1$ in the ambient space. On a generic manifold $\widehat{\mathrm{H}\Lambda}_i$, the discriminant locus has 200 nodes, of which $3 \times 24 = 72$ correspond to lines, 72 to quadrics, and 56 to cubics. We obtain all curves up to degree 3 this way. In addition, the fibres containing lines and quadrics also contain degree-4 and -5 curves, respectively, as the second component. These account for all rational curves with multi-degrees $(0,0,1,1,2)$, $(0,0,1,2,2)$, and permutations thereof.

In this way we confirm the predictions from mirror symmetry, and provide details of the elliptic fibrations $\widehat{\mathrm{H}\Lambda}_i$ that may see future use in study of M/F-theory compactifications.

A comment on indices

To give concise accounts of the different subjects that we touch upon, we adopt a specific index convention in chapters 6 and 7, and also within individual sections of chapter 5. While these conventions are strictly followed in their respective sections, they are not the same in different sections of this part. The conventions are explicitly given in table 4.1.

Chapter	Index Convention
5	Varies by section.
6	Greek indices run from 0 to 5. Latin indices run from 1 to 5.
7	Latin indices run from 0 to 4. Distinct indices are understood to take distinct values.

Table 4.1: *Index conventions in each section.*

We collect some symbols appearing in multiple sections, together with their definitions, in table 4.2.

Symbol	Definition/Description	Ref.
φ	The coordinates φ^a on the complex structure moduli space of HV.	(5.1)
HV	The family of Hulek-Verrill manifolds.	(5.3)
HΛ	The family of mirror Hulek-Verrill manifolds, which are complete intersections in $\left(\mathbb{P}^1\right)^5$.	(5.3)
$\widehat{\text{HV}}$	Family of singular manifolds birational to HV.	(5.3)
$\widehat{\text{H}\Lambda}$	Family of singular manifolds birational to HΛ.	(5.3)
$\widehat{\text{H}\Lambda}_i$	Families of singular manifolds birational to HΛ, obtained by projecting out the i'th $\mathbb{P}^1$ coordinate axis.	(7.2)
P	Laurent polynomial defining $\widehat{\text{HV}}$ in $\mathbb{T}^4$.	(5.1)
P^1, P^2	Laurent polynomials defining the small resolution of $\widehat{\text{HV}}$ in $\mathbb{P}^5$.	(5.2)
Q^1, Q^2	Multi-degree $(1,1,1,1,1)$ polynomials that together define HΛ in $\left(\mathbb{P}^1\right)^5$.	(5.17)
$\widehat{Q}$	A multi-degree $(2,2,2,2)$ polynomial defining $\widehat{\text{H}\Lambda}$ in $\left(\mathbb{P}^1\right)^4$.	(5.13)
$\widehat{Q}^i$	A multi-degree $(2,2,2,2)$ polynomial defining $\widehat{\text{H}\Lambda}_i$ in $\left(\mathbb{P}^1\right)^4$.	(7.4)
E	The locus in $\mathbb{P}^5$ where any of the homogeneous coordinates vanish.	(6.1)
E_μ	The irreducible component of E on which the μ'th homogenous coordinate vanishes.	(6.2)
D_I	Irreducible components of the discriminant locus $\mathbb{\Delta} = 0$ in variables $\sqrt{\varphi^\mu}$.	(6.4)
Π	The HV complex structure period vector expressed in the integral symplectic basis. A superscript as in $\Pi^{(\mu)}$ denotes the expansion about the μ'th large complex structure point.	(6.34)
ϖ	The HV period vector in the Frobenius basis.	(6.29)
$\pi^{(\mu)}$	The HV period vector in the μ'th "Bessel integral basis".	(6.23)
$\text{T}_{u\,v}$	The matrix effecting the basis change between period vectors u, v.	Various
M_s	Matrix giving the monodromy transformation of Π about the locus s.	§6.3
Δ	In chapter 5 and appendix A, a polytope. In chapter 7, the discriminant of an elliptic fibration.	Various
$\mathbb{\Delta}$	The discriminant. $\mathbb{\Delta} = 0$ is the conifold locus in the moduli space of HV.	(5.15)

Table 4.2: *Some symbols that are used throughout the paper with references to where they are defined.*

Chapter 5

Toric Geometry and Mirror Symmetry

We review the construction of Hulek and Verrill's manifold [14] following in part [10]. The starting point of their analysis is the five-parameter family $\widehat{\mathrm{HV}}_{(\varphi^0,\ldots,\varphi^5)}$ of singular varieties embedded in the projective torus $\mathbb{T}^4 = \mathbb{P}^4 \setminus \{X_1 \cdots X_5 = 0\}$ as the vanishing locus of

$$P(\boldsymbol{X};\boldsymbol{\varphi}) \;=\; (X_1+X_2+X_3+X_4+X_5)\left(\frac{\varphi^1}{X_1}+\frac{\varphi^2}{X_2}+\frac{\varphi^3}{X_3}+\frac{\varphi^4}{X_4}+\frac{\varphi^5}{X_5}\right)-\varphi^0\ . \tag{5.1}$$

These varieties can be compactified by using the standard methods of toric geometry (see for example [79]), giving in general a variety with 30 singularities. Outside of the discriminant locus[1] these have small resolutions, which constitute a smooth family of Hulek-Verrill manifolds $\mathrm{HV}_{(\varphi^0,\ldots,\varphi^5)}$.

Particularly interesting examples of such manifolds are provided by a highly symmetric one-parameter subfamily, where $\varphi^0 = 1$ and $\varphi^1 = \cdots = \varphi^5 = \varphi$. These are characterised by a $\mathbb{Z}_5 \times \mathbb{Z}_2$ symmetry, with the group action on the coordinates generated by

$$\mathfrak{A}\ :\ X_i \mapsto X_{i+1}\ , \qquad \mathfrak{B}\ :\ X_i \mapsto \frac{1}{X_i}\ ,$$

where the indices are understood to take values in $\mathbb{Z}_5$. The action on the manifold is free outside of the points $\varphi \in \{\frac{1}{25}\,,\,\frac{1}{9}\,,\,1\}$ in moduli space where fixed points are present. This allows one to take a quotient with respect to these symmetries to get a one-parameter family of Calabi-Yau manifolds, which are smooth for moduli outside these isolated points.

As noted in [14], the varieties on $\mathbb{T}^4$ defined by (5.1) are birational to complete intersection varieties in $\mathbb{P}^5$ defined as the vanishing locus of two polynomials:

$$P^1(\mathbf{X}) \;=\; \sum_{\mu=0}^{5} X_\mu\ , \qquad P^2(\mathbf{X};\varphi) \;=\; \sum_{\mu=0}^{5}\frac{\varphi^\mu}{X_\mu}\ . \tag{5.2}$$

This innocuous transformation turns out to be useful for finding the (non-singular) mirror manifolds $\mathrm{H}\Lambda$ of the (non-singular) Hulek-Verrill Manifolds HV. Combined with the methods of Batyrev and

[1] The situation is a little more involved on the discriminant locus, for details see [14].

Borisov [33–35], which we have briefly reviewed in §2.3.3, they allow us to find the mirror Calabi-Yau manifold as a subvariety of a suitable toric variety.

Using Batyrev's construction [33], we can find the mirror manifolds $\widehat{\mathrm{H}\Lambda}$ and $\mathrm{H}\Lambda$ of $\widehat{\mathrm{HV}}$ and HV. As expected, we find that $\widehat{\mathrm{H}\Lambda}$ is singular and birational to $\mathrm{H}\Lambda$. figure 5.1 outlines the pairings.

$$\begin{array}{ccc} \mathrm{HV} & \longleftrightarrow & \mathrm{H}\Lambda \\ \updownarrow & & \updownarrow \\ \widehat{\mathrm{HV}} & \longleftrightarrow & \widehat{\mathrm{H}\Lambda} \end{array}$$

Figure 5.1: *Relations between the various families of manifolds we study: the singular Hulek-Verrill manifolds are denoted by $\widehat{HV}$, Hulek-Verrill manifolds by HV, the singular mirror Hulek-Verrill manifolds by $\widehat{H\Lambda}$, and mirror Hulek-Verrill manifolds by $H\Lambda$. The horizontal arrows denote mirror maps, and the vertical arrows birational equivalences (blow-ups/-downs).*

5.1 The polytopes corresponding to singular varieties

Quantity	$\widehat{N}$, N	$\widehat{M}$, M
Basis	$\boldsymbol{e}_i$	$\boldsymbol{e}^i$
Coordinates on $\mathbb{T}$	X_i	Y_i
Coordinates on $N_{\mathbb{R}}/M_{\mathbb{R}}$	x_i	y_i
Cox coordinates	ξ_n	η_n
Polytopes	$\widehat{\Delta}^*$, Δ_1, Δ_2, Δ, ∇^*	$\widehat{\Delta}$, ∇_1, ∇_2, ∇, Δ^*
Polytope vertex labels	v_n	u_n
Polytope face labels	ρ_n	τ_n

Table 5.1: *Quantities associated to the lattices $\widehat{N}$, N, $\widehat{N}^* = \widehat{M}$ and $N^* = M$.*

We group the symbols denoting various polytopes, Cox coordinates, and other related information by their associated lattices in table 5.1. The lattices $\widehat{N}$ and $\widehat{M}$ associated to the singular varieties $\widehat{\mathrm{HV}}$ and $\widehat{\mathrm{H}\Lambda}$ are four-dimensional, and consequently for them the index i runs from 1 to 4. The lattices N and M are five-dimensional and for them the indices take values $i = 1, \ldots, 5$.

5.1.1 Five-dimensional description

The polynomial $P(\mathbf{X}; \mathbf{a})$ contains 21 monomials in coordinates $X_1, \ldots, X_5$. Writing these monomials using multi-index notation defines 21 vectors $v_n = (v_n^1, v_n^2, v_n^3, v_n^4, v_n^5)$, $n = 0, \ldots, 20$, in $\mathbb{Z}^5$. We write X^{v_n} for the monomial

$$X^{v_n} \;=\; X_1^{v_n^1} X_2^{v_n^2} X_3^{v_n^3} X_4^{v_n^4} X_5^{v_n^5} \;.$$

The vectors v_n make up the set

$$\big\{(0,0,0,0,0)\big\} \cup \big\{\mathbf{e}_i - \mathbf{e}_j \mid i,j = 1,\ldots,5 \;,\quad i \neq j\big\} \;,$$

with $\mathbf{e}_i$ denoting the standard orthonormal basis for $\mathbb{Z}^5$. These vectors in fact lie in a four-dimensional sublattice

$$A_4 = \left\{ (n_1, n_2, n_3, n_4, n_5) \in \mathbb{Z}^5 \;\middle|\; \sum_{i=1}^{5} n_i = 0 \right\} \subset N \simeq \mathbb{Z}^5 \ ,$$

We take as a basis for the sublattice A_4 the vectors

$$\mathbf{e}_{2,1} \ , \mathbf{e}_{3,2} \ , \mathbf{e}_{4,3} \ , \mathbf{e}_{5,4} \ , \qquad \text{where} \qquad \mathbf{e}_{i,j} = \mathbf{e}_i - \mathbf{e}_j \ .$$

The dual lattice can be realised as a sublattice of $M = N^* \simeq \mathbb{Z}^5$, with the basis given by

$$\mathbf{e}^{i+1,i} \ = \ \frac{i}{5} \sum_{t=i+1}^{5} \mathbf{e}^t - \frac{5-i}{5} \sum_{t=1}^{i} \mathbf{e}^t \ ,$$

where $\mathbf{e}^i$ is the canonical basis of $M \simeq \mathbb{Z}^5$. With these definitions we have that the canonical inner product gives a non-degenerate pairing:

$$\langle \mathbf{e}_{i+1,1}, \mathbf{e}^{j+1,j} \rangle \ = \ \delta_{ij} \ .$$

To find a convenient four-dimensional description for these lattices, we project $N \mapsto \widehat{N} \simeq \mathbb{Z}^4$ and $M \mapsto \widehat{M} \simeq (\mathbb{Z}^4)^*$ with

$$\begin{aligned} &\mathbf{e}_i \mapsto \mathbf{e}_i \ , \quad i = 1, \ldots, 4 \ , \qquad \mathbf{e}_5 \mapsto 0 \ , \\ &\mathbf{e}^i \mapsto \mathbf{e}^i \ , \quad i = 1, \ldots, 4 \ , \qquad \mathbf{e}^5 \mapsto -\mathbf{e}^1 - \mathbf{e}^2 - \mathbf{e}^3 - \mathbf{e}^4 \ . \end{aligned} \tag{5.3}$$

5.1.2 Four-dimensional description of $\widehat{\Delta}$

An equivalent way of arriving at the form of the four-dimensional polytope starts with going to an affine patch, say $X_5 = 1$, where the polynomial $P(\mathbf{X}; \varphi)$ contains 21 monomials that are now of the form

$$1 \ , \qquad X_i \ , \qquad \frac{1}{X_i} \ , \qquad \frac{X_i}{X_j} \ , \qquad i \neq j \ , \qquad i, j \neq 5 \ . \tag{5.4}$$

These monomials correspond to lattice points in $\widehat{N}^4$ that are given by the 21 vectors in the set

$$\big\{(0,0,0,0)\big\} \cup \big\{ \pm \mathbf{e}_i \;\big|\; i = 1, \ldots, 4 \big\} \cup \big\{ \mathbf{e}_i - \mathbf{e}_j \;\big|\; i, j = 1, \ldots, 4 \ , \ \ i \neq j \big\} \ .$$

For the numbering of these lattice points, see appendix A. The convex hull of these points in the real span $\widehat{N}_{\mathbb{R}}$ of $\widehat{N}$,

$$\widehat{\Delta} \ = \ \mathrm{Conv}(u_0, \ldots, u_{20}) \ , \tag{5.5}$$

is a four-dimensional reflexive polytope. The only internal lattice point is the origin u_0, and the vertices are exactly $u_1, \ldots, u_{20}$, which are the only lattice points in $\widehat{\Delta}$. The faces of $\widehat{\Delta}$ consist of 10 tetrahedra and 20 triangular prisms lying on the boundary planes defined by the equations

$$\delta_1 y_1 + \delta_2 y_2 + \delta_3 y_3 + \delta_4 y_4 + \epsilon_0 \ = \ 0 \ , \qquad \delta_i \in \{0, 1\} \ , \qquad \epsilon_0 \in \{-1, 1\}.$$

For the labelling of the faces, see appendix A. The 20 triangular prisms break up into two $\mathbb{Z}_5 \times \mathbb{Z}_2$ transitive orbits, under the actions $\mathfrak{A}$ and $\mathfrak{B}$ given in (5.6), and the tetrahedra form one such orbit. The facets meet as displayed in figure 5.2.

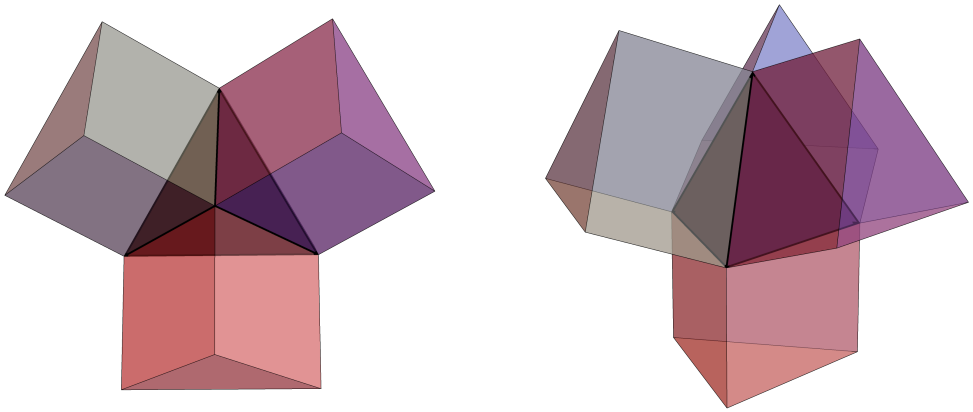


Figure 5.2: *At each of the ten tetrahedra, four of the twenty prisms meet in the above configuration (depicted twice). For each pair of prisms above there is a third (not pictured) sharing a face with both. The altitudes of prisms that share a face are perpendicular. This figure corrects Fig. 13 of [10].*

The polytope $\widehat{\Delta}$ defines a fan whose cones are exactly those supported by the faces of $\widehat{\Delta}$. This fan, however, is not simplicial, and consequently we wish to find a triangulation of $\widehat{\Delta}$, which corresponds to a smooth fan. We find that there are two triangulations that respect the $\mathbb{Z}_5 \times \mathbb{Z}_2$ symmetry. In the four-dimensional description, the action is a composition of the $\mathbb{Z}_5 \times \mathbb{Z}_2$ action in five dimensions and the projection to four dimensions. This gives

$$\begin{aligned} \mathfrak{A} &: (m_1, m_2, m_3, m_4) \mapsto \begin{cases} (\ \ 0, m_1, m_2, m_3)\ , & \text{if } \sum_{i=1}^4 m_i \ = \ 0\ , \\ (\pm 1, m_1, m_2, m_3)\ , & \text{if } \sum_{i=1}^4 m_i \ = \ \mp 1\ , \end{cases} \\ \mathfrak{B} &: \mathbf{e}^i \mapsto -\mathbf{e}^i\ . \end{aligned} \tag{5.6}$$

The cones in the first triangulation are given by

$$\begin{aligned} \sigma_1 &= \Big\langle (1,0,0,0),\ (1,0,\ \ 0,-1),\ (1,0,-1,\ \ 0),\ (0,1,-1,0) \Big\rangle\ , \\ \sigma_2 &= \Big\langle (1,0,0,0),\ (0,1,\ \ 0,\ \ 0),\ (0,1,\ \ 0,-1),\ (0,1,-1,0) \Big\rangle\ , \\ \sigma_3 &= \Big\langle (1,0,0,0),\ (1,0,\ \ 0,-1),\ (0,1,\ \ 0,-1),\ (0,1,-1,0) \Big\rangle\ , \\ \sigma_4 &= \Big\langle (1,0,0,0),\ (1,0,-1,\ \ 0),\ (0,1,-1,\ \ 0),\ (0,0,-1,1) \Big\rangle\ , \\ \sigma_5 &= \Big\langle (1,0,0,0),\ (0,1,\ \ 0,\ \ 0),\ (0,1,-1,\ \ 0),\ (0,0,\ \ 0,1) \Big\rangle\ , \\ \sigma_6 &= \Big\langle (1,0,0,0),\ (0,0,\ \ 0,\ \ 1),\ (0,1,-1,\ \ 0),\ (0,0,-1,1) \Big\rangle\ , \end{aligned} \tag{5.7}$$

and their images under $\mathbb{Z}_2 \times \mathbb{Z}_5$, together with the 10 simplicial cones supported by the tetrahedra. The cones σ_1, σ_2 and σ_3 correspond to the triangulation of the triangular prism $y_1 + y_2 = 1$ and σ_4, σ_5 and σ_6 give a triangulation of the prism $y_3 + y_5 = -1$.

5.1.3 The dual polytope $\widehat{\Delta}^*$

The polytope $\widehat{\Delta}$ has a dual reflexive polytope $\widehat{\Delta}^*$ which is bounded by 20 planes

$$\epsilon_0 + x_i \;=\; 0\;, \qquad 1 + x_i - x_j \;=\; 0\;, \qquad i,j \in \{1,2,3,4\}\;, \quad i \;\neq\; j\;, \qquad \epsilon_0 \in \{-1,1\}\;.$$

These planes intersect $\widehat{\Delta}^*$ in 20 cubical faces. For the explicit numbering of the faces, which manifests the explicit duality between these faces and the vertices of $\widehat{\Delta}$, see appendix A. It follows that $\widehat{\Delta}^*$ is a convex hull of 31 lattice points that we label $v_0, \ldots, v_{30}$.

$$\widehat{\Delta}^* \;=\; \mathrm{Conv}(v_0,\ldots,v_{30}) = \mathrm{Conv}\left(\left\{\,\pm(\delta_1,\delta_2,\delta_3,\delta_4)\;\middle|\;\delta_i \in \{0,1\}\right\}\right)\;. \tag{5.8}$$

The corresponding fan is again non-simplicial, and thus requires triangulation to give a non-singular ambient toric variety. Hulek and Verrill [14] consider a triangulation that is invariant under the S_5 permutations of the lattice coordinates. All of the top-dimensional cones in this triangulation are obtained by acting on the vertices of a single cone with S_5:

$$\left\{\varsigma\langle(1,0,0,0),(1,1,0,0),(1,1,1,0),(1,1,1,1)\rangle\;\middle|\;\varsigma \in S_5\right\}\;.$$

Note that the action of $\varsigma \in S_5$ on $\widehat{N}$ is subtle: we have to consider the action of S_5 on the five-dimensional lattice and then project this to back to the four-dimensional lattice. Doing this, one is left with the following action on the basis

$$\varsigma(\mathbf{e}_i) = \begin{cases} \mathbf{e}_{\varsigma(i)} & \text{if } \varsigma(i) \neq 5\;, \\ -\mathbf{e}_1 - \mathbf{e}_2 - \mathbf{e}_3 - \mathbf{e}_4 & \text{if } \varsigma(i) = 5\;. \end{cases}$$

The triangulation data serves as input for Batyrev's formula [33] for the Hodge numbers of smooth members of the families of Calabi-Yau manifolds corresponding to the polytopes $\widehat{\Delta}$ and $\widehat{\Delta}^*$:

$$h^{12} \;=\; \mathrm{pts}\big(\widehat{\Delta}^*\big) - \sum_{\mathrm{codim}\,\widehat{\Theta}^*=1} \mathrm{int}\big(\widehat{\Theta}^*\big) \;\; + \sum_{\mathrm{codim}\,\widehat{\Theta}=2} \mathrm{int}\big(\widehat{\Theta}^*\big)\,\mathrm{int}\big(\widehat{\Theta}\big) - 5\;,$$

$$h^{11} \;=\; \mathrm{pts}\big(\widehat{\Delta}\big) \;\; - \sum_{\mathrm{codim}\,\widehat{\Theta}=1} \mathrm{int}\big(\widehat{\Theta}\big) \;\; + \sum_{\mathrm{codim}\,\widehat{\Theta}=2} \mathrm{int}\big(\widehat{\Theta}^*\big)\,\mathrm{int}\big(\widehat{\Theta}\big) - 5\;,$$

where $\mathrm{pts}(\widehat{\Theta})$ and $\mathrm{int}(\widehat{\Theta})$ denote the number of lattice points and interior lattice points of $\widehat{\Theta}$. $\widehat{\Theta}$ and $\widehat{\Theta}^*$ are faces of $\widehat{\Delta}$ and $\widehat{\Delta}^*$, respectively. These formulae are manifestly compatible with mirror symmetry. From the toric descriptions for the manifolds $\widehat{\mathrm{HV}}$ and $\widehat{\mathrm{H}\Lambda}$, we find the Hodge numbers

$$h^{p,q}\left(\widehat{\mathrm{HV}}\right) = \begin{array}{ccccccc} & & & 1 & & & \\ & & 0 & & 0 & & \\ & 0 & & 26 & & 0 & \\ 1 & & 16 & & 16 & & 1 \\ & 0 & & 26 & & 0 & \\ & & 0 & & 0 & & \\ & & & 1 & & & \end{array}\;, \qquad h^{p,q}\left(\widehat{\mathrm{H}\Lambda}\right) = \begin{array}{ccccccc} & & & 1 & & & \\ & & 0 & & 0 & & \\ & 0 & & 16 & & 0 & \\ 1 & & 26 & & 26 & & 1 \\ & 0 & & 16 & & 0 & \\ & & 0 & & 0 & & \\ & & & 1 & & & \end{array}\;.$$

5.2 The polytopes corresponding to small resolutions

5.2.1 The small polytopes Δ_1 and Δ_2

To find the toric descriptions of the non-singular manifolds HV and HΛ, we study the polytopes $\Delta_1, \Delta_2 \subset \mathbb{Z}^5$. Their vertices correspond to monomials in the polynomials P^1 and P^2, defined in (5.2), that define on $\mathbb{P}^5$ a variety birational to $\widehat{\text{HV}}$. We work directly in an affine patch where $X_0 = 1$. Then the two polytopes can be expressed as

$$\Delta_1 \;=\; \text{Conv}(\mathbf{0},\, \mathbf{e}_1,\, \mathbf{e}_2,\, \mathbf{e}_3,\, \mathbf{e}_4,\, \mathbf{e}_5)\;, \qquad \Delta_2 \;=\; \text{Conv}(\mathbf{0},\, -\mathbf{e}_1,\, -\mathbf{e}_2,\, -\mathbf{e}_3,\, -\mathbf{e}_4,\, -\mathbf{e}_5) \;=\; -\Delta_1\;.$$

These, and the other polytopes defined this subsection, are schematically represented in two dimensions in figure 5.3. Using these two, we can construct two larger polytopes as their Minkowski sum and the convex hull of their union

$$\Delta \;\stackrel{\text{def}}{=}\; \text{Mink}(\Delta_1,\, \Delta_2)\;, \qquad \nabla^* \;\stackrel{\text{def}}{=}\; \text{Conv}(\Delta_1,\, \Delta_2)\;.$$

From the definition of convex hull, it follows immediately that the vertices of ∇^* are exactly $\pm\mathbf{e}_i$ with $i = 1, \ldots, 5$. Its 32 faces are the four-dimensional simplices of the form

$$\tau_n \;=\; \text{Conv}\left(\epsilon_1\mathbf{e}_1,\, \epsilon_2\mathbf{e}_2,\, \epsilon_3\mathbf{e}_3,\, \epsilon_4\mathbf{e}_4,\, \epsilon_5\mathbf{e}_5\right)\;, \qquad \epsilon_i \in \{-1, 1\}\;,$$

given by intersections of ∇^* with bounding planes

$$\epsilon_1 x_1 + \epsilon_2 x_2 + \epsilon_3 x_3 + \epsilon_4 x_4 + \epsilon_5 x_5 \;=\; 1\;, \qquad \epsilon_i \in \{-1, 1\}\;.$$

The polytope Δ contains in total 31 lattice points,

$$\big\{(0,0,0,0)\big\} \cup \big\{\, \pm\,\mathbf{e}_i \;\big|\; i = 1, \ldots, 5\big\} \cup \big\{\mathbf{e}_i - \mathbf{e}_j \;\big|\; i, j = 1, \ldots, 5\;,\;\; i \neq j\big\}\;.$$

Thus it can be written as a convex hull of 30 lattice points

$$\Delta \;=\; \text{Conv}(v_1, \ldots, v_{30})\;.$$

Its only internal point is the origin, and it has 62 faces that are hypercubes, given by intersections with planes

$$\epsilon_0 + \delta_1 x_1 + \delta_2 x_2 + \delta_3 x_3 + \delta_4 x_4 + \delta_5 x_5 \;=\; 0\;, \qquad \text{with} \qquad \epsilon_0 \in \{-1, 1\}\;,\;\; \delta_i \in \{0, 1\}\;.$$

It can be shown that $\{\Delta_1, \Delta_2\}$ is a nef-partition of Δ.

5.2.2 The small polytopes ∇_1 and ∇_2

Finally, to find the equations defining the mirror Hulek-Verrill manifold, we need the two polytopes ∇_1 and ∇_2. These can be obtained by first finding the duals of ∇^* and Δ. The polytope ∇ is a hypercube centred at the origin. Its vertices are given by the 32 points of the form

$$\nabla = \text{Conv}\left(\{(\epsilon_1, \epsilon_2, \epsilon_3, \epsilon_4, \epsilon_5)\} \mid \epsilon_i \in \{-1, 1\}\right)\;.$$

The faces are the 10 four-dimensional hypercubes given by intersections with the planes

$$y_i = \pm 1 \ .$$

The remaining polytope Δ^* has a slightly more complicated structure. It can be written as the convex hull of 62 vertices of the form

$$\Delta^* \ = \ \mathrm{Conv}\left(\{\pm(\delta_1,\delta_2,\delta_3,\delta_4,\delta_5) \mid \delta_i \in \{0,1\}\}\right) \ .$$

The labelling of all vertices in given in appendix A. It has 30 faces, given by intersections with the planes

$$1 \pm y_i \ = \ 0 \ , \qquad 1 + y_i - y_j \ = \ 0 \ .$$

Like their duals, ∇ and Δ^* can be given in terms of two smaller polytopes ∇_1 and ∇_2:

$$\nabla = \mathrm{Mink}(\nabla_1,\, \nabla_2) \ , \qquad \Delta^* = \mathrm{Conv}(\nabla_1,\, \nabla_2) \ .$$

Here ∇_1 and ∇_2 are hypercubes with one vertex at origin, given by

$$\nabla_1 \ = \ \mathrm{Conv}\left(\{(\delta_2,\ldots,\delta_5) \,|\, \delta_i \in \{0,1\}\}\right) \ , \qquad \nabla_2 \ = \ \mathrm{Conv}\left(\{-(\delta_1,\ldots,\delta_5) \,|\, \delta_i \in \{0,1\}\}\right) \ = -\nabla_1 \ .$$

By the prescription of Batyrev and Borisov, the ambient variety $\mathbb{P}_{\Delta^*}$ for the Hulek-Verrill manifold is given by triangulating Δ^*. We leave most of the details to the reader, but the upshot is that, as in [14], we can take the triangulation to be invariant under permutations $\varsigma \in S_5$ of the coordinates X_i as well as under the $\mathbb{Z}_2$ inversion symmetry $X_i \mapsto \frac{1}{X_i}$.

The fan associated to Δ^* consists of 720 top-dimensional cones. There are three simplicial cones σ_1, σ_2 and σ_3, whose images under S_5 and $\mathbb{Z}_2$ generate the whole fan. These are given by

$$\begin{aligned}
\sigma_1 \ &= \ \Big\langle (\ \ 1,0,0,0,0),\, (\ \ 1,\ \ 1,0,0,0),\, (1,1,1,0,0),\, (1,1,1,1,0),\, (1,1,1,1,1) \Big\rangle \ , \\
\sigma_2 \ &= \ \Big\langle (-1,0,0,0,0),\, (\ \ 0,\ \ 0,0,0,1),\, (0,0,0,1,1),\, (0,0,1,1,1),\, (0,1,1,1,1) \Big\rangle \ , \\
\sigma_3 \ &= \ \Big\langle (-1,0,0,0,0),\, (-1,-1,0,0,0),\, (0,0,0,0,1),\, (0,0,0,1,1),\, (0,0,1,1,1) \Big\rangle \ .
\end{aligned} \tag{5.9}$$

The first cone, together with the 119 distinct cones generated by permuting the coordinates, $\{\varsigma(\sigma_1) \mid \varsigma \in S_5\}$, give a triangulation of the hypercube ∇_1. The $\mathbb{Z}_2$ inversion symmetry acts on these cones by $\varsigma(\sigma_1) \mapsto \varsigma(-\sigma_1)$. The hypercube ∇_2 is triangulated by the $\mathbb{Z}_2$ image of $\{\varsigma(\sigma_1) \mid \varsigma \in S_5\}$. The rest of the polytope ∇ is triangulated by σ_2, σ_3, and their images under $S_5 \times \mathbb{Z}_2$.

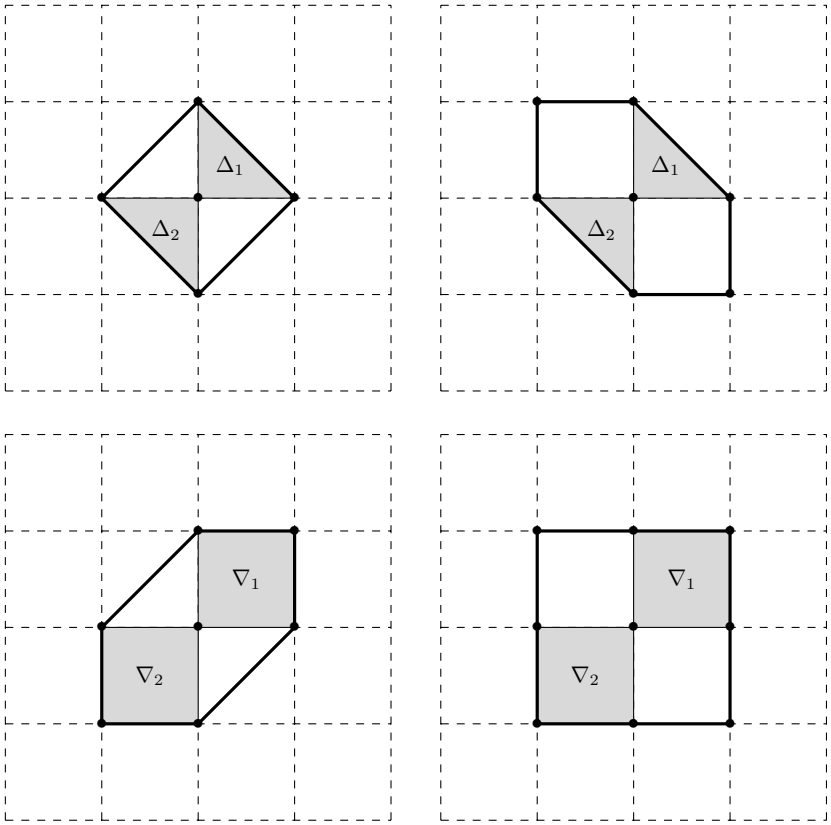


Figure 5.3: *Two-dimensional analogues of the polytopes Δ, ∇, their duals, and their nef-partitions. Clockwise from top-left, we have Conv(Δ_1, Δ_2), Mink(Δ_1, Δ_2), Mink(∇_1, ∇_2), and Conv(∇_1, ∇_2).*

5.3 The Hulek-Verrill manifolds and their mirrors

Having studied the relevant lattice geometry, we are ready to turn to the toric geometry associated to the triangulations of the fans corresponding to the triangulated polytopes that were found in the previous sections. We will give both the singular manifolds $\widehat{\mathrm{HV}}$ and $\widehat{\mathrm{H}\Lambda}$ and their resolutions HV and HΛ as a vanishing locus of a set of polynomials inside the relevant ambient toric variety. We also find some basic properties of these manifolds, which will be relevant in the following chapters. The quantities associated to each manifold are summarised in table 5.2.

Quantity	$\widehat{\mathrm{HV}}$	$\widehat{\mathrm{H}\Lambda}$	HV	HΛ
Defining polynomials	P	Q	P^1, P^2	Q^1, Q^2
Polytopes defining monomials	$\widehat{\Delta}$	$\widehat{\Delta}^*$	Δ_1, Δ_2	∇_1, ∇_2
Ambient toric variety	$\mathbb{P}_{\widehat{\Delta}^*}$	$\mathbb{P}_{\widehat{\Delta}}$	$\mathbb{P}_{\Delta^*}$	$\mathbb{P}_{\nabla^*}$
Coordinates	$X_1, \ldots X_5$	$Y_1, \ldots, Y_4$	$X_0, \ldots, X_5$	$Y_0, \ldots, Y_4$

Table 5.2: *Quantities associated to the manifolds $\widehat{HV}$, $\widehat{H\Lambda}$, HV, and HΛ.*

5.3.1 The singular Hulek-Verrill manifold $\widehat{\mathrm{HV}}$

The ambient toric variety $\mathbb{P}_{\widehat{\Delta}^*}$ in which $\widehat{\mathrm{HV}}$ can be embedded corresponds to the polytope $\widehat{\Delta}^*$. To the vertices we associate Cox coordinates $\xi_1, \ldots, \xi_{30}$. As in (2.18), the ambient variety can then be given by the usual construction as

$$\mathbb{P}_{\widehat{\Delta}^*} \;=\; \frac{\mathbb{C}^{30} \setminus Z_\Delta}{(\mathbb{C}^*)^{26}} \;. \tag{5.10}$$

To study the Calabi-Yau manifold $\widehat{\mathrm{HV}} \subset \mathbb{P}_{\widehat{\Delta}^*}$, we identify the coordinates $X_1, \ldots, X_4$ with the coordinates $\Xi_1, \ldots, \Xi_4$ on the torus, which we define in terms of Cox coordinates in appendix A. Then the Calabi-Yau manifold can be written as as a subset

$$\left\{ \sum_{i \neq j} a_{i,j} \, \frac{X_i}{X_j} + a_0 \;=\; 0 \right\} \subset \mathbb{P}_{\widehat{\Delta}^*}. \tag{5.11}$$

We are chiefly concerned with the five-parameter subfamily

$$a_{i,j} = a_j \qquad \text{for all } i \neq j \;,$$

where the polynomial in (5.11) takes the form P given in (4.1). The generic manifold in this family contains 30 nodal singularities on $\widehat{\mathrm{HV}} \setminus \mathbb{T}^4$, which can be seen by considering the local patches corresponding to the triangulation of the polytope $\widehat{\Delta}^*$ [14]. They have, however, small projective resolutions $\mathrm{HV}_{(a_0,\ldots,a_5)}$, which are smooth Calabi-Yau manifolds. We will discuss the toric description of these manifolds later in this section.

5.3.2 The singular mirror Hulek-Verrill manifold $\widehat{\mathrm{H}\Lambda}$

We can use Batyrev's construction [33] to find the mirror manifolds of the singular Hulek-Verrill manifolds which are birational to the mirror manifolds of the small resolutions mentioned above. The construction of the resolved manifold in this way is somewhat complicated, but in §5.3.3 we give another method of finding this resolution.

We have already found the vertices of the dual polytope $\widehat{\Delta}^*$ in (5.8). These, together with the interior point, correspond to the monomials

$$1 \;, \quad Y_i \;, \quad Y_i Y_j \;, \quad Y_i Y_j Y_k \;, \quad Y_i Y_j Y_k Y_l \;, \quad \frac{1}{Y_i} \;, \quad \frac{1}{Y_i Y_j} \;, \quad \frac{1}{Y_i Y_j Y_k} \;, \quad \frac{1}{Y_i Y_j Y_k Y_l} \;. \tag{5.12}$$

Each of the indices i, j, k, l are distinct and take values in $\{1, 2, 3, 4\}$. The intersection of a generic mirror singular Hulek-Verrill manifold with the torus $\mathbb{T}^4$ is given by the closure of the vanishing locus

$$\widehat{Q} \;\stackrel{\text{def}}{=}\; \sum_{i,j,k,l=0}^{2} A_{i,j,k,l} Y_1^i Y_2^j Y_3^k Y_4^l \;=\; 0 \;. \tag{5.13}$$

One obtains this by taking the most general polynomial with monomials (5.12) and multiplying through by $Y_1 Y_2 Y_3 Y_4$, which gives the same variety on $\mathbb{T}^4$.

Given the triangulation (5.7) of $\widehat{\Delta}$ discussed in §5.1, we can consider the local affine patches $\mathbb{A}_{\sigma_i}$ corresponding to the simplicial cones σ_i. Equivalently, we can choose suitable 4-tuples of the Cox coordinates η_i to act as the local coordinates on patches isomorphic to $\mathbb{A}^4$. It is only necessary to study the six local patches related to the fans given in (5.7) and a single patch generated by any tetrahedron. The other local patches are obtained from these by the action of the $\mathbb{Z}_5 \times \mathbb{Z}_2$ symmetry.

As an example, let us consider the cone σ_1. The coordinates associated to the generators of this cone are

$$x \stackrel{\text{def}}{=} \eta_{20} \ , \quad y \stackrel{\text{def}}{=} \eta_{19} \ , \quad z \stackrel{\text{def}}{=} \eta_{18} \ , \quad w \stackrel{\text{def}}{=} \eta_{14} \ .$$

Since the generators corresponding to these coordinates belong to the same simplicial cone, we can set the other coordinates to unity, and thus identify the local coordinates with those on the torus as (see appendix A)

$$H^1 \ = \ xyz \ , \qquad H^2 \ = \ w \ , \qquad H^3 \ = \ \frac{1}{wz} \ , \qquad H^4 \ = \ \frac{1}{y} \ .$$

We can immediately find the local coordinates on

$$\mathfrak{A}\,\sigma_1 \ = \ \big\langle (-1,1,0,0),\ (0,1,0,0),\ (0,1,0,-1),\ (0,0,1,-1) \big\rangle$$

by noting that the $\mathbb{Z}_5$ action on the Cox coordinates inherited from the action on the vertices maps

$$\eta_{20} \mapsto \eta_4 \ = \ x \ , \qquad \eta_{19} \mapsto \eta_{16} \ = \ y \ , \qquad \eta_{18} \mapsto \eta_{15} \ = \ z \ , \qquad \eta_{14} \mapsto \eta_{12} \ = \ w.$$

The equalities denote identifications with the coordinates on the affine patch $\mathbb{A}_{\mathfrak{A}\sigma_1}$. Thus on this patch, we can make the identifications with the torus coordinates as

$$H_1 \ = \ \frac{1}{x} \ , \qquad H_2 \ = \ xyz \ , \qquad H_3 \ = \ w \ , \qquad H_4 \ = \ \frac{1}{wz} \ .$$

Note that this corresponds to $\mathbb{Z}_5$ acting on the global coordinates as

$$H_i \mapsto H_{i+1} \ , \quad i \neq 4 \ , \qquad\qquad H_4 \mapsto \frac{1}{H_1 H_2 H_3 H_4} \ ,$$

which of course corresponds to the $\mathbb{Z}_5$ action $\mathbf{e}^i \mapsto \mathbf{e}^{i+1}$ of the five-dimensional lattice M, projected down to four dimensions by (5.3).

Writing the polynomial Q in the global coordinates gives, for generic values of the moduli, an irreducible multi-degree $(2,4,4,4)$ polynomial. A member of this family is generically smooth, but smooth members are not birational to mirrors of Hulek-Verrill manifolds $\mathrm{H}\Lambda_{(a_0,\ldots,a_5)}$.

Instead, it turns out that we must only consider those whose defining polynomials can be written in the form

$$\widehat{Q} \ = \ \alpha\,\delta - \beta\,\gamma \ ,$$

where α, β, γ, and δ are multi-degree $(1,1,1,1)$ polynomials in the coordinates $Y_1, \ldots, Y_4$. A manifold with this property has exactly 24 singularities, which can be resolved to obtain a smooth variety.

5.3.3 The Hulek-Verrill manifold HV

As we have already remarked, Hulek and Verrill noted that the singular variety $\widehat{\mathrm{HV}}_{(\varphi^0,\ldots,\varphi^5)}$ defined by the equation

$$\left(\sum_{i=1}^{5} X_i\right)\left(\sum_{i=1}^{5} \frac{\varphi^i}{X_i}\right) \;=\; \varphi^0 \tag{5.14}$$

on the toric variety $\mathbb{P}_{\widehat{\Delta}^*}$ is birational to the subvariety of $\mathbb{P}^5$ defined by the two polynomials

$$P^1 \stackrel{\text{def}}{=} \sum_{\mu=0}^{5} X_\mu \;, \qquad P^2 \stackrel{\text{def}}{=} \sum_{\mu=0}^{5} \frac{\varphi^\mu}{X_\mu} \;.$$

It is possible to develop this further by studying the two equations $P^1 = P^2 = 0$ on the torus $\mathbb{T}^5$ and finding the toric closure of this variety. This can be achieved using the techniques reviewed briefly in §2.3.3. In §5.1, we have studied the polytopes Δ_1 and Δ_2 whose vertices correspond to the monomials in P^1 and P^2, and found the polytope Δ^* which gives the ambient space $\mathbb{P}_{\Delta^*}$. The Cox coordinates and coordinate scalings defining the ambient variety are given in appendix A.

We can analyse this variety further by specialising to various local patches. We only need to analyse the patches that are not related by symmetry. The Cox coordinates associated to the generators of the cone σ_1 in (5.9) are

$$\xi_1 \stackrel{\text{def}}{=} x \;, \qquad \xi_5 \stackrel{\text{def}}{=} y \;, \qquad \xi_{13} \stackrel{\text{def}}{=} z \;, \qquad \xi_{29} \stackrel{\text{def}}{=} w \;, \qquad \xi_{61} \stackrel{\text{def}}{=} v \;.$$

Using the leftover scalings to set the other 57 Cox coordinates ξ to unity, we can identify the invariants $\Xi_1, \ldots, \Xi_5$ as

$$\Xi_1 \;=\; xyzwv \;, \qquad \Xi_2 \;=\; yzwv \;, \qquad \Xi_3 \;=\; zwv \;, \qquad \Xi_4 \;=\; wv \;, \qquad \Xi_5 \;=\; v \;.$$

By further identifying these Ξ_i with the coordinates X_i on the torus, we can write the polynomials P^1 and P^2 as

$$\begin{aligned} P^1 \;&=\; 1 + v + wv + zwv + yzwv + xyzwv \;, \\ P^2 \;&=\; \varphi^0 + \frac{\varphi^1}{xyzwv} + \frac{\varphi^2}{yzwv} + \frac{\varphi^3}{zwv} + \frac{\varphi^4}{wv} + \frac{\varphi^5}{v} \;. \end{aligned}$$

The analogous relations for the remaining cones, σ_2 and σ_3, can be found in a similar manner.

By studying the equations $P^1 = P^2 = \mathrm{d}P^1 \wedge \mathrm{d}P^2 = 0$, it is not difficult to see that, generically, the variety HV does not have singularities. As in the original analysis of Hulek and Verrill [14], we find that there are singularities if and only if

$$\mathbb{\Delta} \stackrel{\text{def}}{=} \prod_{\epsilon_i \in \{\pm 1\}} \left(\sqrt{\varphi^0} + \epsilon_1\sqrt{\varphi^1} + \epsilon_2\sqrt{\varphi^2} + \epsilon_3\sqrt{\varphi^3} + \epsilon_4\sqrt{\varphi^4} + \epsilon_5\sqrt{\varphi^5}\right) \;=\; 0 \;. \tag{5.15}$$

The algorithm of [36, 37], implemented in PALP [38], gives the Hodge numbers of this variety as

$$h^{p,q} = \begin{array}{ccccccc} & & & 1 & & & \\ & & 0 & & 0 & & \\ & 0 & & 45 & & 0 & \\ 1 & & 5 & & 5 & & 1 \\ & 0 & & 45 & & 0 & \\ & & 0 & & 0 & & \\ & & & 1 & & & \end{array} .$$

Thus we identify these manifolds as the small projective resolutions of the singular manifolds $\widehat{\text{HV}}$.

When $\varphi^0 = 1$ and $\varphi^i = \varphi$ for $i \neq 0$, the manifold admits a $\mathbb{Z}_5 \times \mathbb{Z}_2 \subset S_5 \times \mathbb{Z}_2$ symmetry group, which acts freely outside of the singular locus $\mathbb{\Delta} = 0$. The actions of $\mathbb{Z}_5$ and $\mathbb{Z}_2$ on the coordinates can be written as

$$\mathfrak{A} \ : \ X_i \mapsto X_{i+1} \ , \qquad \mathfrak{B} \ : X_i \ \mapsto \frac{1}{X_i} \ , \tag{5.16}$$

with the indices understood to take values in $\mathbb{Z}_5$. The Hodge numbers of the varieties obtained by taking the quotients are given in table 5.3. The one-parameter manifolds $\text{HV}/\mathbb{Z}_5$ and $\text{HV}/\mathbb{Z}_{10}$ have a Picard-Fuchs equation given by the operator number 34 in the AESZ list [80], and were studied in connection to modularity in [1, 10, 13]. For convenience, we will call these manifolds simply as AESZ34, specifying the particular quotient taken, if needed.

Manifold	HV	$\text{HV}/\mathbb{Z}_5$	$\text{HV}/\mathbb{Z}_{10}$
(h^{11}, h^{12})	(45,5)	(9,1)	(5,1)

Table 5.3: *The Hodge numbers h^{11} and h^{12} for the free quotients of HV.*

5.3.4 The mirror Hulek-Verrill manifold HΛ

The family of mirror Hulek-Verrill manifolds can be defined as the vanishing loci of two polynomials corresponding to the polytopes ∇_1 and ∇_2 inside the ambient variety $\mathbb{P}_{\nabla^*}$ associated to the triangulated polytope ∇^*.

The monomials associated to the vertices of ∇_1 are

$$1 \ , \qquad Y_i \ , \qquad Y_i Y_j \ , \qquad Y_i Y_j Y_k \ , \qquad Y_i Y_j Y_k Y_l \ , \qquad Y_i Y_j Y_k Y_l Y_m \ ,$$

with distinct indices understood to take distinct values. The monomials associated to ∇_2 are simply the inverses of these.

$$1 \ , \qquad \frac{1}{Y_i} \ , \qquad \frac{1}{Y_i Y_j} \ , \qquad \frac{1}{Y_i Y_j Y_k} \ , \qquad \frac{1}{Y_i Y_j Y_k Y_l} \ , \qquad \frac{1}{Y_i Y_j Y_k Y_l Y_m} \ .$$

Looking at the vertices of ∇^* listed in appendix A, we see that the ambient variety $\mathbb{P}_{\nabla^*}$ is nothing but the product $(\mathbb{P}^1)^5$. The Cox coordinates are the homogeneous coordinates on each $\mathbb{P}^1$, which we

often denote by $\mathbb{P}^1_i$ with $i = 0, \ldots, 4$ if there is a need to distinguish between different factors in the product $(\mathbb{P}^1)^5$. The coordinates Y_i on the torus are identified with the affine coordinates

$$Y_i = \frac{Y_{i,1}}{Y_{i,0}},$$

with $[Y_{i,0} : Y_{i,1}]$ giving the homogeneous coordinates on $\mathbb{P}^1_i$. It is convenient to intoduce the following monomials of homogeneous coordinates

$$M_{abcde} \;=\; Y_{1,a} Y_{2,b} Y_{3,c} Y_{4,d} Y_{5,e} \ ,$$

where $a, b, c, d, e \in \{0, 1\}$. Using these, the most general polynomials associated to ∇_1 and ∇_2 can be written as

$$Q^1 = \sum_{a,b,c,d,e} A_{abcde} M_{abcde} \ , \qquad Q^2 = \sum_{a,b,c,d,e} B_{abcde} M_{abcde} \ . \tag{5.17}$$

For a special choice of coefficients A and B, the vanishing locus of Q^1 and Q^2 admits $\mathbb{Z}_5$, $\mathbb{Z}_5 \times \mathbb{Z}_2$ or $\mathbb{Z}_5 \times \mathbb{Z}_2 \times \mathbb{Z}_2$ symmetry [73]. These act freely, and thus can be used to obtain smooth quotient manifolds. Denoting the generator of the $\mathbb{Z}_5$ as S, the generator of the first $\mathbb{Z}_2$ as U and the second $\mathbb{Z}_2$ as V, we can take the symmetry transformations to act on the coordinates as

$$S \,:\, Y_{i,a} \mapsto Y_{i+1,a} \ , \qquad U \,:\, Y_{i,a} \mapsto (-1)^a Y_{i,a} \ , \qquad V \,:\, Y_{i,0} \leftrightarrow Y_{i,1} \ , \tag{5.18}$$

where the index i is again understood to take values in $\mathbb{Z}_5$. The symmetries S and V can be seen to descend from the $\mathbb{Z}_5$ and $\mathbb{Z}_2$ symmetries acting on the polytope ∇^*. To write down the polynomials invariant under there symmetries, it is convenient to introduce the $\mathbb{Z}_5$ invariant combinations of the monomials M_{abcde},

$$m_{abcde} \;=\; \sum_{i=1}^{5} Y_{i,a} Y_{i+1,b} Y_{i+2,c} Y_{i+3,d} Y_{i+4,e} \ .$$

The polynomials defining the $\mathbb{Z}_5$ symmetric manifolds can be found by specialising the coefficients A and B so that the vanishing locus $Q^1 = Q^2 = 0$ is invariant under $\mathbb{Z}_5$, or equivalently by finding the $\mathbb{Z}_5$ orbits of Q^1 and Q^2. In this manner, we find

$$\begin{aligned} Q^1 \;&= A_{00000}\, m_{00000} + A_{10000}\, m_{10000} + A_{11000}\, m_{11000} + A_{10100}\, m_{10100} + A_{11100}\, m_{11100} \\ &\quad + A_{11010}\, m_{11010} + A_{11110}\, m_{11110} + A_{11111}\, m_{11111} \ , \\ Q^2 \;&= B_{00000}\, m_{00000} + B_{10000}\, m_{10000} + B_{11000}\, m_{11000} + B_{10100}\, m_{10100} + B_{11100}\, m_{11100} \\ &\quad + B_{11010}\, m_{11010} + B_{11110}\, m_{11110} + B_{11111}\, m_{11111} \ . \end{aligned} \tag{5.19}$$

To find the defining polynomials in the $\mathbb{Z}_5 \times \mathbb{Z}_2$ symmetric case, we can further demand that the vanishing locus of the polynomials is invariant under the $\mathbb{Z}_2$ generated by V, which gives us two polynomials of the form

$$Q^1 \;= A_0\, m_{00000} + A_1\, m_{10000} + A_2\, m_{11000} + A_3\, m_{10100} + A_4\, m_{11100} + A_5\, m_{11010} + A_6\, m_{11110} + A_7\, m_{11111} \ ,$$

$$Q^2 \;= A_0\, m_{11111} + A_1\, m_{11110} + A_2\, m_{11100} + A_3\, m_{11010} + A_4\, m_{11000} + A_5\, m_{10100} + A_6\, m_{10000} + A_7\, m_{00000} \ .$$

Alternatively, we can demand that the vanishing locus is invariant under the second $\mathbb{Z}_2$ generated by U. In this case, the polynomials can be written as

$$\begin{aligned} Q^1 &= A_0\, m_{00000}+A_1\, m_{11000}+A_2\, m_{10100}+A_3\, m_{11110}\ , \\ Q^2 &= B_0\, m_{11111}+B_1\, m_{11100}+B_2\, m_{11010}+B_3\, m_{10010}\ . \end{aligned}$$

Note that the actions of U and V are exchanged under a suitable redefinition of coordinates, and therefore we can choose either of these two forms for the polynomials defining the $\mathbb{Z}_5 \times \mathbb{Z}_2$ invariant variety. Note also that in the latter case the polynomials Q^1 and Q^2 are not each $\mathbb{Z}_2$ invariant, but instead are mapped to each other under the action on $\mathbb{Z}_2$, thus keeping their mutual vanishing locus invariant.

Finally, we can consider the variety invariant under the full $\mathbb{Z}_5 \times \mathbb{Z}_2 \times \mathbb{Z}_2$. In this case we can write the defining polynomials as

$$\begin{aligned} Q^1 &= \frac{A_0}{5}\, m_{00000}+A_1\, m_{11000}+A_2\, m_{10100}+A_3\, m_{11110}\ , \\ Q^2 &= \frac{A_0}{5}\, m_{11111}+A_1\, m_{11100}+A_2\, m_{11010}+A_3\, m_{10010}\ . \end{aligned} \tag{5.20}$$

It turns out that the varieties defined in this way and their quotients under their respective symmetry groups are smooth Calabi-Yau manifolds, which we can identify as mirror manifolds of the five-parameter family $\mathrm{HV}_{(a_0,\ldots,a_5)}$. We call these *mirror Hulek-Verrill manifolds* HΛ. The Hodge numbers of the corresponding quotient varieties were already found in [73]. We reproduce these in table 5.4.

Manifold	HΛ	HΛ/$\mathbb{Z}_2$	HΛ/$\mathbb{Z}_2\times\mathbb{Z}_2$	HΛ/$\mathbb{Z}_5$	HΛ/$\mathbb{Z}_5\times\mathbb{Z}_2$	HΛ/$\mathbb{Z}_5\times\mathbb{Z}_2\times\mathbb{Z}_2$
(h^{11}, h^{12})	(5,45)	(5,25)	(5,15)	(1,9)	(1,5)	(1,3)

Table 5.4: *The Hodge numbers h^{11} and h^{12} of the different free quotients of HΛ.*

Counting the parameters in the polynomials seems naïvely to produce too many parameters compared to the Hodge numbers. However, on taking into account rescalings; remaining automorphisms of the ambient variety $(\mathbb{P}^1)^5$; and $\mathrm{SL}(2,\mathbb{C})$ transformation of the polynomials; we find that the number of free parameters in the defining polynomials agrees with the Hodge numbers.

Finally, we note that this variety is birational to the singular $\widehat{\mathrm{H}\Lambda}$. This is most easily seen by observing that the intersection $\widehat{\mathrm{H}\Lambda} \cap \mathbb{T}^4$ can be obtained from HΛ by blowing down a suitable set of degree-1 rational lines, as we will discuss in detail in chapter 7.

Chapter 6

The Mirror Map and Moduli Space

6.1 Periods

The periods of the HV manifold are essential for understanding both the geometry and physics of the Hulek-Verrill manifolds as well as their mirrors. The series expansions of periods about large complex structure points allow for a mirror symmetry computation of the instanton numbers for the manifold HΛ. In this section, we derive series expressions that we utilise to perform this computation in §6.2. Additionally, the periods as functions of the complex structure moduli of HV are instrumental in describing string theory compactifications on HV. We return to this point in part III where flux vacua in type IIB string theory compactified on HV are studied.

Our approach begins with investigating some differential equations satisfied by the fundamental period ϖ^0, which is long known to admit concise descriptions [14, 76]. We find a set of partial differential equations which, together with asymptotic data coming from mirror symmetry considerations, allow us to find all periods within the large complex structure regions of the complex structure moduli space. We go further by using the methods of [76] to study an ordinary differential equation satisfied by the fundamental, and indeed all, periods. This latter equation is used to analytically continue the periods, and with the data obtained from this, it is possible to give expressions for the periods in all regions of the moduli space.

We derive also formulae that express all periods using integrals of products of Bessel functions. To our knowledge, this is the first appearance of such expressions and we anticipate that these also have applications in the study of banana graph amplitudes. For instance, the integral expressions that we use to describe the periods can also be used to express non-equal-mass four-loop banana integrals in the large momentum region of parameter space. Appropriate generalisations of those expressions relevant to higher-dimensional Hulek-Verrill manifolds will perform the same task for higher-loop banana diagrams.

6.1.1 Moduli space

The parameters $\varphi^0, \cdots, \varphi^5$ in the equation (5.2) defining the manifold HV constitute a set of projective coordinates for $\mathbb{P}^5$. The parameters $\varphi^0, \cdots, \varphi^5$ appear symmetrically, which we can use to great effect to describe different regions in the moduli space. A convenient atlas for $\mathbb{P}^5$ is given by the six sets where one of the projective coordinates is nonvanishing. In the following sections, we mostly work in the patch where $\varphi^0 \neq 0$, but the arguments go through in the other five patches *mutatis mutandis*. Accordingly, the Latin subscripts $i, j, k, \ldots$ are always understood to run from 1 to 5, whereas the Greek subscripts $\mu, \nu, \lambda, \ldots$ are taken to run from 0 to 5.

It is not difficult to see that the manifold HΛ is singular on the locus

$$E \;=\; \varphi^0\,\varphi^1\,\varphi^2\,\varphi^3\,\varphi^4\,\varphi^5 \;=\; 0\;. \tag{6.1}$$

We denote the irreducible components in this locus by

$$E_\mu \;=\; \left\{(\varphi^0,\varphi^1,\varphi^2,\varphi^3,\varphi^4,\varphi^5)\in\mathbb{P}^5 \;\middle|\; \varphi^\mu = 0\right\} \tag{6.2}$$

The intersections of 5 of these hypersurfaces turn out to be large complex structure points, or points of maximal unipotent monodromy, as we will verify in §6.2 by computing the monodromies around these hypersurfaces explicitly.

As we have reviewed earlier in §5.3.4, the Hulek-Verrill manifold has conifold singularities on the locus

$$\mathbb{\Delta} \;\stackrel{\text{def}}{=}\; \prod_{\epsilon_i\in\{\pm1\}} \left(\sqrt{\varphi^0} + \epsilon_1\sqrt{\varphi^1} + \epsilon_2\sqrt{\varphi^2} + \epsilon_3\sqrt{\varphi^3} + \epsilon_4\sqrt{\varphi^4} + \epsilon_5\sqrt{\varphi^5}\right) \;=\; 0\;. \tag{6.3}$$

It is often useful to consider the square roots $\sqrt{\varphi^i}$ as coordinates on the moduli space. This of course gives rise to a multiple cover. We can, to start, choose branches for the square roots with $\mathrm{Re}[\sqrt{\varphi^i}] > 0$. The functions that we study are related to those in other branches via monodromy transformations $\varphi^i \mapsto \mathrm{e}^{2\pi\mathrm{i}}\varphi^i$ around the large complex structure point.

In the coordinates $\sqrt{\varphi^i}$ it is convenient to study the vanishing loci of the individual factors in $\mathbb{\Delta}$. Let I be a subset of indices in $\{0,\ldots,5\}$ and I^c be its complement in $\{0,\ldots,5\}$. Then we define the following closed components D_I corresponding to each set I, sketched in figure 6.1:

$$D_I \;=\; \left\{(\varphi^0,\cdots,\varphi^5)\in\mathbb{P}^5 \;\middle|\; \sum_{i\in I}\mathrm{Re}\left[\sqrt{\varphi^i}\,\right] = \sum_{j\in I^c}\mathrm{Re}\left[\sqrt{\varphi^j}\,\right]\right\}. \tag{6.4}$$

6.1.2 The fundamental period

The holomorphic period for $\mathrm{HV}_{(\varphi^0,\ldots,\varphi^5)}$ can be found by integrating the holomorphic three-form over the torus. We briefly review this procedure. It is enough consider the torus, so we can use the

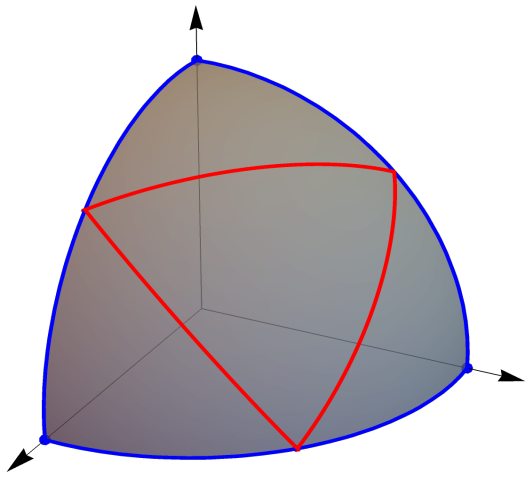


Figure 6.1: *A heuristic sketch of the complex structure moduli space in coordinates $\sqrt{\varphi^\mu}$, with the branch choice of $\sqrt{\varphi^i} > 0$. The grey shell is the moduli space $\mathbb{P}^2$, the red lines represent the irreducible components $D_{\{\mu\}}$ of the discriminant locus $\mathbb{\Delta} = 0$, the blue lines are the loci E_μ, and the blue points are the large complex structure points. The four triangular regions between these lines correspond to the sets $U_{\{\mu\}}$ and $U_{\{0,1\}} \cap U_{\{0,2\}} \cap U_{\{1,2\}}$, which we define in* (6.21).

equation (5.14) defining $\widehat{\mathrm{H}\Lambda}$ in order to obtain this period by the Dwork-Katz-Griffiths method [81].

$$\varpi^{(0);0}(\boldsymbol{\varphi}) \;=\; -\frac{\varphi^0}{(2\pi\mathrm{i})^5}\int\prod_{i=1}^{5}\frac{\mathrm{d}X_i}{X_i}\,\frac{1}{P(\mathbf{X};\boldsymbol{\varphi})} \;=\; -\frac{\varphi^0}{(2\pi\mathrm{i})^5}\int\prod_{i=1}^{5}\frac{\mathrm{d}X_i}{X_i}\left[\sum_{i=1}^{5}\frac{\varphi^i}{X_i}\sum_{j=1}^{5}X_j-\varphi^0\right]^{-1}\,.$$

Near the large complex structure point at $\varphi^1 = \varphi^2 = \cdots = \varphi^5 = 0$, one finds the series expansion

$$\begin{aligned}
\varpi^{(0);0}(\boldsymbol{\varphi}) \;&=\; \sum_{n=0}^{\infty}(\varphi^0)^{-n}\,\frac{1}{(2\pi\mathrm{i})^5}\int\prod_{i=1}^{5}\frac{\mathrm{d}X_i}{X_i}\left(\sum_{i=1}^{5}\frac{\varphi^i}{X_i}\sum_{j=1}^{5}X_j\right)^n \\
&=\; \sum_{n=0}^{\infty}(\varphi^0)^{-n}\sum_{|\boldsymbol{p}|=n}\sum_{|\boldsymbol{q}|=n}\binom{n}{\boldsymbol{p}}\binom{n}{\boldsymbol{q}}\prod_{i=1}^{5}\frac{1}{2\pi\mathrm{i}}\int\frac{\mathrm{d}X_i}{X_i}\,\boldsymbol{X}^{\boldsymbol{p}-\boldsymbol{q}}\,\boldsymbol{\varphi}^{\boldsymbol{q}} \\
&=\; \sum_{n=0}^{\infty}(\varphi^0)^{-n}\sum_{|\boldsymbol{p}|=n}\binom{n}{\boldsymbol{p}}^2\boldsymbol{\varphi}^{\boldsymbol{p}} \\
&\stackrel{\mathrm{def}}{=}\; \sum_{n=0}^{\infty}c_n(\boldsymbol{\varphi})\,(\varphi^0)^{-n}\,.
\end{aligned} \tag{6.5}$$

We will next identify a set of differential operators that annihilate this fundamental period, the expectation being that the other periods should satisfy the same equations. Although this set of equations is demonstrably *not* the full Picard-Fuchs system, we can proceed using the high degree of symmetry and the asymptotics for the periods found from mirror symmetry considerations. In this way, we are able to find expressions for the periods as particular linear combinations of the 32 solutions to this partial Picard-Fuchs system.

6.1.3 The ordinary differential equation obeyed by the fundamental period

Consider the sequence of c_n which gives the coefficients in the series (6.5). In principle, one could use a recurrence relation that c_n satisfies in order to write down an ordinary differential equation — containing derivatives only with respect to φ^0, but whose coefficients are functions of all φ^μ — which is satisfied by the fundamental period. Such recurrence relations were studied by Verrill in [76], wherein a method for determining such a recurrence was given. It was shown that c_n is a holonomic sequence, solving a linear recurrence with polynomial coefficients.

Unfortunately, the fully general case with all φ^i set to indeterminates is not amenable to a computer analysis as the rational functions of the φ^i that appear are prohibitively large. Nonetheless, finding this recurrence for fixed values of φ^i is possible with the methods of [76]. Although this recurrence can be used to obtain a differential equation annihilating ϖ^0, this is not generally of minimal order[1]. We get around this by using the recurrence relation to generate a large number of terms in the series efficiently, and then use these to fix a lower-degree differential equation. One example we will use later is given by the line $(\varphi^0, \ldots, \varphi^5) = (1, \varphi, \varphi/20, \ldots, \varphi/20)$, where the differential operator takes the form

$$\mathcal{L}^{(6)} \;=\; S_6\,\theta^6 + S_5\,\theta^5 + S_4\,\theta^4 + S_3\,\theta^3 + S_2\,\theta^2 + S_1\,\theta + S_0 \;, \tag{6.6}$$

with coefficients polynomials S_n of degree 11.

$$\begin{aligned}
S_6 = {} & -4393216\,\varphi^{11} + 367906816\,\varphi^{10} + 2766668800\,\varphi^9 - 39077007900\,\varphi^8 + 206484873000\,\varphi^7 - 612252422500\,\varphi^6 \\
& + 898848500000\,\varphi^5 - 698473812500\,\varphi^4 + 301613125000\,\varphi^3 - 63023437500\,\varphi^2 + 1968750000\,\varphi + 781250000 \;,
\end{aligned}$$

$$\begin{aligned}
S_5 = {} & -52718592\,\varphi^{11} + 2701502528\,\varphi^{10} + 35940053200\,\varphi^9 - 311032483500\,\varphi^8 + 1552596065500\,\varphi^7 - 3847452445000\,\varphi^6 \\
& + 3932465125000\,\varphi^5 - 1862764937500\,\varphi^4 + 296554687500\,\varphi^3 + 111468750000\,\varphi^2 - 33250000000\,\varphi - 1562500000 \;,
\end{aligned}$$

$$\begin{aligned}
S_4 = {} & -254806528\,\varphi^{11} + 7499038076\,\varphi^{10} + 150742085265\,\varphi^9 - 1014941685775\,\varphi^8 + 5431523295000\,\varphi^7 - 11316503848750\,\varphi^6 \\
& + 9307004090625\,\varphi^5 - 4235035421875\,\varphi^4 + 739773593750\,\varphi^3 + 87307812500\,\varphi^2 + 10281250000\,\varphi + 781250000 \;,
\end{aligned}$$

$$\begin{aligned}
S_3 = {} & -632623104\,\varphi^{11} + 9348961064\,\varphi^{10} + 303965630550\,\varphi^9 - 1813508252350\,\varphi^8 + 10679775875000\,\varphi^7 - 18511281897500\,\varphi^6 \\
& + 13297668268750\,\varphi^5 - 5361295718750\,\varphi^4 + 157421562500\,\varphi^3 + 235818750000\,\varphi^2 - 5250000000\,\varphi \;,
\end{aligned}$$

$$\begin{aligned}
S_2 = {} & -847890688\,\varphi^{11} + 4174802636\,\varphi^{10} + 326073152765\,\varphi^9 - 1845417676975\,\varphi^8 + 11974702116500\,\varphi^7 - 17568183998750\,\varphi^6 \\
& + 11730618440625\,\varphi^5 - 4223423609375\,\varphi^4 - 204717031250\,\varphi^3 + 170156250000\,\varphi^2 - 937500000\,\varphi \;,
\end{aligned}$$

$$\begin{aligned}
S_1 = {} & -579904512\,\varphi^{11} - 1001197360\,\varphi^{10} + 180117501740\,\varphi^9 - 1000845945900\,\varphi^8 + 7134958504500\,\varphi^7 - 9085888402500\,\varphi^6 \\
& + 5823431700000\,\varphi^5 - 1860707500000\,\varphi^4 - 250435000000\,\varphi^3 + 61875000000\,\varphi^2 \;,
\end{aligned}$$

$$\begin{aligned}
S_0 = {} & -158155776\,\varphi^{11} - 992481296\,\varphi^{10} + 40441278660\,\varphi^9 - 224468019900\,\varphi^8 + 1746333878500\,\varphi^7 - 1982812512500\,\varphi^6 \\
& + 1243608875000\,\varphi^5 - 349708500000\,\varphi^4 - 79745000000\,\varphi^3 + 9250000000\,\varphi^2 \;.
\end{aligned}$$

[1] The recurrence provided by this method is of lowest possible order, but without any constraint on the degree of the polynomial coefficients. This leads to extraneous factors in the differential equation provided.

6.1.4 The partial Picard-Fuchs system

We adopt the following notation:

$$\partial_i \;=\; \frac{\partial}{\partial\varphi^i}, \qquad \theta_i \;=\; \varphi^i\partial_i, \qquad \Theta \;=\; \sum_{i=1}^{5}\theta_i \;. \tag{6.7}$$

Note that on a single term $\boldsymbol{\varphi}^{\boldsymbol{p}}\,(\varphi^0)^{-n}$, where $|\boldsymbol{p}| = n$, the action of the operator Θ is the same as that of $-\varphi^0\,\partial_0$. Using this fact, we find that the fundamental period ϖ^0 obeys the following five differential equations:

$$\mathcal{L}_i\varpi^0(\boldsymbol{\varphi}) \;\stackrel{\text{def}}{=}\; \left(\frac{1}{\varphi^0}\,(\Theta+1)^2 - \frac{1}{\varphi^i}\theta_i^2\right)\varpi^0(\boldsymbol{\varphi}) \;=\; 0 \;. \tag{6.8}$$

These equations are, after a change of variables, equivalent to the differential equations (4.8) of [72]. In addition, we have equations obtained by taking differences of the above equations, or by directly inspecting (4.3):

$$\mathcal{L}_{i,j}\varpi^0(\boldsymbol{\varphi}) \;\stackrel{\text{def}}{=}\; \left(\frac{1}{\varphi^i}\theta_i^2 - \frac{1}{\varphi^j}\theta_j^2\right)\varpi^0(\boldsymbol{\varphi}) \;=\; 0 \;. \tag{6.9}$$

These equations (6.9) are manifestly separable, which is suggestive of a route to the other periods.

6.1.5 The Frobenius method

We prove that the fundamental period $\varpi^0(\boldsymbol{\varphi})$ is (up to scale) the sole holomorphic power series solution to (6.8). Make the projective choice $\varphi^0 = 1$, and suppose that the series

$$f(\boldsymbol{\varphi}) \;=\; \sum_{\boldsymbol{p}} f_{\boldsymbol{p}}\,\boldsymbol{\varphi}^{\boldsymbol{p}}$$

solves (6.8). After comparing the powers of φ^i in $\mathcal{L}_1\,f(\boldsymbol{\varphi}) = 0$, we obtain

$$p_1^2\,f_{(p_1,p_2,p_3,p_4,p_5)} \;=\; (p_1+p_2+p_3+p_4+p_5)^2\,f_{(p_1-1,p_2,p_3,p_4,p_5)} \;, \qquad |\boldsymbol{p}| \geq 1. \tag{6.10}$$

There is a similar relation obtained from the other four equations $\mathcal{L}_i\,f(\boldsymbol{\varphi}) = 0$. Together these five relations (6.10) require

$$f_{\boldsymbol{p}} \;=\; \left(\frac{(p_1+p_2+p_3+p_4+p_5)!}{p_1!p_2!p_3!p_4!p_5!}\right)^2\; f_{\boldsymbol{0}} \;. \tag{6.11}$$

While the system of equations $\mathcal{L}_iF = 0$ has a unique holomorphic solution, it is shown below that the system has a solution-space of dimension greater than $\dim\,H^3\,(\mathrm{HV}) = 12$. Therefore it cannot be the entire Picard-Fuchs system, since it is not sufficiently constrained. The solution space can be suitably restricted by the differential equation discussed in §6.1.3, but this is too difficult to write down in full generality. More simply, one can appeal to the method of Frobenius and its relation to (co-)homology discussed in §2.2.2. Equivalently, one can fix the system of 12 periods by imposing boundary conditions consistent with mirror symmetry.

The Frobenius method reveals that there are 32 functions, sums of power series multiplied by logarithms of the φ^i, which solve (6.8). To see this, we set up an indicial equation. With $f_{\boldsymbol{p}}$ from (6.11) and $f_{\mathbf{0}} = 1$, take a solution ansatz

$$\varpi^{\boldsymbol{\epsilon}}(\boldsymbol{\varphi}) \;=\; \sum_{\boldsymbol{p}} \frac{f_{\boldsymbol{p}+\boldsymbol{\epsilon}}}{f_{\boldsymbol{\epsilon}}}\, \boldsymbol{\varphi}^{\boldsymbol{p}+\boldsymbol{\epsilon}}, \tag{6.12}$$

where the $\boldsymbol{\epsilon} = (\epsilon_1, \ldots, \epsilon_5)$ is a five-component multi-index consisting of as-yet undetermined algebra elements, which we refer to here as *Frobenius elements*, and $f_{\boldsymbol{p}+\boldsymbol{\epsilon}}$ is defined by replacing $x!$ by $\Gamma(1+x)$ in (6.11). One can compute

$$\mathcal{L}_i\, \varpi^{\boldsymbol{\epsilon}}(\boldsymbol{\varphi}) \;=\; -\frac{\epsilon_i^2}{\varphi^i}\Big(1 + \mathcal{O}(\mathbf{a})\Big) + \mathcal{O}(\epsilon_i^3)\ . \tag{6.13}$$

The original series solution $\varpi^0(\boldsymbol{\varphi})$ is recovered by taking $\boldsymbol{\epsilon} \to \mathbf{0}$. Additionally, there are new solutions obtained by first differentiating $\varpi^{\boldsymbol{\epsilon}}(\boldsymbol{\varphi})$ once with respect to any number of the ϵ_i and then taking $\boldsymbol{\epsilon} \to \mathbf{0}$. Each such derivative introduces a logarithmic dependence on the φ^i. There are five ϵ_i with respect to which we can differentiate either zero or one times. In total all such choices give us $2^5 = 32$ independent solutions.

The Taylor expansion of $\varpi^{\boldsymbol{\epsilon}}$ in $\boldsymbol{\epsilon}$ is infinite, but only terms not containing the square of an ϵ_i have coefficients that are solutions of (6.8). Introduce the algebraic relation $\epsilon_i^2 = 0$ for the ϵ_i. The Taylor expansion of $\varpi^{\boldsymbol{\epsilon}}$ then truncates, and every coefficient left is a solution to (6.8).

$$\varpi^{\boldsymbol{\epsilon}} = \varpi^0 + \varpi^i\epsilon_i + \frac{1}{2!}\varpi^{ij}\epsilon_i\epsilon_j + \frac{1}{3!}\varpi^{ijk}\epsilon_i\epsilon_j\epsilon_k + \frac{1}{4!}\varpi^{ijkl}\epsilon_i\epsilon_j\epsilon_k\epsilon_l + \frac{1}{5!}\varpi^{ijklm}\epsilon_i\epsilon_j\epsilon_k\epsilon_l\epsilon_m\ . \tag{6.14}$$

In the above implicit sums, the terms with any two indices equal are absent. To obtain the 12 periods among these solutions, we will later in §6.1.8 impose that ϵ_i satisfy the cohomology relations (2.12). Equivalently, we can impose boundary conditions consistent with mirror symmetry.

6.1.6 Separation of variables

Upon expanding the operators θ_i, the differential equations $\mathcal{L}_{i,j}F = 0$ become

$$\left[\partial_i - \partial_j + \varphi^i\partial_i^2 - \varphi^j\partial_j^2\right] F \;=\; 0\ . \tag{6.15}$$

Making a separation-of-variables ansatz $F(\boldsymbol{\varphi}) = \prod_{j=1}^5 G_j(\varphi^j)$ and simplifying $\mathcal{L}_{i,j}F = 0$, one obtains

$$\frac{\partial_i G_i(\varphi^i) + \varphi^i\,\partial_i^2 G_i(\varphi^i)}{G_i(\varphi^i)} \;=\; \frac{\partial_j G_j(\varphi^j) + \varphi^j\,\partial_j^2 G_j(\varphi^j)}{G_j(\varphi^j)}\ .$$

The traditional separation of variables logic can be employed: both sides of this equation respectively depend only on φ^i and φ^j, and so both must be constant. With a certain prescience, we denote this constant by $z^2/4$. Attention should then be turned to the ordinary differential equation that the G_i satisfy:

$$x\,\frac{\mathrm{d}^2}{\mathrm{d}x^2}G(x) + \frac{\mathrm{d}}{\mathrm{d}x}G(x) \;=\; \frac{z^2}{4}G(x).$$

This has the general solution

$$G(x) \;=\; C_1(z)I_0(z\sqrt{x}) + C_2(z)K_0(z\sqrt{x}) \;,$$

where $C_1(z)$ and $C_2(z)$ are arbitrary functions of the parameter z. Therefore, for any choice of the functions $C_1(z)$, $C_2(z)$, the equations $\mathcal{L}_{i,j}F = 0$ for $i, j = 1, \ldots, 5$ have solutions of the form

$$F(\boldsymbol{\varphi}) \;=\; \int \mathrm{d}z\, C(z) \prod_{j=1}^{5} B_j\Big(z\sqrt{\varphi^j}\Big) \;, \tag{6.16}$$

where the five functions B_j are each taken to be modified Bessel functions I_0 or K_0. This brings us closer to the periods, but at this stage of our reasoning, only looking at the system $\mathcal{L}_{i,j}F = 0$, there is still a considerable degree of ignorance as to what the function C should be and which combinations of these solutions we should take to give the periods.

In the regime

$$\mathrm{Re}\left[\sum_{i=1}^{5}\sqrt{\varphi^i}\right] < \mathrm{Re}\left[\sqrt{\varphi^0}\right]$$

the following expression for the fundamental period is valid:

$$\varpi^{(0);0}(\boldsymbol{\varphi}) \;=\; \varphi^0 \int_0^\infty \mathrm{d}z\, z\, K_0\left(\sqrt{\varphi^0}z\right) \prod_{i=1}^{5} I_0\left(\sqrt{\varphi^i}z\right) \;. \tag{6.17}$$

This claim is easy to prove by using the identities listed in appendix B. The identity (6.17) suggests that $C(z)$ should be taken to be $K_0(\sqrt{\varphi^0}z)$. Indeed, by replacing the I_0 functions in the above integral with K_0 functions, we can form 32 functions f that obey the equations $\mathcal{L}_{i,j}\, f = 0$. These 32 functions can be seen to be linearly independent and satisfy the system $\mathcal{L}_i f = 0$, and therefore furnish a basis of series solutions of the system $\mathcal{L}_i f = \mathcal{L}_{i,j} f = 0$. To be sure, the 32 functions obtained in this way have powers series that form a basis for the linear span of the 32 Frobenius solutions given by the construction in §6.1.5.

On symmetry grounds, there will be a role for functions obtained by replacing the K_0 with an I_0 in patches $\varphi^i = 1$ in the moduli space. The reason for this is that, from the global perspective, φ^0 is not distinguished from the φ^i.

6.1.7 Determining closed form expressions for all periods

We have seen that the partial Picard-Fuchs system given by (6.8) and (6.9) should have exactly 32 solutions. Furthermore, we have seen that the integrals of Bessel functions of the form

$$\frac{\varphi^0}{\mathrm{i}\pi} \int_0^\infty \mathrm{d}z\, z\, B_0(\sqrt{\varphi^0}z) \prod_{i=1}^{5} B_i(\sqrt{\varphi^i}z) \tag{6.18}$$

furnish a set of solutions to the partial differential equations (6.8) and (6.9). The $B_\mu(\sqrt{\varphi^\nu}\, z)$ above are understood to be replaced by a conveniently normalised modified Bessel function: either $K_0(\sqrt{\varphi^\mu}\, z)$

or $\mathrm{i}\pi\ I_0(\sqrt{\varphi^\mu}\ z)$. Naïvely it seems that this would give us 64 solutions. However, not all of these converge simultaneously. Indeed, an integral of this form converges in the region of the moduli space where

$$\pm\mathrm{Re}\left[\sqrt{\varphi^0}\right] \pm \mathrm{Re}\left[\sqrt{\varphi^1}\right] \pm \mathrm{Re}\left[\sqrt{\varphi^2}\right] \pm \mathrm{Re}\left[\sqrt{\varphi^3}\right] \pm \mathrm{Re}\left[\sqrt{\varphi^4}\right] \pm \mathrm{Re}\left[\sqrt{\varphi^5}\right] < 0\ . \tag{6.19}$$

The negative sign for $\mathrm{Re}[\sqrt{\varphi^i}]$ is chosen when $B_0(z\sqrt{\varphi^\mu}) = K_0(z\sqrt{\varphi^\mu})$, and the positive sign when $B_0(z\sqrt{\varphi^\mu}) = \mathrm{i}\pi I_0(z\sqrt{\varphi^\mu})$. This follows from demanding that the product of Bessel functions decays exponentially in the limit $z \to \infty$ and recalling the asymptotics of the Bessel functions for large z:

$$K_0(z)\ \sim\ \sqrt{\frac{\pi}{2z}}\,\mathrm{e}^{-z}\ , \qquad \mathrm{i}\pi I_0(z)\ \sim\ \mathrm{i}\sqrt{\frac{\pi}{2z}}\,\mathrm{e}^{z}\ .$$

The boundary between the different regions of convergence is exactly the restriction of the conifold locus $\mathbb{\Delta} = 0$ to the real plane.

On a generic[2] point in the moduli space corresponding to a non-singular manifold, there are exactly 32 convergent integrals of Bessel functions of the form (6.18). This is seen as follows: every curve of the form

$$\mathrm{Re}\left[\sqrt{\varphi^0}\right] \pm \mathrm{Re}\left[\sqrt{\varphi^1}\right] \pm \mathrm{Re}\left[\sqrt{\varphi^2}\right] \pm \mathrm{Re}\left[\sqrt{\varphi^3}\right] \pm \mathrm{Re}\left[\sqrt{\varphi^4}\right] \pm \mathrm{Re}\left[\sqrt{\varphi^5}\right]\ =\ 0 \tag{6.20}$$

divides the space into two regions, those 'above' and 'below'. The curve itself belongs to the discriminant locus. There is exactly one Bessel function integral of the form (6.18) that converges almost everywhere above the curve (6.20) and exactly one converging almost everywhere below the curve. As there are 32 such curves we find exactly 32 convergent integrals at any given point. We can find an almost[3] open covering, where every open subset of the covering corresponds to a different set of Bessel functions.

We can express these covering sets as intersections of suitably defined sets U_I. Let I be a set of indices in $\{0,\ldots,5\}$ and I^c be its complement in $\{0,\ldots,5\}$. Then we define open sets in the moduli space corresponding to each set I:

$$U_I\ =\ \left\{(\varphi^0,\cdots,\varphi^5)\in\mathbb{P}^5\ \middle|\ \sum_{i\in I}\mathrm{Re}\left[\sqrt{\varphi^i}\right] > \sum_{j\in I^c}\mathrm{Re}\left[\sqrt{\varphi^j}\right]\right\}. \tag{6.21}$$

These have the following convenient properties[4]

$$U_I \subset U_J \quad \text{if} \quad J\subset I\subset\{0,\ldots,5\}\ , \qquad\qquad U_I^c\ =\ U_{I^c}\setminus \mathrm{Re}\,\mathbb{\Delta}\ ,$$

where $\mathrm{Re}\,\mathbb{\Delta}$ denotes the space of all points that satisfy any of the equations (6.20).

[2] In addition to the restriction of the discriminant locus to the real plane, the Bessel function integrals also diverge on points whose real parts satisfy the equation (6.20).

[3] The open sets cover the moduli space apart from points which satisfy (6.20).

[4] Recall that we have restricted to the branch $\mathrm{Re}\sqrt{\varphi^\mu} \geq 0$.

In the subset of each patch where they converge, these Bessel function integrals satisfy the partial differential equations (6.9) and (6.8). There are exactly 32 solutions to these equations, so it follows that the periods, which should solve the differential equations, can be expressed in terms of the convergent Bessel function integrals in any patch. In the next subsection we will present an argument to fix the periods as sums of these Bessel integrals in the regions $U_{\{i\}}$ and $U_{\{0\}}$. To find the correct linear combinations of these integrals to give the periods in other regions we study the ordinary differential equations obtained using the techniques of §6.1.3. Choosing the values $\varphi^i = s^i\varphi$, this ODE gives a differential equation that the restrictions of the periods to these lines must satisfy. Given enough lines, we can always find enough equations to completely fix the periods in terms of the Bessel integrals.

To find the relation between the bases of periods in different patches, we analytically continue the Bessel integrals from one region to another. In practice, the easiest way to do this is to numerically integrate the Picard-Fuchs equation along a line crossing multiple regions, and then find the relations between each pair of bases. We have chosen the normalisations of the Bessel function integrals so that these matrices relating different bases are integral. In what follows, we will not need most of these relations, and hence we do not record them here. However, an important special case that we will be using relates the basis of periods near the large complex structure point in the patch $U_{\{0\}}$ to the basis in the patch $U_{\{i\}}$, where there is another large complex structure point.

For instance, we can study the line $(1, \varphi, \frac{\varphi}{20}, \ldots, \frac{\varphi}{20})$ where the periods satisfy the Picard-Fuchs equation $\mathcal{L}^{(6)} f = 0$, with the operator $\mathcal{L}^{(6)}$ given by (6.6). The Bessel function integrals near $\varphi^i = 0$ that satisfy this equation are given by

$$\widehat{\pi}^{(0)} \;=\; \frac{1}{\mathrm{i}\pi}\int_0^\infty \mathrm{d}z\;\frac{z}{\varphi}\;\begin{pmatrix} \mathcal{A}_0\mathcal{B}_1\mathcal{B}^4 \\ \mathcal{B}_0\mathcal{B}_1\mathcal{A}^4 \\ 4\,\mathcal{B}_0\mathcal{A}_1\mathcal{B}\mathcal{A}^3 \\ 6\,\mathcal{B}_0\mathcal{A}_1\mathcal{B}^2\mathcal{A}^2 \\ 12\,\mathcal{B}_0\mathcal{B}_1\mathcal{B}\mathcal{A}^3 + 12\,\mathcal{B}_0\mathcal{A}_1\mathcal{B}^2\mathcal{A}^2 \\ 4\mathcal{B}_0\mathcal{A}_1\mathcal{B}^3\mathcal{A} + 6\mathcal{B}_0\mathcal{B}_1\mathcal{B}^2\mathcal{A}^2 \end{pmatrix},$$

where we have used the following shorthand for the Bessel functions appearing here

$$\mathcal{A}_0 \;=\; \mathrm{i}\pi I_0\left(\varphi^{-1/2}z\right)\;,\quad \mathcal{B}_0 \;=\; K_0\left(\varphi^{-1/2}z\right)\;,\qquad \mathcal{A}_1 \;=\; \mathrm{i}\pi I_0(z)\;,\quad \mathcal{B}_1 \;=\; K_0(z)\;,$$
$$\mathcal{A} \;=\; \mathrm{i}\pi I_0\left(20^{-1/2}z\right)\;,\qquad \mathcal{B} \;=\; K_0\left(20^{-1/2}z\right)\;.$$

On the line, the discriminant locus $\mathbb{\Delta} = 0$ has singularities at five points:

$$\varphi \;\simeq\; 0.2786\;,\quad \varphi \;\simeq\; 0.4775\;,\quad \varphi \;=\; 1\;,\quad \varphi \;\simeq\; 3.2725\;,\quad \text{and}\quad \varphi \;\simeq\; 89.7214\;.$$

The region $|\varphi| > 89.7214$ lies in the region $U_{\{1\}}$, which contains the large complex structure point at $\varphi^0 = \varphi^2 = \varphi^3 = \varphi^4 = \varphi^5 = 0$. By symmetry, we can deduce that the Bessel function integrals giving

a basis of solutions to the Picard-Fuchs equation $\mathcal{L}^{(6)} f = 0$ are

$$\widehat{\pi}^{(1)} \;=\; \frac{1}{\mathrm{i}\pi} \int_0^\infty \mathrm{d}z \; \frac{z}{\varphi} \; \begin{pmatrix} \mathcal{B}_1 \mathcal{A}_0 \mathcal{A}^4 \\ \mathcal{B}_1 \mathcal{B}_0 \mathcal{A}^4 \\ 4\,\mathcal{B}_1 \mathcal{A}_0 \mathcal{B} \mathcal{A}^3 \\ 6\,\mathcal{B}_1 \mathcal{A}_0 \mathcal{B}^2 \mathcal{A}^2 \\ 12\,\mathcal{B}_1 \mathcal{B}_0 \mathcal{B} \mathcal{A}^3 + 12\,\mathcal{B}_1 \mathcal{A}_0 \mathcal{B}^2 \mathcal{A}^2 \\ 4 \mathcal{B}_1 \mathcal{A}_0 \mathcal{B}^3 \mathcal{A} + 6 \mathcal{B}_1 \mathcal{B}_0 \mathcal{B}^2 \mathcal{A}^2 \end{pmatrix} .$$

Given the operator $\mathcal{L}^{(6)}$ it is easy to check that these integrals indeed satisfy the equation.

By integrating the Picard-Fuchs operator $\mathcal{L}^{(6)}$ numerically, we can find the continuation of the period vector $\widehat{\pi}^{(0)}$ to the region $|\varphi| > 89.7214$, giving the following relation between the vectors $\widehat{\pi}^{(0)}$ and $\widehat{\pi}^{(1)}$:

$$\widehat{\pi}^{(0)} \;=\; \widehat{\mathrm{T}}\, \widehat{\pi}^{(1)} \;, \qquad \text{with} \qquad \widehat{\mathrm{T}} \;=\; \begin{pmatrix} -1 & 0 & 0 & 0 & 0 & 0 \\ 0 & 1 & 0 & 0 & 0 & 0 \\ -4 & -4 & -1 & 0 & 0 & 0 \\ -6 & -6 & -3 & 1 & -1 & 0 \\ -12 & -12 & -6 & 0 & -1 & 0 \\ -4 & -4 & -3 & 0 & -1 & -1 \end{pmatrix} . \tag{6.22}$$

We have written the Bessel function integrals in $\widehat{\pi}^0$ and $\widehat{\pi}^1$ in this particular way because these are the natural restrictions of the 12 periods to the line $(\varphi^0, \ldots, \varphi^5) \;=\; (1, \varphi, \frac{\varphi}{20}, \ldots, \frac{\varphi}{20})$. The generic 12-component period vectors are given by

$$\pi^{(0)} \;=\; \frac{\varphi^0}{\mathrm{i}\pi} \int_0^\infty \mathrm{d}z \, z \; \left(\pi^{(0);0}, \pi^{(0);1}, \ldots, \pi^{(0);5}, \pi_1^{(0)}, \ldots, \pi_5^{(0)}, \pi_0^{(0)} \right)^T \;, \tag{6.23}$$

in which

$$\begin{aligned} \pi^{(0);0} \;&=\; \mathcal{B}_0 \mathcal{A}_1 \mathcal{A}_2 \mathcal{A}_3 \mathcal{A}_4 \mathcal{A}_5 \;, & \pi^{(0);i} \;&=\; \mathcal{B}_0 \mathcal{B}_i \prod_{j \neq i} \mathcal{A}_j \;, \\ \pi_i^{(0)} \;&=\; \sum_{\substack{m<n \\ m,n \neq i}} \mathcal{B}_0 \mathcal{B}_m \mathcal{B}_n \prod_{j \neq m,n} \mathcal{A}_j \;, & \pi_0^{(0)} \;&=\; \sum_{l<m<n} \mathcal{B}_0 \mathcal{B}_l \mathcal{B}_m \mathcal{B}_n \prod_{j \neq l,m,n} \mathcal{A}_j \;, \\ \mathcal{A}_\mu \;&=\; \mathrm{i}\pi \; I_0 \left(\sqrt{\varphi^\mu} \; z \right) \;, & \mathcal{B}_\mu \;&=\; K_0 \left(\sqrt{\varphi^\mu} \; z \right) \;. \end{aligned}$$

The vector $\pi^{(1)}$ is given by interchanging the indices 0 and 1. In terms of these quantities, restricted to the line, we have a natural way of writing the relations (6.22) in a symmetric form. For example, the relation corresponding to the third row of the matrix can be written as

$$\pi^{(0);2} + \pi^{(0);3} + \pi^{(0);4} + \pi^{(0);5} \;=\; -4\pi^{(1);0} - 4\pi^{(1);1} - \pi^{(1);2} - \pi^{(1);3} - \pi^{(1);4} - \pi^{(1);5} \;.$$

The coordinates φ^2, φ^3, φ^4, and φ^5 must appear symmetrically in all of these relations. Thus we are able to guess that the relations in the case where all of the coordinates are unequal are

$$\pi^{(0);j} \;=\; -\pi^{(1);0} - \pi^{(1);1} - \pi^{(1);j} \;.$$

We can verify this expectation by studying the line $(\varphi^0, \ldots, \varphi^5) = (1, \varphi, \frac{\varphi}{50}, \frac{\varphi}{100}, \ldots, \frac{\varphi}{100})$, which singles out the period $\pi^{(0);2}$, and allows us to verify the above relation in the case $j = 2$. The other relations

then follow by symmetry. Working in this way, we find that in general the period vectors $\pi^{(0)}$ and $\pi^{(1)}$ are related by

$$\pi^{(0)} \;=\; \mathrm{T}_{\pi^{(0)}\pi^{(1)}}\pi^{(1)}\;, \qquad \text{with} \qquad \mathrm{T}_{\pi^{(0)}\pi^{(1)}} \;=\; \begin{pmatrix} -1 & 0 & 0 & 0 & 0 & 0 & 0 & 0 & 0 & 0 & 0 & 0 \\ 0 & 1 & 0 & 0 & 0 & 0 & 0 & 0 & 0 & 0 & 0 & 0 \\ 1 & -1 & -1 & 0 & 0 & 0 & 0 & 0 & 0 & 0 & 0 & 0 \\ 1 & -1 & 0 & -1 & 0 & 0 & 0 & 0 & 0 & 0 & 0 & 0 \\ 1 & -1 & 0 & 0 & -1 & 0 & 0 & 0 & 0 & 0 & 0 & 0 \\ 1 & -1 & 0 & 0 & 0 & -1 & 0 & 0 & 0 & 0 & 0 & 0 \\ -6 & 6 & 3 & 3 & 3 & 3 & 1 & -1 & -1 & -1 & -1 & 0 \\ -3 & 3 & 0 & 2 & 2 & 2 & 0 & -1 & 0 & 0 & 0 & 0 \\ -3 & 3 & 2 & 0 & 2 & 2 & 0 & 0 & -1 & 0 & 0 & 0 \\ -3 & 3 & 2 & 2 & 0 & 2 & 0 & 0 & 0 & -1 & 0 & 0 \\ -3 & 3 & 2 & 2 & 2 & 0 & 0 & 0 & 0 & 0 & -1 & 0 \\ 4 & -4 & -3 & -3 & -3 & -3 & 0 & 1 & 1 & 1 & 1 & -1 \end{pmatrix} . \tag{6.24}$$

6.1.8 The Frobenius elements as cohomology

As reviewed in §2.2.2, the Frobenius elements ϵ_i have an interpretation in the (co-)homology of the mirror manifold HΛ [27, 28]. These relations are instructive in the present case, so we work through them here. The Frobenius elements ϵ_i are taken to satisfy the (co-)homology relations

$$\epsilon_i\epsilon_j \;=\; \epsilon_j\epsilon_i\;, \qquad \epsilon_i^2 \;=\; 0\;, \qquad \epsilon_i\epsilon_j\epsilon_k \;=\; Y_{ijk}\eta\;, \qquad \eta\,\epsilon_i \;=\; 0\;. \tag{6.25}$$

The elements ϵ_i can be understood as cohomology two-forms, or as their duals, which are four-surfaces. If we think of ϵ_i as four-surfaces, then the products corresponds to intersections, the Y_{ijk} are the intersection numbers, and η is a point. If we think of ϵ_i as two-forms, the products correspond to the wedge product, and η is the volume form. As surfaces, the intersection $\epsilon_i\epsilon_j$ is a curve. These are not all independent, since we know that $b^2(\mathrm{H}\Lambda) = 5$. We can choose a basis μ^j to be dual to the ϵ_i so that we have the relations

$$\epsilon_i\mu^j \;=\; \delta_i^j\eta\;, \qquad \epsilon_i\epsilon_j \;=\; Y_{ijk}\mu^k\;. \tag{6.26}$$

The form of the second relation is dictated by the intersection relation in (6.25). Now the Frobenius period is

$$\varpi \;=\; \varpi^0 + \varpi^i\,\epsilon_i + \varpi_i\,\mu^i + \varpi_0\,\eta\;. \tag{6.27}$$

Comparing with (6.14), we obtain expressions for ϖ^i, ϖ_i, and ϖ_0. The ϵ_i have also explicit representations as 12×12 matrices, which follow from the monodromy matrices given in (6.49)

$$\mathrm{M}_{E_j} \;=\; \mathrm{I}_{12} + 2\pi\mathrm{i}\,\epsilon_j\;,$$

with I_{12} the identity matrix. It is a pleasure to check the algebra above for these matrices.

6.1.9 The periods near large complex structure points

The set $U_{\{0\}}$ is a neighbourhood of the large complex structure point at $E_1\cap\cdots\cap E_5$, and the $U_{\{i\}}$ are neighbourhoods of other large complex structure points. In the region $U_{\{0\}}$, according to the discussion above, the convergent integrals are of the form.

$$\frac{\varphi^0}{\mathrm{i}\pi}\int_0^\infty \mathrm{d}z\,z\,K_0\Big(\sqrt{\varphi^0}z\Big)\prod_{i=1}^5 B_i\Big(\sqrt{\varphi^i}z\Big)\;. \tag{6.28}$$

A basis for the periods can be given as 12 linear combinations of these functions. To fix the precise combinations, we compare the equation (6.27) with the result of applying the relations (6.26) to the expansion (6.14). It is a matter of direct comparison to express the coefficients of the ϵ-series (6.27) in terms of Bessel integrals. The relation between the periods in the Bessel integral basis $\pi^{(\mu)}$ and the periods in the Frobenius basis $\varpi^{(\mu)}$ is

$$\varpi^{(\mu)} \;=\; \mathrm{T}_{\varpi\pi}\pi^{(\mu)}, \qquad \text{with} \qquad \mathrm{T}_{\varpi\pi} \;=\; \begin{pmatrix} \frac{1}{\pi^4} & \mathbf{0}^T & \mathbf{0}^T & 0 \\ \mathbf{0} & -\frac{2\mathrm{i}}{\pi^3}\mathbb{I} & \mathbb{0} & \mathbf{0} \\ -\frac{4}{\pi^2}\mathbf{1} & \mathbb{0} & -\frac{8}{\pi^2}\mathbb{I} & \mathbf{0} \\ 80\frac{\zeta(3)}{\pi^4} & \frac{8\mathrm{i}}{\pi}\mathbf{1}^T & \mathbf{0}^T & \frac{16\mathrm{i}}{\pi} \end{pmatrix}. \tag{6.29}$$

Explicitly, this means that the single-logarithm periods near the large complex structure point at $\varphi^1 = \cdots = \varphi^5 = 0$ are given by

$$\varpi^{(0);j}(\boldsymbol{\varphi}) \;=\; -2\varphi^0 \int \mathrm{d}z\, z\, K_0\Big(\sqrt{\varphi^0}z\Big) K_0\Big(\sqrt{\varphi^j}z\Big) \prod_{i\neq j} I_0\Big(\sqrt{\varphi^i}z\Big)\ . \tag{6.30}$$

For the double-logarithm periods, we have

$$\varpi_j^{(0)}(\boldsymbol{\varphi}) \;=\; 8\varphi^0 \int \mathrm{d}z\, z \sum_{\substack{m<n \\ m,n\neq j}} K_0\Big(\sqrt{\varphi^0}z\Big) K_0\Big(\sqrt{\varphi^m}z\Big) K_0\Big(\sqrt{\varphi^n}z\Big) \prod_{i\neq m,n} I_0\Big(\sqrt{\varphi^i}z\Big) - 4\pi^2\varpi^{(0)}(\boldsymbol{\varphi})\ .$$

The period that is cubic in logarithms is

$$\begin{aligned} \varpi_0^{(0)}(\boldsymbol{\varphi}) \;=\; -16 \sum_{l<m<n} \varphi^0 \int \mathrm{d}z\, z\, K_0\Big(\sqrt{\varphi^0}z\Big) K_0\Big(\sqrt{\varphi^l}z\Big) K_0\Big(\sqrt{\varphi^m}z\Big) K_0\Big(\sqrt{\varphi^n}z\Big) \prod_{i\neq l,m,n} I_0\Big(\sqrt{\varphi^i}z\Big) \\ - 4\pi^2 \sum_{k=1}^{5} \varpi^{(0);k}(\boldsymbol{\varphi}) + 80\zeta(3)\, \varpi^{(0);0}(\boldsymbol{\varphi})\ . \end{aligned} \tag{6.31}$$

Series expansions

We collect some expressions below that are used to express the periods as series. Denote by $H_n^{(r)}$ the n^{th} harmonic number of order r:

$$H_n^{(r)} \;=\; \sum_{k=1}^{n} \frac{1}{k^r}\ , \qquad H_n \;=\; H_n^{(1)}\ .$$

We shall express the periods using the following intermediate series:

$$h_i^{(0)}(\boldsymbol{\varphi}) = \sum_{n=0}^{\infty} \sum_{|\boldsymbol{p}|=n} 2\left(H_n - H_{p_i}\right) \binom{n}{\boldsymbol{p}}^2 \boldsymbol{\varphi}^{\boldsymbol{p}}\, (\varphi^0)^{-n}\ ,$$

$$h_{ij}^{(0)}(\boldsymbol{\varphi}) = \sum_{n=0}^{\infty} \sum_{|\boldsymbol{p}|=n} \Big[4\left(H_n - H_{p_i}\right)\left(H_n - H_{p_j}\right) - 2H_n^{(2)}\Big] \binom{n}{\boldsymbol{p}}^2 \boldsymbol{\varphi}^{\boldsymbol{p}}\, (\varphi^0)^{-n}\ ,$$

$$\begin{aligned} h_{ijk}^{(0)}(\boldsymbol{\varphi}) = \sum_{n=0}^{\infty} \sum_{|\boldsymbol{p}|=n} \Big[8\left(H_n - H_{p_i}\right)\left(H_n - H_{p_j}\right)\left(H_n - H_{p_k}\right) - 4\left(3H_n - H_{p_i} - H_{p_j} - H_{p_k}\right) H_n^{(2)} \\ + 4H_n^{(3)}\Big] \binom{n}{\boldsymbol{p}}^2 \boldsymbol{\varphi}^{\boldsymbol{p}}\, (\varphi^0)^{-n}\ . \end{aligned}$$

The periods (6.30)-(6.31) can be expressed near the point $\varphi^i = 0$ in terms of the above series and logarithms. These results can be derived by considering the Frobenius expansion (6.14), or using the relations in appendix B.

$$\begin{aligned}
\varpi^{(0);j}(\boldsymbol{\varphi}) &= \varpi^{(0);0}(\boldsymbol{\varphi}) \log \frac{\varphi^j}{\varphi^0} + h_j^{(0)}(\boldsymbol{\varphi}) \ , \\
\varpi_j^{(0)}(\boldsymbol{\varphi}) &= 2 \sum_{\substack{m<n \\ m,n\neq j}} \left[\varpi^{(0);0}(\boldsymbol{\varphi}) \log \frac{\varphi^m}{\varphi^0} \ \log \frac{\varphi^n}{\varphi^0} + h_n^{(0)}(\boldsymbol{\varphi}) \log \frac{\varphi^m}{\varphi^0} + h_m^{(0)}(\boldsymbol{\varphi}) \log \frac{\varphi^n}{\varphi^0} + h_{mn}^{(0)}(\boldsymbol{\varphi}) \right] \ , \\
\varpi_0^{(0)}(\boldsymbol{\varphi}) &= 2 \sum_{l<m<n} \Big[\varpi^{(0);0}(\boldsymbol{\varphi}) \log \frac{\varphi^l}{\varphi^0} \ \log \frac{\varphi^m}{\varphi^0} \ \log \frac{\varphi^n}{\varphi^0} \\
&\quad + h_n^{(0)}(\boldsymbol{\varphi}) \log \frac{\varphi^l}{\varphi^0} \ \log \frac{\varphi^m}{\varphi^0} + h_l^{(0)}(\boldsymbol{\varphi}) \log \frac{\varphi^m}{\varphi^0} \ \log \frac{\varphi^n}{\varphi^0} + h_m^{(0)}(\boldsymbol{\varphi}) \log \frac{\varphi^n}{\varphi^0} \ \log \frac{\varphi^l}{\varphi^0} \\
&\quad + h_{mn}^{(0)}(\boldsymbol{\varphi}) \log \frac{\varphi^l}{\varphi^0} + h_{lm}^{(0)}(\boldsymbol{\varphi}) \log \frac{\varphi^n}{\varphi^0} + h_{nl}^{(0)}(\boldsymbol{\varphi}) \log \frac{\varphi^m}{\varphi^0} + h_{lmn}^{(0)}(\boldsymbol{\varphi}) \Big] \ .
\end{aligned} \tag{6.32}$$

6.2 Mirror map and instanton numbers

To determine the mirror map, we recall that near the large complex structure limit the period vector takes the form (2.4) with the prepotential given by

$$\mathcal{F}(z^0, \ldots, z^5) = -\frac{1}{3!} \sum_{a,b,c=0}^{5} Y_{abc} \frac{z^a z^b z^c}{z^0} + (z^0)^2 \sum_{\boldsymbol{p}\neq \boldsymbol{0}} n_{\mathfrak{p}} \, \mathrm{Li}_3(\boldsymbol{q}^{\boldsymbol{p}}) \ , \qquad q_i \stackrel{\mathrm{def}}{=} \exp(2\pi \mathrm{i}\, t^i).$$

The Y_{abc} are given by topological quantities as in (2.9).

To find the triple intersection numbers Y_{ijk}, we first note that $\mathrm{e}_i \wedge \mathrm{e}_i = 0$ for every i. Therefore the only non-vanishing triple intersection numbers are those with all indices different. To find these numbers, we recall that e_i is dual to a hypersurface $\{Y_i - y_i = 0\} \subset \mathrm{H}\Lambda$, where y_i is a constant. The intersection of two of these hyperplanes gives an elliptic curve, which in turn intersects a third hyperplane generically in two points. Therefore the Y_{ijk} are given by

$$Y_{ijk} \ = \ \int_{\mathrm{H}\Lambda} \mathrm{e}_i \wedge \mathrm{e}_j \wedge \mathrm{e}_k \ = \ \begin{cases} 2 \ , & i,\, j,\, k \ \text{ distinct}, \\ 0 & \text{otherwise} \end{cases} \tag{6.33}$$

For the quantities Y_{i00}, we need to compute the second Chern class of $\mathrm{H}\Lambda$. A simple application of the adjunction formula gives the total Chern class as

$$c(\mathrm{H}\Lambda) \ = \ \frac{\prod_{r=1}^5 (1+\mathrm{e}_r)^2}{(1+\sum_{r=1}^5 \mathrm{e}_r)^2} \ .$$

From this we can verify the Calabi-Yau condition $c_1(\mathrm{H}\Lambda) = 0$, and find that the second Chern class $c_2(\mathrm{H}\Lambda)$ can be written as

$$c_2(\mathrm{H}\Lambda) \ = \ 2 \sum_{r<s} \mathrm{e}_s \wedge \mathrm{e}_r \ .$$

Integrating this against e_i using the integral computed in (6.33) gives

$$Y_{i00} \;=\; -\frac{1}{12}\int_{\mathrm{H}\Lambda} c_2(\mathrm{H}\Lambda)\wedge \mathrm{e}_i = -2\ .$$

Naïvely, the numbers Y_{ij0} would equal $\int_{\mathrm{H}\Lambda} c_1(\mathrm{H}\Lambda)\wedge \mathrm{e}_i\wedge \mathrm{e}_j$ and thus vanish. This argument is not correct, and in fact Y_{ij0} can in some cases take the value $1/2$. Based on the gamma class [82], it is expected that in the one-parameter case one can have $Y_{110}=0$ exactly when Y_{111} is even. On the quotient $\mathrm{H}\Lambda/\mathbb{Z}_5$ the triple intersection number Y_{111} is 24, so $Y_{110}=0$. The five-parameter prepotential is related to the prepotential for one-parameter manifolds essentially by setting $t^1=\cdots=t^5=t$ and dividing by 5. Thus we concretely deduce that the quantities Y_{ij0} do in fact vanish.

$$Y_{ij0} \;=\; 0\ .$$

As we know the Hodge numbers $h^{11}=5$ and $h^{12}=45$ of $\mathrm{H}\Lambda$, the Euler characteristic is immediately given by the formula $\chi(\mathrm{H}\Lambda)=2(h^{11}-h^{12})=-80$. Thus the last quantity Y_{000} is given by

$$Y_{000} \;=\; 240\frac{\zeta(3)}{(2\pi\mathrm{i})^3}\ .$$

Note that as a consequence of the highly symmetric nature of the manifold $\mathrm{H}\Lambda$, none of the couplings depend on the particular values of the indices i,j,k, apart from the fact that they need to be distinct for the triple intersection numbers to be non-vanishing. It is then convenient to write the non-vanishing quantities Y_{abc} as

$$Y_{ijk} \;\stackrel{\text{def}}{=}\; Y\ , \qquad\qquad Y_{i00} \;\stackrel{\text{def}}{=}\; Y_{00}\ .$$

As mentioned earlier, the large complex structure points are located on loci where all but one of the parameters φ^i vanish. For concreteness, we are going to concentrate on the large complex structure point at $\varphi^1=\cdots=\varphi^5=0$ in the affine patch $\varphi^0=1$. We denote the integral period vector in this patch by $\Pi^{(0)}$. The other cases are related to this one by the permutation symmetry.

As usual, we identify the affine coordinates t^i of the Kähler moduli space with the periods ϖ by

$$t^i \;=\; \frac{1}{2\pi\mathrm{i}}\frac{\varpi^i}{\varpi^0} \;\sim\; \frac{1}{2\pi\mathrm{i}}\log\varphi^i + \mathcal{O}(\boldsymbol{\varphi})\ .$$

The last expression gives the asymptotic form in the limit $\varphi^1,\ldots,\varphi^5\to 0$, and $\mathcal{O}(\boldsymbol{\varphi})$ denotes terms that are of order 1 or higher in any φ^i. Inverting this map order-by-order one finds the coordinates φ^i in terms of t^i. It is useful to write the resulting map in terms of the elementary symmetric

polynomials[5] $\sigma_i(\boldsymbol{q})$:

$$\begin{aligned}\varphi^i \;=\; & q_i\Big[1-\big(2\sigma_1+2q_i\big)+\Big(\sigma_1^2{+}2\sigma_2{-}2\sigma_1 q_i{+}q_i^2\Big)-\Big(2\sigma_1\sigma_2{+}14\sigma_3{-}\big(16\sigma_2{+}2\sigma_1^2\big)\,q_i{+}10\sigma_1 q_i^2{-}12q_i^3\Big)\\ & +\Big(\sigma_2^2{+}26\sigma_1\sigma_3{-}174\sigma_4+\big(2\sigma_1^3{-}22\sigma_2\sigma_1{+}130\sigma_3\big)\,q_i+\big(18\sigma_1^2{-}136\sigma_2\big)\,q_i^2+116\sigma_1 q_i^3-136q_i^4\Big)\\ & +\Big(-12\sigma_3\sigma_1^2{+}192\sigma_4\sigma_1{-}28\sigma_2\sigma_3+\big(4\sigma_2\sigma_1^2{-}132\sigma_3\sigma_1{+}28\sigma_2^2{-}1376\sigma_4\big)\,q_i\\ & +\big(-10\sigma_1^3{+}122\sigma_2\sigma_1{+}1346\sigma_3\big)\,q_i^2+\big(-128\sigma_1^2{-}1328\sigma_2\big)\,q_i^3+1488\sigma_1 q_i^4-1350q_i^5\Big)\Big]+\mathcal{O}(\boldsymbol{q})^7\end{aligned}$$

As in (2.16), by requiring that the asymptotic forms match[6], we find that the period vectors must be related by

$$\Pi^{(0)} \;=\; \mathrm{T}_{\Pi^{(0)}\varpi^{(0)}}\varpi^{(0)} \;=\; \rho\nu^{-1}\varpi^{(0)}, \tag{6.34}$$

with matrices

$$\rho=\begin{pmatrix} -\frac{1}{3}Y_{000} & \mathbf{1}^T & \mathbf{0}^T & 2\\ \mathbf{1} & \mathbb{0} & -\frac{1}{2}\mathbb{I} & \mathbf{0}\\ 1 & \mathbf{0}^T & \mathbf{0}^T & 0\\ \mathbf{0} & \mathbb{I} & \mathbb{0} & \mathbf{0}\end{pmatrix} \qquad \text{and} \qquad \nu \;=\; \mathrm{diag}(1,(2\pi\mathrm{i})\mathbf{1},(2\pi\mathrm{i})^2\mathbf{1},(2\pi\mathrm{i})^3)\ .$$

6.2.1 Yukawa couplings and instanton numbers

To find the instanton numbers, we compute the Yukawa couplings

$$y_{IJK} \;=-\int_{\mathrm{H}\Lambda}\Omega\wedge\frac{\partial^3\,\Omega}{\partial\varphi^I\partial\varphi^J\partial\varphi^K}\ ,$$

where the indices I,J,K run from 1 to 5. The couplings can be computed using the relation between forms on the manifold $\mathrm{H}\Lambda$ and the ring of defining polynomials modulo the Jacobian ideal [83]. Alternatively, one can find the y_{ijk} as a series in $\boldsymbol{q}$ by a direct computation. As we are mostly interested in finding the instanton numbers, the latter method is sufficient. We express the Yukawa couplings in terms of the period vectors as

$$y_{IJK} \;=\; -(\Pi^{(0)})^T\Sigma\,\partial_{IJK}\Pi^{(0)} \;=\; -(\varpi^{(0)})^T\,\nu^{-1}\,\rho^T\Sigma\rho\,\nu\,\partial_{IJK}\varpi^{(0)}\ .$$

Using the period formulae, we compute y_{IJK} to order 20 in the variables φ^i. It is expected that the Yukawa couplings are rational functions of the moduli a. A natural first guess for the denominator is the discriminant $\mathbb{\Delta}$ as given in (6.3), which is a polynomial of order 16. In fact, we find that

$$y_{IJK}=\frac{P_{IJK}}{\varphi^I\varphi^J\varphi^K\mathbb{\Delta}}\ , \tag{6.35}$$

where the P_{IJK} are degree-14 polynomials in the moduli. Fully expanded, P_{123} is a sum of 11628 monomials while P_{111} and P_{112} each have 8568. Given this large size, and the fact that we have no

[5]Due to the identity $q_1^5-q_1^4\sigma_1+q_1^3\sigma_2-q_1^2\sigma_3+q_1\sigma_4-\sigma_5=0$, this expression is not unique. Unique expressions are obtained, for example, by using this identity to eliminate occurrences of σ_5, or explicit appearances of powers of q_1 higher than four.

[6]Note that we have identified $z^0=\varpi^{(0);0}$, which has asymptotics $1+O(\boldsymbol{\varphi})$.

essential need of them in what follows, we omit their display. Simpler expressions can be arrived at by exploiting symmetries. For example, P_{111} is symmetric in φ^2, φ^3, φ^4, φ^5. This allows one to write P_{111} as a degree-4 polynomial in φ^1 with coefficients that are polynomials in the five elementary symmetric polynomials in the five φ^i. The resulting expression contains 730 monomials when fully expanded. Further simplification is obtained by reintroducing the sixth variable φ^0. This reduces P_{111} to an expression comprising of 212 monomials. Similar simplifications are possible for P_{112} and P_{123}.

We then express the Yukawa coupling in terms of the quantities q_i. The y_{ijk} above is computed in the gauge $z^0 = \varpi^{(0);0}$. To be able to compare this to the expression (6.37) we need to transform to the gauge $z^0 = 1$ in addition to the tensor transformation:

$$y_{ijk} \;=\; \frac{(2\pi\mathrm{i})^3}{(\varpi^{(0);0})^2}\, q_i q_j q_k \sum_{I,J,K} \frac{\partial\varphi^I}{\partial q_i}\frac{\partial\varphi^J}{\partial q_j}\frac{\partial\varphi^K}{\partial q_k}\; y_{IJK}\;. \tag{6.36}$$

Due to the symmetries, there are only three independent Yukawa couplings, up to a permutation of coordinates. For the purposes of finding the instanton numbers, we need only one of these, say y_{111}, this being somewhat simpler to compute. Expressing it as series in $\boldsymbol{q}$, we find

$$\begin{aligned} y_{111} \;=\; 24q_1\Big[1 + \sigma_1 + \frac{1}{3}\left(-14q_1\sigma_1 + 17q_1^2 + 14\sigma_2\right) + \left(-36q_1^3 + 37q_1^2\sigma_1 - 38q_1\sigma_2 + \sigma_1\sigma_2 + 43\sigma_3\right) \\ + \left(-36q_1^3\sigma_1 + 37q_1^2\sigma_1^2 - 2q_1\left(19\sigma_1\sigma_2 + 3\sigma_3\right) + \sigma_2^2 + 44\sigma_1\sigma_3 + 306\sigma_4 + \frac{312\sigma_5}{q_1}\right) + \mathcal{O}(\boldsymbol{q}^5)\Big]\;. \end{aligned}$$

Similar expressions hold for y_{112} and y_{123}. The series expansions for the Yukawa couplings can be written in terms of the instanton numbers as

$$y_{ijk} \;=\; Y_{ijk} + \sum_{\boldsymbol{p}} p_i p_j p_k\, n_{\boldsymbol{p}}\, \frac{\boldsymbol{q}^{\boldsymbol{p}}}{1-\boldsymbol{q}^{\boldsymbol{p}}}\;. \tag{6.37}$$

By comparing this to the series expansion (6.36), which we are able to compute to order 29 in q_i, we can identify the instanton numbers up to degree 29 as listed in table C.1. The first few instanton numbers are listed in 6.1.

6.2.2 Genus-1 instanton numbers

It is possible [84] to define a genus-1 prepotential, which effectively counts the genus-1 curves. In the topological limit it can be expressed as

$$F_1 \;=\; \log\left[\left(\frac{1}{\varpi^{(0);0}}\right)^{3+h^{11}(\mathrm{H}\Lambda)-\chi(\mathrm{H}\Lambda)/12} \det\left(\frac{\partial\boldsymbol{\varphi}}{\partial\boldsymbol{t}}\right) f\right] + \text{const.}\;,$$

where f is a holomorphic function which can be fixed by imposing appropriate boundary conditions. In particular, the prepotential F_1 must be regular at the points inside the Kähler moduli space corresponding to nonsingular manifolds. In the large complex structure limit, F_1 has an expansion [96]

$$F_1 \;=\; 2\pi\mathrm{i}\sum_{i=1}^{5} Y_{i00}t^i - 2\sum_{\boldsymbol{p}}\left(d_{\boldsymbol{p}} + \frac{1}{12}n_{\boldsymbol{p}}\right)\mathrm{Li}_1\left(\boldsymbol{q}^{\boldsymbol{p}}\right) + \text{const.} \tag{6.38}$$

where $d_{\boldsymbol{p}}$ are the genus-1 instanton numbers.

To get the correct growth in the large complex structure limit, f must contain a factor of $\prod_{i=1}^{5}(\varphi^i)^{-3}$. Outside the loci $\varphi^\mu = 0$, we require that F_1 is singular only on the discriminant locus (6.3).

Up to an overall constant, these considerations fix the form of the holomorphic ambiguity f as

$$f = \mathbb{\Delta}^c \prod_{i=1}^{5}(\varphi^i)^{-3} \ .$$

In the one-parameter cases, where the singularities appear as points φ_* in the moduli space, conifold singularities produce a factor of $(\varphi - \varphi_*)^{-1/6}$. We assume that a straightforward generalisation of this holds in the multiparameter case, and thus we take $c = -\frac{1}{6}$. With this choice we find the genus-1 instanton numbers up to degree 29, given in table C.1.

$\boldsymbol{p}$	$n_{\boldsymbol{p}}$	$d_{\boldsymbol{p}}$	$\boldsymbol{p}$	$n_{\boldsymbol{p}}$	$d_{\boldsymbol{p}}$
(1, 0, 0, 0, 0)	24	0	(1, 1, 0, 0, 0)	24	0
(1, 1, 1, 0, 0)	112	0	(2, 1, 1, 0, 0)	24	0
(1, 1, 1, 1, 0)	1104	0	(2, 2, 1, 0, 0)	24	0
(2, 1, 1, 1, 0)	1104	0	(1, 1, 1, 1, 1)	19200	0
(3, 1, 1, 1, 0)	112	0	(2, 2, 2, 0, 0)	80	4
(2, 2, 1, 1, 0)	2800	0	(2, 1, 1, 1, 1)	45408	0
(3, 2, 2, 0, 0)	24	0	(3, 2, 1, 1, 0)	1104	0
(3, 1, 1, 1, 1)	19200	0	(2, 2, 2, 1, 0)	14496	-48
(2, 2, 1, 1, 1)	212880	0	(4, 2, 1, 1, 0)	24	0
(4, 1, 1, 1, 1)	1104	0	(3, 3, 2, 0, 0)	24	0
(3, 3, 1, 1, 0)	1104	0	(3, 2, 2, 1, 0)	14496	-48
(3, 2, 1, 1, 1)	212880	0	(2, 2, 2, 2, 0)	122352	-2292
(2, 2, 2, 1, 1)	1691856	528	(4, 3, 1, 1, 0)	112	0
(4, 2, 2, 1, 0)	2800	0	(4, 2, 1, 1, 1)	45408	0
(3, 3, 3, 0, 0)	112	0	(3, 3, 2, 1, 0)	30624	-224
(3, 3, 1, 1, 1)	434688	0	(3, 2, 2, 2, 0)	234048	-5600
(3, 2, 2, 1, 1)	3222112	928	(2, 2, 2, 2, 1)	20299992	29808
(5, 2, 2, 1, 0)	24	0	(5, 2, 1, 1, 1)	1104	0
(4, 4, 1, 1, 0)	24	0	(4, 3, 3, 0, 0)	24	0
(4, 3, 2, 1, 0)	14496	-48	(4, 3, 1, 1, 1)	212880	0
(4, 2, 2, 2, 0)	122352	-2292	(4, 2, 2, 1, 1)	1691856	528
(3, 3, 3, 1, 0)	122448	-2208	(3, 3, 2, 2, 0)	795936	-29136
(3, 3, 2, 1, 1)	10883712	4320	(3, 2, 2, 2, 1)	63576576	104352
(2, 2, 2, 2, 2)	341681280	3666312			

Table 6.1: *The genus-0 and genus-1 instanton numbers of total degree* ≤ 10. *A multi-index* $\boldsymbol{p}$ *is not displayed if both* $n_{\boldsymbol{p}}$ *and* $d_{\boldsymbol{p}}$ *vanish.*

6.2.3 Relations between the instanton numbers

Inspecting the instanton numbers, it is striking that there are many recurrences of the numbers, for example 24, 80 and, on closer inspection, many other numbers as well, repeat. In fact if

$$\boldsymbol{p} \;=\; (i,\, j,\, k,\, l,\, m) \quad \text{and} \quad \widetilde{\boldsymbol{p}} \;=\; (d-2i,\, j,\, k,\, l,\, m)\;, \quad \text{where} \;\; d \;=\; i+j+k+l+m\;, \tag{6.39}$$

and all the components of $\boldsymbol{p}$ and $d-2i$ are nonnegative, then

$$n_{\boldsymbol{p}} \;=\; n_{\widetilde{\boldsymbol{p}}}\;. \tag{6.40}$$

This identity has many ramifications, and a proper understanding of these devolves upon a discussion of the *web of indices* related to $\boldsymbol{p}$, $W[\boldsymbol{p}]$, obtained by composing the operations $\boldsymbol{p} \mapsto \widetilde{\boldsymbol{p}}$ with permutations. We discuss this is detail in the following subsection. The only $\boldsymbol{p}$ in our tables such that $\widetilde{\boldsymbol{p}}$ has a negative entry is $(1,0,0,0,0)$ and its permutations. The symmetry (6.39), which we will here refer to as a duality, has its origin in the presentation (4.2) of the Hulek-Verrill manifold. In this presentation the six coordinates φ^μ, $\mu = 0,1,\ldots,5$ are projective coordinates that enter on an equal footing. We subsequently passed to five affine coordinates φ^i by setting $\varphi^0 \;=\; 1$. Clearly we could have chosen coordinates by setting any of the φ^μ to unity and using the other φ^μ as coordinates. Now we have taken the large complex structure point to be the point $\varphi^0 \;=\; 1$, $\boldsymbol{\varphi} \;=\; (1,0,0,0,0,0)$, and a consequence of the symmetry of the presentation (4.2) is that there are in fact six large complex structure points, corresponding to taking one of the φ^μ to be unity and the other φ^μ to vanish. We could equally expand the Yukawa coupling about any of these points. We will study the effect of this below, but it is this choice, coupled with the fact that the form of the instanton expansion must remain invariant, that enforces (6.40).

After making such a change in choice of large complex structure point, the new period vector is obtained using the transition matrix $\mathrm{T}_{\Pi^{(0)}\Pi^{(1)}}$ given in (6.55). This matrix can be seen to act on the complex structure moduli space coordinates as

$$z^0 \mapsto -z^0\;, \qquad z^1 \mapsto z^1\;, \qquad z^i \mapsto -z^i - z^1 - z^0 \quad i \neq 0,1\;.$$

This can be stated equivalently in terms of the quantities t^i or q_i:

$$t^1 \mapsto -t^1\;, \quad t^i \mapsto t^i + t^1 + 1\;; \qquad \text{or equivalently} \qquad q_1 \mapsto q_1^{-1}\;, \quad q_i \mapsto q_i q_1\;; \quad i \neq 1\;. \tag{6.41}$$

We can combine these transformations with monodromies around the loci E_i to find a simpler form for them. Consider the matrix

$$\mathrm{M}_{E_5}^{-1}\mathrm{M}_{E_4}^{-1}\mathrm{M}_{E_3}^{-1}\mathrm{M}_{E_2}^{-1}\mathrm{T}_{\Pi^{(0)}\Pi^{(1)}} \;=\; -\begin{pmatrix} 1 & 0 & \mathbf{0}_4^T & 0 & 0 & \mathbf{0}_4^T \\ 0 & -1 & \mathbf{1}_4^T & 0 & 12 & \mathbf{0}_4^T \\ \mathbf{0}_4 & \mathbf{0}_4 & \mathbb{I}_4 & \mathbf{0}_4 & \mathbf{0}_4 & 0 \\ 0 & 0 & \mathbf{0}_4^T & 1 & 0 & \mathbf{0}_4^T \\ 0 & 0 & \mathbf{0}_4^T & 0 & -1 & \mathbf{0}_4^T \\ \mathbf{0} & \mathbf{0} & \mathbb{0}_4 & \mathbf{0} & \mathbf{1} & \mathbb{I}_4 \end{pmatrix},$$

where $\mathbf{0}_4 = (0,0,0,0)^T$, $\mathbf{1} = (1,1,1,1)^T$, $\mathbb{0}_4$ is a 4×4 zero matrix, and $\mathbb{1}_4$ a 4×4 identity matrix. The other matrices, corresponding to the other large complex structure points, are obtained by swapping the second and $(i+2)$'th column and row and the seventh and $(i+7)$'th column and row with each other.

Rather than discussing the Yukawa coupling to see the consequences of these symmetries on instanton numbers, it is simpler to consider the prepotential, bearing in mind the symplectic symmetries. The genus-0 prepotential is

$$\mathcal{F}^{(0)}(\boldsymbol{t}) \;= -(z^0)^2 \left(\frac{1}{6} Y_{ijk}\, t^i t^j t^k + \frac{1}{2} Y_{i00}\, t^i - \frac{\zeta(3)}{2(2\pi\mathrm{i})^3}\, \chi(\mathrm{H}\Lambda) + \frac{1}{(2\pi\mathrm{i})^3} \sum_{\boldsymbol{p}} n_{\boldsymbol{p}}\, \mathrm{Li}_3(\boldsymbol{q}^{\boldsymbol{p}}) \right) . \tag{6.42}$$

The sum is over *positive* multi-indices $\boldsymbol{p}$, where by *positive* we mean that all of its entries are nonnegative and at least one is positive. We now make a change of coordinates,

$$t^i \mapsto \widetilde{t}^i \;, \qquad \widetilde{t}^1 \;=\; -t^1 \;, \quad \widetilde{t}^i \;=\; t^i + t^1 \;, \quad i > 1 \;, \tag{6.43}$$

which differs from the transformation (6.41) by a constant term $\widetilde{t}^i \mapsto t^i - 1$, amounting to an action of a monodromy transformation, which simplifies the following analysis.

Writing $\widetilde{q}_i = \mathrm{e}^{2\pi\mathrm{i}\widetilde{t}^i}$, and $\boldsymbol{q}^{\boldsymbol{p}} = q_1^i q_2^j q_2^k q_4^l q_5^m$, we have $\boldsymbol{q}^{\boldsymbol{p}} = \widetilde{\boldsymbol{q}}^{\widetilde{\boldsymbol{p}}}$, with $\widetilde{\boldsymbol{p}}$ obtained from $\boldsymbol{p}$ by (6.39). Writing the prepotential $\mathcal{F}^{(0)}(\boldsymbol{t})$ in terms of the coordinates $\widetilde{t}^i$, we find

$$\mathcal{F}^{(0)}(\boldsymbol{t}) \;=\; \mathcal{F}^{(0)}\big(\widetilde{\boldsymbol{t}}\big) - 4(\widetilde{t}^1)^3 - 2\widetilde{t}^1 \tag{6.44}$$

The differences arises as

$$\frac{1}{6} Y_{ijk} \left(\widetilde{t}^i \widetilde{t}^j \widetilde{t}^k - t^i t^j t^k \right) + \frac{1}{2} Y_{i00} \left(\widetilde{t}^i - t^i \right) \;.$$

In making the change of coordinates (6.43), we have given the expansion of the prepotential around a different large complex structure point to that of (6.42). Due to the S_6 symmetry, the functional form of the prepotential should be, up to an effect of a symplectic transformation, invariant under the change of coordinates from t^i to $\widetilde{t}^i$. In other words, the functional dependence of the left-hand side of (6.44) on $\boldsymbol{t}$ should be the same as the functional dependence of the right-hand side of (6.44) on $\widetilde{\boldsymbol{t}}$. Requiring this, we obtain

$$4t_1^3 + 2t_1 - \frac{1}{(2\pi\mathrm{i})^3} \sum_{\boldsymbol{p}} n_{\boldsymbol{p}} \mathrm{Li}_3\Big(\boldsymbol{q}^{\widetilde{\boldsymbol{p}}}\Big) \simeq -\frac{1}{(2\pi\mathrm{i})^3} \sum_{\boldsymbol{p}} n_{\boldsymbol{p}} \mathrm{Li}_3(\boldsymbol{q}^{\boldsymbol{p}}) \;, \tag{6.45}$$

with the equality holding up to a symplectic transformation. One now needs to rewrite the sum on the left-hand side. The map (6.39) is an involution, i.e. $\widetilde{\widetilde{\boldsymbol{p}}} = \boldsymbol{p}$, but the sums above are over positive $\boldsymbol{p}$. The only $\boldsymbol{p}$ such that $\widetilde{\boldsymbol{p}}$ has a negative entry is $(1,0,0,0,0)$. Therefore, we have an equality

$$\sum_{\boldsymbol{p}>0} n_{\boldsymbol{p}} \mathrm{Li}_3\Big(\boldsymbol{q}^{\widetilde{\boldsymbol{p}}}\Big) = \left[\sum_{\substack{\boldsymbol{p}, \\ \boldsymbol{p},\, \widetilde{\boldsymbol{p}}>0}} n_{\widetilde{\boldsymbol{p}}}\, \mathrm{Li}_3(\boldsymbol{q}^{\boldsymbol{p}}) + n_{(1,0,0,0,0)}\, \mathrm{Li}_3(q_1) \right] + n_{(1,0,0,0,0)} \left(\mathrm{Li}_3\big(q_1^{-1}\big) - \mathrm{Li}_3(q_1) \right) . \tag{6.46}$$

Substituting (6.46) into (6.45) one obtains

$$4t_1^3 + 2t_1 \simeq \frac{1}{(2\pi\mathrm{i})^3} n_{(1,0,0,0,0)} \left(\mathrm{Li}_3\left(q_1^{-1}\right) - \mathrm{Li}_3(q_1)\right) - \frac{1}{(2\pi\mathrm{i})^3} \sum_{\substack{\boldsymbol{p},\\ \boldsymbol{p},\widetilde{\boldsymbol{p}}>0}} (n_{\boldsymbol{p}} - n_{\widetilde{\boldsymbol{p}}}) \mathrm{Li}_3(\boldsymbol{q}^{\boldsymbol{p}}) \ , \tag{6.47}$$

This imposes that $n_{\boldsymbol{p}} = n_{\widetilde{\boldsymbol{p}}}$ for positive $\boldsymbol{p}, \widetilde{\boldsymbol{p}}$. The left hand side can then be uniquely cancelled by taking $n_{(1,0,0,0,0)} = 24$, in light of the identity

$$\frac{24}{(2\pi\mathrm{i})^3}\left(\mathrm{Li}_3\left(\mathrm{e}^{-2\pi\mathrm{i}t_1}\right) - \mathrm{Li}_3\left(\mathrm{e}^{2\pi\mathrm{i}t_1}\right)\right) \ = \ 2t_1 - 6t_1^2 + 4t_1^3 \ , \qquad \mathrm{Im}[t_1] > 0 \ ,$$

and the fact that the quadratic term $-6t_1^2$ can be removed by a change of symplectic integral basis of $H^3(\mathrm{HV}, \mathbb{Z})$. It is interesting that we have derived the instanton number $n_{(1,0,0,0,0)} = 24$ purely on the grounds of symmetry, without performing a mirror computation or curve-counting. (6.47) then imposes (6.40), which applies for all positive $\boldsymbol{p}$. This includes all $\boldsymbol{p}$ in our tables besides $(1,0,0,0,0)$ and its permutations.

Analogous relations can be seen to hold for the genus-1 instanton numbers that we compute. Indeed, the above argument holds, *mutatis mutandis*, for higher-genus prepotentials.

6.2.4 Duality webs

We refer to the operation in (6.39) as a duality operation on the indices, and denote the set of all multi-indices related to $\boldsymbol{p}$ by these dualities as $W[\boldsymbol{p}]$, the *duality web* containing $\boldsymbol{p}$.

We begin with some elementary properties of the webs, and will observe later that the duality relations correspond to the action of a Coxeter group.

- These duality relations are equivalence relations, so if $\boldsymbol{l} \in W[\boldsymbol{p}]$, then $W[\boldsymbol{l}] = W[\boldsymbol{p}]$.
- If an integer r divides $\boldsymbol{p}$, that is r divides each component of $\boldsymbol{p}$, then r divides $\widetilde{\boldsymbol{p}}$. It follows that the greatest common divisor of the elements of $\boldsymbol{p}$, $\gcd \boldsymbol{p}$, is preserved by the duality transformation and that $\gcd \boldsymbol{l} = \gcd \boldsymbol{p}$, for all $\boldsymbol{l} \in W[\boldsymbol{p}]$. Moreover, for an integer r, the web of $r\boldsymbol{p}$ is obtained by multiplying each multi-index in $W[\boldsymbol{p}]$ by r. We can say that $W[r\boldsymbol{p}] = r\, W[\boldsymbol{p}]$. This observation shows, for example, that $(1,1,1,0,0)$ and $(3,3,3,0,0)$ belong to different webs.

The webs have interesting properties mod 3. We denote the sum of elements of a multi-index I by $|\boldsymbol{p}|$. If the operation takes $\boldsymbol{p}$ to $\widetilde{\boldsymbol{p}}$, as in (6.39), then

$$|\widetilde{\boldsymbol{p}}| \ = \ 2\,|\boldsymbol{p}| - 3i \ = -|\boldsymbol{p}| \mod 3 \ .$$

- It follows that $|\boldsymbol{p}|^2$ is an invariant of the web, so either $|\boldsymbol{l}| = 0 \mod 3$, for all $\boldsymbol{l} \in W[\boldsymbol{p}]$, or $|\boldsymbol{l}|^2 = 1$ for all $\boldsymbol{l} \in W[\boldsymbol{p}]$. Moreover, if $|\boldsymbol{p}| = 0 \mod 3$, we see from (6.39) that $\boldsymbol{l} = \boldsymbol{p} \mod 3$ for all $\boldsymbol{l} \in W[\boldsymbol{p}]$.

We call $\boldsymbol{p}$ is *positive* if all the components of $\boldsymbol{p}$ are nonnegative and at least one is strictly positive, and say that $\boldsymbol{p}$ is *negative* if $-\boldsymbol{p}$ is positive. A multi-index that is neither positive nor negative has both strictly positive and strictly negative components and we refer to such a multi-index as *mixed*.

Analogously, we say that a web W is *positive* if all its multi-indices are positive. A web W is *negative* if $-W$ is positive. A web that is neither positive nor negative is *mixed*.

- The only multi-index in table C.1 that has a duality transform that is not positive is $(1,0,0,0,0)$ which has among its transforms the multi-index $(-1,0,0,0,0)$. Denoting this web by $\mathcal{W}$, we have

  $$\mathcal{W} \;=\; \mathcal{W}_+ \cup \mathcal{W}_- \;,$$

  where

  $$\mathcal{W}_+ \;=\; \Big\{(1,0,0,0,0),\;(1,1,0,0,0),\;(2,1,1,0,0)\;,\ldots\;\Big\}$$

  consists entirely of positive multi-indices, and $\mathcal{W}_- = -\mathcal{W}_+$.

- The argument in the previous subsection 6.2.3 shows that instanton numbers $n_{\boldsymbol{p}}$ are nonzero precisely for multi-indices that lie in $\mathcal{W}_+$, and in the positive webs. This is indeed, what we observe based on extensive computations. For $\boldsymbol{p} \in \mathcal{W}_+$, $n_{\boldsymbol{p}} = 24$, and for $\boldsymbol{l}$ in a positive web $W[\boldsymbol{p}]$ we have $n_{\boldsymbol{l}} = n_{\boldsymbol{p}}$.

There are some intriguing identities that are explained by the duality operations. For example:

$$n_{(i,\,j,\,k,\,0,\,0)} \;=\; n_{(2-i,\,2-j,\,2-k,\,0,\,0)}\;,\quad \text{for}\;\; 0 \le i,j,k \le 2\;,\quad \text{and}\;\; (i,j,k) \neq (0,0,0) \text{ or } (2,2,2)\;.$$

For $(i,j,k) = (1,1,1)$, the identity is trivial, and for the other values of i,j,k this is explained by the fact that all these multi-indices are in the web $\mathcal{W}_+$. This equality can also be explained as a consequence of the elliptic fibration structure of the HΛ manifold as we will see in chapter 7.

Another identity, some aspects of which can be explained by the dualities, is that for a given triple (i,j,k), the genus-0 numbers corresponding to multi-degrees

$$(i,j,k,0,0) + r\,(2,2,2,0,0)\;,\qquad r = 0,1,2,3,\ldots$$

are all equal (to 0, 24, 80, or 112). To illustrate this note that if $(i,j,k) = (1,1,1)$, then the set is $(2r+1)(1,1,1,0,0)$ and for these $n = 112$. If $(i,j,k) = (2,2,2)$, then the set is $r(2,2,2,0,0)$, and for these $n = 80$. For the remaining cases the multi-indices for which $n \neq 0$, are all in $\mathcal{W}_+$, for which $n = 24$.

Table 6.2 sets out an intriguing relation among the instanton numbers that are not explained in this way. There are distinct positive webs W and W' such that $n_W = n_{W'}$. Moreover, precisely when this happens (to the extent of the tables) we have also $d_W = d_{W'}$, where d here denote the genus one instanton numbers. The instanton numbers involved in these relations are highly nontrivial.

While it is possible that some of the webs that are stated to be distinct could in fact coincide, we should state that, in all cases, we have checked the webs up to total degree 250, and these partial webs are distinct. Moreover, in many cases, the webs are demonstrably distinct. The webs in the first two rows of the table, for example, are all distinct since each multi-index $\boldsymbol{p}$ has a distinct greatest common divisor. Apart from these two rows, which are special, there are 7 rows of the table for which the multi-indices $\boldsymbol{p}$ have degrees that are zero mod 3. For these cases the $\boldsymbol{p}$'s mod 3 are invariants of the webs, and in 5 of these cases these invariants are distinct. The remaining 2 of these 7 cases are rows 7 and 18 of the table for which each $\boldsymbol{p}$ reduces to $(2, 1, 0, 0, 0)$ mod 3, up to permutation.

We denote the operation (6.39) by g_1, and the analogous relation acting on the r'th coordinate by g_r. These operations, combined with permutations of the indices, form a group $\mathfrak{W}$. The S_5 subgroup, corresponding to the permutations, can be generated by the transpositions (r, s), in fact it can be generated by the four transpositions $s_r = (r, r+1)$, $r = 1, 2, 3, 4$. Once we admit the permutations, then the dualities g_r can all be obtained from g_1, say; for example $g_2 = s_1 g_1 s_1$.

We have

$$g_1^2 \;=\; s_1^2 \;=\; s_2^2 \;=\; s_3^2 \;=\; s_4^2 \;=\; 1 \;.$$

and it is clear that the generators $\mathfrak{S} = \{g_1,\, s_1,\, s_2,\, s_3,\, s_4\}$ commute, apart from g_1 with s_1, and s_r with s_{r+1}, $r = 1, 2, 3$. The operation $s_r s_{r+1}$ amounts to a cyclic permutation of the three indices $(I_r I_{r+1} I_{r+2}) \to (I_{r+2} I_r I_{r+1})$, so $(s_r s_{r+1})^3 = 1$ and one checks also that $(g_1 s_1)^6 = 1$.

In this way, we observe that $\mathfrak{W}$ is a Coxeter group corresponding to the graph

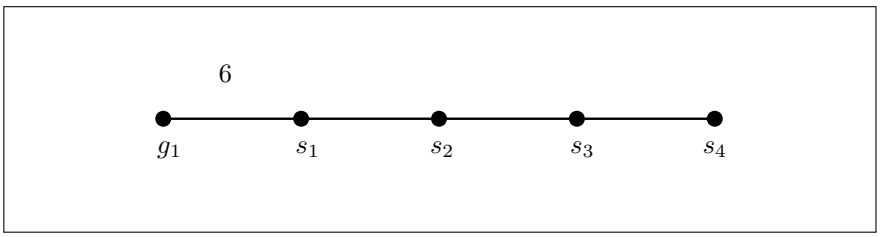


Figure 6.2: *The Coxeter graph corresponding to* $\mathfrak{W}$

#	n	d	Webs
1	112	0	$(2k+1)\,W[(1,1,1,0,0)]$; $k=1,2,\ldots$
2	80	4	$k\,W[(2,2,2,0,0)]$; $k=1,2,\ldots$
3	234048	-5600	(3,2,2,2,0) (4,4,3,1,0)
4	795936	-29136	(3,3,2,2,0) (4,4,4,1,0)
5	4326048	-251520	(3,3,3,2,0) (5,5,5,1,0)
6	33777312	-3031872	(3,3,3,3,0) (5,5,3,2,0) (7,7,6,1,0)
7	7371792	-484896	(4,3,3,2,0) (6,6,5,1,0)
8	88179456	-9395616	(4,3,3,3,0) (7,7,7,1,0)
9	20578560	-1679040	(4,4,3,2,0) (6,6,6,1,0)
10	347078520	-46049040	(4,4,3,3,0) (5,5,4,2,0) (8,8,8,1,0)
11	1935300720	-327015680	(4,4,4,3,0) (6,5,5,2,0) (6,6,3,3,0)
12	14386855920	-3110590260	(4,4,4,4,0) (6,6,6,2,0)
13	539120544	-76342880	(5,4,3,3,0) (9,9,8,1,0)
14	140436672	-16170272	(5,4,4,2,0) (8,8,7,1,0)
15	4392333792	-824199120	(5,4,4,3,0) (6,6,5,2,0)
16	45007048752	-11043084816	(5,4,4,4,0) (6,6,4,3,0) (7,7,6,2,0)
17	1272585120	-203310240	(5,5,3,3,0) (5,5,5,2,0) (9,9,9,1,0)
18	193411225936	-55127514240	(5,5,4,4,0) (8,7,7,2,0)
19	65215603200	-16642969280	(5,5,5,3,0) (7,7,4,3,0)
20	1096632180480	-368134832160	(5,5,5,4,0) (7,7,5,3,0)
21	7888589144400	-3138370134624	(5,5,5,5,0) (7,7,6,3,0) (9,9,9,2,0)
22	65215569408	-16642956928	(6,4,4,4,0) (8,8,6,2,0)
23	21143067840	-4775506080	(6,5,4,3,0) (7,6,6,2,0)
24	391409808576	-119442727776	(6,5,4,4,0) (6,6,5,3,0) (8,8,7,2,0)
25	135171775392	-37176746592	(6,5,5,3,0) (7,7,7,2,0)
26	2981800050480	-1093125957120	(6,5,5,4,0) (7,6,6,3,0) (7,7,4,4,0) (9,9,8,2,0)
27	27765085214112	-12215408263200	(6,5,5,5,0) (7,7,7,3,0) (9,9,6,3,0)
28	1096632086784	-368134868160	(6,6,4,4,0) (8,8,8,2,0)
29	10848408360480	-4429601736480	(6,6,5,4,0) (8,7,6,3,0)
30	126532108859856	-62415555336480	(6,6,5,5,0) (7,6,6,4,0) (8,8,5,4,0) (8,8,7,3,0)
31	1535514818112	-531223501536	(6,6,6,3,0) (7,6,4,4,0) (8,8,5,3,0) (9,8,8,2,0)
32	725912434085952	-405156007308576	(6,6,6,5,0) (8,7,6,4,0) (9,8,8,3,0)
33	51294957112992	-23657221999872	(7,5,5,5,0) (7,7,5,4,0) (8,7,7,3,0)
34	553728279360	-174588053440	(7,6,5,3,0) (9,9,7,2,0)
35	20350993239840	-8738280013680	(7,6,5,4,0) (8,8,6,3,0)
36	305922925426848	-160791639748800	(7,6,5,5,0) (9,9,7,3,0)
37	2235977596096128	-1345692401785920	(7,6,6,5,0) (9,8,6,4,0)
38	19503820669876800	-13461969999093600	(7,6,6,6,0) (8,7,6,5,0) (9,8,7,4,0)
39	408865565088240	-219322647849280	(7,7,6,4,0) (8,6,5,5,0) (8,8,8,3,0)
40	8765016259161504	-5758034709276000	(7,7,6,5,0) (9,9,5,5,0)
41	92700939550359360	-70199768003592720	(7,7,6,6,0) (9,8,6,5,0) (9,8,8,4,0)
42	1692511362069504	-1000067627051904	(7,7,7,4,0) (8,7,5,5,0) (9,9,8,3,0)
43	42801528146793216	-30974226462689184	(7,7,7,5,0) (9,9,7,4,0)
44	3704581973944705776	-3435204329200397376	(7,7,7,7,0) (9,7,7,6,0)
45	3881643757375656	-2421429008571216	(8,6,6,5,0) (8,7,7,4,0) (8,8,5,5,0) (9,9,6,4,0)
46	42801528135993600	-30974226462442944	(8,6,6,6,0) (8,8,8,4,0)
47	1810611871504105272	-1616941505273075616	(8,7,7,6,0) (8,8,8,5,0) (9,8,6,6,0)
48	55456767284050560	-40752668020556480	(8,8,6,5,0) (9,6,6,6,0)
49	419093788958668992	-345708325307878560	(8,8,7,5,0) (9,7,6,6,0)
50	5101035246140064	-3238317072282240	(9,7,7,4,0) (9,8,5,5,0)
51	198280729061595552	-156843054827785632	(9,7,7,5,0) (9,9,6,5,0)
52	170193515484672	-85781801925696	(9,8,7,3,0) (9,9,5,4,0)

Table 6.2: *Pairs (n_W, d_W) that arise for the distinct webs that are shown on the right.*

For two multi-indices $\boldsymbol{p}, \boldsymbol{l}$ let $H(\boldsymbol{p}, \boldsymbol{l})$ denote the bilinear form

$$H(\boldsymbol{p}, \boldsymbol{l}) \;=\; \frac{3}{2}\,\boldsymbol{p}\cdot\boldsymbol{l} - \frac{1}{2}\,|\boldsymbol{p}||\boldsymbol{l}|$$

where $\boldsymbol{p}\cdot\boldsymbol{l}$ denotes the standard inner product. This bilinear form is Lorentzian with signature $(-,+,+,+)$.

The squared length of a multi-index $\boldsymbol{p}$ with respect to H is denoted by $h(\boldsymbol{p})$

$$h(\boldsymbol{p}) \;=\; H(\boldsymbol{p},\boldsymbol{p}) \;.$$

In addition let us define root vectors $\alpha^{(r)}$, $r = 0,\ldots,4$. These are all spacelike and normalised to unity.

$$\begin{aligned}
\alpha^{(0)} &= \qquad (1,\quad 0,0,0,0)\\
\alpha^{(1)} &= \frac{1}{\sqrt{3}}\,(1,-1,0,0,0)\\
\alpha^{(2)} &= \frac{1}{\sqrt{3}}\,(0,1,-1,0,0)\\
\alpha^{(3)} &= \frac{1}{\sqrt{3}}\,(0,0,1,-1,0)\\
\alpha^{(4)} &= \frac{1}{\sqrt{3}}\,(0,0,0,1,-1)\;.
\end{aligned}$$

- The action of the generators on the multi-indices are realised as reflections relative to the metric H

  $$\begin{aligned}
  g_1(\boldsymbol{p}) &= \boldsymbol{p} - 2H(\alpha^{(0)},\boldsymbol{p})\,\alpha^{(0)}\\
  s_r(\boldsymbol{p}) &= \boldsymbol{p} - 2H(\alpha^{(r)},\boldsymbol{p})\,\alpha^{(r)}\;,\;\; r \;=\; 1,2,3,4\;.
  \end{aligned}$$

  Clearly H is invariant under permutations of the indices and so under the actions of the s_r. It is also an immediate check, from the first of the relations above, that

  $$H\big(g_1(\boldsymbol{p}),\, g_1(\boldsymbol{l})\big) \;=\; H(\boldsymbol{p},\boldsymbol{l})\;.$$

  Thus $h(\boldsymbol{p})$ is an invariant of a web and $h(\boldsymbol{l}) = h(\boldsymbol{p})$ for all $\boldsymbol{l} \in W[\boldsymbol{p}]$.

Consider now a positive multi-index $\boldsymbol{p} = (i,j,k,l,m)$, with its indices in *standard order*, that is with $i \geq j \geq k \geq l \geq m$. We shall refer to such a vector as an *ordered source*, if

$$i \leq \frac{|\boldsymbol{p}|}{3}\;.$$

More generally, a *source* is an ordered source up to permutation of indices with the condition on the indices becoming $\max(\boldsymbol{p}) \leq |\boldsymbol{p}|/3$.

- The importance of a source is that $\big|g_r(\boldsymbol{p})\big| \geq |\boldsymbol{p}|$ for $r = 1,\ldots,5$.

  To see this it is sufficient to consider the action of g_1. As previously, set $d = |\boldsymbol{p}|$ and $\widetilde{d} = \big|g_1(\boldsymbol{p})\big|$. Then

  $$g_1(\boldsymbol{p}) \;=\; (d-2i,j,k,l,m) \qquad \text{and} \qquad \widetilde{d} \;=\; 2d-3i\;.$$

  The quantity $d - 2i \geq d/3$, so $g_1(\boldsymbol{p})$ is again a positive multi-index. Moreover

  $$\widetilde{d} \;=\; d + (d-3i) \geq d\;.$$

There is extensive computational evidence to suggest that the degree of a source $\boldsymbol{p}$ cannot be lowered by the action of any word in the g_r, and this may well be an elementary fact, but we currently know of no proof.

- A source $\boldsymbol{p}$ has $h(\boldsymbol{p}) \le 0$, so is future pointing and timelike, or future pointing and null.

  To see this it is perhaps simplest to change coordinates and write

  $$x \;=\; i-j\;, \quad y \;=\; j-k\;, \quad z \;=\; k-l\;, \quad u \;=\; l-m\;, \quad v \;=\; m\;.$$

  In virtue of the standard ordering of $\boldsymbol{p}$, all of the coordinates (x, y, z, u, v) are nonnegative. The condition $i \le |\boldsymbol{p}|/3$ translates into the inequality

  $$u + 2v \;\ge\; 2x + y\;,$$

  and we have

  $$\begin{aligned} h(\boldsymbol{p}) \;&=\; x^2 + xy + y^2 - (u+2v)(x+2y+3z) - (2u^2 + 8uv + 5v^2) \\ &= -\Big\{ \frac{1}{4}\left[(u+2v)^2 - (2x+y)^2\right] + \frac{3}{4}\left[(u+2v)^2 - y^2\right] + (u+2v)(x+2y+3z) \\ &\qquad + u^2 + 4uv + v^2 \Big\}\;. \end{aligned}$$

  In the second equality there is an overall minus sign and the quantity within braces is a sum of manifestly nonnegative terms.

Examples of sources are the multi-index $(1,1,1,0,0)$, which is null, and $(1,1,1,1,0)$, which has $h = -2$. Note that the special index $(1,0,0,0,0)$ is not a source, and in fact has $h = 1$.

If $\boldsymbol{p}$ is a source and $i = |\boldsymbol{p}|/3$ then $g_1(\boldsymbol{p}) = \boldsymbol{p}$. We can exclude this case by requiring $i < |\boldsymbol{p}|/3$.

- Note that if $\boldsymbol{p}$ is a source, and $g_r(\boldsymbol{p}) \ne \boldsymbol{p}$, then $g_r(\boldsymbol{p})$ is not a source.

  We show this for $r = 1$, but the other cases are parallel. Distinguishing quantities pertaining to $g_1(\boldsymbol{p})$ by a tilde, we have, as above,

  $$\widetilde{\imath} \;=\; d - 2i \qquad \text{and} \qquad \widetilde{d} \;=\; 2d - 3i\;.$$

  Set $\xi = i/d$ and $\widetilde{\xi} = \widetilde{\imath}/\widetilde{d}$, then

  $$\widetilde{\xi} \;=\; f(\xi) \;=\; \frac{1-2\xi}{2-3\xi} \qquad \text{and} \qquad f'(\xi) \;=\; -\frac{1}{(2-3\xi)^2}\;.$$

  Since f decreases monotonically for ξ in the range $[0, 1/3)$ we find that

  $$\frac{1}{3} \;< \widetilde{\xi} \le\; \frac{1}{2}\;.$$

  Since $\widetilde{\xi} > 1/3$, $\widetilde{\boldsymbol{p}}$ is not a source.

- While it is not always possible to decrease the degree a multi-index by acting with the generators, it is always possible to increase the degree. For example $\left|g_5(\boldsymbol{p})\right| > |\boldsymbol{p}|$. This observation shows that the positive webs are infinite.

  To see this, suppose that $\boldsymbol{p} = (i, j, k, l, m)$ is a member of a positive web and its components are written in standard order. Since m is the smallest component we have $m \leq |\boldsymbol{p}|/5$, so

$$|\widetilde{\boldsymbol{p}}| \;=\; 2|\boldsymbol{p}| - 3m \;\geq\; \frac{7|\boldsymbol{p}|}{5} \;>\; |\boldsymbol{p}| \;.$$

We wish now to describe the positive webs. Based on extensive calculation, we conjecture that the positive webs are in one-one correspondence with sources. This characterisation is surprisingly simple, since the sources are easily listed. We expect the multi-indices to form a cone, which is specified by identifying its generators.

First note that the condition for an ordered source, $i \leq |\boldsymbol{p}|/3$, is linear, so a linear combination with positive coefficients of ordered sources is again an ordered source. For the converse, that every ordered source can be written as a linear combination with positive coefficients of basis elements, we can proceed by adding sources to the basis as necessary as we increase the degree, say. Though it is not clear a priori that such a process will lead to a finite basis. However on the basis of explicit calculation up to the extent of the tables have the following conjecture:

- Each source may be written as a positive linear combination with integer coefficients of the following 16 sources

$$(1,1,1,0,0) + \text{permutations}$$

$$(1,1,1,1,0) + \text{permutations}$$

$$(1,1,1,1,1) \;.$$

  These elements are certainly necessary. At degree three it is clear that none of the permutations of (1,1,1,0,0) can be written as a positive linear combination of the other permutations. Similarly at degree four the permutations of (1,1,1,1,0) cannot be written as positive linear combinations of the other permutations and the degree three sources. At degree 5 it is clear that a degree five multi-index cannot be written as a positive linear combination of multi-indices of degree three and four.

  At degree six we meet the sources

$$\begin{aligned}(2,2,2,0,0) \;&=\; 2\,(1,1,1,0,0)\\ (2,2,1,1,0) \;&=\; (1,1,1,0,0) + (1,1,0,1,0)\\ (2,1,1,1,1) \;&=\; (1,1,1,0,0) + (1,0,0,1,1)\end{aligned}$$

  which can be written in terms of the basis. Up to degree 29 all the sources can be written as positive linear combinations with integer coefficients of the given basis elements.

If we accept the conjectures made thus far, then we have that

- The multi-indices that belong to the positive webs form a cone whose generators are the multi-index vectors that lie in union of the webs determined by the generators of the web of sources, given above, that is by

$$W[(1,1,1,0,0)] \cup W[(1,1,1,1,0)] \cup W[(1,1,1,1,1)] \ .$$

To see this, note first that all the multi-index vectors in $W[(1,1,1,0,0)]$ are necessary. We give two arguments; the first is immediately clear, the second is an argument that can be applied to other webs also. For the first argument note that all the multi-indices of $W[(1,1,1,0,0)]$ are future pointing and null, and no two are linearly dependant. This being so, any nontrivial positive linear combination of multi-indices in this web yields a multi-index that is timelike so cannot be a member of this web.

For the second argument suppose that some multi-index $\boldsymbol{l}$ can be written as a positive integral combination of other multi-indices $\boldsymbol{k}_a$ so that

$$\boldsymbol{l} \ = \ \sum_a \alpha^a \, \boldsymbol{k}_a \ , \qquad \boldsymbol{k}_a \in W[(1,1,1,0,0)] \ ,$$

with positive integral coefficients α^a. By acting with some element $g \in \mathfrak{W}$ we can transform $\boldsymbol{l}$ to the source $(1,1,1,0,0)$. So now the relation reads

$$(1,1,1,0,0) \ = \ \sum_a \alpha^a \, \widetilde{\boldsymbol{k}}_a \ ,$$

where $\widetilde{\boldsymbol{k}}_a = g\boldsymbol{k}_a$. Now the source has degree 3 and each $|\widetilde{\boldsymbol{k}}_a| \geq 3$ for each a, and this relation is impossible for nontrivial combinations.

To show that all the multi-indices of $W[(1,1,1,1,0)]$ are needed as generators of the cone, suppose that some multi-index $\boldsymbol{p} \in W[(1,1,1,1,0)]$ can be expressed as a nontrivial integral linear combination of the indices in $W[(1,1,1,0,0)] \cup W[(1,1,1,1,0)]$, so that we may write

$$\boldsymbol{p} \ = \ \sum_a \alpha^a \boldsymbol{k}_a + \sum_b \beta^b \boldsymbol{l}_b \ , \qquad \boldsymbol{k}_a \in W[(1,1,1,0,0)] \ , \quad \boldsymbol{l}_b \in W[(1,1,1,1,0)] \ .$$

Again, we transform $\boldsymbol{p}$ to the source, which is now $(1,1,1,1,0)$ and we see that now

$$(1,1,1,1,0) \ = \ \sum_a \alpha^a \widetilde{\boldsymbol{k}}_a + \sum_b \beta^b \, \widetilde{\boldsymbol{l}}_b \ .$$

The degree of the source is 4 while $|\widetilde{\boldsymbol{l}}_b| \geq 4$ and the $|\widetilde{\boldsymbol{k}}_a|$ are multiples of three, so this relation is also impossible.

It can be shown in a similar way that all the multi-indices in $W[(1,1,1,1,1)]$ are also generators.

For the remaining positive webs, we reverse the argument. Let $\boldsymbol{p}$ be the source of such a web; we know that it may be written in terms of the 16 generators of the cone of sources

$$\boldsymbol{p} \;=\; \sum_a \alpha^a \boldsymbol{k}_a + \sum_b \beta^b \boldsymbol{r}_b + \gamma\,(1,1,1,1,1)\ ,$$

where, in this relation, the $\boldsymbol{k}_a$ are the permutations of $(1,1,1,0,0)$ and the $\boldsymbol{r}_b$ are the permutations of $(1,1,1,1,0)$. For $\boldsymbol{l}$ any index in $W[\boldsymbol{p}]$ we choose $g_{\boldsymbol{l}} \in \mathfrak{W}$ that transforms $\boldsymbol{p}$ to $\boldsymbol{l}$. Then, by applying $g_{\boldsymbol{l}}$ to the relation above, we express $\boldsymbol{l}$ as a sum of multi-indices in $W[(1,1,1,0,0)] \cup W[(1,1,1,1,0)] \cup W[(1,1,1,1,1)]$.

6.2.5 Recovering the results on quotient manifolds

Using these results, the genus-0 instanton numbers on the quotient manifolds $\mathrm{H}\Lambda_{\mathbb{Z}_5}$ and $\mathrm{H}\Lambda_{\mathbb{Z}_{10}}$ can be recovered. The first few instanton numbers for the one-parameter manifolds are reproduced from [10] in table 6.3.

We fix attention here to the $\mathbb{Z}_5$ quotient. The action of $\mathbb{Z}_5$ on the cohomology $H^2(\mathrm{H}\Lambda, \mathbb{Z})$ is given by

$$\mathrm{e}_i \mapsto \mathrm{e}_{i+1}\ ,$$

where the index is understood to take values in $\mathbb{Z}_5$, and we have taken this action to be consistent with the choice (5.16) for the action of $\mathbb{Z}_5$ on HV. This also induces an action on $H^4(\mathrm{H}\Lambda, \mathbb{Z})$ via Hodge duality. The $\mathbb{Z}_5$ action on the periods of HV is

$$\varpi^0 \mapsto \varpi^0\ , \qquad \varpi^i \mapsto \varpi^{i+1}\ , \qquad \varpi_i \mapsto \varpi_{i+1}\ , \qquad \varpi_0 \mapsto \varpi_0\ ,$$

with the indices understood to take values in $\mathbb{Z}_5$. The locus of $\mathbb{Z}_5$ symmetric Hulek-Verrill manifolds is $\varphi^1 = \cdots = \varphi^5 \stackrel{\mathrm{def}}{=} \varphi$, and the corresponding mirror manifolds are found on the locus $t^1 = \cdots = t^5 \stackrel{\mathrm{def}}{=} t$. Thus one identifies the generator of the second cohomology of the one-parameter manifold with

$$\mathrm{e} \;=\; \mathrm{e}_1 + \mathrm{e}_2 + \mathrm{e}_3 + \mathrm{e}_4 + \mathrm{e}_5\ .$$

The prepotential on the one-parameter family is identified with that of the five-parameter family by

$$\mathcal{F}(t) \;=\; \frac{1}{5}\,\mathcal{F}(t,t,t,t,t)\ .$$

Indeed, this agrees with the following relatively simple computation on the $\mathbb{Z}_5$ quotient:

$$Y_{111} \;=\; \int_{\mathrm{H}\Lambda/\mathbb{Z}_5} \mathrm{e}\wedge\mathrm{e}\wedge\mathrm{e} \;=\; \frac{1}{5}\sum_{i,j,k=1}^{5}\int_{\mathrm{H}\Lambda} \mathrm{e}_i\wedge\mathrm{e}_j\wedge\mathrm{e}_k \;=\; \frac{1}{5}\sum_{i,j,k=1}^{5} Y_{ijk} \;=\; 24\ .$$

We can identify the other topological numbers Y_{abc} and the instanton numbers in a similar fashion. Since the group $\mathbb{Z}_5$ has no proper subgroups, curves on the manifold must either belong to an orbit of 5 curves or be mapped to themselves. If a curve with Euler character χ is mapped to itself by $\mathbb{Z}_5$ then

the quotient map will take said curve to a curve with Euler character $\chi/5$. In particular, the Euler character of a genus-0 curve is 2, and so there cannot be any genus-0 curves fixed by the $\mathbb{Z}_5$ action.

The relation between the $n_{\boldsymbol{p}}$ of table C.1 and the n_s of table 6.3 is simply

$$\frac{\kappa}{10}\sum_{|\boldsymbol{p}|=s}\widetilde{n}_{\boldsymbol{p}} \;=\; n_s \;. \tag{6.48}$$

The fact that all the instanton numbers we have computed agree with those computed on the one-parameter families through increasingly intricate relations provides a yet another non-trivial consistency check of the results of this chapter.

k	n_k	d_k
1	12κ	$20-10\kappa$
2	24κ	$102-30\kappa$
3	112κ	$1180-438\kappa$
4	624κ	$12096-4428\kappa$
5	4200κ	$133780-48938\kappa$
6	31408κ	$1511730-550266\kappa$
7	258168κ	$17647076-6407530\kappa$
8	2269848κ	$210201644-76161400\kappa$
9	21011260κ	$2545255572-920643442\kappa$
10	202527600κ	$31212421126-11273118446\kappa$
11	2017537884κ	$386727907536-139494386712\kappa$
12	20654747200κ	$4832555488984-1741106040676\kappa$
13	216372489804κ	$60820504439296-21890039477888\kappa$
14	2311525544064κ	$770125991800110-276916193102934\kappa$
15	25115533695300κ	$9802710122549832-3521744606381596\kappa$

Table 6.3: *n_k and d_k are respectively the genus-0 and genus-1 degree-k instanton numbers for the quotient manifolds. The quantity κ is taken to equal 1 or 2 depending on whether one is working on the $\mathbb{Z}_{10}$ or $\mathbb{Z}_5$ quotient. This table is reproduced from [10], where these numbers were given up to degree 20, with thousands being computable.*

6.3 Monodromies

We wish to find the monodromies around the loci E_μ and D_I defined in (6.2) and (6.4). In the next subsection, we will compute the monodromy around the varieties E_i using the series expansions for the periods around the large complex structure point. For the loci D_I, we use numerical integration of the Picard-Fuchs equation to find the monodromies. As we do not have the general five-parameter Picard-Fuchs equation and such an equation would in any case be impractical for this purpose, we use the Picard-Fuchs equations for one-parameter subfamilies as discussed in §6.1.3. Finally, using the relation between the natural basis of periods in the patches $\varphi^0 \neq 0$ and $\varphi^i \neq 0$, we are able to compute the monodromies around E_0 in §6.3.3.

6.3.1 Monodromies around the large complex structure points E_i

The matrices giving the monodromies around the loci E_i can be read directly from the asymptotics of the period vector $\Pi^{(0)}$ in the integral basis, or by using the general formula (2.17). These correspond to coordinate transformations $\varphi^i \to \mathrm{e}^{2\pi \mathrm{i}}\varphi^i$, or alternatively $t^i \to t^i + 1$. These transformations give the following monodromies.

$$\mathrm{M}_{E_1} \;=\; \begin{pmatrix} 1 & -1 & \mathbf{0}_4^T & 2 & 0 & \mathbf{0}_4^T \\ 0 & 1 & \mathbf{0}_4^T & 0 & 0 & \mathbf{0}_4^T \\ \mathbf{0}_4 & \mathbf{0}_4 & \mathbb{I}_4 & \mathbf{0}_4 & \mathbf{0}_4 & 2\mathbb{I}_4 - \mathbb{2}_4 \\ 0 & 0 & \mathbf{0}_4^T & 1 & 0 & \mathbf{0}_4^T \\ 0 & 0 & \mathbf{0}_4^T & 1 & 1 & \mathbf{0}_4^T \\ \mathbf{0}_4 & \mathbf{0}_4 & \mathbb{0}_4 & \mathbf{0}_4 & \mathbf{0}_4 & \mathbb{I}_4 \end{pmatrix} . \tag{6.49}$$

The monodromies around the other loci E_i are obtained by swapping the second and $(i+2)$'th column and row and the seventh and $(i+7)$'th column and row with each other.

6.3.2 Monodromies around the loci D_I

We now set $\varphi^i = s^i\varphi$, $\varphi^0 = 1$ with s^i complex constants. With this, $\mathbb{\Delta}$ becomes a polynomial of degree 16 in φ. This has 16 roots, which are the intersections of the singular locus $\mathbb{\Delta} = 0$ with the plane $\varphi^i = s^i\varphi$. We will find particularly simple Picard-Fuchs operators when some of the s^i are equal. In these cases some of the periods become equal, and hence there exists an operator of degree < 12, whose independent solutions are exactly the distinct periods. These differential equations can be integrated numerically, yielding the monodromy matrices for the independent periods.

Of course the matrices found this way do not give the complete monodromy, as not all of the 12 periods are independent on the lines that we study. However, there is a natural relation between these 'reduced' matrices and the full monodromy matrices, which can be used, together with the S_5 symmetry, to find the full monodromy. To exemplify this process, let us consider the case where $s^1 \neq s^2 = s^3 = s^4 = s^5$. This leaves a set of 6 independent periods, as

$$\begin{aligned} \varpi^{(0);2}(\varphi) &= \varpi^{(0);3}(\varphi) = \varpi^{(0);4}(\varphi) = \varpi^{(0);5}(\varphi) \;, \\ \varpi_2^{(0)}(\varphi) &= \varpi_3^{(0)}(\varphi) = \varpi_4^{(0)}(\varphi) = \varpi_5^{(0)}(\varphi) \;. \end{aligned}$$

The most general monodromy matrix, giving the monodromy transformation of the periods around a singularity φ_*, can be written as

$$\mathrm{M}_{\varphi_*} \;=\; (\boldsymbol{u}_0, \boldsymbol{u}_1, \ldots, \boldsymbol{u}_{10}, \boldsymbol{u}_{11}) \;, \tag{6.50}$$

where $\boldsymbol{u}_i$ are 12-component column vectors

$$\boldsymbol{u}_i \;=\; (u_i^0, u_i^1, \ldots, u_i^{10}, u_i^{11})^T \;.$$

Since some of the periods are equal, we cannot find their individual contributions to this matrix from the reduced monodromy matrix. Instead, the reduced matrix takes the form

$$\widehat{\mathrm{M}}_{\varphi^*} \;=\; (\hat{\boldsymbol{u}}_0, \hat{\boldsymbol{u}}_1, \hat{\boldsymbol{u}}_2 + \hat{\boldsymbol{u}}_3 + \hat{\boldsymbol{u}}_4 + \hat{\boldsymbol{u}}_5, \hat{\boldsymbol{u}}_6, \hat{\boldsymbol{u}}_7, \hat{\boldsymbol{u}}_8 + \hat{\boldsymbol{u}}_9 + \hat{\boldsymbol{u}}_{10} + \hat{\boldsymbol{u}}_{11}) \;, \tag{6.51}$$

where now $\hat{u}_i$ are 6 component column vectors

$$\hat{\boldsymbol{u}}_i \;=\; (u_i^0, u_i^1, u_i^2, u_i^6, u_i^7, u_i^8)^T \ .$$

Relations like this constrain the full 12×12 monodromy matrices. We can construct the full matrices from this data by numerically integrating the Picard-Fuchs equation along several paths in the complex line.

Finally, to make the computation slightly simpler, we use the fact that the singularities at $\mathbb{\Delta} = 0$ correspond to conifolds. It is expected that the matrices corresponding to monodromies around the conifold loci take the form

$$\mathrm{M} \;=\; \mathrm{I}_{12} - \boldsymbol{w}(\Sigma \boldsymbol{w})^T, \tag{6.52}$$

where $\boldsymbol{w}$ is a 12-component vector that gives the cycle vanishing at the conifold point. Thus we can reduce the problem to finding 16 vectors corresponding to the different components D_I of the singular locus.

To get an idea of how the computation proceeds, we briefly explain the computation of some monodromies in a relatively simple example. To be precise, we study the case

$$s^1 = 1 \ , \qquad s^2 \;=\; s^3 \;=\; s^4 \;=\; s^5 = \frac{95}{100} \ .$$

There are six independent periods and so we can find, using the procedure outlined in §6.1.3, a Picard-Fuchs operator of degree 6. This operator has solutions $\varpi^{(0);0}(\varphi)$, $\varpi^{(0);1}(\varphi)$, $\varpi^{(0);2}(\varphi)$, $\varpi_1^{(0)}(\varphi)$, $\varpi_2^{(0)}(\varphi)$, and $\varpi_3^{(0)}(\varphi)$. In the ensuing discussion, we use the shorthands

$$\mathbb{\mu} \;=\; 5\,\frac{81-4\sqrt{95}}{5041} \ , \qquad \overline{\mathbb{\mu}} \;=\; 5\,\frac{81+4\sqrt{95}}{5041} \ , \qquad \mathbb{\nu} \;=\; 5\,\frac{12-\sqrt{95}}{98} \ , \qquad \overline{\mathbb{\nu}} \;=\; 5\,\frac{12+\sqrt{95}}{98} \ . \tag{6.53}$$

The discriminant expressed in terms of φ is in this case, up to a multiplicative constant,

$$\mathbb{\Delta} \;=\; \big(\varphi-1\big)^6\big(\varphi-\mathbb{\mu}\big)\big(\varphi-\overline{\mathbb{\mu}}\big)\big(\varphi-\mathbb{\nu}\big)^4\big(\varphi-\overline{\mathbb{\nu}}\big)^4 \ .$$

Each of these factors corresponds to an intersection of a component D_I with the line. In this way, we can associate each factor with such a component:

$$\begin{aligned}
D_{\{0\}} \;&=\; \{\varphi \;=\; \mathbb{\mu}\} \ , \\
D_{\{0,2\}} \;&=\; D_{\{0,3\}} \;=\; D_{\{0,4\}} \;=\; D_{\{0,5\}} \;=\; \{\varphi \;=\; \mathbb{\nu}\} \ , \\
D_{\{0,1\}} \;&=\; \{\varphi \;=\; \overline{\mathbb{\mu}}\} \ , \\
D_{\{0,2,3\}} \;&=\; D_{\{0,2,4\}} \;=\; D_{\{0,2,5\}} \;=\; D_{\{0,3,4\}} \;=\; D_{\{0,3,5\}} \;=\; D_{\{0,4,5\}} \;=\; \{\varphi = 1\} \ , \\
D_{\{0,1,2\}} \;&=\; D_{\{0,1,3\}} \;=\; D_{\{0,1,4\}} \;=\; D_{\{0,1,5\}} \;=\; \{\varphi \;=\; \overline{\mathbb{\nu}}\} \ .
\end{aligned}$$

The matrices giving the monodromies around these points are given by

$$\widehat{\mathrm{M}}_{\mathbb{µ}} = \begin{pmatrix} 1 & 0 & 0 & 0 & 0 & 0 \\ 0 & 1 & 0 & 0 & 0 & 0 \\ 0 & 0 & 1 & 0 & 0 & 0 \\ -1 & 0 & 0 & 1 & 0 & 0 \\ 0 & 0 & 0 & 0 & 1 & 0 \\ 0 & 0 & 0 & 0 & 0 & 1 \end{pmatrix}, \qquad \widehat{\mathrm{M}}_{\mathbb{ν}} = \begin{pmatrix} 9 & 0 & -8 & 16 & 0 & 0 \\ 0 & 1 & 0 & 0 & 0 & 0 \\ 0 & 0 & 1 & 0 & 0 & 0 \\ -4 & 0 & 4 & -7 & 0 & 0 \\ 0 & 0 & 0 & 0 & 1 & 0 \\ 1 & 0 & -1 & 2 & 0 & 1 \end{pmatrix},$$

$$\widehat{\mathrm{M}}_{\overline{\mathbb{µ}}} = \begin{pmatrix} 3 & -2 & 0 & 4 & 0 & 0 \\ 0 & 1 & 0 & 0 & 0 & 0 \\ 0 & 0 & 1 & 0 & 0 & 0 \\ -1 & 1 & 0 & -1 & 0 & 0 \\ 1 & -1 & 0 & 2 & 1 & 0 \\ 0 & 0 & 0 & 0 & 0 & 1 \end{pmatrix}, \qquad \widehat{\mathrm{M}}_{1} = \begin{pmatrix} 25 & 0 & -48 & 96 & 48 & 96 \\ 12 & 1 & -24 & 48 & 24 & 48 \\ 6 & 0 & -11 & 24 & 12 & 24 \\ -6 & 0 & 12 & -23 & -12 & -24 \\ 0 & 0 & 0 & 0 & 1 & 0 \\ 3 & 0 & -6 & 12 & 6 & 13 \end{pmatrix},$$

$$\widehat{\mathrm{M}}_{\overline{\mathbb{ν}}} = \begin{pmatrix} 17 & -16 & -16 & 64 & 0 & 96 \\ 0 & 1 & 0 & 0 & 0 & 0 \\ 6 & -6 & -5 & 24 & 0 & 36 \\ -4 & 4 & 4 & -15 & 0 & -24 \\ 4 & -4 & -4 & 16 & 1 & 24 \\ 1 & -1 & -1 & 4 & 0 & 7 \end{pmatrix}.$$

To find the full monodromy matrix corresponding to the monodromy around $D_{\{0\}}$, we use

$$\widehat{\mathrm{M}}_{\mathbb{µ}} = \widehat{\mathrm{M}}_{\{0\}}, \tag{6.54}$$

where $\mathrm{M}_{\{0\}}$ is of the form (6.52), and $\widehat{\mathrm{M}}_{\{0\}}$ of the form (6.51). This equation allows us to partially fix the vector $\boldsymbol{w}$, which we denote by $\boldsymbol{w}_{\{0\}}$, giving conditions which can be solved by

$$\boldsymbol{w}_{\{0\}} = (0,\, 0,\, 0,\, w^4,\, w^5,\, -w^4,\, -w^5,\, 1,\, 0,\, 0,\, w^{10},\, w^{11},\, -w^{10} - w^{11}) \,.$$

To proceed, we can compute the monodromies on other similar lines, such as $s^1 = s^3 = s^4 = s^5 = \frac{95}{100}$, $s^2 = 1$. Alternatively, we could impose the S_5 symmetry, whereby all the periods related by a permutations of the indices 2,3,4 and 5 must contribute equally. In this way, we see that the cycle vanishing at $D_{\{0\}}$ has sixth component 1, and all other components zero:

$$\boldsymbol{w}_{\{0\}} = (0,\, 0,\, 0,\, 0,\, 0,\, 0,\, 1,\, 0,\, 0,\, 0,\, 0,\, 0) \,.$$

Next, we concentrate on the singularities at $\varphi = \overline{\mathbb{µ}}$ and $\varphi = \mathbb{ν}$. The latter lies on four singular loci, $D_{\{0,2\}}$, $D_{\{0,3\}}$, $D_{\{0,4\}}$, and $D_{\{0,5\}}$, while the former lies solely in $D_{\{0,1\}}$. Therefore we can use an expression of the form (6.52) for the monodromy matrix around the singularity at $\mathbb{ν}$, while around $\overline{\mathbb{µ}}$ the monodromy is a product of four similar matrices. By comparing to $\mathrm{M}_{\mathbb{ν}}$, we find

$$\boldsymbol{w}_{\{0,1\}} = (-2,\, 0,\, 0,\, w^4,\, w^5,\, -w^4 - w^5,\, 1,\, -1,\, 0,\, w^{10},\, w^{11},\, -w^{10} - w^{11}) \,.$$

By either computing monodromies with different values of s^i, or by a symmetry argument, we find that the vector is given by

$$\boldsymbol{w}_{\{0,1\}} = (-2, 0, 0, 0, 0, 0, 1, -1, 0, 0, 0, 0) \,,$$

which allows us to compute the monodromy matrix $\mathrm{M}_{\{0,1\}}$. Again, by symmetry or considering different values of weights, it can be shown that the vectors giving the monodromy matrices $\mathrm{M}_{\{0,2\}}$,

$\mathrm{M}_{\{0,3\}}$, $\mathrm{M}_{\{0,4\}}$ and $\mathrm{M}_{\{0,5\}}$ are given by permuting the components of the vector $\boldsymbol{w}_{\{0,1\}}$:

$$\begin{aligned}
\boldsymbol{w}_{\{0,2\}} &= (-2,\,0,\,0,\,0,\,0,\,0,\,1,\,0,\,-1,\,0,\,0,\,0)\ , \\
\boldsymbol{w}_{\{0,3\}} &= (-2,\,0,\,0,\,0,\,0,\,0,\,1,\,0,\,0,\,-1,\,0,\,0)\ , \\
\boldsymbol{w}_{\{0,4\}} &= (-2,\,0,\,0,\,0,\,0,\,0,\,1,\,0,\,0,\,0,\,-1,\,0)\ , \\
\boldsymbol{w}_{\{0,5\}} &= (-2,\,0,\,0,\,0,\,0,\,0,\,1,\,0,\,0,\,0,\,0,\,-1)\ .
\end{aligned}$$

As a consistency check, it can be seen that the matrix corresponding to the monodromy around $\mathbb{v}$ is given by a product of reduced monodromy matrices:

$$\mathrm{M}_{\mathbb{v}} \;=\; \widehat{\mathrm{M}}_{\{0,2\}}\,\widehat{\mathrm{M}}_{\{0,3\}}\,\widehat{\mathrm{M}}_{\{0,4\}}\,\widehat{\mathrm{M}}_{\{0,5\}}\ .$$

The matrices corresponding to the remaining loci can be found using similar techniques. This is made slightly more complicated by the fact that paths on the lines $s^1 \neq s^2 = s^3 = s^4 = s^5$ meet these at common intersections of multiple loci. Perhaps the easiest way to circumvent this is to consider a new case where $s^1 \neq s^2 \neq s^3 = s^4 = s^5 \neq s^1$, and permutations thereof. In the case $s_1 \neq s_2 \neq s_3$, $D_{\{0,1,2\}}$ intersects the plane $\varphi^i = s^i\varphi$ in a point that is distinct from the other components. This computation, together with symmetry considerations, leads us to a form of the monodromy matrix where the vanishing cycle is given by

$$\boldsymbol{w}_{\{0,1,2\}} \;=\; (4,\,0,\,0,\,2,\,2,\,2,\,-1,\,1,\,1,\,0,\,0,\,0)\ .$$

The vectors in other cases are given by permuting the components of this vector. One can check that the matrices $\widehat{\mathrm{M}}_1$ and $\widehat{\mathrm{M}}_{\overline{\mathbb{v}}}$ can be written in terms of the reduced matrices associated to these vectors:

$$\begin{aligned}
\widehat{\mathrm{M}}_1 &= \widehat{\mathrm{M}}_{\{0,2,3\}}\,\widehat{\mathrm{M}}_{\{0,2,4\}}\,\widehat{\mathrm{M}}_{\{0,2,5\}}\,\widehat{\mathrm{M}}_{\{0,3,4\}}\,\widehat{\mathrm{M}}_{\{0,3,5\}}\,\widehat{\mathrm{M}}_{\{0,4,5\}}\ , \\
\widehat{\mathrm{M}}_{\overline{\mathbb{v}}} &= \widehat{\mathrm{M}}_{\{0,1,2\}}\,\widehat{\mathrm{M}}_{\{0,1,3\}}\,\widehat{\mathrm{M}}_{\{0,1,4\}}\,\widehat{\mathrm{M}}_{\{0,1,5\}}\ .
\end{aligned}$$

We have found 16 matrices $M_{\{0\}}$, $M_{\{0,i\}}$, and $M_{\{0,i,j\}}$, and there remain 16 still unaccounted for. These, however, can be constructed from the known 16 by a change of indices $0 \leftrightarrow i$. By symmetry, the matrices that are related to each other by such a permutation must be equal. We must, however, take into account that the monodromy transformations obtained in this way are expressed in different bases. Changing all to a common basis, which we take to be the symplectic integral basis where $\Pi^{(0)}$ is given by (6.34), gives matrices with different entries. Thus, for example

$$\mathrm{M}_{\{1\}} \;=\; \mathrm{T}^{-1}_{\Pi^{(1)}\Pi^{(0)}}\,\mathrm{M}_{\{0\}}\mathrm{T}_{\Pi^{(1)}\,\Pi^{(0)}}\ ,$$

where $\mathrm{T}_{\Pi^{(1)}\Pi^{(0)}}$, given explicitly in (6.55), is a change of basis matrix from the canonical integral basis in the patch $\varphi^0 = 1$ to the canonical integral basis in the patch $\varphi^1 = 1$. We will see another explicit example of this in the next subsection where we use this observation to compute the monodromy around the locus E_0 'at infinity'.

6.3.3 Monodromy around infinity, E_0

The remaining singular locus is $\varphi^0 = 0$, which, seen from the patch $\varphi^0 = 1$ corresponds to the monodromy around infinity. Due to the S_5 symmetry, we know that the locus $\varphi^0 = 0$ is on a par with the other loci $\varphi^i = 0$. The only essential difference to the earlier computation is the use of a different basis for the periods.

To find the appropriate change of basis, we use the matrix $\mathrm{T}_{\pi^{(0)}\pi^{(1)}}$ from (6.24), which gives the relation between the period vectors $\pi^{(1)}$ and $\pi^{(0)}$, whose components give the periods as combinations of Bessel function integrals. Using the matrices $\mathrm{T}_{\varpi^{(\mu)}\pi^{(\mu)}}$ and $\mathrm{T}_{\Pi^{(\mu)}\varpi^{(\mu)}}$, we can change from this basis to the integral basis. Note that due to the symmetry, the relation of the vectors $\pi^{(1)}$ to the integral period vector $\Pi^{(1)}$ is same as that of $\pi^{(0)}$ to $\Pi^{(0)}$, so that $\mathrm{T}_{\Pi^{(1)}\pi^{(1)}} = \mathrm{T}_{\Pi^{(0)}\pi^{(0)}}$. The transformation from $\Pi^{(1)}$ to $\Pi^{(0)}$ is thus given by

$$\begin{aligned}\mathrm{T}_{\Pi^{(0)}\Pi^{(1)}} &= \mathrm{T}_{\Pi^{(0)}\varpi^{(0)}}\mathrm{T}_{\varpi^{(0)}\pi^{(0)}}\mathrm{T}_{\pi^{(0)}\pi^{(1)}}\left(\mathrm{T}_{\Pi^{(1)}\varpi^{(1)}}\mathrm{T}_{\varpi^{(1)}\pi^{(1)}}\right)^{-1} \\ &= \begin{pmatrix} -1 & 0 & 1 & 1 & 1 & 1 & -16 & -12 & -6 & -6 & -6 & -6 \\ 0 & 1 & -1 & -1 & -1 & -1 & 12 & 12 & 6 & 6 & 6 & 6 \\ 0 & 0 & -1 & 0 & 0 & 0 & 6 & 6 & 0 & 4 & 4 & 4 \\ 0 & 0 & 0 & -1 & 0 & 0 & 6 & 6 & 4 & 0 & 4 & 4 \\ 0 & 0 & 0 & 0 & -1 & 0 & 6 & 6 & 4 & 4 & 0 & 4 \\ 0 & 0 & 0 & 0 & 0 & -1 & 6 & 6 & 4 & 4 & 4 & 0 \\ 0 & 0 & 0 & 0 & 0 & 0 & -1 & 0 & 0 & 0 & 0 & 0 \\ 0 & 0 & 0 & 0 & 0 & 0 & 0 & 1 & 0 & 0 & 0 & 0 \\ 0 & 0 & 0 & 0 & 0 & 0 & -1 & -1 & -1 & 0 & 0 & 0 \\ 0 & 0 & 0 & 0 & 0 & 0 & -1 & -1 & 0 & -1 & 0 & 0 \\ 0 & 0 & 0 & 0 & 0 & 0 & -1 & -1 & 0 & 0 & -1 & 0 \\ 0 & 0 & 0 & 0 & 0 & 0 & -1 & -1 & 0 & 0 & 0 & -1 \end{pmatrix}. \end{aligned} \tag{6.55}$$

The monodromy of $\Pi^{(0)}$ around $\varphi^0 = 0$ is, by symmetry, equal to the mondromy of $\Pi^{(1)}$ around $\varphi^1 = 0$, which directly allows us to find the monodromy of $\Pi^{(1)}$ around the locus $\varphi^0 = 0$:

$$\mathrm{M}_{E_1} = \left(\mathrm{T}_{\Pi^{(1)}\Pi^{(0)}}\right)^{-1}\left(\mathrm{M}_{E_0}\right)^{-1}\mathrm{T}_{\Pi^{(1)}\Pi^{(0)}} = \begin{pmatrix} 1 & -1 & 1 & 1 & 1 & 1 & -2 & -12 & 0 & 0 & 0 & 0 \\ 0 & 1 & 0 & 0 & 0 & 0 & -12 & 24 & 6 & 6 & 6 & 6 \\ 0 & 0 & 1 & 0 & 0 & 0 & 0 & 6 & 0 & 2 & 2 & 2 \\ 0 & 0 & 0 & 1 & 0 & 0 & 0 & 6 & 2 & 0 & 2 & 2 \\ 0 & 0 & 0 & 0 & 1 & 0 & 0 & 6 & 2 & 2 & 0 & 2 \\ 0 & 0 & 0 & 0 & 0 & 1 & 0 & 6 & 2 & 2 & 2 & 0 \\ 0 & 0 & 0 & 0 & 0 & 0 & 1 & 0 & 0 & 0 & 0 & 0 \\ 0 & 0 & 0 & 0 & 0 & 0 & 0 & 1 & 1 & 0 & 0 & 0 \\ 0 & 0 & 0 & 0 & 0 & 0 & -1 & 0 & 1 & 0 & 0 & 0 \\ 0 & 0 & 0 & 0 & 0 & 0 & -1 & 0 & 0 & 1 & 0 & 0 \\ 0 & 0 & 0 & 0 & 0 & 0 & -1 & 0 & 0 & 0 & 1 & 0 \\ 0 & 0 & 0 & 0 & 0 & 0 & -1 & 0 & 0 & 0 & 0 & 1 \end{pmatrix}.$$

We have used the inverse of the matrix M_{E_0} because the direction of the contour is reversed when changing patches.

6.3.4 Recovering monodromies for the quotient manifolds

Finally, let us briefly comment on the relation of the results presented here to those found for the quotient manifolds in [10]. Specialising to the locus $\varphi^i = \varphi$, $\varphi^0 = 1$, the discriminant vanishes for $\varphi \in \{\frac{1}{25}, \frac{1}{9}, 1\}$. The locus $D_{\{0\}}$ is associated to the first of these points, the loci $D_{\{0,i\}}$ to the second, and the loci $D_{\{0,i,j\}}$ to the last.

On the locus $\varphi^i = \varphi$, $\varphi^0 = 1$, only four of the elements of $\Pi^{(0)}$ are independent. We collect these into the reduced period vector $\widehat{\Pi}^{(0)}$. This is related to the integral period vector $\Pi_{\mathbb{Z}_{10/\kappa}}$ of the quotient

manifold $\mathrm{HV}/\mathbb{Z}_{10/\kappa}$ by a matrix T_κ.

$$\Pi^{(0)} \stackrel{\text{def}}{=} \begin{pmatrix} \Pi_0^{(0);0} \\ \Pi^{(0);1} \\ \Pi_0^{(0)} \\ \Pi_1^{(0)} \end{pmatrix} , \qquad \Pi_{\mathbb{Z}_{10/\kappa}} \;=\; \mathrm{T}_\kappa \widehat{\Pi}^{(0)} , \qquad \mathrm{T}_\kappa \;=\; \begin{pmatrix} 10/\kappa & 0 & 0 & 0 \\ 0 & 2/\kappa & 0 & 0 \\ 0 & 0 & 1 & 0 \\ 0 & 0 & 0 & 1 \end{pmatrix} .$$

We can now give the monodromies M_1, $\mathrm{M}_{\frac{1}{9}}$, and $\mathrm{M}_{\frac{1}{25}}$ of $\Pi_{\mathbb{Z}_{10/\kappa}}$. First, take the product of the relevant matrices $\widehat{\mathrm{M}}_s$ which give the monodromies of $\widehat{\Pi}^0$, and then conjugate by T_κ to obtain the monodromies of $\Pi_{\mathbb{Z}_{10/\kappa}}$. For instance, for the $\mathbb{Z}_{10}$ quotient

$$\mathrm{M}_{\frac{1}{25}} \;=\; \mathrm{T}_1^{-1} \widehat{\mathrm{M}}_{\{0\}} \mathrm{T}_1 \;=\; \begin{pmatrix} 1 & 0 & 0 & 0 \\ 0 & 1 & 0 & 0 \\ -10 & 0 & 1 & 0 \\ 0 & 0 & 0 & 1 \end{pmatrix} .$$

Chapter 7

Counting Curves on the Mirror Hulek-Verrill Manifold

There is an interesting problem in directly counting the numbers of various curves of different degrees on the Hulek-Verrill manifold and its quotients. This serves multiple purposes, such as confirming the predictions of mirror symmetry and counting microstates corresponding to some configurations of branes wrapped on various cycles on the manifold. In this section, we will find the rational curves up to degree 5, and verify that their number agrees with the instanton numbers of §6.2.

It is useful to recognise that the manifolds in HΛ can be realised as blowups of singular tetraquadrics $\widehat{\mathrm{H}\Lambda}_i$ with 24 nodes, using the procedure of [85]. The varieties $\widehat{\mathrm{H}\Lambda}_i$ are limits of the family corresponding to the configuration

$$\begin{bmatrix} \mathbb{P}^1 & 2 \\ \mathbb{P}^1 & 2 \\ \mathbb{P}^1 & 2 \\ \mathbb{P}^1 & 2 \end{bmatrix}_{\chi=-128} . \tag{7.1}$$

Members of the family HΛ are elliptically fibred manifolds, and we are able to compute the discriminant of the fibration using standard methods [86]. It turns out that the the first few low-degree rational curves appear as irreducible components of singular fibres of the elliptic fibration (see figure 7.1).

$$\begin{array}{ccccc} & & L_i & \hookrightarrow & \mathrm{H}\Lambda \\ & & & & \downarrow{\scriptstyle \pi_j} \\ \mathbb{P}^1 & \overset{\varphi}{\hookrightarrow} & F_j & \hookrightarrow & \widehat{\mathrm{H}\Lambda}_j \\ & & \downarrow{\scriptstyle \pi_{m,n}} & & \downarrow{\scriptstyle \pi_{m,n}} \\ & & B & \hookrightarrow & \mathbb{P}^1_m \times \mathbb{P}^1_n \end{array}$$

Figure 7.1: *Structure of the fibrations relevant to counting some rational and elliptic curves. L_i denote the lines on HΛ that are blown down to obtain the singular mirror Hulek-Verrill manifold $\widehat{H\Lambda}_j$ with the birational map denoted by π_j. $\widehat{H\Lambda}_j$ is an elliptically fibred manifold with base $\mathbb{P}^1 \times \mathbb{P}^1$, and a generic fibre F_j. On the discriminant locus $\Delta = 0$ of the elliptic fibration, the fibre becomes singular. On a special set of points B, corresponding to nodes of the discriminant locus, the degenerate fibre is a union of two rational curves.*

The explicit embeddings of curves depend non-trivially on the coefficients in the defining polynomials, but the curve counts for generic members of the family of mirror manifolds agree. For this reason we will, in place of explicit expressions, discuss properties of a generic member of the family HΛ.

Parts of our discussion are best framed in terms of various embedding maps with different degrees. Among these appear numerous context-specific rational functions. For this reason, we will often use the symbols $r_k(z)$, $\widetilde{r}_k(z)$, to denote a ratio of two *situation-dependent* polynomials of degree k. Two instances of these symbols in this section should not automatically be understood as referring to the same function. In this section the Latin indices generically run from 0 to 4. When two different indices appear in an expression, they are understood to refer to distinct numerical values.

7.1 Blow-down and elliptic fibration

The configuration matrix of HΛ is of the form considered in [85], which means that we can use the contraction procedure to obtain a quadric manifold $\widehat{\mathrm{H}\Lambda}_i$ defined by one equation:

$$\begin{matrix}\mathbb{P}^1\\ \mathbb{P}^1\\ \mathbb{P}^1\\ \mathbb{P}^1\\ \mathbb{P}^1\end{matrix}\begin{bmatrix}1 & 1\\ 1 & 1\\ 1 & 1\\ 1 & 1\\ 1 & 1\end{bmatrix}_{\chi=-80} \qquad \longleftrightarrow \qquad \begin{matrix}\mathbb{P}^1\\ \mathbb{P}^1\\ \mathbb{P}^1\\ \mathbb{P}^1\end{matrix}\begin{bmatrix}2\\ 2\\ 2\\ 2\end{bmatrix}_{\chi=-128}\,. \tag{7.2}$$

We frequently distinguish the five $\mathbb{P}^1$ factors in the product $(\mathbb{P}^1)^5$ by subscripts. For example, $\mathbb{P}^1_i$ denotes the i'th such $\mathbb{P}^1$, and has projective coordinates $Y_{i,0}, Y_{i,1}$. Throughout this section, we use the affine coordinates $Y_i = \frac{Y_{i,1}}{Y_{i,0}}$. This makes the equations simpler, and the instances where projective coordinates are needed for statements to be strictly correct are few. Nonetheless, all polynomials in this section can be homogenised using projective coordinates and in this way any minor ambiguities relating to points at infinity are cleared up.

To see in detail how the process depicted in (7.2) works, let us consider the contraction with respect to $\mathbb{P}^1_i$. The equations defining the manifold HΛ can be written as

$$\begin{aligned} Q^1(\boldsymbol{Y}) &= \alpha_i Y_i + \beta_i\,,\\ Q^2(\boldsymbol{Y}) &= \gamma_i Y_i + \delta_i\,, \end{aligned} \tag{7.3}$$

with $\alpha_i, \beta_i, \gamma_i, \delta_i$ multilinear functions of the four coordinates Y_j, $j \neq i$, and no sum over the repeated i is implied. The pair of conditions (7.3) is equivalent to the single matrix equation

$$\begin{pmatrix}\alpha_i & \beta_i\\ \gamma_i & \delta_i\end{pmatrix}\begin{pmatrix}Y_i\\ 1\end{pmatrix} = \mathbf{0}\,.$$

Existence of a solution is equivalent to the vanishing of the determinant of the matrix, that is

$$\widehat{Q}^i \stackrel{\text{def}}{=} \alpha_i\,\delta_i - \beta_i\,\gamma_i = 0\,, \tag{7.4}$$

We denote the variety defined by $\{\widehat{Q}^i = 0\} \subset (\mathbb{P}^1)^4$ as $\widehat{\mathrm{H}\Lambda}_i$. One can see from (7.4) that $\widehat{\mathrm{H}\Lambda}_i$ is a conifold. Since the functions $\alpha_i, \beta_i, \gamma_i, \delta_i$ are multilinear, the corresponding configuration matrix is indeed of the form (7.2).

Note that the varieties $\widehat{\mathrm{H}\Lambda}_i$ are birational to $\mathrm{H}\Lambda$. The projection $\pi_i : \mathrm{H}\Lambda \to \widehat{\mathrm{H}\Lambda}_i$ defined by

$$\pi_i(Y_i, Y_j, Y_k, Y_m, Y_n) \;=\; (Y_j, Y_k, Y_m, Y_n)$$

gives a birational map between the varieties. Given a point $(Y_j, Y_k, Y_m, Y_n) \in \widehat{\mathrm{H}\Lambda}_i$, with $\alpha_i \neq 0$ or $\gamma_i \neq 0$, the equations $Q^1 = Q^2 = 0$ are solved by the unique point $Y_i = -\frac{\beta_i}{\alpha_i}$ or $Y_i = -\frac{\delta_i}{\gamma_i}$, respectively (when $\alpha_i, \gamma_i \neq 0$, these agree), and the inverse π_i^{-1} is well-defined. However, when $\alpha_i = \gamma_i = 0$, the conditions $Q^1 = Q^2 = 0$ are satisfied at the point at infinity, and otherwise if and only if $\beta_i = \delta_i = 0$. If this is the case, the equation $Q^1 = Q^2 = 0$ is true for all values of Y_i, and the inverse image of the point in $\widehat{\mathrm{H}\Lambda}_i$ is a line $\alpha_i = \beta_i = \gamma_i = \delta_i = 0$ on $\mathrm{H}\Lambda$. For generic values of parameters, including generic $\mathbb{Z}_5$, $\mathbb{Z}_5\times\mathbb{Z}_2$ and $\mathbb{Z}_5\times\mathbb{Z}_2\times\mathbb{Z}_2$ symmetric cases, these equations have 24 solutions. From the definition of $\widehat{Q}^i$, (7.4), it is clear that the points satisfying this condition are exactly the singularities of $\widehat{\mathrm{H}\Lambda}_i$.

The manifold $\mathrm{H}\Lambda$ is generically a smooth elliptic threefold, while $\widehat{\mathrm{H}\Lambda}_i$ is an elliptically fibred singular variety (see figure 7.2). To see this explicitly, let us choose the base of the fibration to be $\mathbb{P}^1_m \times \mathbb{P}^1_n$. We can view the polynomial $\widehat{Q}^i$ as a biquadratic whose coefficients depend on Y_m and Y_n.

$$\widehat{Q}^i(Y_j, Y_k) \;=\; \sum_{a,b=0}^{2} A_{a,b}(Y_m, Y_n)\, Y_j^a\, Y_k^b, \tag{7.5}$$

where $A_{a,b}$ are functions of the base coordinates Y_m, Y_n. The exact form of these functions depends on the choice of the Calabi-Yau manifold $\mathrm{H}\Lambda$. This defines a biquadric subvariety $E_{i;m,n}$ of $\mathbb{P}^1_j \times \mathbb{P}^1_k$, which is a Calabi-Yau variety of dimension one, and thus an elliptic curve.

$$\begin{array}{ccc} & & \mathrm{H}\Lambda \\ & & \big\downarrow{\scriptstyle \pi_i} \\ E_{i;m,n} & \hookrightarrow & \widehat{\mathrm{H}\Lambda}_i \\ & & \big\downarrow{\scriptstyle \pi_{m,n}} \\ & & \mathbb{P}^1_m \times \mathbb{P}^1_n. \end{array}$$

Figure 7.2: *The Elliptic Fibration on $H\Lambda_i$ with base $\mathbb{P}^1_m \times \mathbb{P}^1_n$.*

Any biquadratic in $\mathbb{P}^1_m \times \mathbb{P}^1_n$ can be transformed into the Weierstrass form [86]. To this end, one first computes the quadratic discriminant of (7.5) with respect to Y_j.

$$\mathcal{D}_n(Y_k) = \left(\sum_{a=0}^{2} A_{a,1} Y_k^i\right)^2 - 4\left(\sum_{a=0}^{2} A_{i,2} Y_k^i\right)\left(\sum_{i=0}^{2} A_{i,0} Y_k^i\right) \;\stackrel{\text{def}}{=}\; b_4 Y_k^4 + 4b_3 Y_k^3 + 6b_2 Y_k^2 + 4b_1 Y_k + b_0 \ .$$

One computes the two "Eisenstein invariants of plane quartics" defined in [86] for this polynomial:

$$D_{m,n} \;=\; b_4 b_0 + 3b_2^2 - 4b_3 b_1 \ ,$$

$$E_{m,n} \;=\; b_4 b_1^2 + b_3^2 b_0 - b_4 b_2 b_0 - 2b_3 b_2 b_1 + b_2^3 \ ,$$

where each b_a is a function of Y_m and Y_n. These can be used to write the Weierstrass form of the elliptic fibre as

$$y^2 \;=\; x^3 - D_{m,n} x + 2E_{m,n} \ .$$

The discriminant of this elliptic curve is

$$\Delta_{i;\,m,n} \;=\; -D_{m,n}^3 + 27 E_{m,n}^2 \ ,$$

where the index i refers to the coordinate with respect to which we have contracted HΛ in order to obtain the singular manifold $\widehat{\mathrm{H}\Lambda}_i$, and the indices m and n refer to the choice of the base of the fibration. It is useful to observe that the discriminants satisfy the relations

$$\Delta_{i;\,m,n} \;=\; \Delta_{j;\,m,n} \;=\; \Delta_{k;\,m,n} \ ,$$

In other words, for the purposes of computing the discriminant on the base $\mathbb{P}_m \times \mathbb{P}_n$, it does not matter which contraction we choose. We plot the zero loci for three $\Delta_{i;\,m,n}$ in figure 7.4.

In a generic case, $\Delta_{i;\,m,n}$ is an irreducible bidegree $(24, 24)$ polynomial.

$$\Delta_{i;\,m,n}(Y_m, Y_n) \;=\; \sum_{a,b=0}^{24} \alpha_{a,b} Y_m^a \, Y_n^b \ .$$

In case the manifold is symmetric under $\mathbb{Z}_2$ or $\mathbb{Z}_2 \times \mathbb{Z}_2$, the discriminant satisfies one or both of the following symmetry relations:

$$Y_m^{24} \, Y_n^{24} \, \Delta_{i;\,m,n}\left(\frac{1}{Y_m}, \frac{1}{Y_n}\right) \;=\; \Delta_{i;\,m,n}(Y_m, Y_n) \ , \qquad \Delta_{i;\,m,n}(-Y_m, -Y_n) \;=\; \Delta_{i;\,m,n}(Y_m, Y_n) \ .$$

A sketch of Δ for such a $\mathbb{Z}_2 \times \mathbb{Z}_2$ symmetric case is given in figure 7.3. The vanishing locus of Δ corresponds to the singular locus of elliptic fibres. The types of singular fibres on elliptic surfaces have been classified by Kodaira [77, 78]. Table 7.1 below contains the cases relevant for us.

Type	Ord(D)	Ord(E)	Ord(Δ)	Dynkin Label	Fibre	Number
I_1	0	0	1	A_1	1 nodal curve	Continuum
I_2	0	0	2	A_2	2 curves meeting at 2 points	200
II	1	1	2	A_1	1 cuspidal curve	192

Table 7.1: *The Kodaira classification of singular fibres that appear in the elliptic fibration over the base* $\mathbb{P}^1_m \times \mathbb{P}^1_n$.

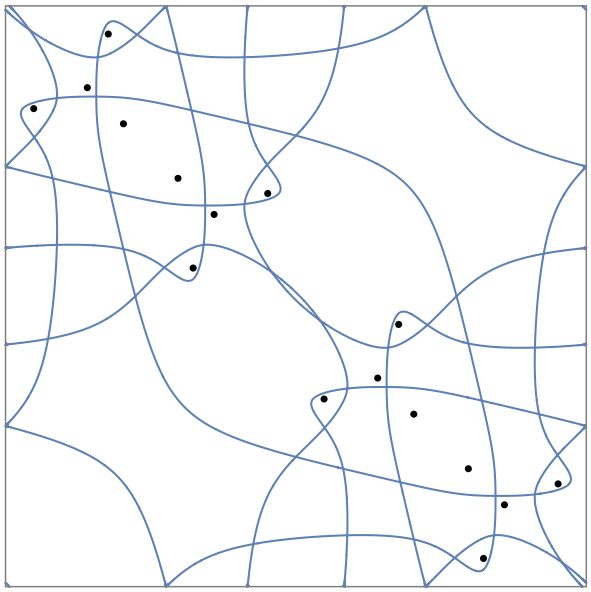


Figure 7.3: *A sketch of the discriminant locus in $\mathbb{P}^1\times\mathbb{P}^1$. Opposite edges of the figure are understood to be identified. The real section is drawn. The isolated dots that do not appear to lie on the discriminant locus are 'space invaders' that lie on suppressed complex branches of the curve. The sketch is made for a $\mathbb{Z}_2\times\mathbb{Z}_2$-symmetric variety as in* (5.20)*, and so the figure is invariant under two reflections. For the values of the parameters for which the sketch is drawn, none of the 192 cusps lie in the real section.*

Generically $\Delta_{i;\,m,n}$ is irreducible, so a generic point on the curve $\Delta_{i;\,m,n}=0$ corresponds to a singularity of the type I_1. In other words, the fibre over a generic point over $\{\Delta_{i;\,m,n}=0\}\subset\mathbb{P}^1_m\times\mathbb{P}^1_n$ is a nodal curve. This is related to the fibration structure of the manifold. Namely, the generic fibre over the projection $\mathrm{H}\Lambda\to\mathbb{P}^1_n$ is a K3 surface. Furthermore, a K3 surface can be realised as an elliptic fibration over $\mathbb{P}^1_m$ with exactly 24 nodal curves. As $\Delta_{i;\,m,n}$ is a bidegree-24 polynomial, a generic fibre over $\mathbb{P}^1_n$ is an elliptically fibred $\mathbb{P}^1_m$ with 24 nodal fibres.

In addition to these generic points, the discriminant curve $\Delta_{i;\,m,n}=0$ itself has singularities. We find that on $\widehat{\mathrm{H}\Lambda}_i$ these fall into two categories, corresponding to cases I_2 and II in the Kodaira classification. In the generic case, there are 200 points of type I_2 and 192 of type II. These account for all 392 singularities on a generic curve. In accordance with the Kodaira classification, on singularities of type I_2, the polynomials $\widehat{Q}^i(Y_m,Y_n)$ factorise, with each factor corresponding to an irreducible rational curve. The two components meet at two points, which are the singularities of the fibre. The only exceptions to this are fibres which contain degree-5 rational curves on $\mathrm{H}\Lambda$ — the second component of such a fibre is a degree-1 rational curve. When this curve is parallel to $\mathbb{P}_i$, it is exactly the line which has been blown down to obtain $\widehat{\mathrm{H}\Lambda}_i$, and thus does not appear in the fibres on $\widehat{\mathrm{H}\Lambda}_i$.

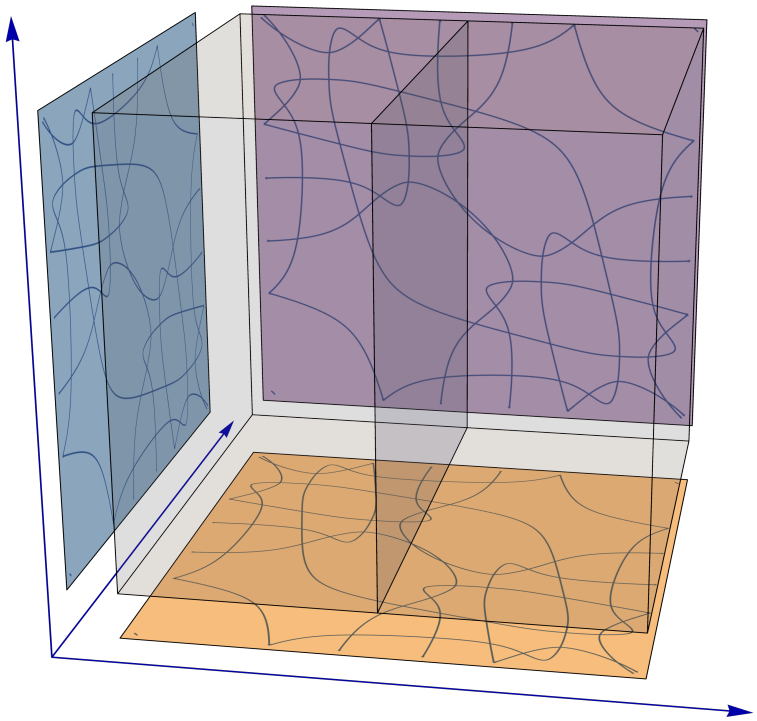


Figure 7.4: *A heuristic sketch of the multiple fibrations. Each axis corresponds to a* $\mathbb{P}^1$*, and the indicated plane corresponds to a K3 fibre of a projection to one of the* $\mathbb{P}^1$*'s.*

In what follows, we mostly study the fibres on the singular varieties $\widehat{\mathrm{H}\Lambda}_i$. However, using the birational map between $\widehat{\mathrm{H}\Lambda}_i$ and $\mathrm{H}\Lambda$ we can lift the curves on $\widehat{\mathrm{H}\Lambda}_i$ found this way to curves on $\mathrm{H}\Lambda$. Outside of the exceptional divisors the lift preserves the structure of the fibres. The two-component fibres of Kodaira type I_2 are unions of degree-1, -2, -3, -4, and -5 rational curves. In particular, the singular fibres include all lines, quadrics and cubics. We discuss each of these cases in detail in the following sections §7.3, §7.4, and §7.5. First, however, it is convenient to briefly review some general aspects of curves on $(\mathbb{P}^1)^5$.

7.2 Complete intersection curves on $(\mathbb{P}^1)^5$

It turns out that the curves we consider in the following can be expressed as complete intersections of four polynomials in $(\mathbb{P}^1)^5$. The degrees and Euler characteristics of such curves are calculable by elementary techniques. Complete intersections on $(\mathbb{P}^1)^5$ can be systematically searched for, and doing this we obtain some evidence, consistent with the predictions of mirror symmetry, that there are no more curves than those we find here. We consider one-dimensional varieties defined by four equations

$$p^1 \;=\; p^2 \;=\; p^3 \;=\; p^4 \;=\; 0\;, \qquad \text{with} \qquad \deg_i\left(p^\alpha\right) = n_i^\alpha . \tag{7.6}$$

The two-form dual to the subvariety $p^\alpha = 0$ is given by

$$\mathcal{P}^\alpha \;=\; \sum_{i=0}^{4} n_i^\alpha J_i\;,$$

where J_i is the Kähler, or equivalently volume, form of $\mathbb{P}^1_i$. Then the dual form of the curve $p^1 = p^2 = p^3 = p^4 = 0$ is

$$C \stackrel{\text{def}}{=} \mathcal{P}^1 \wedge \mathcal{P}^2 \wedge \mathcal{P}^3 \wedge \mathcal{P}^4 = \sum_{\varsigma\in S_5} n^1_{\varsigma(1)} n^2_{\varsigma(2)} n^3_{\varsigma(3)} n^4_{\varsigma(4)}\, J_{\varsigma(1)} \wedge J_{\varsigma(2)} \wedge J_{\varsigma(3)} \wedge J_{\varsigma(4)} \ ,$$

where the sum runs over all permutations of $\{0,\ldots,4\}$. The i'th degree of a curve $\mathcal{C}$ dual to C is

$$\deg_i(\mathcal{C}) = \int_{(\mathbb{P}^1)^5} J_i \wedge \mathcal{C} = \sum_{\substack{\varsigma\in S_4\\ a,b,c,d\neq i}} n^1_{\varsigma(a)} n^2_{\varsigma(b)} n^3_{\varsigma(c)} n^4_{\varsigma(d)} \ . \tag{7.7}$$

The total Chern class of the curve (7.6) is given by

$$c(\mathcal{C}) = \frac{\prod_{i=0}^4 (1+J_i)^2}{\prod_{\alpha=1}^4 (1+\sum_{i=0}^4 n_i^\alpha J_i)} \ .$$

It is straightforward to compute the Euler characteristic from the first Chern class:

$$\chi(\mathcal{C}) = \sum_{\varsigma\in S_5} \left(2 - \sum_{\alpha=1}^4 n^\alpha_{\varsigma(0)}\right) n^1_{\varsigma(1)} n^2_{\varsigma(2)} n^3_{\varsigma(3)} n^4_{\varsigma(4)} = 2\deg(\mathcal{C}) - \sum_{i=0}^4 \sum_{\alpha=1}^4 n_i^\alpha \deg_i(\mathcal{C}) \ . \tag{7.8}$$

These formulae give the degrees and genera of various curves in the following sections. The degrees defined in this way will also agree with the degrees of isomorphisms $\varphi : \mathbb{P}^1 \to \mathcal{C}$.

As we are interested in curves in the Calabi-Yau manifold HΛ, we need to make sure that the curve $\mathcal{C}$ lies completely within this manifold. In the language of algebraic geometry, this is equivalent to requiring that the radical of the ideal generated by the polynomials p_i contains the polynomials Q^1 and Q^2 which define the HΛ manifold.

It is often convenient to study the lines and other curves on the singular spaces $\widehat{\text{H}\Lambda}_i$, where their connection to the elliptic fibration can be immediately appreciated. Given a curve $\mathcal{C}$, and a projection π to a base B, $\mathcal{C}$ may project to a curve of B or to a point. If $\mathcal{C}$ projects to a curve, it is said to be *horizontal* with respect to the projection π, and if it projects to a point it is said to be *vertical* with respect to π. We study each case in turn, and show that the lines can be uniquely associated to a unique degree-5 line and to a node in the discriminant $\Delta_{i;\,m,n}$.

7.3 Lines

Every degree-1 rational curve in $(\mathbb{P}^1)^5$ is given by a set of four linear equations, each in a single variable. These read, for some $j \in \{0,1,2,3,4\}$ and each $s \in \{0,1,2,3,4\} \setminus j$,

$$Y_s - y_s = 0 \ . \tag{7.9}$$

In this way a point $\boldsymbol{y} = (y_i, y_k, y_m, y_n)$ defines a line L_j which is parallel to $\mathbb{P}^1_j$. Using the data of equations (7.9), the formulae (7.7) and (7.8) tell us that

$$\deg_i(L_j) = \delta_{ij} \ , \qquad \chi(L_j) = 2 \ ,$$

which is exactly as expected for a line. For a line L_j to lie on HΛ, the solutions to (7.9) must additionally satisfy $Q^1 = Q^2 = 0$. A substitution reveals that this condition amounts to

$$\alpha_j(\boldsymbol{y})Y_j + \beta_j(\boldsymbol{y}) \;=\; 0 \;, \qquad \gamma_j(\boldsymbol{y})Y_j + \delta_j(\boldsymbol{y}) \;=\; 0 \;.$$

Therefore the $\boldsymbol{y}$ must solve $\alpha_j = \beta_j = \gamma_j = \delta_j = 0$, and so gives a singularity on $\widehat{\mathrm{H}\Lambda}_j$. As has already been mentioned, these equations have 24 solutions for each j. There are therefore $5 \times 24 = 120$ lines. In the $\mathbb{Z}_5$ symmetric case, the permissible values of $\boldsymbol{y}$ group into $\mathbb{Z}_5$ orbits and the quotient procedure leaves us with 24 lines. Similarly, in the $\mathbb{Z}_2$ symmetric cases, the involution $Y_i \mapsto -Y_i$ (or equivalently $Y_{i,0} \leftrightarrow Y_{i,1}$) identifies two lines. On $\mathrm{H}\Lambda/(\mathbb{Z}_5 \times \mathbb{Z}_2)$ there are therefore 12 lines, each descending from a family of 10 lines on the covering space. The generic $\mathbb{Z}_5 \times \mathbb{Z}_2 \times \mathbb{Z}_2$ quotient contains exactly 6 lines.

7.3.1 Horizontal lines

For definiteness, let us consider the projection π_4, the lines L_2, and take the elliptic fibration $E_{4;0,1}$ with base $\mathbb{P}^1_0 \times \mathbb{P}^1_1$. The lines L_2 on HΛ can be understood to arise as blow-ups of singular points $\boldsymbol{y}$ on $\widehat{\mathrm{H}\Lambda}_2$, and can be given by the embedding

$$z \mapsto (y_0, y_1, z, y_3, y_4) \;.$$

The projection π_4 then takes this line to a line in $\widehat{\mathrm{H}\Lambda}_4$, given by the embedding

$$z \mapsto (y_0, y_1, z, y_3) \;.$$

Thus L_2 forms part of the fibre of $E_{4;0,1}$ lying over the basepoint (y_0, y_1). Tautologically, this fibre can be realised as the curve defined by the equation

$$\widehat{Q}^4(y_0, y_1, Y_2, Y_3) \;=\; 0 \;.$$

Reflecting the fact that this fibre contains a line and hence is reducible, the above polynomial factorises into degree-1 and degree-3 pieces (in homogeneous coordinates). The first factor is of course the equation of the image of the line L_2 in $\widehat{\mathrm{H}\Lambda}_4$.

The second factor of $\widehat{Q}^4$ has degree $(1, 2)$ with respect to Y_2, Y_3, and thus is a multi-degree $(0, 0, 1, 2)$ curve $\widehat{\mathcal{C}}_{(0,0,1,2)}$, which meets the line at two points. The map

$$z \mapsto (y_0, y_1, z, r_2(z)) \tag{7.10}$$

is a degree-$(0, 0, 1, 2)$ isomorphism taking $\mathbb{P}^1$ to $\widehat{\mathcal{C}}_{(0,0,1,2)}$.

These curves lift to degree-5 curves $\mathcal{C}_{(0,0,1,2,2)}$ on HΛ. The equations $Q^1 = Q^2 = 0$ are solved by setting $Y_4 = -\frac{\beta_4}{\alpha_4} = -\frac{\delta_4}{\gamma_4}$. Note that α_4 and β_4 are both linear in Y_0 and Y_1, so substituting in the values of Y_0 and Y_1 in terms of z from (7.10) into the ratio $\frac{\beta_4(z)}{\alpha_4(z)}$ gives a rational function $\widetilde{r}_2(z)$ of

degree 2, as the quantities $\alpha_4(z)$ and $\beta_4(z)$ have exactly one linear factor in common. We arrive at a curve $\mathcal{C}_{(0,0,1,2,2)}$ with an isomorphism $\psi_{4;,0,1;2} : \mathbb{P}^1 \to \mathcal{C}_{(0,0,1,2,2)}$ given by

$$\psi_{4;0,1;2}(z) \;=\; (y_0, y_1, z, r_2(z), \widetilde{r}_2(z)) \;\; . \tag{7.11}$$

Therefore, on HΛ the fibre over basepoint (y_0, y_1) consists of two rational curves that meet in two points. According to Kodaira's classification, the point (y_0, y_1) must be a node on the discriminant of this elliptic fibration. Upon projection to $\widehat{\mathrm{H}\Lambda}_4$, this becomes a node of $\Delta_{4;\,0,1}$, which is indeed what we find in the examples we have studied.

Other maps $\psi_{i;m,n;j}$ are defined similarly, with the privileged role of Y_4, Y_0, Y_1, Y_2 in this construction replaced by Y_i, Y_m, Y_n, Y_j. We display the interplay between these maps and projections in figure 7.5.

$$\begin{array}{ccccc}
 & & \mathrm{H}\Lambda \supset L_i & \xleftarrow[\pi_j^{-1}]{} & \boldsymbol{y} \subset \widehat{\mathrm{H}\Lambda}_j \\
 & & \downarrow{\scriptstyle \pi_i} & & \\
\mathbb{P}^1 & \xrightarrow{\psi_{i;m,n;j}} & L_j \subset E_{i;m,n} & \hookrightarrow & \widehat{\mathrm{H}\Lambda}_i \\
 & & & & \downarrow{\scriptstyle \pi_{m,n}} \\
 & & & & \mathbb{P}^1_m \times \mathbb{P}^1_n
\end{array}$$

Figure 7.5: *A chain of birational maps allows us to see lines $L_i^{(a)}$, corresponding to a singularity of $\widehat{H\Lambda}_j$ at $\boldsymbol{y}^{(a)}$ explicitly as singular fibres on $\widehat{H\Lambda}_i$ viewed as a fibration over $\mathbb{P}^1_m \times \mathbb{P}^1_n$. The polynomial $\widehat{Q}^i(Y_m, Y_n)$ factorises into two factors, one of degree $(0,1)$, corresponding to the line, and the other of degree $(2,1)$. This latter factor corresponds to a projection of a degree-5 curve down to $\widehat{H\Lambda}_i$.*

7.3.2 Vertical lines

Let us now focus our attention to the line L_4, which is mapped to point[1] $\boldsymbol{y}$ by π_4. By symmetry, over the point (y_0, y_1) on the base $\mathbb{P}^1_0 \times \mathbb{P}^1_1$ in HΛ, the fibre is given by the union of the line L_4 together with a degree-5 curve $\mathcal{C}_{(0,0,2,2,1)}$, which meets the line in two points. Projecting this fibre down to $\widehat{\mathrm{H}\Lambda}_4$ maps the line to a point $\boldsymbol{y}$, and the degree-5 curve to a degree-4 curve $\widehat{\mathcal{C}}_{(0,0,2,2)}$, which intersects itself at the point $\boldsymbol{y}$. So there exists a birational map $\mathbb{P}^1 \to \mathcal{C}_{(0,0,2,2)}$

$$z \mapsto \left(y_0^{(a)}, y_1^{(a)}, r_2(z), \widetilde{r}_2(z)\right) \;\; , \tag{7.12}$$

which is not, however, an isomorphism due to the self-intersection. Such a curve will not fit Kodaira's classification, which can be traced back to the fact that $\widehat{\mathrm{H}\Lambda}_4$ is singular. Indeed, the lift of the fibre is a union of two rational curves meeting at two points, and thus corresponds to a node in the discriminant locus of the fibration HΛ. Upon projecting down to HΛ, this becomes a node of the locus $\Delta_{4;\,0,1} = 0$. An alternative way of arriving at the same conclusion is by noting that, as we

[1] This point is not necessarily the same as the $\boldsymbol{y}$ in the previous subsection.

have remarked previously, $\Delta_{4;\,0,1} = \Delta_{2;\,0,1}$, and by the previous subsection, L_4 corresponds to a node of $\Delta_{2;\,0,1} = 0$.

A straightforward generalisation of the the results of the last two subsections reveals that the 72 lines L_i, L_j, and L_k, together with the degree-5 curves, account for 72 of the nodes of the discriminant locus $\Delta_{i;\,m,n} = 0$. The locus has in total 200 nodes, the rest of which turn out to correspond to curves of degrees 2, 3, and 4, as we show shortly.

Figure 7.6 displays the lifts of singular fibres in $\widehat{\mathrm{H}\Lambda}_4$ to $\mathrm{H}\Lambda$.

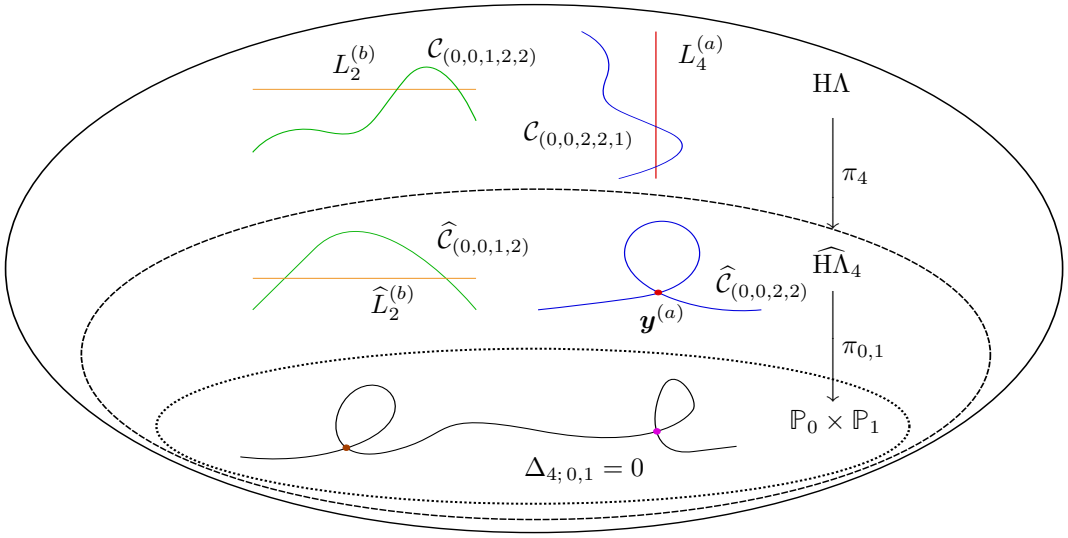


Figure 7.6: *Schematic representation of elliptic fibres containing lines on HΛ. For concreteness, we have chosen here $i = 4$, $m = 0$, and $n = 1$. The largest oval represents the smooth manifold HΛ, on which the elliptic fibres over $\mathbb{P}_0 \times \mathbb{P}_1$ contain unions of two rational curves. Here we have pictures of the fibres which consist of one line and a degree-5 curve.*

7.4 Quadrics

The analysis of irreducible degree-2 curves proceeds largely along the same lines. Algebraic quadrics on HΛ can be expressed, for a triple k, m, n and with constants q_k, q_m, q_n, as the complete intersections

$$Y_k - q_k \;=\; 0\;, \quad Y_m - q_m \;=\; 0\;, \quad Y_n - q_n \;=\; 0\;, \quad p\,(Y_0, Y_1, Y_2, Y_3, Y_4) \;=\; 0\;. \tag{7.13}$$

Here, p is an irreducible multi-degree $(1,1,1,1,1)$ polynomial. With i, j denoting the pair in

$$\{0,1,2,3,4\} \setminus \{k,m,n\}\;,$$

the equations (7.13) define a curve $\mathcal{C}$ with

$$\deg_s(\mathcal{C}) \;=\; \delta_{s,i} + \delta_{s,j}, \qquad \chi(\mathcal{C}) \;=\; 2.$$

While this is not the most general form of degree-2 curve on $(\mathbb{P}^1)^5$, it can be shown that only curves of this form lie in HΛ. To ensure that a curve defined by (7.13) lies in HΛ, we must have that,

specialising to $Y_i = q_i, Y_j = q_j, Y_k = q_k$,

$$Q^1, Q^2 \in \sqrt{\langle p \rangle} \;=\; \langle p \rangle \;.$$

The square root indicates the radical of the ideal $\langle p \rangle$, which in this case is the ideal itself. As p is irreducible and all three polynomials Q^1, Q^2, p are multi-degree (1,1,1,1,1), this requires $p = CQ^1$ or $p = CQ^2$, with C a constant. Further, we must have either $Q^1 = Q^2$ or one of the Q's vanishing at $Y_k = q_k, Y_m = q_m, Y_n = q_n$. We cannot have both Q's vanishing after this specialisation. In general there are 24 values of $\{q_k, q_m, q_n\}$ for which these conditions are satisfied. There are 10 ways of choosing the triple k, m, n, and so we find 240 curves of degree 2 on HΛ. In the $\mathbb{Z}_5$, $\mathbb{Z}_5\times\mathbb{Z}_2$, and $\mathbb{Z}_5\times\mathbb{Z}_2\times\mathbb{Z}_2$ symmetric cases, these curves come in families of 5, 10, and 20, respectively, so taking the quotient by $\mathbb{Z}_5$ gives exactly 48 curves on H$\Lambda/\mathbb{Z}_5$, 24 on H$\Lambda/\mathbb{Z}_5\times\mathbb{Z}_2$, and 12 on H$\Lambda/\mathbb{Z}_5\times\mathbb{Z}_2\times\mathbb{Z}_2$. This agrees with the results of [10].

Again, an alternative point-of-view can be obtained by viewing these quadrics as fibres of the elliptic fibrations $\widehat{\mathrm{H}\Lambda}_i \to \mathbb{P}^1_m \times \mathbb{P}^1_n$. Consider the case $(i, j, k, m, n) = (4, 2, 3, 0, 1)$. The quadrics $\mathcal{C}_{(0,0,1,1,0)}$ are isomorphic to $\mathbb{P}^1$ with the map given by

$$z \mapsto (q_0, q_1, z, r_1(z), q_4)\,.$$

Upon projection by π_4, this becomes a quadric on $\widehat{\mathrm{H}\Lambda}_4$ with embedding

$$z \mapsto (q_0, q_1, z, r_1(z))\,.$$

The fibre to which this belongs is given by $\widehat{Q}^4(q_0, q_1, Y_2, Y_3)$, which factorises into two degree $(1,1)$ factors, with the first one corresponding to the quadric $\widehat{\mathcal{C}}_{(0,0,1,1)}$. The second curve $\widehat{\mathcal{C}}_{(0,0,1,1)}$ is also a quadric on $\widehat{\mathrm{H}\Lambda}_4$, but can be lifted to H$\Lambda$. To do this, set $Y_4 = -\frac{\beta_4}{\alpha_4}$, to ensure that the lifted curve lies in HΛ. Expressing α_4 and β_4 in terms of z, the parameter on the curve, this is generically a degree-2 rational function. Thus the lift $\mathcal{C}_{(0,0,1,1,2)}$ is a degree-4 curve isomorphic to $\mathbb{P}^1$ via

$$z \mapsto (q_0, q_1, z, r_1(z), r_2(z))\,.$$

Similarly, by symmetry, we know that there exists a fibre on HΛ which consists of the curves $\mathcal{C}_{(0,0,0,1,1)}$ and $\mathcal{C}_{(0,0,2,1,1)}$. Projecting them down to $\widehat{\mathrm{H}\Lambda}_4$ gives a line and cubic, $\widehat{\mathcal{C}}_{(0,0,0,1)}$ and $\widehat{\mathcal{C}}_{(0,0,2,1)}$, meeting in two points. By symmetry, the curves $\mathcal{C}_{(0,0,1,1,2)}$ and $\mathcal{C}_{(0,0,1,1,0)}$ studied above also meet in two points, in accordance with Kodaira's classification. Thus the 72 quadrics of the form $\mathcal{C}_{(0,0,1,1,0)}$, $\mathcal{C}_{(0,0,1,0,1)}$, and $\mathcal{C}_{(0,0,0,1,1)}$ also each correspond to a unique node of the discriminant locus $\Delta_{4;\,0,1}$.

7.5 Cubics

Cubic curves whose multi-degree is a permutation of $(1,1,1,0,0)$ can be expressed as complete intersections. The most general cubic curves that can be defined by four multilinear equations are of the form

$$\begin{aligned} Y_m - c_m &= 0\,, \\ Y_n - c_n &= 0\,, \\ p \stackrel{\text{def}}{=} a_0 + a_1 Y_i + a_2 Y_j + a_3 Y_i Y_j &= 0\,, \\ q \stackrel{\text{def}}{=} b_0 + b_1 Y_k + b_2 Y_j + b_3 Y_k Y_j &= 0\,, \end{aligned}$$

This defines a curve $\mathcal{C}_3$ with

$$\deg_i(\mathcal{C}_3) \;=\; \delta_{i,l} + \delta_{i,m} + \delta_{i,n}, \qquad \chi(\mathcal{C}_3) \;=\; 2.$$

Curves of this form include all cubics lying in HΛ. To sit in HΛ, the ideal generated by these polynomials must contain the polynomials Q^1 and Q^2. This condition is equivalent to requiring that there are coefficients d_a, e_b such that when $Y_m = c_m$, $Y_n = c_n$

$$Q^1 \;=\; d_1\,p + d_2\,q + d_3\,p\,Y_k + d_4\,q\,Y_i\;, \qquad Q^2 \;=\; e_1\,p + e_2\,q + e_3\,p\,Y_k + e_4\,q\,Y_i\;.$$

For a quintuple (i,j,k,m,n) there are in general exactly 112 solutions to these equations. Summing over the 10 distinct choices of (i,j,k,m,n) gives us 1120 curves of degree 3, which once again come in $\mathbb{Z}_5$, $\mathbb{Z}_5\times\mathbb{Z}_2$, and $\mathbb{Z}_5\times\mathbb{Z}_2\times\mathbb{Z}_2$ invariant families in the symmetric cases. Taking the quotients with respect to $\mathbb{Z}_5$, $\mathbb{Z}_5\times\mathbb{Z}_2$, and $\mathbb{Z}_5\times\mathbb{Z}_2\times\mathbb{Z}_2$ leave 224, 112, and 56 curves of degree 3, respectively, in agreement with [10].

As was the case with the lines and quadrics, the cubics also appear as singular fibres of elliptic fibrations, and in fact account for the remaining 56 nodes of the discriminant locus $\Delta_{i;\,m,n} = 0$. Take again $(i,j,k,m,n) = (4,2,3,0,1)$ to expedite the discussion, and consider the cubic curves $\mathcal{C}_{(0,0,1,1,1)}$. The projection of this curve to $\widehat{\text{H}\Lambda}_4$ is a quadric $\widehat{\mathcal{C}}_{(0,0,1,1)}$. As before, this indicates that the polynomial $\widehat{Q}^4(Y_2,Y_3)$ factorises into two components, both of degree $(1,1)$. The isomorphisms with $\mathbb{P}^1$ are of the form

$$z \mapsto (c_0, c_1, z, r_1(z))\,.$$

The quantity $\frac{\beta_4}{\alpha_4}$ determining the lift to a curve on HΛ is a priori a ratio of two degree-2 polynomials. However, this is a component of a reducible elliptic fibre inside of which we already have a curve of total degree 3, therefore the two polynomials α_4, β_4 must share a factor so that the lifts are curves $\mathcal{C}_{(0,0,1,1,1)}$. The isomorphisms with $\mathbb{P}^1$ are given by

$$z \mapsto (c_0, c_1, z, r_1(z), \widetilde{r}_1(z))\,.$$

7.6 Summary

This completes the classifications of fibres over the nodes of the discriminant curves on singular varieties $\widehat{\mathrm{H}\Lambda}_i$ (over the base $\mathbb{P}_m \times \mathbb{P}_n$), and their lifts to H$\Lambda$. We summarise our findings in table 7.2 and table 7.3, taking $i = 4$, $m = 0$, $n = 1$ for concreteness.

Type	Degree 1	Degree 2	Curve 1	Curve 2	Number
Line	(0,0,0,0)	(0,0,2,2)	L_4	$\mathcal{C}_{(0,0,2,2,1)}$	24
Line	(0,0,1,0)	(0,0,1,2)	L_2	$\mathcal{C}_{(0,0,1,2,2)}$	24
Line	(0,0,0,1)	(0,0,2,1)	L_3	$\mathcal{C}_{(0,0,2,1,2)}$	24
Quadric	(0,0,1,1)	(0,0,1,1)	$\mathcal{C}_{(0,0,1,1,0)}$	$\mathcal{C}_{(0,0,1,1,2)}$	24
Quadric	(0,0,1,0)	(0,0,1,2)	$\mathcal{C}_{(0,0,1,0,1)}$	$\mathcal{C}_{(0,0,1,2,1)}$	24
Quadric	(0,0,0,1)	(0,0,2,1)	$\mathcal{C}_{(0,0,0,1,1)}$	$\mathcal{C}_{(0,0,2,1,1)}$	24
Cubic	(0,0,1,1)	(0,0,1,1)	$\mathcal{C}_{(0,0,1,1,1)}$	$\mathcal{C}_{(0,0,1,1,1)}$	56

Table 7.2: *Factorisations of $\widehat{Q}_4$ over the nodes of the discriminant curve $\Delta_{4;\,0,1} = \Delta_{3;\,0,1} = \Delta_{2;\,0,1}$ and the corresponding curves on the non-singular variety HΛ.*

$\mathfrak{p}$	$n_{\mathfrak{p}}$
(0,0,0,0,1)	24
(0,0,0,1,1)	24
(0,0,0,0,2)	0
(0,0,1,1,1)	112
(0,0,0,1,2)	0
(0,0,0,0,3)	0
(0,0,1,1,2)	24
(0,0,0,1,3)	0
(0,0,0,0,4)	0
(0,0,1,2,2)	24
(0,0,0,1,4)	0
(0,0,0,0,5)	0

Table 7.3: *The results of this section, giving the curve-counts for some low degrees. The numbers that are related to these by a cyclic permutation are omitted. Note the agreement with table 6.2.*

Part III

Supersymmetric Flux Vacua on Hulek-Verrill Manifolds

We study supersymmetric flux vacua in compactifications of type IIB string theory and F-theory on the five-parameter Hulek-Verrill manifolds. Supersymmetric flux vacua and rank-two attractor points have a close relation to modularity of the compactification manifolds. This connection can be seen explicitly by finding the zeta functions of the compactification manifolds as functions of the complex structure parameters. To achieve this, we generalise the methods of Candelas, de la Ossa, and van Straten to multiparameter manifolds. We compile tables of zeta function numerators of symmetric Hulek-Verrill manifolds with all complex structure parameters equal. Corresponding to the existence of supersymmetric flux vacua, these numerators factorise, and we can associate the flux vacua with elliptic, Hilbert or Bianchi modular forms, depending on whether the complex structure moduli are rational numbers or belong to totally real or imaginary quadratic number fields.

Chapter 8

Introduction

8.1 Introduction

The Hulek-Verrill manifolds have been shown [14] to display modular properties, which are reflected in physics of string theory compactifications on these manifolds. For instance, in [10] rank-two attractor points in Calabi-Yau compactifications of IIB string theory on the $\mathbb{Z}_5$ and $\mathbb{Z}_{10}$ quotients of the S_5 symmetric subfamily of the five-parameter Hulek-Verrill manifolds were studied. The rank-two attractor points can be associated to weight-four modular forms, thus giving a concrete realisation of an idea of Moore's [8, 9] that such attractor points should have a relation to the arithmetic and number theoretic properties of the compactification manifolds.

Rank-two attractor points and the associated BPS black holes are, however, not the only physically interesting objects related to number theoretic aspects of Calabi-Yau manifolds. It was pointed out in [10] and elaborated in detail in [11, 12] that supersymmetric flux compactifications — that is, compactifications of IIB supergravity theory on a Calabi-Yau manifold with a non-trivial three-form flux background — also correspond to the compactification manifold having modular properties, but with the associated modular forms being of weight two.

The physical quantities associated to both rank-two attractor points and supersymmetric flux vacua have been observed to display intriguing relations to number theoretic quantities. For example, the entropy of black holes associated to rank-two attractor points studied in [10] was shown to be expressible in terms of ratios of L-functions associated to the modular forms related to the zeta function at the rank-two attractor points in the moduli space. The solutions with non-trivial three-form fluxes can be lifted to F-theory solutions, and the modular form associated to the F-theory fibre can be identified with the modular form related to the zeta function.

Unfortunately, the number of examples of both modular supersymmetric flux vacua and rank-two attractor points currently available is rather limited, which might raise doubts about the generality of some of the observations made from this data. To amend the deficiency of explicit examples,

we construct novel families of supersymmetric, modular flux vacua on certain class of Hulek-Verrill manifolds. The S_5 or, more generally the $\mathbb{Z}_2$ symmetry, of the manifolds corresponding to certain loci in the five-parameter moduli space can be used to show that these manifolds support supersymmetric flux vacua. The existence of these solutions hinges only on the manifold having of a certain type of $\mathbb{Z}_2$ symmetry, and is thus not limited to Hulek-Verrill manifolds.

To show that the flux vacua we construct are indeed modular, by which we mean that the zeta function numerator factorises and there is a modular form associated to the coefficients appearing in the numerator, we need to develop a practical method of computing zeta functions of multiparameter Calabi-Yau manifolds. A computational method for doing this on one-parameter threefolds was given by Candelas, de la Ossa and van Straten [13], whose method we generalise to cover multiparamater manifolds. This generalisation works for any three-dimensional Calabi-Yau manifold, and in addition to studying flux vacua on Hulek-Verrill manifolds can be used, for example, to search for rank-two attractor points, although we will not undertake such a search here.

8.2 Outline

Zeta functions for multiparameter threefolds

The chapter 9 is devoted to generalising the methods developed by Candelas, de la Ossa and van Straten [13] for computing zeta functions of one-parameter Calabi-Yau threefolds to multiparameter manifolds: We find a suitable basis of the third cohomology, a particularly convenient basis turns out to be given by

$$\left\{\vartheta_0\Omega\ ,\vartheta_i\Omega,\ \vartheta^i\Omega,\ \vartheta^0\Omega\right\}\ ,\quad \text{with}\quad (\vartheta_0,\ \vartheta_i,\ \vartheta^i,\ \vartheta^0)\stackrel{\text{def}}{=}\left(1,\theta_i,\ \widehat{Y}^{ijk}\theta_j\theta_k,\ \frac{\widehat{Y}^{ijk}}{m}\theta_i\theta_j\theta_k\right).$$

The properties of the Frobenius map and Gauss-Manin connection acting on this basis to makes it possible to derive a differential equation satisfied by the matrix $\mathrm{F}_p(\boldsymbol{\varphi})$ representing the action of the Frobenius map Fr_p (see (3.9)) on the third (p-adic) cohomology $H^3(X_{\boldsymbol{\varphi}},\mathbb{Q}_p)$ as a function of the moduli space coordinates $\boldsymbol{\varphi}$. The key to obtaining suitably generalised quantities lies in the analysis of multiparameter mirror maps we undertook in section 2.2. Rather pleasantly, careful study of the conditions the Frobenius map has to satisfy restricts the matrix $\mathrm{U}(\boldsymbol{\varphi}) = \mathrm{F}(\boldsymbol{\varphi})^{-1}$ representing the action of the inverse Frobenius map to take a form analogous to the one-parameter case

$$\mathrm{U}(\boldsymbol{\varphi})\ =\ \mathrm{E}^{-1}(\boldsymbol{\varphi}^p)\mathrm{U}(0)\mathrm{E}(\boldsymbol{\varphi})\ ,$$

where the matrices are given in terms of the (arithmetic) Frobenius basis periods ϖ_a and ϖ^a, and indicial algebra elements ϵ_i, μ^i, and η defined in §2.2.2 by

$$\mathrm{E}(\boldsymbol{\varphi})_a{}^b=\vartheta^b\,\varpi_a(\boldsymbol{\varphi})\ ,\qquad \mathrm{U}(0)=u\Lambda\left(\mathrm{I}+\alpha^i\,\epsilon_i+\beta_i\,\mu^i+\gamma\,\eta\right)\ ,\qquad \Lambda\ =\ \mathrm{diag}(1,p\,\mathbf{1},p^2\,\mathbf{1},p^3)\ , \quad (8.1)$$

where, in the first expression, the indices a and b are understood to stand for both upper and lower indices, making $\mathrm{E}(\boldsymbol{\varphi})$ a $(2m+2)\times(2m+2)$ matrix, and $\mathbf{1}$ is an m-parameter vector with all components equal to 1. The constant u can be set to unity, and β_i can be shown to depend on α_i via relation

$$u \;=\; 1 \;, \qquad \beta_i \;=\; \frac{1}{2}\, Y_{ijk}\alpha^j\alpha^k \;.$$

Unlike in the one-parameter case, the constants α_i do not vanish in general. Rather, they can be found by demanding that the matrix $\mathrm{U}(\boldsymbol{\varphi})$ takes on the rational form

$$\mathrm{U}(\boldsymbol{\varphi}) \;=\; \frac{\mathcal{U}(\boldsymbol{\varphi})}{P(\boldsymbol{\varphi})^p} + \mathcal{O}(p^n) \;,$$

when working to the p-adic accuracy p^n, which in practice means computing the coefficients in the polynomials modulo p^n. Here $\mathcal{U}(\varphi)$ is a matrix the entries of which are polynomials in $\boldsymbol{\varphi}$, and $P(\boldsymbol{\varphi})$ is a polynomial in $\boldsymbol{\varphi}$.

To test our methods and provide useful data for study of modularity of supersymmetric flux vacua, we study two example families of manifolds: As the first example, we take the two-parameter mirror Octic manfolds whose zeta function was studied in [70], the results of which we are able to reproduce and extend. The second example is the S_5 symmetric subfamily of the five-parameter family of Hulek-Verrill manifolds where all complex structure parameters are set equal, $\varphi^i = \varphi$. We provide tables of the zeta function numerators for these manifolds in appendix D.

Supersymmetric flux vacua on Hulek-Verrill manifolds

The zeta function numerators $R(T)$ corresponding to the S_5-symmetric Hulek-Verrill manifolds display a striking factorisation property: over the integers, the degree-12 polynomials $R(T)$ factorise to quadratic and quartic polynomials $R_2(T)$ and $R_4(T)$ to take the form

$$R(T) \;=\; R_2(T)^4 R_4(T) \;.$$

These factorisations can, in fact, be traced back to the S_5 symmetry. This suggests that the manifolds are weight-two modular, and support supersymmetric flux vacua, although, as pointed out in [12], this is not guaranteed by existence of such factorisations alone. However, the S_5 symmetry also guarantees existence of supersymmetric flux vacua corresponding to these manifolds.

In fact, existence of a $\mathbb{Z}_2$ symmetry which exchanges two of the moduli space coordinates is enough to provide solutions to the supersymmetric flux vacuum equations. Consider a $\mathbb{Z}_2$ transformation $\mathfrak{A}_{k,l}$ on the complex structure moduli $\boldsymbol{\varphi}$

$$\mathfrak{A}_{k,l} \,:\, \mathbb{C}^m \to \mathbb{C}^m \,:\, \varphi^k \mapsto \varphi^l \;, \quad \varphi^l \mapsto \varphi^k \;, \quad \varphi^s \mapsto \varphi^s \text{ for } s \neq k,l$$

such that the periods satisfy

$$\widehat{\varpi}^i(\boldsymbol{\varphi}) \;=\; \widehat{\varpi}^j(\mathfrak{A}_{k,l}\boldsymbol{\varphi}) \;, \qquad \widehat{\varpi}_i(\boldsymbol{\varphi}) \;=\; \widehat{\varpi}_j(\mathfrak{A}_{k,l}\boldsymbol{\varphi}) \;.$$

If such a symmetry exists, we choose the flux vectors F and H introduced in (3.19) so that

$$\widehat{F} \stackrel{\text{def}}{=} (\rho^T\Sigma)^{-1}\Sigma F \;=\; \delta_i - \delta_j \;, \qquad \widehat{H} \stackrel{\text{def}}{=} (\rho^T\Sigma)^{-1}\Sigma H \;=\; \delta_{2+m+i} - \delta_{2+m+j} \;,$$

where δ_i are $(2m+2)$-component vectors with i'th component equal to 1, and the others equalling zero. Then by giving τ the value

$$\tau \;=\; \frac{1}{2\pi\mathrm{i}}\,\frac{\partial_{z^k}\left(\varpi^i-\varpi^j\right)}{\partial_{z^k}\left(\varpi^i-\varpi^j\right)}\bigg|_{z^k=z^l}$$

one obtains a solution to the supersymmetric flux vacuum equations.

The flux vacua found this way can be lifted to F-theory solutions with modulus τ of the F-theory curve identified with the axiodilaton, as reviewed in section 3.5.3. Analogously to the results of [11], based on extensive numerical experimentation, we find that the F-theory fibre $\mathcal{E}_F$ agrees, up to a simple modulus-dependent twist, with the elliptic curve $\mathcal{E}_R$ associated to the modular form related to the quadratic factor $R_2(T)$ of the zeta function denominator. This fibre can be written in the Weierstrass form as

$$y^2 \;=\; x^3 + \frac{(1{+}3\varphi)(1{-}15\varphi{+}75\varphi^2{+}3\varphi^3)}{12288}x + \frac{(-1{+}6\varphi{+}3\varphi^3)(1{-}12\varphi{+}30\varphi^2{-}540\varphi^3{+}9\varphi^4)}{3538944}\;. \qquad (8.2)$$

We can test this result by computing the zeta function for various rational values of φ, as well as values in totally real and imaginary quadratic field extensions of $\mathbb{Q}$. In the first case, we find elliptic modular forms, whose associated elliptic curve agrees exactly with the fibre (8.2). In the latter two cases, the associated modular forms are Hilbert and Bianchi modular forms, respectively, and we find a perfect agreement between $\mathcal{E}_R$ and $\mathcal{E}_F$ in all cases we have studied.

These results can be seen as providing extensive evidence for the conjecture made in [12], where a relation between the complex structure modulus in totally real and quadratic imaginary fields and Hilbert and Bianchi modular forms was proposed. In appendix E, we provide tables of points in the complex structure moduli space, together with the modular forms associated to the the elliptic curves $\mathcal{E}_F$ and $\mathcal{E}_R$ corresponding to these points. In each case, we have checked that the Hecke eigenvalues of the modular forms agree at least to the first 50 primes (excluding a small number of bad primes).

8.2.1 Conventions

To avoid cluttering equations with long formulae, we adopt a number of nonstandard conventions. We denote $m \times m$ matrices by symbols in blackboard bold, and m-component vectors with symbols in bold.

Unless otherwise stated, we employ the Einstein summation convention, with the indices $a, b, c, \ldots$ from the beginning of the Latin alphabet taking values $0, \ldots, m$, and the indices $i, j, k, \ldots$ from the middle of the alphabet taking values $1, \ldots, m$.

Chapter 9

Zeta Function

9.1 Frobenius map

Following [13], which builds on the work of Dwork and Lauder [47, 87, 88], we compute the zeta function of a Calabi-Yau manifold X by finding the matrix $\mathrm{F}(\boldsymbol{\varphi})$ representing the action of the Frobenius map defined in (3.8), and then using the relation (3.10) between the Frobenius map and the zeta function.

To better understand how this works, we first define a vector bundle $\mathcal{H}$, whose base is the complex structure moduli space $\mathcal{M}_{\mathbb{C}S}$ of the family $X_{\boldsymbol{\varphi}}$ of Calabi-Yau manifolds we are studying. The fibre over a point $\boldsymbol{\varphi} \in \mathcal{M}_{\mathbb{C}S}$ is the middle cohomology group $H^3(X_{\boldsymbol{\varphi}})$ of the manifold $X_{\boldsymbol{\varphi}}$ corresponding to that point.

$$\begin{array}{ccc} H^3(X_{\boldsymbol{\varphi}}, \mathbb{C}) & \longhookrightarrow & \mathcal{H} \\ & & \big\downarrow \pi \\ & & \mathcal{M}_{\mathbb{C}S} \end{array}$$

Figure 9.1: *The vector bundle $\mathcal{H}$.*

On this bundle, we can define the action of the Frobenius maps $\mathrm{Fr}_{p^n} : \Gamma(\mathcal{M}_{\mathbb{C}S}, H^3) \to \Gamma(\mathcal{M}_{\mathbb{C}S}, H^3)$. There is also a canonical Gauss-Manin connection $\nabla : \Gamma(\mathcal{M}_{\mathbb{C}S}, H^3) \to \Gamma(\mathcal{M}_{\mathbb{C}S}, H^3 \otimes T^*\mathcal{M}_{\mathbb{C}S})$ on $H^3(X_{\mathrm{Teich}(\boldsymbol{\varphi})})$. For our purposes, it will be enough to study the covariant derivatives along the vector fields θ_i. Define the covariant derivatives

$$\nabla_i \stackrel{\mathrm{def}}{=} \nabla_{\theta_i} : \Gamma(\mathcal{M}_{\mathbb{C}S}, H^3) \to \Gamma(\mathcal{M}_{\mathbb{C}S}, H^3) \ . \tag{9.1}$$

The Frobenius map and these derivatives satisfy a compatibility relation, as well as Leibniz rule and linearity relation. For any section $v \in \Gamma(\mathcal{M}_{\mathbb{C}S}, H^3)$ and any function $f : \mathcal{M}_{\mathbb{C}S} \to \mathbb{C}$ on the moduli space, the following relations hold

$$\begin{aligned} p\,\mathrm{Fr}(\nabla_i v) &= \nabla_i(\mathrm{Fr}\, v) \ , \\ \nabla_i\,(f(\boldsymbol{\varphi})v) &= (\theta_i f)(\boldsymbol{\varphi})\, v + f(\boldsymbol{\varphi})\nabla_i v \ , \\ \mathrm{Fr}\,(f(\boldsymbol{\varphi})v) &= f(\boldsymbol{\varphi}^p)\,\mathrm{Fr}(v) \ . \end{aligned} \tag{9.2}$$

Over a generic point in the moduli space, the action of the Frobenius map Fr_{p^n} cannot be reduced, in a natural way, to an action on the middle cohomology as the fibre is not kept fixed under $\boldsymbol{\varphi} \mapsto \boldsymbol{\varphi}^{p^n}$, and the Frobenius map can be viewed as a map between distinct fibres $\mathrm{Fr}_{p^n} : \mathcal{H}_{\boldsymbol{\varphi}} \to \mathcal{H}_{\boldsymbol{\varphi}^{p^n}}$. However, at fixed points of Fr_{p^n}, such as at the Teichmüller representatives $\mathrm{Teich}(\boldsymbol{\varphi})$ of integral vectors $\boldsymbol{\varphi} \in \mathbb{Z}^m$, it is indeed possible to identify the action of Fr_{p^n} on the middle cohomology $H^3(X_{\mathrm{Teich}(\boldsymbol{\varphi})})$. We denote the matrix describing this action, in the basis defined by (9.3) below, by $\mathrm{F}(\boldsymbol{\varphi})$. The Teichmüller representative $\mathrm{Teich}(\boldsymbol{\varphi})$ provides a natural embedding of $\mathbb{Z}_p$ to $\mathbb{Q}_p$, and hence we can identify $X_{\mathrm{Teich}(\boldsymbol{\varphi})}$ with the manifold $X_{\boldsymbol{\varphi}}(\mathbb{F}_p)$ defined over the finite field $\mathbb{F}_p$.

We have thus far purposefully left unspecified the type of the cohomology theory we study. We will be concentrating on two types of cohomologies: The first one is the usual Dolbeault cohomology $H^{i,j}(X, \mathbb{C})$ of a complex manifold, which we can use for performing various computations in a familiar manner. However, for the purposes of finding the zeta function, we need a p-adic cohomology theory, such as the Dwork cohomology [89], which is a more natural theory to study on a manifold defined over a finite field. These cohomology groups $H^3(X, \mathbb{Q}_p)$ are finite-dimensional vector spaces over the field $\mathbb{Q}_p$ of p-adic numbers. Importantly, many of the properties we need to find the action of the Frobenius map are essentially independent of the choice of the cohomology theory [10].

Reformatting this in slightly more pedestrian language, we wish to find the matrix $\mathrm{F}(\boldsymbol{\varphi})$, which can be done by solving a differential equation that follows from the compatibility conditions of the Gauss-Manin connection and the Frobenius map. Having found this map, the zeta function can be computed as the characteristic polynomial of its inverse $\mathrm{U}(\boldsymbol{\varphi})$. As the matrix $\mathrm{F}(\boldsymbol{\varphi})$ is defined in such a way that it is only well-defined when $\boldsymbol{\varphi}$ is a fixed point of the Frobenius maps Fr_{p^n}, we have to evaluate the matrix F at $\mathrm{Teich}(\boldsymbol{\varphi})$.

9.1.1 Basis of the vector bundle $\mathcal{H}$

In order to study the Frobienus map, we need to find a basis of sections of the vector bundle $\mathcal{H}$. A natural choice of sections is given by the holomorphic three-form Ω together with a suitable set of its logarithmic derivatives. These derivatives must be chosen so that the Frobenius map in the given basis is regular in the large complex structure limit. In particular, this implies that the basis must have a certain asymptotic form, and that the sections must be linearly independent in the large complex structure limit.

We will shortly show that such set of sections is given by

$$\Omega\ , \qquad \theta_i\Omega\ , \qquad \widehat{Y}^{ijk}\theta_j\theta_k\Omega\ , \qquad \widehat{Y}^{ijk}\theta_i\theta_j\theta_k\Omega\ . \tag{9.3}$$

It is useful to gather the combinations of derivatives appearing here into a vector

$$\vartheta \stackrel{\text{def}}{=} (\vartheta_0, \vartheta_i, \vartheta^i, \vartheta^0) \stackrel{\text{def}}{=} \left(1, \theta_i, \widehat{Y}^{ijk}\theta_j\theta_k, \frac{\widehat{Y}^{ijk}}{m}\theta_i\theta_j\theta_k\right) \ .$$

Let us denote by $\mathrm{E}(\boldsymbol{\varphi})$ the change-of-basis matrix from the constant basis to this basis. Explicitly, the components of this matrix are given by

$$\mathrm{E}(\boldsymbol{\varphi})_a^{\ b} = \vartheta^b \, \varpi_a(\boldsymbol{\varphi}) \ ,$$

where the indices a and b are understood to stand for both upper and lower indices. With this definition, the asymptotic form of $\mathrm{E}(\boldsymbol{\varphi})$ in the large complex structure limit, $\varphi_i \to 0$ for all i, is given by

$$\mathrm{E}(\boldsymbol{\varphi}) \ = \ \begin{pmatrix} 1 & \mathbf{0}^T & \mathbf{0}^T & 0 \\ \boldsymbol{\ell} & \mathbb{I} & 0 & \mathbf{0} \\ \frac{1}{2!}\,\boldsymbol{\ell}^T\mathbb{Y}_i\boldsymbol{\ell} & \ell^i\mathbb{Y}_i & \mathbb{I} & \mathbf{0} \\ \frac{1}{6!}\,Y_{ijk}\ell^i\ell^j\ell^k & \frac{1}{2!}\,\boldsymbol{\ell}^T\mathbb{Y}_i\boldsymbol{\ell} & \boldsymbol{\ell}^T & 1 \end{pmatrix} + \mathcal{O}(\boldsymbol{\varphi}\log^3\boldsymbol{\varphi}) \ = \ \boldsymbol{\varphi}^{\boldsymbol{\epsilon}} + \mathcal{O}(\boldsymbol{\varphi}\log^3\boldsymbol{\varphi}) \ ,$$

where a free index i corresponds to a row or a column vector.

We also note that the logarithmic derivatives of E can be written in the form

$$(\theta_i \mathrm{E})(\boldsymbol{\varphi}) = \mathrm{E}(\boldsymbol{\varphi})\mathrm{B}_i(\boldsymbol{\varphi}) \ ,$$

which follows from the fact that the basis corresponding to E spans the third cohomology, and can be seen as the statement that $\mathrm{B}_i(\boldsymbol{\varphi})$ are the connection matrices of the Gauss-Manin connections (9.1). We can work out the asymptotics of the matrices B_i in the large complex structure limit by studying the asymptotic form of $\theta_i E$.

$$\theta_i \mathrm{E} \sim \begin{pmatrix} 0 & \mathbf{0} & \mathbf{0} & 0 \\ \boldsymbol{\delta}_i & 0 & 0 & \mathbf{0} \\ \boldsymbol{\ell}\cdot\mathbb{Y}_j\cdot\boldsymbol{\ell} & \mathbb{Y}_i & 0 & \mathbf{0} \\ \frac{1}{2!}\boldsymbol{\ell}\cdot\mathbb{Y}_i\cdot\boldsymbol{\ell} & \boldsymbol{Y}_{ij}\cdot\boldsymbol{\ell} & \boldsymbol{\delta}_i & 1 \end{pmatrix} \ = \ \boldsymbol{\varphi}^{\boldsymbol{\epsilon}}\epsilon_i \ .$$

Comparing this to the asymptotics of $\mathrm{E}(\boldsymbol{\varphi})$, we deduce that in the large complex structure limit

$$\mathrm{B}_i(0) \ = \ \epsilon_i \ .$$

9.1.2 The differential equation satisfied by the Frobenius map

The basic idea is to derive a differential equation satisfied by $\mathrm{F}(\boldsymbol{\varphi})$, and find the solution given the value of the matrix F at some point φ_0 as an initial condition.

Using the compatability conditions (9.2), one can derive the following differential equation for the matrix of the Frobenius action

$$\theta_i(\mathrm{F})(\boldsymbol{\varphi}) \ = \ p\,\mathrm{F}(\boldsymbol{\varphi})\left(\mathrm{B}_i(\boldsymbol{\varphi})\big|_{\boldsymbol{\varphi}\to\boldsymbol{\varphi}^p}\right) - \mathrm{B}_i(\boldsymbol{\varphi})\mathrm{F}(\boldsymbol{\varphi}) \ .$$

The solution to these equations is given by

$$\mathrm{F}(\boldsymbol{\varphi}) \;=\; \mathrm{E}^{-1}(\boldsymbol{\varphi})\mathrm{F}(\boldsymbol{\varphi}_0)\mathrm{E}(\boldsymbol{\varphi}^p)\;, \tag{9.4}$$

where $\boldsymbol{\varphi}_0$ is a fixed initial value. In the following, we will take $\mathrm{F}(\boldsymbol{\varphi}_0)$ to be the limiting value $\mathrm{F}(\mathbf{0}) \stackrel{\mathrm{def}}{=} \lim_{\varphi_i \to 0} \mathrm{F}(\boldsymbol{\varphi})$, as it turns out that it is possible to highly constrain the form that the matrix $\mathrm{F}(\mathbf{0})$ takes in this limit. For computing the zeta function, it is moreover more convenient to work with the inverse Frobenius map

$$\mathrm{U}(\boldsymbol{\varphi}) \stackrel{\mathrm{def}}{=} \mathrm{F}^{-1}(\boldsymbol{\varphi}) \;=\; \mathrm{E}^{-1}(\boldsymbol{\varphi}^p)\mathrm{U}(0)\mathrm{E}(\boldsymbol{\varphi})\;.$$

The large complex structure limit

Taking the limit $\boldsymbol{\varphi} \to \mathbf{0}$ of (9.4), one obtains the following relations, the one-parameter analogue of which was used in [13] to constrain the form of the matrix $\mathrm{U}(\mathbf{0})$

$$p\,\epsilon_i \mathrm{U}(\mathbf{0}) \;=\; \mathrm{U}(\mathbf{0})\,\epsilon_i\;, \qquad i = 1, \ldots, m\;. \tag{9.5}$$

The most general solution to these conditions can be written in a convenient form as

$$\mathrm{U}(\mathbf{0}) = u\Lambda\left(\mathrm{I} + \alpha^i\,\epsilon_i + \beta_i\,\mu^i + \gamma\,\eta\right)\;, \qquad \Lambda \;=\; \mathrm{diag}(1, p\,\mathbf{1}, p^2\,\mathbf{1}, p^3)\;. \tag{9.6}$$

To see this, we denote the components of $\mathrm{U}(\mathbf{0})$ by

$$\mathrm{U}(\mathbf{0}) \;=\; \begin{pmatrix} u_0^0 & u_0^{1,i} & u_0^{2,i} & u_0^3 \\ u_{1,i}^0 & u_{1,i}^{1,j} & u_{1,i}^{2,j} & u_{1,i}^3 \\ u_{2,i}^0 & u_{2,i}^{1,j} & u_{2,i}^{2,j} & u_{2,i}^3 \\ u_3^0 & u_3^{1,j} & u_3^{2,j} & u_3^3 \end{pmatrix}\;,$$

and note that from (9.5) it is possibly to obtain commutation relations of $\mathrm{U}(\mathbf{0})$ with matrices η and μ^i:

$$p^3\eta\mathrm{U}(\mathbf{0}) \;=\; \mathrm{U}(\mathbf{0})\eta\;, \qquad p^2\mu^i\mathrm{U}(\mathbf{0}) \;=\; \mathrm{U}(\mathbf{0})\mu^i\;. \tag{9.7}$$

The first of which is equivalent to requiring

$$u_0^{1,i} \;=\; u_0^{2,i} \;=\; u_0^3 \;=\; 0\;, \qquad u_0^3 \;=\; u_{1,i}^3 \;=\; u_{2,i}^3 \;=\; 0\;, \qquad p^3 u_0^0 \;=\; u_3^3\;.$$

Substituting these conditions into the second equation in (9.7), and contracting with $\widehat{Y}_{ijk}$ where needed, the following conditions are found:

$$u_{1,i}^{1,j} \;=\; p\,u_0^0\,\delta_i^j\;, \quad u_{1,i}^{2,j} \;=\; u_{1,i}^3 \;=\; 0\;, \quad u_{2,i}^{2,j} = p^2\,u_0^0\,\delta_i^j\;, \quad u_{2,i}^3 \;=\; 0\;, \quad u_3^{2,i} \;=\; 3p^2 u_{1,i}^0\;.$$

Finally, with these conditions, the original commutation relations (9.5) are equivalent to

$$u_{2,i}^{1,j} \;=\; p u_{1,k}^0 Y_{ijk}\;, \qquad u_3^{1,i} \;=\; p u_{2,i}^0\;.$$

Denoting the independent constants appearing here as

$$u_0^0 = u \ , \qquad u_{i,1}^0 = up\alpha^i \ , \qquad u_{2,i}^0 = up^2\beta_i \ , \qquad u_3^0 \ = \ up^3\gamma \ ,$$

we obtain the result (9.6).

In addition, we can impose consistency relation with inner product $H^3 \times H^3 \to \mathbb{C}$

$$(\xi, \omega) \ = \ \int_X \xi \wedge \omega \ .$$

In the Frobenius basis where the period vector is ϖ, the matrix corresponding to the inner product is given by

$$\sigma \ = \ \nu^{-1}\rho^T\Sigma\rho\nu^{-1} \ = \ \frac{1}{(2\pi\mathrm{i})^3}\begin{pmatrix} 0 & \mathbf{0}^T & \mathbf{0}^T & -1 \\ \mathbf{0} & \mathbb{0} & \mathbb{I} & \mathbf{0} \\ \mathbf{0} & -\mathbb{I} & \mathbb{0} & \mathbf{0} \\ 1 & \mathbf{0}^T & \mathbf{0}^T & 0 \end{pmatrix} .$$

The matrix $\mathrm{U}(\mathbf{0})$ should satisfy

$$\mathrm{U}(\mathbf{0})\,\sigma\,\mathrm{U}(\mathbf{0})^T \ = \ p^3\sigma \ .$$

This imposes the conditions

$$u^2 \ = \ 1 \ , \qquad \beta_i \ = \ \frac{1}{2}\,Y_{ijk}\alpha^j\alpha^k \ .$$

In the one-parameter case of [13] it was conjectured, supported with extensive numerical evidence that the correct solution is obtained by imposing (in the basis we are using)

$$u \ = \ 1 \ , \quad \alpha \ = \ 0 \ , \quad \gamma \ = \ 6\chi(X)\zeta_p(3) \ .$$

However, by studying various examples, the straightforward generalisation of these relations to the multiparameter case does not seem to be always true. Rather, p-adic expansions for the coefficients α_i and γ can be found order-by-order by requiring that the matrix $\mathrm{U}(\boldsymbol{\varphi})$ takes the rational form given in (9.9). It is tempting to speculate that they are given in terms of topological data of the family of manifolds in question, but we have not been able to find an universal expression for these constants.

9.1.3 Inversion of $\mathrm{E}(\boldsymbol{\varphi})$

To compute the matrix $\mathrm{U}(\boldsymbol{\varphi})$, we need an efficient way of inverting the matrix $\mathrm{E}(\boldsymbol{\varphi})$. Luckily a practical method of doing this is given in [90]. The idea is that the inner products

$$(\vartheta_a\Omega, \vartheta_b\Omega) = \int_X \vartheta_a\Omega \wedge \vartheta_b\Omega \ , \quad (\vartheta^a\Omega, \vartheta^b\Omega) = \int_X \vartheta^a\Omega \wedge \vartheta^b\Omega \ , \quad \text{and} \quad (\vartheta_a\Omega, \vartheta^b\Omega) = \int_X \vartheta_a\Omega \wedge \vartheta^b\Omega$$

can be expressed as simple rational functions of the parameters $\boldsymbol{\varphi}$. These product are exactly the components of the matrix

$$\mathrm{W}(\boldsymbol{\varphi}) \stackrel{\mathrm{def}}{=} \mathrm{E}(\boldsymbol{\varphi})^T\sigma\mathrm{E}(\boldsymbol{\varphi}) \ . \tag{9.8}$$

Using this matrix, the inverse matrix $\mathrm{E}^{-1}(\boldsymbol{\varphi})$ can be expressed as

$$\mathrm{E}^{-1}(\boldsymbol{\varphi}) \;=\; (\sigma \mathrm{E}(\boldsymbol{\varphi})\mathrm{W}^{-1}(\boldsymbol{\varphi}))^T \;.$$

This is convenient to compute in practice because, as a matrix of rational functions, $\mathrm{W}(\boldsymbol{\varphi})$ is relatively easy to invert.

9.1.4 The form of $\mathrm{U}(\boldsymbol{\varphi})$

The matrix $\mathrm{U}(\boldsymbol{\varphi}) = \mathrm{E}^{-1}(\boldsymbol{\varphi}^p)\mathrm{U}(\mathbf{0})\mathrm{E}(\boldsymbol{\varphi})$ is naturally expressed as a matrix of series in variables $\boldsymbol{\varphi}$. In all of the cases we have studied, the coefficients in the series, which have p-adic integers as their coefficients, are p-adically convergent. However, they converge only slowly, so it is useful to note [87, 88] that $\mathrm{U}(\boldsymbol{\varphi})$ can be expressed as a matrix of rational functions. To do this in practice, we fix a p-adic accuracy and ignore any contributions smaller than this accuracy, or in other words, we compute the coefficients in the series appearing in $\mathrm{U}(\boldsymbol{\varphi})$ modulo p^n for some integer $n < p$. Then the matrices $\mathrm{U}(\boldsymbol{\varphi})$ can be expressed in the form

$$\mathrm{U}(\boldsymbol{\varphi}) \;=\; \frac{\mathcal{U}(\boldsymbol{\varphi})}{P(\boldsymbol{\varphi})^p} + \mathcal{O}(p^n) \;, \tag{9.9}$$

where $\mathcal{U}(\varphi)$ is a matrix with entries that are polynomials in $\boldsymbol{\varphi}$ and $P(\boldsymbol{\varphi})$ is a polynomial in $\boldsymbol{\varphi}$ that depends on the p-adic accuracy n. In all cases we have studied, this polynomial takes the form

$$P(\boldsymbol{\varphi}) \;=\; \mathcal{W}(\boldsymbol{\varphi})\mathcal{Y}(\boldsymbol{\varphi})^2\left(\Delta(\boldsymbol{\varphi})\mathcal{Y}(\boldsymbol{\varphi})\right)^{n-5} \;, \qquad n \geq 5 \;, \tag{9.10}$$

where $\Delta(\boldsymbol{\varphi})$ is the discriminant of the family of Calabi-Yau manifolds we are studying, $\mathcal{W}(\boldsymbol{\varphi})$ the denominator of the matrix $\mathrm{W}^{-1}(\boldsymbol{\varphi})$, and $\mathcal{Y}(\boldsymbol{\varphi})$ represents additional factors in the denominator of the (quantum corrected) Yukawa couplings y_{ijk}.

9.2 Constraints from the Weyl conjectures

The functional equation (3.7) satisfied by the zeta function of a Calabi-Yau threefold implies that its numerator $R(X,T)$ satisfies the following functional equation:

$$R(X,T) \;=\; p^{3(h^{12}+1)}\,T^{2(h^{12}+1)}R\left(X,p^{-3}T^{-1}\right) \;.$$

This relation halves the number of independent parameters, imposing the following relations among the coefficients

$$a_{2(h^{12}+1)-i} \;=\; p^{3(h^{12}+1-i)}a_i \;, \qquad a_{2(h^{12}+1)} \;=\; p^{3(h^{12}+1)} \;. \tag{9.11}$$

Our aim is to fix the remaining independent coefficients by using the relation (3.10) between the zeta function and the inverse Frobenius map acting on the third cohomolgy, which fully determines the

zeta function of a Calabi-Yau threefold. The relation (3.10) can be explicitly restated in terms of the matrix $\mathrm{U}(\boldsymbol{\varphi})$ as

$$R(X_{\boldsymbol{\varphi}}, T) \;=\; \mathrm{Det}(1 - T\,\mathrm{U}(\boldsymbol{\varphi}))\ ,$$

which could in principle used directly to compute the zeta function numerator. However, in practice, finding the determinant of a matrix whose entries are multivariate series is computationally very taxing. In addition, these results would necessarily only give the coefficients a_i up to certain p-adic accuracy. To resolve the first issue, it is more convenient to be able to express the independent coefficients a_i as traces of powers of $\mathrm{U}(\boldsymbol{\varphi})$. To address the second, using the Riemann hypothesis, we can derive bounds for the norms of a_i. This allows us to fix an p-adic accuracy to which the series need to be computed in order to obtain exact results for the a_i. This is also a crucial piece of information needed to accelerate convergence of the series in $\mathrm{U}(\boldsymbol{\varphi})$, as only when working with a fixed p-adic accuracy and ignoring any coefficients of higher p-adic order, will we find that the *a priori* infinite series appearing as elements of $\mathrm{U}(\boldsymbol{\varphi})$ are actually rational functions with $\mathrm{U}(\boldsymbol{\varphi})$ taking the form (9.9), which allows computing its values exactly to a given p-adic accuracy.

It is possible to find the coefficients of the characteristic polynomial by considering the following standard identities

$$\det\left(1 - T\mathrm{U}(\boldsymbol{\varphi})\right) \;=\; \exp\left(\mathrm{Tr}\log(1 - T\mathrm{U}(\boldsymbol{\varphi}))\right) \;=\; \exp\left(-\sum_{n=1}^{\infty} T^n \frac{\mathrm{Tr}\,\mathrm{U}(\boldsymbol{\varphi})^n}{n}\right)\ .$$

Expanding this in powers of T gives a each coefficient a_i as a function of traces of powers of $\mathrm{U}(\boldsymbol{\varphi})$ in a way reminiscent of computing Chern classes. As the entries of $\mathrm{U}(\boldsymbol{\varphi})$ are series whose coefficients are p-adic integers, when $\boldsymbol{\varphi}$ is evaluated at Teichmüller lifts $\mathrm{Teich}(\boldsymbol{\varphi}) = (\mathrm{Teich}(\varphi_1), \ldots, \mathrm{Teich}(\varphi_m))$, the a_i are seen to be p-adic, and thus rational, integers.

By the Riemann hypothesis, if we diagonalise the matrix $\mathrm{U}(\boldsymbol{\varphi})$, the eigenvalues will be algebraic integers λ_j of absolute value $|\lambda_j| = p^{3/2}$. The coefficients of the characteristic polynomial $R(T)$ can be expressed as symmetric polynomials of these eigenvalues.

$$a_i \;=\; (-1)^i\,\sigma_i(\lambda_1, \ldots, \lambda_{2m+2})\ ,$$

where σ_i is the i'th elementary symmetric polynomial, and no sum over i is implied. From the Riemann hypothesis it immediately follows that every monomial in σ_i has an absolute value of $p^{3i/2}$, whereas the number of monomials is $\binom{2m+2}{i}$. This gives a simple bound on the magnitude of a_i

$$|a_i| < \binom{2m+2}{i} p^{3i/2}\ . \tag{9.12}$$

Thus, if we are interested in computing a_i, we only need to compute it modulo p^n, where n is an integer such that $\binom{2m+2}{i} p^{3i/2} \leq p^n$. This gives the p-adic accuracy mentioned in §9.1.4 to which we need to know $\mathrm{U}(\boldsymbol{\varphi})$.

9.3 Examples

To illustrate the methods developed here in concrete cases, we study two relatively different cases: the two-parameter mirror manifold of the octic hypersurface in the weighted projective space $\mathbb{P}^{(1,1,2,2,2)}$, and the five-parameter family of mirror Hulek-Verrill manifolds. Our main interest is in the Hulek-Verrill manifolds, as in the next chapter the zeta function data will be essential for analysis of modularity of flux vacua. However, both of these two cases also act as checks of our methods, as some results for the family of mirror octics has been obtained in [70], and the symmetries of the Hulek-Verrill manifold, together with the point-counting formula given in [14], can be used to obtain partial results for these manifolds as well.

Treating these two examples also requires use of different strategies due to the computational complexity of various matrices involved, and the p-adic accuracy required to obtain exact results numerically. It is possible to study the two-parameter example by expanding the periods as a series in two parameters, which makes it easy to obtain results for any values of the parameters. However, for a larger number of parameters this becomes quickly computationally too cumbersome to be practical. These cases can be treated by studying lines inside of the multiparameter moduli space in a manner similar to how monodromy matrices were computed in 6.3. This allows expressing the periods and their derivatives as series in one parameter, greatly reducing the computational complexity of the problem. By considering a suitable line, it is possible to obtain the zeta function at any point in this way.

9.3.1 Two-parameter example: the mirror octic

We begin with a study of the mirror octic. Mirror symmetry for this manifold has been studied in detail in [91], and the zeta function has been computed in some special cases in [70]. This allows us to make highly non-trivial checks of the method presented above by comparing the results to those obtained in [70].

The family of octic Calabi-Yau manifolds is given by resolving the singularities of a varieties defined as degree-8 hypersurfaces in the weighted projective space $\mathbb{P}^{(1,1,2,2,2)}$.

The Hodge diamond of the family of octics is given by

$$h^{p,q} \;=\; \begin{array}{ccccccc} & & & 1 & & & \\ & & 0 & & 0 & & \\ & 0 & & 2 & & 0 & \\ 1 & & 86 & & 86 & & 1 \\ & 0 & & 2 & & 0 & \\ & & 0 & & 0 & & \\ & & & 1 & & & \end{array} .$$

Thus the mirror of this family gives a two-parameter model. These manifolds have been explicitly constructed in [91], where they were identified with the manifolds given by $\{P = 0\}/\mathbb{Z}_4^3$ with

$$P \;=\; x_1^8 + x_2^8 + x_3^4 + x_4^4 + x_5^4 - 2\phi x_1^4 x_2^4 - 8\psi x_1 x_2 x_3 x_4 x_5 \;=\; 0 \;,$$

and with the group $\mathbb{Z}_4^3$ is realised as the group with generators

$$(0,3,1,0,0)\ , \qquad (0,3,0,1,0)\ , \qquad (0,3,0,0,1)\ .$$

The complex structure moduli space $\mathcal{M}_{\mathbb{C}S}$ of mirror octics can be identified as

$$\mathcal{M}_{\mathbb{C}S} \ = \ \mathrm{Spec}\left[\frac{\mathbb{C}[\widehat{x},\widehat{y},\widehat{z}]}{\langle\widehat{x}\widehat{z}-\widehat{y}^2\rangle}\right]\ ,$$

where the coordinates $\widehat{x}$, $\widehat{y}$, and $\widehat{z}$ can be related to ψ and ϕ by

$$\widehat{x} \ = \ \psi^8\ , \qquad \widehat{y} \ = \ \psi^4\phi\ , \qquad \widehat{z} \ = \ \phi^2\ .$$

The natural coordinates to use near the large complex structure point are

$$u \stackrel{\mathrm{def}}{=} \frac{1}{\phi^2}\ , \qquad w \stackrel{\mathrm{def}}{=} \frac{\phi}{\psi^4}\ ,$$

in terms of which the large complex structure point is located as $u = w = 0$.

The triple intersection numbers Y_{ijk} are given by

$$Y_{111} \ = \ 0\ , \quad Y_{112} \ = \ 0\ , \quad Y_{122} \ = \ 4\ , \quad Y_{222} \ = \ 8\ ,$$

where the index 1 refers to the linear system of divisors inherited from the vanishing loci of degree-1 polynomials generated by the x_1 and x_2 in the ambient space, whereas the index 2 refers to the linear system generated by the degree 2 polynomials.

We take the quantities $\widehat{Y}^{ijk}$ to be symmetric in the last two indices, with the independent values given by

$$\widehat{Y}^{121} \ = \ -\frac{1}{4}\ , \quad \widehat{Y}^{122} \ = \ \frac{1}{4}\ , \quad \widehat{Y}^{212} \ = \ \frac{1}{8}\ , \quad \widehat{Y}^{111} \ = \ 0\ , \quad \widehat{Y}^{112} \ = \ 0\ , \quad \widehat{Y}^{222} \ = \ 0\ .$$

The discriminant Δ and the additional factor $\mathcal{Y}$ appearing in the Yukawa coupling denominators are given by

$$\Delta \ = \ 64 + 16w + (1-u)w^2\ , \qquad \mathcal{Y} \ = \ u - 1\ .$$

The Picard-Fuchs system

In the coordinates adapted to the large complex structure point, the fundamental period is

$$\varpi_0(u,w) \ = \ \sum_{r,s=0}^{\infty} \frac{(8r+4s)!(-2)^s}{\left((2r+s)!\right)^3 (r!)^2 s! 8^{8r+4s}} u^r w^{2r+s}\ .$$

In these coordinates, two of the differential operators giving the Picard-Fuchs system found in [91] can be written as

$$\mathcal{L}_1 \ = \ 128uw^2\partial_u\partial_w^2 - 8w^3(8{+}w)\partial_w^3 + 64uw\partial_u\partial_w - w^2(160{+}30w)\partial_w^2 - (36w{+}15w^2)\partial_w + 8u\partial_u\ ,$$

$$\mathcal{L}_2 \ = \ 1 - 16uw^2\partial_w^2 + 48u(1-u)\partial_u + 64u^2w\partial_u\partial_w + 64u^2(1-u)\partial_u^2\ .$$

Alternatively, these equations can be written as relations between the basis of $H^3(X,\mathbb{C})$ spanned by the derivatives $\vartheta_a\Omega$ and $\vartheta^a\Omega$ of the holomorphic three-form.

$$\begin{aligned} 64\vartheta_1 + (w-32)\vartheta_2 + 1024\vartheta^1 - 128(8+w)\theta_w\vartheta^1 - 256w\theta_w\vartheta^2 &= 0 \ , \\ 256u\vartheta^2 - 128u\vartheta^1 + 64(1-u)\theta_u\vartheta_1 - 32(1+u)\vartheta_1 + 16u\vartheta_2 + 4 &= 0 \ , \\ \theta_w\vartheta_1 - 8\vartheta^2 = 0 \ , \qquad \theta_w\vartheta_2 - 8\vartheta^1 - 16\vartheta^2 &= 0 \ , \qquad \theta_u\vartheta_2 - 8\vartheta^2 = 0 \ , \\ 4\theta_u\vartheta^1 + 4\theta_w\vartheta^2 - 24\vartheta^0 &= 0 \ , \end{aligned}$$

where the first two relations are the Picard-Fuchs equations, and we have also included a few additional relations that are identically true due to the way ϑ_a and ϑ^a are defined.

To obtain series expressions for the periods around the large complex structure point, we use series ansätze for the functions f^I appearing in the expression (2.13) for the period vector:

$$f^I = \sum_{\mu,\nu=0}^{\infty} c^I_{\mu\nu} u^\mu w^\nu \ .$$

Here I can be a one-, two, or three-component index. Substituting the Frobenius basis periods ϖ_a, ϖ^a expressed in terms of these series into the first two differential equations, we obtain recurrence relations for the coefficients $c^I_{\mu\nu}$, which can be used to quickly compute the series f^I to high order. To get a better idea how this works in practice, let us consider the fundamental period. The recurrence relations can in this case be expressed as

$$c^0_{\mu\nu} = \frac{(1+\nu-2\mu)(2+\nu-2\mu)}{4\mu^2} c^0_{\mu-1,\nu} \ , \qquad c^0_{0\nu} = \frac{-32\nu^3+48\nu^2-22\nu+3}{256\nu^3} c^0_{0,\nu-1} \ .$$

Together with the boundary conditions

$$c^0_{00} = 1 \ , \qquad c^0_{\mu\nu} = 0 \quad \text{if } \mu<0 \text{ or } \nu<0 \ ,$$

these are enough to solve for all coefficients $c^0_{\mu\nu}$. The coefficients appearing in the other periods satisfy similar, albeit more intricate, recurrence relations, which we will refrain from displaying here.

U(u,w) and the zeta function

Having obtained the periods via recurrence relations, we only need to find the matrix $\mathrm{W}^{-1}(u,w)$ defined in (9.8) to be able to compute the matrix $\mathrm{U}(u,w)$. In the present case, it is not difficult to compute the required inner products of derivatives of periods to show that

$$\mathrm{W}^{-1} = \frac{(2\pi\mathrm{i})^3}{2048} \begin{pmatrix} 0 & -12(u-1)w & \frac{Cuw}{\mathcal{W}} & \frac{64Bu}{\mathcal{W}} & \frac{128Aw}{\mathcal{W}} & \frac{1536D(u-1)}{\mathcal{W}} \\ 12(u-1)w & 0 & 32(u-1)w & 512(u-1)(w+8) & 1024(u-1)w & 0 \\ -\frac{Cuw}{\mathcal{W}} & -32(u-1)w & 0 & -512u(w+4) & -512(uw+w+8) & 0 \\ -\frac{64Bu}{\mathcal{W}} & -512(u-1)(w+8) & 512u(w+4) & 0 & 0 & 0 \\ -\frac{128Aw}{\mathcal{W}} & -1024(u-1)w & 512(uw+w+8) & 0 & 0 & 0 \\ -\frac{1536D(u-1)}{\mathcal{W}} & 0 & 0 & 0 & 0 & 0 \end{pmatrix} ,$$

where we have denoted

$$\begin{aligned} A &= 3u^2w - 9uw - 32u + 2w + 16 \ , \qquad B = 5uw^2 - 8uw - 9w^2 - 40w - 128 \ , \\ C &= 11uw - 24u - 27w - 40 \ , \qquad D = uw^2 - w^2 - 16w - 64 \ , \\ \mathcal{W} &= 8 - 4u + w \ . \end{aligned}$$

With this expression, computing the inverse matrix $\mathrm{E}^{-1}(u^p, w^p)$ is simple. It is then also easy to compute the matrix $\mathrm{U}(u, w)$ for the first few primes p. As examples, we take $p = 7, 11, 13$. Before specifying the values of α_1 and α_2, the series coefficients appearing in $\mathrm{U}(u, w)$ are not p-adic integers, nor will the series converge to a rational function with the denominator (9.9), which would in practice be seen as series multiplied by (9.10) becoming finite polynomials.

Imposing the requirement that the entries of $\mathrm{U}(u, w)$ be rational functions with p-adic integers as coefficients of polynomials in the numerator and denominator, gives an overconstrained system, which can be used to solve the constants α_1, α_2, and γ to appropriate p-adic accuracies. From (9.12), it follows that we need to compute $\mathrm{U}(u, w)$ to p-adic accuracy p^6, which in turn implies, that α_i need to be computed up to order p^5 or higher, and γ need to be computed up to order p^3. We gather the values computed in this way in table 9.1.

p	α_1	α_2	γ
7	$44306 + \mathcal{O}(7^6)$	$8385 + \mathcal{O}(7^6)$	$42 + \mathcal{O}(7^3)$
11	$1752874333 + \mathcal{O}(11^9)$	$1387991913 + \mathcal{O}(11^9)$	$28653 + \mathcal{O}(11^5)$
13	$275282911 + \mathcal{O}(13^8)$	$290459929 + \mathcal{O}(13^8)$	$23300 + \mathcal{O}(13^4)$

Table 9.1: *The values of the prime-dependent constants α_1, α_2 and γ appearing in the most general form* (9.6) *of the matrix $U(0,0)$ for the cases $p = 7, 11, 13$ we include in appendix D.*

Using these values to compute the matrices $\mathrm{U}(u, w)$, one finds that these take exactly the form (9.9), which allows computing the independent coefficients a_1, a_2, and a_3 appearing in the zeta function numerators $R(T)$. The numerators are listed in appendix D.

9.3.2 Five-parameter example: the Hulek-Verrill manifold

As an example of a case where it is beneficial to study zeta functions on complex lines in the moduli space, consider the five-parameter Hulek-Verrill manifolds, focusing on the S_5-symmetric complex lines on the patch $\varphi^0 = 1$ with $\boldsymbol{\varphi} = (\varphi, \varphi, \varphi, \varphi, \varphi)$, $\varphi \in \mathbb{C}$. This example will also turn out to be useful for the study of supersymmetric flux vacua.

Recalling the values (6.33) that the triple intersection numbers Y_{ijk} take, we can choose the quantities $\widehat{Y}^{ijk}$ so that the $\mathbb{Z}_5$ symmetry of is preserved:

$$\widehat{Y}^{iii} \;=\; \widehat{Y}^{iji} \;=\; \widehat{Y}^{jii} \;=\; -\frac{1}{24}\,, \qquad \widehat{Y}^{ijk} \;=\; \frac{1}{24}\,, \tag{9.13}$$

On this line the discriminant (5.15) becomes

$$\Delta_5 \;=\; (1-\varphi)^{10}(1-9\varphi)^5(1-25\varphi)\,.$$

However, for the purposes of computing the zeta function on the line, we do not need to account for the multiplicities, so we can take the discriminant to be

$$\Delta = (1-\varphi)(1-9\varphi)(1-25\varphi) \ .$$

Recalling (6.35), we see that the denominators in the Yukawa couplings are given by the discriminant above, apart from the factor φ^3, which does not affect the convergence of the series. Thus we can take

$$\mathcal{Y} \ = \ 1 \ . \tag{9.14}$$

Univariate series expansions

We could in principle use the series expressions (6.32) to compute the matrix $\mathrm{E}(\varphi)$. However, these series are rather cumbersome which makes this method very inefficient for computing the series to a high order.

As we are interested in series expressions on the symmetric lines $\varphi^i = \varphi$, we only need the periods and their logarithmic derivatives as series in one variable. Having to first compute a five-variable series and then specialise to this line is a computationally expensive process. Instead of having to do this, it is possible to derive recurrences for the periods and their derivatives directly as univariate series.

Let $\mathfrak{t}$ be a list of elements of $\{1,2,3,4,5\}$ (allowing duplicates) of length ≤ 3, and denote

$$\theta_{\mathfrak{t}} \ = \ \prod_{i\in\mathfrak{t}} \theta_i \ ,$$

$$\theta_{\mathfrak{t}}\varpi^a|_{\varphi^i\to\varphi,\,\log\varphi\to 0} \ = \ f^a_{\mathfrak{t}} \ , \qquad \theta_{\mathfrak{t}}\varpi_a|_{\varphi^i\to\varphi,\,\log\varphi\to 0} \ = \ f_{\mathfrak{t},a} \ .$$

We seek an efficient way to compute a large number of terms in the power series $f^a_{\mathfrak{t}}$ and $f_{\mathfrak{t},a}$. With these, we are able to compute the periods and their derivatives because the power series that multiply the logarithms in each are formed from known combinations of the above series. This problem can be broken up to computing the series expansions of the following sets:

$$A \ = \ \{f_{\mathfrak{t},0},\, f^0_{\mathfrak{t}} |\ \mathfrak{t} \text{ contains no repeated elements}\} \ ,$$

$$B \ = \ \{f_{\mathfrak{t},i},\, f^i_{\mathfrak{t}} |\ \mathfrak{t} \text{ contains no repeated elements and } i>0\} \ ,$$

$$C \ = \ \{f_{\mathfrak{t},a}, f^a_{\mathfrak{t}} \mid \mathfrak{t} \text{ contains repeated elements and } a\geq 0\} \ .$$

In [76], Verrill gave a recursive method for computing the coefficients

$$c^{\boldsymbol{\epsilon}}_n \ = \ \sum_{|\boldsymbol{p}|=n} \left(\frac{n!}{p_1!p_2!p_3!p_4!p_5!}\right)^2 \boldsymbol{p}^{\boldsymbol{\epsilon}} \ = \ \sum_{|\boldsymbol{p}|=n} \binom{n}{\boldsymbol{p}}^2 \boldsymbol{p}^{\boldsymbol{\epsilon}} \ , \tag{9.15}$$

where $\boldsymbol{\epsilon}$ is a five-component multi-index with $\epsilon_i \in \{0,1\}$. These appear as coefficients of the fundamental period ϖ^0 and its non-repeated logarithmic derivatives, which is the set A. The method in [76] thus can be used to efficiently compute the functions in A.

Recurrences for the coefficients of the series in B can be derived by considering the ordinary differential equations

$$\mathcal{L}^{\mathfrak{t}}(F) \;=\; 0 \tag{9.16}$$

satisfied by the functions $f^0_{\mathfrak{t}} = \theta_{\mathfrak{t}}\varpi^0$ on the S_5-symmetric line. These equations are obtained in the standard way from the recurrences for the functions in A that can be computed by Verrill's method.

About $\varphi = 0$, there is a Frobenius basis of solutions to each of the equations (9.16) consisting of a single holomorphic solution, $f^0_{\mathfrak{t}}$, in addition to which there are solutions containing logarithms of φ. Let us denote the holomorphic part of each of these solutions by $g_{\mathfrak{t},k}$, bearing in mind that the range of k varies with $\boldsymbol{t}$. The coefficients of these functions satisfy almost the same recurrence relations as the corresponding functions in A, but with an inhomogeneity that can be computed in terms of functions $g_{\mathfrak{t},l}$, with $l < k$. It can be shown that $f^a_{\mathfrak{t}}$ and $f_{\mathfrak{t},a}$ are sums of functions $g_{\mathfrak{t},k}$, $f_{\mathfrak{r},a}$, and $f^a_{\mathfrak{r}}$, where $\mathfrak{r} \subsetneq \mathfrak{t}$. As an example of this principle, consider the function $f^1_{\{1\}}$, which has a series expansion

$$f^1_{\{1\}} \;=\; 2\sum_{n=0}^{\infty}\sum_{|\boldsymbol{p}|=n}\left(\frac{n!}{p_1!p_2!p_3!p_4!p_5!}\right)^2 p_1\left(H_n - H_{p_1}\right)\varphi^n \;.$$

The function $f^0_{\{1\}}$ has an expansion

$$f^0_{\{1\}} \;=\; \sum_{n=0}^{\infty}\sum_{|\boldsymbol{p}|=n}\left(\frac{n!}{p_1!p_2!p_3!p_4!p_5!}\right)^2 p_1\varphi^n \;, \tag{9.17}$$

and by applying the Frobenius method to this function, we can obtain a logarithmic solution to (9.16) with $\boldsymbol{t} = \{1\}$, which has a holomorphic part

$$g_{\{1\},1} \;=\; \partial_{\epsilon_1}\left(f^0_{\{1\}}\big|_{p_i\to p_i+\epsilon_i,\; n\to n+\sum\epsilon_i}\right)\Big|_{\epsilon_i\to 0,\,\log\to 0} \;=\; f^1_{\{1\}} + f^0_{\{0\}} \;.$$

We see that it is possible compute $f^1_{\{1\}}$ in terms of two functions that we already defined recursively: $g_{\{1\},1}$, which satisfies the inhomogenous recurrence relation just derived, and $f^0_{\{0\}}$ which is a member of A.

Recursion in $\mathfrak{t}$ allows for the functions in B to be expressed in terms of solutions to a recurrence relation and functions in A, which we can already compute.

To better illustrate the recurrences for the functions g, consider $\varpi^1 = f^0_{\{\}}\log\varphi + f^1_{\{\}}$. By substituting this into the differential equation (9.16) with $\mathfrak{t} = \{\}$, we obtain an inhomogeneous differential equation for the functions $f^1_{\{\}}$:

$$\mathcal{L}^{\{\}}(f^1_{\{\}}) \;=\; -\mathcal{L}^{\{\}}(\log\varphi\, f^0_{\{\}}) \;.$$

From this equation, we can read off an inhomogeneous recurrence relation satisfied by the coefficients d_n appearing in the expansion

$$f^1_{\{\}} \;=\; \sum_{n=1}^{\infty} d_n\varphi^n \;.$$

The inhomogeneity involves the coefficients of $f^0_{\{\}}$, which is a member of A and can be computed quickly. This solves the problem for the functions in B.

Finally, we turn to the functions in C. Luckily, there are identities that give these functions in terms of functions belonging to A or B. For example, consider the derivatives $\theta_1^2\theta_2\varpi^0$. From the series expansion (6.5), it follows that

$$\theta_1^2\theta_2\varpi^0 \;=\; \sum_{n=0}^{\infty}\sum_{|\boldsymbol{p}|=n}\binom{n}{\boldsymbol{p}}^2 p_1^2 p_2\,\boldsymbol{\varphi}^n \;=\; \sum_{n=0}^{\infty} n^2 \sum_{|\boldsymbol{p}|=n}\binom{n-1}{\boldsymbol{p}-\boldsymbol{\delta}_1}^2 p_2\,\varphi^n \;=\; \sum_{n=0}^{\infty} n^2 c^{(2)}_{n-1}\varphi^n\ ,$$

where the coefficients $c^{(2)}_{n-1}$ are those appearing in the series expansion of $\theta_2\varpi^0$. It is possible to find an exhaustive list of such identities, one for each function in C, thus finishing the problem of finding a fast method of computing the periods and their derivatives on a line in the moduli space.

This problem is made simpler by working on the line with the full S_5 symmetry, where not all of the functions $f^a_{\mathfrak{t}}$ and $f_{\mathfrak{t},a}$ are independent. For instance $f^0_{\{1,2,3\}} = f^0_{\{3,4,5\}}$ on this line. However, the method described above can be used to work on any line $\varphi^i = s^i\varphi$, where s^i are constants. The main difference is that there are in full generality ten periods ϖ^i and ϖ_i, and so 12 functions and their numerous derivatives to consider. The series expansions of all of these can be computed with the above method, but the recurrence relations and intermediate differential equations (9.16) become more complicated the less symmetry one has.

Inversion of $\mathbf{E}(\boldsymbol{\varphi})$

To compute the inverse matrix $\mathrm{E}^{-1}(\varphi)$, we need to compute the inner products $(\vartheta_a\Omega,\vartheta_b\Omega)$, $(\vartheta_a\Omega,\vartheta^b\Omega)$, and $(\vartheta^a\Omega,\vartheta^b\Omega)$. Due to the symmetries, there are only five independent such inner products that do not vanish:

$$\begin{aligned}
(\vartheta_0\Omega,\vartheta^0\Omega) &= -\frac{1}{(2\pi\mathrm{i})^3}\frac{5(18\varphi-1)}{12(\varphi-1)(9\varphi-1)(25\varphi-1)}\ ,\\
(\vartheta_i\Omega,\vartheta^i\Omega) &= \frac{1}{(2\pi\mathrm{i})^3}\frac{18\varphi-1}{2(\varphi-1)(9\varphi-1)(25\varphi-1)}\ ,\\
(\vartheta_i\Omega,\vartheta^j\Omega) &= -\frac{1}{(2\pi\mathrm{i})^3}\frac{7\varphi}{2(\varphi-1)(9\varphi-1)(25\varphi-1)}\ ,\\
(\vartheta_i\Omega,\vartheta^0\Omega) &= -\frac{1}{(2\pi\mathrm{i})^3}\frac{1800\varphi^4+1915\varphi^3-462\varphi^2+11\varphi}{12(\varphi-1)^2(9\varphi-1)^2(25\varphi-1)^2}\ ,\\
(\vartheta^i\Omega,\vartheta^0\Omega) &= \frac{1}{(2\pi\mathrm{i})^3}\frac{1215\varphi^4-415\varphi^3+16\varphi^2}{72(\varphi-1)^2(9\varphi-1)^2(25\varphi-1)^2}
\end{aligned}$$

With these, it is easy to compute the matrix $\mathrm{W}^{-1}(\varphi)$, which we refrain from giving here due to its size. However, by computing the matrix, the denominator can be identified as

$$\mathcal{W} \;=\; (10\varphi+1)(18\varphi-1)\ .$$

U(φ) and the zeta function

With the information above, it is straightforward to construct the matrices $\mathrm{E}(\varphi)$ and $\mathrm{E}(\varphi)^{-1}$. The S_5 symmetry of the manifolds we are studying admit corresponds to permutations of the coordinates $\varphi^i \to \varphi^{\varsigma(i)}$, $\varsigma \in S_5$, and acts on the periods as

$$\varpi_0 \mapsto \varpi_0 \ , \qquad \varpi_i \mapsto \varpi_{\varsigma(i)} \ , \qquad \varpi^i \mapsto \varpi^{\varsigma(i)} \ , \qquad \varpi^0 \mapsto \varpi^0 \ ,$$

but keeps the period vector invariant, implying that there are only four independent periods. The choice (9.13) of the quantities $\widehat{Y}^{ijk}$ guarantees a similar symmetry property for the derivative vector ϑ under the action of the permutations ς:

$$\vartheta_0 \mapsto \vartheta_0 \ , \qquad \vartheta_i \mapsto \vartheta_{\varsigma(i)} \ , \qquad \vartheta^i \mapsto \vartheta^{\varsigma(i)} \ , \qquad \vartheta^0 \mapsto \vartheta^0 \ .$$

As a consequence, the matrices $\mathrm{E}(\varphi)$ and $\mathrm{E}^{-1}(\varphi)$ have a corresponding symmetry property: applying simultaneously the same permutation $\varsigma \in S_5$ to the columns and rows $2, \ldots, 6$ and $7, \ldots, 11$ keeps the matrices invariant. Due to these symmetries, it is natural to assume that the matrix $\mathrm{U}(0)$ has the form

$$\mathrm{U}(0) = u\Lambda \left(\mathrm{I} + \alpha\, \epsilon_i + 12\alpha^2\, \mu^i + 6\chi(X)\zeta_p(3)\, \eta \right) \ ,$$

which can be verified, at least to the p-adic accuracy we are working to, by starting with the most general form (9.6) of $\mathrm{U}(0)$, and imposing requirements that the coefficients in the series appearing in $\mathrm{U}(\varphi)$ are p-adic integers. Further, from this requirement we find that $\alpha = 0$, to the accuracy we are working to.

With this form of $\mathrm{U}(0)$, the matrix $\mathrm{U}(\varphi)$ has also the same S_5 symmetry as the matrices $\mathrm{E}(\varphi)$ and $\mathrm{E}^{-1}(\varphi)$. This permutation symmetry implies that its characteristic polynomials factorises over integers as

$$\mathrm{Det}(\mathrm{I} - \mathrm{U}(\varphi)T) \ = \ R_2(T)^4 R_4(T) \ ,$$

where $R_2(T)$ is a quadratic and $R_4(T)$ a quadric polynomial. Further, from the Weyl conjectures it follows that these polynomials take the form

$$R_2(T) \ = \ 1 + a_1 pT + p^3 T^3 \ , \qquad R_4(T) \ = \ 1 + b_1 T + b_2 pT^2 + b_1 p^3 T^3 + p^6 T^4 \ ,$$

leaving three undertermined coefficients. It turns out that in all cases we have studied the polynomial $R_4(T)$ is exactly the numerator of the zeta function of $\mathbb{Z}_5$ quotient, studied for example in [10], of the manifolds on the completely symmetric line.

The polynomials $R_4(T)$ can be therefore found in the tables of [13]. Thus leaves us with one parameter, a_1, to fix. Apart from using the matrix $\mathrm{U}(\varphi)$, this coefficient can be found by using the relation of the

coefficients of the zeta function numerator to the number of points on the manifold defined over finite fields. The number of points on Hulek-Verrill manifolds over the field $\mathbb{F}_p$ was computed by Hulek and Verrill [14]. On the non-singular manifolds the number of points over $\mathbb{F}_p$ is given by

$$\#_p \mathrm{HV}_{(\varphi^1,\varphi^2,\varphi^3,\varphi^4,\varphi^5)} \;=\; 48p^2 + 46p + 14 + \sum_{x,y,z=1}^{p-1} \left(\frac{\Upsilon}{p}\right) + \rho(\varphi^1)\#_p(\mathcal{E}) \;,$$

where

$$\Upsilon \;=\; \left((1+x+y+z)\left(\frac{\varphi^2}{x}+\frac{\varphi^3}{y}+\frac{\varphi^4}{z}+\varphi^5\right)-\varphi^1-1\right)^2 - 4\varphi^1 \;,$$

$\left(\frac{\Upsilon}{p}\right)$ denotes the Kronecker symbol, and in this context

$$\rho(\varphi^1) \;=\; \begin{cases} p & \text{if } \varphi^1 \equiv 1 \bmod p \;, \\ 0 & \text{otherwise.} \end{cases}$$

$\#_p(\mathcal{E})$ denotes the number of points over $\mathbb{F}_p$ on the elliptic curve

$$(x+y+z)\left(\frac{\varphi^2}{x}+\frac{\varphi^3}{y}+\frac{\varphi^4}{z}\right) \;=\; \varphi^5 \;.$$

Using the relation between the series expansion of the zeta function and the number of points on the manifold, we find that the coefficients a_1 should be given by

$$a_1 \;=\; \frac{1}{4}\left(b_1 + 1 + 45p + 45p^2 + p^3 - \#_p \mathrm{HV}_{(\varphi,\varphi,\varphi,\varphi,\varphi)}\right) \;.$$

Thus the zeta function for the S_5-symmetric family of Hulek-Verrill manifolds can be computed in two ways: using the point-counting formula together with the tables in [13], and alternatively by computing the traces of powers of $\mathrm{U}(\varphi)$. Comparing the results gives intricate consistency checks of our methods, and we indeed find a perfect agreement.

Chapter 10

Supersymmetric Flux Vacua on Hulek-Verrill Manifolds

10.1 The supersymmetric flux vacuum equations

We can use a class of $\mathbb{Z}_2$ symmetries to find solutions to the equations (3.21) that must be satisfied in order for a supersymmetric flux vacuum to exist. In particular, the five-parameter Hulek-Verrill manifolds on the S_5-symmetric locus in the moduli space exhibit such symmetries. To find a non-trivial solution to the flux vacuum equations (3.21), one must specify a pair of integral flux vectors F and H satisfying

$$F^T \, \Sigma \, H \, \neq \, 0 \; .$$

In terms of these the flux vector corresponding to the complexified field strength G_3 is $F - \tau H$, so the superpotential can be written as

$$W \; = \; (F - \tau H)^T \, \Sigma \, \Pi \; .$$

The flux vectors F and H are constrained by the requirement that equations

$$W \; = \; 0 \; , \qquad \partial_\tau W \; = \; 0 \; , \qquad \partial_{z^i} W \; = \; 0 \tag{10.1}$$

can be solved for complex scalar field τ and complex structure moduli z^i. The second of the equations (10.1) is equivalent to the condition that H is symplectic orthogonal to the period vector Π whence the first equation reduces to demand that F be symplectic orthogonal to Π. Thus we must find vectors F and H satisfying the following thee conditions

$$F^T \, \Sigma \, H \, \neq \, 0 \; , \qquad H^T \, \Sigma \, \Pi \; = \; 0 \; , \qquad F^T \, \Sigma \, \Pi \; = \; 0 \; .$$

Once a pair of fluxes has been specified, it is necessary to constrain the moduli z^i and τ so that there exists a solution to the remaining $m = h^{2,1}$ equations

$$\partial_{z^i} \, (F - \tau H)^T \, \Sigma \, \Pi \; = \; 0 \; .$$

For the purposes of finding solutions to the supersymmetric flux vacuum equations, instead of working with the period vector in the integral basis Π, it is convenient to use the complex Frobenius basis where the periods are given by the vector $\widehat{\varpi}$ defined in (2.15). For this purpose, we introduce vectors $\widehat{F}$ and $\widehat{H}$ adapted to this basis. Define

$$\widehat{F}^{\,T} \;=\; F^T\,\Sigma\,(\Sigma\rho)^{-1}\ , \qquad \widehat{H}^{\,T} \;=\; H^T\,\Sigma\,(\Sigma\rho)^{-1}\ .$$

Note, however, that these are not the vectors F and H expressed in the complex Frobenius basis, but rather auxiliary vectors, whose utility comes from the fact that the flux vacuum equations become simple when expressed using them and the periods in the complex Frobenius basis. To be precise, the flux vacuum equations

$$F^T\,\Sigma\,H\;\neq\;0\ , \qquad F^T\,\Sigma\,\Pi\;=\;0\ , \qquad H^T\,\Sigma\,\Pi\;=\;0\ , \qquad \partial_{z^i}\,(F-\tau H)^T\,\Sigma\,\Pi\;=\;0\ ,$$

then read

$$\widehat{F}^{\,T}\,\Sigma\rho^{-1}\Sigma(\rho^T)^{-1}\Sigma\,\widehat{H}\;\neq\;0\ , \quad \widehat{F}^{\,T}\,\Sigma\,\widehat{\varpi}\;=\;0\ , \quad \widehat{H}^{\,T}\,\Sigma\,\widehat{\varpi}\;=\;0\ , \quad \partial_{z^i}\left(\widehat{F}-\tau\widehat{H}\right)\,\Sigma\,\widehat{\varpi}\;=\;0\ . \tag{10.2}$$

We shall specify our solution in terms of the vectors $\widehat{F}$ and $\widehat{H}$, taking care that the vectors F and H in the integral basis defined by this choice have rational entries. The physical quantization condition demands that F and H have integral entries, but this can always be accomplished by a scaling.

10.2 Solutions from $\mathbb{Z}_2$ symmetry

Suppose that there exsists a point $\boldsymbol{\varphi}$ in the complex structure moduli space and a pair of integers $i\neq j$ so that the following equalities hold:

$$\widehat{\varpi}^i(\boldsymbol{\varphi})\;=\;\widehat{\varpi}^j(\boldsymbol{\varphi}')\ , \qquad \widehat{\varpi}_i(\boldsymbol{\varphi})\;=\;\widehat{\varpi}_j(\boldsymbol{\varphi}')\ , \tag{10.3}$$

where $\boldsymbol{\varphi}'$ is obtained by acting on $\boldsymbol{\varphi}$ by a $\mathbb{Z}_2$ permutation $\mathfrak{A}_{k,l}$ defined by

$$\mathfrak{A}_{k,l}\,:\,\mathbb{C}^m\to\mathbb{C}^m\,:\,\varphi^k\mapsto\varphi^l\ , \quad \varphi^l\mapsto\varphi^k\ , \quad \varphi^s\mapsto\varphi^s \text{ for } s\neq k,l$$

for some integers $k\neq l$. This happens, for instance, on manifolds whose complex structure moduli space is symmetric under $\varphi^k\leftrightarrow\varphi^l$.

Let δ_n denote the $(2m{+}2)$-component vector with n'th entry 1 and all other entries zero. When the vector $\widehat{\varpi}$ has the symmetry (10.3), it is possible to solve (10.2) by first choosing the fluxes as

$$\widehat{F}\;=\;\delta_i-\delta_j\ , \qquad \widehat{H}\;=\;\delta_{m+1+i}-\delta_{m+1+j}\ ,$$

Then a solution to the equations (10.2) is found by imposing $\varphi^k=\varphi^l$, which is the fixed locus of the involution $\mathfrak{A}_{k,l}$, but leaving the remaining φ^s free, and giving τ the value

$$\tau\;=\;\left.\frac{\widehat{F}^{\,T}\,\Sigma\,\partial_{\varphi^k}\widehat{\varpi}}{\widehat{H}^{\,T}\,\Sigma\,\partial_{\varphi^k}\widehat{\varpi}}\right|_{\varphi^k=\varphi^l}\;=\;-\frac{1}{2\pi\mathrm{i}}\left.\frac{\partial_{\varphi^k}\,(\varpi_i-\varpi_j)}{\partial_{\varphi^k}\,(\varpi^i-\varpi^j)}\right|_{\varphi^k=\varphi^l}\ . \tag{10.4}$$

We now proceed to investigate such solutions on the S_5-symmetric locus of the family of Hulek-Verrill manifolds. Using the Bessel function expressions (6.30)-(6.31), we are able to give a formula for τ as a ratio of Bessel function integrals. These latter expressions allow us, after some numerical work, to find the j-invariant of the associated F-theory curve as a rational function of the complex structure moduli:

$$j(\tau(\varphi)) \;=\; R(\varphi)\;,$$

where R is a rational function. We have verified this identity to 200 figures for hundreds of values of φ in each case.

10.2.1 The Hulek-Verrill manifold

The five-parameter Hulek-Verrill manifolds support supersymmetric flux vacua on the loci where any two complex structure moduli φ^i are equal. For definiteness, let us set two of the φ^1 and φ^2 equal to a value b^0, and relabel the three remaining φ^i as b^1, b^2, b^3. Use of standard Bessel function identities reveals that the axiodilaton in (10.4) is

$$\tau\left(b^1,\,b^2,\,b^3\right) \;=\; \frac{2\mathrm{i}}{\pi}\,\frac{\int_0^\infty \mathrm{d}z\; z\,\mathrm{K}_0(z)\left[\mathrm{K}_0\left(\sqrt{b^1}z\right)\,\mathrm{I}_0\left(\sqrt{b^2}z\right)\,\mathrm{I}_0\left(\sqrt{b^3}z\right)\;+\text{cyclic}\right]}{\int_0^\infty \mathrm{d}z\; z\,\mathrm{K}_0(z)\,\mathrm{I}_0\left(\sqrt{b^1}z\right)\,\mathrm{I}_0\left(\sqrt{b^2}z\right)\,\mathrm{I}_0\left(\sqrt{b^3}z\right)}\;. \tag{10.5}$$

Perhaps curiously, the dependence on b^0 cancels.

The dependence of the j-invariant can be found numerically by computing the value of j on numerous points on the moduli space, and fitting the points on a rational function. It turns out that the j-function takes a remarkably simple form

$$j\left(\frac{1}{2}\tau\left(b^1,\,b^2,\,b^3\right)\right) \;=\; \frac{\left(\Delta_F + 256\;b^1b^2b^3\right)^3}{\Delta_F^2\;b^1b^2b^3}\;, \tag{10.6}$$

where we have used $\tau/2$ instead of τ, as this gives a slightly more convenient form of j-function. This rescaling corresponds to an isogeny of the F-theory curve, or equivalently to a rescaling of fluxes, as discussed in §10.3, and thus gives also a valid solution. The polynomial Δ_F related to the discriminant (5.15) is given by

$$\begin{aligned}\Delta_F \;&=\; \prod_{\epsilon_i=\pm 1}\left(1+\epsilon_1\sqrt{b^1}+\epsilon_2\sqrt{b^2}+\epsilon_3\sqrt{b_3}\right)\\ &=\; \left(\left(1-b^1-b^2-b^3\right)^2-4\left(b^1b^2+b^2b^3+b_3b^1\right)\right)^2-64\;b^1b^2b^3\end{aligned}$$

To derive (10.5) and then subsequently arrive at (10.6), we have used the expressions (6.30)-(6.31) for the periods valid in the region Re $\left[\sum_{i=1}^5\sqrt{\varphi^i}\right] < 1$. Since the expression (10.6) is well-defined everywhere outside of the discriminant locus, this is the unique analytic continuation of the left-hand side into this region and the expression (10.6) is correct throughout moduli space.

To fix the F-theory fibre $\mathcal{E}_F$, which was shown in §3.5.3 to take on the general form (3.25)

$$y^2 \;=\; x^3 + (C-3)x + (C-2) \;,$$

we must choose $C = C(b^1,\, b^2,\, b^3)$ such that the j-invariant of this curve agrees with (10.6). Requiring this, the resulting equation is cubic in C and has three solutions. Among these three, only one is a rational function of the moduli b_i. In this way we are led to

$$C(b^1,\, b^2,\, b^3) \;=\; \frac{9}{4} - \frac{144\; b^1 b^2 b^3}{\Delta_F + 64\; b^1 b^2 b^3} \;. \tag{10.7}$$

10.3 Flux vacuum modularity

10.3.1 The S_5 symmetric family $\varphi^i = \varphi$

As an interesting example of these families of supersymmetric flux vacua, we study the solutions on the locus in the complex structure moduli space where all complex structure moduli are equal, $\varphi^i = \varphi$ for $i = 1, \ldots, 5$. As shown in chapter 9, then the polynomial $R(T)$ determining the zeta function takes the form

$$R(T) \;=\; R_2(T)^4 R_4(T) \;,$$

where the polynomials $R_2(T)$ and $R_4(T)$ are determined up to three constants a_p, b_p, and c_p:

$$R_2(T) \;=\; 1 - c_p p T + p^3 T \;, \qquad R_4(T) \;=\; 1 + a_p T + b_p T^2 + a_p p^3 T^3 + p^6 T^4 \;.$$

These have been tabulated for primes up to $p = 47$ in appendix D, and more can be easily computed using the methods developed in the previous chapter.

Based on the modularity conjecture of [11, 12] the coefficients c_p appearing in the quadratic polynomial $R_2(T)$ should be coefficients of a modular form, at least when p is not a prime of bad reduction. These may be elliptic modular forms, but also other types of modular forms should appear. For instance, we should have Hilbert or Bianchi modular forms appearing when φ belongs to a totally real or an imaginary quadratic number field, respectively. To test this expectation, we can fix the value of φ, compute the coefficients c_p for the primes, say, $p < 100$, and we should be able to find a modular form whose coefficients are given by the c_p.

On the S_5-symmetric locus, there exists a supersymmetric flux vacuum for any value of φ, apart from the values $\varphi = 1/25, 1/9, 1$ corresponding to singular Hulek-Verrill manifolds. This is reflected by the fact that the zeta function numerator $R(T)$ has always a quadratic piece when factorised over integers. We can therefore search for modular forms with coefficients c_p for any φ, and should always be able to find such a modular form — and thus a corresponding elliptic curve. What makes the search significantly easier is that based on on the arguments and observations of [11, 12] we expect that

the axiodilaton τ, which can be solved from the equation (10.5), can be identified with the complex structure modulus of this elliptic curve, and thus these modular forms have the j-invariants given by (10.6), which on the S_5-symmetric locus is given by

$$j\left(\frac{1}{2}\tau(\varphi,\varphi,\varphi)\right) \stackrel{\text{def}}{=} j(\varphi) \;=\; \frac{(1+3\varphi)^3(1-15\varphi+75\varphi^2+3\varphi^3)^3}{(1-9\varphi)^2(1-\varphi)^6\varphi^3}\ .$$

The corresponding F-theory fibre is

$$y^2 = x^3 - \left(\frac{144\varphi^3}{\left(3\varphi^2+6\varphi-1\right)^2}+\frac{3}{4}\right)x + \frac{1}{4} - \frac{144\varphi^3}{\left(3\varphi^2+6\varphi-1\right)^2}\ . \tag{10.8}$$

Scaling of fluxes and isogenies

The relation between the flux vectors F and H and the axiodilaton τ seemingly produces a paradox when the axio-dilaton is identified with the complex structure parameter of the F-theory fibre $\mathcal{E}_F$, or more generally, with the complex structure parameter of the curve $\mathcal{E}_R$ associated to the zeta function. Namely, given a point $\boldsymbol{\varphi}$ in the moduli space, the zeta function and thus the coefficients $a_p(\mathcal{E}_R)$ related to the number of points on $\mathcal{E}_R$ over finite fields $\mathbb{F}_p$ are uniquely determined, and in particular do not depend on the flux vectors $\widehat{F}$ and $\widehat{H}$. However, under a scaling $\widehat{F} \to \alpha\widehat{F}$, $\widehat{H} \mapsto \beta\widehat{H}$ with $\alpha,\beta \in \mathbb{N}$, which preserves the quantisation conditions, the parameter τ scales as $\tau \to \alpha/\beta\tau$, thus giving a different elliptic curve associated to the flux vacuum.

The resolution to this apparent tension is that a rational scaling of τ gives an *isogeny* of elliptic curves. Isogenous elliptic curves $\mathcal{E}$ and $\mathcal{E}'$ have, in particular, same number of points over all finite fields $\mathbb{F}_p$. Thus the modular form coefficients associated to these elliptic curves satisfy $a_p(\mathcal{E}) = a_p(\mathcal{E}')$ for every good p. Even more is actually true. By the Faltings-Tate theorem [92], if $a_p(\mathcal{E}) = a_p(\mathcal{E}')$ for all but finitely many primes, then $\mathcal{E}$ and $\mathcal{E}'$ are isogenous. Thus the zeta function does not actually determine the elliptic curve $\mathcal{E}_R$ uniquely, but only up to isogeny. In the IIB theory this is reflected by the freedom to scale the fluxes by integers. Note that the charge quantisation plays a central role in this argument; elliptic curves related by an irrational scaling of τ are not isogenous.

In the case of elliptic curves and zeta functions associated to flux vacua, we conjecture that it is always possible to choose $\mathcal{E}_R$ among the isogeny class so that its j-invariant agrees with the j-invariant of the F-theory curve $\mathcal{E}_F$. This j-invariant is uniquely determined by the coordinates in the moduli space and the flux vectors.

10.3.2 Rational points and elliptic modular forms

Returning to the relation of the F-theory fibre $\mathcal{E}_F$ and the elliptic curve $\mathcal{E}_R$ corresponding to the quadratic factor $R_2(T)$, the flux vacuum equations only fix the modulus τ or equivalently the j-invariant of $\mathcal{E}_F$, and thus a particular complex isomorphism class. However, these arguments do not

fix a particular rational model for the elliptic curve, leaving us with the freedom to to twist this curve. From physical perspective this can be thought of as the gauge freedom to choose complex coordinates on the fibre.

From this point of view, it seems evident that the physical theory will not distinguish between different rational models as each fibre differs just by a gauge transformation. However, following [12], we can ask if there exists a 'natural', choice of coordinates on the elliptic fibre, which makes the F-theory fibre and the curve $\mathcal{E}_R$ corresponding to $R_2(T)$ agree everywhere. Existence of such a set of coordinates that should be a given by some 'simple' function on the moduli space, or even in any open subset in the moduli space, is not at all obvious, as the coordinate transformation needed is not a priori required to even be continuous. Nevertheless, we remarkably find that in this case there exists a coordinate transformation (10.9) that is given by a root of a simple rational function.

To find the required change of coordinates so that $\mathcal{E}_F$ has the same rational structure as the curve $\mathcal{E}_R$, we fix the value of φ and compute the coefficients $c_p(\varphi)$ for the first few primes, say $p < 100$. This is enough to find the corresponding elliptic curve which has the correct j-invariant, and thus is related to $\mathcal{E}_F$ by a twist

$$x \to c_t(\varphi)^2 x \ , \qquad y \to c_t(\varphi)^3 y \ , \tag{10.9}$$

which can be found explicitly by comparing the equations defining the curves $\mathcal{E}_F$ and $\mathcal{E}_R$.

For example, consider the case $\varphi = \frac{15}{2}$. The j-invariant corresponding to the F-theory curve at this point is

$$j\left(\frac{15}{2}\right) \ = \ \frac{8244868726038180601}{576324614706750} \ .$$

The L-functions and modular forms database LMFDB [41] lists 5 elliptic curves and corresponding modular forms with this j-invariant. We expect to find the modular form associated to the zeta function at $\varphi = \frac{15}{2}$ among these. To fix the modular form, we compute the coefficients c_p for the primes $p < 100$. With the zeta function numerators on hand, this is straightforward, apart from the slight subtlety associated with the representing the rational number r/s in the finite fields $\mathbb{F}_p$. When $p \nmid s$, there is an unique element $x \in \mathbb{F}_p$ such that $xs = 1 \bmod p$. This x gives the representative of $1/s$ in $\mathbb{F}_p$, and r/s is represented by $rx \in \mathbb{F}_p$. With this, it is easy to compute the coefficients and compare them to the modular form coefficients (see table 10.1). We find perfect agreement with the modular form with LMFDB label **51870.bs3**, whereas the coefficient of other modular forms differ at various primes by a sign, as is expected for modular forms given by twists.

The modular form **51870.bs3** corresponds to the elliptic curve

$$y + xy + y^2 \ = \ x^3 - 42088x + 3112688 \ , \tag{10.10}$$

defined up to a rational isomorphism of the form (10.9) with $c_t(\varphi)$ a rational number. The elliptic curve (10.10) can be obtained from the expression (10.8) for $\mathcal{E}_F$ by affecting a twist (10.9) on the fibre coordinates x and y with

$$c_t\left(\frac{15}{2}\right) \;=\; -\mathrm{i}\sqrt{\frac{851}{6}}\;,$$

defined up to a rational number.

p	$\varphi \in \mathbb{F}_p$	c_p
5	0	—
7	4	1
11	2	6
13	1	—
17	16	−6
19	17	1
23	19	0
29	22	−6
31	23	2
37	26	2
41	28	0
43	29	8
47	31	0
53	34	0
59	37	−6
61	38	8
67	41	8
71	43	0
73	44	2
79	47	−10
83	49	−12
89	52	0
97	56	8

p	c_p
5	1
7	1
11	6
13	1
17	−6
19	1
23	0
29	−6
31	2
37	2
41	0
43	8
47	0
53	0
59	−6
61	8
67	8
71	0
73	2
79	−10
83	−12
89	0
97	8

Table 10.1: *On the left, we list the coefficients c_p appearing in the quadratic factor $R_2(T)$ of the zeta function numerator at $\varphi = 15/2$. The second column displays the image of $\varphi = 15/2$ in the finite field $\mathbb{F}_p$. Where the value for coefficient c_p is not displayed, this is due to φ corresponding to an apparent singularity (see [13]) for that prime. On the right we display the Hecke eigenvalues c_p corresponding to a prime p of the weight-two modular form with LMFDB label **51870.bs3**. Note the perfect agreement when c_p is listed.*

This procedure can be repeated for various values of φ. In all cases we find that, as expected by the modularity conjecture, the elliptic curve obtained from flux compactifications is a twist of the curve associated to the zeta function. We tabulate these twists along with the corresponding curves for a few rational values of φ in table 10.2. Many more points can be studied, and we include more complete data in appendix E.

φ	Elliptic Curve	Modular Form	c_t	Elliptic Curve Equation
3	**156.b3**	**156.2.a.b**	$-\mathrm{i}\sqrt{\frac{22}{3}}$	$y^2 = x^3 + x^2 - 148x + 644$
$\frac{7}{2}$	**4270.c3**	**4270.2.a.c**	$-\mathrm{i}\sqrt{\frac{227}{6}}$	$y + xy + y^2 = x^3 - 3818x + 89958$
4	**210.d5**	**210.2.a.d**	$-\mathrm{i}\sqrt{\frac{71}{6}}$	$xy + y^2 = x^3 - 361x + 2585$
$\frac{9}{2}$	**3318.e3**	**3318.2.a.e**	$-\mathrm{i}\sqrt{\frac{347}{6}}$	$y + xy + y^2 = x^3 - 8341x + 288230$
5	**220.a4**	**220.2.a.a**	$-\mathrm{i}\sqrt{\frac{13}{3}}$	$y^2 = x^3 + x^2 - 45x + 100$
$\frac{11}{2}$	**6402.f3**	**6402.2.a.f**	$-\mathrm{i}\sqrt{\frac{491}{6}}$	$y + xy + y^2 = x^3 - 15671x + 733052$
6	**1590.u3**	**1590.2.a.u**	$-\mathrm{i}\sqrt{\frac{143}{6}}$	$xy + y^2 = x^3 - 1290x + 17100$
$\frac{13}{2}$	**32890.b3**	**32890.2.a.b**	$-\mathrm{i}\sqrt{\frac{659}{6}}$	$y + xy + y^2 = x^3 - 26624x + 1596972$
7	**2604.d3**	**2604.2.a.d**	$-\mathrm{i}\sqrt{\frac{94}{3}}$	$y^2 = x^3 + x^2 - 2108x + 34596$
$\frac{15}{2}$	**51870.bs3**	**51870.2.a.bs**	$-\mathrm{i}\sqrt{\frac{851}{6}}$	$y + xy + y^2 = x^3 - 42088x + 3112688$
8	**994.e3**	**994.2.a.e**	$-\mathrm{i}\sqrt{\frac{239}{6}}$	$xy + y^2 = x^3 - 3238x + 65508$

Table 10.2: *Some modular forms corresponding to the quadratic factors of the numerator of the zeta function, the corresponding elliptic curves and twists relating these curves to the F-theory fibre* (10.8).

Based on the data in table 10.2, we can find a root of a simple rational function

$$c_t(\varphi) \;=\; \sqrt{\frac{3}{2(1-6\varphi-3\varphi^2)}}\,.$$

that gives the twists up to a rational number, twisting by which does not change the rational model. Based on this, we conjecture that choosing the F-theory fibre over a generic point on the Calabi-Yau manifold to be

$$y^2 \;=\; x^3 - \frac{(1{+}3\varphi)(1{-}15\varphi{+}75\varphi^2{+}3\varphi^3)}{3}x + \frac{2(-1{+}6\varphi{+}3\varphi^2)(1{-}12\varphi{+}30\varphi^2{-}540\varphi^3{+}9\varphi^4)}{27} \qquad (10.11)$$

the F-theory curve $\mathcal{E}_F$ coincides with $\mathcal{E}_R$, with both curves having the same rational model. With the zeta function data on hand, we can test this conjecture for hundreds of rational values of φ. The results agree perfectly, giving a strong indication of veracity of this conjecture. We tabulate the values of φ, along with the corresponding modular forms and elliptic curves in appendix E.

Note that this only fixes the curves up to a rational isomorphism, and there is no unique way of making this choice. One such choice is to use the convention used by LMFDB, where the elliptic curves are displayed in Weierstrass form with integral coefficients. To get to this form will in general require a further rational change of coordinates.

One interesting observation that can be made from the data gathered in E is that the curves with equal j-invariant $j(\varphi)$, the one corresponding to the correct modular form is, for all examples we have studied, given by the curve with the smallest conductor. This phenomenon does not appear in the examples studied in [12].

10.3.3 Real quadratic points and Hilbert modular forms

With the conjecture that the elliptic curve $\mathcal{E}_R$ associated to the quadratic factor $R_2(T)$ of the zeta function is given by (10.11), we can investigate cases where this elliptic curve is defined over an extended number field. A particularly interesting case is given by real quadratic fields $\mathbb{Q}(\sqrt{\alpha})$, where α is a positive square-free integer. Elliptic curves defined over these fields have been proven to be modular [93] in a sense that for an elliptic curve $E(\mathbb{Q}(\sqrt{\alpha}))$ defined over $\mathbb{Q}(\sqrt{\alpha})$, there exists a Hilbert cusp form f over $\mathbb{Q}(\sqrt{\alpha})$ of weight $(2,2)$ so that $L(E) = L(f)$. Consequently, we expect to again have a correspondence between the coefficients appearing in the quadratic factor of the zeta function numerator agree with the Fourier series coefficients of Hilbert modular forms.

By studying the zeta function at points in the moduli space where φ and j take on real quadratic values, we will see that the coefficients c_p of the quadratic factors $R_2(T)$ indeed correspond to Fourier coefficients of a Hilbert cusp form of parallel weight $(2,2)$ and the corresponding elliptic curve is given by $\mathcal{E}_F$, as we would expect based on the analogous study of rational points and elliptic curves conducted above. An analogous prediction in the case of a family of octic Calabi-Yau manifolds was made in [12]. However, in that case the lack of zeta function data prevented the authors from explicitly verifying their predictions.

To see explicitly how the correspondence works in the real quadratic case, let us take as an example the case $\varphi = 2+\sqrt{3}$. In this case the j-invariant is given by

$$j(2+\sqrt{3}) \;=\; \frac{35168888}{529} + \frac{15980748}{529}\sqrt{3}\;,$$

and the fibre $\mathcal{E}_F$ is given by, up to an isomorphism over $\mathbb{Q}(\sqrt{3})$, by

$$y^2 + \left(1+\sqrt{3}\right)xy + \left(1+\sqrt{3}\right) \;=\; x^3 - \left(11-4\sqrt{3}\right)x + 12 - 8\sqrt{3}\;.$$

This is the elliptic curve with LMFDB label **92.1-a3**, whose corresponding Hilbert cusp forms have labels **2.2.12.1-92.1-a** and **2.2.12.1-92.1-b**, which differ only by a relative sign of some eigenvalues. The Hecke eigenvalues corresponding to the first few primes of $\mathbb{Q}(\sqrt{3})$ are given in table 10.3.

To find the corresponding coefficients c_p in the quadratic factor of the zeta function, we must find a representative of $\sqrt{3}$ in $\mathbb{F}_p$. By this we mean an element $\alpha \in \mathbb{F}_p$ that satisfies the equation $x^2-3=0$ in $\mathbb{F}_p$. This equation can only be satisfied if 3 is a quadratic residue mod p, in which case there are exactly two solutions we can think of corresponding to $\pm\sqrt{3}$. However, we need to keep in mind that the choice of the representative is arbitrary and, thus we should think of both solutions as representing $\sqrt{3}$.

Using the solutions α, we can form, for every p such that 3 is a quadratic residue mod p, two representatives of $2+\sqrt{3} \in \mathbb{F}_p$. We can then find the corresponding coefficients c_p, and thus obtain a pair of coefficients c_p for every such prime. We collect the data for primes $5 \leq p < 100$ in table 10.3.

$\mathfrak{p}$	$N(\mathfrak{p})$	$c_{\mathfrak{p}}$
$(11, 1-2\sqrt{3})$	11	-6
$(11, 1+2\sqrt{3})$	11	0
$(13, 4+\sqrt{3})$	13	-4
$(13, 4-\sqrt{3})$	13	-4
$(23, 2-3\sqrt{3})$	23	-1
$(23, 2+3\sqrt{3})$	23	0
$(37, -7+2\sqrt{3})$	37	-4
$(37, -7-2\sqrt{3})$	37	2
$(47, -1+4\sqrt{3})$	47	0
$(47, -1-4\sqrt{3})$	47	0
$(59, -4+5\sqrt{3})$	59	12
$(59, -4-5\sqrt{3})$	59	-12
$(61, -8+\sqrt{3})$	61	8
$(61, -8-\sqrt{3})$	61	-10
$(71, -2+5\sqrt{3})$	71	0
$(71, -2-5\sqrt{3})$	71	12
$(73, -10+3\sqrt{3})$	73	2
$(73, -10-3\sqrt{3})$	73	-10
$(83, -5+6\sqrt{3})$	83	-12
$(83, -5-6\sqrt{3})$	83	-6
$(97, -10-\sqrt{3})$	97	2
$(97, -10+\sqrt{3})$	97	14

p	$\varphi \in \mathbb{F}_p$	c_p
11	8	-6
11	7	0
13	6	-4
13	11	-4
23	18	-1
23	9	0
37	24	-4
37	17	2
47	14	0
47	37	0
59	50	12
59	13	-12
61	10	8
61	55	-10
71	45	0
71	30	12
73	54	2
73	23	-10
83	72	-12
83	15	-6
97	89	2
97	12	14

Table 10.3: *On the left, we list the Hecke eigenvalues $c_{\mathfrak{p}}$ of the Hilbert cusp form with the LMFDB label **2.2.12.1-92.1-b**, corresponding to primes $\mathfrak{p}$ of $\mathbb{Q}(\sqrt{3})$ with norms $N(\mathfrak{p})$. On the right, we display the representatives of $\varphi = 2+\sqrt{3}$ in the finite fields $\mathbb{F}_p$ and the coefficients c_p in the quadratic factor of the zeta function numerator corresponding to these representatives. If a prime is not listed, it means that the representative of $2+\sqrt{3}$ does not exist for that prime. Note again the perfect agreement of $c_{\mathfrak{p}}$ with c_p.*

These considerations can be repeated for multiple values of the complex structure modulus φ in totally real number fields. As expected, in every case we have studied where the F-theory curve given by (10.11) can be found on LMFDB, the Hilbert modular form associated to the F-theory curve agrees with the modular form related to the zeta function. We list more values of φ in totally real field extensions together with the corresponding Hilbert modular forms in appendix E.

10.3.4 Imaginary quadratic fields and Bianchi modular forms

In the case of imaginary quadratic field extensions $\mathbb{Q}(\sqrt{-\alpha})$ with $\alpha > 0$ a square-free integer. For these, the corresponding elliptic curves are conjectured to be modular like those defined over real quadratic field extensions, with the difference being that now the corresponding modular forms should be Bianchi

cusp forms. The identification of the quadratic factor $R_2(T)$ and the relevant Bianchi modular form works completely analogously to the case of real quadratic fields. As a simple example, consider the F-theory fibre over $\varphi = \mathrm{i}$. The fibre is an elliptic curve with the LMFDB label **164.1-a1**, given by

$$y^2 + (1+\mathrm{i})xy + (1+\mathrm{i})y \;=\; x^3 + (1+\mathrm{i})x^2 + 5\mathrm{i}x + 1 + 4\mathrm{i}\ .$$

Its j-invariant is

$$j(\mathrm{i}) \;=\; -\frac{16234000}{1681} + \frac{31900500}{1681}\,\mathrm{i}\ .$$

This elliptic curve has an associated Bianchi modular form with LMFDB label **164.1-a**, whose Hecke eigenvalues $c_{\mathfrak{p}}$ are listed in table 10.4. As with Hilbert modular forms, we can find representatives of $\varphi = \mathrm{i}$ in finite fields $\mathbb{F}_p$ by finding solutions to the equation $x^2 + 1 = 0 \bmod p$. When such solutions exist, this allows us to associate two coefficients c_p appearing in the quadratic factor of the zeta function numerator to the point $\varphi = \mathrm{i}$. As expected, we find agreement with these coefficients and the Hecke eigenvalues of the Bianchi modular form **164.1-a**. We display the coefficients $c_{\mathfrak{p}}$ and c_p for primes $5 \leq p \leq 100$ in table 10.4, although we have checked the agreement up to the 100 first primes.

$\mathfrak{p}$	$N(\mathfrak{p})$	$c_{\mathfrak{p}}$
$(-2-\mathrm{i})$	5	0
$(1+2\mathrm{i})$	5	0
$(-2-3\mathrm{i})$	13	2
$(3+2\mathrm{i})$	13	-4
$(4+\mathrm{i})$	17	6
$(-4+\mathrm{i})$	17	-6
$(5-2\mathrm{i})$	29	6
$(5+2\mathrm{i})$	29	0
$(6+\mathrm{i})$	37	8
$(-6+\mathrm{i})$	37	-4
$(5+4\mathrm{i})$	41	-6
—	41	—
$(7-2\mathrm{i})$	53	6
$(7+2\mathrm{i})$	53	12
$(-5-6\mathrm{i})$	61	2
$(6+5\mathrm{i})$	61	-10
$(-8-3\mathrm{i})$	73	14
$(-8+3\mathrm{i})$	73	-10
$(8-5\mathrm{i})$	89	6
$(5+8\mathrm{i})$	89	6
$(9-4\mathrm{i})$	97	2
$(9+4\mathrm{i})$	97	2

p	$\phi \in \mathbb{F}_p$	c_p
5	3	0
5	2	0
13	8	2
13	5	-4
17	13	6
17	4	-6
29	17	6
29	12	0
37	31	8
37	6	-4
41	9	-6
41	32	-1
53	30	6
53	23	12
61	50	2
61	11	-10
73	46	14
73	27	-10
89	55	6
89	34	6
97	75	2
97	22	2

Table 10.4: *On the left, we tabulate the Hecke eigenvalues $c_{\mathfrak{p}}$ corresponding to primes $\mathfrak{p}$ of $\mathbb{Q}(i)$ with norm $N(\mathfrak{p})$ of the Bianchi cusp form with LMFDB label **164.1-a**. On the right, the coefficients c_p appearing in the quadratic part of the zeta function numerator are listed together with the representatives of $\varphi = i$ in finite fields $\mathbb{F}_p$. The Hecke eigenvalues and the zeta function coefficients agree again.*

This procedure can be repeated for various values of φ in quadratic imaginary number fields. In all cases we have studied, when the F-theory fibre is found in LMFDB, agreement between the elliptic

curves $\mathcal{E}_F$ and $\mathcal{E}_R$ is found. We compile the points studied, together with their associated elliptic curves and modular forms in appendix E.

10.3.5 Base changes, from Hilbert and Bianchi to elliptic modular forms

In some cases, even if the value of the complex structure modulus takes on a value in a totally real or quadratic imaginary field extension of $\mathbb{Q}$, the j-invariant may still lay in the base field $\mathbb{Q}$, and further the F-theory curve $\mathcal{E}_F$ itself may be defined over $\mathbb{Q}$. In this case $\mathcal{E}_F$ is a *base change* of an elliptic curve in $\mathbb{Q}$. To such a curve we thus can associate two modular forms: the Hilbert or Bianchi modular form of the base-change curve, and the elliptic modular form of the curve defined over $\mathbb{Q}$.

In this case, one can again find multiple representatives of the complex structure modulus φ, and thus multiple coefficients c_p associated to these representatives. As expected, these turn out to be coefficients of a Hilbert or a Bianchi modular form. However, these modular forms are related to an elliptic modular form by the base change. Explicitly, the Hecke eigenvalues $c_{\mathfrak{p}}$ are equal for all $\mathfrak{p}$ with same norm, and are coefficients of an elliptic modular form.

For example, consider $\varphi = -1 + \mathrm{i}\sqrt{3} \in \mathbb{Q}\left(\sqrt{-3}\right)$. The j-invariant of the fibre corresponding to this elliptic curve is a rational number

$$j\left(-1+\mathrm{i}\sqrt{3}\right) \;=\; \frac{4956477625}{941192}\ ,$$

and indeed $\mathcal{E}_F$ is defined over $\mathbb{Q}$, being given by

$$y^2 \;=\; x^3 + \frac{1705}{3}x + \frac{115414}{27}\ .$$

Thus we can think this as a base-change curve.

As in the previous subsection 10.3.4, we can find the coefficients c_p in the zeta function corresponding to $\varphi = -1 + \mathrm{i}\sqrt{3}$. We list them in table 10.5 and identify them with the coefficients of the Bianchi modular form **196.2-a**. The Hecke eigenvalues corresponding to primes with the same norm are equal, which is a reflection of the base change, as these are exactly the Hecke eigenvalues $c_{N(\mathfrak{p})}$ of the elliptic modular forms **14.2.a.a** and **126.2.a.b**.

p	13	13	19	19	31	31	37	37	43	43	61	61	67	67	73	73	79	79	97	97
$\phi \in \mathbb{F}_p$	5	6	3	14	10	19	15	20	12	29	26	33	7	58	16	55	31	46	25	70
c_p	−4	−4	2	2	−4	−4	2	2	8	8	8	8	−4	−4	2	2	8	8	−10	−10

Table 10.5: *The coefficients c_p appearing in the quadratic part of the zeta function numerator are listed together with the representatives of $\varphi = -1 + i\sqrt{3}$ in finite fields $\mathbb{F}_p$. These numbers can be identified with the Hecke eigenvalues of the Bianchi cusp form **196.2-a**, and of the newforms **14.2.a.a** and **126.2.a.b**.*

Part IV

Towards Microscopic Interpretation: Attractors with Large Complex Structure

We study the attractor equations for an arbitrary one-parameter family of Calabi-Yau manifolds in the large complex structure region. These equations can be solved iteratively, generating what we term an N-expansion, which is a power series in the Gromov-Witten invariants of the manifold. The coefficients of this series are associated with integer partitions. In important cases we are able to find closed-form expressions for the general term of this expansion. To our knowledge, these are the first generic solutions to attractor equations that incorporate instanton contributions. In particular, we find a simple closed-form formula for the entropy associated to rank-two attractor points that includes all genus-0 instanton corrections.

Chapter 11

Introduction

11.1 Preamble

In general, finding exact attractor equation solutions that correspond to black holes with non-vanishing central charge is not as easy as finding solutions to the supersymmetric flux vacuum equations, due to the fact that the space $H^{(3,0)}(X,\mathbb{C})\oplus H^{(0,3)}(X,\mathbb{C})$ is always two-dimensional. However, by making certain simplifications, such as taking the complex structure of the compactification manifold to be large so that the instanton corrections to the prepotential (2.8) can be ignored, solutions can be found [15, 94] relatively easily. In this part, we concentrate on the region of the moduli space that is near the large complex structure point. In this region, the instanton corrections cannot be ignored, but it is possible to solve the instanton-corrected attractor equations using perturbative methods.

Given the intricate nature of instanton-corrected equations, it is very surprising that, in some important special cases, we are able to find a closed-form expression for the instanton corrections. With the help of these solutions, we are able to give interesting formulae for locations of attractor points in the moduli space, and some physical quantities of interest. For example, it is possible to give a formula for the entropy of a black hole that, in the large charge limit, is fully quantum- and instanton-corrected.

Our aim in this part is to develop what we term *N-expansions*, by which we mean expansions in terms of the Gromov-Witten invariants $N_k^{\rm GW}$, which include all perturbative and non-perturbative terms. The prototypical quantity that exhibits such an N-expansion is the prepotential (2.8), which, in the one-parameter case, takes the form

$$\begin{aligned}\mathcal{F} &= -\frac{1}{3!}Y_{abc}\frac{z^a z^b z^c}{z^0} - (z^0)^2\mathcal{I}\left(\frac{z^1}{z^0}\right)\\ &= (z^0)^2\left(-\frac{1}{6}Y_{111}t^3 - \frac{1}{2}Y_{110}t^2 - \frac{1}{2}Y_{100}t - \frac{1}{6}Y_{000} - \mathcal{I}\left(t\right)\right).\end{aligned} \tag{11.1}$$

The quantity $\mathcal{I}(t)$, which we call the *instanton sum*, corresponds to the exponentially small terms, and has the form

$$\mathcal{I}(t) \;=\; \frac{1}{(2\pi\mathrm{i})^3}\sum_{k=1}^{\infty} n_k \mathrm{Li}_3(\mathrm{e}^{2\pi\mathrm{i}kt}) \;=\; \frac{1}{(2\pi\mathrm{i})^3}\sum_{k=1}^{\infty}\frac{N_k}{k^3}\mathrm{e}^{2\pi\mathrm{i}kt}\ , \tag{11.2}$$

where the integral coefficients n_k are the instanton numbers or Gopakumar-Vafa invariants [95, 96] and in the second expression we have written the instanton sum in terms of what we shall call the *scaled Gromov-Witten invariants* N_k, which are given by

$$N_k \;=\; \sum_{d|k} d^3 n_d \;, \qquad N_k \;=\; k^3 N_k^{GW} \;, \tag{11.3}$$

with N_k^{GW} the usual Gromov-Witten invariants. The form of the prepotential has long been known. However, we have recalled this to emphasise that $\mathcal{F}$ has a *universal* form. Given the topological quantities Y_{ijk} and the instanton numbers n_k corresponding to a given manifold X, one can write down the prepotential and its N-expansion converges in a neighbourhood of the large complex structure point. What we seek here are similar universal expansions for quantities of interest such as the coordinate t and the central charge corresponding to an attractor point. In the general case, the expressions for these quantities are somewhat detailed. However, in simple cases, they can be concisely stated. For example, for the case of a D6-D0 brane system, which we specify completely in chapter 14, the attractor point location is given by

$$t = \mathrm{i}y, \qquad \text{where} \quad \frac{y}{y_0} = 1 - \sum_{m=1}^{\infty} \sum_{\mathfrak{p}\in \mathrm{pt}(m)} a_{\mathfrak{p}} N_{\mathfrak{p}} \left(\frac{m}{2\pi y_0 Y_{111}}\right)^{\boldsymbol{\ell}(\mathfrak{p})} \boldsymbol{k}_{\boldsymbol{\ell}(\mathfrak{p})-1}(2\pi m y_0). \tag{11.4}$$

In this expression y_0 is the perturbative solution for y, obtained by solving the perturbative attractor equations, where the non-perturbative terms $\mathcal{I}$ are set to zero. The quantity m is an integer while $\mathfrak{p}$ runs over the partitions of m. If $\mathfrak{p} = \{j^{\mu_j}\}$, with $\sum_j \mu_j j = m$, is such a partition, then $\boldsymbol{\ell}(\mathfrak{p}) = \sum_j \mu_j$ is the length of the partition. Surprisingly, the functions $\boldsymbol{k}_n$ that arise here are the modified spherical Bessel function $\boldsymbol{k}_n(z) = \sqrt{\frac{2}{\pi z}} K_{n+\frac{1}{2}}(z)$. The coefficient $a_{\mathfrak{p}}$ is a combinatorial factor related to the partition, and the quantity $N_{\mathfrak{p}}$ is a combination of scaled Gromov-Witten invariants

$$a_{\mathfrak{p}} \;=\; \prod_j \frac{1}{\mu_j!\, j^{2\mu_j}} \;, \qquad N_{\mathfrak{p}} \;=\; \prod_j N_j^{\mu_j} \;. \tag{11.5}$$

Our results apply, in particular, to one of the rank-two attractor points of [10]. In that case, y is known explicitly to high precision, and this formula has been checked for integers m up to 75 and so for over 80 million partitions, giving an accuracy of over 50 decimal places. The sum also responds well to the techniques of accelerated convergence, and using an iterated Shanks transformation of order 11, the agreement can be extended to 80 decimal places. The difficulty in checking this to a higher degree of accuracy lies in the need to work with a large numbers of partitions.

A similarly concise expression can be given for $|\mathcal{Z}|^2$, where $\mathcal{Z}$ is the central charge associated to a certain class of rank-two attractor points,

$$|\mathcal{Z}(Q_1)|^2 \;=\; \frac{\kappa^2 y}{2} |\Upsilon - \Lambda| \;, \tag{11.6}$$

where y is as in the expression given above, and the rank-two attractor point corresponds to the two charge vectors

$$Q_1 \;=\; \kappa \begin{pmatrix} 0 \\ \Upsilon \\ 1 \\ 0 \end{pmatrix}, \qquad Q_2 \;=\; \lambda \begin{pmatrix} \Lambda \\ 0 \\ 0 \\ 1 \end{pmatrix}.$$

In (11.6), we have given an expression for $|\mathcal{Z}(Q_1)|^2$. The corresponding expression for $|\mathcal{Z}(Q_2)|^2$ is

$$|\mathcal{Z}(Q_2)|^2 \;=\; \frac{\lambda^2}{2y}|\Upsilon - \Lambda| \; .$$

Though the expression (11.6) appears simpler, it is clear that the quantity $1/y$ can be re-expressed as an N-expansion.

These N-expansions have a compelling interpretation in terms of microstate counting, and this is particularly clear in virtue of the appearance of the instanton numbers. The $\mathcal{N} = 4$ case was famously studied by Strominger and Vafa [97]. Important early papers on microstate counting of black holes in $\mathcal{N} = 2$ theories are [15] by Maldacena, Strominger and Witten, the papers [98–105] and the extensive research of Sen (see for example [106] and references therein). These calculations take into account the leading term with the coefficient Y_{111} of the prepotential and also, in the case of [15], the term with coefficient Y_{100}, which is important owing to its relation to the genus-one correction to the prepotential. Here our aim is to take into account also the remaining terms, namely the perturbative Y_{000} term, and the instanton corrections, whose importance for the application to counting is manifest.

The utility of the prepotential for us is that, as in (2.3), we can write the holomorphic 3-form in terms of its derivatives so that that the period vector Π is

$$\Pi(t) = \begin{pmatrix} \frac{\partial}{\partial z^0}\mathcal{F} \\ \frac{\partial}{\partial z^1}\mathcal{F} \\ z^0 \\ z^1 \end{pmatrix} = z^0 \begin{pmatrix} \frac{1}{6}Yt^3 - \frac{1}{2}Y_{100}t - \frac{1}{3}\mathrm{i}Y\sigma - 2\mathcal{I}(t) + t\mathcal{I}'(t) \\ -\frac{1}{2}Yt^2 - Y_{110}t - \frac{1}{2}Y_{100} - \mathcal{I}'(t) \\ 1 \\ t \end{pmatrix}. \tag{11.7}$$

Here we have used the fact that the period vector is only defined up to a scale, and is a homogeneous of degree one as a function of z_0, z_1. For brevity, we shall write in the following

$$Y_{111} \;=\; Y \qquad \text{and} \qquad Y_{000} \;=\; \mathrm{i}Y\sigma \; .$$

Black holes in type II supergravity theories compactified on Calabi-Yau manifolds can be viewed as consisting of D0-, D2-, D4-, and D6-branes wrapped on 0-, 2-, 4-, and 6-cycles in the type IIA theory, or alternatively as D3-branes wrapping 3-cycles in the type IIB theory. This implies that the charge vector of the black hole can be viewed as an element of $H^0(X,\mathbb{Z})\oplus H^2(X,\mathbb{Z})\oplus H^4(X,\mathbb{Z})\oplus H^6(X,\mathbb{Z})$ or $H^3(X,\mathbb{Z})$. We will concentrate on one-parameter families of Calabi-Yau manifolds and usually choose a basis for these vector spaces so that we can think of the charge vector Q as an element of $\mathbb{Z}^4$ and the period vector Π as an element of $\mathbb{C}^4$.

A generic element $\Gamma \in H^0(X,\mathbb{Z})\oplus H^2(X,\mathbb{Z})\oplus H^4(X,\mathbb{Z})\oplus H^6(X,\mathbb{Z})$ can be written as

$$\Gamma \;=\; p^0 + p\, e_1 + q\,\frac{e_1^2}{Y} + q_0\,\frac{e_1^3}{Y}\ .$$

The corresponding charge vector is

$$Q \;=\; \begin{pmatrix} q_0 \\ q \\ p^0 \\ p \end{pmatrix} \;=\; \begin{pmatrix} q_{\mathrm{D0}} \\ q_{\mathrm{D2}} \\ q_{\mathrm{D6}} \\ q_{\mathrm{D4}} \end{pmatrix}, \tag{11.8}$$

where the last equality reminds us of the relation of the components to the D-brane charges[1]. This choice of basis coincides with the choice that resulted in the expression (11.7) for the period vector, so that we are allowed to think of the charge and period vectors both as elements of same vector space isomorphic to $\mathbb{C}^4$, although due to charge quantisation the elements of Q are integral.

11.2 Outline

In this part, our aim is to solve the attractor equations for an arbitrary one-parameter family of Calabi-Yau manifolds by developing N-expansions for the attractor point coordinate t. Although we consider an arbitrary manifold, for simplicity we specialise the form of the charge vector and concentrate on two important special cases that correspond to the D6-D2-D0 and D4-D2-D0 brane systems. The main reason for this choice is that restricting to a case where one of the charges vanishes makes the resulting equations much more tractable. In addition, these systems are of particular interest with microstate counting in mind, as their microstate indices can be viewed either as Donaldson-Thomas invariants or as Witten indices of divisor moduli spaces [16, 17, 107].

In chapter 12, we discuss the general method that will be used to derive N-expansions. We use chapter section to set notation, find expressions that are later specialised, and review some basic facts concerning partitions. We also define operations on partitions that are useful for expressing various functions as perturbative expansions.

Following these preliminaries, in §13.1 and §13.2 we are able to calculate fully instanton-corrected solutions to the attractor equations for the general D4-D2-D0 and D6-D2-D0 configurations. The alignment and orthogonality equations are considered separately. The solutions are separated into a perturbative part and instanton corrections.

Our strategy is to express the instanton corrections as series in $q_y = \mathrm{e}^{-2\pi y_0}$. These series have coefficients which are polynomials in the perturbative coordinates x_0, y_0, as well as the related quantities $\sin 2\pi x_0$ and $\cos 2\pi x_0$. The polynomials are most conveniently expressed as solutions to recurrence relations. These relations can be quite complicated, but in chapter 14 we see that in some important

[1] In these conventions the D-brane charges do not include the charges induced on various branes by the coupling to the world-volume curvature. Often it is useful to switch to conventions where these charges are included. For the relation between the two conventions, see §15.2.1.

cases there exist closed-form expressions. In particular, the polynomials appearing in the solutions to the D4-D2-D0 orthogonality equation and a special case of the D6-D2-D0 alignment equations can be written in terms of modified spherical Bessel functions.

This special case of the D6-D2-D0 alignment equations is of particular interest since the rank-two attractor points of AESZ34, found in [10], are included in this case. The highly constrained nature of the rank-two attractor points allows one, for example, to write the entropy in the particularly simple form (11.6). Combining the solutions obtained here to the formulae in [10], where the entropy at rank two attractor points was related to L-function values, we are able to derive an intriguing formula relating L-function values to Gromov-Witten invariants and Bessel functions.

We also provide some intuition on the rather abstract solutions by studying the limit charge ratio limits where the attractor points tend towards the large complex structure point. As a consequence of working in these limits, it is possible to deduce some universal properties of the solutions that are true on any one-parameter manifold. For example, we are able, based on consideration of the black hole charge alone, to determine whether solutions to the alignment or orthogonality equations exist near the large complex structure point.

To conclude this part and consequently the thesis, in chapter 15 we consider an important, but very speculative, open problem that connects to many promising directions for future research: is there a connection between the arithmetic properties of the compactification manifold and the physical properties of the corresponding black hole solutions? To take some first steps towards potentially addressing this problem, we study our entropy formulae from the perspective of microstate counting and verify that in leading order these expressions agree with those in [15] and with modular form asymptotics. We are, however, considering a limit that is different from that in [15] and so differences appear in subleading orders. In this sense, our results extend those in [15, 94, 98]. We conclude with a brief discussion of potential approaches of making headway toward answering this and other related problems.

11.3 Notation

We introduce some notation in an attempt to streamline otherwise complicated equations, and collect the notation which is used throughout this part, in the tables below.

$Y_{111} = Y$	$\mathrm{Im}\, Y_{000} = Y\sigma$	$\zeta = \frac{\sigma}{y_0^3}$	$\widehat{\sigma} = \frac{\sigma}{\beta^3}$
$\alpha = -\frac{Y_{110}+\Upsilon}{\widetilde{\beta}Y}$	$\beta = \sqrt{\frac{Y_{100}+2\Upsilon}{Y}}$	$\widetilde{\beta} = \sqrt{\frac{Y_{100}+2\Lambda}{Y}}$	$\gamma = -\frac{3\Lambda}{\beta^3 Y}$

Table 11.1: *Shorthand for Y_{abc}- and charge-related quantities. We take β and $\widetilde{\beta}$ to have argument 0 or $\pi/2$, depending on the argument of the square root.*

These quantities appear naturally as they are independent under monodromies. To see this, consider the symplectic transformations from section 2.2.1. In the one-parameter case such a transformation is defined by three integers, which we denote by $\mathbb{A} = A$, $\boldsymbol{B} = B$, and C. As this is a transformation of the cohomology basis, it also acts on the charge forms and vectors. The symplectic transformation S acts on the charge vector by

$$S \begin{pmatrix} q_0 \\ q \\ p^0 \\ p \end{pmatrix} = \begin{pmatrix} q_0 + Bp + Cp^0 \\ q \ + Ap + Bp^0 \\ p^0 \\ p \end{pmatrix}.$$

It follows that p^0 and p are fixed and the first two components give the transformations of q_0 and q. We work with two cases: the D6-case where $p^0 = 1$ and $p = 0$, and the D4-case where $p^0 = 0$ and $p = 1$. Recalling the transformation laws (2.11), in the D6-case the combinations

$$q + \frac{1}{2}Y_{100} \qquad \text{and} \qquad q_0 + \frac{1}{3}\mathrm{Re}[Y_{000}]$$

are invariant, while for the D4-case the invariant combinations are

$$q + Y_{110} \qquad \text{and} \qquad q_0 + \frac{1}{2}Y_{100}\ .$$

Table 11.2: *Quantities that are used throughout the part with references to where they are defined.*

Notation	**Definition**	**Description**	**Ref**
Π	$(\partial_0\mathcal{F}, \partial_1\mathcal{F}, z^0, z^1)^T$	integral period vector of X	(11.7)
Q	$(q_0, q, p_0, p)^T$	charge vector	(11.8)
$\mathcal{F}$	$-\frac{1}{3!}Y_{abc}\frac{z^a z^b z^c}{z^0} - (z^0)^2\mathcal{I}\left(\frac{z^1}{z^0}\right)$	Calabi-Yau prepotential	(11.1)
$t = x + \mathrm{i}y$	z^1/z^0	attractor point coordinate	§11.1
t_0, x_0, y_0	$t_0 = x_0 + \mathrm{i}y_0$	perturbative coordinates	§12.4
x_{00}, y_{00}	$x_0\vert_{\sigma=0}$, $y_0\vert_{\sigma=0}$	coordinates at $\sigma = 0$	§12.4
$\mathcal{I}$	$\frac{1}{(2\pi\mathrm{i})^3}\sum_{k=1}^{\infty} n_k \mathrm{Li}_3(\mathrm{e}^{2\pi\mathrm{i}kt})$	instanton sum	(11.2)
$\mathcal{I}_1$, $\mathcal{I}_2$	$\mathrm{Re}[\mathcal{I}]$, $\mathrm{Im}[\mathcal{I}]$	real and imaginary parts	§12.3

table 11.2 continued.

Notation	Definition	Description	Ref
Y_{abc}		topological quantities	(2.9)
$\mathcal{Z}$	$\frac{Q^T\Sigma\Pi}{\sqrt{-\mathrm{i}\Pi^\dagger\Sigma\Pi}}$	central charge	(3.13)
n_k		instanton numbers	(11.2)
N_k^{GW}		Gromov-Witten invariants	(11.3)
N_k	$\sum_{d\|k} d^3 n_d = k^3 N_k^{GW}$	scaled GW-invariants	(11.3)
q_t	$\mathrm{e}^{2\pi\mathrm{i}t_0}$	small expansion parameter	(12.8)
q_x, q_y	$q_x = \mathrm{e}^{2\pi\mathrm{i}x_0}$, $q_y = \mathrm{e}^{-2\pi y_0}$	phase and modulus of q_t	(12.8)
t_i	$t = \sum_{j=0}^{\infty} t_j q_t^j$	q_t-expansion of t	(12.8)
x_i, y_i	$x = \sum_{j=0}^{\infty} x_j q_y^j$, $y = \sum_{j=0}^{\infty} y_j q_y^j$	real and imaginary parts	(12.6)
$R^t_{\mathfrak{p}}$	$t_j = \sum_{\mathfrak{p}\in\mathrm{pt}(j)} N_{\mathfrak{p}} R^{(t)}_{\mathfrak{p}}$	rational functions	(12.7)
$R^x_{\mathfrak{p}}$, $R^y_{\mathfrak{p}}$	$\mathrm{Re}\left[R^t_{\mathfrak{p}}\right]$, $\mathrm{Im}\left[R^t_{\mathfrak{p}}\right]$	real and imaginary parts	(12.7)
$\mathfrak{p}, \mathfrak{q}$	$\sum_j \mu_j j$, $\sum_j \nu_j j$	partitions	§12.5
$c_{\mathfrak{p}}$	$\frac{(\sum_{j=1}^{\infty}\mu_j)!}{\prod_{j=1}^{\infty}\mu_j!}$; $\quad \mathfrak{p} = \sum_j \mu_j j$	multinomial coefficient	(12.14)
$a_{\mathfrak{p}}$	$\prod_{j=1}^{\infty} \frac{1}{j^{2\mu_j}\mu_j!}$, when $\mathfrak{p} = \sum_{j=1}^{\infty}\mu_j j$	combinatorial coefficients	(14.3)
$(F*G)_{\mathfrak{p}}$	$\sum_{\mathfrak{q}\subseteq\mathfrak{p}} F_{\mathfrak{p}-\mathfrak{q}}\, G_{\mathfrak{q}}$	natural convolution-like product	(12.12)
$(F\circ G)_{\mathfrak{p}}$	$\sum_{\mathfrak{q}\subset\mathfrak{p}} F_{\mathfrak{p}-\mathfrak{q}}\, G_{\mathfrak{q}}$	above, empty partitions excluded	(12.12)
Λ, Υ	varies according to context	charge ratios	(12.2)
$\|\mathfrak{p}\|$	the integer with partition $\mathfrak{p}$		§12.5
$\boldsymbol{\ell}(\mathfrak{p})$	number of parts of a partition $\mathfrak{p}$	length of $\mathfrak{p}$	§12.5
$\mathrm{pt}(k)$	$\left\{ \mathfrak{p} \;\middle\vert\; \|\mathfrak{p}\| = k \right\}$	set of all partitions of k	(12.10)
$\mathrm{pt}_s(k)$	$\{ \mathfrak{p} \mid \|\mathfrak{p}\| = k \text{ and } \boldsymbol{\ell}(\mathfrak{p}) = s \}$	all partitions of length s	(12.11)
η_k	$\sum_{j=0}^{k} \frac{(-1)^j}{y_0^{j+1}} \sum_{\mathfrak{p}\in\mathrm{pt}_j(k)} c_{\mathfrak{p}} y_{\mathfrak{p}}$	coeffs. in the q_y-expansion of $1/y$	(12.15)
$\boldsymbol{\eta}_{\mathfrak{p}}$	$\frac{1}{y_0}\sum_{j=0}^{l(\mathfrak{p})} \frac{(-1)^j}{y_0^j} r^y_{(j,j),\mathfrak{p}}$	coeffs. in the expansion of $1/y$	(12.17)
$\mathrm{e}^y(\alpha)$	$\sum_{j=0}^{k} \frac{(2\pi m)^j}{j!} \sum_{\mathfrak{p}\in\mathrm{pt}_j(k)} c_{\mathfrak{p}} y_{\mathfrak{p}}$	coeffs. in the q_y-expansion of $\mathrm{e}^{2\pi y}$	(12.15)
$\mathbf{e}^y_{\mathfrak{p}}$	$\sum_{j=0}^{l(\mathfrak{p})} \frac{(2\pi\alpha)^j}{j!} r^y_{(j,j),\mathfrak{p}}$	coeffs. in the expansion of $\mathrm{e}^{2\pi y}$	(12.17)
$r^x_{(m,n),\mathfrak{p}}$	$\sum_{\substack{\sum_{j=1}^{n}\mathfrak{p}_j=\mathfrak{p} \\ \mathfrak{p}_1,\ldots,\mathfrak{p}_m\neq\emptyset}} c\big(\{\mathfrak{p}_j\}_{j=1}^{i}\big) \prod_{j=1}^{i} R^x_{\mathfrak{p}_j}$	combinations of functions R^x	(12.16)
$\boldsymbol{k}_n(z)$	$\sqrt{\frac{2}{\pi z}} K_{n+\frac{1}{2}}(z)$	modified spherical Bessel functions	(14.4)
$f_n(y)$	$\mathrm{e}^y y^{n+1} \boldsymbol{k}_n(y)$	polynomials associated to $\boldsymbol{k}_n$	(14.4)

Chapter 12

Solving the Attractor Equations: a General Overview

Our strategy for solving the attractor equations relies on using the expression (11.7) for the period vector Π to express both the alignment equations (3.17) and the orthogonality equation (3.16) explicitly as a set of equalities involving geometric data, that is the topological quantities Y_{abc} and Gromov-Witten invariants of the Calabi-Yau manifold, and the black hole charges.

In the following sections §13.1 and §13.2, we solve these equations perturbatively in the instanton corrections. We first find the zeroth-order solution corresponding to what we shall refer to as the *perturbative* part of the prepotential, where only the Y_{abc}-terms are included, ignoring the contributions of the instanton sums. This gives a pair of polynomial equations of degree at most four. Explicit solutions of such polynomial equations are of course known since the Renaissance, but we dedicate some discussion to giving the most concise solutions: in most cases these can be given by simple trigonometric expressions.

12.1 The large complex structure region

We use the term *large complex structure region* to refer to a region in the Calabi-Yau moduli space where our solutions, such as (11.4), converge. We will later, in appendix H, argue that such a region exists and contains an open neighbourhood of the large complex structure point.

There are also at least two other closely related, but ultimately different, regions in the moduli space that could reasonably be called large complex structure regions. One is the region where the instanton sum $\mathcal{I}(t)$ converges. This is determined by the asymptotic growth of the Gromov-Witten invariants (see for example [26, 108–110])

$$\log N_k^{\mathrm{GW}} \;\sim\; 2\pi y_{\mathrm{sing}} k \ ,$$

where y_{sing} is the coordinate of the singularity nearest to the large complex structure point. Thus the instanton sum $\mathcal{I}(t)$ converges if and only if $\mathrm{Im}\, t > y_{\mathrm{sing}}$.

It is also possible to study this region using the mirror symmetry relation to the complex structure moduli space on the mirror manifold. As usual, the coordinates on the complex structure moduli space can be chosen so that the point of maximal unipotent monodromy is located at $\varphi = 0$, and the complexified Kähler moduli space coordinate t can be written in terms of periods $\varpi_a(\varphi)$, which are solutions to a Picard-Fuchs equation:[1]

$$t \;=\; \frac{1}{2\pi\mathrm{i}}\frac{\varpi_1(\varphi)}{\varpi_0(\varphi)} \;=\; \frac{1}{2\pi\mathrm{i}}\log\varphi + \mathcal{O}(\varphi)\ . \tag{12.1}$$

The solutions $\varpi_a(\varphi)$ have a radius of convergence determined by the singularities of the Picard-Fuchs operator. This determines yet another region that could be reasonably called the large complex structure region. Applying the mirror map (12.1), this region gets mapped to a neighbourhood of $t \to \infty$, bounded by a circle around the nearest singularity, unless the Picard-Fuchs operator has apparent singularities. However, this image does not in general coincide with the $\mathrm{Im}\, t > y_{\mathrm{sing}}$ region, as the correction terms of order $\mathcal{O}(\varphi)$ affect the relation. In figure 12.1, we have sketched the region around $\varphi = 0$, its image under the mirror map, and image of the resulting region under the map $t \to 1/t$.

12.2 Particular brane systems

We study extremal charged black holes that, in the string theory picture, arise from wrappings of D-branes on cycles on the internal Calabi-Yau manifold. Let us restrict our attention to arrangements containing some D2- and D0-branes bound to either D6- or D4-branes but not both. Recalling the form of a generic charge vector (11.8), this means that the charge vectors are of the form

$$Q_{\mathrm{D4}} = \kappa\begin{pmatrix}\Lambda\\ \Upsilon\\ 0\\ 1\end{pmatrix}, \qquad\qquad Q_{\mathrm{D6}} = \kappa\begin{pmatrix}\Lambda\\ \Upsilon\\ 1\\ 0\end{pmatrix}. \tag{12.2}$$

The physical charge vectors have integral components, so Λ and Υ are rational numbers, and κ is a suitable integer. The charge vectors are written in this way partly to simplify later expressions since the locations of attractor points depend only on the *charge ratios* Υ and Λ. Furthermore, this decomposition allows us to make an important distinction between what we call the *large charge limit*, where $|\kappa| \to \infty$ and the *large charge ratio limits*, where either $|\Lambda|$ or $|\Upsilon|$ is large.

In [10], where rank-two attractor points for one-parameter families were first explicitly identified, the associated charge vectors were of this type, and charge vectors of this form have received much attention in the literature. Microstate counting has been performed both for black holes of charge Q_{D4} using elliptic genera [16, 17] and D6-D0 bound states using Donaldson-Thomas invariants [59, 107].

[1] In this part we are only concerned with one-parameter families, so we adopt the standard notation $\varpi^0 = \varpi_0$, $\varpi^1 = \varpi_1$, $\varpi_1 = \varpi_2$, and $\varpi_0 = \varpi_3$ for the periods. Similar notation is applied to the periods Π_i in the integral basis.

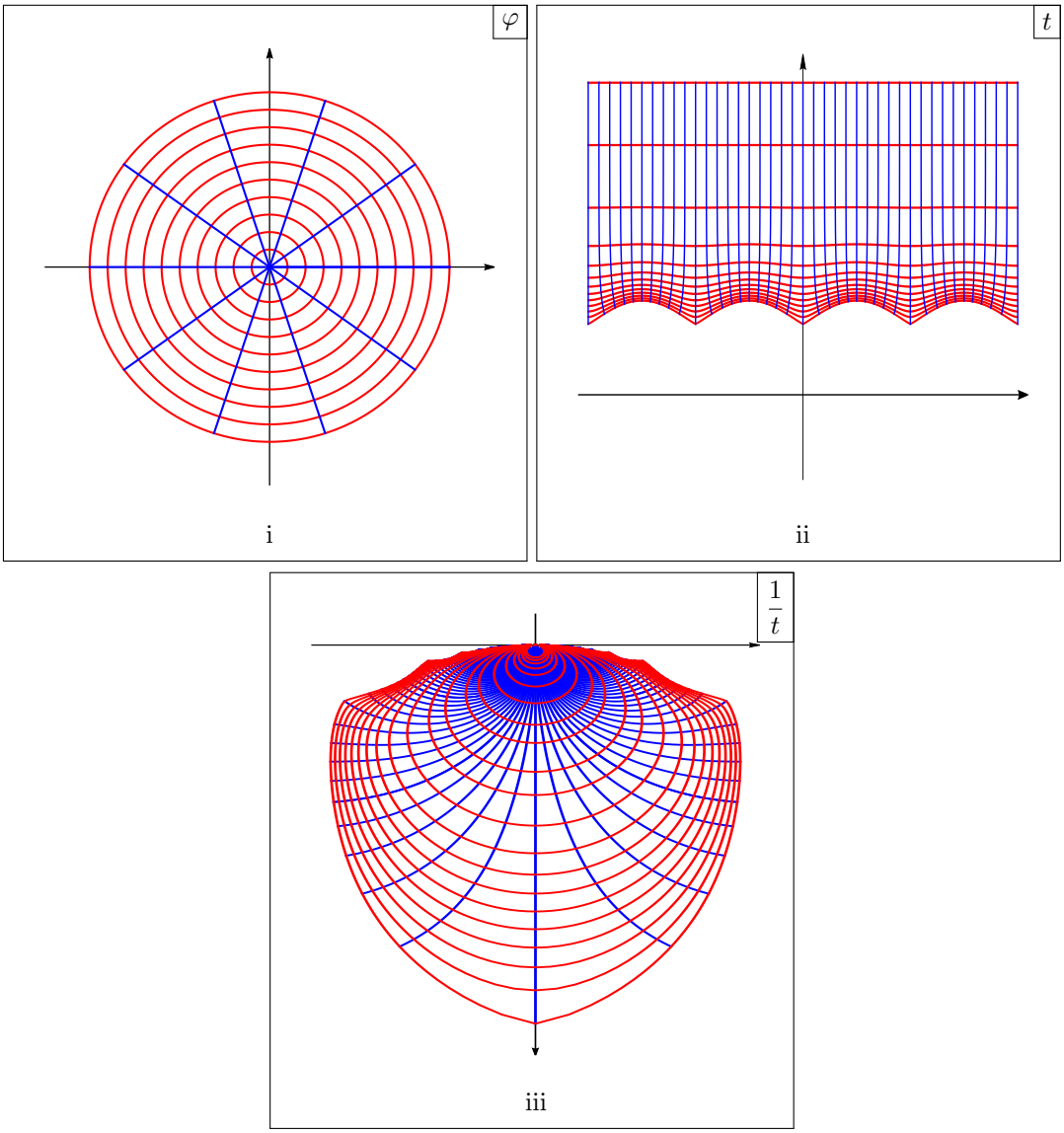


Figure 12.1: *A sketch of three different views on the large complex structure region. Figure i displays the large complex structure region on the complex structure moduli space $\mathcal{M}_{\mathbb{C}S}$ of an one-parameter Calabi-Yau threefold. The region is centred around the large complex structure singularity at $\varphi = 0$ and bounded by a circle through the singularity nearest to the $\varphi = 0$ singularity. Under the mirror map, this gets mapped to the subset of the t upper half plane displayed in Figure ii, bounded from below and extending to imaginary infinity. This figure contains multiple copies of the fundamental domain, corresponding to the multiples branches of the mirror map. This can be more conveniently displayed by making a transformation $t \to 1/t$, resulting in the region displayed in Figure iii. Note that the exact shapes of these regions depend on the manifold in question, but the qualitative features of these regions are similar for any one-parameter family of Calabi-Yau manifolds.*

By utilising the monodromy around the large complex structure point we can extend our solutions to any brane system where the D6-charge divides the D4-charge, as we will show in detail in appendix F.

12.3 General comments concerning the alignment equations

The alignment equations (3.15) depend on the quantity $\mathrm{Im}[C\Pi]$, which is manifestly not holomorphic in t, so it becomes useful to decompose the coordinate t into its real and imaginary parts, $t = x + \mathrm{i}y$.

Similarly, the constant C can be written as $a+\mathrm{i}b$. In the basis we have chosen, all Y_{abc} are real, apart from $Y_{000} = \mathrm{i}Y\sigma$ which is pure imaginary. The instanton sum $\mathcal{I}(t)$ and its derivative $\mathcal{I}'(t)$ can be decomposed as $\mathcal{I}(t) = \mathcal{I}_1(x,y) + \mathrm{i}\mathcal{I}_2(x,y)$ and $\mathcal{I}'(t) = \mathcal{I}'_1(x,y) + \mathrm{i}\mathcal{I}'_2(x,y)$.

In terms of these quantities, the alignment equations (3.17) are

$$Q \;=\; a\begin{bmatrix} \frac{1}{6}Yy\big(3x^2-y^2\big) - \frac{1}{2}Y_{100}y - \frac{1}{3}Y\sigma + y\mathcal{I}'_1 + x\mathcal{I}'_2 - 2\mathcal{I}_2 \\ -Yxy - Y_{110}y - \mathcal{I}'_2 \\ 0 \\ y \end{bmatrix} + b\begin{bmatrix} \frac{1}{6}Yx\big(x^2-3y^2\big) - \frac{1}{2}Y_{100}x + x\mathcal{I}'_1 - y\mathcal{I}'_2 - 2\mathcal{I}_1 \\ \frac{1}{2}Y(y^2-x^2) - Y_{110}x - \frac{1}{2}Y_{100} - \mathcal{I}'_1 \\ 1 \\ x \end{bmatrix} \tag{12.3}$$

The lower two components of this vector equation determine a and b

$$(a,b) = \begin{cases} \frac{\kappa}{y}\,(-x\,,y)\,, & \text{D6-system} \\ \\ \frac{\kappa}{y}\,(\;\;1\,,0)\,, & \text{D4-system.} \end{cases} \tag{12.4}$$

Substituting these two values into the upper two components of equation (12.3) leaves two equations for x and y. This offers one perspective on the ubiquity of rank one attractor points and rarity of those of rank-two: the alignment equations written in the form (12.3) can be solved very often, but satisfying this equation for two linearly independent charge vectors involves four equations and only two unknowns. This latter system is overdetermined and usually insoluble.

After substituting in (12.4), there is an overall factor of κ on both sides of (12.3) which cancels. This leaves the equations with which we begin the discussion of the alignment equations in §13.1 and §13.2.

12.4 Setting up the iteration

To set up the perturbative problem, we will separate, in the period vector, those terms that do not contain instanton corrections from those that do.

$$\Pi = \Pi_0 + \Delta_{\mathcal{I}}\Pi,$$

$$\Pi_0 = \begin{pmatrix} \frac{1}{6}Yt^3 - \frac{1}{2}Y_{100}t - \frac{1}{3}\mathrm{i}Y\sigma \\ -\frac{1}{2}Yt^2 - Y_{110}t - \frac{1}{2}Y_{100} \\ 1 \\ t \end{pmatrix}, \qquad \Delta_{\mathcal{I}}\Pi = \begin{pmatrix} t\mathcal{I}' - 2\mathcal{I} \\ -\mathcal{I}' \\ 0 \\ 0 \end{pmatrix}.$$

As stated above, we wish to treat the instanton terms as small corrections, and so in all cases we first solve the zeroth-order *perturbative equations*. These are obtained from the full alignment or orthogonality equations by simply replacing the full period vector Π by Π_0,

$$\mathrm{Im}[C\,\Pi_0] \;=\; Q\;, \qquad\qquad \Pi_0^T\,\Sigma\,Q \;=\; 0\;. \tag{12.5}$$

We denote the solutions to the perturbative alignment equations by $t_0 = x_0 + \mathrm{i}y_0$, and largely work directly with the real and imaginary parts. These solutions are usually most conveniently expressed

in terms of trigonometric functions, although it is also possible to give x_0 and y_0 as power series in σ. To this end, we define the quantities x_{00} and y_{00} as the $\sigma \to 0$ limits of x_0 and y_0:

$$x_{00} \;=\; x_0\big|_{\sigma=0} \;, \qquad y_{00} \;=\; y_0\big|_{\sigma=0} \;.$$

The utility of this expansion will be seen in chapter 15, where it is the natural expansion to use for comparing supergravity results to microscopic formulae.

Near the large complex structure point the instanton corrections are exponentially small and can be expanded in terms of the quantity $q_y = \mathrm{e}^{-2\pi y_0}$, where y_0 is the perturbative value of the attractor coordinate, found by using the procedure outlined above. We find that the instanton corrections take the form of a series in q_y,

$$x \;=\; \sum_{j=0}^{\infty} x_j q_y^j \;, \qquad y \;=\; \sum_{j=0}^{\infty} y_j q_y^j \;, \tag{12.6}$$

with coefficients x_j and y_j that are rational functions of x_0, y_0, $\sin 2\pi x_0$, and $\cos 2\pi x_0$.

$$x_j \;=\; \sum_{\mathfrak{p}\in \mathrm{pt}(j)} N_{\mathfrak{p}} R^x_{\mathfrak{p}}\,(x_0, y_0), \qquad y_j \;=\; \sum_{\mathfrak{p}\in \mathrm{pt}(j)} N_{\mathfrak{p}} R^y_{\mathfrak{p}}\,(x_0, y_0), \tag{12.7}$$

where $\mathfrak{p}$ is a partition of $j \in \mathbb{Z}_+$, $R^x_{\mathfrak{p}}\,(x_0, y_0)$ and $R^y_{\mathfrak{p}}\,(x_0, y_0)$ are rational functions of x_0, y_0, $\sin(2\pi x_0)$, and $\cos(2\pi x_0)$ and are independent of the Gromov-Witten invariants. We give recurrence relations for the $R^x_{\mathfrak{p}}$ and $R^y_{\mathfrak{p}}$, which are amenable to rapid computer calculation. Since the individual terms in the sum are exponentially small, the first few terms suffice for many practical purposes.

Solving the orthogonality equation proceeds in a very similar manner. The principal difference is that, as the orthogonality equation (3.16) depends on t holomorphically, it is most convenient to work directly with t itself instead of splitting it into real and imaginary parts. Similarly, we do not split the instanton sums $\mathcal{I}$ and $\mathcal{I}'$ into their real and imaginary parts. We denote the solution to the perturbative equations (12.5) by t_0 and express this both as a closed-form expression involving trigonometric functions, as well as a Taylor series expansion around $\sigma = 0$. To include the instanton corrections we make the ansatz

$$t \;=\; \sum_{j=0}^{\infty} t_j q_t^j \;, \tag{12.8}$$

where $q_t = \mathrm{e}^{2\pi \mathrm{i} t_0}$ is the small parameter. As before, we are able to derive recurrence relations for the coefficients t_j. In (12.8) the t_j can be expressed in terms of rational functions and Gromov-Witten invariants in the form

$$t_j \;=\; \sum_{\mathfrak{p}\in \mathrm{pt}(j)} N_{\mathfrak{p}} R^t_{\mathfrak{p}}(t_0) \;. \tag{12.9}$$

12.5 Partitions

Since many of the formulae we will come across while solving the attractor equations involve partitions, it is useful to introduce some terminology and notation from the domain of enumerative combinatorics and provide a rudimentary introduction to the theory of partitions. This serves to fix our notation and give some of the basic results that will be extensively used in the following. A more thorough treatment can be found in, for example, [111], whose notation we largely follow.

12.5.1 Basic definitions and notation

A *partition* $\mathfrak{p}$ of a positive integer $k \in \mathbb{Z}_+$ is a sequence of positive integers

$$0 < p_1 \leq p_2 \leq \ldots \leq p_m \quad \text{such that} \quad \sum_{i=1}^{m} p_i \;=\; k \;.$$

If $\mathfrak{p}$ is a partition of k, we write $|\mathfrak{p}| = k$ and refer to the terms p_i as the *parts* of $\mathfrak{p}$. The number of parts is called the *length* of the partition, which is denoted by $\boldsymbol{\ell}(\mathfrak{p})$. If μ_i denotes the number of parts equal to i, we can write partitions by means of a multiset notation $\mathfrak{p} = \{1^{\mu_1}, 2^{\mu_2}, ...\}$, where only a finite number of μ_i are non-zero.

The partitions of an integer k can be also viewed as the different ways of expressing k as a sum of positive integers without distinguishing the order of the summands. In virtue of this, partitions are often also written using a summation notation:

$$\mathfrak{p} \;=\; \sum_{i=1}^{\infty} \mu_i i \;.$$

Every integer k is a partition of itself, so we can regard integers as special cases of partitions.

Although partitions are defined as sequences of positive numbers, it is sometimes convenient to generalise the notion of partition to include *partitions with zeros*. A partition with zeros $\mathfrak{p}$ of $k \in \mathbb{Z}_+$ is a sequence of non-negative integers

$$0 \leq p_1 \leq p_2 \leq ... \leq p_m \quad \text{such that} \quad \sum_{i=1}^{m} p_i \;=\; k \;.$$

The definitions of $\boldsymbol{\ell}(\mathfrak{p})$ and $|\mathfrak{p}|$ are as before.

There is an important special case where the partition corresponds to an empty multiset $\mathfrak{p} = \emptyset$. This is the *empty partition*, and we take $\boldsymbol{\ell}(\emptyset) = 0$ and $|\emptyset| = 0$. It is important to distinguish the empty partition $\emptyset$ from the partition with zeros $\{0^n\}$. For example, we have $\boldsymbol{\ell}(\emptyset) = 0$, while $\boldsymbol{\ell}(\{0^n\}) = n$.

12.5.2 Operations on partitions

In this subsection

$$\mathfrak{p} \;=\; \sum_{i=0}^{\infty} \mu_i i \;=\; \{0^{\mu_0}, 1^{\mu_1}, 2^{\mu_2}, ...\} \qquad \text{and} \qquad \mathfrak{q} \;=\; \sum_{i=0}^{\infty} \nu_i i \;=\; \{0^{\nu_0}, 1^{\nu_1}, 2^{\nu_2}, ...\}$$

are either partitions or partitions with zeros, for which the multiset or sum notation is used depending on the context.

We write $\mathfrak{p} \subseteq \mathfrak{q}$ if, as multisets, $\mathfrak{p} \subseteq \mathfrak{q}$, which means that $\mu_i \leq \nu_i$ for all i. We use $\subset$ when $\mu_i < \nu_i$.

We can always define a sum of two partitions as a union of the partitions: $\mathfrak{p} + \mathfrak{q} = \mathfrak{p} \cup \mathfrak{q}$, where in writing $\mathfrak{p} \cup \mathfrak{q}$ we understand $\mathfrak{p}$ and $\mathfrak{q}$ as multisets. Alternatively, in the sum notation,

$$\mathfrak{p} + \mathfrak{q} \;=\; \sum_{i=0}^{\infty} (\mu_i + \nu_i)\, i \;.$$

It is clear that this is always a partition, and that $|\mathfrak{p} + \mathfrak{q}| = |\mathfrak{p}| + |\mathfrak{q}|$, and $\boldsymbol{\ell}(\mathfrak{p} + \mathfrak{q}) = \boldsymbol{\ell}(\mathfrak{p}) + \boldsymbol{\ell}(\mathfrak{q})$.

When $\mathfrak{p} \subseteq \mathfrak{q}$, the difference of these partitions can be defined as $\mathfrak{q} - \mathfrak{p} = \mathfrak{q} \setminus \mathfrak{p}$ or, slightly informally, using the sum notation, as

$$\mathfrak{q} - \mathfrak{p} \;=\; \sum_{i=0}^{\infty} (\nu_i - \mu_i)\, i \;.$$

Note that there is a potential source of confusion here with the treatment of zeros. We emphasise that this sum is just an informal way of writing the difference, and the unambiguous definition is given via the multiset difference. Similarly to the sum, $|\mathfrak{q} - \mathfrak{p}| = |\mathfrak{q}| - |\mathfrak{p}|$ and $\boldsymbol{\ell}(\mathfrak{q} - \mathfrak{p}) = \boldsymbol{\ell}(\mathfrak{q}) - \boldsymbol{\ell}(\mathfrak{p})$. In the special case $\mathfrak{p} = \mathfrak{q}$, we have

$$\mathfrak{p} - \mathfrak{p} \;=\; \emptyset,$$

which follows unambiguously by taking the multiset difference.

It is useful also to define notation for some important sets of partitions. The set of all partitions of k, of any length, is denoted by

$$\mathrm{pt}(k) \;\stackrel{\text{def}}{=}\; \big\{\, \mathfrak{p} \;\big|\; |\mathfrak{p}| = k \big\} \;, \tag{12.10}$$

whereas set of all partitions of k with length s is denoted by

$$\mathrm{pt}_s(k) \;\stackrel{\text{def}}{=}\; \{\, \mathfrak{p} \;\big|\; |\mathfrak{p}| = k \;\text{ and }\; \boldsymbol{\ell}(\mathfrak{p}) = s \} \;. \tag{12.11}$$

In addition, we define some unions of the above sets:

$$\mathrm{pt}_{\leq s}(k) \;\stackrel{\text{def}}{=}\; \bigcup_{r=1}^{s} \mathrm{pt}_r(k)\,, \quad \text{and} \quad \mathrm{pt}_{< s}(k) \;\stackrel{\text{def}}{=}\; \bigcup_{r=1}^{s-1} \mathrm{pt}_r(k) \;,$$

with the sets $\mathrm{pt}_{\geq s}(k)$ and $\mathrm{pt}_{> s}(k)$ defined similarly.

The set of partitions of k with zeros is denoted by $\mathrm{pt}^0(k)$, and the definitions of the variants such as $\mathrm{pt}^0_{\leq s}(k)$ are given straightforwardly, as in the above. To avoid any confusion arising from the somewhat subtle issue of the empty partition, we take $\mathrm{pt}(0) = \{\emptyset\}$, and $\emptyset \notin \mathrm{pt}^0_i(k)$ for any i or k.

It is sometimes convenient to use a partition $\mathfrak{p}$ as a multi-index, specifying a product. This is understood exclusively for the following five quantities:

$$x_{\mathfrak{p}} \;=\; \prod_{j=0}^{\infty} x_j^{\mu_j} \;, \qquad y_{\mathfrak{p}} \;=\; \prod_{j=0}^{\infty} y_j^{\mu_j} \;, \qquad t_{\mathfrak{p}} \;=\; \prod_{j=0}^{\infty} t_j^{\mu_j} \;, \qquad N_{\mathfrak{p}} \;=\; \prod_{j=0}^{\infty} N_j^{\mu_j} \;, \qquad \boldsymbol{m}_{\mathfrak{p}} \;=\; \prod_{j=0}^{\infty} \boldsymbol{m}_j^{\mu_j} \;.$$

In all other cases where $\mathfrak{p}$ appears in a subscript, such as the later $\mathcal{E}_{j,\mathfrak{p}}$, it is meant as an index that associates a quantity to a partition in some other way specific to that symbol. In other words, each such symbol is a different function of $\mathfrak{p}$.

Functions arise that depend on partitions and also Gromov-Witten invariants. Using the partition notation, these can be written as N-expansions

$$F \;=\; \sum_{\mathfrak{p}} N_{\mathfrak{p}} F_{\mathfrak{p}} \;.$$

The coefficients $F_{\mathfrak{p}}$ can be thought of as functions of the partitions $\mathfrak{p}$. For two such functions $F_{\mathfrak{p}}$ and $G_{\mathfrak{p}}$, there is a natural convolution-like product

$$(F*G)_{\mathfrak{p}} \;\stackrel{\text{def}}{=}\; \sum_{\mathfrak{q}\subseteq\mathfrak{p}} F_{\mathfrak{p}-\mathfrak{q}}\, G_{\mathfrak{q}} \;. \tag{12.12}$$

This product is clearly commutative and associative, so we write

$$F*(G*H) \;=\; (F*G)*H \;=\; F*G*H \;.$$

The main utility of this product is that if

$$F(j) \;=\; \sum_{\mathfrak{p}\in\mathrm{pt}(j)} F_{\mathfrak{p}}\, N_{\mathfrak{p}} \;, \qquad \text{and} \qquad G(j) \;=\; \sum_{\mathfrak{p}\in\mathrm{pt}(j)} G_{\mathfrak{p}}\, N_{\mathfrak{p}} \;,$$

then the following identity holds

$$\sum_{j=0}^{k} F(j)\, G(k-j) \;=\; \sum_{\mathfrak{p}\in\mathrm{pt}(k)} (F*G)_{\mathfrak{p}}\, N_{\mathfrak{p}} \;.$$

This identity finds frequent use in formulating different recurrence relations.

The sum in the convolution-like product includes the cases $\mathfrak{q}=\mathfrak{p}$ and $\mathfrak{q}=\emptyset$, which both correspond to the empty partition. It is sometimes useful to consider a convolution-like product which does not include these two terms. We denote this product by $\circ$.

$$(F\circ G)_{\mathfrak{p}} \;\stackrel{\text{def}}{=}\; \sum_{\mathfrak{q}\subset\mathfrak{p},\mathfrak{q}\neq\emptyset} F_{\mathfrak{p}-\mathfrak{q}}\, G_{\mathfrak{q}} \;=\; (F*G) - F_{\emptyset}G_{\mathfrak{p}} - F_{\mathfrak{p}}G_{\emptyset} \;.$$

12.5.3 Series expansions

The main utility of the theory of partitions to the discussion of the attractor equations is that the generating functions of many series that arise may be expressed in terms of the quantities defined

above. The prototypical quantities where sums or series can be written with the help of partitions are the powers of sums. For example

$$\left(\sum_{j=1}^{\infty} x_j q^j\right)^n \;=\; \sum_{k=1}^{\infty} q^k \sum_{\mathfrak{p}\in \mathrm{pt}_n(k)} c_{\mathfrak{p}} x_{\mathfrak{p}} \;, \tag{12.13}$$

where $c_{\mathfrak{p}}$ is the multinomial coefficient associated to the partition $\mathfrak{p} = \sum_{j=1}^{\infty} \mu_j j$

$$c_{\mathfrak{p}} \;=\; \frac{\left(\sum_{j=1}^{\infty} \mu_j\right)!}{\prod_{j=1}^{\infty} \mu_j!} \;. \tag{12.14}$$

Expressions like this will be appear repeatedly in what follows. In this way, recalling the q-expansions

$$x \;=\; \sum_{i=0}^{\infty} x_i \, q_y^i \;, \quad y \;=\; \sum_{i=0}^{\infty} y_i \, q_y^i \;, \quad t \;=\; \sum_{i=0}^{\infty} t_i \, q_t^i \;,$$

we are led to series expansions, following straightforwardly from (12.13), for the following quantities:

$$\begin{aligned}
x^n \;&=\; \sum_{k=0}^{\infty} q_y^k \sum_{\mathfrak{p}\in \mathrm{pt}_n^0(k)} c_{\mathfrak{p}} x_{\mathfrak{p}} \;, \qquad n>0 \;, \\
\frac{1}{y} \;&=\; \sum_{k=0}^{\infty} \eta_k \, q_y^k \;, \qquad\qquad \text{where} \qquad\qquad \eta_k \;\stackrel{\text{def}}{=}\; \sum_{j=0}^{k} \frac{(-1)^j}{y_0^{j+1}} \sum_{\mathfrak{p}\in \mathrm{pt}_j(k)} c_{\mathfrak{p}} y_{\mathfrak{p}} \;, \\
\mathrm{e}^{-2\pi m y} \;&=\; \sum_{k=0}^{\infty} \mathrm{e}_k^y(-m) \, q_y^{k+m} \;, \qquad \text{where} \qquad \mathrm{e}_k^y(m) \;\stackrel{\text{def}}{=}\; \sum_{j=0}^{k} \frac{(2\pi m)^j}{j!} \sum_{\mathfrak{p}\in \mathrm{pt}_j(k)} c_{\mathfrak{p}} y_{\mathfrak{p}} \;, \\
\mathrm{e}^{2\pi \mathrm{i} m x} \;&=\; \sum_{k=0}^{\infty} \mathrm{e}_k^x(\mathrm{i}m) \, q_y^k q_x^m \;, \qquad \text{where} \qquad \mathrm{e}_k^x(m) \;\stackrel{\text{def}}{=}\; \sum_{j=0}^{k} \frac{(2\pi m)^j}{j!} \sum_{\mathfrak{p}\in \mathrm{pt}_j(k)} c_{\mathfrak{p}} x_{\mathfrak{p}} \;, \\
\mathrm{e}^{2\pi \mathrm{i} m t} \;&=\; \sum_{k=0}^{\infty} \mathrm{e}_k^t(\mathrm{i}m) \, q_t^{k+m} \;, \qquad \text{where} \qquad \mathrm{e}_k^t(m) \;\stackrel{\text{def}}{=}\; \sum_{j=0}^{k} \frac{(2\pi m)^j}{j!} \sum_{\mathfrak{p}\in \mathrm{pt}_j(k)} c_{\mathfrak{p}} t_{\mathfrak{p}} \;.
\end{aligned} \tag{12.15}$$

It is also useful to express these in terms of the N-expansions (12.7) and (12.9). Substituting these expansions for x and y, we find a set of expressions listed below. In the intermediate expressions, the following quantity appears often:

$$r^x_{(m,n),\mathfrak{p}} \;\stackrel{\text{def}}{=}\; \sum_{\substack{\sum_{j=1}^n \mathfrak{p}_j = \mathfrak{p} \\ \mathfrak{p}_1,\ldots,\mathfrak{p}_m \neq \emptyset}} c\Big(\{\mathfrak{p}_j\}_{j=1}^n\Big) \prod_{j=1}^n R^x_{\mathfrak{p}_j} \;. \tag{12.16}$$

The sum here is over all partitions such that their sum is equal to $\mathfrak{p}$, with the condition that the partitions $\mathfrak{p}_1, ..., \mathfrak{p}_m$ are non-empty (or equivalently that there are between 0 and $n-m$ empty partitions). The coefficients $c(\{\mathfrak{p}_j\})$ are given by $c_{\mathfrak{q}}$, where $\mathfrak{q}$ is the partition $\sum_{j=1}^n q_j$ formed out of the multiplicities q_j of distinct partitions in the set $\{\mathfrak{p}_j\}_{j=1}^n$. We define functions $r^y_{(m,n),\mathfrak{p}}$ and $r^t_{(m,n),\mathfrak{p}}$ similarly, with the only difference being that R^x is replaced by R^y or R^t.

With the help of these quantities, various quantities appearing in (12.15) can be expressed in a form that is convenient for later computations. For example:

$$\eta_k \;=\; \sum_{\mathfrak{p}\in \mathrm{pt}(k)} N_{\mathfrak{p}} \sum_{j=1}^{l(\mathfrak{p})} \frac{(-1)^j}{y_0^{j+1}} r^y_{(j,j),\mathfrak{p}} \;\stackrel{\text{def}}{=}\; \sum_{\mathfrak{p}\in \mathrm{pt}(k)} \boldsymbol{\eta}_{\mathfrak{p}} N_{\mathfrak{p}} \;,$$

$$\eta'_k \;=\; \sum_{\mathfrak{p}\in \mathrm{pt}(k)} N_{\mathfrak{p}} \sum_{j=2}^{l(\mathfrak{p})} \frac{(-1)^j}{y_0^{j+1}} r^y_{(j,j),\mathfrak{p}} \;\stackrel{\mathrm{def}}{=}\; \sum_{\mathfrak{p}\in \mathrm{pt}(k)} \boldsymbol{\eta}'_{\mathfrak{p}} N_{\mathfrak{p}} \ , \tag{12.17}$$

$$\mathrm{e}^x_k(\alpha) \;=\; \sum_{\mathfrak{p}\in \mathrm{pt}(k)} N_{\mathfrak{p}} \sum_{j=0}^{l(\mathfrak{p})} \frac{(2\pi\alpha)^j}{j!} r^x_{(j,j),\mathfrak{p}} \;\stackrel{\mathrm{def}}{=}\; \sum_{\mathfrak{p}\in \mathrm{pt}(k)} \mathbf{e}^x_{\mathfrak{p}}(\alpha)\, N_{\mathfrak{p}} \ ,$$

with similar expressions holding for $\mathrm{e}^y_k(\alpha)$ and $\mathrm{e}^t_k(\alpha)$. When $\mathfrak{p}=\emptyset$, we define the exceptional values

$$\boldsymbol{\eta}_\emptyset \;=\; \frac{1}{y_0} \ , \qquad \boldsymbol{\eta}'_\emptyset \;=\; 1 \ .$$

We give some combinations of these functions their own names due to the fact that these will appear in the instanton sums.

$$\mathcal{C}_j(k) \;=\; \sum_{\mathfrak{p}\in \mathrm{pt}(k)} N_{\mathfrak{p}}\, \mathcal{C}_{j,\mathfrak{p}} \ , \qquad \mathcal{S}_j(k) \;=\; \sum_{\mathfrak{p}\in \mathrm{pt}(k)} N_{\mathfrak{p}} \mathcal{S}_{j,\mathfrak{p}} \ , \qquad \mathcal{E}_j(k) \;=\; \sum_{\mathfrak{p}\in \mathrm{pt}(k)} N_{\mathfrak{p}} \mathcal{E}_{j,\mathfrak{p}} \ , \tag{12.18}$$

where

$$\mathcal{C}_{j,\mathfrak{p}} \;=\; \frac{1}{Y(2\pi)^j} \sum_{m\in\mathfrak{p}} \frac{1}{2m^j} \Big(q_x^m \big(\mathbf{e}^x(\mathrm{i}m) * \mathbf{e}^y(-m)\big)_{\mathfrak{p}-m} + q_x^{-m} \big(\mathbf{e}^x(-\mathrm{i}m) * \mathbf{e}^y(-m)\big)_{\mathfrak{p}-m} \Big) \ ,$$

$$\mathcal{S}_{j,\mathfrak{p}} \;=\; \frac{1}{Y(2\pi)^j} \sum_{m\in\mathfrak{p}} \frac{1}{2\mathrm{i}m^j} \Big(q_x^m \big(\mathbf{e}^x(\mathrm{i}m) * \mathbf{e}^y(-m)\big)_{\mathfrak{p}-m} - q_x^{-m} \big(\mathbf{e}^x(-\mathrm{i}m) * \mathbf{e}^y(-m)\big)_{\mathfrak{p}-m} \Big) \ ,$$

$$\mathcal{E}_{j,\mathfrak{p}} \;=\; \frac{1}{Y(2\pi\mathrm{i})^j} \sum_{m\in\mathfrak{p}} \frac{1}{m^j} \mathbf{e}^t(\mathrm{i}m)_{\mathfrak{p}-m} \ ,$$

where the sums over $m\in\mathfrak{p}$ denote the sum where every i with $\mu_i\neq 0$ is counted once. Now the instanton sums and their derivatives can be written compactly as

$$\mathcal{I}_1 \;=\; -Y \sum_{k=1}^\infty q_y^k\, \mathcal{S}_3(k) \ , \qquad \mathcal{I}_2 \;=\; Y \sum_{k=1}^\infty q_y^k\, \mathcal{C}_3(k) \ ,$$

$$\mathcal{I}'_1 \;=\; -Y \sum_{k=1}^\infty q_y^k\, \mathcal{C}_2(k) \ , \qquad \mathcal{I}'_2 \;=\; -Y \sum_{k=1}^\infty q_y^k\, \mathcal{S}_2(k) \ ,$$

$$\mathcal{I} \;=\; Y \sum_{k=1}^\infty q_t^k \mathcal{E}_3(k) \ , \qquad \mathcal{I}' \;=\; Y \sum_{k=1}^\infty q_t^k \mathcal{E}_2(k) \ .$$

Chapter 13

Brane Systems

In this chapter, we use the methods outlined previously to find the perturbative solutions to the zeroth-order attractor equations and the recurrence relations for the instanton corrections. The orthogonality and alignment equations are considered separately.

13.1 The D4-D2-D0 system

Let us start with the case where the charge vector takes the following form, corresponding to the D4-D2-D0 system:

$$Q_{\mathrm{D4}} = \kappa \begin{pmatrix} \Lambda \\ \Upsilon \\ 0 \\ 1 \end{pmatrix}.$$

The orthogonality equation for a charge vector of this form turns out to be the simplest among the four different cases we study in this part. Consequently, this is one of the cases where we are able to find a closed-form solution for the instanton corrections, as will be shown in detail in chapter 14.

With regards to microstate counting, the alignment equations in this case are particularly interesting. For example, in [16, 17] the microstates of black holes with these charges are counted by the coefficients of modular forms. Using these results, it is possible to express the Bekenstein-Hawking entropy in terms of the perturbative corrections corresponding to σ as well as the instanton corrections. This can be used to compare the macroscopic expression to the asymptotics of modular forms. We discuss this in a little more detail in chapter 15.

13.1.1 The orthogonality equation

The orthogonality equation depends only on the complex period vector Π and not on its real and imaginary parts separately. Therefore, it is most natural to write the orthogonality equation as a condition on the complex coordinate t instead of separating this into the real and imaginary parts x and y as we are obliged to do for the non-holomorphic alignment equations later.

The orthogonality equation $\Pi^T \Sigma Q_{\rm D4} = 0$ can be written as

$$t^2 - 2t\alpha\widetilde{\beta} + \widetilde{\beta}^2 + \frac{2}{Y}\mathcal{I}' \;=\; 0 \;. \tag{13.1}$$

The perturbative equations

Ignoring the instanton corrections, the equation is just a quadratic. Moreover, it is independent of σ. Of the two solutions, the solution that can, for suitable values of Λ and Υ, lie near the large complex structure point is

$$t_0 \;=\; \widetilde{\beta}\left(\alpha + \sqrt{\alpha^2 - 1}\right). \tag{13.2}$$

For this to give a solution that lies in the large complex structure region, t_0 needs to have a large imaginary part. As $\alpha\widetilde{\beta} = -\frac{Y_{110}+\Lambda}{Y}$ is always real and $\widetilde{\beta}$ has a phase 0 or $\frac{\pi}{2}$, the pair α and $\widetilde{\beta}$ are either both real or both purely imaginary. In fact, in the large complex structure region they cannot both be imaginary, for then t_0 would be real. Thus we require that $\widetilde{\beta} > 0$ and $-1 < \alpha < 1$, in order for t_0 to have a positive imaginary part. We will discuss the conditions for existence of perturbative solutions near the large complex structure point in more detail in §14.4. This said, the real and imaginary parts x_0 and y_0 can be written as

$$x_0 \;=\; \widetilde{\beta}\alpha \;, \qquad y_0 \;=\; \widetilde{\beta}\sqrt{1-\alpha^2} \;. \tag{13.3}$$

Instanton corrections

The instanton corrections to the solutions of the orthogonality equation are included as a series in q_t by writing $t = \sum_j t_j\, q_t^j$ and substituting this to (13.1), including the instanton sum. To solve the attractor equations, we require that the coefficient of every power of q_t vanishes. This requirement can be written as

$$0 \;=\; \frac{1}{2}\sum_{\mathfrak{p}\in \mathrm{pt}_2^0(k)} c_{\mathfrak{p}} t_{\mathfrak{p}} - \alpha\widetilde{\beta} t_k + \mathcal{E}_2(k) \;.$$

It is simple to solve this equation for t_k in terms of t_i with $i < k$. As $\mathcal{E}_2(k)$ is independent of t_k, the above equation contains t_k multiplied by the factor $(t_0 - \alpha\widetilde{\beta})$. Thus t_k is given by

$$t_k \;=\; \frac{1}{\alpha\widetilde{\beta} - t_0}\left(\frac{1}{2}\sum_{\mathfrak{p}\in \mathrm{pt}_2(k)} c_{\mathfrak{p}} t_{\mathfrak{p}} + \mathcal{E}_2(k)\right).$$

We now express t_k in terms of the Gromov-Witten invariants in the form (12.9). The rational functions $R^t_{\mathfrak{p}}$ are chosen to be independent of the scaled Gromov-Witten invariants N_k. This leads to a recurrence relation

$$R^t_{\mathfrak{p}}(t_0) \;=\; \frac{1}{\alpha\widetilde{\beta} - t_0}\left(\frac{1}{2}\left(R^t \circ R^t\right)_{\mathfrak{p}} + \mathcal{E}_{2,\mathfrak{p}}\right). \tag{13.4}$$

From this we see that the $R^t_{\mathfrak{p}}$ are rational functions of t_0. The denominators of these rational functions are due to the overall prefactor $1/(\alpha\widetilde{\beta}-t_0)$, and can be written explicitly. We can concentrate on the numerators by introducing polynomials $P^t_{\mathfrak{p}}$

$$P^t_{\mathfrak{p}}(w) \;=\; -\frac{\mathrm{i}\pi\mathbb{\Delta}(w)^{\boldsymbol{\ell}(\mathfrak{p})}}{w}R^t_{\mathfrak{p}}\left(\alpha\widetilde{\beta}+\mathrm{i}\frac{w}{\pi}\right),$$

where, in this subsection,

$$\mathbb{\Delta}(w) \;=\; -4Yw^2\ .$$

With this definition, we can later substitute $w = \pi y_0$ to re-obtain the rational functions $R^t_{\mathfrak{p}}(t_0)$ satisfying the recurrence relation (13.4). This is a consequence of the fact that the instanton corrections depend essentially on y_0 only.

It is easy to write down the first few polynomials. These have a simple form, and will later play an important role in finding solutions to the attractor equations in closed form.

$$\begin{aligned}
P^t_{\{1\}}(w) &= 1\ ,\\
P^t_{\{2\}}(w) &= \frac{1}{4}\ ,\\
P^t_{\{1^2\}}(w) &= -\frac{1}{2}\ (1+4w)\,,\\
P^t_{\{1,2\}}(w) &= -\frac{1}{4}\ (1+6w)\,,\\
P^t_{\{1^3\}}(w) &= \frac{1}{2}\ \left(1+6w+12w^2\right),\\
P^t_{\{1^2,2\}}(w) &= \frac{1}{8}\ \left(3+24w+64w^2\right),\\
P^t_{\{1^4\}}(w) &= -\frac{1}{24}\left(15+120w+384w^2+512w^3\right).
\end{aligned}$$

Combining these observations, and recalling from (13.3) that $\alpha\widetilde{\beta}-t_0=-\mathrm{i}y_0$, we are able to write the coordinate t in the form

$$t \;=\; t_0+\mathrm{i}y_0\sum_{k=1}^{\infty}\mathrm{e}^{2\pi\mathrm{i}kt_0}\sum_{\mathfrak{p}\in\mathrm{pt}(k)}\frac{N_{\mathfrak{p}}}{\mathbb{\Delta}\left(\pi y_0\right)^{\boldsymbol{\ell}(\mathfrak{p})}}P^t_{\mathfrak{p}}\left(\pi y_0\right).$$

Let us also consider the real and imaginary parts of t. The polynomials $P^t_{\mathfrak{p}}(v)$ are real for real v, as can be seen from the recurrence (13.4), so the real and imaginary parts of t are given by

$$\begin{aligned}
x &= x_0-y_0\sum_{k=0}^{\infty}\mathrm{e}^{-2\pi ky_0}\sin(2\pi kx_0)\sum_{\mathfrak{p}\in\mathrm{pt}(k)}\frac{N_{\mathfrak{p}}}{\mathbb{\Delta}\left(\pi y_0\right)^{\boldsymbol{\ell}(\mathfrak{p})}}P^t_{\mathfrak{p}}\left(\pi y_0\right),\\
y &= y_0+y_0\sum_{k=0}^{\infty}\mathrm{e}^{-2\pi ky_0}\cos(2\pi kx_0)\sum_{\mathfrak{p}\in\mathrm{pt}(k)}\frac{N_{\mathfrak{p}}}{\mathbb{\Delta}\left(\pi y_0\right)^{\boldsymbol{\ell}(\mathfrak{p})}}P^t_{\mathfrak{p}}\left(\pi y_0\right).
\end{aligned}\tag{13.5}$$

13.1.2 The alignment equations

The alignment equations are most conveniently expressed in terms of the real coordinates x and y. After replacing a and b in the equations (12.3) via (12.4), we are left with two nontrivial conditions:

$$\begin{aligned}(3x^2-y^2)y-2\sigma+\frac{6}{Y}\left(x\mathcal{I}_2'-2\mathcal{I}_2+y\mathcal{I}_1'\right)-3\widetilde{\beta}^2y &= 0\ ,\\ x+\frac{1}{Yy}\mathcal{I}_2'-\alpha\widetilde{\beta} &= 0\ .\end{aligned} \tag{13.6}$$

The perturbative equations

Neglecting the instanton contributions, the attractor equations become

$$\left(3x_0^2-y_0^2\right)y_0-2\sigma-3\widetilde{\beta}^2y_0 = 0\ ,\qquad x_0-\alpha\widetilde{\beta} = 0\ . \tag{13.7}$$

The second of these equations is solved trivially, and substituting this solution into the first equation yields a cubic for y_0:

$$y_0^3-3\widetilde{\beta}^2(\alpha^2-1)y_0+2\sigma = 0\ .$$

This makes it possible to give a simple solution for y_0 in terms of trigonometric functions. When $\widetilde{\beta}\neq 0$ and $|\alpha|\neq 1$, we make the substitution

$$y_0 = 2\widetilde{\beta}\sqrt{\alpha^2-1}\sin\theta\ , \tag{13.8}$$

which brings the equation to the form

$$-4\sin^3\theta+3\sin\theta = \frac{\sigma}{\widetilde{\beta}^3(\alpha^2-1)^{3/2}}\ .$$

The left-hand side can be recognised as $\sin 3\theta$, with θ defined by

$$\sin 3\theta = \frac{\sigma}{\widetilde{\beta}^3(\alpha^2-1)^{3/2}}\ . \tag{13.9}$$

A cubic has three solutions, corresponding here to the freedom to replace θ by $\theta+\frac{2\pi}{3}$ or $\theta+\frac{4\pi}{3}$. We want to choose a branch so that y_0 is real and $x_0+\mathrm{i}y_0$ lies in the large complex structure region. This choice depends on the values of the charges and Yukawa couplings, and so on $\alpha,\widetilde{\beta}$, and σ, and on the size of the large complex structure region. To better describe these various possibilities we tabulate different relevant cases in table 13.1. As we do not have a general formula for the radius of the large complex structure region, we will include all solutions for which a positive solution for y_0 exists.

In addition to the cases listed in table 13.1, there are degenerate cases with $\widetilde{\beta}=0$ or $\alpha^2=1$. In the case $\widetilde{\beta}=0$, we take $\alpha\to\infty$ in such a way that

$$\alpha\widetilde{\beta} = -\frac{Y_{110}+\Upsilon}{Y_{111}}\ ,\qquad \text{and}\qquad \widetilde{\beta}\sqrt{\alpha^2-1}\to\left|\frac{Y_{110}+\Upsilon}{Y_{111}}\right|.$$

These resolve the ambiguities in table 13.1.

Charge data	Positive solutions for y_0	Definition of θ
$0\leq\sigma\leq\widetilde{\beta}^3(\alpha^2-1)^{3/2}$	$2\widetilde{\beta}\sqrt{\alpha^2-1}\sin\theta,\ 2\widetilde{\beta}\sqrt{\alpha^2-1}\sin\left(\theta+\frac{2\pi}{3}\right)$	$\theta=\frac{1}{3}\sin^{-1}\frac{\sigma}{(\widetilde{\beta}\sqrt{\alpha^2-1})^3}$
$\widetilde{\beta}^3(\alpha^2-1)^{3/2}\leq\sigma\leq 0$	$2\widetilde{\beta}\sqrt{\alpha^2-1}\sin\left(\theta+\frac{4\pi}{3}\right)$	$\theta=\frac{1}{3}\sin^{-1}\frac{\sigma}{(\widetilde{\beta}\sqrt{\alpha^2-1})^3}$
$-\widetilde{\beta}^3(\alpha^2-1)^{3/2}\leq\sigma\leq 0$	$2\widetilde{\beta}\sqrt{\alpha^2-1}\sin\left(\theta+\frac{2\pi}{3}\right)$	$\theta=\frac{1}{3}\sin^{-1}\frac{\sigma}{(\widetilde{\beta}\sqrt{\alpha^2-1})^3}$
$0\leq\sigma\leq-\widetilde{\beta}^3(\alpha^2-1)^{3/2}$	$2\widetilde{\beta}\sqrt{\alpha^2-1}\sin\theta,\ 2\widetilde{\beta}\sqrt{\alpha^2-1}\sin\left(\theta+\frac{4\pi}{3}\right)$	$\theta=\frac{1}{3}\sin^{-1}\frac{\sigma}{(\widetilde{\beta}\sqrt{\alpha^2-1})^3}$
$\sigma<\widetilde{\beta}^3(\alpha^2-1)^{3/2}<0$	$-2\widetilde{\beta}\sqrt{\alpha^2-1}\cosh\nu$	$\theta=\frac{3\pi}{2}+\mathrm{i}\nu,\ \nu=\frac{1}{3}\cosh^{-1}\frac{\sigma}{(\widetilde{\beta}\sqrt{\alpha^2-1})^3}$
$\sigma<-\widetilde{\beta}^3(\alpha^2-1)^{3/2}<0$	$2\widetilde{\beta}\sqrt{\alpha^2-1}\sin\theta$	$\theta=\frac{5\pi}{6}+\mathrm{i}\nu\ \nu=\frac{1}{3}\cosh^{-1}\frac{\sigma}{(\widetilde{\beta}\sqrt{\alpha^2-1})^3}$
$\sigma<0,\ \mathrm{i}\widetilde{\beta}\sqrt{\alpha^2-1}\in\mathbb{R}$	$2\lvert\widetilde{\beta}\sqrt{\alpha^2-1}\sinh\nu\rvert$	$\theta=\mathrm{i}\nu,\ \nu=\frac{1}{3}\sinh^{-1}\frac{\sigma}{\lvert\widetilde{\beta}\sqrt{\alpha^2-1}\rvert^3}$

Table 13.1: *Solutions to the perturbative attractor equations* (13.7). *Whenever an inverse trigonometric function appears in this list, it should be understood to take the principal branch value. The list only includes the solutions for which $y_0>0$, as these are the only solutions that can possibly lie within the large complex structure region. However, even if a solution is included here, it may not lie near the large complex structure point for all Calabi-Yau manifolds.*

In the two cases where either $\alpha^2=1$ or $\widetilde{\beta}=\widetilde{\beta}\alpha=0$, both with $\sigma<0$, the only possibly admissible solution is

$$x_0 \;=\; 0\,, \qquad y_0 \;=\; |\sigma|^{1/3}.$$

The values of charges that are not included in the table 13.1, or among the two degenerate cases, do not have a solution which lies near the large complex structure point. Figure 13.1 provides some intuition in the situations where multiple solutions for y_0 exist for a set of charges.

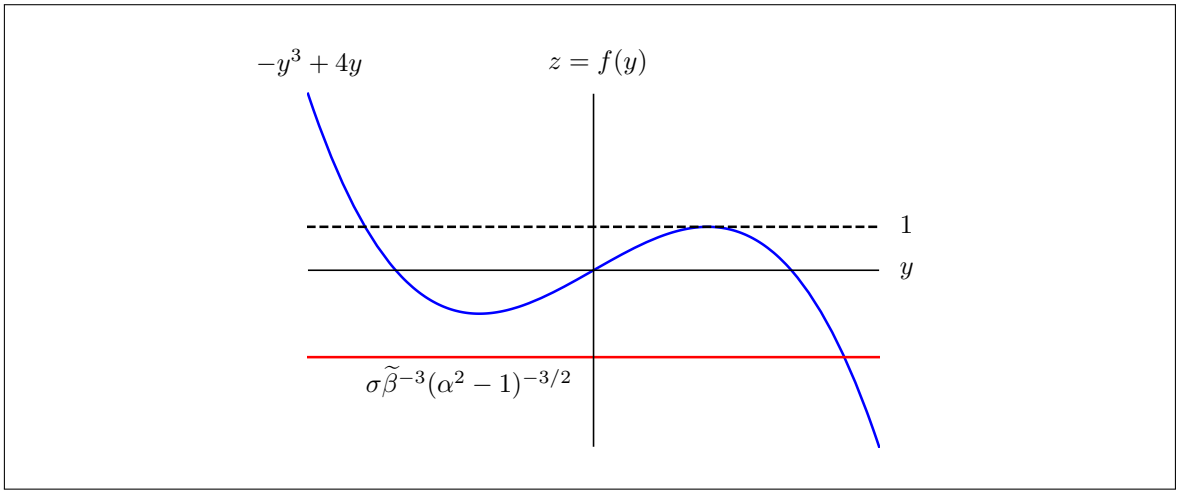


Figure 13.1: *In the case where $\beta\in\mathbb{R}$ and $|\alpha|>1$ the number of positive solutions for y_0 varies, subject to the value of σ. The red line moves up and down as σ is varied, with the solution being the value of y such that the red line intersects the blue curve. When the red line lies in the region $0<z<1$, there are two positive solutions, but when $z>1$ there are no positive solutions. A similar plot can be drawn for other charge ranges.*

It is also useful to expand y_0 as a series in σ. This gives a perturbative expansion for y_0 which is convergent when $\sigma/(\widetilde{\beta}\sqrt{\alpha^2-1})$ is small, which happens, for example, in the large charge ratio limits.

If $\sigma = 0$, then there are solutions to (13.7) with positive y_0 only if $\widetilde{\beta}^2\left(\alpha^2-1\right) > 0$. These solutions with $\sigma = 0$ are

$$x_{00} \;=\; \widetilde{\beta}\alpha \;, \qquad y_{00} \;=\; \sqrt{3}\left|\widetilde{\beta}\sqrt{\alpha^2-1}\right| .$$

This y_{00} is the zeroth-order term in the σ expansion, with the full series given by

$$y_0 \;=\; y_{00}\left[1 - \frac{1}{12\pi}\sum_{n=1}^{\infty}\frac{\Gamma(\frac{n}{2}-\frac{1}{6})\,\Gamma(\frac{n}{2}+\frac{1}{6})}{n!}\left(\frac{2\sqrt{27}\,\sigma}{y_{00}^3}\right)^n\right] . \tag{13.10}$$

This can also be expressed in terms of hypergeometric functions:

$$\frac{y_0}{y_{00}} \;=\; {}_2F_1\left(\begin{matrix}\frac{1}{6},\,-\frac{1}{6}\\ \frac{1}{2}\end{matrix};\;\frac{27\sigma^2}{y_{00}^6}\right) - \frac{\sigma}{y_{00}^3}\,{}_2F_1\left(\begin{matrix}\frac{1}{3},\,\frac{2}{3}\\ \frac{3}{2}\end{matrix};\;\frac{27\sigma^2}{y_{00}^6}\right) .$$

Instanton corrections

Having written the alignment equations in terms of x and y, the instanton corrections are naturally included as a series in q_y. Then the procedure for solving the alignment equations is nearly identical to that used to solve the orthogonality equation.

Using the q_y expansions (12.6) for x and y, the second instanton-corrected equation (13.6) becomes

$$\sum_{k=1}^{\infty} q_y^k\left(x_k - \sum_{j=1}^{k}\eta_{k-j}\,\mathcal{S}_2(j)\right) \;=\; 0 \;.$$

Demanding that the coefficient of q_y^k vanishes gives that

$$x_k \;=\; \sum_{j=1}^{k}\eta_{k-j}\,\mathcal{S}_2(j) \;.$$

This lends itself to an iterative solution as the left-hand side only involves x_j and y_j with $j < k$.

Next we use the N-expansions (12.7), (12.17), and (12.18) to give x_j, η_j, and $\mathcal{S}_2(j)$ in terms of the rational functions $R^x_{\mathfrak{p}}$ and $R^y_{\mathfrak{p}}$:

$$\sum_{\mathfrak{p}\in\mathrm{pt}(k)} N_{\mathfrak{p}} R^x_{\mathfrak{p}} \;=\; \sum_{\mathfrak{p}\in\mathrm{pt}(k)} N_{\mathfrak{p}}(\boldsymbol{\eta}*\mathcal{S}_2)_{\mathfrak{p}} \;.$$

The convolution $(\boldsymbol{\eta}*\mathcal{S}_2)_{\mathfrak{p}}$ involves $R^x_{\mathfrak{q}}$ and $R^y_{\mathfrak{q}}$ with $|\mathfrak{q}| < k$, so $R^x_{\mathfrak{p}}$ with $|\mathfrak{p}| = k$ appears only on the right-hand side. By construction, the $R^x_{\mathfrak{p}}$ are themselves independent of the Gromov-Witten invariants, so the coefficients of different $N_{\mathfrak{p}}$ satisfy the equation independently. Thus we have a relation which determines the $R^x_{\mathfrak{p}}$ recursively:

$$R^x_{\mathfrak{p}} \;=\; (\boldsymbol{\eta}*\mathcal{S}_2)_{\mathfrak{p}} \;, \tag{13.11}$$

The requirement that the coefficient of q_y^k vanishes in the first instanton-corrected equation (13.6) is

$$0 \;=\; \frac{1}{6}\sum_{\mathfrak{p}\in\mathrm{pt}_2^0(k)} c_{\mathfrak{p}}(3x_{\mathfrak{p}} - y_{\mathfrak{p}}) - \frac{\sigma}{3}\eta_k - 2\sum_{i=1}^{k}\eta_{k-i}\,\mathcal{C}_3(i) - \mathcal{C}_2(k) - \sum_{0\le j\le i\le k-1} x_{i-j}\,\eta_j\,\mathcal{S}_2(k-i) \;.$$

Here y_k appears only in η_k and in the first sum when $\mathfrak{p}$ takes the value $\mathfrak{p} = k + 0$. Thus y_k appears multiplied by the factor

$$\frac{\sigma}{3y_0^2} - \frac{1}{3}y_0 \;=\; -\frac{1}{3}y_0(1-\zeta)\;.$$

We rearrange the equation to express y_k in terms of x_i with $i \le k$ and y_i with $k < i$.

$$y_k = \frac{3}{y_0(1-\zeta)}\left(\frac{1}{6}\sum_{\mathfrak{p}\in \mathrm{pt}_2(k)} c_{\mathfrak{p}}(3x_{\mathfrak{p}} - y_{\mathfrak{p}}) + x_0x_k - \frac{\sigma}{3}\eta'_k - 2\sum_{i=1}^{k}\eta_{k-i}\,\mathcal{C}_3(i) - \mathcal{C}_2(k) - \sum_{0\le j\le i\le k-1} x_{i-j}\,\eta_j\,\mathcal{S}_2(k-i)\right).$$

We have solved for x_k in terms of x_i, y_i with $i < k$ above. This is therefore a well-defined recurrence relation for y_k. To find the recurrence for $R^y_{\mathfrak{p}}$, we use the expressions (12.7) to obtain

$$R^y_{\mathfrak{p}}(x_0,y_0) = \frac{3}{y_0(1-\zeta)}\left(\frac{1}{2}r^x_{(2,2),\mathfrak{p}} - \frac{1}{6}r^y_{(2,2),\mathfrak{p}} + x_0R^x_{\mathfrak{p}} - \frac{y_0^3\zeta}{3}\boldsymbol{\eta}'_{\mathfrak{p}} - 2\left(\mathcal{C}_3 * \boldsymbol{\eta}\right)_{\mathfrak{p}} - \mathcal{C}_{2\mathfrak{p}} - \left(\mathcal{S}_2 * R^x * \boldsymbol{\eta}\right)_{\mathfrak{p}}\right). \quad (13.12)$$

The denominators are again simple, given essentially by the prefactor appearing in the expression above. We can therefore easily extract the numerators to give us polynomials.

$$\begin{aligned}
P^x_{\mathfrak{p}}(u,v) &= Y\pi v R^x_{\mathfrak{p}}\left(\frac{u}{\pi},\frac{v}{\pi}\right), && l(\mathfrak{p}) = 1\;,\\
P^x_{\mathfrak{p}}(u,v) &= -\frac{\pi\mathbb{\Delta}(v)^{\boldsymbol{\ell}(\mathfrak{p})}}{v^2(1-\zeta)^3}R^x_{\mathfrak{p}}\left(\frac{u}{\pi},\frac{v}{\pi}\right), && l(\mathfrak{p}) > 1\;,\\
P^y_{\mathfrak{p}}(u,v) &= -\frac{\pi\mathbb{\Delta}(v)^{\boldsymbol{\ell}(\mathfrak{p})}}{v(1-\zeta)}R^y_{\mathfrak{p}}\left(\frac{u}{\pi},\frac{v}{\pi}\right),
\end{aligned} \quad (13.13)$$

where, in this subsection,

$$\mathbb{\Delta}(v) \;=\; Yv^3(1-\zeta)^2.$$

The first few polynomials are

$$\begin{aligned}
P^x_{\{1\}}(u,v) &= \frac{1}{4}\sin(2u)\;,\\
P^x_{\{2\}}(u,v) &= \frac{1}{16}\sin(4u)\;,\\
P^x_{\{1^2\}}(u,v) &= -\frac{1}{32}\Big(3+9v+2(4-\zeta)v^2\Big)\sin(4u)\;,\\
P^y_{\{1\}}(u,v) &= \frac{3}{4}(1+v)\cos(2u)\;,\\
P^y_{\{2\}}(u,v) &= \frac{3}{32}(1+2v)\cos(4u)\;,\\
P^y_{\{1^2\}}(u,v) &= \frac{3}{64}\Big(9+6(4-\zeta)v+3(8-4\zeta-\zeta^2)v^2+4(2-\zeta-\zeta^2)v^3\\
&\qquad +\big(9+6(4-\zeta)v+3(10-8\zeta+\zeta^2)v^2+4(4-5\zeta+\zeta^2)v^3\big)\cos(4u)\Big)\;.
\end{aligned}$$

In summary, the full solution is

$$\begin{aligned}
x &= x_0 - \sum_{k=0}^{\infty}\mathrm{e}^{-2\pi k y_0}\left(\sum_{\mathfrak{p}\in\mathrm{pt}_{>1}(k)} N_{\mathfrak{p}}\frac{\pi y_0^2(1-\zeta)^3}{\mathbb{\Delta}(\pi y_0)^{\boldsymbol{\ell}(\mathfrak{p})}}P^x_{\mathfrak{p}}(\pi x_0,\pi y_0) - \frac{N_kP^x_k(\pi x_0,\pi y_0)}{Y\pi^2y_0}\right),\\
y &= y_0 - \sum_{k=0}^{\infty}\mathrm{e}^{-2\pi k y_0}\sum_{\mathfrak{p}\in\mathrm{pt}(k)} N_{\mathfrak{p}}\frac{y_0(1-\zeta)}{\mathbb{\Delta}(\pi y_0)^{\boldsymbol{\ell}(\mathfrak{p})}}P^y_{\mathfrak{p}}(\pi x_0,\pi y_0)\;,
\end{aligned}$$

where x_0 and y_0 are the perturbative solutions to (13.7). The polynomials $P^x_{\mathfrak{p}}$ and $P^y_{\mathfrak{p}}$ are given in terms of the rational functions $R^x_{\mathfrak{p}}$ and $R^y_{\mathfrak{p}}$ in (13.13). These, in turn, are given by the recurrence relations (13.11) and (13.12).

13.2 The D6-D2-D0 system

Let us now consider a charge vector that corresponds to a black hole consisting of some D6 branes bound to a set of D2- and D0-branes. In other words, take the charge vector to be

$$Q_{D6} \;=\; \kappa \begin{pmatrix} \Lambda \\ \Upsilon \\ 1 \\ 0 \end{pmatrix} .$$

Although for generic charges of this form the alignment equations are the most complicated of the four cases studied here, these will simplify considerably when we specialise to the important special case $\Lambda = 0$. The equations in this section are of interest for studying rank-two attractor points as the explicit example found in [10] has a charge vector of this form with $\Lambda = 0$.

13.2.1 The orthogonality equation

The condition that the central charge vanishes is again best written as a single complex equation

$$t^3 - 3\beta^2 t - 2\mathrm{i}\sigma + 2\beta^3\gamma - \frac{12}{Y}\,\mathcal{I} + \frac{6}{Y}\,t\mathcal{I}' \;=\; 0 \; . \tag{13.14}$$

The perturbative equations

Neglecting the instanton contributions leaves a cubic equation, which is already of a form that can, when $\beta \neq 0$, be solved using a trigonometric substitution as in §13.1. Writing the equation as

$$-4\left(\frac{t_0}{2\beta}\right)^3 + 3\frac{t_0}{2\beta} \;=\; \gamma - \mathrm{i}\frac{\sigma}{\beta^3} \; , \tag{13.15}$$

it is clear that the solution is given by

$$t_0 \;=\; 2\beta \sin\theta \; , \qquad \text{where} \qquad \sin 3\theta \;=\; \gamma - \mathrm{i}\frac{\sigma}{\beta^3} \; . \tag{13.16}$$

Again, the three solutions correspond to θ, $\theta + \frac{2\pi}{3}$ and $\theta + \frac{4\pi}{3}$. We are only concerned with the values of θ that give a t_0 potentially lying in the large complex structure region, that is with $\mathrm{Im}\, t_0 > 0$.

This analysis runs slightly differently when β vanishes. When this occurs, γ necessarily tends to infinity in such a way that $\beta^3\gamma \to -\frac{3\Lambda}{Y}$, which is a finite constant. In this case, the perturbative equations are

$$t_0^3 \;\stackrel{\text{def}}{=}\; r_0^3\, \mathrm{e}^{3\mathrm{i}\phi_0} = -2\beta^3\gamma + 2\mathrm{i}\sigma \; , \qquad \text{where } r_0 > 0 \text{ and } 0 \leq \phi_0 < \frac{2}{3}\pi \; .$$

The solutions with a positive imaginary part are then obtained by choosing the correct branch of the cube root, and are given in table 13.2.

Charge Data	t_0
$\beta^3\gamma < 0$ and $\sigma = 0$	$r_0\,\mathrm{e}^{\mathrm{i}\left(\phi_0+\frac{2}{3}\pi\right)}$
$\sigma > 0$	$r_0\,\mathrm{e}^{\mathrm{i}\phi_0}$, $r_0\,\mathrm{e}^{\mathrm{i}\left(\phi_0+\frac{2}{3}\pi\right)}$
otherwise	$r_0\,\mathrm{e}^{\mathrm{i}\phi_0}$

Table 13.2: *Solutions with positive imaginary part when β vanishes.*

As before, it is occasionally useful to write the solution for t_0 as a series expansion in σ, but we leave the details to appendix G.

Instanton corrections

As before, we require that the coefficient of every power vanishes in the q_t expansion. This leads to recurrence relations for $R^t_{\mathfrak{p}}$. Explicitly, the condition that the coefficient of q_t^k vanishes can be written compactly as

$$\frac{1}{6}\sum_{\mathfrak{p}\in \mathrm{pt}_3^0(k)} c_{\mathfrak{p}} t_{\mathfrak{p}} - \frac{1}{2}\beta^2 t_k + \sum_{i=0}^{k} t_{k-i}\mathcal{E}_2(i) - 2\mathcal{E}_3(k) \;=\; 0\ .$$

Here t_k appears in the first term when $\mathfrak{p} = 0+0+k$, with the coefficient $c_{0+0+k} = 3$, and also in the second term, so overall it is multiplied by $\frac{1}{2}(t_0^2 - \beta^2)$. Using this, it is easy to write down the recurrence relation for t_k:

$$t_k \;=\; \frac{2}{\beta^2 - t_0^2}\left(\frac{1}{6}\sum_{\mathfrak{p}\in \mathrm{pt}_3(k)} c_{\mathfrak{p}} t_{\mathfrak{p}} + \frac{1}{2} t_0 \sum_{\mathfrak{p}\in \mathrm{pt}_2(k)} t_{\mathfrak{p}} + \sum_{i=0}^{k} t_{k-i}\mathcal{E}_2(i) - 2\mathcal{E}_3(k)\right).$$

This can be used to derive the recurrence relation for the functions $R^t_{\mathfrak{p}}$,

$$R^t_{\mathfrak{p}} \;=\; \frac{2}{\beta^2 - t_0^2}\left(\frac{1}{6} r^t_{(2,3),\mathfrak{p}} + \left(\mathcal{E}_2 * R^t\right)_{\mathfrak{p}} - 2\mathcal{E}_{3,\mathfrak{p}}\right)\ . \tag{13.17}$$

Once again we can define functions $P^t_{\mathfrak{p}}$, which are polynomials in t_0, that correspond to the numerators of $R^t_{\mathfrak{p}}$. The denominators of $R^t_{\mathfrak{p}}$ with t_0 dependence come from the overall prefactor in (13.17), so we define

$$P^t_{\mathfrak{p}}(w) \;=\; \frac{\mathrm{i}\pi\,\mathbb{\Delta}(\mathrm{i}w)^{\boldsymbol{\ell}(\mathfrak{p})}}{\pi^2\beta^2 + w^2} R^t_{\mathfrak{p}}\left(\mathrm{i}\frac{w}{\pi}\right),$$

where, in this section,

$$\mathbb{\Delta}(w) \;=\; Y\left(\pi^2\beta^2 - w^2\right)^2.$$

These polynomials can be then computed from the recurrence relation (13.17), together with the above relation between the rational functions $R^t_{\mathfrak{p}}$ and the polynomials $P^t_{\mathfrak{p}}$. The first few polynomials

are listed below:

$$\begin{aligned}
P^t_{\{1\}}(w) &= \frac{1}{2}\,(1+w)\,,\\
P^t_{\{2\}}(w) &= \frac{1}{16}\,(1+2w)\,,\\
P^t_{\{1^2\}}(w) &= \frac{1}{4}\,(1+w)\Big(w+2w^2+2w^3+\pi^2\beta^2\,(1+2w)\Big),\\
P^t_{\{1,2\}}(w) &= \frac{1}{32}\Big(2w+9w^2+18w^3+12w^4+\pi^2\beta^2\,\big(3+14w+12w^2\big)\Big)\,.
\end{aligned}$$

The location of the attractor point t can be written in terms of these polynomials, giving us a relatively simple solution to the attractor equations.

$$t \;=\; t_0 - \mathrm{i}\pi\,\big(\beta^2 - t_0^2\big)\sum_{k=1}^{\infty}\mathrm{e}^{2\pi\mathrm{i}kt_0}\sum_{\mathfrak{p}\in\mathrm{pt}(k)}\frac{N_{\mathfrak{p}}}{\mathbb{\Delta}(\pi t_0)^{\ell(\mathfrak{p})}}P^t_{\mathfrak{p}}(-\mathrm{i}\pi t_0)\;.$$

13.2.2 The alignment equations

As discussed in chapter 12, we can use (12.4) to reduce the alignment equations to a pair:

$$\begin{aligned}
x(x^2+y^2) - \frac{\sigma x}{y} + \frac{3}{Y}\left(2\mathcal{I}_1 - \frac{2x}{y}\mathcal{I}_2 + \frac{x^2+y^2}{y}\mathcal{I}_2'\right) - \beta^3\gamma &= 0\;,\\
x^2+y^2 + \frac{2}{Y}\left(\frac{x}{y}\mathcal{I}_2' - \mathcal{I}_1'\right) - \beta^2 &= 0\;.
\end{aligned} \tag{13.18}$$

The perturbative equations

In this case, solving the perturbative equations reduces to finding the roots of a quartic recorded in (13.22), which allows for a closed-form solution in terms of radicals. However, the resulting expression is not particularly illuminating. It is useful to first solve the equations in the special case $\sigma = 0$ and use the solutions x_{00}, y_{00} to give the explicit solution in terms of radicals, as well as an expansion in σ. Each of these formulations of the solution is useful for different purposes although ultimately both solutions are of course equivalent.

Neglecting instantons, the equations for x_0 and y_0 read

$$x_0\,y_0 \;=\; \beta\gamma\,y_0 + \frac{\sigma}{\beta^2}\,x_0\;, \qquad\qquad x_0^2 + y_0^2 \;=\; \beta^2\;.$$

In the special case $\sigma = 0$, these are solved by

$$x_0 \;=\; x_{00} \;=\; \beta\gamma\;, \qquad\qquad y_0 \;=\; y_{00} \;=\; \beta\sqrt{1-\gamma^2}\;. \tag{13.19}$$

Note for later use that the second equation in (13.19) implies that an attractor point only exists for this brane configuration if β is real, and therefore so is γ. The modulus $|t_0| = \beta$ is independent of σ. For $\sigma = 0$, we are also forced to have $|\gamma| < 1$, so it is possible introduce a real angle $\phi_{00} \in (0,\pi)$ by defining

$$\gamma \;=\; \cos\phi_{00}\;, \qquad \text{so that} \qquad x_{00} \;=\; \beta\cos\phi_{00} \quad\text{and}\quad y_{00} \;=\; \beta\sin\phi_{00}\;.$$

It is optimal to work with the rescaled parameter $\widehat{\sigma} = \frac{\sigma}{\beta^3}$. We define also the rescaled coordinates

$$\widehat{x} \;=\; \frac{x_0}{\beta}\;, \qquad\qquad \widehat{y} \;=\; \frac{y_0}{\beta}\;.$$

In these variables the alignment equations are

$$\widehat{x}\widehat{y} - \gamma\widehat{y} - \widehat{\sigma}\widehat{x} \;=\; 0\;, \qquad\qquad \widehat{x}^2 + \widehat{y}^2 \;=\; 1\;. \tag{13.20}$$

The first equation above provides an expression for $\widehat{x}$ in terms of $\widehat{y}$:

$$\widehat{x} \;=\; \frac{\gamma\widehat{y}}{\widehat{y} - \widehat{\sigma}}\;. \tag{13.21}$$

Substituting this into the second of equations (13.20), one obtains a quartic equation for $\widehat{y}$:

$$(\widehat{y}^2 - 1)\,(\widehat{y} - \widehat{\sigma})^2 + \widehat{y}^2\gamma^2 \;=\; 0\;. \tag{13.22}$$

This can be solved in terms of radicals using standard methods, or otherwise as an expansion in σ. We relegate the somewhat lengthy details and results to appendix G.

Instanton corrections

The instanton corrections to the alignment equations take again the form of a series in q_y. To solve these equations perturbatively, we again require that the coefficient of every power of q_y vanishes. This leads to two conditions

$$\begin{aligned} 0 \;=\; & -\frac{1}{3}\sum_{0\le j\le i\le k}(x_{k-i}x_{i-j}x_j + x_{k-i}y_{i-j}y_j) + \frac{\sigma}{3}\sum_{i=0}^{k}\eta_{k-i}x_i + 2\mathcal{S}_3(k) \\ & + 2\sum_{0\le j\le i\le k}\mathcal{C}_3(k-i)\eta_{i-j}x_j + \sum_{0\le l\le j\le i\le k}x_{k-i}x_{i-j}\eta_{j-l}\mathcal{S}_2(l) + \sum_{i=0}^{k}y_{k-i}\mathcal{S}_2(i)\;, \end{aligned}$$

$$0 \;=\; \frac{1}{2}\sum_{i=0}^{k}(x_{k-i}x_i + y_{k-i}y_i) + \mathcal{C}_2(k) - \sum_{0\le j\le i\le k}x_{k-i}\eta_{i-j}\mathcal{S}_2(j)\;.$$

In the first equation, x_k and y_k appear in the first three terms, while other terms contain only x_i and y_i with $i < k$. The prefactors of x_k and y_k are

$$\frac{1}{3}\Big((1-\zeta)y_0^2 - 3x_0^2\Big), \qquad \text{and} \qquad -\frac{1}{3}(2+\zeta)x_0y_0\;.$$

In the second equation the coefficients are x_0 and y_0, respectively. We can then solve the two equations above for x_k and y_k. In this way, we get a recurrence relation for x_k and y_k in terms of y_i and x_i with $i < k$, which is of the form

$$x_k \;=\; \frac{A(k) + (2+\zeta)B(k)x_0}{(1-\zeta)\beta^2}\;, \qquad\qquad y_k \;=\; -\frac{A(k)x_0 + B(k)\big(3x_0^2 + (1-\zeta)y_0^2\big)}{y_0(1-\zeta)\beta^2}\;,$$

where $A(k)$ and $B(k)$ can be written as N-expansions

$$A(k) \;=\; \sum_{\mathfrak{p}\in\mathrm{pt}(k)}N_{\mathfrak{p}}A_{\mathfrak{p}}\;, \qquad B(k) \;=\; \sum_{\mathfrak{p}\in\mathrm{pt}(k)}N_{\mathfrak{p}}B_{\mathfrak{p}}\;,$$

with the coefficients $A_{\mathfrak{p}}$ and $B_{\mathfrak{p}}$ given by

$$\begin{aligned} A_{\mathfrak{p}} &= -r^x_{(2,3),\mathfrak{p}} - \left(r^y_{(1,2)} \circ R^x\right)_{\mathfrak{p}} - r^y_{(2,2),\mathfrak{p}} x_0 + \zeta y_0^3 \left((\boldsymbol{\eta} \circ R^x)_{\mathfrak{p}} + \boldsymbol{\eta}'_{\mathfrak{p}} x_0\right) \\ &\qquad + 6\,\mathcal{S}_{3,\mathfrak{p}} + 6\,(\mathcal{C}_3 * \boldsymbol{\eta} * R^x)_{\mathfrak{p}} + 3\,(\mathcal{S}_2 * \boldsymbol{\eta} * R^x * R^x)_{\mathfrak{p}} + 3\,(\mathcal{S}_2 * R^y)_{\mathfrak{p}}\ , \\ B_{\mathfrak{p}} &= \frac{1}{2}\,(R^y \circ R^y\ + R^x \circ R^x)_{\mathfrak{p}} + \mathcal{C}_{2,\mathfrak{p}} - (\mathcal{S}_2 * \boldsymbol{\eta} * R^x)_{\mathfrak{p}}\ . \end{aligned} \tag{13.23}$$

The quantities $A(k)$ and $B(k)$ can be seen to only depend on $R^x_{\mathfrak{q}}$ and $R^y_{\mathfrak{q}}$ with $|\mathfrak{q}| < k$. This leads immediately to the following recurrences:

$$R^x_{\mathfrak{p}} = \frac{A_{\mathfrak{p}} + (\zeta+2)B_{\mathfrak{p}} x_0}{(1-\zeta)\beta^2}\ , \qquad R^y_{\mathfrak{p}} = -\frac{A_{\mathfrak{p}} x_0 + B_{\mathfrak{p}}(3x_0^2 + (1-\zeta)y_0^2)}{y_0(1-\zeta)\beta^2}\ . \tag{13.24}$$

It is clear that in general $R^x_{\mathfrak{p}}$ and $R^y_{\mathfrak{p}}$ are rational functions. Furthermore, their denominators take on a simple form. This allows us, by a suitable scaling, to find functions $P^x_{\mathfrak{p}}$ and $P^y_{\mathfrak{p}}$ which are polynomials in the quantities x_0, y_0, $\sin(2\pi x_0)$, and $\cos(2\pi y_0)$,

$$P^x_{\mathfrak{p}}(u,v) = -\frac{\pi \mathbb{\Delta}(v)^{\boldsymbol{\ell}(\mathfrak{p})}}{v^2(1-\zeta)} R^x_{\mathfrak{p}}\left(\frac{u}{\pi}, \frac{v}{\pi}\right), \qquad P^y_{\mathfrak{p}}(u,v) = -\frac{\pi \mathbb{\Delta}(v)^{\boldsymbol{\ell}(\mathfrak{p})}}{v(1-\zeta)} R^y_{\mathfrak{p}}\left(\frac{u}{\pi}, \frac{v}{\pi}\right), \tag{13.25}$$

where, in this section, $\mathbb{\Delta}$ denotes the quantity

$$\mathbb{\Delta}(v) = Y(1-\zeta)^2 v^3 \beta^2\ .$$

These polynomials get rather complicated quite quickly. We list the first few polynomials:

$$\begin{aligned} P^x_1(u,v) &= -\frac{1}{4}\left(\left((1-\zeta)u^2 + 3v(v+1)\right)\sin(2u) + u\left((2+\zeta)v+3\right)\cos(2u)\right), \\ P^x_2(u,v) &= -\frac{1}{32}\Big(\left(2(1-\zeta)u^2 + 3v(2v+1)\right)\sin(4u) + u(2(2+\zeta)v+3)\cos(4u)\Big), \\ P^y_1(u,v) &= \frac{1}{4}\left(\left(3u^2(v+1) + (1-\zeta)v^3\right)\cos(2u) + uv((2+\zeta)v+3)\sin(2u)\right), \\ P^y_2(u,v) &= \frac{1}{32}\Big(\left(u^2(6v+3) + 2(1-\zeta)v^3\right)\cos(4u) + uv(2(2+\zeta)v+3)\sin(4u)\Big). \end{aligned}$$

Writing (12.7) in terms of these gives the following N-expansions for x and y

$$\begin{aligned} x &= x_0 - \pi y_0^2(1-\zeta)\sum_{k=1}^{\infty} \mathrm{e}^{-2\pi k y_0} \sum_{\mathfrak{p}\in \mathrm{pt}(k)} \frac{N_{\mathfrak{p}}}{\mathbb{\Delta}(\pi y_0)^{\boldsymbol{\ell}(\mathfrak{p})}} P^x_{\mathfrak{p}}(\pi x_0, \pi y_0)\ , \\ y &= y_0 - \ y_0(1-\zeta)\sum_{k=1}^{\infty} \mathrm{e}^{-2\pi k y_0} \sum_{\mathfrak{p}\in \mathrm{pt}(k)} \frac{N_{\mathfrak{p}}}{\mathbb{\Delta}(\pi y_0)^{\boldsymbol{\ell}(\mathfrak{p})}} P^y_{\mathfrak{p}}(\pi x_0, \pi y_0)\ . \end{aligned}$$

Chapter 14

Solutions

In the previous sections, we have introduced the general formalism for solving attractor equations, which is used in this section to study some important special cases for which this formalism undergoes considerable simplification.

We first consider the D6-D2-D0 alignment equations in the case $x = 0$. In this case, the perturbative equations (13.19) do not, in fact, involve σ, so $y_0 = \beta$, which is a great simplification compared to the analysis of §13.2.2. The slightly more involved D4-D2-D0 orthogonality equation is also studied. In this case, the attractor equations can be solved without any additional assumptions. These solutions have a similar form to those of the D6-D2-D0 case, which can be understood by examining intersections of linear subspaces with the charge lattice.

One of the most interesting consequences of these solutions is that with them it is possible to give a relatively simple systematic expansion, which includes the instanton corrections, for the central charge and thus for the entropy of the black holes corresponding to the aforementioned systems.

Although the solutions are not limited to rank-two attractor points, an important class of concrete examples are provided by the rank two attractor points found in [10]. We briefly review some central properties related to these points before verifying that our method reproduces these from a different point of view. The intriguing number theoretic properties of the rank two attractor points provide us with an interesting identity (14.11) connecting Bessel functions and Gromov-Witten invariants to L-functions.

14.1 The D6-D2-D0 alignment equations

The alignment equations (13.18) simplify considerably when restricted to the special case where $\Lambda = 0$. By looking at the equations, it can be easily verified that γ vanishes so that the perturbative solution for x is given by $x_0 = 0$. It can be verified that $x = 0$ is a solution to the instanton-corrected equations as well. Thus we can take $x_i = 0$ for all i and $R^x_{\mathfrak{p}} = 0$ for all $\mathfrak{p}$.

As σ only appears multiplied by x, it drops out of the equations. The perturbative coordinate y_0 is then simply

$$y_0 \;=\; \beta \;=\; \sqrt{\frac{Y_{100}+2\Upsilon}{Y}}\ .$$

More significantly, upon setting $x=0$ the recurrence relation for the instanton corrections, given by (13.24) together with (13.23), simplifies considerably. One is left with the relation

$$R^y_{\mathfrak{p}}(y_0) \;=\; -\frac{1}{2y_0}(R^y\circ R^y)_{\mathfrak{p}} - \frac{1}{y_0}\mathcal{C}_{2,\mathfrak{p}}\ . \tag{14.1}$$

To proceed, we write out $\mathcal{C}_{2,\mathfrak{p}}$ in terms of the functions $R^y_{\mathfrak{p}}$. When $x=0$, the coefficients $\mathcal{C}_{2,\mathfrak{p}}$ simplify:

$$\mathcal{C}_{2,\mathfrak{p}} \;=\; \frac{1}{Y}\sum_{m\in\mathfrak{p}}\sum_{j=0}^{l(\mathfrak{p})-1}\frac{(-2\pi m)^{j-2}}{j!}r^y_{(j,j),\mathfrak{p}-m} \;=\; \frac{1}{Y}\sum_{m\in\mathfrak{p}}\sum_{j=1}^{l(\mathfrak{p})-1}\frac{(-2\pi m)^{j-2}}{j!}\overbrace{(R^y\circ R^y\circ\ldots\circ R^y)}^{j\text{ times}}_{\mathfrak{p}-m}\ . \tag{14.2}$$

Thus the recurrence relation is brought to the form

$$R^y_{\mathfrak{p}}(y_0) \;=\; -\frac{1}{2y_0}(R^y\circ R^y)_{\mathfrak{p}} - \frac{1}{y_0}\sum_{m\in\mathfrak{p}}\sum_{j=1}^{l(\mathfrak{p})-1}\frac{(-2\pi m)^{j-2}}{j!}\overbrace{(R^y\circ R^y\circ\ldots\circ R^y)}^{j\text{ times}}_{\mathfrak{p}-m}\ .$$

As previously, it is most convenient to define a set of polynomials $P^y_{\mathfrak{p}}(v)$ by separating the denominators of $R^y_{\mathfrak{p}}$. We could in principle use the definition (13.25), but here it is useful to give a slightly different definition adapted to this special case:

$$\widetilde{P}^y_{\mathfrak{p}}(v) \;\stackrel{\text{def}}{=}\; -\frac{(4\pi^2v^2Y)^{l(\mathfrak{p})}}{a_{\mathfrak{p}}v}R^y_{\mathfrak{p}}(v)\ ,$$

where $a_{\mathfrak{p}}$ are partition-dependent rational constants that we will later fix to get a convenient form for the solution. With this definition, it can be seen that $\widetilde{P}^y_{\mathfrak{p}}(v)$ are polynomials with coefficients in $\mathbb{Q}(\pi)$. In particular, for partitions of length 1, $\mathfrak{p}=\{p_1\}$, we find that

$$\widetilde{P}^y_{\{p_1\}}(v) \;=\; 4\pi^2vYR^y_{\{p_1\}}(v) \;=\; \frac{1}{a_{\{p_1\}}p_1^2}\ .$$

An important observation is that the polynomials $\widetilde{P}^y_{\mathfrak{p}}(v)$ depend on the partition $\mathfrak{p}$ only via its length $l(\mathfrak{p})$ and modulus $|\mathfrak{p}|$. This motivates us to define a second set of polynomials

$$\widetilde{P}^y_{\mathfrak{p}}\left(\frac{v}{2\pi|\mathfrak{p}|}\right) \;\stackrel{\text{def}}{=}\; f_{\ell(\mathfrak{p})}(v)\ .$$

The polynomials $f_s(v)$ only depend on the length $\ell(\mathfrak{p})=s$ of the partition $\mathfrak{p}$. In addition, f_s turn out to have rational coefficients that depend on the $a_{\mathfrak{p}}$. By a suitable choice of these constants the polynomials $f_s(v)$ have integral coefficients.

By numerical experimentation, we find that the $a_{\mathfrak{p}}$ fit a combinatorial pattern. Any coefficient associated to the partition $\sum_{j=1}^{\infty}\mu_j j=\{1^{\mu_1},2^{\mu_2},\ldots\}$ factorises into coefficients associated to the partitions $\{1^{\mu_1}\},\{2^{\mu_2}\},\ldots$, and moreover

$$a_{\{1^{\mu_1},2^{\mu_2},\ldots\}} \;=\; \prod_{j=1}^{\infty}a_{\{j^{\mu_j}\}} \;=\; \prod_{j=1}^{\infty}\frac{1}{j^{2\mu_j}(\mu_j!)}\ . \tag{14.3}$$

The first few functions $f_s(z)$ are

$$\begin{aligned}
f_1(z) &= z+1 \ , \\
f_2(z) &= z^2+3z+3 \ , \\
f_3(z) &= z^3+6z^2+15z+15 \ , \\
f_4(z) &= z^4+10z^3+45z^2+105z+105 \ , \\
f_5(z) &= z^5+15z^4+105z^3+420z^2+945z+945 \ , \\
f_6(z) &= z^6+21z^5+210z^4+1260z^3+4725z^2+10395z+10395 \ , \\
f_7(z) &= z^7+28z^6+378z^5+3150z^4+17325z^3+62370z^2+135135z+135135 \ .
\end{aligned}$$

These are seen to obey a second-order differential equation of confluent hypergeometric type

$$z\frac{d^2}{dz^2}f_s - 2(s+z)\frac{d}{dz}f_s + 2sf_s \ = \ 0 \ ,$$

which implies that they have the expansion:

$$f_s(z) \ = \ \sum_{j=0}^{s} \frac{(2s-j)!}{2^{s-j}(s-j)!j!}\, z^j \ .$$

The fact that the differential equation is of confluent hypergeometric type suggests a connection with Bessel functions. Indeed, the polynomials f_s can be expressed in terms of the modified spherical Bessel functions of the third kind, $\boldsymbol{k}_n(z)$:

$$f_s(y) \ = \ \mathrm{e}^y y^{s+1}\boldsymbol{k}_s(y) \ , \quad \text{where} \quad \boldsymbol{k}_n(z) \ = \ \sqrt{\frac{2}{\pi z}}K_{n+\frac{1}{2}}(z) \ , \tag{14.4}$$

with $K_\nu(z)$ the modified Bessel functions of the second kind [112]. These functions have useful properties. Among others, they satisfy the following recurrence relation and differential identity:

$$\boldsymbol{k}_n(z) \ = \ \boldsymbol{k}_{n-2}(z) + \frac{2n-1}{z}\boldsymbol{k}_{n-1}(z) \ , \qquad \boldsymbol{k}_{n+1}(z) \ = -z^n\frac{d}{dz}\left(z^{-n}\boldsymbol{k}_n(z)\right) \ .$$

As a consequence of the first identity, there is a recurrence relation for the polynomials f_s,

$$f_s(z) \ = \ z^2 f_{s-2}(z) + (2s-1)f_{s-1}(z) \ .$$

Incorporating these results, we find the following expression for t:

$$t \ = \ \mathrm{i}\beta\left(1 - \sum_{j=1}^{\infty}\mathrm{e}^{-2\pi j\beta}\sum_{\mathfrak{p}\in\mathrm{pt}(j)}\frac{a_{\mathfrak{p}}N_{\mathfrak{p}}}{(4\pi^2\beta^2Y)^{\boldsymbol{\ell}(\mathfrak{p})}}f_{\boldsymbol{\ell}(\mathfrak{p})-1}(2\pi j\beta)\right) , \tag{14.5}$$

where the polynomials are given by (14.4), and we have recalled that $y_0 = \beta$. Expressing this in terms of the Bessel functions $\boldsymbol{k}_n(y)$ gives an equivalent formula, in which the relevance of the Bessel functions is obvious.

$$t \ = \ \mathrm{i}y \ , \qquad \text{where} \qquad \frac{y}{\beta} \ = \ 1 - \sum_{j=1}^{\infty}\sum_{\mathfrak{p}\in\mathrm{pt}(j)} a_{\mathfrak{p}}N_{\mathfrak{p}}\left(\frac{j}{2\pi\beta Y}\right)^{\boldsymbol{\ell}(\mathfrak{p})}\boldsymbol{k}_{\boldsymbol{\ell}(\mathfrak{p})-1}(2\pi j\beta) \ . \tag{14.6}$$

Summarising, we have found the fully instanton-corrected solutions for the attractor point coordinate t when the charge vector Q takes the form

$$Q \;=\; \kappa \begin{pmatrix} 0 \\ \Upsilon \\ 1 \\ 0 \end{pmatrix} . \tag{14.7}$$

Strictly speaking, as we had to resort to numerical experimentation to arrive at this result, the result remains a conjecture rather than a rigorously proven result. We have, however, verified the validity of (14.6) formula in a number of cases, involving both rank-one and rank-two attractor points, to a numerical accuracy of at least 50 digits, with sums containing over 8.1×10^7 partitions. For the rank two attractor point of [10], using 11 iterations of a Shanks transformation, we find agreement to 80 digits. Rank one attractor points can be found arbitrarily close to the large complex structure point, which makes it easy to find agreement to hundreds of digits in many cases.

These formulae can be applied for any one-parameter family of Calabi-Yau manifolds by substitution of the Gromov-Witten invariants and the correct topological quantities Y_{abc}. However, care must be taken as not all charge vectors correspond to t_0 that lies near the large complex structure point. Below, in appendix H, we discuss the conditions for the series (14.5) and (14.6) to converge, and thus lie in the large complex structure region.

14.2 The D4-D2-D0 orthogonality equation

In addition to the alignment equations, it is also possible to find similarly simple solutions to the D4-D2-D0 orthogonality equation. In this case it is not necessary to make the assumption $x = 0$ to simplify the equations, since we can formulate them in terms of a single coordinate t, which allows using the methods from the previous section to reduce the functions $R^t_{\mathfrak{p}}$ to the polynomials f_s.

We found in §13.1 that the recurrence relation for the rational functions $R^t_{\mathfrak{p}}$ is given by (13.4),

$$R^t_{\mathfrak{p}}(t_0) \;=\; \frac{1}{\alpha\widetilde{\beta} - t_0} \left(\frac{1}{2} (R^t \circ R^t)_{\mathfrak{p}} + \mathcal{E}_{2,\mathfrak{p}} \right) ,$$

which is reminiscent of (14.1), especially when we recall that $\alpha\widetilde{\beta} - t_0 = -y_0$. Writing out $\mathcal{E}_{2,\mathfrak{p}}$ gives

$$\mathcal{E}_{2,\mathfrak{p}} \;=\; \frac{1}{Y} \sum_{m \in \mathfrak{p}} \sum_{j=1}^{l(\mathfrak{p})-1} \frac{(2\pi \mathrm{i} m)^{j-2}}{j!} \overbrace{(R^t \circ R^t \circ \ldots \circ R^t)}^{j \text{ times}}_{\mathfrak{p}-m} ,$$

which differs from the relation (14.2) only by factors of i and the replacement of $R^y_{\mathfrak{p}}$ by $R^t_{\mathfrak{p}}$. It follows that the solution to the recurrence relation for $R^t_{\mathfrak{p}}$ is also determined by the polynomials f_s. In fact,

$$\mathrm{i} \frac{2\pi|\mathfrak{p}|}{a_{\mathfrak{p}} v} \left(\frac{Y v^2}{|\mathfrak{p}|^2} \right)^{\boldsymbol{\ell}(\mathfrak{p})} R^t_{\mathfrak{p}} \left(\alpha\widetilde{\beta} + \mathrm{i} \frac{v}{2\pi|\mathfrak{p}|} \right) \;=\; f_{\boldsymbol{\ell}(\mathfrak{p})-1}(v) \; .$$

Similarly to the previous section, the left-hand side of this relation depends on the partitions $\mathfrak{p}$ only through their lengths. Using the relation (14.4) between the polynomials $f_s(v)$ and the Bessel functions $\boldsymbol{k}_s(v)$, we can give N-expansions for t:

$$\begin{aligned} t \;&=\; t_0 - \mathrm{i}y_0 \sum_{j=1}^{\infty} \mathrm{e}^{2\pi\mathrm{i}jt_0} \sum_{\mathfrak{p}\in\mathrm{pt}(j)} \frac{a_{\mathfrak{p}} N_{\mathfrak{p}}}{(4\pi^2 y_0^2 Y)^{\boldsymbol{\ell}(\mathfrak{p})}} f_{\boldsymbol{\ell}(\mathfrak{p})-1}(2\pi j y_0) \;, \\ &=\; t_0 - \mathrm{i}y_0 \sum_{j=1}^{\infty} \mathrm{e}^{2\pi\mathrm{i}jx_0} \sum_{\mathfrak{p}\in\mathrm{pt}(j)} a_{\mathfrak{p}} N_{\mathfrak{p}} \left(\frac{j}{2\pi y_0 Y}\right)^{\boldsymbol{\ell}(\mathfrak{p})} \boldsymbol{k}_{\boldsymbol{\ell}(\mathfrak{p})-1}(2\pi j y_0) \;, \end{aligned}$$

where the perturbative solution t_0 is given by

$$t_0 \;=\; \widetilde{\beta}\left(\alpha + \sqrt{\alpha^2-1}\right).$$

This is very similar to the solution (14.6). The only differences are due to the different zeroth-order solutions and that this expansion is in terms of q_t instead of q_y. Indeed, when $x_0 = 0$ but $y_0 \neq 0$, that is, when $\alpha = 0$, this actually reduces to (14.6).

14.3 Entropy at rank-two attractor points

A particularly interesting consequence of the formula (14.6) is that we can compute the area of black holes corresponding to rank-two attractor points. At rank two attractor points, the plane V spanned by $\mathrm{Re}\,\Pi$ and $\mathrm{Im}\,\Pi$ intersects the charge lattice in a lattice plane. As a consequence, there is a simple relation between the central charge and t, which, combined with earlier formulae, allows us to write a relatively simple expression for the black hole area.

To find the relation, consider a rank-two attractor point with coordinate t, corresponding to a charge lattice basis given by

$$Q_1 \;=\; \kappa \begin{pmatrix} 0 \\ \Upsilon \\ 1 \\ 0 \end{pmatrix}, \qquad Q_2 \;=\; \lambda \begin{pmatrix} \Lambda \\ 0 \\ 0 \\ 1 \end{pmatrix}.$$

These two charge vectors satisfying the alignment equations (3.15) at t are charge vectors respectively corresponding to D6-D2-D0 and D4-D2-D0 brane configurations[1]. For attractor points on the imaginary axis, these charges are proportional to the real and imaginary parts of the period vector, respectively. Therefore it is possible to write the charge vectors and so the central charge directly in terms of the period vector. We have

$$Q_1 \;=\; \kappa \mathrm{Re}\,\Pi \;, \qquad Q_2 \;=\; \frac{\lambda}{y}\mathrm{Im}\,\Pi \;, \qquad \frac{1}{z_0}\Pi \;=\; \frac{1}{\kappa}Q_1 + \mathrm{i}\,\frac{y}{\lambda}Q_2 \;.$$

Now, consider a black hole with a charge vector Q_1. It follows from the expressions above, together with the definition (3.13), that the central charge $\mathcal{Z}_1 \stackrel{\mathrm{def}}{=} \mathcal{Z}(Q_1)$ satisfies the relations

$$|\mathcal{Z}_1|^2 \;=\; \frac{y}{2}\left|\frac{\kappa}{\lambda}\, Q_1^T \Sigma Q_2\right| \;=\; \frac{y\kappa^2}{2}|\Lambda - \Upsilon| \;, \tag{14.8}$$

[1] See §12.2 and §15.2.1 for the relation of charge vectors and branes.

where y is given by (14.6). In a similar way, a black hole with charge vector Q_2 has central charge $\mathcal{Z}_2 \stackrel{\text{def}}{=} \mathcal{Z}(Q_2)$, which satisfies the relation

$$|\mathcal{Z}_2|^2 \;=\; \frac{1}{2y}\left|\frac{\lambda}{\kappa}Q_1^T\Sigma Q_2\right| \;=\; \frac{\lambda^2}{2y}|\Lambda-\Upsilon|\;. \tag{14.9}$$

This formula depends only on the charge ratios Υ and Λ, and the topological data of the Calabi-Yau manifold. Given a pair of charge vectors corresponding to a rank-two attractor point, we can immediately find the central charge associated to one of the charges. In practice this formula also gives numerical results to good accuracy, since near the large complex structure point the coefficients $a_{\mathfrak{p}}$ decrease rapidly and ensure the rapid convergence of the sum.

One of the main reasons for the interest in the central charge is that, as will be discussed further in section 15, the central charge is directly related to the Bekenstein-Hawking entropy in the supergravity theory with at most two-derivative corrections as

$$S_{\text{BH}}(Q_1) \;=\; \pi|\mathcal{Z}_1|^2\;.$$

14.3.1 An example: a rank-two attractor point on AESZ34

It was found in [10] that there is a rank two attractor point in the large complex structure region of the one-parameter family of Calabi-Yau manifolds which is the number 34 on the AESZ list [80]. This gives an explicit example of a very interesting attractor point to study using the methods developed in the preceding sections. By studying the zeta function and its factorisation, the authors of [10] found that there is a rank-two attractor point located at

$$\varphi \;=\; 33-8\sqrt{17} \;=\; 0.0151...\;,$$

which we should compare with the φ value at the nearest singularity to the origin, $\varphi=\frac{1}{25}=0.04$. Therefore this lies in the large complex structure region in the sense discussed in §11.1. It will also be argued in appendix H that the series (14.6) converges for the corresponding value of y_0.

Using the mirror map, the t coordinate corresponding to the attractor point was found to be

$$t \;=\; \mathrm{i}\frac{5}{16\cdot 17}(9+\sqrt{17})\frac{\pi\lambda_4(1)}{\lambda_4(2)}\;, \tag{14.10}$$

where λ_4 is the real part of the L-function associated to the modular form with the LMFDB [41] designation **34.4.b.a**. The charges associated to this attractor point are

$$Q_1 \;=\; \kappa\begin{pmatrix}0\\3c\\1\\0\end{pmatrix}, \qquad Q_2 \;=\; \kappa\begin{pmatrix}-2c\\0\\0\\5\end{pmatrix},$$

where $c=1$ or $c=2$ correspond to taking different quotients in the construction of the manifold (see [10]). Without any essential loss of generality, we take $c=1$ for the following discussion. We

note that Q_1 has exactly the form (14.7), which makes it possible to apply the formula (14.6) to find both the attractor point location and the value of the central charge at this attractor point. To specialise to AESZ34 we need only to substitute in these charges, the Yukawa couplings, and the Gromov-Witten invariants.

In this case, the quantities appearing in the perturbative part of the prepotential are given by

$$Y \;=\; 12\;,\quad Y_{110} \;=\; 0\;,\quad Y_{100} \;=\; -1\;,\quad \sigma \;=\; -\frac{2\zeta(3)}{(2\pi)^3}\;,$$

To Q_1 correspond a set of values for our shorthand Greek symbols.

$$\alpha_1 \;=\; \frac{\sqrt{3}}{2}\mathrm{i}\;,\quad \widetilde{\beta}_1 \;=\; \frac{\sqrt{3}}{6}\mathrm{i}\;,\quad \beta_1 \;=\; \frac{\sqrt{15}}{6}\;,\quad \gamma_1 \;=\; 0\;.$$

The first few instanton numbers n_k and scaled Gromov-Witten invariants are listed in table 14.1.

$\boldsymbol{k}$	$\boldsymbol{n_k}$	$\boldsymbol{N_k}$
1	12	12
2	24	204
3	112	3036
4	624	40140
5	4200	525012
6	31408	6787356
7	258168	88551636
8	2269848	1162202316
9	21011260	15317211576
10	202527600	202528125204

Table 14.1: *The first 10 instanton numbers n_k and the scaled Gromov-Witten invariants N_k for the manifold AESZ34.*

The perturbative solution to the alignment equations is given by

$$y_0 \;=\; \beta_1 \;=\; \frac{\sqrt{15}}{6}\;.$$

The solution formula (14.6), together with the expression (14.10) for t, implies the following relation between the L-function values and the Gromov-Witten invariants:

$$\frac{1}{17}(9+\sqrt{17})\frac{\pi\lambda_4(1)}{\lambda_4(2)} \;=\; \frac{8}{\sqrt{15}}\left\{1-\sum_{j=1}^{\infty}\sum_{\mathfrak{p}\in\mathrm{pt}(j)} a_{\mathfrak{p}}N_{\mathfrak{p}}\left(\frac{j}{4\pi\sqrt{15}}\right)^{\boldsymbol{\ell}(\mathfrak{p})}\boldsymbol{k}_{\boldsymbol{\ell}(\mathfrak{p})-1}\left(\frac{\sqrt{15}}{3}\pi j\right)\right\}. \qquad (14.11)$$

This remarkable identity works also as a check of our results. We can compute the sum on the right-hand side as far as $j = 75$, which includes over 8.1×10^7 partitions and is enough to give us an accuracy of over 55 digits. We see that there is indeed an equality, to this accuracy. After applying eleven Shanks transformations to our sequence of partial sums we get agreement to 80 digits. The above identity is also an interesting companion to the those relating to the rank-two attractor points on AESZ34 found in [10].

A curious aspect of this relation is that the quantities on the left-hand side, the coordinate values and L-function values, correspond to the number field $\mathbb{Q}(\sqrt{17})$ while the right-hand side involves y_0, which is an element of $\mathbb{Q}(\sqrt{15})$.

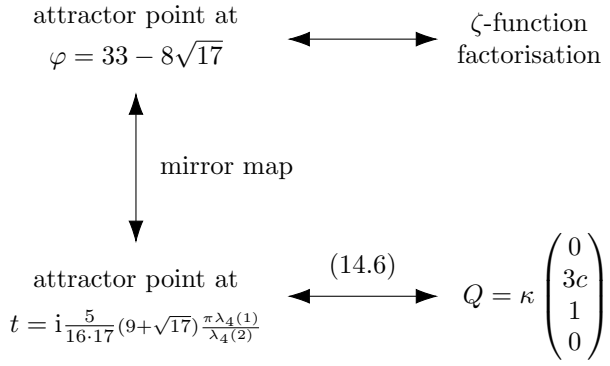


Figure 14.1: *Summary of the relations between different quantities associated to the rank-two attractor point at $\varphi = 33 - 8\sqrt{17}$. Roughly speaking, the method used in [10] to study the attractor point moves anti-clockwise in the figure whereas our method moves clockwise.*

14.4 Solutions with large charge ratios

To end this chapter, let us provide some intuition on the behaviour of the rather abstract solutions to the attractor equations by considering behaviour of families of solutions obtained when the charge ratios Λ and Υ are varied. To ensure that the perturbative solutions converge, we concentrate on the case where the absolute value of at least one of the charge ratios Λ or Υ is large, and further $\big||\Upsilon| - |\Lambda|\big|$ is also large[2]. In this regime the attractor points approach the large complex structure limit, which allows making statements that are true for any one-parameter family. We are then able to derive simple conditions for existence of attractor points with large complex structure.

As a byproduct of these considerations, we also obtain a classification of attractor points into those with vanishing and non-vanishing central charges, based on the charge data alone. This is of importance if the BPS state existence conjecture holds [8, 9, 59–61]. As discussed in greater detail in §3.5.2, the conjecture states that the existence of BPS states in the full quantum theory of gravity can be deduced from the existence of attractor flows. Note that near enough to large complex structure point, when the charge ratios are large, every attractor point is obtained by our perturbative method, as given a solution t, there exists $t_0 \approx t$ which solves the zeroth-order equations. Every such solution leads then to an associated solution to the fully instanton-corrected equations, having t_0 as the zeroth-order term.

[2]In this section, "large" can be usually somewhat tautologically taken to mean "large enough so that the solution in question converges". In practice, Λ and Υ can often even have absolute values smaller than unity. For example, in figure 14.2, we plot solutions with $(\Lambda, \Upsilon) = (0, 1), (0, -1/4)$ and, both of which can be seen to lie near the large complex structure point.

14.4.1 The D4-D2-D0 system

The perturbative solution to the D4-D2-D0 alignment equations is given by (13.7), (13.8), and (13.9):

$$x_0 \;=\; \alpha\widetilde{\beta}\;, \qquad \text{and} \qquad y_0 \;=\; 2\widetilde{\beta}\sqrt{\alpha^2-1}\sin\theta\;, \quad \text{with} \quad \sin 3\theta \;=\; \frac{\sigma}{\widetilde{\beta}^3(\alpha^2-1)^{3/2}}\;.$$

In the large charge ratio limits where $|\widetilde{\beta}|$ or $|\alpha|$ is large, $\sin 3\theta$ is small and the leading-order solution is given by choosing $\theta = \frac{\pi}{3}$. So we have

$$x_0 \;=\; \alpha\widetilde{\beta}\;, \qquad y_0 \;=\; \widetilde{\beta}\sqrt{3(\alpha^2-1)} + \mathcal{O}\left(\frac{\sigma}{\widetilde{\beta}^3(\alpha^2-1)^{3/2}}\right),$$

where the full expansion of y_0 as a series in σ is given by (13.10).

In order for this to be a valid solution that lies near the large complex structure limit, both x_0 and y_0 need to be real, and in addition y_0 should be large. Writing out the shorthand in terms of the manifestly real Y, Y_{100}, Y_{110}, and the charge ratios, we see that x_0 is real for any charge ratios Λ, Υ and any Y_{abc}. The condition for y_0 to be large and real becomes

$$(Y_{110}+\Upsilon)^2 \;\gg\; Y(Y_{100}+2\Lambda)\;. \tag{14.12}$$

Here and in the following we use $A \gg B$ to indicate that for every one-parameter Calabi-Yau manifold, there exists a manifold-specific constant C so that when $A - B > C$, then an attractor point exists in the large complex structure region.

The orthogonality equation can be treated in a similar manner. In this case, σ does not enter the equations, and the perturbative solution to the orthogonality equation is simply given by (13.2). We require again that the imaginary part of t_0 is positive and large. As noted previously, $\alpha\widetilde{\beta}$ is manifestly real, so the condition for the imaginary part to be large is

$$\widetilde{\beta}^2(\alpha^2-1) \;\ll\; 0\;.$$

Expanding the shorthand, we find the condition that is the opposite to (14.12):

$$Y(Y_{100}+2\Lambda) \;\gg\; (Y_{110}+\Upsilon)^2\;. \tag{14.13}$$

Significantly, in large charge ratio limits where $\big||\Upsilon| - |\Lambda|\big|$ is sufficiently large, one these conditions is always satisfied, and the solutions to the orthogonality and alignment equations are mutually exclusive. If a solution with vanishing central charge exists, then there is no solution with non-vanishing central charge, and vice versa. While one may expect a result like this based on the BPS state existence conjecture, a different result would not necessarily contradict the conjecture as there can in principle be basin boundaries in the moduli space. Crossing these walls can change the BPS spectrum discontinuously. Thus having two attractor points for the same charge near the large complex structure point with both vanishing and non-vanishing central charge would not violate the conjecture,

but rather imply that there is a boundary between the basins of attraction of the two distinct attractor points. However, our analysis implies that sufficiently near the large complex structure we have only one attractor point, which can be of either kind, and no such wall exists.

We illustrate the solutions to the alignment equations in the case of AESZ34 by using the recurrence relations uncovered in §13.1.2 to solve the attractor equations to order 10 in q_y. In figure 14.2 families of solutions are plotted, where either Λ or Υ is fixed, and the other parameter is varied. The exact form these plots take depends on the choice of the family of Calabi-Yau manifolds, but most of the qualitative properties are similar for any family of manifolds.

In figure 14.2 (i), $1/t$, the reciprocal of the attractor point coordinate, is plotted. keeping Λ fixed and varying Υ from -1000 to 1000. This illustrates several qualitative aspects of the solutions. In particular, as $\Lambda \to \pm\infty$ or $\Upsilon \to \infty$, the attractor points approach the large complex structure point at $t = \infty$. For $\Lambda < 0$, the curves traced out as Υ varies are closed, while for $\Lambda > 0$ the curves end on the boundary of the large complex structure region, beyond which a solution no longer exists. This is in accord with the conditions (14.12) and (14.13), from which we see that if Λ too greatly exceeds $|\Upsilon|$, then there are no solutions to the alignment equations. Finally, note that the plot is symmetric about the vertical axis following from the fact that when $Y_{110} = 0$, x_0 is proportional to Υ and y_0 depends on Υ only through Υ^2.

A similar figure can be drawn keeping Υ fixed and varying Λ. In figure 14.2 (ii), we let Υ to vary from -10000 to 10000 and plot the solutions where they exist. Again some of the properties of the conditions (14.12) and (14.13) are reflected in the plot. For example, solutions do not exist when Λ greatly exceeds Υ and $\Lambda > 0$, while for large negative Λ, they exist for all values of Υ. As expected, the attractor points tend towards the origin for $\Upsilon \to -\infty$ and $|\Lambda| \to \infty$. Note also the symmetry under $\Upsilon \to -\Upsilon$, which maps one family of solutions to another.

14.4.2 The D6-D2-D0 system

The perturbative solution to the alignment equations (13.19) is given by one of the somewhat complicated expressions (G.4), (G.5), and (G.6). While it is possible to use these expressions to study the existence of solutions with large imaginary part, it is more convenient to directly work on the equations (13.19) in different limits,

$$x_0 y_0 \;=\; \beta\gamma y_0 + \frac{\sigma}{\beta^2} x_0 \;, \qquad\qquad x_0^2 + y_0^2 \;=\; \beta^2 \;.$$

The different cases are $(|\Lambda|, |\Upsilon|) \to (\infty, c)$, $(|\Lambda|, |\Upsilon|) \to (\infty, \infty)$ and $(|\Lambda|, |\Upsilon|) \to (c, \infty)$, with c a finite, possibly zero, constant. It is straightforward to check that in all these cases, we can neglect σ. Thus in all cases

$$x_0 \;=\; \beta\gamma \;, \qquad y_0 \;=\; \beta\sqrt{1-\gamma^2} \;.$$

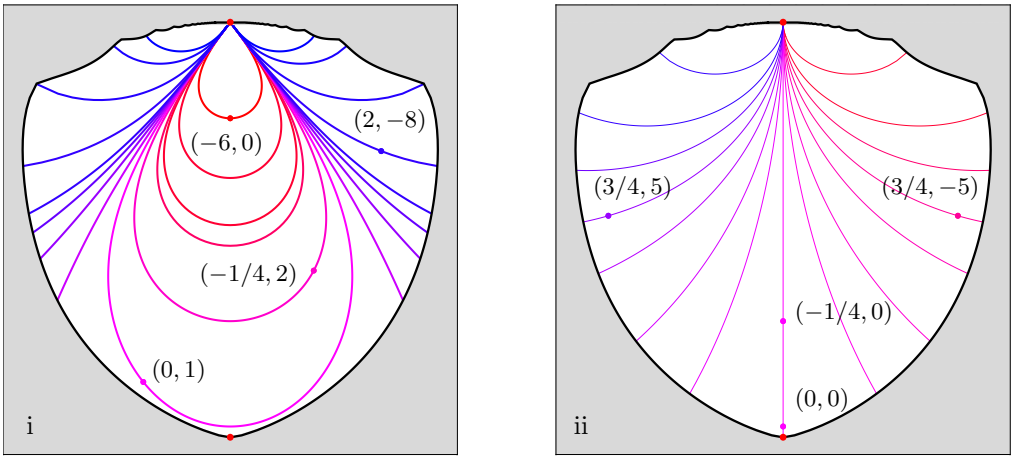


Figure 14.2: *i) Families of solutions to the D4-D2-D0 alignment equations on the* $1/t$ *plane. The origin is the large complex structure point, and the large complex structure region (see §11.1) is the region with white background. On each curve,* Λ *is fixed with* Υ *ranging from* -1000 *to* 1000*. For large positive values of* Λ*, solutions do not exist when* $|\Upsilon|$ *is small.* Λ *takes values* $\Lambda \in \{-6, -2, -1, -3/4, -1/4, 0, 1/4, 1/2, 3/4, 1, 2, 6, 20, 40\}$*. We have also highlighted some points along the curves. The labels are the values of the charge ratios in the form* (Λ, Υ)*. The two unlabelled red points denote the singularities at* $t = \infty$ *and* $t = iy_{\rm sing} \approx 2.4i$*.*

ii) Here Υ *is kept fixed on each curve as* Λ *varies from -10 000 to 10 000. Some attractor points on the curves are highlighted. These are labelled by the charge ratios* (Υ, Λ)*.* Υ *takes the values* $\Upsilon \in \pm\{0, 1, 2, 7/2, 5, 7, 10, 20\}$*, with each distinct value corresponding to a separate curve.*

The combination $\beta\gamma$ is manifestly real, so to have a valid solution near the large complex structure point, we need to demand that y_0 is real, large, and positive. This requires that

$$(2\Upsilon + Y_{100})^3 \;\gg\; 9Y\Lambda^2 \ .$$

We can analyse the orthogonality equation in a similar manner. With instantons neglected, the complex coordinate t_0 satisfies the equation (13.15). It is again possible to neglect σ in this context, and use the results collected in table G.1; When $\beta \in \mathbb{R}^+$, the condition for y_{00} to be large and positive is that either $|\gamma|$ is large, or β is large with $|\gamma| > 1$, whereas when $\beta \in \mathrm{i}\mathbb{R}^+$, we just need that either $|\beta|$ or $|\gamma|$ is large. In the large charge ratio limits, these conditions can be equivalently expressed as a single condition

$$9Y\Lambda^2 \;\gg\; (Y_{100} + 2\Upsilon)^3 \ .$$

We see that the solutions with $|\mathcal{Z}| = 0$ and $|\mathcal{Z}| \neq 0$ are again mutually exclusive in the same manner as in the D4-D2-D0 case. This implies that, at least in the cases we consider here, for every charge vector, an attractor point is uniquely of either type, and the type can be read from the charge vector.

Chapter 15

Outlook: Comparison with Microscopic Entropy

We dedicate the last chapter of this thesis to a brief exploration of the boundary of what is currently known. As the topics covered in this thesis could be developed in many directions, we mainly concentrate to future directions with connection to one of the questions that motivated development of many techniques and results presented in this thesis, and which has connections to many other open questions in the realm of Calabi-Yau modularity: do the modular forms related to the zeta function of the compactification manifold have a natural physical or geometric interpretation?

In various physical theories, modular forms appear naturally, for instance as supersymmetric indices whose coefficients can be interpreted as counting microstates. Therefore, a natural guess for a quantity that could be related to these modular forms is the entropy of black holes associated to rank-two attractor points. It is known that in many cases, such as in the case of black holes in $\mathcal{N}$=4 supersymmetric theories [97], the entropy can be expressed in terms of a modular form (see, for example, [106, 113, 114] and references therein). However, in the case of $\mathcal{N}$=2 theories, the microstate counting producing the correct entropy is not known, except for a few particular models [16, 17, 106, 115]. Black holes associated to rank-two attractor points are under particularly good control due to the stringent conditions they have to satisfy, and might thus provide an ideal case for addressing this problem.

To take some first steps towards understanding the microstate counting of black holes in Calabi-Yau compactifications with an eye on its potential relation to arithmetic and geometry, and develop some appreciation of the type of difficulties one is likely to encounter when studying this problem, we briefly review some results concerning entropy of black holes associated to attractor points. As an indication of how the results presented in this part may find application in this study, we compare the entropy formulae derived in the previous sections to the counting of microstates.

15.1 The central charge and entropy

In the case of Calabi-Yau compactifications, the attractor equations not only make it possible to find the complex (or complexified Kähler) structure of the internal manifold, but also can be used to compute the central charge (3.13) of the supergravity theory, which in turn is related to the Bekenstein-Hawking entropy of the black hole associated to the attractor point.

$$S_{\text{BH}} \;=\; \frac{A}{4} \;=\; \pi|\mathcal{Z}|^2.$$

Solutions to the attractor equations in the approximation where the instanton corrections to the prepotential are ignored, but the genus-1 perturbative contribution is included, were found in [94, 103] and used to give an approximate formula for the Bekenstein-Hawking entropy in any Calabi-Yau compactification, where the internal manifold has a large complex structure. For black holes for which $p^0 = 0$ but the other charges are large,

$$S_{\text{BH}} \approx \pi\sqrt{-\frac{2}{3}Y(\widetilde{p}^3 + c_2\widetilde{p})\left(\widetilde{q}_0 - \frac{1}{2\widetilde{p}Y}\widetilde{q}^2\right)}\,. \tag{15.1}$$

Here $\widetilde{p}$, $\widetilde{q}$ and $\widetilde{q}_0$ are the microscopic charges, that is the numbers of D4-, D2-, and D0-branes. The relation to the macroscopic charges p, q and q_0 can be found in the next section 15.2.1.

The existence of such a result, which bears a resemblance to Cardy growth [116], raises the question whether there is a modular form related to the microstate counting, whose asymptotics reproduce the above formula in a manner similar to the celebrated results of Strominger and Vafa [97]. This question was first tackled in [15], where the authors showed that this entropy can be reproduced, under some mild assumptions, by counting the massless degrees of freedom in an M-theory scenario with fivebranes wrapping a four-cycle on X and the M-theory circle, together with momentum q_0 around the circle. This setup gives rise to a two-dimensional $\mathcal{N} = (4, 0)$ conformal field theory on the fivebrane world-volume. It is possible to define a *modified elliptic genus* [16, 17], which is a supersymmetric index which is invariant under continuous deformations of the theory, at least for small enough deformations. This modified elliptic genus can be expressed in terms of a vector-valued modular form. The coefficients of this modular form contain information about the number of microstates. The asymptotic growth of the number of microstates is then given by the Cardy formula [116] with the central charges

$$c_R = Y\left(\widetilde{p}^3 + c_2\widetilde{p}\right), \qquad c_L = Y\left(\widetilde{p}^3 + \frac{1}{2}c_2\widetilde{p}\right).$$

In the large charge limit $\widetilde{p} \to \infty$, this correctly reproduces (15.1).

In the cases where the charge $\widetilde{p}$ is small, the corresponding modified elliptic genera have been found explicitly, for some simple but interesting Calabi-Yau manifolds, in [16, 17]. To do this, one can consider the geometry of divisors, curves, and points on the manifold. The fivebranes are understood as divisors, and the lower-dimensional branes as curves or points on these. The coefficients in the

modular form that appears in the modified elliptic genus can then be found by studying the moduli spaces of various such configurations of branes and computing their Witten indices.

There is also an alternative method, which uses *split attractor flows* [60, 61, 117] to compute elliptic genera. This was used in [107] to repeat the calculation for the Calabi-Yau manifolds referred to above. This technique is based on the observation that at least some of the coefficients count microscopic degrees of freedom in situations where the black hole can be viewed as a bound state of a D6- and an anti-D6-brane [59]. Such microstate indices can be expressed in terms of Donaldson-Thomas invariants [118, 119], which in turn can be expressed in terms of the Gromov-Witten invariants. Interestingly, these invariants also appear in our macroscopic expressions, such as (11.4). Unfortunately, the modified elliptic genus is not currently known for the family of AESZ34 manifolds, which we have used as the main example of a one-parameter Calabi-Yau manifold in this part owing to the fact that these manifolds are obtained as quotients of the S_5-symmetric Hulek-Verrill manifolds and admit rank-two attractor points.

15.2 Entropy from conformal field theory

15.2.1 Microscopic charge vector

The discussion in this part has been thus far mostly cast in terms of the charge vector Q defined by (11.8), which is a convenient quantity when considering black holes from the macroscopic supergravity perspective. For the purposes of discussing the microstructure of the black holes, it is more convenient to define a microscopic charge vector

$$\widetilde{Q} \;=\; \begin{pmatrix} \widetilde{q}_0 \\ -\widetilde{q} \\ \widetilde{p}^0 \\ -\widetilde{p} \end{pmatrix} .$$

The charges that appear here correspond to the couplings to the RR-potentials in the D-brane world-volume action. Consider first a D6-brane with a world-volume flux F, a two-form field B and RR-potentials C^{2n+1}, $n = 0, 1, 2, 3$. Its world-volume action has the Wess-Zumino term given by

$$S_{\rm WZ} \;=\; \int_{\widetilde{X}} C \wedge e^{F-B} \wedge \sqrt{\widehat{A}(\widetilde{X})} \;,$$

where C is a multiform built out of the RR-potentials, $C = C^{(7)}+C^{(5)}+C^{(3)}+C^{(1)}$. The world-volume flux F and the B-field can be combined into a single tensor $\mathcal{F} = F - B$. The charges coupling to the RR-potentials can be computed from this action either directly or by writing down a charge multiform. To do this, we note that

$$\frac{\delta S_{\rm WZ}}{\delta C^{2n+1}} \;=\; \left[\, e^{\mathcal{F}} \wedge \sqrt{\widehat{A}(\widetilde{X})} \,\right]_{6-2n} = \quad \left[\left(1 + \mathcal{F} + \frac{1}{2}\mathcal{F}^2 + \frac{1}{6}\mathcal{F}^3\right) \wedge \left(1 + \frac{c_2(\widetilde{X})}{24}\right)\right]_{6-2n} ,$$

where $[*]_{6-2n}$ denotes the $(6-2n)$-form part of the multiform. This motivates defining a microscopic charge multiform $\widetilde{\Gamma}$.

$$\widetilde{\Gamma} \;=\; \sum_{n=0}^{3} \frac{\delta S_{\rm WZ}}{\delta C^{2n+1}} \;=\; e^{\mathcal{F}} \wedge \sqrt{\widehat{A}(\widetilde{X})}\;.$$

Since X is a one-parameter manifold, $b^2(\widetilde{X}) = 1$, and we can write $\mathcal{F} = f\mathrm{e}$, where f is a scalar, and e generates $H^2(\widetilde{X}, \mathbb{Z})$. Then the charge form becomes

$$\widetilde{\Gamma} \;=\; 1 + f\mathrm{e} + \left(\frac{1}{2}f^2 + \frac{c_2}{24}\right)\mathrm{e}^2 + \left(\frac{1}{6}f^3 + \frac{c_2}{24}f\right)\mathrm{e}^3\;.$$

The form $\mho$, defining the microscopic period vector $\widetilde{\Pi}$ (see [21]), is given by the mirror of the holomorphic three form Ω on X:

$$\mho \;=\; e^{B+\mathrm{i}J} \;=\; e^{t\mathrm{e}} \;=\; 1 + t\,\mathrm{e} + \frac{1}{2}t^2\,\mathrm{e}^2 + \frac{1}{6}t^3\,\mathrm{e}^3\;.$$

The appropriate [59] inner product to use to compute the central charge is the Dirac-Schwinger-Zwanziger product, defined by

$$\widetilde{\Gamma}\cdot\mho \;=\; \int_{\widetilde{X}} \widetilde{\Gamma}\wedge\mho^*\;,$$

where $\mho^*$ is the form obtained by inverting the signs of the 2- and 6-form components of $\mho$, so that $\mho^* = e^{-t\mathrm{e}}$.

Alternatively, we can identify the components of the vectors $\widetilde{Q}$ and $\widetilde{\Pi}$ corresponding to $\widetilde{\Gamma}$ and $\mho$.

$$\widetilde{Q} \;=\; \begin{pmatrix} \frac{1}{6}Yf^3 - \frac{Y_{100}}{2}f \\ -\frac{1}{2}Yf^2 + \frac{Y_{100}}{2} \\ 1 \\ -f \end{pmatrix}, \qquad \widetilde{\Pi} \;=\; \begin{pmatrix} \frac{1}{6}Yt^3 \\ \frac{1}{2}Yt^2 \\ 1 \\ t \end{pmatrix},$$

where c_2 has been expressed in terms of Y_{100}. With this definition, the Dirac-Schwinger-Zwanziger product becomes the familiar symplectic inner product between these vectors:

$$\widetilde{\Gamma}\cdot\mho \;=\; \widetilde{Q}^T\Sigma\widetilde{\Pi}\;.$$

As a simple consistency check, we note that this is invariant under the monodromy $t \to t+1$ and $B \to B+1$, which acts as $f \to f+1$ [1].

To find the relation between the microscopic charge vector $\widetilde{Q}$ and the macroscopic vector Q, note the relation between the corresponding period vectors

$$\Pi_0\big|_{\sigma=0} \;=\; \mathrm{T}_\Pi\widetilde{\Pi}\;, \qquad \text{with} \qquad \mathrm{T}_\Pi \;=\; \begin{pmatrix} 1 & 0 & 0 & -\frac{1}{2}Y_{100} \\ 0 & -1 & -\frac{1}{2}Y_{100} & -Y_{110} \\ 0 & 0 & 1 & 0 \\ 0 & 0 & 0 & 1 \end{pmatrix}.$$

[1] Note that this is the action of the monodromy despite the fact that $\mathcal{F} = F - B$, owing to the sign change in the vector $\widetilde{Q}$.

The central charge should be basis independent, requiring that $\widetilde{Q}^T\Sigma\widetilde{\Pi} = Q^T\Sigma\Pi_0\big|_{\sigma=0}$, which allows the identification

$$\widetilde{Q} \;=\; \mathrm{T}_Q^{-1}Q\;, \qquad \text{with} \qquad \mathrm{T}_Q \;=\; \left(\Sigma^{-1}\mathrm{T}_\Pi^{-1}\Sigma\right)^T \;=\; \begin{pmatrix} 1 & 0 & 0 & \frac{1}{2}Y_{100} \\ 0 & 1 & -\frac{1}{2}Y_{100} & Y_{110} \\ 0 & 0 & 1 & 0 \\ 0 & 0 & 0 & -1 \end{pmatrix}.$$

15.2.2 Entropy from modular form asymptotics

It is believed (see [15]) that the microscopic theory describing the D4-D2-D0-brane system is a two-dimensional $\mathcal{N} = (4,0)$ superconformal field theory. In [15–17], it is proposed that the microstate numbers for a system of $\widetilde{p}$ D4-branes bound to $\widetilde{q}$ D2 and $\widetilde{q}_0$ D0 branes can be read from the coefficients $c_\mu(n) = c_\mu\left(\widetilde{q}_0 + \widetilde{q}^2/(2\widetilde{p}Y)\right)$ of a modified elliptic genus.

The famous Cardy formula [116] gives the asymptotic growth of the modular form coefficients $c_\mu(n)$ for large n in terms of the central charge and the charges $\widetilde{q}$ and $\widetilde{q}_0$

$$c\,(n) \;\sim\; \exp\left[4\pi\sqrt{\frac{c_R}{24}\left(-\widetilde{q}_0 + \frac{\widetilde{q}^2}{2\widetilde{p}Y}\right)}\,\right],$$

which is valid in the limit where the quantity $-\widetilde{q}_0 + \widetilde{q}^2/(2\widetilde{p}Y)$ is much larger than the conformal field theory central chare c_R. Here we also ignored the index μ as the different $c_\mu(n)$ have the same leading term in the large n limit. In [15], it was shown, under some relatively mild assumptions, that the central charge c_R can be expressed in terms of the black hole charges as

$$c_R \;=\; Y\left(\widetilde{p}^3 + c_2\,\widetilde{p}\right)\;.$$

To compare this to N-expansions, recall the form (12.2) the charge vector corresponding to the D4-D2-D0 system takes. We identify $\widetilde{p} = \kappa$, $\widetilde{q} = -\kappa\,(\Upsilon + Y_{110})$, and $\widetilde{q}_0 = \frac{\kappa}{2}\,(2\Lambda + Y_{100})$, concentrating on the special case where $\widetilde{q} = 0$ for clarity. The Cardy formula gives the asymptotic expression

$$c\,(n) \;\sim\; \exp\left[\pi\sqrt{-\frac{Y}{3}\,(\kappa^4 + c_2\kappa^2)\,(2\Lambda + Y_{100})}\,\right].$$

In the large charge limit $\kappa \to \infty$, the expression simplifies to give the asymptotic formula for the microscopic entropy as

$$S \;=\; \log c(\widetilde{q}_0) \;\sim\; \pi\kappa^2\sqrt{-\frac{Y}{3}\,(2\Lambda + Y_{100})}\;. \tag{15.2}$$

The relative sign between the D4 charge κ and the D0 charge $\frac{\kappa}{2}(2\Lambda+Y_{100})$ is determined by $(2\Lambda+Y_{100})$. The above formula is only sensible when this factor is negative, which conforms with the expectation that D4-branes bind to anti-D0-branes, and anti-D4-branes bind to D0-branes. This is the case for which we will derive the macroscopic formula below.

15.3 Entropy from supergravity

To compare this leading-order microscopic result to the expression for the central charge, it is in principle enough to solve the attractor equations in the approximation where we disregard the instanton corrections and set $\sigma = 0$. This is essentially equivalent to the approach taken in [15, 94], except that we here ignore the higher-genus corrections, as we are interested in the large charge limit. It is interesting, however, to see explicitly how the result, in this limit is, just the leading term in the N-expansion for the central charge. This general formula will also contain the subleading corrections and, in this sense, extend the results of [15, 94]. It is also intriguing to ponder on how the N-expansion might relate to the celebrated Rademacher expansion [120], which provides asymptotic expressions for modular form coefficients.

As with the expressions for the recurrence relations (13.12) for the rational functions R_x and R_y, we expect the general formula for $|\mathcal{Z}|^2$ to be rather complicated. To make the essential structure of the expansion and comparison clear, we will concentrate on the special case where $\Upsilon = 0$, $Y_{110} = 0$ and $2\Lambda + Y_{100} < 0$. This situation is somewhat analogous to that which allowed finding the explicit solutions in chapter 14. Once again, the rank-two attractor points discovered in [10] satisfy this condition. The generalisation is conceptually straightforward.

The conditions $\Upsilon = 0$ and $Y_{110} = 0$ imply that $\alpha = 0$, and so $x_0 = 0$. Looking at the alignment equations (13.6), this implies $x = 0$ even when the instanton corrections are taken into account. The central charge is given by (3.13), which simplifies when $x = 0$ to take the form

$$\mathcal{Z}(Q_{D4}) \;=\; -\kappa\,\frac{-\frac{1}{2}Yy^2 + \frac{1}{2}Y\widetilde{\beta}^2 + \mathcal{I}_1'}{\sqrt{\frac{4}{3}Yy^3 + \frac{2}{3}Y\sigma + 4\mathcal{I}_2 - 4y\mathcal{I}_1'}} \;\stackrel{\text{def}}{=}\; -\kappa L\sqrt{\frac{Y}{M}}\ ,$$

where

$$L \;=\; -\frac{1}{2}y^2 + \frac{1}{2}\widetilde{\beta}^2 + \frac{1}{Y}\mathcal{I}_1'\ , \qquad M \;=\; \frac{4}{3}y^3 + \frac{2}{3}\sigma + \frac{4}{Y}\mathcal{I}_2 - \frac{4y}{Y}\mathcal{I}_1'\ .$$

Using the expansions in §12.5, the quantities K and M appearing here can be written as N-expansions:

$$L \;=\; -\frac{1}{2}y_0^2 + \frac{1}{2}\widetilde{\beta}^2 + \sum_{k=1}^{\infty} q_y^k \sum_{\mathfrak{p}\in \mathrm{pt}(k)} N_{\mathfrak{p}}\boldsymbol{L}_{\mathfrak{p}}\ ,$$

$$\frac{1}{\sqrt{M}} \;=\; \frac{1}{\sqrt{\frac{2}{3}\left(\sigma + 2y_0^3\right)}} + \sum_{k=1}^{\infty} q_y^k \sum_{\mathfrak{p}\in \mathrm{pt}(k)} N_{\mathfrak{p}}\boldsymbol{M}_{\mathfrak{p}}\ .$$

We have written the q_y-independent part explicitly, as this will be important for comparing the leading-order result in this expansion with the modular form asymptotics and results of [15, 94]. The

coefficients of the invariants $N_{\mathfrak{p}}$ can be expressed as

$$\boldsymbol{L}_{\mathfrak{p}} \;=\; -\frac{1}{2}\left(R^y * R^y\right)_{\mathfrak{p}} - \mathcal{C}_{2,\mathfrak{p}} \;, \qquad \boldsymbol{L}_{\emptyset} \;=\; \frac{1}{2}\left(\widetilde{\beta}^2 - y_0^2\right)$$

$$\boldsymbol{M}_{\mathfrak{p}} \;=\; \sum_{i=0}^{\infty} \frac{(-1)^i \left(\frac{1}{2}\right)_i}{Y^i \left(\frac{2}{3}\sigma + \frac{4}{3}y_0^3\right)^{i+1/2} i!} \sum_{\substack{\sum_{j=1}^i \mathfrak{p}_j = \mathfrak{p} \\ \mathfrak{p}_j \neq \emptyset}} c\big(\{\mathfrak{p}_j\}_{j=1}^i\big) \prod_{j=1}^i \boldsymbol{m}_{\mathfrak{p}_j} \;,$$

where the sum is defined as in (12.16) and the quantities $\boldsymbol{m}_{\mathfrak{p}}$ are given by

$$\boldsymbol{m}_{\mathfrak{p}} \;=\; \frac{4}{3} Y r^y_{(1,3),\mathfrak{p}} + 4Y\mathcal{C}_{3,\mathfrak{p}} + 4Y\left(\mathcal{C}_2 * R^y\right)_{\mathfrak{p}} \;.$$

In terms of these quantities, the central charge becomes

$$\mathcal{Z}(Q_{D4}) \;=\; \kappa \frac{\sqrt{3Y}\widetilde{\beta}^2\left(1 + 4\sin^2\left(\theta + \frac{4\pi}{3}\right)\right)}{\sqrt{8\sigma + 128\mathrm{i}\widetilde{\beta}^3 \sin^3\left(\theta + \frac{4\pi}{3}\right)}} - \kappa\sqrt{Y}\sum_{k=1}^{\infty} \mathrm{e}^{-2\pi k y_0} \sum_{\mathfrak{p}\in \mathrm{pt}(k)} N_{\mathfrak{p}} \left(\boldsymbol{M} * \boldsymbol{L}\right)_{\mathfrak{p}} \;, \tag{15.3}$$

where we have written out the σ-corrected coordinates x_0 and y_0 in the first term explicitly in terms of $\widetilde{\beta} = \sqrt{(2\Lambda + Y_{100})/Y}$, the Yukawa coupling Y, and the angle θ defined in (13.9). It is θ that contains the contribution of σ. As θ is defined as a particular value of an arcsine, we have incorporated a shift by $\frac{4\pi}{3}$ in (15.3), as per the first row of table 13.1. This solution is the correct one to use in the limit where σ is neglected, in the case where $2\Lambda + Y_{100} < 0$.

Since we are only interested in the leading order here, we can disregard instanton corrections, and also set $\sigma = 0$, and thus $\theta = 0$. The expression for the central charge then becomes

$$\mathcal{Z}(Q_{D4}) \;\sim\; \mathrm{i}\frac{\kappa}{3^{1/4}}\sqrt{Y|\widetilde{\beta}|} \;=\; \mathrm{i}\kappa\left(\frac{Y}{3}\right)^{1/4} |Y_{100} + 2\Lambda|^{1/4}.$$

Finally, the leading term in the expression for the Bekenstein-Hawking entropy is

$$S_{\mathrm{BH}} \;=\; \pi|\mathcal{Z}(Q_{\mathrm{D4}})|^2 \;\sim\; \pi\kappa^2\sqrt{-\frac{Y}{3}(2\Lambda + Y_{100})} \;,$$

which agrees precisely with the modular form asymptotics (15.2), as expected. Of course this result just verifies that the formulae here agree with the well-known results of [15, 94] in the large charge limit. However, our approach to deriving the entropy from supergravity allows writing down a systematic expansions, similar to (15.3), for the subleading terms that were not included in [15, 94].

It is intriguing that these terms involve Gromov-Witten invariants, which have a natural interpretation as counting microscopic D-brane configurations. This also shows a striking similarity to results relating to the asymptotics of modular forms, see for example [120, 121].

15.4 Open questions

It would be interesting to develop the comparison with modular form asymptotics further. In principle it should be possible to proceed as in [16, 17], and identify the space of vector-valued modular forms

that appear in the expression for the modified elliptic genus. One of the main difficulties is that to compare the asymptotics with the entropy formula derived from supergravity, one would need to find this space for a large charge. The number of polar terms, and thus independent vector-valued modular forms quickly increases with increasing charge, making it difficult to find a basis. In addition, the geometries of D-brane configurations corresponding to the black hole become very complicated very quickly when the magnetic charge is increased, which makes it difficult to fix the modified elliptic genus in terms of the basis of vector-valued modular forms.

We have seen in chapter 7 that at least some aspects of the enumerative geometry of the mirror Hulek-Verrill manifolds, which must be understood in order to find the modified elliptic genus, are significantly easier to understand than those on the quotient manifolds AESZ34. Thus it would be interesting to use generalisation of the methods of [16, 17] to find the modified elliptic genus corresponding to various D4-brane configurations on the mirror Hulek-Verrill manifold.

The currently known explicit examples of rank-two attractor points are limited to the three attractor points on AESZ34 [10] and points on hypergeometric families [122]. These have been observed to have many fascinating properties. It would be interesting to see how general these properties are, and possibly identify additional ones. The method presented in chapter 9 opens up a possibility of a systematic study of zeta functions on a wide variety of multiparameter manifolds. The techniques of [10] could be used to search for rank-two attractor points utilising factorisations of the zeta function. For instance, these might include attractor points whose microscopic geometry is simpler than that of the currently known examples.

Additionally, it would be interesting to understand the generalisation of various modularity-related results appearing in chapters 10 and 14 to cases where the modularity does not arise from two-dimensional Galois representations, but from higher-dimensional ones. Such cases are provided, for example, by black holes corresponding to rank-one attractor points. Based on Langlands correspondence, it is believed that also in these cases it is possible to associate an automorphic form to the zeta function. However, in general, these will not be modular forms associated to elliptic curves, which we have exclusively studied in this thesis. Exploring the correspondence of zeta function and more general class of physical solutions will thus likely require improvements to the current understanding of other automorphic forms, such as Siegel modular forms.

Appendices

Appendix A

Toric Geometry Data

In this appendix, we gather the combinatorial data defining various polytopes and toric varieties discussed in chapter 5. This allows easy checking of some results alluded to in the main body of text.

The polytope $\widehat{\Delta}$ and the ambient variety $\mathbb{P}_{\widehat{\Delta}}$

Vertices of $\widehat{\Delta}$			
u_1	(-1, 0, 0, 0)	u_{11}	(0, 0, 0, 1)
u_2	(-1, 0, 0, 1)	u_{12}	(0, 0, 1,-1)
u_3	(-1, 0, 1, 0)	u_{13}	(0, 0, 1, 0)
u_4	(-1, 1, 0, 0)	u_{14}	(0, 1,-1, 0)
u_5	(0,-1, 0, 0)	u_{15}	(0, 1, 0,-1)
u_6	(0,-1, 0, 1)	u_{16}	(0, 1, 0, 0)
u_7	(0,-1, 1, 0)	u_{17}	(1,-1, 0, 0)
u_8	(0, 0,-1, 0)	u_{18}	(1, 0,-1, 0)
u_9	(0, 0,-1, 1)	u_{19}	(1, 0, 0,-1)
u_{10}	(0, 0, 0,-1)	u_{20}	(1, 0, 0, 0)

Faces of $\widehat{\Delta}$			
ρ_1	$y_1 = 1$	ρ_{16}	$-y_4 = 1$
ρ_2	$-y_1 = 1$	ρ_{17}	$y_1 + y_4 = 1$
ρ_3	$y_2 = 1$	ρ_{18}	$-y_1 - y_4 = 1$
ρ_4	$-y_2 = 1$	ρ_{19}	$y_2 + y_4 = 1$
ρ_5	$y_1 + y_2 = 1$	ρ_{20}	$-y_2 - y_4 = 1$
ρ_6	$-y_1 - y_2 = 1$	ρ_{21}	$y_1 + y_2 + y_4 = 1$
ρ_7	$y_3 = 1$	ρ_{22}	$-y_1 - y_2 - y_4 = 1$
ρ_8	$-y_3 = 1$	ρ_{23}	$y_3 + y_4 = 1$
ρ_9	$y_1 + y_3 = 1$	ρ_{24}	$-y_3 - y_4 = 1$
ρ_{10}	$-y_1 - y_3 = 1$	ρ_{25}	$y_1 + y_3 + y_4 = 1$
ρ_{11}	$y_2 + y_3 = 1$	ρ_{26}	$-y_1 - y_3 - y_4 = 1$
ρ_{12}	$-y_2 - y_3 = 1$	ρ_{27}	$y_2 + y_3 + y_4 = 1$
ρ_{13}	$y_1 + y_2 + y_3 = 1$	ρ_{28}	$-y_2 - y_3 - y_4 = 1$
ρ_{14}	$-y_1 - y_2 - y_3 = 1$	ρ_{29}	$y_1 + y_2 + y_3 + y_4 = 1$
ρ_{15}	$y_4 = 1$	ρ_{30}	$-y_1 - y_2 - y_3 - y_4 = 1$

There are 16 relations between these vectors, expressed in a convenient basis as:

$$u_i + u_{21-i} = 0, \qquad 1 \le i \le 10 \ ,$$

$$u_1 - u_5 + u_{17} = 0 \ , \qquad u_1 - u_8 + u_{18} = 0 \ , \qquad u_1 - u_{10} + u_{19} = 0 \ ,$$

$$u_5 - u_8 + u_{14} = 0 \ , \qquad u_5 - u_{10} + u_{15} = 0 \ , \qquad u_8 - u_{10} + u_{12} = 0 \ .$$

As in (2.20), each of these relations corresponds to a scaling symmetry $\mathbb{C}^* \subset (\mathbb{C}^*)^{16}$. There are four invariant combinations of coordinates that we can identify with the coordinates on the torus $\mathbb{T}^4 \subset \mathbb{P}_{\widehat{\Delta}}$. These can be taken to be

$$\begin{aligned} H_1 &= \eta^{o_1} = \frac{\eta_{17}\eta_{18}\eta_{19}\eta_{20}}{\eta_1\eta_2\eta_3\eta_4} \ , \qquad H_2 = \eta^{o_2} = \frac{\eta_4\eta_{14}\eta_{15}\eta_{16}}{\eta_5\eta_6\eta_7\eta_{17}} \ , \\ H_3 &= \eta^{o_3} = \frac{\eta_3\eta_7\eta_{12}\eta_{13}}{\eta_8\eta_9\eta_{14}\eta_{18}} \ , \qquad H_4 = \eta^{o_4} = \frac{\eta_2\eta_6\eta_9\eta_{11}}{\eta_{10}\eta_{12}\eta_{15}\eta_{19}} \ . \end{aligned} \tag{A.1}$$

The dual polytope $\widehat{\Delta}^*$ and the ambient variety $\mathbb{P}_{\widehat{\Delta}^*}$

Vertices of $\widehat{\Delta}^*$			
v_1	(1, 0, 0, 0)	v_{16}	(0, 0, 0,-1)
v_2	(-1, 0, 0, 0)	v_{17}	(1, 0, 0, 1)
v_3	(0, 1, 0, 0)	v_{18}	(-1, 0, 0,-1)
v_4	(0,-1, 0, 0)	v_{19}	(0, 1, 0, 1)
v_5	(1, 1, 0, 0)	v_{20}	(0,-1, 0,-1)
v_6	(-1,-1, 0, 0)	v_{21}	(1, 1, 0, 1)
v_7	(0, 0, 1, 0)	v_{22}	(-1,-1, 0,-1)
v_8	(0, 0,-1, 0)	v_{23}	(0, 0, 1, 1)
v_9	(1, 0, 1, 0)	v_{24}	(0, 0,-1,-1)
v_{10}	(-1, 0,-1, 0)	v_{25}	(1, 0, 1, 1)
v_{11}	(0, 1, 1, 0)	v_{26}	(-1, 0,-1,-1)
v_{12}	(0,-1,-1, 0)	v_{27}	(0, 1, 1, 1)
v_{13}	(1, 1, 1, 0)	v_{28}	(0,-1,-1,-1)
v_{14}	(-1,-1,-1, 0)	v_{29}	(1, 1, 1, 1)
v_{15}	(0, 0, 0, 1)	v_{30}	(-1,-1,-1,-1)

Faces of $\widehat{\Delta}^*$			
τ_1	$-x_1 = 1$	τ_{11}	$x_4 = 1$
τ_2	$-x_1 + x_4 = 1$	τ_{12}	$x_3 - x_4 = 1$
τ_3	$-x_1 + x_3 = 1$	τ_{13}	$x_3 = 1$
τ_4	$-x_1 + x_2 = 1$	τ_{14}	$x_2 - x_3 = 1$
τ_5	$-x_2 = 1$	τ_{15}	$x_2 - x_4 = 1$
τ_6	$-x_2 + x_4 = 1$	τ_{16}	$x_2 = 1$
τ_7	$-x_2 + x_3 = 1$	τ_{17}	$x_1 - x_2 = 1$
τ_8	$-x_3 = 1$	τ_{18}	$x_1 - x_3 = 1$
τ_9	$-x_3 + x_4 = 1$	τ_{19}	$x_1 - x_4 = 1$
τ_{10}	$-x_4 = 1$	τ_{20}	$x_1 = 1$

We find 26 independent relations between the 30 vectors.

$$
\begin{aligned}
v_{2i} + v_{2i-1} &= 0\ , \quad 1 \le i \le 15\ , \\
v_7 + v_{15} + v_{24} &= 0\ , \qquad v_3 + v_7 + v_{15} + v_{28} = 0\ , \\
v_3 + v_{15} + v_{20} &= 0\ , \qquad v_1 + v_7 + v_{15} + v_{26} = 0\ , \\
v_1 + v_{15} + v_{18} &= 0\ , \qquad v_1 + v_3 + v_{15} + v_{22} = 0\ , \\
v_3 + v_7 + v_{12} &= 0\ , \qquad v_1 + v_3 + v_7 + v_{14} = 0\ , \\
v_1 + v_7 + v_{10} &= 0\ , \qquad v_3 + v_7 + v_{15} + v_{28} = 0\ , \\
v_1 + v_3 + v_6 &= 0\ .
\end{aligned}
$$

Again, each of these relations corresponds to a scaling symmetry $\mathbb{C}^* \subset (\mathbb{C}^*)^{26}$. There are four invariant combinations of coordinates that we can identify with the coordinates on the torus $\mathbb{T}^4 \subset X_{\widehat{\Delta}^*}$. These can be taken to be

$$
\begin{aligned}
\Xi_1 &= \xi^{w_1} = \frac{\xi_1\xi_5\xi_9\xi_{13}\xi_{17}\xi_{21}\xi_{25}\xi_{29}}{\xi_2\xi_6\xi_{10}\xi_{14}\xi_{18}\xi_{22}\xi_{26}\xi_{30}}\ , \qquad \Xi_2 = \xi^{w_2} = \frac{\xi_3\xi_5\xi_{11}\xi_{13}\xi_{19}\xi_{21}\xi_{27}\xi_{29}}{\xi_4\xi_6\xi_{12}\xi_{14}\xi_{20}\xi_{22}\xi_{28}\xi_{30}}\ , \\
\Xi_3 &= \xi^{w_3} = \frac{\xi_7\xi_9\xi_{11}\xi_{13}\xi_{23}\xi_{25}\xi_{27}\xi_{29}}{\xi_8\xi_{10}\xi_{12}\xi_{14}\xi_{24}\xi_{26}\xi_{28}\xi_{30}}\ , \qquad \Xi_4 = \xi^{w_4} = \frac{\xi_{15}\xi_{17}\xi_{19}\xi_{21}\xi_{23}\xi_{25}\xi_{27}\xi_{29}}{\xi_{16}\xi_{18}\xi_{20}\xi_{22}\xi_{24}\xi_{26}\xi_{28}\xi_{30}}\ .
\end{aligned}
\tag{A.2}
$$

The polytope ∇^* and the ambient variety $\mathbb{P}_{\nabla^*}$

Vertices of ∇^*	
u_1	(1, 0, 0, 0, 0)
u_2	(-1, 0, 0, 0, 0)
u_3	(0, 1, 0, 0, 0)
u_4	(0,-1, 0, 0, 0)
u_5	(0, 0, 1, 0, 0)
u_6	(0, 0,-1, 0, 0)
u_7	(0, 0, 0, 1, 0)
u_8	(0, 0, 0,-1, 0)
u_9	(0, 0, 0, 0, 1)
u_{10}	(0, 0, 0, 0,-1)

Faces of ∇^*			
τ_1	$-x_1-x_2-x_3-x_4-x_5=1$	τ_{17}	$x_1-x_2-x_3-x_4-x_5=1$
τ_2	$-x_1-x_2-x_3-x_4+x_5=1$	τ_{18}	$x_1-x_2-x_3-x_4+x_5=1$
τ_3	$-x_1-x_2-x_3+x_4-x_5=1$	τ_{19}	$x_1-x_2-x_3+x_4-x_5=1$
τ_4	$-x_1-x_2-x_3+x_4+x_5=1$	τ_{20}	$x_1-x_2-x_3+x_4+x_5=1$
τ_5	$-x_1-x_2+x_3-x_4-x_5=1$	τ_{21}	$x_1-x_2+x_3-x_4-x_5=1$
τ_6	$-x_1-x_2+x_3-x_4+x_5=1$	τ_{22}	$x_1-x_2+x_3-x_4+x_5=1$
τ_7	$-x_1-x_2+x_3+x_4-x_5=1$	τ_{23}	$x_1-x_2+x_3+x_4-x_5=1$
τ_8	$-x_1-x_2+x_3+x_4+x_5=1$	τ_{24}	$x_1-x_2+x_3+x_4+x_5=1$
τ_9	$-x_1+x_2-x_3-x_4-x_5=1$	τ_{25}	$x_1+x_2-x_3-x_4-x_5=1$
τ_{10}	$-x_1+x_2-x_3-x_4+x_5=1$	τ_{26}	$x_1+x_2-x_3-x_4+x_5=1$
τ_{11}	$-x_1+x_2-x_3+x_4-x_5=1$	τ_{27}	$x_1+x_2-x_3+x_4-x_5=1$
τ_{12}	$-x_1+x_2-x_3+x_4+x_5=1$	τ_{28}	$x_1+x_2-x_3+x_4+x_5=1$
τ_{13}	$-x_1+x_2+x_3-x_4-x_5=1$	τ_{29}	$x_1+x_2+x_3-x_4-x_5=1$
τ_{14}	$-x_1+x_2+x_3-x_4+x_5=1$	τ_{30}	$x_1+x_2+x_3-x_4+x_5=1$
τ_{15}	$-x_1+x_2+x_3+x_4-x_5=1$	τ_{31}	$x_1+x_2+x_3+x_4-x_5=1$
τ_{16}	$-x_1+x_2+x_3+x_4+x_5=1$	τ_{32}	$x_1+x_2+x_3+x_4+x_5=1$

A brief inspection reveals that the ten vertices of this polytope share precisely five relations, $u_{2i}+u_{2i-1}=0$. Each pair of vertices entering into these relations form a set of homogeneous coordinates for a $\mathbb{P}^1$.

The polytope Δ^* and the ambient variety $\mathbb{P}_{\Delta^*}$

Vertices of Δ^*			
u_1	(1, 0, 0, 0, 0)	u_{32}	(0, 0, 0, 0,-1)
u_2	(-1, 0, 0, 0, 0)	u_{33}	(1, 0, 0, 0, 1)
u_3	(0, 1, 0, 0, 0)	u_{34}	(-1, 0, 0, 0,-1)
u_4	(0,-1, 0, 0, 0)	u_{35}	(0, 1, 0, 0, 1)
u_5	(1, 1, 0, 0, 0)	u_{36}	(0,-1, 0, 0,-1)
u_6	(-1,-1, 0, 0, 0)	u_{37}	(1, 1, 0, 0, 1)
u_7	(0, 0, 1, 0, 0)	u_{38}	(-1,-1, 0, 0,-1)
u_8	(0, 0,-1, 0, 0)	u_{39}	(0, 0, 1, 0, 1)
u_9	(1, 0, 1, 0, 0)	u_{40}	(0, 0,-1, 0,-1)
u_{10}	(-1, 0,-1, 0, 0)	u_{41}	(1, 0, 1, 0, 1)
u_{11}	(0, 1, 1, 0, 0)	u_{42}	(-1, 0,-1, 0,-1)
u_{12}	(0,-1,-1, 0, 0)	u_{43}	(0, 1, 1, 0, 1)
u_{13}	(1, 1, 1, 0, 0)	u_{44}	(0,-1,-1, 0,-1)
u_{14}	(-1,-1,-1, 0, 0)	u_{45}	(1, 1, 1, 0, 1)
u_{15}	(0, 0, 0, 1, 0)	u_{46}	(-1,-1,-1, 0,-1)
u_{16}	(0, 0, 0,-1, 0)	u_{47}	(0, 0, 0, 1, 1)
u_{17}	(1, 0, 0, 1, 0)	u_{48}	(0, 0, 0,-1,-1)
u_{18}	(-1, 0, 0,-1, 0)	u_{49}	(1, 0, 0, 1, 1)
u_{19}	(0, 1, 0, 1, 0)	u_{50}	(-1, 0, 0,-1,-1)
u_{20}	(0,-1, 0,-1, 0)	u_{51}	(0, 1, 0, 1, 1)
u_{21}	(1, 1, 0, 1, 0)	u_{52}	(0,-1, 0,-1,-1)
u_{22}	(-1,-1, 0,-1, 0)	u_{53}	(1, 1, 0, 1, 1)
u_{23}	(0, 0, 1, 1, 0)	u_{54}	(-1,-1, 0,-1,-1)
u_{24}	(0, 0,-1,-1, 0)	u_{55}	(0, 0, 1, 1, 1)
u_{25}	(1, 0, 1, 1, 0)	u_{56}	(0, 0,-1,-1,-1)
u_{26}	(-1, 0,-1,-1, 0)	u_{57}	(1, 0, 1, 1, 1)
u_{27}	(0, 1, 1, 1, 0)	u_{58}	(-1, 0,-1,-1,-1)
u_{28}	(0,-1,-1,-1, 0)	u_{59}	(0, 1, 1, 1, 1)
u_{29}	(1, 1, 1, 1, 0)	u_{60}	(0,-1,-1,-1,-1)
u_{30}	(-1,-1,-1,-1, 0)	u_{61}	(1, 1, 1, 1, 1)
u_{31}	(0, 0, 0, 0, 1)	u_{62}	(-1,-1,-1,-1,-1)

Faces of Δ^*	
ρ_1	$y_1=1$
ρ_2	$y_2=1$
ρ_3	$y_3=1$
ρ_4	$y_4=1$
ρ_5	$y_5=1$
ρ_6	$-y_1=1$
ρ_7	$-y_2=1$
ρ_8	$-y_3=1$
ρ_9	$-y_4=1$
ρ_{10}	$-y_5=1$
ρ_{11}	$y_1-y_2=1$
ρ_{12}	$y_1-y_3=1$
ρ_{13}	$y_1-y_4=1$
ρ_{14}	$y_1-y_5=1$
ρ_{15}	$-y_1+y_2=1$
ρ_{16}	$y_2-y_3=1$
ρ_{17}	$y_2-y_4=1$
ρ_{18}	$y_2-y_5=1$
ρ_{19}	$-y_1+y_3=1$
ρ_{20}	$-y_2+y_3=1$
ρ_{21}	$y_3-y_4=1$
ρ_{22}	$y_3-y_5=1$
ρ_{23}	$-y_1+y_4=1$
ρ_{24}	$-y_2+y_4=1$
ρ_{25}	$-y_3+y_4=1$
ρ_{26}	$y_4-y_5=1$
ρ_{27}	$-y_1+y_5=1$
ρ_{28}	$-y_2+y_5=1$
ρ_{29}	$-y_3+y_5=1$
ρ_{30}	$-y_4+y_5=1$

There are 57 independent relations between these 62 vectors.

$$u_{2i} + u_{2i-1} \;=\; 0, \qquad 1 \le i \le 31 \ ,$$

$$\begin{array}{rrr}
u_1{+}u_3{+}u_6 = 0 \ , & u_1{+}u_7{+}u_{10} = 0 \ , & u_1{+}u_{15}{+}u_{18} = 0 \ , \\
u_1{+}u_{31}{+}u_{34} = 0 \ , & u_3{+}u_7{+}u_{12} = 0 \ , & u_3{+}u_{15}{+}u_{20} = 0 \ , \\
u_3{+}u_{31}{+}u_{36} = 0 \ , & u_7{+}u_{15}{+}u_{24} = 0 \ , & u_7{+}u_{31}{+}u_{40} = 0 \ , \\
u_{15}{+}u_{31}{+}u_{48} = 0 \ , & u_1{+}u_3{+}u_7{+}u_{14} = 0 \ , & u_1{+}u_3{+}u_{15}{+}u_{22} = 0 \ , \\
u_1{+}u_3{+}u_{31}{+}u_{38} = 0 \ , & u_1{+}u_7{+}u_{15}{+}u_{26} = 0 \ , & u_1{+}u_7{+}u_{31}{+}u_{42} = 0 \ , \\
u_1{+}u_{15}{+}u_{31}{+}u_{50} = 0 \ , & u_3{+}u_7{+}u_{15}{+}u_{28} = 0 \ , & u_3{+}u_7{+}u_{31}{+}u_{44} = 0 \ , \\
u_3{+}u_{15}{+}u_{31}{+}u_{52} = 0 \ , & u_7{+}u_{15}{+}u_{31}{+}u_{56} = 0 \ , & u_1{+}u_3{+}u_7{+}u_{15}{+}u_{30} = 0 \ , \\
u_1{+}u_3{+}u_7{+}u_{31}{+}u_{46} = 0 \ , & u_1{+}u_3{+}u_{15}{+}u_{31}{+}u_{54} = 0 \ , & u_1{+}u_7{+}u_{15}{+}u_{31}{+}u_{58} = 0 \ , \\
u_3{+}u_7{+}u_{15}{+}u_{31}{+}u_{60} = 0 \ , & u_1{+}u_3{+}u_7{+}u_{15}{+}u_{31}{+}u_{62} = 0 \ . &
\end{array}$$

Each of these relations corresponds to a scaling symmetry $\mathbb{C}^* \subset (\mathbb{C}^*)^{57}$. There are five independent invariant combinations of coordinates that we can identify as coordinates on the torus $\mathbb{T}^5 \subset \mathbb{P}_{\Delta^*}$.

$$\begin{aligned}
\Xi_1 \;=\; \xi^{w_1} \;&=\; \frac{\xi_1\xi_5\xi_9\xi_{13}\xi_{17}\xi_{21}\xi_{25}\xi_{29}\xi_{33}\xi_{37}\xi_{41}\xi_{45}\xi_{49}\xi_{53}\xi_{57}\xi_{61}}{\xi_2\xi_6\xi_{10}\xi_{14}\xi_{18}\xi_{22}\xi_{26}\xi_{30}\xi_{34}\xi_{38}\xi_{42}\xi_{46}\xi_{50}\xi_{54}\xi_{58}\xi_{62}} \ , \\
\Xi_2 \;=\; \xi^{w_2} \;&=\; \frac{\xi_3\xi_5\xi_{11}\xi_{13}\xi_{19}\xi_{21}\xi_{27}\xi_{29}\xi_{35}\xi_{37}\xi_{43}\xi_{45}\xi_{51}\xi_{53}\xi_{59}\xi_{61}}{\xi_4\xi_6\xi_{12}\xi_{14}\xi_{20}\xi_{22}\xi_{28}\xi_{30}\xi_{36}\xi_{38}\xi_{44}\xi_{46}\xi_{52}\xi_{54}\xi_{60}\xi_{62}} \ , \\
\Xi_3 \;=\; \xi^{w_3} \;&=\; \frac{\xi_7\xi_9\xi_{11}\xi_{13}\xi_{23}\xi_{25}\xi_{27}\xi_{29}\xi_{39}\xi_{41}\xi_{43}\xi_{45}\xi_{55}\xi_{57}\xi_{59}\xi_{61}}{\xi_8\xi_{10}\xi_{12}\xi_{14}\xi_{24}\xi_{26}\xi_{28}\xi_{30}\xi_{40}\xi_{42}\xi_{44}\xi_{46}\xi_{56}\xi_{58}\xi_{60}\xi_{62}} \ , \\
\Xi_4 \;=\; \xi^{w_4} \;&=\; \frac{\xi_{15}\xi_{17}\xi_{19}\xi_{21}\xi_{23}\xi_{25}\xi_{27}\xi_{29}\xi_{47}\xi_{49}\xi_{51}\xi_{53}\xi_{55}\xi_{57}\xi_{59}\xi_{61}}{\xi_{16}\xi_{18}\xi_{20}\xi_{22}\xi_{24}\xi_{26}\xi_{28}\xi_{30}\xi_{48}\xi_{50}\xi_{52}\xi_{54}\xi_{56}\xi_{58}\xi_{60}\xi_{62}} \ , \\
\Xi_5 \;=\; \xi^{w_5} \;&=\; \frac{\xi_{31}\xi_{33}\xi_{35}\xi_{37}\xi_{39}\xi_{41}\xi_{43}\xi_{45}\xi_{47}\xi_{49}\xi_{51}\xi_{53}\xi_{55}\xi_{57}\xi_{59}\xi_{61}}{\xi_{32}\xi_{34}\xi_{36}\xi_{38}\xi_{40}\xi_{42}\xi_{44}\xi_{46}\xi_{48}\xi_{50}\xi_{52}\xi_{54}\xi_{56}\xi_{58}\xi_{60}\xi_{62}} \ .
\end{aligned} \tag{A.3}$$

The polytope ∇

Vertices of ∇					
u_1	(-1,-1,-1,-1,-1)	u_{13}	(-1, 1, 1,-1,-1)	u_{25}	(1, 1,-1,-1,-1)
u_2	(-1,-1,-1,-1, 1)	u_{14}	(-1, 1, 1,-1, 1)	u_{26}	(1, 1,-1,-1, 1)
u_3	(-1,-1,-1, 1,-1)	u_{15}	(-1, 1, 1, 1,-1)	u_{27}	(1, 1,-1, 1,-1)
u_4	(-1,-1,-1, 1, 1)	u_{16}	(-1, 1, 1, 1, 1)	u_{28}	(1, 1,-1, 1, 1)
u_5	(-1,-1, 1,-1,-1)	u_{17}	(1,-1,-1,-1,-1)	u_{29}	(1, 1, 1,-1,-1)
u_6	(-1,-1, 1,-1, 1)	u_{18}	(1,-1,-1,-1, 1)	u_{30}	(1, 1, 1,-1, 1)
u_7	(-1,-1, 1, 1,-1)	u_{19}	(1,-1,-1, 1,-1)	u_{31}	(1, 1, 1, 1,-1)
u_8	(-1,-1, 1, 1, 1)	u_{20}	(1,-1,-1, 1, 1)	u_{32}	(1, 1, 1, 1, 1)
u_9	(-1, 1,-1,-1,-1)	u_{21}	(1,-1, 1,-1,-1)		
u_{10}	(-1, 1,-1,-1, 1)	u_{22}	(1,-1, 1,-1, 1)		
u_{11}	(-1, 1,-1, 1,-1)	u_{23}	(1,-1, 1, 1,-1)		
u_{12}	(-1, 1,-1, 1, 1)	u_{24}	(1,-1, 1, 1, 1)		

Faces of ∇	
ρ_1	$y_1 = 1$
ρ_2	$-y_1 = 1$
ρ_3	$y_2 = 1$
ρ_4	$-y_2 = 1$
ρ_5	$y_3 = 1$
ρ_6	$-y_3 = 1$
ρ_7	$y_4 = 1$
ρ_8	$-y_4 = 1$
ρ_9	$y_5 = 1$
ρ_{10}	$-y_5 = 1$

The polytope Δ

Vertices of Δ	
v_1	(1, 0, 0, 0, 0)
v_2	(0, 1, 0, 0, 0)
v_3	(0, 0, 1, 0, 0)
v_4	(0, 0, 0, 1, 0)
v_5	(0, 0, 0, 0, 1)
v_6	(-1, 0, 0, 0, 0)
v_7	(0,-1, 0, 0, 0)
v_8	(0, 0,-1, 0, 0)
v_9	(0, 0, 0,-1, 0)
v_{10}	(0, 0, 0, 0,-1)
v_{11}	(1,-1, 0, 0, 0)
v_{12}	(1, 0,-1, 0, 0)
v_{13}	(1, 0, 0,-1, 0)
v_{14}	(1, 0, 0, 0,-1)
v_{15}	(-1, 1, 0, 0, 0)
v_{16}	(0, 1,-1, 0, 0)
v_{17}	(0, 1, 0,-1, 0)
v_{18}	(0, 1, 0, 0,-1)
v_{19}	(-1, 0, 1, 0, 0)
v_{20}	(0,-1, 1, 0, 0)
v_{21}	(0, 0, 1,-1, 0)
v_{22}	(0, 0, 1, 0,-1)
v_{23}	(-1, 0, 0, 1, 0)
v_{24}	(0,-1, 0, 1, 0)
v_{25}	(0, 0,-1, 1, 0)
v_{26}	(0, 0, 0, 1,-1)
v_{27}	(-1, 0, 0, 0, 1)
v_{28}	(0,-1, 0, 0, 1)
v_{29}	(0, 0,-1, 0, 1)
v_{30}	(0, 0, 0,-1, 1)

Faces of Δ			
τ_1	$x_1 = 1$	τ_{32}	$-x_5 = 1$
τ_2	$-x_1 = 1$	τ_{33}	$x_1 + x_5 = 1$
τ_3	$x_2 = 1$	τ_{34}	$-x_1 - x_5 = 1$
τ_4	$-x_2 = 1$	τ_{35}	$x_2 + x_5 = 1$
τ_5	$x_1 + x_2 = 1$	τ_{36}	$-x_2 - x_5 = 1$
τ_6	$-x_1 - x_2 = 1$	τ_{37}	$x_1 + x_2 + x_5 = 1$
τ_7	$x_3 = 1$	τ_{38}	$-x_1 - x_2 - x_5 = 1$
τ_8	$-x_3 = 1$	τ_{39}	$x_3 + x_5 = 1$
τ_9	$x_1 + x_3 = 1$	τ_{40}	$-x_3 - x_5 = 1$
τ_{10}	$-x_1 - x_3 = 1$	τ_{41}	$x_1 + x_3 + x_5 = 1$
τ_{11}	$x_2 + x_3 = 1$	τ_{42}	$-x_1 - x_3 - x_5 = 1$
τ_{12}	$-x_2 - x_3 = 1$	τ_{43}	$x_2 + x_3 + x_5 = 1$
τ_{13}	$x_1 + x_2 + x_3 = 1$	τ_{44}	$-x_2 - x_3 - x_5 = 1$
τ_{14}	$-x_1 - x_2 - x_3 = 1$	τ_{45}	$x_1 + x_2 + x_3 + x_5 = 1$
τ_{15}	$x_4 = 1$	τ_{46}	$-x_1 - x_2 - x_3 - x_5 = 1$
τ_{16}	$-x_4 = 1$	τ_{47}	$x_4 + x_5 = 1$
τ_{17}	$x_1 + x_4 = 1$	τ_{48}	$-x_4 - x_5 = 1$
τ_{18}	$-x_1 - x_4 = 1$	τ_{49}	$x_1 + x_4 + x_5 = 1$
τ_{19}	$x_2 + x_4 = 1$	τ_{50}	$-x_1 - x_4 - x_5 = 1$
τ_{20}	$-x_2 - x_4 = 1$	τ_{51}	$x_2 + x_4 + x_5 = 1$
τ_{21}	$x_1 + x_2 + x_4 = 1$	τ_{52}	$-x_2 - x_4 - x_5 = 1$
τ_{22}	$-x_1 - x_2 - x_4 = 1$	τ_{53}	$x_1 + x_2 + x_4 + x_5 = 1$
τ_{23}	$x_3 + x_4 = 1$	τ_{54}	$-x_1 - x_2 - x_4 - x_5 = 1$
τ_{24}	$-x_3 - x_4 = 1$	τ_{55}	$x_3 + x_4 + x_5 = 1$
τ_{25}	$x_1 + x_3 + x_4 = 1$	τ_{56}	$-x_3 - x_4 - x_5 = 1$
τ_{26}	$-x_1 - x_3 - x_4 = 1$	τ_{57}	$x_1 + x_3 + x_4 + x_5 = 1$
τ_{27}	$x_2 + x_3 + x_4 = 1$	τ_{58}	$-x_1 - x_3 - x_4 - x_5 = 1$
τ_{28}	$-x_2 - x_3 - x_4 = 1$	τ_{59}	$x_2 + x_3 + x_4 + x_5 = 1$
τ_{29}	$x_1 + x_2 + x_3 + x_4 = 1$	τ_{60}	$-x_2 - x_3 - x_4 - x_5 = 1$
τ_{30}	$-x_1 - x_2 - x_3 - x_4 = 1$	τ_{61}	$x_1 + x_2 + x_3 + x_4 + x_5 = 1$
τ_{31}	$x_5 = 1$	τ_{62}	$-x_1 - x_2 - x_3 - x_4 - x_5 = 1$

Appendix B

Series Expressions and Bessel Integrals

The symbol $\boldsymbol{p}$ is understood to denote a multi-index $(p_1, p_2, p_3, p_4, p_5)$. We adopt a notation $c_{\mathbf{p}}$ for the multinomial coefficients. Recall also the harmonic numbers H_n and Polygamma functions ψ.

$$c_{\mathbf{p}} \stackrel{\text{def}}{=} \binom{|\boldsymbol{p}|}{\boldsymbol{p}}^2 = \left(\frac{\left(\sum_{i=1}^5 p_i\right)!}{\prod_{i=1}^5 p_i!}\right)^2 , \qquad H_n = \sum_{k=1}^{n} \frac{1}{k} , \qquad \psi(z) = \frac{\mathrm{d}}{\mathrm{d}z} \log\Gamma(z) .$$

For positive integers m one has the following special values for ψ and its derivatives:

$$\psi(m) = H_{m-1} - \gamma , \qquad \psi^{(1)}(m) = \frac{\pi^2}{6} - \sum_{k=1}^{m-1} \frac{1}{k^2} , \qquad \psi^{(2)}(m) = 2\left(-\zeta(3) + \sum_{k=1}^{m-1} \frac{1}{k^3}\right),$$

with γ the Euler-Mascheroni constant.

With n understood to be a positive integer, we will make frequent use of the following integrals, valid for $\mathrm{Re}[a_0] > 0$.

$$\begin{aligned}
\int_0^\infty \mathrm{d}z\, K_0(\sqrt{a_0}z) z^{2n+1} &= 4^n (n!)^2 a_0^{-1-n} , \\
\int_0^\infty \mathrm{d}z\, K_0(\sqrt{a_0}z) \log\left(\frac{z}{2}\right) z^{2n+1} &= 4^n (n!)^2 a_0^{-1-n} \left(\psi(n+1) - \frac{1}{2}\log(a_0)\right), \\
\int_0^\infty \mathrm{d}z\, K_0(\sqrt{a_0}z) \log\left(\frac{z}{2}\right)^2 z^{2n+1} &= 4^{n-1} (n!)^2 a_0^{-1-n} \left(2\psi^{(1)}(n+1) - 2\psi(n+1) + \log(a_0)\right), \qquad \text{(B.1)} \\
\int_0^\infty \mathrm{d}z\, K_0(\sqrt{a_0}z) \log\left(\frac{z}{2}\right)^3 z^{2n+1} &= 4^{n-1} (n!)^2 a_0^{-1-n} \Big(\psi^{(2)}(n+1) \\
&\quad -3\left(\log a_0 - 2\psi(n+1)\right)\psi^{(1)}(n+1) - \frac{1}{2}\left(\log a_0 - 2\psi(n+1)\right)^3\Big) .
\end{aligned}$$

Recall the following series expressions for the Bessel functions $I_0(x)$ and $K_0(x)$, which can be substituted in the integrals (6.30)-(6.31) giving periods in terms of integrals of Bessel functions. Then integrating termwise applying the above identities allows one obtain the formulae(6.32).

$$I_0(x) = \sum_{n=0}^{\infty} \frac{1}{(n!)^2} \left(\frac{x}{2}\right)^{2n} , \qquad K_0(x) = -\log\left(\frac{x}{2}\right) I_0(x) + \sum_{n=0}^{\infty} \frac{\psi(n+1)}{(n!)^2} \left(\frac{x}{2}\right)^{2n} . \qquad \text{(B.2)}$$

Appendix C

Instanton Numbers of Mirror Hulek-Verrill Manifolds

As discussed in §6.2.3, the instanton numbers can be arranged into duality webs generated by the duality operation

$$\boldsymbol{p} \;=\; (i,j,k,l,m) \;\;\mapsto\;\; \widetilde{\boldsymbol{p}} \;=\; (d-2i,\, j,\, k,\, l,\, m)\;, \qquad \text{with}\;\; d \;=\; i+j+k+l+m\;,$$

together with S_5 permutations of indices. The instanton numbers in a given duality web are equal, so we can compactly present the instanton numbers up to degree 29 by tabulating distinct duality webs, corresponding to non-zero instanton numbers, together with the genus-0 instanton numbers $n_{\boldsymbol{p}}$ and $d_{\boldsymbol{p}}$. The full list of instanton numbers can be found in [2].

Table C.1: *The positive webs, together with $\mathcal{W}_+$, and the instanton numbers n_W and d_W.*

Web	$\lvert\boldsymbol{p}\rvert$	$h(\boldsymbol{p})$	n	d
$\mathcal{W}_+$[(1,0,0,0,0)]	1	1	24	0
W[(1,1,1,0,0)]	3	0	112	0
W[(1,1,1,1,0)]	4	-2	1104	0
W[(1,1,1,1,1)]	5	-5	19200	0
W[(2,1,1,1,1)]	6	-6	45408	0
W[(2,2,1,1,0)]	6	-3	2800	0
W[(2,2,1,1,1)]	7	-8	212880	0
W[(2,2,2,0,0)]	6	0	80	4
W[(2,2,2,1,0)]	7	-5	14496	-48
W[(2,2,2,1,1)]	8	-11	1691856	528
W[(2,2,2,2,0)]	8	-8	122352	-2292
W[(2,2,2,2,1)]	9	-15	20299992	29808
W[(2,2,2,2,2)]	10	-20	341681280	3666312
W[(3,2,2,1,1)]	9	-12	3222112	928
W[(3,2,2,2,0)]	9	-9	234048	-5600
W[(3,2,2,2,1)]	10	-17	63576576	104352
W[(3,2,2,2,2)]	11	-23	1599622824	22958688
W[(3,3,1,1,1)]	9	-9	434688	0

Continued on next page

Table C.1 – continued

Web	$\lvert\boldsymbol{p}\rvert$	$h(\boldsymbol{p})$	n	d
W[(3,3,2,1,0)]	9	-6	30624	-224
W[(3,3,2,1,1)]	10	-14	10883712	4320
W[(3,3,2,2,0)]	10	-11	795936	-29136
W[(3,3,2,2,1)]	11	-20	316997280	679968
W[(3,3,2,2,2)]	12	-27	11032046624	230549312
W[(3,3,3,0,0)]	9	0	112	0
W[(3,3,3,1,0)]	10	-8	122448	-2208
W[(3,3,3,1,1)]	11	-17	59097600	30720
W[(3,3,3,2,0)]	11	-14	4326048	-251520
W[(3,3,3,2,1)]	12	-24	2322325968	6953664
W[(3,3,3,2,2)]	13	-32	105371446464	3347625888
W[(3,3,3,3,0)]	12	-18	33777312	-3031872
W[(3,3,3,3,1)]	13	-29	23351460864	99761664
W[(3,3,3,3,2)]	14	-38	1326841710624	65707393920
W[(3,3,3,3,3)]	15	-45	21228933784320	1668835805184
W[(4,2,2,2,2)]	12	-24	2624447520	40083960
W[(4,3,2,2,1)]	12	-21	529392832	1194656
W[(4,3,2,2,2)]	13	-29	27607031136	652777584
W[(4,3,3,1,1)]	12	-18	100919904	42560
W[(4,3,3,2,0)]	12	-15	7371792	-484896
W[(4,3,3,2,1)]	13	-26	5950086192	19494816
W[(4,3,3,2,2)]	14	-35	377080188864	14105356368
W[(4,3,3,3,0)]	13	-20	88179456	-9395616
W[(4,3,3,3,1)]	14	-32	85495746528	411633120
W[(4,3,3,3,2)]	15	-42	6446376071472	385951211712
W[(4,3,3,3,3)]	16	-50	134508124418928	13029814091424
W[(4,4,2,1,1)]	12	-15	19420400	10400
W[(4,4,2,2,0)]	12	-12	1423104	-61760
W[(4,4,2,2,1)]	13	-23	1426637712	3692400
W[(4,4,2,2,2)]	14	-32	103492041648	2937953580
W[(4,4,3,1,0)]	12	-9	234048	-5600
W[(4,4,3,1,1)]	13	-20	282674592	73824
W[(4,4,3,2,0)]	13	-17	20578560	-1679040
W[(4,4,3,2,1)]	14	-29	22951602432	86694528
W[(4,4,3,2,2)]	15	-39	1912895782008	87650018048
W[(4,4,3,3,0)]	14	-23	347078520	-46049040
W[(4,4,3,3,1)]	15	-36	443961562528	2496782816
W[(4,4,3,3,2)]	16	-47	42411173392368	3154648420512
W[(4,4,3,3,3)]	17	-56	1112487680575968	135453779066496
W[(4,4,4,0,0)]	12	0	80	4
W[(4,4,4,1,0)]	13	-11	795936	-29136
W[(4,4,4,1,1)]	14	-23	1218252960	-317232
W[(4,4,4,2,0)]	14	-20	88177920	-9396672
W[(4,4,4,2,1)]	15	-33	126121309632	561090816
W[(4,4,4,2,2)]	16	-44	13138629854976	755118268080
W[(4,4,4,3,0)]	15	-27	1935300720	-327015680
W[(4,4,4,3,1)]	16	-41	3114669545280	20875131744
W[(4,4,4,3,2)]	17	-53	363393804317664	34155140507184
W[(4,4,4,3,3)]	18	-63	11630106886504344	1803381971700144
W[(4,4,4,4,0)]	16	-32	14386855920	-3110590260

Continued on next page

Table C.1 – continued

Web	$\lvert\boldsymbol{p}\rvert$	$h(\boldsymbol{p})$	n	d
W[(4,4,4,4,1)]	17	-47	28258960027296	228415121472
W[(4,4,4,4,2)]	18	-60	3920585033699328	470537427014352
W[(4,4,4,4,3)]	19	-71	149583407202367176	29809312235610960
W[(4,4,4,4,4)]	20	-80	2315758601706011520	597237294763420872
W[(5,3,3,2,2)]	15	-36	570360079168	22327107072
W[(5,3,3,3,1)]	15	-33	130194945024	646886400
W[(5,3,3,3,2)]	16	-44	13834674726336	894337855968
W[(5,3,3,3,3)]	17	-53	389973010495488	41704406393856
W[(5,4,2,2,2)]	15	-33	158730945984	4750051104
W[(5,4,3,2,1)]	15	-30	35487082592	138982240
W[(5,4,3,2,2)]	16	-41	4183230238656	208350582720
W[(5,4,3,3,0)]	15	-24	539120544	-76342880
W[(5,4,3,3,1)]	16	-38	980247769056	5848333440
W[(5,4,3,3,2)]	17	-50	125365423769760	10348372749216
W[(5,4,3,3,3)]	18	-60	4272828104425920	586171325733792
W[(5,4,4,1,1)]	15	-24	1944767152	-1114976
W[(5,4,4,2,0)]	15	-21	140436672	-16170272
W[(5,4,4,2,1)]	16	-35	285207114048	1342319904
W[(5,4,4,2,2)]	17	-47	39692266181304	2545705442112
W[(5,4,4,3,0)]	16	-29	4392333792	-824199120
W[(5,4,4,3,1)]	17	-44	9502910875584	68863079616
W[(5,4,4,3,2)]	18	-57	1423524718242752	151342528026688
W[(5,4,4,3,3)]	19	-68	57309129620711136	10159668608774304
W[(5,4,4,4,0)]	17	-35	45007048752	-11043084816
W[(5,4,4,4,1)]	18	-51	114110495895360	1011188967744
W[(5,4,4,4,2)]	19	-65	19680157760407104	2707370108500416
W[(5,4,4,4,3)]	20	-77	920246692052672448	211913083229294304
W[(5,4,4,4,4)]	21	-87	17389206433621316832	5224733955268106112
W[(5,5,2,2,1)]	15	-24	2306418848	6414464
W[(5,5,2,2,2)]	16	-35	366406656528	12168742800
W[(5,5,3,1,1)]	15	-21	464696832	75776
W[(5,5,3,2,0)]	15	-18	33777312	-3031872
W[(5,5,3,2,1)]	16	-32	83099778720	351706176
W[(5,5,3,2,2)]	17	-44	13073262151968	733831612704
W[(5,5,3,3,0)]	16	-26	1272585120	-203310240
W[(5,5,3,3,1)]	17	-41	3100342138368	20194851840
W[(5,5,3,3,2)]	18	-54	507096396665312	47693058783296
W[(5,5,3,3,3)]	19	-65	21671962905320448	3417190702574592
W[(5,5,4,1,0)]	15	-12	1423616	-61920
W[(5,5,4,1,1)]	16	-26	4826161680	-6126048
W[(5,5,4,2,0)]	16	-23	347078520	-46049040
W[(5,5,4,2,1)]	17	-38	931163905728	4741984896
W[(5,5,4,2,2)]	18	-51	164605655104880	12091316695232
W[(5,5,4,3,0)]	17	-32	14386869840	-3110582880
W[(5,5,4,3,1)]	18	-48	39821013536096	318330381792
W[(5,5,4,3,2)]	19	-62	7371081117191712	903625742797728
W[(5,5,4,3,3)]	20	-74	362176732991882256	74503089764268384
W[(5,5,4,4,0)]	18	-39	193411225936	-55127514240
W[(5,5,4,4,1)]	19	-56	609209937409968	6007581031968
W[(5,5,4,4,2)]	20	-71	126656377507736616	20254395759934128

Continued on next page

Table C.1 – continued

Web	$\|\boldsymbol{p}\|$	$h(\boldsymbol{p})$	n	d
W[(5,5,4,4,3)]	21	-84	7079567101109436512	1905129808949968992
W[(5,5,4,4,4)]	22	-95	159832960277398698312	56439747241501122192
W[(5,5,5,0,0)]	15	0	112	0
W[(5,5,5,1,0)]	16	-14	4326048	-251520
W[(5,5,5,1,1)]	17	-29	17798444544	-46978560
W[(5,5,5,2,0)]	17	-26	1272585120	-203310240
W[(5,5,5,2,1)]	18	-42	4217701870608	23350187616
W[(5,5,5,2,2)]	19	-56	905275754212800	77522333436960
W[(5,5,5,3,0)]	18	-36	65215603200	-16642969280
W[(5,5,5,3,1)]	19	-53	221145135246336	1974181959168
W[(5,5,5,3,2)]	20	-68	48949713376347552	7011987726247008
W[(5,5,5,3,3)]	21	-81	2860072289627444736	689915910456635392
W[(5,5,5,4,0)]	19	-44	1096632180480	-368134832160
W[(5,5,5,4,1)]	20	-62	4162140562025760	46131775979616
W[(5,5,5,4,2)]	21	-78	1017289744237857120	190939831236687552
W[(5,5,5,4,3)]	22	-92	66573482065327669440	21104661093843211008
W[(5,5,5,4,4)]	23	-104	1763388068567027864736	736557199694836925664
W[(5,5,5,5,0)]	20	-50	7888589144400	-3138370134624
W[(5,5,5,5,1)]	21	-69	35306571598392576	442883019280896
W[(5,5,5,5,2)]	22	-86	9952370045915290464	2206547301748229184
W[(5,5,5,5,3)]	23	-101	749974117128947225088	281693674984303028736
W[(5,5,5,5,4)]	24	-114	22958958469178899286112	1139890245435959261 3184
W[(5,5,5,5,5)]	25	-125	347718598088041789328640	205994740015586336392704
W[(6,3,3,3,3)]	18	-54	552486590320032	60862991224384
W[(6,4,3,3,2)]	18	-51	178677828494464	15219924472416
W[(6,4,3,3,3)]	19	-62	8236673292611808	1190848151512512
W[(6,4,4,2,2)]	18	-48	56949598227232	3775716012840
W[(6,4,4,3,1)]	18	-45	13674852866304	101366312448
W[(6,4,4,3,2)]	19	-59	2768640614245200	310831260169488
W[(6,4,4,3,3)]	20	-71	145074948270672288	27569906261747088
W[(6,4,4,4,0)]	18	-36	65215569408	-16642956928
W[(6,4,4,4,1)]	19	-53	224917616990784	2072265197088
W[(6,4,4,4,2)]	20	-68	50310287851264512	7431936473155680
W[(6,4,4,4,3)]	21	-81	2968386268852263168	742174782726416480
W[(6,4,4,4,4)]	22	-92	69702170473826178048	22962634839334473072
W[(6,5,3,2,2)]	18	-45	18954386538304	1103727042528
W[(6,5,3,3,1)]	18	-42	4510722900128	30154035584
W[(6,5,3,3,2)]	19	-56	1000740719949936	99761061359136
W[(6,5,3,3,3)]	20	-68	55724768553096576	9449678610817056
W[(6,5,4,2,1)]	18	-39	1367836823744	7112117856
W[(6,5,4,2,2)]	19	-53	328447354833120	25630803734064
W[(6,5,4,3,0)]	18	-33	21143067840	-4775506080
W[(6,5,4,3,1)]	19	-50	79804026346992	665062141248
W[(6,5,4,3,2)]	20	-65	19159936729163904	2530955656217280
W[(6,5,4,3,3)]	21	-78	1187054464752608224	265869597857942752
W[(6,5,4,4,0)]	19	-41	391409808576	-119442727776
W[(6,5,4,4,1)]	20	-59	1608297381675072	16731712682064
W[(6,5,4,4,2)]	21	-75	419478239436537264	73138223025414832
W[(6,5,4,4,3)]	22	-89	28814753795787304128	8521174156401735360
W[(6,5,4,4,4)]	23	-101	790863904443723569376	309132463141878510000

Continued on next page

Table C.1 – continued

Web	$\lvert\boldsymbol{p}\rvert$	$h(\boldsymbol{p})$	n	d
W[(6,5,5,1,1)]	18	-30	27120466144	-87015936
W[(6,5,5,2,0)]	18	-27	1935300720	-327015680
W[(6,5,5,2,1)]	19	-44	8748592415904	49806889344
W[(6,5,5,2,2)]	20	-59	2428815576573408	225463832566752
W[(6,5,5,3,0)]	19	-38	135171775392	-37176746592
W[(6,5,5,3,1)]	20	-56	596073535387056	5619611350656
W[(6,5,5,3,2)]	21	-72	165119843412344816	25872896752378400
W[(6,5,5,3,3)]	22	-86	11833136668383611040	3144478089605250720
W[(6,5,5,4,0)]	20	-47	2981800050480	-1093125957120
W[(6,5,5,4,1)]	21	-66	14258867760974432	168513518883456
W[(6,5,5,4,2)]	22	-83	4252005327651223776	879997438952410320
W[(6,5,5,4,3)]	23	-98	334370838391810248432	117552717975524482368
W[(6,5,5,4,4)]	24	-111	10565118218002014469248	4920814265932180005216
W[(6,5,5,5,0)]	21	-54	27765085214112	-12215408263200
W[(6,5,5,5,1)]	22	-74	152435152838866176	2055320972401920
W[(6,5,5,5,2)]	23	-92	51265779665018065536	12636043517074729152
W[(6,5,5,5,3)]	24	-108	4556958521329222612288	1911288345346635589568
W[(6,5,5,5,4)]	25	-122	163766423699355653551056	91183351722137909496000
W[(6,5,5,5,5)]	26	-134	29101742338304014161626688	1942248611676865375886400
W[(6,6,2,2,2)]	18	-36	551803842816	19270744144
W[(6,6,3,2,1)]	18	-33	125948336640	554248640
W[(6,6,3,2,2)]	19	-47	39360165257928	2461712752416
W[(6,6,3,3,0)]	18	-27	1935300720	-327015680
W[(6,6,3,3,1)]	19	-44	9425697295296	66382892544
W[(6,6,3,3,2)]	20	-59	2713101057421728	294058742512224
W[(6,6,3,3,3)]	21	-72	190193228131870512	35367733329831456
W[(6,6,4,1,1)]	18	-27	7510615200	-12495360
W[(6,6,4,2,0)]	18	-24	539115744	-76341160
W[(6,6,4,2,1)]	19	-41	2910089695872	15766948032
W[(6,6,4,2,2)]	20	-56	903893653068672	76906534439280
W[(6,6,4,3,0)]	19	-35	45007048752	-11043084816
W[(6,6,4,3,1)]	20	-53	220840621188096	1954674541824
W[(6,6,4,3,2)]	21	-69	66233922634330080	9613082109166896
W[(6,6,4,3,3)]	22	-83	5023740750844977792	1243841228095131744
W[(6,6,4,4,0)]	20	-44	1096632086784	-368134868160
W[(6,6,4,4,1)]	21	-63	5658979212554128	63004921310816
W[(6,6,4,4,2)]	22	-80	1795314514514344416	346443574026127704
W[(6,6,4,4,3)]	23	-95	147828049737997120632	48619672420408782672
W[(6,6,4,4,4)]	24	-108	4831190355131709036288	2110546919582910040272
W[(6,6,5,1,0)]	18	-15	7371792	-484896
W[(6,6,5,1,1)]	19	-32	61773182400	-273996960
W[(6,6,5,2,0)]	19	-29	4392333792	-824199120
W[(6,6,5,2,1)]	20	-47	25377635878296	149497953456
W[(6,6,5,2,2)]	21	-63	8718347106041576	894838196834976
W[(6,6,5,3,0)]	20	-41	391409808576	-119442727776
W[(6,6,5,3,1)]	21	-60	2150266975191936	21688029832256
W[(6,6,5,3,2)]	22	-77	721163569257189312	125469245902996512
W[(6,6,5,3,3)]	23	-92	61757539943858380704	18293419124197908384
W[(6,6,5,4,0)]	21	-51	10848408360480	-4429601736480
W[(6,6,5,4,1)]	22	-71	63276065657309280	805991883499728

Continued on next page

Table C.1 – continued

Web	$\lvert\boldsymbol{p}\rvert$	$h(\boldsymbol{p})$	n	d
W[(6,6,5,4,2)]	23	-89	22420496977021999680	5175740190127316160
W[(6,6,5,4,3)]	24	-105	2073506802039240412736	816025913316248333120
W[(6,6,5,4,4)]	25	-119	76746430278444036385392	40163166616613493587568
W[(6,6,5,5,0)]	22	-59	126532108859856	-62415555336480
W[(6,6,5,5,1)]	23	-80	830212985215356432	12132995150259168
W[(6,6,5,5,2)]	24	-99	325919053252224299168	90095498612893458272
W[(6,6,5,5,3)]	25	-116	33557221088952835248384	15832086999292901742336
W[(6,6,5,5,4)]	26	-131	1393776642755701910391504	875590499820813091496688
W[(6,6,5,5,5)]	27	-144	28656849112544426796718608	21652833697465345825473216
W[(6,6,6,0,0)]	18	0	80	4
W[(6,6,6,1,0)]	19	-17	20578560	-1679040
W[(6,6,6,1,1)]	20	-35	203336907216	-1334560224
W[(6,6,6,2,0)]	20	-32	14386855920	-3110590260
W[(6,6,6,2,1)]	21	-51	99894446151552	604322817696
W[(6,6,6,2,2)]	22	-68	40767562975883520	4694772196282128
W[(6,6,6,3,0)]	21	-45	1535514818112	-531223501536
W[(6,6,6,3,1)]	22	-65	10102374952223232	109867633989312
W[(6,6,6,3,2)]	23	-83	3982038442779651984	777895843534310448
W[(6,6,6,3,3)]	24	-99	398117530652334602832	132628671085592097024
W[(6,6,6,4,0)]	22	-56	51294956593632	-23657222126952
W[(6,6,6,4,1)]	23	-77	354725791310991552	4906985498846880
W[(6,6,6,4,2)]	24	-96	145958872012447992432	37906436889576198396
W[(6,6,6,4,3)]	25	-113	15579801166584314831616	6912402731596987607520
W[(6,6,6,4,4)]	26	-128	664776534906643820467776	393169006303652095072272
W[(6,6,6,5,0)]	23	-65	725912434085952	-405156007308576
W[(6,6,6,5,1)]	24	-87	5571858588504821712	88798104825584352
W[(6,6,6,5,2)]	25	-107	2507158978553441682912	782286842060773523040
W[(6,6,6,5,3)]	26	-125	294433074567120966718080	157120006208930268178944
W[(6,6,6,5,4)]	27	-141	13944411721206459640109952	9930103217664737498362752
W[(6,6,6,5,5)]	28	-155	32768461438734929996173876 8	28139610544603882976457033 6
W[(6,6,6,6,0)]	24	-72	5101035241706976	-3238317070364520
W[(6,6,6,6,1)]	25	-95	45075021198059982144	786907500135989952
W[(6,6,6,6,2)]	26	-116	22914149837439123291648	8106453008262631136544
W[(6,6,6,6,3)]	27	-135	3030705830464261116958752	1836744316255728093377504
W[(6,6,6,6,4)]	28	-152	16182365961682789204294665 6	13109862097711964053267764 0
W[(6,6,6,6,5)]	29	-167	43007797210741512414808847 04	42102606163818323057770680 00
W[(7,4,4,3,3)]	21	-72	196866216448867200	38231916995852064
W[(7,4,4,4,2)]	21	-69	68481669752665152	10343926869883680
W[(7,4,4,4,3)]	22	-83	5273427759409817952	1369210879561818480
W[(7,4,4,4,4)]	23	-95	157391952685989052728	54505767240269122368
W[(7,5,3,3,3)]	21	-69	75992812385562624	13183353406838784
W[(7,5,4,3,2)]	21	-66	26217346711258048	3545177906512576
W[(7,5,4,3,3)]	22	-80	2124595552827372432	494845153306899264
W[(7,5,4,4,1)]	21	-60	2211223893638272	23383915823040
W[(7,5,4,4,2)]	22	-77	754387255278771840	136879891485939456
W[(7,5,4,4,3)]	23	-92	65617907601886711296	20425869092209172544
W[(7,5,4,4,4)]	24	-105	2234583126440197477248	928035242813679386880
W[(7,5,5,2,2)]	21	-60	3356453655323136	319546789488192
W[(7,5,5,3,1)]	21	-57	824874647838720	7905805097984
W[(7,5,5,3,2)]	22	-74	299477728365291600	48909204818311680

Continued on next page

Table C.1 – continued

Web	$\lvert\boldsymbol{p}\rvert$	$h(\boldsymbol{p})$	n	d
W[(7,5,5,3,3)]	23	-89	27190620887571766272	7616709702249560064
W[(7,5,5,4,0)]	21	-48	4136092936448	-1559208760288
W[(7,5,5,4,1)]	22	-68	26040136828870752	316717033197408
W[(7,5,5,4,2)]	23	-86	9824161857371476896	2144674430360819712
W[(7,5,5,4,3)]	24	-102	953357306203227960000	356555435715410957376
W[(7,5,5,4,4)]	25	-116	36602428260502812573792	18266693407737182177184
W[(7,5,5,5,0)]	22	-56	51294957112992	-23657221999872
W[(7,5,5,5,1)]	23	-77	358330187751266304	5019686189816832
W[(7,5,5,5,2)]	24	-96	148388879628408287328	38978014973683179264
W[(7,5,5,5,3)]	25	-113	15930480413967177684480	7166819934960635255808
W[(7,5,5,5,4)]	26	-128	683358195482651060173200	410426378940650223011136
W[(7,5,5,5,5)]	27	-141	144014956353093838652737536	10424016378695267249799168
W[(7,6,3,3,2)]	21	-60	3761948244770304	418651558115072
W[(7,6,3,3,3)]	22	-74	346896207708697296	67323025901888832
W[(7,6,4,2,2)]	21	-57	1259132047619264	110090172437152
W[(7,6,4,3,1)]	21	-54	308134225628128	2778335397408
W[(7,6,4,3,2)]	22	-71	121505012171479176	18421518301369920
W[(7,6,4,3,3)]	23	-86	11689593863624674656	3057298493530985568
W[(7,6,4,4,0)]	21	-45	1535514818112	-531223501536
W[(7,6,4,4,1)]	22	-65	10462960782869952	120114507109632
W[(7,6,4,4,2)]	23	-83	4202606608677077184	857299960689895392
W[(7,6,4,4,3)]	24	-99	426992405813739053760	149677043087457971504
W[(7,6,4,4,4)]	25	-113	16950676810888359150336	7947181852777331886432
W[(7,6,5,2,1)]	21	-48	35929933424832	213298398784
W[(7,6,5,2,2)]	22	-65	16270300857476160	1749317561578944
W[(7,6,5,3,0)]	21	-42	553728279360	-174588053440
W[(7,6,5,3,1)]	22	-62	4021264698687264	41786034116160
W[(7,6,5,3,2)]	23	-80	1706830027589928192	314475153857119104
W[(7,6,5,3,3)]	24	-96	180227194372605425904	56981868551941098752
W[(7,6,5,4,0)]	22	-53	20350993239840	-8738280013680
W[(7,6,5,4,1)]	23	-74	150993571342096992	2001252354617280
W[(7,6,5,4,2)]	24	-93	65822715717348500960	16227227828645916976
W[(7,6,5,4,3)]	25	-110	7345251761305389562560	3105932030883925870176
W[(7,6,5,4,4)]	26	-125	324239422338282700223616	183290892867377049167040
W[(7,6,5,5,0)]	23	-62	305922925426848	-160791639748800
W[(7,6,5,5,1)]	24	-84	2483294974158049312	38035145900721056
W[(7,6,5,5,2)]	25	-104	1172715223879828113648	34883658057363657472
W[(7,6,5,5,3)]	26	-122	1430659870599296518820 64	7297740947214374046960 0
W[(7,6,5,5,4)]	27	-138	6979017914791123565948416	4760519298349779631098496
W[(7,6,5,5,5)]	28	-152	167783614906668761262716784	13823704937763195640644499 2
W[(7,6,6,1,1)]	21	-36	299302640864	-2202805408
W[(7,6,6,2,0)]	21	-33	21143067840	-4775506080
W[(7,6,6,2,1)]	22	-53	194378107421760	1179552933984
W[(7,6,6,2,2)]	23	-71	100108346194477248	12276819589743504
W[(7,6,6,3,0)]	22	-47	2981800050480	-1093125957120
W[(7,6,6,3,1)]	23	-68	24863416450991904	281059260470880
W[(7,6,6,3,2)]	24	-87	12017787465197578008	2517326301790872576
W[(7,6,6,3,3)]	25	-104	1445782834458789325920	519156967290582783648
W[(7,6,6,4,0)]	23	-59	126532108859856	-62415555336480
W[(7,6,6,4,1)]	24	-81	1079565550915867008	15666901809220000

Continued on next page

Table C.1 – continued

Web	$\|\boldsymbol{p}\|$	$h(\boldsymbol{p})$	n	d
W[(7,6,6,4,2)]	25	-101	533243466879375407808	149323799470083244320
W[(7,6,6,4,3)]	26	-119	67330722644161744497600	32349736654103967569424
W[(7,6,6,4,4)]	27	-135	3369981367793558156370720	2166849385502855883360624
W[(7,6,6,5,0)]	24	-69	2235977596096128	-1345692401785920
W[(7,6,6,5,1)]	25	-92	20734174826253969312	348635537576206944
W[(7,6,6,5,2)]	26	-113	11001712604766772877568	3721525089274735889952
W[(7,6,6,5,3)]	27	-132	1505729217469676504230592	874186334599890564570432
W[(7,6,6,5,4)]	28	-149	82579048510474932784060128	64187540696210944731760560
W[(7,6,6,5,5)]	29	-164	22408125897758955838844156576	21073924838545795185214923 84
W[(7,6,6,6,0)]	25	-77	19503820669876800	-13461969999093600
W[(7,6,6,6,1)]	26	-101	204289830851585811840	3782526785435078400
W[(7,6,6,6,2)]	27	-123	120468636234042768002112	46465382392154451939072
W[(7,6,6,6,3)]	28	-143	18312063250016785426332456	12132928161031878393585456
W[(7,6,6,6,4)]	29	-161	11185922624472084194947002 24	99326826421425165897506592 0
W[(7,7,3,2,2)]	21	-48	56389985840000	3650629114944
W[(7,7,3,3,1)]	21	-45	13542066341888	97849986048
W[(7,7,3,3,2)]	22	-62	7173870919736064	840536568752160
W[(7,7,3,3,3)]	23	-77	841539378868429824	173735334568551936
W[(7,7,4,2,1)]	21	-42	4216297529824	23296907136
W[(7,7,4,2,2)]	22	-59	2422178398686816	223306712255904
W[(7,7,4,3,0)]	21	-36	65215603200	-16642969280
W[(7,7,4,3,1)]	22	-56	594508678788528	5559537648384
W[(7,7,4,3,2)]	23	-74	297115911452589936	47974716780673152
W[(7,7,4,3,3)]	24	-90	35230204567671156080	9881551554602229408
W[(7,7,4,4,0)]	22	-47	2981800050480	-1093125957120
W[(7,7,4,4,1)]	23	-68	25857038420140320	310320577356576
W[(7,7,4,4,2)]	24	-87	12756877670900976952	2792965386085320880
W[(7,7,4,4,3)]	25	-104	1560763765722117846528	590236080316778614944
W[(7,7,4,4,4)]	26	-119	73760592549207990341160	37482832972502804145504
W[(7,7,5,1,1)]	21	-33	92396257280	-471020544
W[(7,7,5,2,0)]	21	-30	6558863360	-1292723968
W[(7,7,5,2,1)]	22	-50	71274491245200	428753909184
W[(7,7,5,2,2)]	23	-68	40746789567213888	4682747289739200
W[(7,7,5,3,0)]	22	-44	1096632180480	-368134832160
W[(7,7,5,3,1)]	23	-65	10097809547695104	109488862752768
W[(7,7,5,3,2)]	24	-84	5251183397613765152	1040501263302552608
W[(7,7,5,3,3)]	25	-101	666467844013257615360	227671001933190288384
W[(7,7,5,4,0)]	23	-56	51294957112992	-23657221999872
W[(7,7,5,4,1)]	24	-78	468967501173905952	6536958768444736
W[(7,7,5,4,2)]	25	-98	245004909605415502560	65291193554279696544
W[(7,7,5,4,3)]	26	-116	32292308644789613776992	14816698735976435302944
W[(7,7,5,4,4)]	27	-132	1670002775792759585584480	1028056808615702374843808
W[(7,7,5,5,0)]	24	-66	964399018545152	-548768158982912
W[(7,7,5,5,1)]	25	-89	9433084896265973760	152724917794335744
W[(7,7,5,5,2)]	26	-110	5240983985031424336512	169390504234456661 7888
W[(7,7,5,5,3)]	27	-129	743754012075104160058368	413486815490189461567488
W[(7,7,5,5,4)]	28	-146	41952996407118579100732512	31280567724121492258032672
W[(7,7,5,5,5)]	29	-161	11633932524718368688617861 12	10509992132039453093215436 8
W[(7,7,6,1,0)]	21	-18	33777312	-3031872
W[(7,7,6,1,1)]	22	-38	639016897824	-5776067616

Continued on next page

Table C.1 – continued

Web	$\lvert\boldsymbol{p}\rvert$	$h(\boldsymbol{p})$	n	d
W[(7,7,6,2,0)]	22	-35	45007048752	-11043084816
W[(7,7,6,2,1)]	23	-56	515881389602064	3117411980160
W[(7,7,6,2,2)]	24	-75	322136481160659232	42751365570060704
W[(7,7,6,3,0)]	23	-50	7888589144400	-3138370134624
W[(7,7,6,3,1)]	24	-72	80203179581197904	950472340606656
W[(7,7,6,3,2)]	25	-92	46154206945493038080	10495212981639920256
W[(7,7,6,3,3)]	26	-110	6528373563454253739936	2551778870797810769088
W[(7,7,6,4,0)]	24	-63	408865565088240	-219322647849280
W[(7,7,6,4,1)]	25	-86	4182469007721935136	64196301394125984
W[(7,7,6,4,2)]	26	-107	2422666442072438912352	738648123808652479056
W[(7,7,6,4,3)]	27	-126	355021932713338577724288	186191937088342721822720
W[(7,7,6,4,4)]	28	-143	20512359802778934105982824	14433618175802344857159648
W[(7,7,6,5,0)]	25	-74	8765016259161504	-5758034709276000
W[(7,7,6,5,1)]	26	-98	95977233617823957552	1714200026193282432
W[(7,7,6,5,2)]	27	-120	58904390293772710703920	21768872364464612982848
W[(7,7,6,5,3)]	28	-140	92449719645764325833596 80	58773682166729684416405 44
W[(7,7,6,5,4)]	29	-158	57908324967262914509503 0368	49398481686680631621383 7888
W[(7,7,6,6,0)]	26	-83	92700939550359360	-70199768003592720
W[(7,7,6,6,1)]	27	-108	1129438555365292906784	22298898608487186016
W[(7,7,6,6,2)]	28	-131	760089538306826431748976	321577464094704294681456
W[(7,7,6,6,3)]	29	-152	13095657525668962636257 5040	95352673153203400660517280
W[(7,7,7,0,0)]	21	0	112	0
W[(7,7,7,1,0)]	22	-20	88179456	-9395616
W[(7,7,7,1,1)]	23	-41	1927069671936	-22739284992
W[(7,7,7,2,0)]	23	-38	135171775392	-37176746592
W[(7,7,7,2,1)]	24	-60	1823829689450016	10748457996288
W[(7,7,7,2,2)]	25	-80	1329872815417735680	193409949629545344
W[(7,7,7,3,0)]	24	-54	27765085214112	-12215408263200
W[(7,7,7,3,1)]	25	-77	331877990439469056	4142934152742912
W[(7,7,7,3,2)]	26	-98	221273208968851435344	55156658249311147008
W[(7,7,7,3,3)]	27	-117	36027026438881932128256	15448516510046832328704
W[(7,7,7,4,0)]	25	-68	1692511362069504	-1000067627051904
W[(7,7,7,4,1)]	26	-92	20221514209776438144	330197068437575904
W[(7,7,7,4,2)]	27	-114	13449577349429667122112	4498860807385583308224
W[(7,7,7,4,3)]	28	-134	22485111547036656869007 36	12953369360986113230529 60
W[(7,7,7,4,4)]	29	-152	14781836303848871619272 2368	11442461827331289236652 0384
W[(7,7,7,5,0)]	26	-80	42801528146793216	-30974226462689184
W[(7,7,7,5,1)]	27	-105	542448112625738749440	10343645286248254464
W[(7,7,7,5,2)]	28	-128	378607952063724321532320	153782147365152593438592
W[(7,7,7,5,3)]	29	-149	67179875933573491930042368	47005257591061770949294080
W[(7,7,7,6,0)]	27	-90	536474722655969280	-448609384225666560
W[(7,7,7,6,1)]	28	-116	7483863739103052384864	158207445568417102656
W[(7,7,7,6,2)]	29	-140	5668780293104872727438208	2642910651915844284490560
W[(7,7,7,7,0)]	28	-98	3704581973944705776	-3435204329200397376
W[(7,7,7,7,1)]	29	-125	58444196223515692468224	1327111985411944965120
W[(8,4,4,4,4)]	24	-96	205889395932163617312	72441168290052535416
W[(8,5,4,4,3)]	24	-93	86069413996832124352	27232968315848722400
W[(8,5,4,4,4)]	25	-107	3727698169135125498096	1592870480807489129616
W[(8,5,5,3,3)]	24	-90	35767925041629127584	10189105935322611904
W[(8,5,5,4,2)]	24	-87	12945658352928829152	2874629165830386272

Continued on next page

Table C.1 – continued

Web	$\lvert\boldsymbol{p}\rvert$	$h(\boldsymbol{p})$	n	d
W[(8,5,5,4,3)]	25	-104	1597193840680108612560	614995894410428607648
W[(8,5,5,4,4)]	26	-119	76121903698269498879600	3948041810698146653352 0
W[(8,5,5,5,1)]	24	-78	474753531842519136	6730910671190400
W[(8,5,5,5,2)]	25	-98	250363560088071437904	67768604147499442944
W[(8,5,5,5,3)]	26	-116	33298242026156998722144	15578338962013218600864
W[(8,5,5,5,4)]	27	-132	1737004389084229283537184	1092905783425309905030912
W[(8,5,5,5,5)]	28	-146	43981223391578028025767312	33565543023690642272679360
W[(8,6,4,3,3)]	24	-87	15439042985968145360	4109159918573469824
W[(8,6,4,4,2)]	24	-84	5561099164846002688	1154720984430059840
W[(8,6,4,4,3)]	25	-101	719772958474534446912	260001810225111467808
W[(8,6,4,4,4)]	26	-116	35504946591945154063104	17316166253014236259776
W[(8,6,5,3,2)]	24	-81	2266457718090172160	425294962053433344
W[(8,6,5,3,3)]	25	-98	305275969074406465728	99531632175997196352
W[(8,6,5,4,1)]	24	-75	201010148340707968	2697580082412768
W[(8,6,5,4,2)]	25	-95	111802499676622459032	28431306071376793872
W[(8,6,5,4,3)]	26	-113	15467950978366663032576	6808548519814415880000
W[(8,6,5,4,4)]	27	-129	830547124981920578846912	492306078671771466820064
W[(8,6,5,5,0)]	24	-63	408865565088240	-219322647849280
W[(8,6,5,5,1)]	25	-86	4254301857683952288	66591254167125120
W[(8,6,5,5,2)]	26	-107	2490930240945503131824	772032475082783116752
W[(8,6,5,5,3)]	27	-126	368512581418692060268192	197228805113267715996416
W[(8,6,5,5,4)]	28	-143	21480065424682369924330608	15461693507386297016774064
W[(8,6,5,5,5)]	29	-158	61121031290459098512641299 2	53416798018436365202367888 0
W[(8,6,6,2,2)]	24	-72	134490191192202528	16827059517736904
W[(8,6,6,3,1)]	24	-69	33425310221788864	382345702776672
W[(8,6,6,3,2)]	25	-89	20678681485694660736	4476560442767249184
W[(8,6,6,3,3)]	26	-107	3087105410543684178144	1156070611877661822288
W[(8,6,6,4,0)]	24	-60	170193514498560	-85781801535360
W[(8,6,6,4,1)]	25	-83	1864566688856423904	27663244132912416
W[(8,6,6,4,2)]	26	-104	1142319760025546317200	333685276507832498868
W[(8,6,6,4,3)]	27	-123	174894056440451268167776	88255562432100365628448
W[(8,6,6,4,4)]	28	-140	1045675654920590535945830 4	7101369488031789966243504
W[(8,6,6,5,0)]	25	-71	3881643757375656	-2421429008571216
W[(8,6,6,5,1)]	26	-95	44858935490060258472	776764446454911264
W[(8,6,6,5,2)]	27	-117	28841649917004887522080	10255257716817787654800
W[(8,6,6,5,3)]	28	-137	4698818465684165361643776	2882884240831835131741344
W[(8,6,6,5,4)]	29	-155	3031939576952955741679723 68	2501740290241521326129418 72
W[(8,6,6,6,0)]	26	-80	42801528135993600	-30974226462442944
W[(8,6,6,6,1)]	27	-105	546003716872720702848	10474506505204294080
W[(8,6,6,6,2)]	28	-128	382713191877285462148512	156242327334663646224888
W[(8,6,6,6,3)]	29	-149	6816111497229587524170604 8	4800028244917346285884809 6
W[(8,7,3,3,3)]	24	-78	1126346577851592960	237188563748902272
W[(8,7,4,3,2)]	24	-75	398660145480045856	65682988009064448
W[(8,7,4,3,3)]	25	-92	60590920000179493056	17566723688872737408
W[(8,7,4,4,1)]	24	-69	34807080531177792	423655401709600
W[(8,7,4,4,2)]	25	-89	22012186784542835520	4983325664622060480
W[(8,7,4,4,3)]	26	-107	3345260435684206623648	1320063534010559077776
W[(8,7,4,4,4)]	27	-123	192443720708788001680608	102771309648644620264992
W[(8,7,5,2,2)]	24	-69	55084399995750144	6466615047655104
W[(8,7,5,3,1)]	24	-66	13661798641742976	150108480756288

Continued on next page

Table C.1 – continued

Web	$\lvert\boldsymbol{p}\rvert$	$h(\boldsymbol{p})$	n	d
W[(8,7,5,3,2)]	25	-86	9117897040377080832	1869909171436016640
W[(8,7,5,3,3)]	26	-104	1437664544143525963632	512903625458504140800
W[(8,7,5,4,0)]	24	-57	69468841810240	-32779917518560
W[(8,7,5,4,1)]	25	-80	817746667654917168	11668379661795360
W[(8,7,5,4,2)]	26	-101	530380950844598802240	147653937102100467360
W[(8,7,5,4,3)]	27	-120	84779574976667980526368	40909136655697997550496
W[(8,7,5,4,4)]	28	-137	5236870677368742358091328	3408941234035601841250272
W[(8,7,5,5,0)]	25	-68	1692511362069504	-1000067627051904
W[(8,7,5,5,1)]	26	-92	20644575230653895136	344594558995733856
W[(8,7,5,5,2)]	27	-114	13895992208920106396544	4727639000530609605248
W[(8,7,5,5,3)]	28	-134	2346380263735039996887072	1380187929485720284723200
W[(8,7,5,5,4)]	29	-152	15564288314565360744968337 6	12332017180252710906786115 2
W[(8,7,6,2,1)]	24	-57	710229601026304	4272120540288
W[(8,7,6,2,2)]	25	-77	571128202199454336	78667271480859264
W[(8,7,6,3,0)]	24	-51	10848408360480	-4429601736480
W[(8,7,6,3,1)]	25	-74	142342287006477504	1722815728418688
W[(8,7,6,3,2)]	26	-95	101657485900434092424	24205677459521479872
W[(8,7,6,3,3)]	27	-114	17421547466353577240096	7175765870665787614560
W[(8,7,6,4,0)]	25	-65	725912434085952	-405156007308576
W[(8,7,6,4,1)]	26	-89	9254014284061822464	146449762016579712
W[(8,7,6,4,2)]	27	-111	6488505552963384035984	2085054959697204491664
W[(8,7,6,4,3)]	28	-131	1130432594965350429319440	627928503566826840282528
W[(8,7,6,4,4)]	29	-149	76752707872006994882755104	57440210392521975531302352
W[(8,7,6,5,0)]	26	-77	19503820669876800	-13461969999093600
W[(8,7,6,5,1)]	27	-102	259867472483449630240	4813453384531950048
W[(8,7,6,5,2)]	28	-125	189389511540055226332992	74184255759899839436832
W[(8,7,6,5,3)]	29	-146	34795170486545493534538224	23538032787827317440430848
W[(8,7,6,6,0)]	27	-87	254791938658803840	-204417944244944160
W[(8,7,6,6,1)]	28	-113	3705422029800182188416	76233400110735695520
W[(8,7,6,6,2)]	29	-137	2913373653270128828358720	1313382488163858590583360
W[(8,7,7,1,1)]	24	-42	2760956499680	-35309984768
W[(8,7,7,2,0)]	24	-39	193411225936	-55127514240
W[(8,7,7,2,1)]	25	-62	3377194221012096	19460158766688
W[(8,7,7,2,2)]	26	-83	3047920567708923264	466497292363869360
W[(8,7,7,3,0)]	25	-56	51294957112992	-23657221999872
W[(8,7,7,3,1)]	26	-80	761479183438470384	9764259633947136
W[(8,7,7,3,2)]	27	-102	612363334253114849568	161547529688023582240
W[(8,7,7,3,3)]	28	-122	118167437729899245359856	53848312436074659256320
W[(8,7,7,4,0)]	26	-71	3881643757375656	-2421429008571216
W[(8,7,7,4,1)]	27	-96	56225444916409818816	952690031556127200
W[(8,7,7,4,2)]	28	-119	44276794310053780437840	15741021131132583500640
W[(8,7,7,4,3)]	29	-140	86444902852829367395477 76	53108241399502791864130 56
W[(8,7,7,5,0)]	27	-84	119602242975339008	-91914770340089280
W[(8,7,7,5,1)]	28	-110	1805398290592460769984	35900356719080933088
W[(8,7,7,5,2)]	29	-134	1469714544745529210370240	636966041838597182072352
W[(8,7,7,6,0)]	28	-95	1810611871504105272	-1616941505273075616
W[(8,7,7,6,1)]	29	-122	29632320884127789040512	655738370875420162368
W[(8,7,7,7,0)]	29	-104	15060587910821007264	-15002076051597343200
W[(8,8,3,3,2)]	24	-63	9867511282052976	1185430621063936
W[(8,8,3,3,3)]	25	-80	2006276928131711424	439198792163267520

Continued on next page

Table C.1 – continued

Web	$\lvert\boldsymbol{p}\rvert$	$h(\boldsymbol{p})$	n	d
W[(8,8,4,2,2)]	24	-60	3345447617629184	316457581635168
W[(8,8,4,3,1)]	24	-57	822222499846400	7826902863232
W[(8,8,4,3,2)]	25	-77	713471511849776160	122281608111146832
W[(8,8,4,3,3)]	26	-95	135135632721772486224	41111092665529983696
W[(8,8,4,4,0)]	24	-48	4136092740352	-1559208686912
W[(8,8,4,4,1)]	25	-71	62675569121448240	784225690196688
W[(8,8,4,4,2)]	26	-92	49318322079952346112	11721366876475799760
W[(8,8,4,4,3)]	27	-111	9090329485714422369312	3788700251223612606992
W[(8,8,4,4,4)]	28	-128	624198973773146079716784	353812311322644431070252
W[(8,8,5,2,1)]	24	-51	99885127862240	604016711936
W[(8,8,5,2,2)]	25	-71	100010833402440120	12238194838809408
W[(8,8,5,3,0)]	24	-45	1535514818112	-531223501536
W[(8,8,5,3,1)]	25	-68	24840263013168672	280061917894368
W[(8,8,5,3,2)]	26	-89	20610476713078747200	4443062729668252800
W[(8,8,5,3,3)]	27	-108	3937816074403396325984	1485322356047272900832
W[(8,8,5,4,0)]	25	-59	126532108859856	-62415555336480
W[(8,8,5,4,1)]	26	-83	1859138760210276768	27442949686074432
W[(8,8,5,4,2)]	27	-105	1458934381540619175680	429548694784566103072
W[(8,8,5,4,3)]	28	-125	276957561140740817672064	141959405252146760964096
W[(8,8,5,4,4)]	29	-143	20081002987269237834527544	13937339478667000119236400
W[(8,8,5,5,0)]	26	-71	3881643757375656	-2421429008571216
W[(8,8,5,5,1)]	27	-96	57539715512784775920	998655920868343392
W[(8,8,5,5,2)]	28	-119	45903620873883847141776	16604759404714367599872
W[(8,8,5,5,3)]	29	-140	9056138605664527122727872	5683140308380169857515456
W[(8,8,6,1,1)]	24	-39	927231904320	-9200679520
W[(8,8,6,2,0)]	24	-36	65215569408	-16642956928
W[(8,8,6,2,1)]	25	-59	1335301022489328	7932337626384
W[(8,8,6,2,2)]	26	-80	1329629977546611936	193232919723748536
W[(8,8,6,3,0)]	25	-53	20350993239840	-8738280013680
W[(8,8,6,3,1)]	26	-77	331824982853181696	4137353643774720
W[(8,8,6,3,2)]	27	-99	285713812377367900976	72150775131428807216
W[(8,8,6,3,3)]	28	-119	57992334650190556570488	25428538397714935697520
W[(8,8,6,4,0)]	26	-68	1692511359568896	-1000067627325696
W[(8,8,6,4,1)]	27	-93	26146648523244093888	430155649709142688
W[(8,8,6,4,2)]	28	-116	21685078061596939766784	7419452787535790690304
W[(8,8,6,4,3)]	29	-137	4407669387277685669560512	261487861096108941343833 6
W[(8,8,6,5,0)]	27	-81	55456767284050560	-40752668020556480
W[(8,8,6,5,1)]	28	-107	878968309413423252864	17001413171806593504
W[(8,8,6,5,2)]	29	-131	746119098679547758175328	312334294647361791229536
W[(8,8,6,6,0)]	28	-92	875827020273329664	-752251254607854720
W[(8,8,6,6,1)]	29	-119	14913192160928967502416	321538657422443256528
W[(8,8,7,1,0)]	24	-21	140436672	-16170272
W[(8,8,7,1,1)]	25	-44	5601159429504	-83145266112
W[(8,8,7,2,0)]	25	-41	391409808576	-119442727776
W[(8,8,7,2,1)]	26	-65	8359186921934400	46040552189760
W[(8,8,7,2,2)]	27	-87	8999069221638485760	1469239641997479152
W[(8,8,7,3,0)]	26	-59	126532108859856	-62415555336480
W[(8,8,7,3,1)]	27	-84	2251004857405139040	29808201189352224
W[(8,8,7,3,2)]	28	-107	2125395706871678176416	599695012064780172192
W[(8,8,7,3,3)]	29	-128	475983733946283470184480	232464084388228505851296

Continued on next page

Table C.1 – continued

Web	$\lvert\boldsymbol{p}\rvert$	$h(\boldsymbol{p})$	n	d
W[(8,8,7,4,0)]	27	-75	11461248223336400	-7656245352109120
W[(8,8,7,4,1)]	28	-101	196113949182715052160	3469894328671355136
W[(8,8,7,4,2)]	29	-125	179029959278599331183904	68216655150306510669456
W[(8,8,7,5,0)]	28	-89	419093788958668992	-345708325307878560
W[(8,8,7,5,1)]	29	-116	7382355219180836928000	153930935927106810240
W[(8,8,7,6,0)]	29	-101	7505020393627384992	-7217177104026255792
W[(8,8,8,0,0)]	24	0	80	4
W[(8,8,8,1,0)]	25	-23	347078520	-46049040
W[(8,8,8,1,1)]	26	-47	15746747463456	-285485916336
W[(8,8,8,2,0)]	26	-44	1096632086784	-368134868160
W[(8,8,8,2,1)]	27	-69	27132798580132512	137150695673232
W[(8,8,8,2,2)]	28	-92	33641794610965862400	5923901626220768640
W[(8,8,8,3,0)]	27	-63	408865565088240	-219322647849280
W[(8,8,8,3,1)]	28	-89	8424735061429730304	115480640308379520
W[(8,8,8,3,2)]	29	-113	9106787701513392933312	2772036316581728759040
W[(8,8,8,4,0)]	28	-80	42801528135993600	-30974226462442944
W[(8,8,8,4,1)]	29	-107	844343421475958442384	15670595020056748992
W[(8,8,8,5,0)]	29	-95	1810611871504105272	-1616941505273075616
W[(9,5,5,4,4)]	27	-120	96959783616963943030208	50915057095808531822560
W[(9,5,5,5,3)]	27	-117	42482450279496628079616	20127314721021911676928
W[(9,5,5,5,4)]	28	-134	2754129399126265116578688	1771748988189311827248096
W[(9,5,5,5,5)]	29	-149	85113274584443674676815872	669369163519938856522168 32
W[(9,6,4,4,4)]	27	-117	45328721421594382226880	22390120482647854754272
W[(9,6,5,4,3)]	27	-114	19781742107681508906368	8820756832744533115968
W[(9,6,5,4,4)]	28	-131	1321756163879149610446896	80141437984418978904864 0
W[(9,6,5,5,2)]	27	-108	3194412266903770307840	1003282043598184664064
W[(9,6,5,5,3)]	28	-128	588017185467849919723392	32201747245550597794694 4
W[(9,6,5,5,4)]	29	-146	41753519869402757126310048	30986533923874230605211360
W[(9,6,6,3,3)]	27	-108	3965695431311102575520	1505336844006318854880
W[(9,6,6,4,2)]	27	-105	1468942204326701835456	434985047971986769440
W[(9,6,6,4,3)]	28	-125	280190865205345515202656	144746838738025811348976
W[(9,6,6,4,4)]	29	-143	20420265705357860466725736	14305111033066829808964272
W[(9,6,6,5,1)]	27	-96	57866098737278532384	1011424106940266496
W[(9,6,6,5,2)]	28	-119	46407141063611686053552	16899949831877607148848
W[(9,6,6,5,3)]	29	-140	9205492921536158089178400	5827961507523161595876576
W[(9,6,6,6,0)]	27	-81	55456767284050560	-40752668020556480
W[(9,6,6,6,1)]	28	-107	886526887354737645072	17294122346233404288
W[(9,6,6,6,2)]	29	-131	757338998385448742259408	319351886711731639092048
W[(9,7,4,4,3)]	27	-108	4302653199079323937920	1721332405243795563776
W[(9,7,4,4,4)]	28	-125	308970407090480886905664	16896514790488628782876 8
W[(9,7,5,3,3)]	27	-105	1852914051293922601984	670374726927803695104
W[(9,7,5,4,2)]	27	-102	684339544738107833984	193221962896538278144
W[(9,7,5,4,3)]	28	-122	136517982401519160854256	67481808424198752531456
W[(9,7,5,4,4)]	29	-140	10288587378544353628959936	69133047326362921628768 64
W[(9,7,5,5,1)]	27	-93	26729153888914424832	450524230700139520
W[(9,7,5,5,2)]	28	-116	22480410038381810846784	7838457970390311440448
W[(9,7,5,5,3)]	29	-137	4625435952934481006642688	2809517795490346324727808
W[(9,7,6,3,2)]	27	-96	131895336423525168320	31875712216477298048
W[(9,7,6,3,3)]	28	-116	28271565861485256037152	11940345167441877911232
W[(9,7,6,4,1)]	27	-90	12023512502480326944	192137049043395264

Continued on next page

Table C.1 – continued

Web	$\lvert\boldsymbol{p}\rvert$	$h(\boldsymbol{p})$	n	d
W[(9,7,6,4,2)]	28	-113	10547216287172185866240	3475713613337883829632
W[(9,7,6,4,3)]	29	-134	2240131001946976373134464	128569966501792923903350 4
W[(9,7,6,5,0)]	27	-78	25383601647232320	-17802901998922240
W[(9,7,6,5,1)]	28	-104	424552799703766464912	8000113898763198720
W[(9,7,6,5,2)]	29	-128	377337473299364349892128	152785612691569068751872
W[(9,7,6,6,0)]	28	-89	419093788958668992	-345708325307878560
W[(9,7,6,6,1)]	29	-116	7465381920406413655872	157174083455108555904
W[(9,7,7,2,2)]	27	-84	4005072998835530048	623145599186074560
W[(9,7,7,3,1)]	27	-81	1000944581364139008	12940864211175424
W[(9,7,7,3,2)]	28	-104	1010995377658903433280	274043841200077763232
W[(9,7,7,3,3)]	29	-125	238119849054264183598080	112332804021170119948800
W[(9,7,7,4,0)]	27	-72	5101035246140064	-3238317072282240
W[(9,7,7,4,1)]	28	-98	93022849378461001968	1603689039494806080
W[(9,7,7,4,2)]	29	-122	89401881734473077280272	32906148327728452809888
W[(9,7,7,5,0)]	28	-86	198280729061595552	-156843054827785632
W[(9,7,7,5,1)]	29	-113	3667019460175374709248	74648911275455548416
W[(9,7,7,6,0)]	29	-98	3704581973944705776	-3435204329200397376
W[(9,8,4,3,3)]	27	-96	176048749037882981792	54398198798074388800
W[(9,8,4,4,2)]	27	-93	64342058578990962432	15534320958543602432
W[(9,8,4,4,3)]	28	-113	14880953729756521482240	6366888695682697842144
W[(9,8,4,4,4)]	29	-131	1250148843664649970662352	733085308674475362988800
W[(9,8,5,3,2)]	27	-90	26964980823333578944	5907389929476004224
W[(9,8,5,3,3)]	28	-110	6470374366380782830464	2506621507185094907424
W[(9,8,5,4,1)]	27	-84	2436667741602374528	36360838742410016
W[(9,8,5,4,2)]	28	-107	240195348206440929758 4	726440453016521093136
W[(9,8,5,4,3)]	29	-128	556910170480793670482400	295443957082726234710912
W[(9,8,5,5,0)]	27	-72	5101035246140064	-3238317072282240
W[(9,8,5,5,1)]	28	-98	95308266595738550640	1685025369541284480
W[(9,8,5,5,2)]	29	-122	92873867581256305971840	34790520976213893550464
W[(9,8,6,2,2)]	27	-81	1755969430220426496	259636655223086848
W[(9,8,6,3,1)]	27	-78	438395891787545984	5516943176462464
W[(9,8,6,3,2)]	28	-101	475191508986206197632	123424186729923646080
W[(9,8,6,3,3)]	29	-122	117846752322559629255984	53548008570062637417696
W[(9,8,6,4,0)]	27	-69	2235977596096128	-1345692401785920
W[(9,8,6,4,1)]	28	-95	43589536992230477208	730324510146863712
W[(9,8,6,4,2)]	29	-119	44162182140827544636144	15659653975155880831536
W[(9,8,6,5,0)]	28	-83	92700939550359360	-70199768003592720
W[(9,8,6,5,1)]	29	-110	1801675431551746250880	35705455486282123392
W[(9,8,6,6,0)]	29	-95	1810611871504105272	-1616941505273075616
W[(9,8,7,2,1)]	27	-66	11256418126498304	60842853741632
W[(9,8,7,2,2)]	28	-89	15318198529776992064	2579059445631070176
W[(9,8,7,3,0)]	27	-60	170193515484672	-85781801925696
W[(9,8,7,3,1)]	28	-86	3833600055583272480	51494523118178400
W[(9,8,7,3,2)]	29	-110	4421119882261082749248	1296069103156616952768
W[(9,8,7,4,0)]	28	-77	19503820669876800	-13461969999093600
W[(9,8,7,4,1)]	29	-104	408994002687679224816	7411795886398986624
W[(9,8,7,5,0)]	29	-92	875827020316064256	-752251254614400960
W[(9,8,8,1,1)]	27	-48	22072657897776	-425570551040
W[(9,8,8,2,0)]	27	-45	1535514818112	-531223501536
W[(9,8,8,2,1)]	28	-71	48279338403693048	230627260020528

Continued on next page

Table C.1 – continued

Web	$\lvert\boldsymbol{p}\rvert$	$h(\boldsymbol{p})$	n	d
W[(9,8,8,2,2)]	29	-95	72939895256309497680	13404209975769169392
W[(9,8,8,3,0)]	28	-65	725912434085952	-405156007308576
W[(9,8,8,3,1)]	29	-92	18275815076572138848	254920513927767648
W[(9,8,8,4,0)]	29	-83	92700939550359360	-70199768003592720
W[(9,9,3,3,3)]	27	-81	2670197361402514944	595724740895599616
W[(9,9,4,3,2)]	27	-78	951716992566363648	166286435635301824
W[(9,9,4,3,3)]	28	-98	297520326374626846896	94786453063647970848
W[(9,9,4,4,1)]	27	-72	83845604993916000	1063377379790976
W[(9,9,4,4,2)]	28	-95	109036439304691948608	27149794915803480576
W[(9,9,4,4,3)]	29	-116	30907191740331009622272	13740363716226750753600
W[(9,9,5,2,2)]	27	-72	134329574207275104	16773356868339520
W[(9,9,5,3,1)]	27	-69	33386278590988800	381144946134016
W[(9,9,5,3,2)]	28	-92	45945931585469072928	10388937656332753536
W[(9,9,5,3,3)]	29	-113	13510524682548173641728	5442063622506471346176
W[(9,9,5,4,0)]	27	-60	170193515484672	-85781801925696
W[(9,9,5,4,1)]	28	-86	4165834565805729216	63502596678612960
W[(9,9,5,4,2)]	29	-110	5029248618061980310752	1581805356183712228896
W[(9,9,5,5,0)]	28	-74	8765016259161504	-5758034709276000
W[(9,9,5,5,1)]	29	-101	201260631020776796160	3655384754255841792
W[(9,9,6,2,1)]	27	-60	1823776449179136	10747142102848
W[(9,9,6,2,2)]	28	-83	3046779784226901072	465966091929471216
W[(9,9,6,3,0)]	27	-54	27765085214112	-12215408263200
W[(9,9,6,3,1)]	28	-80	761207182511922096	9751729607816928
W[(9,9,6,3,2)]	29	-104	1009523697408684687360	273179253014427444000
W[(9,9,6,4,0)]	28	-71	3881643757375656	-2421429008571216
W[(9,9,6,4,1)]	29	-98	92904071198229763248	1598269886739062400
W[(9,9,6,5,0)]	29	-86	198280729061595552	-156843054827785632
W[(9,9,7,1,1)]	27	-45	7933211814912	-126220459008
W[(9,9,7,2,0)]	27	-42	553728279360	-174588053440
W[(9,9,7,2,1)]	28	-68	20278800720533664	105019516952544
W[(9,9,7,2,2)]	29	-92	33639461017770972672	5921797441909136064
W[(9,9,7,3,0)]	28	-62	305922925426848	-160791639748800
W[(9,9,7,3,1)]	29	-89	8424230964009345024	115413671534048256
W[(9,9,7,4,0)]	29	-80	42801528146793216	-30974226462689184
W[(9,9,8,1,0)]	27	-24	539120544	-76342880
W[(9,9,8,1,1)]	28	-50	42951164308896	-929847901440
W[(9,9,8,2,0)]	28	-47	2981800050480	-1093125957120
W[(9,9,8,2,1)]	29	-74	112932475851555408	486039827347776
W[(9,9,8,3,0)]	29	-68	1692511362069504	-1000067627051904
W[(9,9,9,0,0)]	27	0	112	0
W[(9,9,9,1,0)]	28	-26	1272585120	-203310240
W[(9,9,9,1,1)]	29	-53	113958894140160	-2891432289792
W[(9,9,9,2,0)]	29	-50	7888589144400	-3138370134624

Appendix D

Zeta Function Numerators

D.1 The mirror octic

We collect here the numerators of the zeta function computed for the first few primes at various values of (u, w) using the results outlined above. We omit the values of (u, w) for which the denominator in the matrix $\mathrm{U}(u, w)$ vanishes, as these require more careful treatment, and can be thought of as analogues of the apparent singularities encountered in [13].

$p = 7$			
(u, w)	smooth/sing.	singularity	$R(T)$
$(1, 1)$	smooth*		
$(1, 2)$	smooth*		
$(1, 3)$	singular		
$(1, 4)$	smooth*		
$(1, 5)$	smooth*		
$(1, 6)$	smooth*		
$(2, 1)$	smooth		$p^6T^6 - 2p^5T^5 + 3p^4T^4 - 60p^2T^3 + 3pT^2 - 2T + 1$
$(2, 2)$	smooth		$p^6T^6 + 4p^5T^5 + 19p^4T^4 - 8p^2T^3 + 19pT^2 + 4T + 1$
$(2, 3)$	smooth		$p^6T^6 - 4p^5T^5 + 27p^4T^4 - 88p^2T^3 + 27pT^2 - 4T + 1$
$(2, 4)$	singular		
$(2, 5)$	singular		
$(2, 6)$	smooth		$p^6T^6 + 2p^6T^5 + 43p^4T^4 + 68p^2T^3 + 43pT^2 + 2pT + 1$
$(3, 1)$	smooth		$p^6T^6 + 12p^5T^5 + 15p^4T^4 - 64p^2T^3 + 15pT^2 + 12T + 1$
$(3, 2)$	smooth		$p^6T^6 - 24p^5T^5 + 15p^4T^4 + 120p^2T^3 + 15pT^2 - 24T + 1$
$(3, 3)$	smooth		$p^6T^6 - 18p^5T^5 + 33p^4T^4 - 120p^2T^3 + 33pT^2 - 18T + 1$
$(3, 4)$	smooth*		
$(3, 5)$	smooth		$p^6T^6 - 6p^5T^5 + 89p^4T^4 - 48p^2T^3 + 89pT^2 - 6T + 1$
$(3, 6)$	smooth		$p^6T^6 + 4p^6T^5 + 83p^4T^4 + 216p^2T^3 + 83pT^2 + 4pT + 1$
$(4, 1)$	singular		
$(4, 2)$	singular		
$(4, 3)$	smooth		$p^6T^6 - 4p^5T^5 + p^5T^4 + 8p^2T^3 + p^2T^2 - 4T + 1$
$(4, 4)$	smooth		$p^6T^6 + 16p^5T^5 + 5p^5T^4 - 32p^2T^3 + 5p^2T^2 + 16T + 1$
$(4, 5)$	smooth		$p^6T^6 - 6p^5T^5 + 59p^4T^4 + 44p^2T^3 + 59pT^2 - 6T + 1$
$(4, 6)$	smooth		$p^6T^6 + 2p^6T^5 - 37p^4T^4 - 188p^2T^3 - 37pT^2 + 2pT + 1$
$(5, 1)$	smooth		$p^6T^6 + 26p^5T^5 + 25p^4T^4 - 16p^2T^3 + 25pT^2 + 26T + 1$
$(5, 2)$	smooth		$p^6T^6 - 10p^5T^5 - 5p^5T^4 + 176p^2T^3 - 5p^2T^2 - 10T + 1$
$(5, 3)$	smooth		$p^6T^6 + 10p^5T^5 + 17p^4T^4 + 136p^2T^3 + 17pT^2 + 10T + 1$
$(5, 4)$	smooth		$p^6T^6 - 12p^5T^5 + 15p^4T^4 + 15pT^2 - 12T + 1$
$(5, 5)$	smooth*		

Continued on the following page

$p = 7$, *continued*			
(u, w)	smooth/sing.	singularity	$R(T)$
$(5, 6)$	smooth		$p^6T^6 - 4p^6T^5 + 107p^4T^4 - 296p^2T^3 + 107pT^2 - 4pT + 1$
$(6, 1)$	smooth		$p^6T^6 - 2p^5T^5 - 25p^4T^4 + 132p^2T^3 - 25pT^2 - 2T + 1$
$(6, 2)$	smooth*		
$(6, 3)$	smooth		$p^6T^6 - 4p^5T^5 + 11p^4T^4 + 136p^2T^3 + 11pT^2 - 4T + 1$
$(6, 4)$	smooth		$p^6T^6 + 30p^5T^5 + 95p^4T^4 + 292p^2T^3 + 95pT^2 + 30T + 1$
$(6, 5)$	smooth		$p^6T^6 - 6p^5T^5 + p^5T^4 + 108p^2T^3 + p^2T^2 - 6T + 1$
$(6, 6)$	smooth		$p^6T^6 + 39p^4T^4 - 80p^2T^3 + 39pT^2 + 1$

$p = 11$			
(u, w)	smooth/sing.	singularity	$R(T)$
$(1, 1)$	smooth*		
$(1, 2)$	smooth*		
$(1, 3)$	smooth*		
$(1, 4)$	smooth*		
$(1, 5)$	smooth*		
$(1, 6)$	smooth*		
$(1, 7)$	singular		
$(1, 8)$	smooth*		
$(1, 9)$	smooth*		
$(1, 10)$	smooth*		
$(2, 1)$	smooth		$p^6T^6 + 38p^5T^5 + 181p^4T^4 + 320p^2T^3 + 181pT^2 + 38T + 1$
$(2, 2)$	smooth		$p^6T^6 + 32p^5T^5 + 171p^4T^4 + 272p^2T^3 + 171pT^2 + 32T + 1$
$(2, 3)$	smooth		$p^6T^6 - 8p^5T^5 - 41p^4T^4 - 40p^2T^3 - 41pT^2 - 8T + 1$
$(2, 4)$	smooth		$p^6T^6 - 82p^5T^5 + 365p^4T^4 - 1184p^2T^3 + 365pT^2 - 82T + 1$
$(2, 5)$	smooth		$p^6T^6 + 52p^5T^5 + 223p^4T^4 + 896p^2T^3 + 223pT^2 + 52T + 1$
$(2, 6)$	smooth		$p^6T^6 - 24p^5T^5 + 107p^4T^4 - 64p^2T^3 + 107pT^2 - 24T + 1$
$(2, 7)$	smooth		$p^6T^6 - 2p^5T^5 - 63p^4T^4 - 48p^2T^3 - 63pT^2 - 2T + 1$
$(2, 8)$	smooth		$p^6T^6 - 14p^5T^5 + 3p^5T^4 + 216p^2T^3 + 3p^2T^2 - 14T + 1$
$(2, 9)$	smooth		$p^6T^6 + 6p^5T^5 - 39p^4T^4 + 296p^2T^3 - 39pT^2 + 6T + 1$
$(2, 10)$	smooth		$p^6T^6 - 8p^5T^5 + 119p^4T^4 + 72p^2T^3 + 119pT^2 - 8T + 1$
$(3, 1)$	smooth		$p^6T^6 + 20p^5T^5 + 119p^4T^4 + 136p^2T^3 + 119pT^2 + 20T + 1$
$(3, 2)$	singular		
$(3, 3)$	smooth		$p^6T^6 + 6p^5T^5 + 83p^4T^4 + 68p^2T^3 + 83pT^2 + 6T + 1$
$(3, 4)$	smooth*		
$(3, 5)$	smooth		$p^6T^6 - 46p^5T^5 + 43p^4T^4 + 4p^3T^3 + 43pT^2 - 46T + 1$
$(3, 6)$	singular		
$(3, 7)$	smooth		$p^6T^6 - 4p^5T^5 - 5p^4T^4 - 24p^2T^3 - 5pT^2 - 4T + 1$
$(3, 8)$	smooth		$p^6T^6 - 53p^4T^4 + 320p^2T^3 - 53pT^2 + 1$
$(3, 9)$	smooth		$p^6T^6 + 2p^6T^5 + 67p^4T^4 + 356p^2T^3 + 67pT^2 + 2pT + 1$
$(3, 10)$	smooth		$p^6T^6 - 4p^5T^5 + 91p^4T^4 - 152p^2T^3 + 91pT^2 - 4T + 1$
$(4, 1)$	singular		
$(4, 2)$	smooth		$p^6T^6 + 42p^5T^5 + 75p^4T^4 + 60p^2T^3 + 75pT^2 + 42T + 1$
$(4, 3)$	smooth		$p^6T^6 - 46p^5T^5 + 43p^4T^4 + 172p^2T^3 + 43pT^2 - 46T + 1$
$(4, 4)$	smooth		$p^6T^6 + 46p^5T^5 + 43p^4T^4 - 300p^2T^3 + 43pT^2 + 46T + 1$
$(4, 5)$	smooth		$p^6T^6 + 10p^5T^5 + 9p^5T^4 + 20p^3T^3 + 9p^2T^2 + 10T + 1$
$(4, 6)$	smooth		$p^6T^6 - 2p^6T^5 + 235p^4T^4 - 452p^2T^3 + 235pT^2 - 2pT + 1$
$(4, 7)$	smooth		$p^6T^6 - 28p^5T^5 + 203p^4T^4 - 744p^2T^3 + 203pT^2 - 28T + 1$
$(4, 8)$	singular		
$(4, 9)$	smooth		$p^6T^6 - 28p^5T^5 - 5p^4T^4 + 344p^2T^3 - 5pT^2 - 28T + 1$
$(4, 10)$	smooth		$p^6T^6 + 2p^6T^5 + 91p^4T^4 + 388p^2T^3 + 91pT^2 + 2pT + 1$
$(5, 1)$	smooth*		
$(5, 2)$	smooth		$p^6T^6 + 80p^5T^5 + 283p^4T^4 + 800p^2T^3 + 283pT^2 + 80T + 1$
$(5, 3)$	smooth		$p^6T^6 + 12p^5T^5 + 83p^4T^4 + 24p^3T^3 + 83pT^2 + 12T + 1$
$(5, 4)$	smooth		$p^6T^6 + 107p^4T^4 - 192p^2T^3 + 107pT^2 + 1$

Continued on the following page

$p = 11$, *continued*			
(u, w)	smooth/sing.	singularity	$R(T)$
$(5, 5)$	singular		
$(5, 6)$	smooth		$p^6T^6 - 10p^5T^5 - 69p^4T^4 + 228p^2T^3 - 69pT^2 - 10T + 1$
$(5, 7)$	smooth		$p^6T^6 - 8p^5T^5 + 9p^5T^4 - 16p^3T^3 + 9p^2T^2 - 8T + 1$
$(5, 8)$	smooth		$p^6T^6 - 38p^5T^5 + 19p^4T^4 + 124p^2T^3 + 19pT^2 - 38T + 1$
$(5, 9)$	smooth		$p^6T^6 + 10p^5T^5 + 3p^4T^4 + 284p^2T^3 + 3pT^2 + 10T + 1$
$(5, 10)$	singular		
$(6, 1)$	smooth		$p^6T^6 - 12p^5T^5 + 183p^4T^4 - 144p^2T^3 + 183pT^2 - 12T + 1$
$(6, 2)$	smooth		$p^6T^6 - 14p^5T^5 + 53p^4T^4 - 128p^2T^3 + 53pT^2 - 14T + 1$
$(6, 3)$	smooth		$p^6T^6 + 48p^5T^5 + 23p^4T^4 - 344p^2T^3 + 23pT^2 + 48T + 1$
$(6, 4)$	smooth		$p^6T^6 + 20p^5T^5 + 163p^4T^4 + 296p^2T^3 + 163pT^2 + 20T + 1$
$(6, 5)$	smooth*		
$(6, 6)$	smooth		$p^6T^6 + 2p^5T^5 + 17p^4T^4 + 456p^2T^3 + 17pT^2 + 2T + 1$
$(6, 7)$	smooth		$p^6T^6 - 10p^5T^5 + 113p^4T^4 - 48p^3T^3 + 113pT^2 - 10T + 1$
$(6, 8)$	smooth		$p^6T^6 + 20p^5T^5 + 23p^4T^4 - 288p^2T^3 + 23pT^2 + 20T + 1$
$(6, 9)$	smooth		$p^6T^6 - 40p^5T^5 + 155p^4T^4 - 608p^2T^3 + 155pT^2 - 40T + 1$
$(6, 10)$	smooth		$p^6T^6 + 30p^5T^5 - 83p^4T^4 - 72p^3T^3 - 83pT^2 + 30T + 1$
$(7, 1)$	smooth		$p^6T^6 + 14p^5T^5 + 167p^4T^4 + 100p^2T^3 + 167pT^2 + 14T + 1$
$(7, 2)$	smooth		$p^6T^6 - 42p^5T^5 + 103p^4T^4 - 140p^2T^3 + 103pT^2 - 42T + 1$
$(7, 3)$	smooth		$p^6T^6 - 48p^5T^5 + 339p^4T^4 - 960p^2T^3 + 339pT^2 - 48T + 1$
$(7, 4)$	smooth		$p^6T^6 - 26p^5T^5 + 31p^4T^4 + 180p^2T^3 + 31pT^2 - 26T + 1$
$(7, 5)$	smooth		$p^6T^6 + 68p^5T^5 + 127p^4T^4 - 8p^2T^3 + 127pT^2 + 68T + 1$
$(7, 6)$	smooth		$p^6T^6 - 30p^5T^5 + 5p^5T^4 - 164p^2T^3 + 5p^2T^2 - 30T + 1$
$(7, 7)$	smooth		$p^6T^6 + 32p^5T^5 + 111p^4T^4 + 128p^2T^3 + 111pT^2 + 32T + 1$
$(7, 8)$	smooth		$p^6T^6 + 34p^5T^5 - p^4T^4 - 292p^2T^3 - pT^2 + 34T + 1$
$(7, 9)$	smooth*		
$(7, 10)$	smooth		$p^6T^6 + 12p^5T^5 + 43p^4T^4 - 120p^2T^3 + 43pT^2 + 12T + 1$
$(8, 1)$	smooth		$p^6T^6 - 70p^5T^5 + 25p^5T^4 - 1028p^2T^3 + 25p^2T^2 - 70T + 1$
$(8, 2)$	smooth*		
$(8, 3)$	smooth		$p^6T^6 + 32p^5T^5 + 31p^4T^4 + 80p^2T^3 + 31pT^2 + 32T + 1$
$(8, 4)$	smooth		$p^6T^6 + 16p^5T^5 + 107p^4T^4 - 96p^2T^3 + 107pT^2 + 16T + 1$
$(8, 5)$	smooth		$p^6T^6 + 14p^5T^5 + 163p^4T^4 + 436p^2T^3 + 163pT^2 + 14T + 1$
$(8, 6)$	smooth		$p^6T^6 - 18p^5T^5 + 43p^4T^4 - 4p^3T^3 + 43pT^2 - 18T + 1$
$(8, 7)$	smooth		$p^6T^6 + 52p^5T^5 + 183p^4T^4 + 328p^2T^3 + 183pT^2 + 52T + 1$
$(8, 8)$	smooth		$p^6T^6 + 26p^5T^5 + 115p^4T^4 + 444p^2T^3 + 115pT^2 + 26T + 1$
$(8, 9)$	smooth		$p^6T^6 - 8p^5T^5 - p^4T^4 + 608p^2T^3 - pT^2 - 8T + 1$
$(8, 10)$	smooth		$p^6T^6 - 6p^5T^5 + 67p^4T^4 - 388p^2T^3 + 67pT^2 - 6T + 1$
$(9, 1)$	smooth		$p^6T^6 - 4p^6T^5 + 107p^4T^4 - 72p^2T^3 + 107pT^2 - 4pT + 1$
$(9, 2)$	smooth		$p^6T^6 + 12p^5T^5 + 23p^4T^4 - 520p^2T^3 + 23pT^2 + 12T + 1$
$(9, 3)$	smooth		$p^6T^6 + 24p^5T^5 + 139p^4T^4 + 464p^2T^3 + 139pT^2 + 24T + 1$
$(9, 4)$	singular		
$(9, 5)$	smooth		$p^6T^6 + 4p^5T^5 + 59p^4T^4 + 152p^2T^3 + 59pT^2 + 4T + 1$
$(9, 6)$	smooth*		
$(9, 7)$	smooth		$p^6T^6 + 28p^5T^5 + 167p^4T^4 + 664p^2T^3 + 167pT^2 + 28T + 1$
$(9, 8)$	smooth		$p^6T^6 - 26p^5T^5 - 13p^4T^4 - 60p^2T^3 - 13pT^2 - 26T + 1$
$(9, 9)$	singular		
$(9, 10)$	smooth		$p^6T^6 - 46p^5T^5 + 139p^4T^4 - 340p^2T^3 + 139pT^2 - 46T + 1$
$(10, 1)$	smooth		$p^6T^6 + 48p^5T^5 + 131p^4T^4 + 160p^2T^3 + 131pT^2 + 48T + 1$
$(10, 2)$	smooth		$p^6T^6 - 16p^5T^5 - 3p^5T^4 + 136p^2T^3 - 3p^2T^2 - 16T + 1$
$(10, 3)$	smooth		$p^6T^6 + 60p^5T^5 + 295p^4T^4 + 1088p^2T^3 + 295pT^2 + 60T + 1$
$(10, 4)$	smooth		$p^6T^6 - 54p^5T^5 + 269p^4T^4 - 936p^2T^3 + 269pT^2 - 54T + 1$
$(10, 5)$	smooth		$p^6T^6 - 50p^5T^5 + 105p^4T^4 - 200p^2T^3 + 105pT^2 - 50T + 1$
$(10, 6)$	smooth		$p^6T^6 + 28p^5T^5 + 63p^4T^4 + 288p^2T^3 + 63pT^2 + 28T + 1$
$(10, 7)$	smooth		$p^6T^6 - 18p^5T^5 + 3p^5T^4 - 16p^3T^3 + 3p^2T^2 - 18T + 1$
$(10, 8)$	smooth		$p^6T^6 - 12p^5T^5 + 27p^4T^4 - 456p^2T^3 + 27pT^2 - 12T + 1$
$(10, 9)$	smooth		$p^6T^6 + 2p^5T^5 + 9p^4T^4 + 32p^3T^3 + 9pT^2 + 2T + 1$

Continued on the following page

$p = 11$, *continued*			
(u, w)	smooth/sing.	singularity	$R(T)$
$(10, 10)$	smooth*		

$p = 13$			
(u, w)	smooth/sing.	singularity	$R(T)$
$(1, 1)$	smooth*		
$(1, 2)$	smooth*		
$(1, 3)$	smooth*		
$(1, 4)$	smooth*		
$(1, 5)$	smooth*		
$(1, 6)$	smooth*		
$(1, 7)$	smooth*		
$(1, 8)$	smooth*		
$(1, 9)$	singular		
$(1, 10)$	smooth*		
$(1, 11)$	smooth*		
$(1, 12)$	smooth*		
$(2, 1)$	smooth		$p^6T^6 + 58p^5T^5 + 119p^4T^4 - 164p^2T^3 + 119pT^2 + 58T + 1$
$(2, 2)$	smooth		$p^6T^6 + 2p^5T^5 + 287p^4T^4 - 100p^2T^3 + 287pT^2 + 2T + 1$
$(2, 3)$	smooth		$p^6T^6 - 30p^5T^5 + 163p^4T^4 - 1052p^2T^3 + 163pT^2 - 30T + 1$
$(2, 4)$	smooth		$p^6T^6 + 36p^5T^5 + 199p^4T^4 + 56p^3T^3 + 199pT^2 + 36T + 1$
$(2, 5)$	smooth		$p^6T^6 - 12p^5T^5 + 19p^4T^4 + 80p^2T^3 + 19pT^2 - 12T + 1$
$(2, 6)$	smooth		$p^6T^6 + 56p^5T^5 + 123p^4T^4 + 248p^2T^3 + 123pT^2 + 56T + 1$
$(2, 7)$	smooth		$p^6T^6 + 2p^5T^5 + 27p^4T^4 + 804p^2T^3 + 27pT^2 + 2T + 1$
$(2, 8)$	smooth		$p^6T^6 + 4p^5T^5 - 93p^4T^4 - 464p^2T^3 - 93pT^2 + 4T + 1$
$(2, 9)$	smooth		$p^6T^6 - 46p^5T^5 + 131p^4T^4 - 700p^2T^3 + 131pT^2 - 46T + 1$
$(2, 10)$	smooth		$p^6T^6 + 4p^5T^5 + 55p^4T^4 + 504p^2T^3 + 55pT^2 + 4T + 1$
$(2, 11)$	smooth		$p^6T^6 - 32p^5T^5 + 51p^4T^4 - 40p^2T^3 + 51pT^2 - 32T + 1$
$(2, 12)$	smooth		$p^6T^6 - 28p^5T^5 + 295p^4T^4 - 680p^2T^3 + 295pT^2 - 28T + 1$
$(3, 1)$	singular		
$(3, 2)$	smooth		$p^6T^6 - 10p^5T^5 + 3p^5T^4 - 28p^2T^3 + 3p^2T^2 - 10T + 1$
$(3, 3)$	smooth		$p^6T^6 + 48p^5T^5 + 151p^4T^4 + 128p^2T^3 + 151pT^2 + 48T + 1$
$(3, 4)$	smooth*		
$(3, 5)$	smooth		$p^6T^6 - 18p^5T^5 + 215p^4T^4 + 148p^2T^3 + 215pT^2 - 18T + 1$
$(3, 6)$	smooth		$p^6T^6 + 16p^5T^5 + 63p^4T^4 + 48p^3T^3 + 63pT^2 + 16T + 1$
$(3, 7)$	singular		
$(3, 8)$	smooth		$p^6T^6 + 28p^5T^5 + 55p^4T^4 - 440p^2T^3 + 55pT^2 + 28T + 1$
$(3, 9)$	smooth		$p^6T^6 - 18p^5T^5 + 199p^4T^4 - 908p^2T^3 + 199pT^2 - 18T + 1$
$(3, 10)$	smooth		$p^6T^6 + 24p^5T^5 + 151p^4T^4 - 272p^2T^3 + 151pT^2 + 24T + 1$
$(3, 11)$	smooth		$p^6T^6 - 14p^5T^5 + 127p^4T^4 + 92p^2T^3 + 127pT^2 - 14T + 1$
$(3, 12)$	smooth		$p^6T^6 - 14p^5T^5 - 57p^4T^4 - 4p^3T^3 - 57pT^2 - 14T + 1$
$(4, 1)$	smooth		$p^6T^6 + 46p^5T^5 + 199p^4T^4 + 180p^2T^3 + 199pT^2 + 46T + 1$
$(4, 2)$	smooth		$p^6T^6 + 30p^5T^5 + 327p^4T^4 + 404p^2T^3 + 327pT^2 + 30T + 1$
$(4, 3)$	smooth		$p^6T^6 - 4p^5T^5 - 33p^4T^4 + 696p^2T^3 - 33pT^2 - 4T + 1$
$(4, 4)$	smooth		$p^6T^6 - 24p^5T^5 - 73p^4T^4 + 976p^2T^3 - 73pT^2 - 24T + 1$
$(4, 5)$	smooth		$p^6T^6 + 54p^5T^5 + 119p^4T^4 + 20p^3T^3 + 119pT^2 + 54T + 1$
$(4, 6)$	singular		
$(4, 7)$	smooth		$p^6T^6 - 18p^5T^5 + 135p^4T^4 - 268p^2T^3 + 135pT^2 - 18T + 1$
$(4, 8)$	singular		
$(4, 9)$	smooth		$p^6T^6 - 42p^5T^5 + 251p^4T^4 - 388p^2T^3 + 251pT^2 - 42T + 1$
$(4, 10)$	smooth		$p^6T^6 + 44p^5T^5 - 89p^4T^4 - 1080p^2T^3 - 89pT^2 + 44T + 1$
$(4, 11)$	smooth		$p^6T^6 - 22p^5T^5 + 295p^4T^4 - 292p^2T^3 + 295pT^2 - 22T + 1$
$(4, 12)$	smooth		$p^6T^6 - 49p^4T^4 - 592p^2T^3 - 49pT^2 + 1$
$(5, 1)$	smooth		$p^6T^6 - 12p^5T^5 + 59p^4T^4 + 448p^2T^3 + 59pT^2 - 12T + 1$
$(5, 2)$	smooth		$p^6T^6 - 8p^5T^5 - 9p^4T^4 - 528p^2T^3 - 9pT^2 - 8T + 1$

Continued on the following page

$p = 13$, *continued*			
(u, w)	smooth/sing.	singularity	$R(T)$
$(5, 3)$	smooth		$p^6T^6 - 4p^5T^5 + 115p^4T^4 + 448p^2T^3 + 115pT^2 - 4T + 1$
$(5, 4)$	smooth		$p^6T^6 - 2p^5T^5 - 57p^4T^4 - 556p^2T^3 - 57pT^2 - 2T + 1$
$(5, 5)$	smooth		$p^6T^6 + 48p^5T^5 + 127p^4T^4 + 400p^2T^3 + 127pT^2 + 48T + 1$
$(5, 6)$	smooth		$p^6T^6 - 38p^5T^5 + 19p^5T^4 - 868p^2T^3 + 19p^2T^2 - 38T + 1$
$(5, 7)$	smooth		$p^6T^6 - 28p^5T^5 + 95p^4T^4 - 120p^2T^3 + 95pT^2 - 28T + 1$
$(5, 8)$	smooth		$p^6T^6 - 2p^5T^5 + 251p^4T^4 + 60p^2T^3 + 251pT^2 - 2T + 1$
$(5, 9)$	smooth		$p^6T^6 + 38p^5T^5 + 11p^4T^4 - 132p^2T^3 + 11pT^2 + 38T + 1$
$(5, 10)$	smooth		$p^6T^6 - 92p^5T^5 + 443p^4T^4 - 1536p^2T^3 + 443pT^2 - 92T + 1$
$(5, 11)$	smooth		$p^6T^6 + 22p^5T^5 + 75p^4T^4 + 108p^2T^3 + 75pT^2 + 22T + 1$
$(5, 12)$	smooth*		
$(6, 1)$	smooth		$p^6T^6 + 34p^5T^5 - 9p^4T^4 - 692p^2T^3 - 9pT^2 + 34T + 1$
$(6, 2)$	smooth		$p^6T^6 + 32p^5T^5 + 301p^4T^4 + 680p^2T^3 + 301pT^2 + 32T + 1$
$(6, 3)$	smooth*		
$(6, 4)$	smooth		$p^6T^6 - 58p^5T^5 + 275p^4T^4 - 1356p^2T^3 + 275pT^2 - 58T + 1$
$(6, 5)$	smooth		$p^6T^6 - 36p^5T^5 + 145p^4T^4 - 320p^2T^3 + 145pT^2 - 36T + 1$
$(6, 6)$	smooth		$p^6T^6 - 47p^4T^4 - 56p^2T^3 - 47pT^2 + 1$
$(6, 7)$	smooth		$p^6T^6 + 66p^5T^5 + 67p^4T^4 - 340p^2T^3 + 67pT^2 + 66T + 1$
$(6, 8)$	smooth		$p^6T^6 - 4p^5T^5 + 121p^4T^4 + 32p^2T^3 + 121pT^2 - 4T + 1$
$(6, 9)$	smooth		$p^6T^6 - 12p^5T^5 + 105p^4T^4 - 32p^3T^3 + 105pT^2 - 12T + 1$
$(6, 10)$	smooth		$p^6T^6 + 6p^5T^5 + 191p^4T^4 + 500p^2T^3 + 191pT^2 + 6T + 1$
$(6, 11)$	smooth		$p^6T^6 - 38p^5T^5 + 175p^4T^4 - 932p^2T^3 + 175pT^2 - 38T + 1$
$(6, 12)$	smooth		$p^6T^6 + 2p^5T^5 + 3p^5T^4 + 1068p^2T^3 + 3p^2T^2 + 2T + 1$
$(7, 1)$	smooth		$p^6T^6 + 2p^5T^5 - 101p^4T^4 + 124p^2T^3 - 101pT^2 + 2T + 1$
$(7, 2)$	smooth		$p^6T^6 - 32p^5T^5 - 83p^4T^4 + 912p^2T^3 - 83pT^2 - 32T + 1$
$(7, 3)$	smooth		$p^6T^6 + 100p^5T^5 + 557p^4T^4 + 2008p^2T^3 + 557pT^2 + 100T + 1$
$(7, 4)$	smooth		$p^6T^6 - 36p^5T^5 + 173p^4T^4 - 152p^2T^3 + 173pT^2 - 36T + 1$
$(7, 5)$	smooth		$p^6T^6 + 36p^5T^5 - 83p^4T^4 - 456p^2T^3 - 83pT^2 + 36T + 1$
$(7, 6)$	smooth		$p^6T^6 - 14p^5T^5 + 211p^4T^4 + 124p^2T^3 + 211pT^2 - 14T + 1$
$(7, 7)$	smooth*		
$(7, 8)$	smooth		$p^6T^6 - 6p^5T^5 + 7p^5T^4 + 524p^2T^3 + 7p^2T^2 - 6T + 1$
$(7, 9)$	smooth		$p^6T^6 - 88p^5T^5 + 329p^4T^4 - 880p^2T^3 + 329pT^2 - 88T + 1$
$(7, 10)$	smooth		$p^6T^6 + 2p^6T^5 + 51p^4T^4 + 268p^2T^3 + 51pT^2 + 2pT + 1$
$(7, 11)$	smooth		$p^6T^6 - 20p^5T^5 + 229p^4T^4 - 344p^2T^3 + 229pT^2 - 20T + 1$
$(7, 12)$	smooth		$p^6T^6 - 10p^5T^5 + 339p^4T^4 - 348p^2T^3 + 339pT^2 - 10T + 1$
$(8, 1)$	smooth		$p^6T^6 - 56p^5T^5 + 141p^4T^4 - 488p^2T^3 + 141pT^2 - 56T + 1$
$(8, 2)$	smooth		$p^6T^6 - 18p^5T^5 + 267p^4T^4 - 476p^2T^3 + 267pT^2 - 18T + 1$
$(8, 3)$	smooth		$p^6T^6 + 22p^5T^5 + 11p^5T^4 + 4p^3T^3 + 11p^2T^2 + 22T + 1$
$(8, 4)$	smooth		$p^6T^6 + 38p^5T^5 + 219p^4T^4 + 1044p^2T^3 + 219pT^2 + 38T + 1$
$(8, 5)$	smooth		$p^6T^6 - 48p^5T^5 + 25p^4T^4 + 248p^2T^3 + 25pT^2 - 48T + 1$
$(8, 6)$	smooth		$p^6T^6 + 50p^5T^5 + 151p^4T^4 + 492p^2T^3 + 151pT^2 + 50T + 1$
$(8, 7)$	smooth		$p^6T^6 - 32p^5T^5 + 69p^4T^4 + 376p^2T^3 + 69pT^2 - 32T + 1$
$(8, 8)$	smooth		$p^6T^6 + 18p^5T^5 + 167p^4T^4 - 212p^2T^3 + 167pT^2 + 18T + 1$
$(8, 9)$	smooth		$p^6T^6 + 44p^5T^5 - 87p^4T^4 - 1280p^2T^3 - 87pT^2 + 44T + 1$
$(8, 10)$	smooth		$p^6T^6 - 84p^5T^5 + 505p^4T^4 - 1792p^2T^3 + 505pT^2 - 84T + 1$
$(8, 11)$	smooth*		
$(8, 12)$	smooth		$p^6T^6 + 56p^5T^5 + 209p^4T^4 + 696p^2T^3 + 209pT^2 + 56T + 1$
$(9, 1)$	smooth		$p^6T^6 - 36p^5T^5 + 103p^4T^4 - 344p^2T^3 + 103pT^2 - 36T + 1$
$(9, 2)$	smooth*		
$(9, 3)$	smooth		$p^6T^6 - 30p^5T^5 + 103p^4T^4 - 596p^2T^3 + 103pT^2 - 30T + 1$
$(9, 4)$	singular		
$(9, 5)$	smooth		$p^6T^6 - 54p^5T^5 + 119p^4T^4 - 4p^2T^3 + 119pT^2 - 54T + 1$
$(9, 6)$	smooth		$p^6T^6 + 36p^5T^5 + 7p^4T^4 - 616p^2T^3 + 7pT^2 + 36T + 1$
$(9, 7)$	smooth		$p^6T^6 + 10p^5T^5 - 5p^5T^4 + 172p^2T^3 - 5p^2T^2 + 10T + 1$
$(9, 8)$	smooth		$p^6T^6 - 10p^5T^5 - p^4T^4 - 140p^2T^3 - pT^2 - 10T + 1$
$(9, 9)$	smooth		$p^6T^6 + 46p^5T^5 + 215p^4T^4 + 916p^2T^3 + 215pT^2 + 46T + 1$

Continued on the following page

$p = 13$, *continued*			
(u, w)	smooth/sing.	singularity	$R(T)$
$(9, 10)$	smooth		$p^6T^6 + 40p^5T^5 + 199p^4T^4 + 1264p^2T^3 + 199pT^2 + 40T + 1$
$(9, 11)$	singular		
$(9, 12)$	smooth		$p^6T^6 - 60p^5T^5 + 215p^4T^4 - 392p^2T^3 + 215pT^2 - 60T + 1$
$(10, 1)$	smooth		$p^6T^6 + 10p^5T^5 - 57p^4T^4 - 804p^2T^3 - 57pT^2 + 10T + 1$
$(10, 2)$	smooth		$p^6T^6 + 36p^5T^5 + 399p^4T^4 + 744p^2T^3 + 399pT^2 + 36T + 1$
$(10, 3)$	smooth		$p^6T^6 - 82p^5T^5 + 423p^4T^4 - 1484p^2T^3 + 423pT^2 - 82T + 1$
$(10, 4)$	smooth		$p^6T^6 - 22p^5T^5 - 9p^4T^4 - 388p^2T^3 - 9pT^2 - 22T + 1$
$(10, 5)$	smooth		$p^6T^6 + 18p^5T^5 - 45p^4T^4 + 308p^2T^3 - 45pT^2 + 18T + 1$
$(10, 6)$	smooth*		
$(10, 7)$	smooth		$p^6T^6 + 3p^5T^4 - 544p^2T^3 + 3p^2T^2 + 1$
$(10, 8)$	smooth		$p^6T^6 - 12p^5T^5 - 17p^4T^4 + 584p^2T^3 - 17pT^2 - 12T + 1$
$(10, 9)$	smooth		$p^6T^6 + 74p^5T^5 + 19p^5T^4 + 700p^2T^3 + 19p^2T^2 + 74T + 1$
$(10, 10)$	singular		
$(10, 11)$	smooth		$p^6T^6 + 34p^5T^5 + 135p^4T^4 + 28p^3T^3 + 135pT^2 + 34T + 1$
$(10, 12)$	singular		
$(11, 1)$	smooth		$p^6T^6 + 4p^5T^5 + 67p^4T^4 - 656p^2T^3 + 67pT^2 + 4T + 1$
$(11, 2)$	smooth		$p^6T^6 - 54p^5T^5 + 15p^5T^4 - 140p^2T^3 + 15p^2T^2 - 54T + 1$
$(11, 3)$	smooth		$p^6T^6 - 30p^5T^5 + 111p^4T^4 - 772p^2T^3 + 111pT^2 - 30T + 1$
$(11, 4)$	smooth		$p^6T^6 + 4p^6T^5 + 123p^4T^4 + 256p^2T^3 + 123pT^2 + 4pT + 1$
$(11, 5)$	smooth		$p^6T^6 + 12p^5T^5 + 47p^4T^4 + 280p^2T^3 + 47pT^2 + 12T + 1$
$(11, 6)$	smooth		$p^6T^6 + 60p^5T^5 + 391p^4T^4 + 1384p^2T^3 + 391pT^2 + 60T + 1$
$(11, 7)$	smooth		$p^6T^6 + 16p^5T^5 + 199p^4T^4 + 544p^2T^3 + 199pT^2 + 16T + 1$
$(11, 8)$	smooth		$p^6T^6 - 40p^5T^5 + 55p^4T^4 - 336p^2T^3 + 55pT^2 - 40T + 1$
$(11, 9)$	smooth		$p^6T^6 - 2p^5T^5 + 43p^4T^4 + 556p^2T^3 + 43pT^2 - 2T + 1$
$(11, 10)$	smooth*		
$(11, 11)$	smooth		$p^6T^6 + 4p^6T^5 + 319p^4T^4 + 1192p^2T^3 + 319pT^2 + 4pT + 1$
$(11, 12)$	smooth		$p^6T^6 - 58p^5T^5 + 3p^5T^4 + 132p^2T^3 + 3p^2T^2 - 58T + 1$
$(12, 1)$	smooth*		
$(12, 2)$	singular		
$(12, 3)$	singular		
$(12, 4)$	smooth		$p^6T^6 - 30p^5T^5 + 19p^5T^4 - 180p^2T^3 + 19p^2T^2 - 30T + 1$
$(12, 5)$	smooth		$p^6T^6 - 72p^5T^5 + 359p^4T^4 - 1648p^2T^3 + 359pT^2 - 72T + 1$
$(12, 6)$	smooth		$p^6T^6 - 6p^5T^5 + 199p^4T^4 - 132p^2T^3 + 199pT^2 - 6T + 1$
$(12, 7)$	smooth		$p^6T^6 + 6p^5T^5 - 25p^4T^4 - 60p^2T^3 - 25pT^2 + 6T + 1$
$(12, 8)$	smooth		$p^6T^6 + 36p^5T^5 + 15p^4T^4 + 296p^2T^3 + 15pT^2 + 36T + 1$
$(12, 9)$	smooth		$p^6T^6 + 2p^6T^5 + 15p^4T^4 + 108p^2T^3 + 15pT^2 + 2pT + 1$
$(12, 10)$	smooth		$p^6T^6 + 22p^5T^5 + 95p^4T^4 - 332p^2T^3 + 95pT^2 + 22T + 1$
$(12, 11)$	smooth		$p^6T^6 - 60p^5T^5 + 15p^4T^4 + 552p^2T^3 + 15pT^2 - 60T + 1$
$(12, 12)$	smooth		$p^6T^6 + 8p^5T^5 + 127p^4T^4 + 320p^2T^3 + 127pT^2 + 8T + 1$

D.2 The S_5 symmetric Hulek-Verrill manifolds

$p = 7$			
φ	smooth/sing.	singularity	$R(T)$
1	singular	1	
2	singular	$\frac{1}{25}$	
3	smooth		$\left(p^3T^3 - 2pT + 1\right)^4 \left(p^6T^4 + 2p^3T^3 - 54pT^2 + 2T + 1\right)$
4	singular	$\frac{1}{9}$	
5	smooth		$\left(p^3T^3 + 4pT + 1\right)^4 \left(p^3T^2 - 34T + 1\right) \left(p^3T^2 + 4pT + 1\right)$
6	smooth		$\left(p^3T^3 - 2pT + 1\right)^4 \left(p^6T^4 + 12p^3T^3 - 14pT^2 + 12T + 1\right)$

$p = 11$			
φ	smooth/sing.	singularity	$R(T)$
1	singular	1	
2	smooth		$\left(p^3T^3 - 6pT + 1\right)^4 \left(p^6T^4 + 42p^3T^3 + 194pT^2 + 42T + 1\right)$
3	smooth		$\left(p^3T^3 + 1\right)^4 \left(p^3T^2 + 1\right) \left(p^3T^2 + 28T + 1\right)$
4	singular	$\frac{1}{25}$	
5	singular	$\frac{1}{9}$	
6	smooth		$\left(p^3T^3 + 1\right)^4 \left(p^6T^4 - 2p^3T^3 + 2pT^2 - 2T + 1\right)$
7	smooth		$\left(p^3T^3 + 1\right)^4 \left(p^6T^4 - 22p^3T^3 + 122pT^2 - 22T + 1\right)$
8	smooth*		
9	smooth		$\left(p^3T^3 + 1\right)^4 \left(p^6T^4 - 32p^3T^3 + 2pT^2 - 32T + 1\right)$
10	smooth		$\left(p^3T^3 + 1\right)^4 \left(p^6T^4 - 22p^3T^3 + 2pT^2 - 22T + 1\right)$

$p = 13$			
φ	smooth/sing.	singularity	$R(T)$
1	singular	1	
2	smooth		$\left(p^3T^3 - 2pT + 1\right)^4 \left(p^3T^2 + 34T + 1\right) \left(p^3T^2 - 6pT + 1\right)$
3	singular	$\frac{1}{9}$	
4	smooth		$\left(p^3T^3 - 2pT + 1\right)^4 \left(p^3T^2 + 42T + 1\right) \left(p^3T^2 - 2pT + 1\right)$
5	smooth		$\left(p^3T^3 + 4pT + 1\right)^4 \left(p^6T^4 - 36p^3T^3 + 166pT^2 - 36T + 1\right)$
6	smooth		$\left(p^3T^3 + 4pT + 1\right)^4 \left(p^6T^4 - 26p^3T^3 + 266pT^2 - 26T + 1\right)$
7	smooth		$\left(p^3T^3 + 4pT + 1\right)^4 \left(p^6T^4 + 14p^3T^3 - 54pT^2 + 14T + 1\right)$
8	smooth*		
9	smooth*		
10	smooth		$\left(p^3T^3 - 2pT + 1\right)^4 \left(p^3T^2 + 42T + 1\right) \left(p^3T^2 - 2pT + 1\right)$
11	smooth		$\left(p^3T^3 + 4pT + 1\right)^4 \left(p^3T^2 - 18T + 1\right) \left(p^3T^2 + 4pT + 1\right)$
12	singular	$\frac{1}{25}$	

$p = 17$			
φ	smooth/sing.	singularity	$R(T)$
1	singular	1	
2	singular	$\frac{1}{9}$	
3	smooth		$\left(p^3T^3 + 6pT + 1\right)^4 \left(p^6T^4 + 98p^3T^3 + 674pT^2 + 98T + 1\right)$
4	smooth		$\left(p^3T^3 + 6pT + 1\right)^4 \left(p^3T^2 - 114T + 1\right) \left(p^3T^2 + 6pT + 1\right)$
5	smooth*		
6	smooth		$\left(p^3T^3 + 1\right)^4 \left(p^6T^4 - 44p^3T^3 + 38pT^2 - 44T + 1\right)$
7	smooth		$\left(p^3T^3 + 6pT + 1\right)^4 \left(p^6T^4 - 2p^3T^3 + 194pT^2 - 2T + 1\right)$
8	smooth		$\left(p^3T^3 + 6pT + 1\right)^4 \left(p^3T^2 - 94T + 1\right) \left(p^3T^2 + 6pT + 1\right)$
9	smooth		$\left(p^3T^3 - 6pT + 1\right)^4 \left(p^6T^4 + 4p^3T^3 + 182pT^2 + 4T + 1\right)$
10	smooth		$\left(p^3T^3 - 6pT + 1\right)^4 \left(p^6T^4 + 34p^3T^3 + 2pT^2 + 34T + 1\right)$
11	smooth		$\left(p^3T^3 + 1\right)^4 \left(p^6T^4 - 124p^3T^3 + 518pT^2 - 124T + 1\right)$
12	smooth		$\left(p^3T^3 - 6pT + 1\right)^4 \left(p^3T^2 - 74T + 1\right) \left(p^3T^2 - 6pT + 1\right)$
13	smooth		$\left(p^3T^3 - 6pT + 1\right)^4 \left(p^3T^2 + 78T + 1\right) \left(p^3T^2 - 2pT + 1\right)$
14	smooth		$\left(p^3T^3 + 1\right)^4 \left(p^3T^2 + 1\right) \left(p^3T^2 - 134T + 1\right)$
15	singular	$\frac{1}{25}$	
16	smooth		$\left(p^3T^3 + 6pT + 1\right)^4 \left(p^3T^2 - 2pT + 1\right) \left(p^3T^2 + 6pT + 1\right)$

$p = 19$			
φ	smooth/sing.	singularity	$R(T)$
1	singular	1	
2	smooth		$\left(p^3T^3 + 4pT + 1\right)^4 \left(p^6T^4 + 76p^3T^3 + 2pT^2 + 76T + 1\right)$

Continued on the following page

$p = 19$, *continued*			
φ	smooth/sing.	singularity	$R(T)$
3	smooth		$\left(p^3T^3 - 2pT + 1\right)^4 \left(p^6T^4 - 8p^3T^3 + 242pT^2 - 8T + 1\right)$
4	smooth		$\left(p^3T^3 + 4pT + 1\right)^4 \left(p^3T^2 - 60T + 1\right) \left(p^3T^2 + 4pT + 1\right)$
5	smooth		$\left(p^3T^3 + 4pT + 1\right)^4 \left(p^3T^2 - 60T + 1\right) \left(p^3T^2 + 4pT + 1\right)$
6	smooth		$\left(p^3T^3 - 8pT + 1\right)^4 \left(p^6T^4 + 8p^3T^3 - 318pT^2 + 8T + 1\right)$
7	smooth		$\left(p^3T^3 + 4pT + 1\right)^4 \left(p^6T^4 - 44p^3T^3 - 238pT^2 - 44T + 1\right)$
8	smooth		$\left(p^3T^3 - 2pT + 1\right)^4 \left(p^3T^2 - 80T + 1\right) \left(p^3T^2 - 2pT + 1\right)$
9	smooth		$\left(p^3T^3 + 4pT + 1\right)^4 \left(p^3T^2 - 160T + 1\right) \left(p^3T^2 + 4pT + 1\right)$
10	smooth		$\left(p^3T^3 - 2pT + 1\right)^4 \left(p^6T^4 + 12p^3T^3 + 562pT^2 + 12T + 1\right)$
11	smooth		$\left(p^3T^3 + 4pT + 1\right)^4 \left(p^3T^2 - 140T + 1\right) \left(p^3T^2 + 4pT + 1\right)$
12	smooth		$\left(p^3T^3 - 2pT + 1\right)^4 \left(p^6T^4 + 12p^3T^3 + 82pT^2 + 12T + 1\right)$
13	smooth		$\left(p^3T^3 - 8pT + 1\right)^4 \left(p^6T^4 + 178p^3T^3 + 1082pT^2 + 178T + 1\right)$
14	smooth		$\left(p^3T^3 - 2pT + 1\right)^4 \left(p^6T^4 + 12p^3T^3 - 158pT^2 + 12T + 1\right)$
15	smooth		$\left(p^3T^3 - 2pT + 1\right)^4 \left(p^6T^4 + 42p^3T^3 - 38pT^2 + 42T + 1\right)$
16	singular	$\frac{1}{25}$	
17	singular	$\frac{1}{9}$	
18	smooth*		

$p = 23$			
φ	smooth/sing.	singularity	$R(T)$
1	singular	1	
2	smooth		$\left(p^3T^3 + 1\right)^4 \left(p^6T^4 - 28p^3T^3 + 98pT^2 - 28T + 1\right)$
3	smooth		$\left(p^3T^3 + 1\right)^4 \left(p^6T^4 - 68p^3T^3 + 98pT^2 - 68T + 1\right)$
4	smooth		$\left(p^3T^3 + 1\right)^4 \left(p^3T^2 - 120T + 1\right) \left(p^3T^2 + 4pT + 1\right)$
5	smooth		$\left(p^3T^3 + 6pT + 1\right)^4 \left(p^6T^4 - 90p^3T^3 + 890pT^2 - 90T + 1\right)$
6	smooth		$\left(p^3T^3 + 1\right)^4 \left(p^6T^4 + 72p^3T^3 + 98pT^2 + 72T + 1\right)$
7	smooth		$\left(p^3T^3 + 1\right)^4 \left(p^6T^4 + 52p^3T^3 + 338pT^2 + 52T + 1\right)$
8	smooth		$\left(p^3T^3 + 1\right)^4 \left(p^6T^4 + 12p^3T^3 + 98pT^2 + 12T + 1\right)$
9	smooth*		
10	smooth		$\left(p^3T^3 + 6pT + 1\right)^4 \left(p^3T^2 - 132T + 1\right) \left(p^3T^2 + 4pT + 1\right)$
11	smooth		$\left(p^3T^3 - 6pT + 1\right)^4 \left(p^6T^4 + 94p^3T^3 - 94pT^2 + 94T + 1\right)$
12	singular	$\frac{1}{25}$	
13	smooth		$\left(p^3T^3 + 1\right)^4 \left(p^3T^2 + 1\right) \left(p^3T^2 + 112T + 1\right)$
14	smooth		$\left(p^3T^3 - 6pT + 1\right)^4 \left(p^6T^4 + 94p^3T^3 + 266pT^2 + 94T + 1\right)$
15	smooth		$\left(p^3T^3 + 1\right)^4 \left(p^6T^4 + 2p^3T^3 - 142pT^2 + 2T + 1\right)$
16	smooth*		
17	smooth		$\left(p^3T^3 - 6pT + 1\right)^4 \left(p^6T^4 + 144p^3T^3 + 626pT^2 + 144T + 1\right)$
18	singular	$\frac{1}{9}$	
19	smooth		$\left(p^3T^3 + 1\right)^4 \left(p^6T^4 + 162p^3T^3 + 1178pT^2 + 162T + 1\right)$
20	smooth		$\left(p^3T^3 + 6pT + 1\right)^4 \left(p^6T^4 - 120p^3T^3 + 530pT^2 - 120T + 1\right)$
21	smooth		$\left(p^3T^3 + 6pT + 1\right)^4 \left(p^6T^4 - 120p^3T^3 + 530pT^2 - 120T + 1\right)$
22	smooth		$\left(p^3T^3 - 6pT + 1\right)^4 \left(p^6T^4 + 94p^3T^3 + 866pT^2 + 94T + 1\right)$

$p = 29$			
φ	smooth/sing.	singularity	$R(T)$
1	singular	1	
2	smooth		$\left(p^3T^3 + 1\right)^4 \left(p^6T^4 - 150p^3T^3 + 362pT^2 - 150T + 1\right)$
3	smooth		$\left(p^3T^3 + 6pT + 1\right)^4 \left(p^6T^4 - 6p^3T^3 + 722pT^2 - 6T + 1\right)$
4	smooth		$\left(p^3T^3 + 6pT + 1\right)^4 \left(p^3T^2 - 190T + 1\right) \left(p^3T^2 + 6pT + 1\right)$
5	smooth		$\left(p^3T^3 + 6pT + 1\right)^4 \left(p^6T^4 + 44p^3T^3 + 182pT^2 + 44T + 1\right)$
6	smooth		$\left(p^3T^3 - 6pT + 1\right)^4 \left(p^6T^4 + 96p^3T^3 - 418pT^2 + 96T + 1\right)$

Continued on the following page

$p = 29$, *continued*			
φ	smooth/sing.	singularity	$R(T)$
7	singular	$\frac{1}{25}$	
8	smooth		$\left(p^3T^3+6pT+1\right)^4\left(p^6T^4+24p^3T^3+542pT^2+24T+1\right)$
9	smooth		$\left(p^3T^3+6pT+1\right)^4\left(p^6T^4-16p^3T^3-418pT^2-16T+1\right)$
10	smooth		$\left(p^3T^3+1\right)^4\left(p^6T^4-80p^3T^3+542pT^2-80T+1\right)$
11	smooth		$\left(p^3T^3+6pT+1\right)^4\left(p^6T^4-126p^3T^3+242pT^2-126T+1\right)$
12	smooth		$\left(p^3T^3+1\right)^4\left(p^6T^4+100p^3T^3+182pT^2+100T+1\right)$
13	singular	$\frac{1}{9}$	
14	smooth		$\left(p^3T^3-6pT+1\right)^4\left(p^6T^4-24p^3T^3+542pT^2-24T+1\right)$
15	smooth		$\left(p^3T^3+6pT+1\right)^4\left(p^6T^4-156p^3T^3+1382pT^2-156T+1\right)$
16	smooth		$\left(p^3T^3+6pT+1\right)^4\left(p^6T^4-396p^3T^3+2822pT^2-396T+1\right)$
17	smooth		$\left(p^3T^3-6pT+1\right)^4\left(p^6T^4+6p^3T^3-238pT^2+6T+1\right)$
18	smooth		$\left(p^3T^3+1\right)^4\left(p^6T^4+10p^3T^3-1438pT^2+10T+1\right)$
19	smooth		$\left(p^3T^3+1\right)^4\left(p^6T^4+130p^3T^3+722pT^2+130T+1\right)$
20	smooth		$\left(p^3T^3-6pT+1\right)^4\left(p^6T^4+276p^3T^3+1862pT^2+276T+1\right)$
21	smooth*		
22	smooth		$\left(p^3T^3+6pT+1\right)^4\left(p^6T^4+24p^3T^3+1262pT^2+24T+1\right)$
23	smooth		$\left(p^3T^3-6pT+1\right)^4\left(p^3T^2-294T+1\right)\left(p^3T^2+10pT+1\right)$
24	smooth		$\left(p^3T^3-6pT+1\right)^4\left(p^6T^4+56p^3T^3+782pT^2+56T+1\right)$
25	smooth		$\left(p^3T^3-6pT+1\right)^4\left(p^6T^4-44p^3T^3-58pT^2-44T+1\right)$
26	smooth*		
27	smooth		$\left(p^3T^3-6pT+1\right)^4\left(p^6T^4+6p^3T^3-118pT^2+6T+1\right)$
28	smooth		$\left(p^3T^3-6pT+1\right)^4\left(p^6T^4+136p^3T^3+782pT^2+136T+1\right)$

$p = 31$			
φ	smooth/sing.	singularity	$R(T)$
1	singular	1	
2	smooth		$\left(p^3T^3+4pT+1\right)^4\left(p^6T^4-288p^3T^3+2434pT^2-288T+1\right)$
3	smooth*		
4	smooth		$\left(p^3T^3+4pT+1\right)^4\left(p^6T^4+352p^3T^3+2114pT^2+352T+1\right)$
5	singular	$\frac{1}{25}$	
6	smooth		$\left(p^3T^3+10pT+1\right)^4\left(p^6T^4+258p^3T^3+2122pT^2+258T+1\right)$
7	singular	$\frac{1}{9}$	
8	smooth		$\left(p^3T^3-8pT+1\right)^4\left(p^3T^2+268T+1\right)\left(p^3T^2-8pT+1\right)$
9	smooth		$\left(p^3T^3-8pT+1\right)^4\left(p^3T^2+168T+1\right)\left(p^3T^2-8pT+1\right)$
10	smooth		$\left(p^3T^3+4pT+1\right)^4\left(p^6T^4+52p^3T^3-286pT^2+52T+1\right)$
11	smooth		$\left(p^3T^3+4pT+1\right)^4\left(p^6T^4-98p^3T^3+1514pT^2-98T+1\right)$
12	smooth		$\left(p^3T^3-2pT+1\right)^4\left(p^6T^4-264p^3T^3+1906pT^2-264T+1\right)$
13	smooth		$\left(p^3T^3+4pT+1\right)^4\left(p^6T^4-98p^3T^3+674pT^2-98T+1\right)$
14	smooth		$\left(p^3T^3+4pT+1\right)^4\left(p^6T^4-8p^3T^3+1154pT^2-8T+1\right)$
15	smooth		$\left(p^3T^3-8pT+1\right)^4\left(p^6T^4-200p^3T^3+1058pT^2-200T+1\right)$
16	smooth		$\left(p^3T^3+4pT+1\right)^4\left(p^3T^2-192T+1\right)\left(p^3T^2+4pT+1\right)$
17	smooth		$\left(p^3T^3-8pT+1\right)^4\left(p^6T^4-90p^3T^3-422pT^2-90T+1\right)$
18	smooth		$\left(p^3T^3-8pT+1\right)^4\left(p^3T^2+128T+1\right)\left(p^3T^2-8pT+1\right)$
19	smooth*		
20	smooth		$\left(p^3T^3-8pT+1\right)^4\left(p^3T^2-8pT+1\right)\left(p^3T^2+8pT+1\right)$
21	smooth		$\left(p^3T^3+4pT+1\right)^4\left(p^6T^4+12p^3T^3+754pT^2+12T+1\right)$
22	smooth		$\left(p^3T^3+4pT+1\right)^4\left(p^3T^2-72T+1\right)\left(p^3T^2+4pT+1\right)$
23	smooth		$\left(p^3T^3-2pT+1\right)^4\left(p^6T^4-4p^3T^3+1266pT^2-4T+1\right)$
24	smooth		$\left(p^3T^3+4pT+1\right)^4\left(p^6T^4+82p^3T^3+1394pT^2+82T+1\right)$
25	smooth		$\left(p^3T^3+4pT+1\right)^4\left(p^6T^4+72p^3T^3-446pT^2+72T+1\right)$
26	smooth		$\left(p^3T^3+4pT+1\right)^4\left(p^3T^2-202T+1\right)\left(p^3T^2+4pT+1\right)$
27	smooth		$\left(p^3T^3+10pT+1\right)^4\left(p^6T^4+198p^3T^3+562pT^2+198T+1\right)$

Continued on the following page

$p = 31$, *continued*			
φ	smooth/sing.	singularity	$R(T)$
28	smooth		$\left(p^3T^3 - 8pT + 1\right)^4 \left(p^6T^4 + 1858pT^2 + 1\right)$
29	smooth		$\left(p^3T^3 - 2pT + 1\right)^4 \left(p^6T^4 + 196p^3T^3 + 1346pT^2 + 196T + 1\right)$
30	smooth		$\left(p^3T^3 + 4pT + 1\right)^4 \left(p^6T^4 - 318p^3T^3 + 1954pT^2 - 318T + 1\right)$

$p = 37$			
φ	smooth/sing.	singularity	$R(T)$
1	singular	1	
2	smooth		$\left(p^3T^3 + 4pT + 1\right)^4 \left(p^6T^4 + 54p^3T^3 + 322pT^2 + 54T + 1\right)$
3	singular	$\frac{1}{25}$	
4	smooth		$\left(p^3T^3 - 2pT + 1\right)^4 \left(p^6T^4 - 48p^3T^3 + 2206pT^2 - 48T + 1\right)$
5	smooth		$\left(p^3T^3 - 2pT + 1\right)^4 \left(p^3T^2 - 404T + 1\right) \left(p^3T^2 - 2pT + 1\right)$
6	smooth		$\left(p^3T^3 + 4pT + 1\right)^4 \left(p^6T^4 + 64p^3T^3 + 302pT^2 + 64T + 1\right)$
7	smooth		$\left(p^3T^3 + 10pT + 1\right)^4 \left(p^6T^4 - 204p^3T^3 + 838pT^2 - 204T + 1\right)$
8	smooth		$\left(p^3T^3 + 10pT + 1\right)^4 \left(p^6T^4 - 274p^3T^3 + 2418pT^2 - 274T + 1\right)$
9	smooth		$\left(p^3T^3 - 2pT + 1\right)^4 \left(p^6T^4 + 232p^3T^3 + 1166pT^2 + 232T + 1\right)$
10	smooth		$\left(p^3T^3 + 10pT + 1\right)^4 \left(p^6T^4 - 244p^3T^3 + 2358pT^2 - 244T + 1\right)$
11	smooth*		
12	smooth		$\left(p^3T^3 + 10pT + 1\right)^4 \left(p^6T^4 + 176p^3T^3 + 1758pT^2 + 176T + 1\right)$
13	smooth		$\left(p^3T^3 - 8pT + 1\right)^4 \left(p^6T^4 - 10p^3T^3 + 930pT^2 - 10T + 1\right)$
14	smooth		$\left(p^3T^3 - 2pT + 1\right)^4 \left(p^6T^4 - 18p^3T^3 + 826pT^2 - 18T + 1\right)$
15	smooth		$\left(p^3T^3 - 2pT + 1\right)^4 \left(p^6T^4 + 182p^3T^3 + 186pT^2 + 182T + 1\right)$
16	smooth		$\left(p^3T^3 - 2pT + 1\right)^4 \left(p^6T^4 - 28p^3T^3 - 474pT^2 - 28T + 1\right)$
17	smooth		$\left(p^3T^3 - 2pT + 1\right)^4 \left(p^6T^4 - 18p^3T^3 - 1454pT^2 - 18T + 1\right)$
18	smooth		$\left(p^3T^3 + 10pT + 1\right)^4 \left(p^6T^4 + 316p^3T^3 + 3158pT^2 + 316T + 1\right)$
19	smooth		$\left(p^3T^3 - 2pT + 1\right)^4 \left(p^6T^4 + 162p^3T^3 + 1186pT^2 + 162T + 1\right)$
20	smooth		$\left(p^3T^3 - 2pT + 1\right)^4 \left(p^6T^4 - 188p^3T^3 + 1766pT^2 - 188T + 1\right)$
21	smooth		$\left(p^3T^3 - 2pT + 1\right)^4 \left(p^3T^2 + 346T + 1\right) \left(p^3T^2 - 2pT + 1\right)$
22	smooth		$\left(p^3T^3 - 2pT + 1\right)^4 \left(p^6T^4 - 258p^3T^3 + 2146pT^2 - 258T + 1\right)$
23	smooth		$\left(p^3T^3 - 8pT + 1\right)^4 \left(p^6T^4 + 170p^3T^3 + 1890pT^2 + 170T + 1\right)$
24	smooth		$\left(p^3T^3 + 4pT + 1\right)^4 \left(p^3T^2 + 358T + 1\right) \left(p^3T^2 - 2pT + 1\right)$
25	smooth		$\left(p^3T^3 + 10pT + 1\right)^4 \left(p^6T^4 - 24p^3T^3 + 238pT^2 - 24T + 1\right)$
26	smooth		$\left(p^3T^3 - 2pT + 1\right)^4 \left(p^6T^4 + 12p^3T^3 + 1846pT^2 + 12T + 1\right)$
27	smooth		$\left(p^3T^3 - 2pT + 1\right)^4 \left(p^6T^4 + 432p^3T^3 + 3166pT^2 + 432T + 1\right)$
28	smooth		$\left(p^3T^3 - 2pT + 1\right)^4 \left(p^6T^4 - 88p^3T^3 - 1074pT^2 - 88T + 1\right)$
29	smooth		$\left(p^3T^3 - 2pT + 1\right)^4 \left(p^6T^4 + 432p^3T^3 + 3886pT^2 + 432T + 1\right)$
30	smooth		$\left(p^3T^3 - 2pT + 1\right)^4 \left(p^6T^4 - 8p^3T^3 + 2126pT^2 - 8T + 1\right)$
31	smooth		$\left(p^3T^3 - 8pT + 1\right)^4 \left(p^6T^4 + 30p^3T^3 + 1090pT^2 + 30T + 1\right)$
32	smooth		$\left(p^3T^3 - 8pT + 1\right)^4 \left(p^6T^4 + 30p^3T^3 + 2410pT^2 + 30T + 1\right)$
33	singular	$\frac{1}{9}$	
34	smooth		$\left(p^3T^3 - 2pT + 1\right)^4 \left(p^6T^4 - 28p^3T^3 + 1446pT^2 - 28T + 1\right)$
35	smooth*		
36	smooth		$\left(p^3T^3 - 2pT + 1\right)^4 \left(p^6T^4 - 308p^3T^3 + 2486pT^2 - 308T + 1\right)$

$p = 41$			
φ	smooth/sing.	singularity	$R(T)$
1	singular	1	
2	smooth		$\left(p^3T^3 - 6pT + 1\right)^4 \left(p^6T^4 - 48p^3T^3 + 1214pT^2 - 48T + 1\right)$
3	smooth		$\left(p^3T^3 + 12pT + 1\right)^4 \left(p^6T^4 - 230p^3T^3 + 2018pT^2 - 230T + 1\right)$
4	smooth*		
5	smooth		$\left(p^3T^3 - 6pT + 1\right)^4 \left(p^6T^4 + 192p^3T^3 - 226pT^2 + 192T + 1\right)$

Continued on the following page

$p = 41$, *continued*			
φ	smooth/sing.	singularity	$R(T)$
6	smooth		$\left(p^3T^3 - 12pT + 1\right)^4 \left(p^6T^4 + 396p^3T^3 + 2966pT^2 + 396T + 1\right)$
7	smooth		$\left(p^3T^3 + 1\right)^4 \left(p^6T^4 - 12p^3T^3 + 2342pT^2 - 12T + 1\right)$
8	smooth		$\left(p^3T^3 + 6pT + 1\right)^4 \left(p^6T^4 - 396p^3T^3 + 2390pT^2 - 396T + 1\right)$
9	smooth		$\left(p^3T^3 + 6pT + 1\right)^4 \left(p^6T^4 + 24p^3T^3 - 850pT^2 + 24T + 1\right)$
10	smooth		$\left(p^3T^3 + 6pT + 1\right)^4 \left(p^3T^2 - 422T + 1\right) \left(p^3T^2 + 6pT + 1\right)$
11	smooth		$\left(p^3T^3 + 6pT + 1\right)^4 \left(p^6T^4 - 246p^3T^3 + 1970pT^2 - 246T + 1\right)$
12	smooth		$\left(p^3T^3 + 1\right)^4 \left(p^6T^4 - 282p^3T^3 + 482pT^2 - 282T + 1\right)$
13	smooth		$\left(p^3T^3 + 6pT + 1\right)^4 \left(p^6T^4 - 106p^3T^3 + 290pT^2 - 106T + 1\right)$
14	smooth		$\left(p^3T^3 + 1\right)^4 \left(p^6T^4 + 8p^3T^3 - 2338pT^2 + 8T + 1\right)$
15	smooth		$\left(p^3T^3 - 6pT + 1\right)^4 \left(p^6T^4 + 182p^3T^3 + 1154pT^2 + 182T + 1\right)$
16	smooth*		
17	smooth		$\left(p^3T^3 + 1\right)^4 \left(p^6T^4 + 148p^3T^3 + 422pT^2 + 148T + 1\right)$
18	smooth		$\left(p^3T^3 + 6pT + 1\right)^4 \left(p^6T^4 - 76p^3T^3 - 490pT^2 - 76T + 1\right)$
19	smooth		$\left(p^3T^3 + 12pT + 1\right)^4 \left(p^6T^4 - 30p^3T^3 + 578pT^2 - 30T + 1\right)$
20	smooth		$\left(p^3T^3 - 6pT + 1\right)^4 \left(p^6T^4 - 108p^3T^3 - 106pT^2 - 108T + 1\right)$
21	smooth		$\left(p^3T^3 - 6pT + 1\right)^4 \left(p^6T^4 - 128p^3T^3 - 1186pT^2 - 128T + 1\right)$
22	smooth		$\left(p^3T^3 + 6pT + 1\right)^4 \left(p^6T^4 - 336p^3T^3 + 2030pT^2 - 336T + 1\right)$
23	singular	$\frac{1}{25}$	
24	smooth		$\left(p^3T^3 + 6pT + 1\right)^4 \left(p^6T^4 + 4p^3T^3 + 470pT^2 + 4T + 1\right)$
25	smooth		$\left(p^3T^3 + 6pT + 1\right)^4 \left(p^6T^4 - 36p^3T^3 - 250pT^2 - 36T + 1\right)$
26	smooth		$\left(p^3T^3 + 1\right)^4 \left(p^6T^4 - 312p^3T^3 + 1742pT^2 - 312T + 1\right)$
27	smooth		$\left(p^3T^3 + 1\right)^4 \left(p^6T^4 + 168p^3T^3 - 898pT^2 + 168T + 1\right)$
28	smooth		$\left(p^3T^3 + 1\right)^4 \left(p^6T^4 + 48p^3T^3 - 1138pT^2 + 48T + 1\right)$
29	smooth		$\left(p^3T^3 - 6pT + 1\right)^4 \left(p^6T^4 + 172p^3T^3 + 614pT^2 + 172T + 1\right)$
30	smooth		$\left(p^3T^3 + 1\right)^4 \left(p^6T^4 - 82p^3T^3 + 2642pT^2 - 82T + 1\right)$
31	smooth		$\left(p^3T^3 + 6pT + 1\right)^4 \left(p^6T^4 + 104p^3T^3 + 590pT^2 + 104T + 1\right)$
32	singular	$\frac{1}{9}$	
33	smooth		$\left(p^3T^3 - 6pT + 1\right)^4 \left(p^6T^4 + 292p^3T^3 + 1334pT^2 + 292T + 1\right)$
34	smooth		$\left(p^3T^3 - 6pT + 1\right)^4 \left(p^6T^4 + 282p^3T^3 + 3554pT^2 + 282T + 1\right)$
35	smooth		$\left(p^3T^3 - 6pT + 1\right)^4 \left(p^3T^2 - 162T + 1\right) \left(p^3T^2 - 6pT + 1\right)$
36	smooth		$\left(p^3T^3 - 6pT + 1\right)^4 \left(p^6T^4 + 392p^3T^3 + 3374pT^2 + 392T + 1\right)$
37	smooth		$\left(p^3T^3 + 6pT + 1\right)^4 \left(p^6T^4 + 284p^3T^3 + 1670pT^2 + 284T + 1\right)$
38	smooth		$\left(p^3T^3 - 12pT + 1\right)^4 \left(p^6T^4 - 44p^3T^3 - 154pT^2 - 44T + 1\right)$
39	smooth		$\left(p^3T^3 - 6pT + 1\right)^4 \left(p^6T^4 + 552p^3T^3 + 4334pT^2 + 552T + 1\right)$
40	smooth		$\left(p^3T^3 - 6pT + 1\right)^4 \left(p^6T^4 + 92p^3T^3 + 2054pT^2 + 92T + 1\right)$

$p = 43$			
φ	smooth/sing.	singularity	$R(T)$
1	singular	1	
2	smooth		$\left(p^3T^3 - 8pT + 1\right)^4 \left(p^6T^4 - 212p^3T^3 + 482pT^2 - 212T + 1\right)$
3	smooth		$\left(p^3T^3 + 4pT + 1\right)^4 \left(p^6T^4 + 94p^3T^3 + 2186pT^2 + 94T + 1\right)$
4	smooth		$\left(p^3T^3 - 8pT + 1\right)^4 \left(p^6T^4 + 48p^3T^3 + 1282pT^2 + 48T + 1\right)$
5	smooth		$\left(p^3T^3 - 8pT + 1\right)^4 \left(p^6T^4 - 72p^3T^3 + 1762pT^2 - 72T + 1\right)$
6	smooth		$\left(p^3T^3 - 8pT + 1\right)^4 \left(p^3T^2 + 412T + 1\right) \left(p^3T^2 - 8pT + 1\right)$
7	smooth		$\left(p^3T^3 - 2pT + 1\right)^4 \left(p^6T^4 + 356p^3T^3 + 2994pT^2 + 356T + 1\right)$
8	smooth		$\left(p^3T^3 + 4pT + 1\right)^4 \left(p^6T^4 - 336p^3T^3 + 2626pT^2 - 336T + 1\right)$
9	smooth		$\left(p^3T^3 + 4pT + 1\right)^4 \left(p^6T^4 - 196p^3T^3 + 3666pT^2 - 196T + 1\right)$
10	smooth		$\left(p^3T^3 + 4pT + 1\right)^4 \left(p^3T^2 - 508T + 1\right) \left(p^3T^2 + 4pT + 1\right)$
11	smooth		$\left(p^3T^3 + 4pT + 1\right)^4 \left(p^6T^4 + 84p^3T^3 - 1454pT^2 + 84T + 1\right)$
12	smooth*		
13	smooth		$\left(p^3T^3 + 4pT + 1\right)^4 \left(p^3T^2 - 508T + 1\right) \left(p^3T^2 + 4pT + 1\right)$
14	smooth		$\left(p^3T^3 - 8pT + 1\right)^4 \left(p^6T^4 + 368p^3T^3 + 2562pT^2 + 368T + 1\right)$

Continued on the following page

$p = 43$, *continued*			
φ	smooth/sing.	singularity	$R(T)$
15	smooth		$\left(p^3T^3 - 8pT + 1\right)^4 \left(p^6T^4 + 48p^3T^3 + 1282pT^2 + 48T + 1\right)$
16	smooth		$\left(p^3T^3 + 4pT + 1\right)^4 \left(p^6T^4 - 196p^3T^3 - 654pT^2 - 196T + 1\right)$
17	smooth		$\left(p^3T^3 + 4pT + 1\right)^4 \left(p^6T^4 + 224p^3T^3 + 1986pT^2 + 224T + 1\right)$
18	smooth		$\left(p^3T^3 + 10pT + 1\right)^4 \left(p^6T^4 + 152p^3T^3 + 2418pT^2 + 152T + 1\right)$
19	smooth		$\left(p^3T^3 + 10pT + 1\right)^4 \left(p^6T^4 - 128p^3T^3 + 818pT^2 - 128T + 1\right)$
20	smooth		$\left(p^3T^3 - 8pT + 1\right)^4 \left(p^6T^4 - 12p^3T^3 - 1358pT^2 - 12T + 1\right)$
21	smooth		$\left(p^3T^3 - 8pT + 1\right)^4 \left(p^6T^4 + 168p^3T^3 - 1118pT^2 + 168T + 1\right)$
22	smooth		$\left(p^3T^3 - 8pT + 1\right)^4 \left(p^6T^4 + 38p^3T^3 - 2238pT^2 + 38T + 1\right)$
23	smooth		$\left(p^3T^3 + 4pT + 1\right)^4 \left(p^6T^4 + 44p^3T^3 + 2226pT^2 + 44T + 1\right)$
24	singular	$\frac{1}{9}$	
25	smooth		$\left(p^3T^3 + 4pT + 1\right)^4 \left(p^6T^4 + 124p^3T^3 + 1586pT^2 + 124T + 1\right)$
26	smooth		$\left(p^3T^3 + 10pT + 1\right)^4 \left(p^6T^4 - 178p^3T^3 + 1938pT^2 - 178T + 1\right)$
27	smooth		$\left(p^3T^3 - 8pT + 1\right)^4 \left(p^3T^2 + 292T + 1\right) \left(p^3T^2 - 8pT + 1\right)$
28	smooth		$\left(p^3T^3 - 2pT + 1\right)^4 \left(p^6T^4 + 96p^3T^3 - 1166pT^2 + 96T + 1\right)$
29	smooth		$\left(p^3T^3 - 8pT + 1\right)^4 \left(p^6T^4 - 162p^3T^3 + 1882pT^2 - 162T + 1\right)$
30	smooth*		
31	singular	$\frac{1}{25}$	
32	smooth		$\left(p^3T^3 - 2pT + 1\right)^4 \left(p^6T^4 - 214p^3T^3 - 366pT^2 - 214T + 1\right)$
33	smooth		$\left(p^3T^3 - 2pT + 1\right)^4 \left(p^6T^4 + 326p^3T^3 + 2394pT^2 + 326T + 1\right)$
34	smooth		$\left(p^3T^3 + 10pT + 1\right)^4 \left(p^6T^4 - 498p^3T^3 + 4618pT^2 - 498T + 1\right)$
35	smooth		$\left(p^3T^3 + 4pT + 1\right)^4 \left(p^6T^4 - 176p^3T^3 + 1346pT^2 - 176T + 1\right)$
36	smooth		$\left(p^3T^3 - 8pT + 1\right)^4 \left(p^3T^2 - 244T + 1\right) \left(p^3T^2 + 4pT + 1\right)$
37	smooth		$\left(p^3T^3 + 4pT + 1\right)^4 \left(p^6T^4 - 136p^3T^3 + 3426pT^2 - 136T + 1\right)$
38	smooth		$\left(p^3T^3 - 8pT + 1\right)^4 \left(p^6T^4 + 188p^3T^3 + 3282pT^2 + 188T + 1\right)$
39	smooth		$\left(p^3T^3 + 4pT + 1\right)^4 \left(p^6T^4 + 274p^3T^3 + 3506pT^2 + 274T + 1\right)$
40	smooth		$\left(p^3T^3 + 4pT + 1\right)^4 \left(p^6T^4 + 264p^3T^3 + 1186pT^2 + 264T + 1\right)$
41	smooth		$\left(p^3T^3 + 4pT + 1\right)^4 \left(p^3T^2 - 428T + 1\right) \left(p^3T^2 + 4pT + 1\right)$
42	smooth		$\left(p^3T^3 + 10pT + 1\right)^4 \left(p^6T^4 + 42p^3T^3 - 1982pT^2 + 42T + 1\right)$

$p = 47$			
φ	smooth/sing.	singularity	$R(T)$
1	singular	1	
2	smooth		$\left(p^3T^3 + 1\right)^4 \left(p^3T^2 + 1\right) \left(p^3T^2 - 264T + 1\right)$
3	smooth		$\left(p^3T^3 + 1\right)^4 \left(p^3T^2 + 1\right) \left(p^3T^2 + 136T + 1\right)$
4	smooth		$\left(p^3T^3 + 12pT + 1\right)^4 \left(p^6T^4 - 240p^3T^3 + 1730pT^2 - 240T + 1\right)$
5	smooth		$\left(p^3T^3 - 6pT + 1\right)^4 \left(p^6T^4 - 216p^3T^3 + 1202pT^2 - 216T + 1\right)$
6	smooth		$\left(p^3T^3 + 12pT + 1\right)^4 \left(p^6T^4 - 480p^3T^3 + 3650pT^2 - 480T + 1\right)$
7	smooth		$\left(p^3T^3 + 1\right)^4 \left(p^6T^4 + 376p^3T^3 + 3458pT^2 + 376T + 1\right)$
8	smooth		$\left(p^3T^3 + 1\right)^4 \left(p^6T^4 - 144p^3T^3 + 1538pT^2 - 144T + 1\right)$
9	smooth		$\left(p^3T^3 + 1\right)^4 \left(p^3T^2 + 1\right) \left(p^3T^2 - 444T + 1\right)$
10	smooth		$\left(p^3T^3 - 12pT + 1\right)^4 \left(p^6T^4 + 72p^3T^3 + 866pT^2 + 72T + 1\right)$
11	smooth		$\left(p^3T^3 - 6pT + 1\right)^4 \left(p^3T^2 - 402T + 1\right) \left(p^3T^2 + 8pT + 1\right)$
12	smooth		$\left(p^3T^3 + 1\right)^4 \left(p^6T^4 - 124p^3T^3 + 578pT^2 - 124T + 1\right)$
13	smooth		$\left(p^3T^3 + 6pT + 1\right)^4 \left(p^6T^4 - 2p^3T^3 + 74pT^2 - 2T + 1\right)$
14	smooth*		
15	smooth		$\left(p^3T^3 - 6pT + 1\right)^4 \left(p^6T^4 - 276p^3T^3 + 3842pT^2 - 276T + 1\right)$
16	smooth		$\left(p^3T^3 + 1\right)^4 \left(p^3T^2 + 1\right) \left(p^3T^2 + 136T + 1\right)$
17	smooth		$\left(p^3T^3 - 12pT + 1\right)^4 \left(p^3T^2 + 416T + 1\right) \left(p^3T^2 - 12pT + 1\right)$
18	smooth		$\left(p^3T^3 + 1\right)^4 \left(p^6T^4 - 64p^3T^3 + 3458pT^2 - 64T + 1\right)$
19	smooth		$\left(p^3T^3 + 6pT + 1\right)^4 \left(p^6T^4 + 98p^3T^3 + 1754pT^2 + 98T + 1\right)$
20	smooth		$\left(p^3T^3 + 12pT + 1\right)^4 \left(p^3T^2 - 24T + 1\right) \left(p^3T^2 + 12pT + 1\right)$
21	singular	$\frac{1}{9}$	

Continued on the following page

$p = 47$, *continued*			
φ	smooth/sing.	singularity	$R(T)$
22	smooth		$\left(p^3T^3+1\right)^4\left(p^6T^4+436p^3T^3+3218pT^2+436T+1\right)$
23	smooth		$\left(p^3T^3+6pT+1\right)^4\left(p^6T^4+18p^3T^3+434pT^2+18T+1\right)$
24	smooth		$\left(p^3T^3+12pT+1\right)^4\left(p^6T^4+440p^3T^3+3650pT^2+440T+1\right)$
25	smooth		$\left(p^3T^3+1\right)^4\left(p^6T^4-244p^3T^3+2018pT^2-244T+1\right)$
26	smooth		$\left(p^3T^3-6pT+1\right)^4\left(p^3T^2-32T+1\right)\left(p^3T^2-12pT+1\right)$
27	smooth		$\left(p^3T^3-12pT+1\right)^4\left(p^6T^4-288p^3T^3+1346pT^2-288T+1\right)$
28	smooth		$\left(p^3T^3+1\right)^4\left(p^6T^4-304p^3T^3+3458pT^2-304T+1\right)$
29	smooth		$\left(p^3T^3+1\right)^4\left(p^6T^4+166p^3T^3+218pT^2+166T+1\right)$
30	smooth		$\left(p^3T^3-6pT+1\right)^4\left(p^6T^4-106p^3T^3+3602pT^2-106T+1\right)$
31	smooth		$\left(p^3T^3+1\right)^4\left(p^6T^4+156p^3T^3-382pT^2+156T+1\right)$
32	singular	$\frac{1}{25}$	
33	smooth		$\left(p^3T^3+1\right)^4\left(p^6T^4+536p^3T^3+4898pT^2+536T+1\right)$
34	smooth*		
35	smooth		$\left(p^3T^3+12pT+1\right)^4\left(p^6T^4-560p^3T^3+5570pT^2-560T+1\right)$
36	smooth		$\left(p^3T^3+1\right)^4\left(p^6T^4-304p^3T^3+578pT^2-304T+1\right)$
37	smooth		$\left(p^3T^3+1\right)^4\left(p^6T^4+16p^3T^3-2302pT^2+16T+1\right)$
38	smooth		$\left(p^3T^3+1\right)^4\left(p^6T^4+296p^3T^3+2978pT^2+296T+1\right)$
39	smooth		$\left(p^3T^3+6pT+1\right)^4\left(p^6T^4+708p^3T^3+5714pT^2+708T+1\right)$
40	smooth		$\left(p^3T^3+12pT+1\right)^4\left(p^6T^4+270p^3T^3+2930pT^2+270T+1\right)$
41	smooth		$\left(p^3T^3-12pT+1\right)^4\left(p^6T^4+222p^3T^3+1826pT^2+222T+1\right)$
42	smooth		$\left(p^3T^3-12pT+1\right)^4\left(p^6T^4-168p^3T^3+3266pT^2-168T+1\right)$
43	smooth		$\left(p^3T^3+6pT+1\right)^4\left(p^6T^4+488p^3T^3+3314pT^2+488T+1\right)$
44	smooth		$\left(p^3T^3-12pT+1\right)^4\left(p^6T^4-158p^3T^3+1826pT^2-158T+1\right)$
45	smooth		$\left(p^3T^3-6pT+1\right)^4\left(p^6T^4-366p^3T^3+3122pT^2-366T+1\right)$
46	smooth		$\left(p^3T^3+6pT+1\right)^4\left(p^6T^4-612p^3T^3+5714pT^2-612T+1\right)$

Appendix E

Modular Forms Associated to Flux Vacua

In this appendix, we gather lists of modular forms and elliptic curves corresponding to zeta functions of Hulek-Verrill manifolds $\mathrm{HV}_{(\varphi,\varphi,\varphi,\varphi,\varphi)}$ at various points on in the moduli space. We only display modular forms when they are listed in LMFDB. In the first section, we list elliptic modular forms, which correspond to rational values of φ. In the following two sections we consider Hilbert and Bianchi modular forms, respectively, omitting base-change curves discussed in §10.3.5.

E.1 Rational points and elliptic modular forms

φ	Modular form label	$\mathcal{E}_F$ Weierstrass coefficients	$\mathcal{E}_F$ label
-64	**75010.2.a.k**	$(\frac{6967453259518}{27}, \frac{91349761}{3})$	**75010.k4**
-63	**2982.2.a.j**	$(\frac{6384710311936}{27}, \frac{84885760}{3})$	**2982.j4**
-61	**416020.2.a.b**	$(\frac{5339586557824}{27}, \frac{72973264}{3})$	**416020.b4**
-59	**470820.2.a.o**	$(\frac{4440052584448}{27}, \frac{62334976}{3})$	**470820.o4**
-56	**402990.2.a.cj**	$(\frac{3327929601694}{27}, \frac{48564769}{3})$	**402990.cj4**
-55	**23870.2.a.b**	$(\frac{3012999405568}{27}, \frac{44513536}{3})$	**23870.b4**
-54	**160710.2.a.w**	$(\frac{2723091767278}{27}, \frac{40713841}{3})$	**160710.w4**
-53	**152004.2.a.g**	$(\frac{2456607504256}{27}, \frac{37155280}{3})$	**152004.g4**
-51	**304980.2.a.r**	$(\frac{1987894104064}{27}, \frac{30721024}{3})$	**304980.r4**
-50	**230010.2.a.br**	$(\frac{1782841003198}{27}, \frac{27825601}{3})$	**230010.br4**
$-\frac{149}{3}$	**356706.2.a.i**	$(\frac{46399542075392}{729}, \frac{242151680}{27})$	**356706.i4**
-49	**30940.2.a.g**	$(\frac{1595558555008}{27}, \frac{25131856}{3})$	**30940.g4**
$-\frac{97}{2}$	**224070.2.a.bc**	$(\frac{48262128716843}{864}, \frac{381723049}{48})$	**224070.bc4**

Continued on the following page

continued			
φ	Modular form label	$\mathcal{E}_F$ Weierstrass coefficients	$\mathcal{E}_F$ label
-48	**18186.2.a.e**	$(\frac{1424807592766}{27}, \frac{22630465}{3})$	**18186.e4**
-47	**14946.2.a.m**	$(\frac{1269413896192}{27}, \frac{20312320}{3})$	**14946.m4**
-45	**280140.2.a.bf**	$(\frac{1000312620928}{27}, \frac{16190416}{3})$	**280140.bf4**
$-\frac{133}{3}$	**203490.2.a.t**	$(\frac{24889900802048}{729}, \frac{44878592}{9})$	**203490.t4**
-44	**131010.2.a.i**	$(\frac{884561174638}{27}, \frac{14369521}{3})$	**131010.i4**
-43	**183524.2.a.a**	$(\frac{780074930176}{27}, \frac{12697600}{3})$	**183524.a4**
$-\frac{125}{3}$	**4230.2.a.bb**	$(\frac{17732670365696}{729}, \frac{96176384}{27})$	**4230.bb4**
$-\frac{81}{2}$	**364038.2.a.e**	$(\frac{17999349377867}{864}, \frac{145878505}{48})$	**364038.e4**
-40	**7790.2.a.d**	$(\frac{525638849758}{27}, \frac{8496481}{3})$	**7790.d4**
$-\frac{79}{2}$	**337962.2.a.d**	$(\frac{15705820876499}{864}, \frac{126481465}{48})$	**337962.d4**
-39	**4290.2.a.p**	$(\frac{457896583168}{27}, \frac{7342336}{3})$	**4290.p4**
-38	**10374.2.a.l**	$(\frac{397505869486}{27}, \frac{6299185}{3})$	**10374.l4**
-37	**469604.2.a.a**	$(\frac{343823984512}{27}, \frac{5360080}{3})$	**469604.a4**
-36	**14430.2.a.bj**	$(\frac{296250412174}{27}, \frac{4518289}{3})$	**14430.bj4**
-35	**33180.2.a.r**	$(\frac{254225010688}{27}, \frac{3767296}{3})$	**33180.r4**
-34	**365330.2.a.k**	$(\frac{217226217598}{27}, \frac{3100801}{3})$	**365330.k4**
$-\frac{101}{3}$	**449046.2.a.d**	$(\frac{5559988527104}{729}, \frac{26067200}{27})$	**449046.d4**
-33	**334356.2.a.e**	$(\frac{184769293696}{27}, \frac{2512720}{3})$	**334356.e4**
$-\frac{131}{4}$	**357630.2.a.be**	$(\frac{363133524283739}{55296}, \frac{608578441}{768})$	**357630.be4**
-32	**1122.2.a.j**	$(\frac{156404605822}{27}, \frac{1997185}{3})$	**1122.j4**
-31	**2170.2.a.k**	$(\frac{131715948544}{27}, \frac{1548544}{3})$	**2170.k4**
$-\frac{121}{4}$	**120230.2.a.b**	$(\frac{236297113440659}{55296}, \frac{320687161}{768})$	**120230.b4**
-30	**252030.2.a.p**	$(\frac{110318904718}{27}, \frac{1161361}{3})$	**252030.p4**
-29	**227940.2.a.f**	$(\frac{91859244928}{27}, \frac{830416}{3})$	**227940.f4**
$-\frac{85}{3}$	**16830.2.a.w**	$(\frac{2187614560256}{729}, \frac{1915648}{9})$	**16830.w4**
-28	**102718.2.a.p**	$(\frac{76011365806}{27}, \frac{550705}{3})$	**102718.p4**
-27	**5124.2.a.b**	$(\frac{62476767232}{27}, \frac{317440}{3})$	**5124.b4**
-26	**18330.2.a.w**	$(\frac{50982568414}{27}, \frac{126049}{3})$	**18330.w4**
$-\frac{77}{3}$	**200970.2.a.eu**	$(\frac{1284145258496}{729}, \frac{637184}{27})$	**200970.eu4**
-25	**29380.2.a.b**	$(\frac{41280062848}{27}, -\frac{27824}{3})$	**29380.b4**

Continued on the following page

continued			
φ	Modular form label	$\mathcal{E}_F$ Weierstrass coefficients	$\mathcal{E}_F$ label
$-\frac{49}{2}$	**316302.2.a.g**	$(\frac{1184935602059}{864}, -\frac{1471895}{48})$	**316302.g4**
-24	**6510.2.a.bd**	$(\frac{33143312158}{27}, -\frac{148319}{3})$	**6510.bd4**
$-\frac{47}{2}$	**55930.2.a.b**	$(\frac{947116081043}{864}, -\frac{3156551}{48})$	**55930.b4**
-23	**1794.2.a.e**	$(\frac{26367778816}{27}, -\frac{239360}{3})$	**1794.e4**
-22	**100694.2.a.f**	$(\frac{20768997742}{27}, -\frac{304655}{3})$	**100694.f4**
$-\frac{65}{3}$	**278460.2.a.bt**	$(\frac{516647284736}{729}, -\frac{2891776}{27})$	**278460.bt4**
$-\frac{64}{3}$	**232758.2.a.q**	$(\frac{475407224522}{729}, -\frac{335615}{3})$	**232758.q4**
-21	**87780.2.a.t**	$(\frac{16181286784}{27}, -\frac{347696}{3})$	**87780.t4**
$-\frac{61}{3}$	**25254.2.a.q**	$(\frac{367488180224}{729}, -\frac{1096960}{9})$	**25254.q4**
$-\frac{81}{4}$	**373830.2.a.h**	$(\frac{27267629366339}{55296}, -\frac{94041959}{768})$	**373830.h4**
-20	**38010.2.a.ba**	$(\frac{12456496078}{27}, -\frac{371759}{3})$	**38010.ba4**
$-\frac{77}{4}$	**322014.2.a.bh**	$(\frac{20785788041003}{55296}, -\frac{97075415}{768})$	**322014.bh4**
-19	**16340.2.a.c**	$(\frac{9462796288}{27}, -\frac{379904}{3})$	**16340.c4**
$-\frac{56}{3}$	**96642.2.a.bx**	$(\frac{232383044714}{729}, -\frac{3416215}{27})$	**96642.bx4**
-18	**18582.2.a.l**	$(\frac{7083505726}{27}, -\frac{374975}{3})$	**18582.l4**
$-\frac{53}{3}$	**33390.2.a.f**	$(\frac{173038051328}{729}, -\frac{3337984}{27})$	**33390.f4**
$-\frac{69}{4}$	**50370.2.a.h**	$(\frac{11550693060827}{55296}, -\frac{93257591}{768})$	**50370.h4**
-17	**15708.2.a.g**	$(\frac{5215956352}{27}, -\frac{359600}{3})$	**15708.g4**
$-\frac{49}{3}$	**121212.2.a.n**	$(\frac{113680904192}{729}, -\frac{1034240}{9})$	**121212.n4**
-16	**4930.2.a.e**	$(\frac{3770398654}{27}, -\frac{336191}{3})$	**4930.e4**
$-\frac{46}{3}$	**402822.2.a.bd**	$(\frac{81059759594}{729}, -\frac{317215}{3})$	**402822.bd4**
-15	**510.2.a.g**	$(\frac{2668945408}{27}, -\frac{306944}{3})$	**510.g4**
$-\frac{29}{2}$	**472874.2.a.a**	$(\frac{71229140099}{864}, -\frac{4652135}{48})$	**472874.a4**
-14	**26670.2.a.bf**	$(\frac{1844554318}{27}, -\frac{273839}{3})$	**26670.bf4**
$-\frac{27}{2}$	**6090.2.a.j**	$(\frac{48576965723}{864}, -\frac{4102391}{48})$	**6090.j4**
$-\frac{40}{3}$	**42570.2.a.bd**	$(\frac{38347324586}{729}, -\frac{751517}{9})$	**42570.bd4**
-13	**21476.2.a.c**	$(\frac{1240049536}{27}, -\frac{238640}{3})$	**21476.c4**
$-\frac{25}{2}$	**6810.2.a.e**	$(\frac{32155292411}{864}, -\frac{3531959}{48})$	**6810.e4**
$-\frac{37}{3}$	**23310.2.a.w**	$(\frac{25246048256}{729}, -\frac{214784}{3})$	**23310.w4**
$-\frac{49}{4}$	**330190.2.a.b**	$(\frac{1846551651587}{55296}, -\frac{54222311}{768})$	**330190.b4**

Continued on the following page

continued			
φ	Modular form label	$\mathcal{E}_F$ Weierstrass coefficients	$\mathcal{E}_F$ label
-12	**8502.2.a.e**	$(\frac{807182062}{27}, -\frac{202895}{3})$	**8502.e4**
$-\frac{23}{2}$	**48070.2.a.a**	$(\frac{20552095331}{864}, -\frac{2963879}{48})$	**48070.a4**
$-\frac{45}{4}$	**85890.2.a.h**	$(\frac{1168782613739}{55296}, -\frac{45193559}{768})$	**85890.h4**
-11	**660.2.a.d**	$(\frac{505729024}{27}, -\frac{167936}{3})$	**660.d4**
$-\frac{32}{3}$	**61110.2.a.bs**	$(\frac{11570679626}{729}, -\frac{1409911}{27})$	**61110.bs4**
$-\frac{21}{2}$	**184506.2.a.f**	$(\frac{12598240787}{864}, -\frac{2417735}{48})$	**184506.f4**
$-\frac{41}{4}$	**458790.2.a.g**	$(\frac{708090344819}{55296}, -\frac{36585479}{768})$	**458790.g4**
-10	**10010.2.a.o**	$(\frac{302631838}{27}, -\frac{134879}{3})$	**10010.o4**
$-\frac{29}{3}$	**5742.2.a.t**	$(\frac{6804119552}{729}, -\frac{1120000}{27})$	**5742.t4**
$-\frac{19}{2}$	**138054.2.a.j**	$(\frac{7340529419}{864}, -\frac{1909655}{48})$	**138054.j4**
$-\frac{28}{3}$	**332010.2.a.cx**	$(\frac{5628017978}{729}, -38117)$	**332010.cx4**
-9	**2460.2.a.c**	$(\frac{171173248}{27}, -\frac{104624}{3})$	**2460.c4**
$-\frac{17}{2}$	**100130.2.a.a**	$(\frac{4015983563}{864}, -\frac{1452311}{48})$	**100130.a4**
$-\frac{25}{3}$	**23940.2.a.s**	$(\frac{3042308096}{729}, -\frac{259072}{9})$	**23940.s4**
-8	**438.2.a.g**	$(\frac{90193246}{27}, -\frac{77855}{3})$	**438.g4**
$-\frac{23}{3}$	**376740.2.a.v**	$(\frac{1929607808}{729}, -\frac{628144}{27})$	**376740.v4**
$-\frac{15}{2}$	**69870.2.a.k**	$(\frac{2027378771}{864}, -\frac{1054919}{48})$	**69870.k4**
$-\frac{22}{3}$	**66330.2.a.bn**	$(\frac{1512019466}{729}, -\frac{186557}{9})$	**66330.bn4**
-7	**14.2.a.a**	$(\frac{43343872}{27}, -\frac{55040}{3})$	**14.a6**
$-\frac{27}{4}$	**45942.2.a.r**	$(\frac{72600132203}{55296}, -\frac{12797015}{768})$	**45942.r4**
$-\frac{20}{3}$	**126270.2.a.bk**	$(\frac{893451866}{729}, -\frac{435271}{27})$	**126270.bk4**
$-\frac{13}{2}$	**46410.2.a.bf**	$(\frac{920019491}{864}, -\frac{723239}{48})$	**46410.bf4**
$-\frac{19}{3}$	**218196.2.a.i**	$(\frac{671714432}{729}, -\frac{42160}{3})$	**218196.i4**
$-\frac{25}{4}$	**66410.2.a.a**	$(\frac{47319616979}{55296}, -\frac{10414919}{768})$	**66410.a4**
-6	**2310.2.a.t**	$(\frac{18382894}{27}, -\frac{36431}{3})$	**2310.t4**
$-\frac{23}{4}$	**29118.2.a.e**	$(\frac{29623480451}{55296}, -\frac{8305895}{768})$	**29118.e4**
$-\frac{17}{3}$	**39780.2.a.x**	$(\frac{359591936}{729}, -\frac{280576}{27})$	**39780.x4**
$-\frac{11}{2}$	**28886.2.a.a**	$(\frac{359758907}{864}, -\frac{459575}{48})$	**28886.a4**
$-\frac{16}{3}$	**2394.2.a.l**	$(\frac{254679434}{729}, -\frac{79165}{9})$	**2394.l4**
$-\frac{21}{4}$	**40530.2.a.o**	$(\frac{17651668859}{55296}, -\frac{6467639}{768})$	**40530.o4**

Continued on the following page

continued

φ	Modular form label	$\mathcal{E}_F$ Weierstrass coefficients	$\mathcal{E}_F$ label
-5	**1380.2.a.d**	$(\frac{6506368}{27}, -\frac{22064}{3})$	**1380.d4**
$-\frac{19}{4}$	**30590.2.a.a**	$(\frac{9883815227}{55296}, -\frac{4894391}{768})$	**30590.a4**
$-\frac{14}{3}$	**92106.2.a.bt**	$(\frac{117442922}{729}, -\frac{163735}{27})$	**92106.bt4**
$-\frac{9}{2}$	**5478.2.a.d**	$(\frac{112262939}{864}, -\frac{262775}{48})$	**5478.d4**
$-\frac{13}{3}$	**1170.2.a.h**	$(\frac{75603968}{729}, -\frac{44288}{9})$	**1170.h4**
$-\frac{17}{4}$	**112098.2.a.e**	$(\frac{5101499843}{55296}, -\frac{3576935}{768})$	**112098.e4**
-4	**370.2.a.d**	$(\frac{1720078}{27}, -\frac{11759}{3})$	**370.d4**
$-\frac{15}{4}$	**79230.2.a.h**	$(\frac{2351754899}{55296}, -\frac{2502599}{768})$	**79230.h4**
$-\frac{11}{3}$	**47124.2.a.l**	$(\frac{26858624}{729}, -\frac{82480}{27})$	**47124.l4**
$-\frac{7}{2}$	**2730.2.a.p**	$(\frac{23518403}{864}, -\frac{128231}{48})$	**2730.p4**
$-\frac{10}{3}$	**36270.2.a.bz**	$(\frac{14309306}{729}, -\frac{6959}{3})$	**36270.bz4**
$-\frac{13}{4}$	**4862.2.a.b**	$(\frac{911813291}{55296}, -\frac{1655255}{768})$	**4862.b4**
-3	**84.2.a.b**	$(\frac{249856}{27}, -\frac{5120}{3})$	**84.b4**
$-\frac{11}{4}$	**33990.2.a.r**	$(\frac{255101579}{55296}, -\frac{1015319}{768})$	**33990.r4**
$-\frac{8}{3}$	**990.2.a.i**	$(\frac{2560298}{729}, -\frac{32599}{27})$	**990.i4**
$-\frac{5}{2}$	**3290.2.a.b**	$(\frac{1585331}{864}, -\frac{47879}{48})$	**3290.b4**
$-\frac{7}{3}$	**13860.2.a.t**	$(\frac{526976}{729}, -\frac{7312}{9})$	**13860.t4**
$-\frac{9}{4}$	**6630.2.a.k**	$(\frac{18477107}{55296}, -\frac{559751}{768})$	**6630.k4**
-2	**114.2.a.c**	$(-\frac{9218}{27}, -\frac{1535}{3})$	**114.c4**
$-\frac{7}{4}$	**10318.2.a.b**	$(-\frac{29290717}{55296}, -\frac{262055}{768})$	**10318.b4**
$-\frac{5}{3}$	**90.2.a.a**	$(-\frac{385024}{729}, -\frac{7936}{27})$	**90.a4**
$-\frac{3}{2}$	**870.2.a.c**	$(-\frac{406549}{864}, -\frac{10199}{48})$	**870.c4**
$-\frac{4}{3}$	**1638.2.a.p**	$(-\frac{272998}{729}, -\frac{1325}{9})$	**1638.p4**
$-\frac{5}{4}$	**210.2.a.b**	$(-\frac{17794981}{55296}, -\frac{92279}{768})$	**210.b8**
$-\frac{24}{25}$	**50610.2.a.bc**	$(-\frac{1025271241346}{6591796875}, -\frac{60120191}{1171875})$	**50610.bc4**
$-\frac{23}{25}$	**20010.2.a.w**	$(-\frac{902621241344}{6591796875}, -\frac{52211456}{1171875})$	**20010.w4**
$-\frac{9}{10}$	**51870.2.a.ba**	$(-\frac{1729589653}{13500000}, -\frac{1242071}{30000})$	**51870.ba4**
$-\frac{4}{5}$	**1230.2.a.h**	$(-\frac{37583426}{421875}, -\frac{52031}{1875})$	**1230.h4**
$-\frac{19}{25}$	**29260.2.a.c**	$(-\frac{499886206976}{6591796875}, -\frac{27201536}{1171875})$	**29260.c4**
$-\frac{3}{4}$	**1302.2.a.h**	$(-\frac{4021669}{55296}, -\frac{17015}{768})$	**1302.h4**

Continued on the following page

continued			
φ	Modular form label	$\mathcal{E}_F$ Weierstrass coefficients	$\mathcal{E}_F$ label
$-\frac{18}{25}$	**241230.2.a.cf**	$(-\frac{421268926754}{6591796875}, -\frac{22456991}{1171875})$	**241230.cf4**
$-\frac{7}{10}$	**86870.2.a.b**	$(-\frac{788823757}{13500000}, -\frac{519431}{30000})$	**86870.b4**
$-\frac{16}{25}$	**5330.2.a.d**	$(-\frac{289241090786}{6591796875}, -\frac{14566751}{1171875})$	**5330.d4**
$-\frac{31}{50}$	**305970.2.a.k**	$(-\frac{8359631224813}{210937500000}, -\frac{206480711}{18750000})$	**305970.k4**
$-\frac{3}{5}$	**30.2.a.a**	$(-\frac{15048704}{421875}, -\frac{18176}{1875})$	**30.a8**
$-\frac{14}{25}$	**412230.2.a.cg**	$(-\frac{188399497106}{6591796875}, -\frac{8604431}{1171875})$	**412230.cg4**
$-\frac{11}{20}$	**405790.2.a.d**	$(-\frac{23305890133}{864000000}, -\frac{3269591}{480000})$	**405790.d4**
$-\frac{13}{25}$	**350740.2.a.b**	$(-\frac{148537921664}{6591796875}, -\frac{6268976}{1171875})$	**350740.b4**
$-\frac{1}{2}$	**66.2.a.a**	$(-\frac{17173}{864}, -\frac{215}{48})$	**66.a4**
$-\frac{12}{25}$	**147630.2.a.cc**	$(-\frac{115017022514}{6591796875}, -\frac{4322351}{1171875})$	**147630.cc4**
$-\frac{9}{20}$	**87870.2.a.i**	$(-\frac{12281244013}{864000000}, -\frac{1269191}{480000})$	**87870.i4**
$-\frac{11}{25}$	**20460.2.a.k**	$(-\frac{87271878656}{6591796875}, -\frac{2733056}{1171875})$	**20460.k4**
$-\frac{2}{5}$	**1610.2.a.c**	$(-\frac{4141874}{421875}, -\frac{2351}{1875})$	**1610.c4**
$-\frac{9}{25}$	**54060.2.a.h**	$(-\frac{46755076736}{6591796875}, -\frac{499376}{1171875})$	**54060.h4**
$-\frac{7}{20}$	**17430.2.a.n**	$(-\frac{5624587837}{864000000}, -\frac{122471}{480000})$	**17430.n4**
$-\frac{8}{25}$	**32010.2.a.l**	$(-\frac{32788971074}{6591796875}, \frac{209089}{1171875})$	**32010.l3**
$-\frac{3}{10}$	**14430.2.a.t**	$(-\frac{55540837}{13500000}, \frac{12169}{30000})$	**14430.t3**
$-\frac{7}{25}$	**770.2.a.f**	$(-\frac{22229295104}{6591796875}, \frac{688384}{1171875})$	**770.f3**
$-\frac{27}{100}$	**26670.2.a.q**	$(-\frac{41070994000597}{13500000000000}, \frac{198710569}{300000000})$	**26670.q3**
$-\frac{13}{50}$	**455910.2.a.v**	$(-\frac{577520181757}{210937500000}, \frac{13636249}{18750000})$	**455910.v3**
$-\frac{1}{4}$	**130.2.a.a**	$(-\frac{135901}{55296}, \frac{601}{768})$	**130.a3**
$-\frac{6}{25}$	**73470.2.a.w**	$(-\frac{14505231026}{6591796875}, \frac{971089}{1171875})$	**73470.w3**
$-\frac{21}{100}$	**39270.2.a.bg**	$(-\frac{20982192888133}{13500000000000}, \frac{274899529}{300000000})$	**39270.bg6**
$-\frac{1}{5}$	**420.2.a.c**	$(-\frac{580736}{421875}, \frac{1744}{1875})$	**420.c3**
$-\frac{9}{50}$	**231870.2.a.f**	$(-\frac{225875861893}{210937500000}, \frac{17573449}{18750000})$	**231870.f3**
$-\frac{4}{25}$	**17690.2.a.f**	$(-\frac{5430510866}{6591796875}, \frac{1078129}{1171875})$	**17690.f3**
$-\frac{3}{20}$	**32430.2.a.j**	$(-\frac{621825157}{864000000}, \frac{433609}{480000})$	**32430.j3**
$-\frac{7}{50}$	**450870.2.a.bg**	$(-\frac{132287982877}{210937500000}, \frac{16536409}{18750000})$	**450870.bg3**
$-\frac{3}{25}$	**5460.2.a.e**	$(-\frac{3116969984}{6591796875}, \frac{968704}{1171875})$	**5460.e3**
$-\frac{1}{10}$	**2090.2.a.b**	$(-\frac{4774213}{13500000}, \frac{22729}{30000})$	**2090.b3**

Continued on the following page

continued			
φ	Modular form label	$\mathcal{E}_F$ Weierstrass coefficients	$\mathcal{E}_F$ label
$-\frac{2}{25}$	**1290.2.a.n**	$(-\frac{1732452194}{6591796875}, \frac{795169}{1171875})$	**1290.n3**
$-\frac{3}{50}$	**122430.2.a.ba**	$(-\frac{40997900917}{210937500000}, \frac{11117929}{18750000})$	**122430.ba3**
$-\frac{1}{20}$	**6090.2.a.i**	$(-\frac{144144253}{864000000}, \frac{263449}{480000})$	**6090.i3**
$-\frac{1}{25}$	**4420.2.a.a**	$(-\frac{942432896}{6591796875}, \frac{591184}{1171875})$	**4420.a3**
$-\frac{3}{100}$	**392430.2.a.f**	$(-\frac{1650088716517}{13500000000000}, \frac{138085129}{300000000})$	**392430.f3**
$-\frac{1}{50}$	**30090.2.a.d**	$(-\frac{21962069173}{210937500000}, \frac{7813609}{18750000})$	**30090.d3**
$-\frac{1}{100}$	**110090.2.a.b**	$(-\frac{1190615433373}{13500000000000}, \frac{112277209}{300000000})$	**110090.b3**
$\frac{1}{100}$	**30030.2.a.p**	$(-\frac{829247746573}{13500000000000}, \frac{88322809}{300000000})$	**30030.p5**
$\frac{1}{50}$	**2870.2.a.c**	$(-\frac{10541225773}{210937500000}, \frac{4836409}{18750000})$	**2870.c3**
$\frac{3}{100}$	**212430.2.a.c**	$(-\frac{533228824117}{13500000000000}, \frac{67316329}{300000000})$	**212430.c3**
$\frac{1}{25}$	**30.2.a.a**	$(-\frac{196714496}{6591796875}, \frac{227584}{1171875})$	**30.a6**
$\frac{1}{20}$	**2090.2.a.c**	$(-\frac{18062893}{864000000}, \frac{80569}{480000})$	**2090.c3**
$\frac{3}{50}$	**32430.2.a.k**	$(-\frac{2668954717}{210937500000}, \frac{2733529}{18750000})$	**32430.k3**
$\frac{7}{100}$	**240870.2.a.g**	$(-\frac{68964389677}{13500000000000}, \frac{38542009}{300000000})$	**240870.g3**
$\frac{2}{25}$	**1610.2.a.b**	$(\frac{10786606}{6591796875}, \frac{136369}{1171875})$	**1610.b3**
$\frac{9}{100}$	**51870.2.a.y**	$(\frac{100241285507}{13500000000000}, \frac{32980249}{300000000})$	**51870.y6**
$\frac{1}{10}$	**30.2.a.a**	$(\frac{162467}{13500000}, \frac{3289}{30000})$	**30.a5**
$\frac{11}{100}$	**9790.2.a.a**	$(\frac{204822055547}{13500000000000}, \frac{34778569}{300000000})$	**9790.a3**
$\frac{3}{25}$	**660.2.a.d**	$(\frac{108601216}{6591796875}, \frac{151504}{1171875})$	**660.d3**
$\frac{13}{100}$	**192270.2.a.q**	$(\frac{209391850043}{13500000000000}, \frac{45048649}{300000000})$	**192270.q3**
$\frac{7}{50}$	**39130.2.a.b**	$(\frac{2483040923}{210937500000}, \frac{3356809}{18750000})$	**39130.b3**
$\frac{3}{20}$	**3570.2.a.k**	$(\frac{4041323}{864000000}, \frac{103849}{480000})$	**3570.k3**
$\frac{4}{25}$	**2310.2.a.u**	$(-\frac{42369266}{6591796875}, \frac{307729}{1171875})$	**2310.u7**
$\frac{9}{50}$	**38130.2.a.k**	$(-\frac{9213935293}{210937500000}, \frac{7194649}{18750000})$	**38130.k3**
$\frac{19}{100}$	**40470.2.a.u**	$(-\frac{965671254613}{13500000000000}, \frac{137858089}{300000000})$	**40470.u3**
$\frac{1}{5}$	**20.2.a.a**	$(-\frac{45056}{421875}, \frac{1024}{1875})$	**20.a3**
$\frac{11}{50}$	**30030.2.a.r**	$(-\frac{43008008653}{210937500000}, \frac{14130169}{18750000})$	**30030.r3**
$\frac{6}{25}$	**16530.2.a.y**	$(-\frac{2270202626}{6591796875}, \frac{1183489}{1171875})$	**16530.y2**
$\frac{1}{4}$	**30.2.a.a**	$(-\frac{24013}{55296}, \frac{889}{768})$	**30.a6**
$\frac{13}{50}$	**322270.2.a.b**	$(-\frac{113727665557}{210937500000}, \frac{24727849}{18750000})$	**322270.b2**

Continued on the following page

continued			
φ	Modular form label	$\mathcal{E}_F$ Weierstrass coefficients	$\mathcal{E}_F$ label
$\frac{27}{100}$	**313170.2.a.bb**	$(-\frac{8918727672997}{13500000000000}, \frac{448255369}{300000000})$	**313170.bb2**
$\frac{7}{25}$	**7980.2.a.d**	$(-\frac{5276146304}{6591796875}, \frac{1973584}{1171875})$	**7980.d2**
$\frac{3}{10}$	**3570.2.a.j**	$(-\frac{15415597}{13500000}, \frac{63289}{30000})$	**3570.j2**
$\frac{8}{25}$	**7990.2.a.d**	$(-\frac{10407439874}{6591796875}, \frac{3045889}{1171875})$	**7990.d2**
$\frac{7}{20}$	**39130.2.a.c**	$(-\frac{2117186317}{864000000}, \frac{1661689}{480000})$	**39130.c2**
$\frac{9}{25}$	**210.2.a.d**	$(-\frac{18509275136}{6591796875}, \frac{4436224}{1171875})$	**210.d5**
$\frac{19}{50}$	**64790.2.a.a**	$(-\frac{767492660413}{210937500000}, \frac{84190489}{18750000})$	**64790.a2**
$\frac{2}{5}$	**390.2.a.g**	$(-\frac{1958114}{421875}, \frac{9889}{1875})$	**390.g2**
$\frac{11}{25}$	**56980.2.a.b**	$(-\frac{47857840256}{6591796875}, \frac{8315344}{1171875})$	**56980.b2**
$\frac{9}{20}$	**20130.2.a.e**	$(-\frac{6965097373}{864000000}, \frac{3651289}{480000})$	**20130.e2**
$\frac{23}{50}$	**108330.2.a.d**	$(-\frac{1883303235397}{210937500000}, \frac{152647369}{18750000})$	**108330.d2**
$\frac{12}{25}$	**32370.2.a.be**	$(-\frac{71674613714}{6591796875}, \frac{10876849}{1171875})$	**32370.be2**
$\frac{1}{2}$	**14.2.a.a**	$(-\frac{11341}{864}, \frac{505}{48})$	**14.a4**
$\frac{13}{25}$	**17940.2.a.e**	$(-\frac{103620030464}{6591796875}, \frac{13901824}{1171875})$	**17940.e2**
$\frac{27}{50}$	**133170.2.a.k**	$(-\frac{3942036612397}{210937500000}, \frac{249594169}{18750000})$	**133170.k2**
$\frac{11}{20}$	**26070.2.a.m**	$(-\frac{17560460773}{864000000}, \frac{6757129}{480000})$	**26070.m2**
$\frac{14}{25}$	**77770.2.a.k**	$(-\frac{145472985506}{6591796875}, \frac{17427169}{1171875})$	**77770.k2**
$\frac{3}{5}$	**660.2.a.c**	$(-\frac{12750464}{421875}, \frac{34384}{1875})$	**660.c2**
$\frac{16}{25}$	**3570.2.a.w**	$(-\frac{2670940923 86}{6591796875}, \frac{26127649}{1171875})$	**3570.w6**
$\frac{13}{20}$	**88270.2.a.a**	$(-\frac{37558428517}{864000000}, \frac{11215369}{480000})$	**88270.a2**
$\frac{17}{25}$	**170.2.a.a**	$(-\frac{351523610624}{6591796875}, \frac{31377664}{1171875})$	**170.a2**
$\frac{7}{10}$	**11130.2.a.n**	$(-\frac{820794997}{13500000}, \frac{876649}{30000})$	**11130.n2**
$\frac{18}{25}$	**28770.2.a.bm**	$(-\frac{455201025554}{6591796875}, \frac{37277809}{1171875})$	**28770.bm2**
$\frac{3}{4}$	**138.2.a.b**	$(-\frac{4591477}{55296}, \frac{27625}{768})$	**138.b2**
$\frac{19}{25}$	**83220.2.a.d**	$(-\frac{581061685376}{6591796875}, \frac{43866064}{1171875})$	**83220.d2**
$\frac{4}{5}$	**310.2.a.a**	$(-\frac{46867106}{421875}, \frac{81889}{1875})$	**310.a2**
$\frac{81}{100}$	**358530.2.a.f**	$(-\frac{1586119012101613}{13500000000000}, \frac{13600575289}{300000000})$	**358530.f6**
$\frac{41}{50}$	**392370.2.a.v**	$(-\frac{26192108471293}{210937500000}, \frac{881956249}{18750000})$	**392370.v2**
$\frac{21}{25}$	**17220.2.a.j**	$(-\frac{912370774016}{6591796875}, \frac{59259904}{1171875})$	**17220.j2**
$\frac{17}{20}$	**67830.2.a.q**	$(-\frac{126133966477}{864000000}, \frac{25150969}{480000})$	**67830.q2**

Continued on the following page

continued

φ	Modular form label	$\mathcal{E}_F$ Weierstrass coefficients	$\mathcal{E}_F$ label
$\frac{22}{25}$	**57090.2.a.p**	$(-\frac{1125012532034}{6591796875}, \frac{68142529}{1171875})$	**57090.p2**
$\frac{9}{10}$	**2130.2.a.g**	$(-\frac{2549332333}{13500000}, \frac{1866169}{30000})$	**2130.g2**
$\frac{23}{25}$	**41860.2.a.b**	$(-\frac{1374241430144}{6591796875}, \frac{77867344}{1171875})$	**41860.b2**
$\frac{19}{20}$	**28690.2.a.a**	$(-\frac{208110189493}{864000000}, \frac{35117929}{480000})$	**28690.a2**
$\frac{24}{25}$	**5730.2.a.o**	$(-\frac{1664367159746}{6591796875}, \frac{88473409}{1171875})$	**5730.o2**
$\frac{49}{50}$	**27370.2.a.d**	$(-\frac{58438242389773}{210937500000}, \frac{1505906809}{18750000})$	**27370.d2**
$\frac{99}{100}$	**261030.2.a.s**	$(-\frac{3914878633699573}{13500000000000}, \frac{24839653609}{300000000})$	**261030.s2**
$\frac{11}{10}$	**9790.2.a.b**	$(-\frac{6289904413}{13500000}, \frac{3407449}{30000})$	**9790.b2**
$\frac{6}{5}$	**210.2.a.d**	$(-\frac{290831186}{421875}, \frac{276529}{1875})$	**210.d2**
$\frac{5}{4}$	**410.2.a.a**	$(-\frac{45816661}{55296}, \frac{128041}{768})$	**410.a2**
$\frac{13}{10}$	**41730.2.a.k**	$(-\frac{13348706437}{13500000}, \frac{5627209}{30000})$	**41730.k2**
$\frac{4}{3}$	**198.2.a.d**	$(-\frac{808006}{729}, \frac{5465}{27})$	**198.d2**
$\frac{7}{5}$	**4060.2.a.b**	$(-\frac{582737024}{421875}, \frac{439504}{1875})$	**4060.b2**
$\frac{3}{2}$	**30.2.a.a**	$(-\frac{1629757}{864}, \frac{13849}{48})$	**30.a4**
$\frac{8}{5}$	**2010.2.a.j**	$(-\frac{1065453554}{421875}, \frac{657169}{1875})$	**2010.j3**
$\frac{5}{3}$	**1260.2.a.j**	$(-\frac{2214784}{729}, \frac{3568}{9})$	**1260.j3**
$\frac{17}{10}$	**170170.2.a.c**	$(-\frac{44863548157}{13500000}, \frac{12626329}{30000})$	**170170.c3**
$\frac{7}{4}$	**2478.2.a.c**	$(-\frac{209560429}{55296}, \frac{352825}{768})$	**2478.c3**
$\frac{9}{5}$	**1140.2.a.d**	$(-\frac{1816702976}{421875}, \frac{937984}{1875})$	**1140.d4**
$\frac{19}{10}$	**91770.2.a.x**	$(-\frac{74306509453}{13500000}, \frac{17676409}{30000})$	**91770.x3**
2	**34.2.a.a**	$(-\frac{187634}{27}, \frac{2065}{3})$	**34.a3**
$\frac{21}{10}$	**413490.2.a.bg**	$(-\frac{117143150293}{13500000}, \frac{23946409}{30000})$	**413490.bg3**
$\frac{11}{5}$	**31020.2.a.k**	$(-\frac{4525106816}{421875}, \frac{1723984}{1875})$	**31020.k3**
$\frac{9}{4}$	**2310.2.a.l**	$(-\frac{657131581}{55296}, \frac{756121}{768})$	**2310.l5**
$\frac{7}{3}$	**1260.2.a.d**	$(-\frac{10227712}{729}, \frac{29696}{27})$	**1260.d4**
$\frac{12}{5}$	**21630.2.a.bb**	$(-\frac{6731730434}{421875}, \frac{2247169}{1875})$	**21630.bb3**
$\frac{5}{2}$	**1290.2.a.h**	$(-\frac{16615909}{864}, \frac{65161}{48})$	**1290.h3**
$\frac{13}{5}$	**910.2.a.a**	$(-\frac{9708806144}{421875}, \frac{2869504}{1875})$	**910.a4**
$\frac{8}{3}$	**2070.2.a.p**	$(-\frac{18840214}{729}, \frac{4961}{3})$	**2070.p3**
$\frac{27}{10}$	**118830.2.a.f**	$(-\frac{369336680317}{13500000}, \frac{51533209}{30000})$	**118830.f3**

Continued on the following page

continued

φ	Modular form label	$\mathcal{E}_F$ Weierstrass coefficients	$\mathcal{E}_F$ label
$\frac{11}{4}$	**14630.2.a.b**	$(-\frac{1645608133}{55296}, \frac{1395529}{768})$	**14630.b3**
$\frac{14}{5}$	**2310.2.a.u**	$(-\frac{13637023346}{421875}, \frac{3600529}{1875})$	**2310.u4**
3	**156.2.a.b**	$(-\frac{1198208}{27}, \frac{7120}{3})$	**156.b3**
$\frac{16}{5}$	**15290.2.a.f**	$(-\frac{25195636946}{421875}, \frac{5427889}{1875})$	**15290.f3**
$\frac{13}{4}$	**8814.2.a.b**	$(-\frac{3546914437}{55296}, \frac{2332105}{768})$	**8814.b3**
$\frac{10}{3}$	**18270.2.a.bz**	$(-\frac{52548214}{729}, \frac{88649}{27})$	**18270.bz3**
$\frac{17}{5}$	**37740.2.a.f**	$(-\frac{33317433344}{421875}, \frac{6544384}{1875})$	**37740.f4**
$\frac{7}{2}$	**4270.2.a.c**	$(-\frac{77998789}{864}, \frac{183241}{48})$	**4270.c3**
$\frac{18}{5}$	**61230.2.a.z**	$(-\frac{43375763234}{421875}, \frac{7809889}{1875})$	**61230.z3**
$\frac{11}{3}$	**198.2.a.b**	$(-\frac{81584128}{729}, \frac{39680}{9})$	**198.b4**
$\frac{37}{10}$	**358530.2.a.i**	$(-\frac{1575342271477}{13500000}, \frac{136029289}{30000})$	**358530.i3**
$\frac{15}{4}$	**43230.2.a.n**	$(-\frac{6865654141}{55296}, \frac{3630361}{768})$	**43230.n3**
$\frac{19}{5}$	**220780.2.a.b**	$(-\frac{55689113216}{421875}, \frac{9235024}{1875})$	**220780.b3**
4	**210.2.a.d**	$(-\frac{4518866}{27}, \frac{17329}{3})$	**210.d5**
$\frac{21}{5}$	**4830.2.a.bf**	$(-\frac{88512536576}{421875}, \frac{12607744}{1875})$	**4830.bf4**
$\frac{17}{4}$	**65858.2.a.a**	$(-\frac{12255698989}{55296}, \frac{5358265}{768})$	**65858.a3**
$\frac{13}{3}$	**44460.2.a.l**	$(-\frac{176796544}{729}, \frac{200144}{27})$	**44460.l3**
$\frac{22}{5}$	**360910.2.a.j**	$(-\frac{109820740754}{421875}, \frac{14577649}{1875})$	**360910.j3**
$\frac{9}{2}$	**3318.2.a.e**	$(-\frac{249631453}{864}, \frac{400345}{48})$	**3318.e3**
$\frac{23}{5}$	**139380.2.a.d**	$(-\frac{134982429824}{421875}, \frac{16751824}{1875})$	**139380.d3**
$\frac{14}{3}$	**56826.2.a.u**	$(-\frac{249365926}{729}, \frac{84115}{9})$	**56826.u3**
$\frac{19}{4}$	**95190.2.a.w**	$(-\frac{20535533461}{55296}, \frac{7587241}{768})$	**95190.w3**
$\frac{24}{5}$	**120270.2.a.w**	$(-\frac{164483857586}{421875}, \frac{19141969}{1875})$	**120270.w3**
5	**220.2.a.a**	$(-\frac{12726272}{27}, \frac{34816}{3})$	**220.a4**
$\frac{21}{4}$	**132090.2.a.x**	$(-\frac{32702355253}{55296}, \frac{10392169}{768})$	**132090.x3**
$\frac{16}{3}$	**10998.2.a.r**	$(-\frac{463912438}{729}, \frac{383945}{27})$	**10998.r3**
$\frac{27}{5}$	**78540.2.a.r**	$(-\frac{284445697664}{421875}, \frac{27728464}{1875})$	**78540.r3**
$\frac{11}{2}$	**6402.2.a.f**	$(-\frac{634485421}{864}, \frac{752185}{48})$	**6402.f3**
$\frac{28}{5}$	**397670.2.a.o**	$(-\frac{336917310914}{421875}, \frac{31103809}{1875})$	**397670.o3**
$\frac{17}{3}$	**21420.2.a.o**	$(-\frac{615175552}{729}, \frac{51664}{3})$	**21420.o3**

Continued on the following page

continued			
φ	Modular form label	$\mathcal{E}_F$ Weierstrass coefficients	$\mathcal{E}_F$ label
$\frac{23}{4}$	**177422.2.a.a**	$(-\frac{49944931597}{55296}, \frac{13851385}{768})$	**177422.a3**
$\frac{29}{5}$	**870.2.a.b**	$(-\frac{396729491456}{421875}, \frac{34756864}{1875})$	**870.b4**
6	**1590.2.a.u**	$(-\frac{29734562}{27}, \frac{61921}{3})$	**1590.u3**
$\frac{25}{4}$	**46410.2.a.be**	$(-\frac{73655211421}{55296}, \frac{18046681}{768})$	**46410.be6**
$\frac{19}{3}$	**2394.2.a.k**	$(-\frac{1032871936}{729}, \frac{661760}{27})$	**2394.k4**
$\frac{32}{5}$	**8490.2.a.g**	$(-\frac{627622749074}{421875}, \frac{47513329}{1875})$	**8490.g3**
$\frac{13}{2}$	**32890.2.a.b**	$(-\frac{1381700917}{864}, \frac{1277929}{48})$	**32890.b3**
$\frac{33}{5}$	**337260.2.a.r**	$(-\frac{724423061504}{421875}, \frac{52409344}{1875})$	**337260.r4**
$\frac{20}{3}$	**90270.2.a.x**	$(-\frac{1311847174}{729}, \frac{259763}{9})$	**90270.x3**
$\frac{27}{4}$	**32982.2.a.g**	$(-\frac{105438693349}{55296}, \frac{23063305}{768})$	**32982.g3**
7	**2604.2.a.d**	$(-\frac{60996224}{27}, \frac{101200}{3})$	**2604.d3**
$\frac{36}{5}$	**296670.2.a.ce**	$(-\frac{10868276024 66}{421875}, \frac{69223009}{1875})$	**296670.ce3**
$\frac{29}{4}$	**74530.2.a.b**	$(-\frac{147123549541}{55296}, \frac{28989961}{768})$	**74530.b3**
$\frac{22}{3}$	**244530.2.a.cy**	$(-\frac{2045761222}{729}, \frac{1057241}{27})$	**244530.cy3**
$\frac{37}{5}$	**15170.2.a.i**	$(-\frac{1234904489984}{421875}, \frac{75583744}{1875})$	**15170.i4**
$\frac{15}{2}$	**51870.2.a.bs**	$(-\frac{2692392949}{864}, \frac{2020201}{48})$	**51870.bs3**
$\frac{23}{3}$	**70380.2.a.bk**	$(-\frac{2516783104}{729}, \frac{406528}{9})$	**70380.bk4**
$\frac{31}{4}$	**10230.2.a.o**	$(-\frac{200768505373}{55296}, \frac{35918809}{768})$	**10230.o3**
8	**994.2.a.e**	$(-\frac{113664098}{27}, \frac{155425}{3})$	**994.e3**
$\frac{41}{5}$	**223860.2.a.s**	$(-\frac{1992549380096}{421875}, \frac{105201664}{1875})$	**223860.s4**
$\frac{25}{3}$	**73260.2.a.y**	$(-\frac{3711800704}{729}, \frac{1595984}{27})$	**73260.y3**
$\frac{17}{2}$	**77010.2.a.k**	$(-\frac{4824213229}{864}, \frac{3025081}{48})$	**77010.k3**
$\frac{26}{3}$	**414414.2.a.ck**	$(-\frac{4455627958}{729}, 67115)$	**414414.ck3**
9	**30.2.a.a**	$(-\frac{196714496}{27}, \frac{227584}{3})$	**30.a6**
$\frac{28}{3}$	**52290.2.a.cr**	$(-\frac{6290319334}{729}, \frac{2305529}{27})$	**52290.cr3**
$\frac{19}{2}$	**8398.2.a.c**	$(-\frac{8094667933}{864}, \frac{4342105}{48})$	**8398.c3**
$\frac{49}{5}$	**167860.2.a.b**	$(-\frac{4566856871936}{421875}, \frac{187730944}{1875})$	**167860.b4**
10	**2670.2.a.f**	$(-\frac{321031442}{27}, \frac{320881}{3})$	**2670.f3**
$\frac{31}{3}$	**179676.2.a.f**	$(-\frac{10092679168}{729}, \frac{3215360}{27})$	**179676.f4**
$\frac{21}{2}$	**149226.2.a.u**	$(-\frac{12883191301}{864}, \frac{6024265}{48})$	**149226.u3**

Continued on the following page

continued			
φ	Modular form label	$\mathcal{E}_F$ Weierstrass coefficients	$\mathcal{E}_F$ label
$\frac{53}{5}$	**93810.2.a.j**	$(-\frac{6573251108864}{421875}, \frac{242761984}{1875})$	**93810.j4**
$\frac{32}{3}$	**49590.2.a.bj**	$(-\frac{11693531062}{729}, \frac{1189507}{9})$	**49590.bj3**
$\frac{54}{5}$	**101010.2.a.cc**	$(-\frac{7168085228306}{421875}, \frac{258143089}{1875})$	**101010.cc3**
11	**1540.2.a.a**	$(-\frac{499452032}{27}, \frac{438736}{3})$	**1540.a3**
$\frac{45}{4}$	**493230.2.a.m**	$(-\frac{1135005901381}{55296}, \frac{120949321}{768})$	**493230.m3**
$\frac{23}{2}$	**198030.2.a.bc**	$(-\frac{19631975077}{864}, \frac{8128009}{48})$	**198030.bc3**
$\frac{35}{3}$	**8190.2.a.bq**	$(-\frac{17703460864}{729}, \frac{532736}{3})$	**8190.bq4**
12	**7062.2.a.s**	$(-\frac{746772914}{27}, \frac{584785}{3})$	**7062.s3**
$\frac{61}{5}$	**72590.2.a.a**	$(-\frac{12592868335616}{421875}, \frac{386070784}{1875})$	**72590.a4**
$\frac{49}{4}$	**91770.2.a.be**	$(-\frac{1681996056301}{55296}, \frac{160294201}{768})$	**91770.be6**
$\frac{25}{2}$	**51290.2.a.b**	$(-\frac{28845553789}{864}, \frac{10713241}{48})$	**51290.b3**
$\frac{64}{5}$	**336890.2.a.f**	$(-\frac{15709579574546}{421875}, \frac{452815729}{1875})$	**336890.f3**
13	**4524.2.a.f**	$(-\frac{1079717888}{27}, \frac{762880}{3})$	**4524.f4**
$\frac{53}{4}$	**350966.2.a.a**	$(-\frac{2413508268277}{55296}, \frac{208098025}{768})$	**350966.a3**
$\frac{40}{3}$	**396270.2.a.ep**	$(-\frac{32747945494}{729}, \frac{7470569}{27})$	**396270.ep3**
$\frac{27}{2}$	**7230.2.a.k**	$(-\frac{41089145869}{864}, \frac{13843321}{48})$	**7230.k3**
$\frac{69}{5}$	**53130.2.a.cf**	$(-\frac{22189828284416}{421875}, \frac{581972224}{1875})$	**53130.cf4**
14	**910.2.a.g**	$(-\frac{1516866626}{27}, \frac{977089}{3})$	**910.g3**
$\frac{43}{3}$	**3870.2.a.e**	$(-\frac{45608525824}{729}, \frac{9515264}{27})$	**3870.e4**
$\frac{29}{2}$	**45066.2.a.p**	$(-\frac{56985750613}{864}, \frac{17585065}{48})$	**45066.p3**
15	**28140.2.a.s**	$(-\frac{2078544512}{27}, \frac{1231696}{3})$	**28140.s3**
$\frac{77}{5}$	**99330.2.a.x**	$(-\frac{36608512139264}{421875}, \frac{841156864}{1875})$	**99330.x4**
$\frac{31}{2}$	**498046.2.a.a**	$(-\frac{77212000981}{864}, \frac{22008745}{48})$	**498046.a3**
16	**4290.2.a.bb**	$(-\frac{2786673602}{27}, \frac{1531201}{3})$	**4290.bb6**
$\frac{81}{5}$	**206340.2.a.a**	$(-\frac{46061004763136}{421875}, \frac{998063104}{1875})$	**206340.a4**
$\frac{49}{3}$	**423108.2.a.e**	$(-\frac{82599949696}{729}, \frac{14776400}{27})$	**423108.e3**
17	**646.2.a.b**	$(-\frac{3664584704}{27}, \frac{1880320}{3})$	**646.b4**
$\frac{52}{3}$	**253890.2.a.dh**	$(-\frac{107977284742}{729}, \frac{18077081}{27})$	**253890.dh3**
18	**16422.2.a.x**	$(-\frac{4736790578}{27}, \frac{2283985}{3})$	**16422.x3**
$\frac{93}{5}$	**132990.2.a.q**	$(-\frac{85686325059584}{421875}, \frac{1596561664}{1875})$	**132990.q4**

Continued on the following page

continued			
φ	Modular form label	$\mathcal{E}_F$ Weierstrass coefficients	$\mathcal{E}_F$ label
19	**19380.2.a.i**	$(-\frac{6028720256}{27}, \frac{2747344}{3})$	**19380.i3**
$\frac{59}{3}$	**81774.2.a.r**	$(-\frac{189672841216}{729}, \frac{9276160}{9})$	**81774.r4**
20	**34010.2.a.e**	$(-\frac{7566414482}{27}, \frac{3275761}{3})$	**34010.e3**
$\frac{101}{5}$	**342390.2.a.n**	$(-\frac{123527495622656}{421875}, \frac{2118586624}{1875})$	**342390.n4**
$\frac{81}{4}$	**66990.2.a.bg**	$(-\frac{16368273900973}{55296}, \frac{875182009}{768})$	**66990.bg6**
21	**19740.2.a.w**	$(-\frac{9376182272}{27}, \frac{3874816}{3})$	**19740.w4**
$\frac{85}{4}$	**388110.2.a.j**	$(-\frac{20222389854901}{55296}, \frac{1033290601}{768})$	**388110.j3**
$\frac{64}{3}$	**209718.2.a.bh**	$(-\frac{271199817526}{729}, \frac{36820745}{27})$	**209718.bh3**
22	**91014.2.a.q**	$(-\frac{11484218594}{27}, \frac{4550305}{3})$	**91014.q3**
$\frac{67}{3}$	**6030.2.a.u**	$(-\frac{330956234752}{729}, \frac{43141376}{27})$	**6030.u4**
23	**104236.2.a.c**	$(-\frac{13916183168}{27}, \frac{5308240}{3})$	**104236.c3**
$\frac{117}{5}$	**357630.2.a.cl**	$(-\frac{234144349036544}{421875}, \frac{3522429184}{1875})$	**357630.cl4**
24	**29670.2.a.w**	$(-\frac{16696740386}{27}, \frac{6154849}{3})$	**29670.w3**
$\frac{49}{2}$	**288862.2.a.b**	$(-\frac{583201750573}{864}, \frac{105814585}{48})$	**288862.b3**
25	**210.2.a.b**	$(-\frac{19849060352}{27}, \frac{7096576}{3})$	**210.b6**
$\frac{51}{2}$	**326298.2.a.s**	$(-\frac{690282619741}{864}, \frac{121682905}{48})$	**326298.s3**
26	**30290.2.a.i**	$(-\frac{23394281042}{27}, \frac{8140081}{3})$	**30290.i3**
$\frac{133}{5}$	**198170.2.a.g**	$(-\frac{401841259618304}{421875}, \frac{5511180544}{1875})$	**198170.g4**
27	**1716.2.a.c**	$(-\frac{27350931584}{27}, \frac{9292240}{3})$	**1716.c3**
$\frac{83}{3}$	**231570.2.a.x**	$(-\frac{816074481664}{729}, \frac{30372608}{9})$	**231570.x4**
28	**10542.2.a.p**	$(-\frac{31734316658}{27}, \frac{10560145}{3})$	**10542.p3**
29	**52780.2.a.b**	$(-\frac{36555862016}{27}, \frac{11951104}{3})$	**52780.b4**
$\frac{59}{2}$	**154698.2.a.g**	$(-\frac{1252265115853}{864}, \frac{203121145}{48})$	**154698.g3**
30	**234030.2.a.t**	$(-\frac{41822421122}{27}, \frac{13472641}{3})$	**234030.t3**
$\frac{91}{3}$	**306306.2.a.z**	$(-\frac{1179286233088}{729}, \frac{126091520}{27})$	**306306.z4**
$\frac{153}{5}$	**264180.2.a.s**	$(-\frac{706200797425664}{421875}, \frac{9032157184}{1875})$	**264180.s4**
31	**258540.2.a.f**	$(-\frac{47535542912}{27}, \frac{15132496}{3})$	**258540.f3**
$\frac{125}{4}$	**123310.2.a.a**	$(-\frac{100420020653221}{55296}, \frac{3985919881}{768})$	**123310.a3**
$\frac{157}{5}$	**328130.2.a.b**	$(-\frac{780391212621824}{421875}, \frac{9898088704}{1875})$	**328130.b4**
32	**17794.2.a.f**	$(-\frac{53690700674}{27}, \frac{16938625}{3})$	**17794.f3**

Continued on the following page

continued			
φ	Modular form label	$\mathcal{E}_F$ Weierstrass coefficients	$\mathcal{E}_F$ label
33	**2442.2.a.h**	$(-\frac{60276482048}{27}, \frac{18899200}{3})$	**2442.h4**
34	**342210.2.a.cf**	$(-\frac{67273740146}{27}, \frac{21022609}{3})$	**342210.cf3**
35	**373660.2.a.b**	$(-\frac{74654705792}{27}, \frac{23317456}{3})$	**373660.b3**
$\frac{107}{3}$	**125190.2.a.i**	$(-\frac{2153803866112}{729}, 8315648)$	**125190.i4**
36	**67830.2.a.bz**	$(-\frac{82382060882}{27}, \frac{25792561}{3})$	**67830.bz6**
37	**36852.2.a.g**	$(-\frac{90407972864}{27}, \frac{28456960}{3})$	**36852.g4**
$\frac{189}{5}$	**255990.2.a.bn**	$(-\frac{1515690511671296}{421875}, \frac{19206863104}{1875})$	**255990.bn4**
38	**479446.2.a.r**	$(-\frac{98673090338}{27}, \frac{31319905}{3})$	**479446.r3**
39	**103740.2.a.n**	$(-\frac{107105499776}{27}, \frac{34390864}{3})$	**103740.n3**
40	**140010.2.a.y**	$(-\frac{115619643362}{27}, \frac{37679521}{3})$	**140010.y3**
$\frac{81}{2}$	**344598.2.a.c**	$(-\frac{3836051926381}{864}, \frac{630537145}{48})$	**344598.c3**
41	**9430.2.a.b**	$(-\frac{124115197952}{27}, \frac{41195776}{3})$	**9430.b4**
$\frac{83}{2}$	**371010.2.a.i**	$(-\frac{4106250603037}{864}, \frac{688678489}{48})$	**371010.i3**
$\frac{128}{3}$	**34470.2.a.bi**	$(-\frac{3723561786934}{729}, \frac{142768643}{9})$	**34470.bi3**
$\frac{131}{3}$	**16506.2.a.p**	$(-\frac{3934987706368}{729}, \frac{155288320}{9})$	**16506.p4**
44	**373670.2.a.j**	$(-\frac{148240985906}{27}, \frac{53212369}{3})$	**373670.j3**
$\frac{221}{5}$	**205530.2.a.r**	$(-\frac{2339224763211776}{421875}, \frac{33810290944}{1875})$	**205530.r4**
45	**66660.2.a.g**	$(-\frac{155322232832}{27}, \frac{57742336}{3})$	**66660.g4**
46	**284970.2.a.db**	$(-\frac{161619837122}{27}, \frac{62552641}{3})$	**284970.db3**
48	**121542.2.a.c**	$(-\frac{170981879618}{27}, \frac{73059265}{3})$	**121542.c3**
49	**2310.2.a.u**	$(-\frac{173544513536}{27}, \frac{78778624}{3})$	**2310.u7**
50	**31430.2.a.e**	$(-\frac{174316993202}{27}, \frac{84824401}{3})$	**31430.e3**
51	**233580.2.a.l**	$(-\frac{172981131392}{27}, \frac{91208656}{3})$	**233580.l3**
$\frac{261}{5}$	**254910.2.a.n**	$(-\frac{2626611433250816}{421875}, \frac{62083657984}{1875})$	**254910.n4**
53	**327964.2.a.b**	$(-\frac{162561732608}{27}, \frac{105041920}{3})$	**327964.b4**
54	**154230.2.a.n**	$(-\frac{152687117666}{27}, \frac{112516129}{3})$	**154230.n3**
55	**163020.2.a.o**	$(-\frac{139118713472}{27}, \frac{120379216}{3})$	**163020.o3**
56	**387310.2.a.h**	$(-\frac{121373753762}{27}, \frac{128644321}{3})$	**387310.h3**
57	**798.2.a.d**	$(-\frac{98931482624}{27}, \frac{137324800}{3})$	**798.d4**
60	**136290.2.a.cs**	$(\frac{2394297358}{27}, \frac{165995281}{3})$	**136290.cs3**

Continued on the following page

continued			
φ	Modular form label	$\mathcal{E}_F$ Weierstrass coefficients	$\mathcal{E}_F$ label
64	**4830.2.a.be**	$(\frac{242251704574}{27}, \frac{210885889}{3})$	**4830.be6**
65	**9490.2.a.i**	$(\frac{326184460288}{27}, \frac{223396096}{3})$	**9490.i4**
72	**275622.2.a.h**	$(\frac{1293518287006}{27}, \frac{327119905}{3})$	**275622.h3**
73	**17958.2.a.e**	$(\frac{1500299026432}{27}, \frac{344439040}{3})$	**17958.e4**
76	**389310.2.a.u**	$(\frac{2254347815758}{27}, \frac{400518481}{3})$	**389310.u3**
81	**2730.2.a.bd**	$(\frac{4059342757888}{27}, \frac{508784896}{3})$	**2730.bd6**
82	**181302.2.a.bd**	$(\frac{4519890782926}{27}, \frac{532822225}{3})$	**181302.bd3**
89	**9790.2.a.a**	$(\frac{8952272871424}{27}, \frac{725649664}{3})$	**9790.a4**
96	**491910.2.a.m**	$(\frac{16196039095678}{27}, \frac{966407041}{3})$	**491910.m3**
97	**63438.2.a.d**	$(\frac{17526857261056}{27}, \frac{1005134080}{3})$	**63438.d4**
99	**411180.2.a.m**	$(\frac{20449340577664}{27}, \frac{1086057424}{3})$	**411180.m3**
100	**296670.2.a.ch**	$(\frac{22049566023598}{27}, \frac{1128298801}{3})$	**296670.ch6**

E.2 Totally real number fields and Hilbert modular forms

$\mathbb{Q}(\sqrt{2})$			
φ	Modular form labels		$\mathcal{E}_F$ label
$-10-7\sqrt{2}$	**2.2.8.1-2254.1-f**	**2.2.8.1-2254.2-f**	**2254.1-f2**
$-10+7\sqrt{2}$	**2.2.8.1-2254.1-f**	**2.2.8.1-2254.2-f**	**2254.2-f1**
$-7-8\sqrt{2}$	**2.2.8.1-1106.2-a**	**2.2.8.1-1106.3-a**	**1106.2-a2**
$-7-6\sqrt{2}$	**2.2.8.1-4991.4-e**	**2.2.8.1-4991.5-e**	**4991.4-e2**
$-7-5\sqrt{2}$	**2.2.8.1-644.1-d**	**2.2.8.1-644.4-d**	**644.4-d2**
$-7-4\sqrt{2}$	**2.2.8.1-3196.2-a**	**2.2.8.1-3196.3-a**	**3196.3-a2**
$-7+4\sqrt{2}$	**2.2.8.1-3196.2-a**	**2.2.8.1-3196.3-a**	**3196.2-a2**
$-7+5\sqrt{2}$	**2.2.8.1-644.1-d**	**2.2.8.1-644.4-d**	**644.1-d1**
$-7+6\sqrt{2}$	**2.2.8.1-4991.4-e**	**2.2.8.1-4991.5-e**	**4991.5-e4**
$-7+8\sqrt{2}$	**2.2.8.1-1106.2-a**	**2.2.8.1-1106.3-a**	**1106.3-a3**
$-5-4\sqrt{2}$	**2.2.8.1-3332.1-b**	**2.2.8.1-3332.2-b**	**3332.1-b2**
$-5+4\sqrt{2}$	**2.2.8.1-3332.1-b**	**2.2.8.1-3332.2-b**	**3332.2-b4**
$-4-3\sqrt{2}$	**2.2.8.1-1246.1-d**	**2.2.8.1-1246.4-d**	**1246.1-d2**
$-4+3\sqrt{2}$	**2.2.8.1-1246.1-d**	**2.2.8.1-1246.4-d**	**1246.4-d3**
$-3-2\sqrt{2}$	**2.2.8.1-17.1-a**	**2.2.8.1-17.2-a**	**17.2-a2**
$-3+2\sqrt{2}$	**2.2.8.1-17.1-a**	**2.2.8.1-17.2-a**	**17.1-a1**
$-2-2\sqrt{2}$	**2.2.8.1-574.2-d**	**2.2.8.1-574.3-d**	**574.3-d2**

Continued on the following page

$\mathbb{Q}(\sqrt{2})$, *continued*			
φ	Modular form labels		$\mathcal{E}_F$ label
$-2-1\sqrt{2}$	**2.2.8.1-2786.1-d**	**2.2.8.1-2786.4-d**	**2786.4-d2**
$-2+1\sqrt{2}$	**2.2.8.1-2786.1-d**	**2.2.8.1-2786.4-d**	**2786.1-d2**
$-2+2\sqrt{2}$	**2.2.8.1-574.2-d**	**2.2.8.1-574.3-d**	**574.2-d4**
$-1-2\sqrt{2}$	**2.2.8.1-3836.2-d**	**2.2.8.1-3836.3-d**	**3836.2-d2**
$-1-1\sqrt{2}$	**2.2.8.1-124.1-b**	**2.2.8.1-124.2-b**	**124.1-b2**
$-1+1\sqrt{2}$	**2.2.8.1-124.1-b**	**2.2.8.1-124.2-b**	**124.2-b4**
$-1+2\sqrt{2}$	**2.2.8.1-3836.2-d**	**2.2.8.1-3836.3-d**	**3836.3-d4**
$1-2\sqrt{2}$	**2.2.8.1-511.2-e**	**2.2.8.1-511.3-e**	**511.2-e2**
$1-1\sqrt{2}$	**2.2.8.1-28.1-a**	**2.2.8.1-28.2-a**	**28.1-a2**
$1+1\sqrt{2}$	**2.2.8.1-28.1-a**	**2.2.8.1-28.2-a**	**28.2-a6**
$1+2\sqrt{2}$	**2.2.8.1-511.2-e**	**2.2.8.1-511.3-e**	**511.3-e3**
$2-1\sqrt{2}$	**2.2.8.1-254.1-a**	**2.2.8.1-254.2-a**	**254.2-a4**
$2+1\sqrt{2}$	**2.2.8.1-254.1-a**	**2.2.8.1-254.2-a**	**254.1-a3**
$3-2\sqrt{2}$	**2.2.8.1-28.1-a**	**2.2.8.1-28.2-a**	**28.2-a3**
$3+2\sqrt{2}$	**2.2.8.1-28.1-a**	**2.2.8.1-28.2-a**	**28.1-a5**
$4-3\sqrt{2}$	**2.2.8.1-4194.1-b**	**2.2.8.1-4194.2-b**	**4194.2-b1**
$4-2\sqrt{2}$	**2.2.8.1-1154.1-a**	**2.2.8.1-1154.2-a**	**1154.2-a4**
$4+2\sqrt{2}$	**2.2.8.1-1154.1-a**	**2.2.8.1-1154.2-a**	**1154.1-a2**
$4+3\sqrt{2}$	**2.2.8.1-4194.1-b**	**2.2.8.1-4194.2-b**	**4194.1-b2**
$5-4\sqrt{2}$	**2.2.8.1-1148.2-b**	**2.2.8.1-1148.3-b**	**1148.3-b2**
$5-2\sqrt{2}$	**2.2.8.1-2737.4-e**	**2.2.8.1-2737.5-e**	**2737.5-e3**
$5+2\sqrt{2}$	**2.2.8.1-2737.4-e**	**2.2.8.1-2737.5-e**	**2737.4-e2**
$5+4\sqrt{2}$	**2.2.8.1-1148.2-b**	**2.2.8.1-1148.3-b**	**1148.2-b1**
$6-4\sqrt{2}$	**2.2.8.1-3038.1-d**	**2.2.8.1-3038.2-d**	**3038.1-d6**
$6+4\sqrt{2}$	**2.2.8.1-3038.1-d**	**2.2.8.1-3038.2-d**	**3038.2-d4**
$7-5\sqrt{2}$	**2.2.8.1-2884.2-a**	**2.2.8.1-2884.3-a**	**2884.3-a1**
$7+5\sqrt{2}$	**2.2.8.1-2884.2-a**	**2.2.8.1-2884.3-a**	**2884.2-a1**
$9-8\sqrt{2}$	**2.2.8.1-2914.2-f**	**2.2.8.1-2914.3-f**	**2914.2-f2**
$9-6\sqrt{2}$	**2.2.8.1-639.1-b**	**2.2.8.1-639.2-b**	**639.2-b4**
$9-4\sqrt{2}$	**2.2.8.1-3332.1-d**	**2.2.8.1-3332.2-d**	**3332.2-d6**
$9+4\sqrt{2}$	**2.2.8.1-3332.1-d**	**2.2.8.1-3332.2-d**	**3332.1-d4**
$9+6\sqrt{2}$	**2.2.8.1-639.1-b**	**2.2.8.1-639.2-b**	**639.1-b1**
$9+8\sqrt{2}$	**2.2.8.1-2914.2-f**	**2.2.8.1-2914.3-f**	**2914.3-f1**
$10-7\sqrt{2}$	**2.2.8.1-578.1-b**	**2.2.8.1-578.1-f**	**578.1-f1**
$10+7\sqrt{2}$	**2.2.8.1-578.1-b**	**2.2.8.1-578.1-f**	**578.1-b1**

$\mathbb{Q}(\sqrt{3})$			
φ	Modular form labels		$\mathcal{E}_F$ label
$-9-6\sqrt{3}$	**2.2.12.1-759.1-e**	**2.2.12.1-759.4-e**	**759.1-e2**
$-9+6\sqrt{3}$	**2.2.12.1-759.1-e**	**2.2.12.1-759.4-e**	**759.4-e4**
$-7-4\sqrt{3}$	**2.2.12.1-52.1-b**	**2.2.12.1-52.2-b**	**52.2-b2**
$-7+4\sqrt{3}$	**2.2.12.1-52.1-b**	**2.2.12.1-52.2-b**	**52.1-b1**
$-5-3\sqrt{3}$	**2.2.12.1-426.1-a**	**2.2.12.1-426.2-a**	**426.1-a2**
$-5+3\sqrt{3}$	**2.2.12.1-426.1-a**	**2.2.12.1-426.2-a**	**426.2-a3**
$-3-2\sqrt{3}$	**2.2.12.1-564.1-a**	**2.2.12.1-564.2-a**	**564.1-a2**
$-3+2\sqrt{3}$	**2.2.12.1-564.1-a**	**2.2.12.1-564.2-a**	**564.2-a4**
$-2-2\sqrt{3}$	**2.2.12.1-3666.2-m**	**2.2.12.1-3666.3-m**	**3666.2-m2**
$-2-1\sqrt{3}$	**2.2.12.1-708.1-d**	**2.2.12.1-708.2-d**	**708.1-d2**
$-2+1\sqrt{3}$	**2.2.12.1-708.1-d**	**2.2.12.1-708.2-d**	**708.2-d1**
$-2+2\sqrt{3}$	**2.2.12.1-3666.2-m**	**2.2.12.1-3666.3-m**	**3666.3-m4**
$-1-2\sqrt{3}$	**2.2.12.1-1199.2-e**	**2.2.12.1-1199.3-e**	**1199.3-e2**
$-1-1\sqrt{3}$	**2.2.12.1-286.1-b**	**2.2.12.1-286.4-b**	**286.1-b2**
$-1+1\sqrt{3}$	**2.2.12.1-286.1-b**	**2.2.12.1-286.4-b**	**286.4-b4**
$-1+2\sqrt{3}$	**2.2.12.1-1199.2-e**	**2.2.12.1-1199.3-e**	**1199.2-e3**
$1-1\sqrt{3}$	**2.2.12.1-1074.1-c**	**2.2.12.1-1074.2-c**	**1074.2-c2**
$1+1\sqrt{3}$	**2.2.12.1-1074.1-c**	**2.2.12.1-1074.2-c**	**1074.1-c3**
$2-1\sqrt{3}$	**2.2.12.1-92.1-b**	**2.2.12.1-92.2-b**	**92.2-b3**
$2+1\sqrt{3}$	**2.2.12.1-92.1-b**	**2.2.12.1-92.2-b**	**92.1-b3**
$3-2\sqrt{3}$	**2.2.12.1-111.1-a**	**2.2.12.1-111.2-a**	**111.1-a2**
$3-1\sqrt{3}$	**2.2.12.1-2598.1-d**	**2.2.12.1-2598.2-d**	**2598.2-d4**
$3+1\sqrt{3}$	**2.2.12.1-2598.1-d**	**2.2.12.1-2598.2-d**	**2598.1-d2**
$3+2\sqrt{3}$	**2.2.12.1-111.1-a**	**2.2.12.1-111.2-a**	**111.2-a2**
$4-2\sqrt{3}$	**2.2.12.1-1518.2-e**	**2.2.12.1-1518.3-e**	**1518.2-e6**
$4+2\sqrt{3}$	**2.2.12.1-1518.2-e**	**2.2.12.1-1518.3-e**	**1518.3-e5**
$6-3\sqrt{3}$	**2.2.12.1-3732.1-f**	**2.2.12.1-3732.2-f**	**3732.2-f4**
$6+3\sqrt{3}$	**2.2.12.1-3732.1-f**	**2.2.12.1-3732.2-f**	**3732.1-f1**
$7-4\sqrt{3}$	**2.2.12.1-132.1-b**	**2.2.12.1-132.2-b**	**132.2-b3**
$7+4\sqrt{3}$	**2.2.12.1-132.1-b**	**2.2.12.1-132.2-b**	**132.1-b4**
$8-4\sqrt{3}$	**2.2.12.1-2306.1-c**	**2.2.12.1-2306.2-c**	**2306.1-c4**
$8+4\sqrt{3}$	**2.2.12.1-2306.1-c**	**2.2.12.1-2306.2-c**	**2306.2-c1**
$10-6\sqrt{3}$	**2.2.12.1-4962.1-a**	**2.2.12.1-4962.2-a**	**4962.2-a2**
$10+6\sqrt{3}$	**2.2.12.1-4962.1-a**	**2.2.12.1-4962.2-a**	**4962.1-a1**

$\mathbb{Q}(\sqrt{7})$			
φ	Modular form labels		$\mathcal{E}_F$ label
$-5-2\sqrt{7}$	**2.2.28.1-57.1-d**	**2.2.28.1-57.4-d**	**57.4-d2**
$-5+2\sqrt{7}$	**2.2.28.1-57.1-d**	**2.2.28.1-57.4-d**	**57.1-d3**

Continued on the following page

$\mathbb{Q}(\sqrt{7})$, *continued*			
φ	Modular form labels		$\mathcal{E}_F$ label
$3-1\sqrt{7}$	**2.2.28.1-654.2-b**	**2.2.28.1-654.3-b**	**654.3-b4**
$3+1\sqrt{7}$	**2.2.28.1-654.2-b**	**2.2.28.1-654.3-b**	**654.2-b2**
$5-1\sqrt{7}$	**2.2.28.1-666.1-h**	**2.2.28.1-666.2-h**	**666.2-h6**
$5+1\sqrt{7}$	**2.2.28.1-666.1-h**	**2.2.28.1-666.2-h**	**666.1-h4**

E.3 Imaginary quadratic number fields and Bianchi modular forms

$\mathbb{Q}(\sqrt{-1})$			
φ	Modular form labels		$\mathcal{E}_F$ label
$-7-8\mathrm{i}$	**2.0.4.1-32770.3-a**	**2.0.4.1-32770.6-a**	**32770.3-a1**
$-7+8\mathrm{i}$	**2.0.4.1-32770.3-a**	**2.0.4.1-32770.6-a**	**32770.6-a1**
$-5-2\mathrm{i}$	**2.0.4.1-44225.5-a**	**2.0.4.1-44225.8-a**	**44225.8-a3**
$-5-1\mathrm{i}$	**2.0.4.1-12506.3-a**	**2.0.4.1-12506.4-a**	**12506.3-a3**
$-5+1\mathrm{i}$	**2.0.4.1-12506.3-a**	**2.0.4.1-12506.4-a**	**12506.4-a3**
$-5+2\mathrm{i}$	**2.0.4.1-44225.5-a**	**2.0.4.1-44225.8-a**	**44225.5-a3**
$-3-5\mathrm{i}$	**2.0.4.1-73882.1-a**	**2.0.4.1-73882.8-a**	**73882.1-a1**
$-3-4\mathrm{i}$	**2.0.4.1-1300.3-a**	**2.0.4.1-1300.4-a**	**1300.4-a4**
$-3-2\mathrm{i}$	**2.0.4.1-72020.4-c**	**2.0.4.1-72020.5-b**	**72020.4-c3**
$-3+2\mathrm{i}$	**2.0.4.1-72020.4-c**	**2.0.4.1-72020.5-b**	**72020.5-b3**
$-3+4\mathrm{i}$	**2.0.4.1-1300.3-a**	**2.0.4.1-1300.4-a**	**1300.3-a4**
$-3+5\mathrm{i}$	**2.0.4.1-73882.1-a**	**2.0.4.1-73882.8-a**	**73882.8-a1**
$-2-4\mathrm{i}$	**2.0.4.1-82850.3-b**	**2.0.4.1-82850.4-b**	**82850.3-b2**
$-2-2\mathrm{i}$	**2.0.4.1-17810.1-b**	**2.0.4.1-17810.8-c**	**17810.8-c3**
$-2-1\mathrm{i}$	**2.0.4.1-22100.5-f**	**2.0.4.1-22100.8-f**	**22100.5-f4**
$-2+1\mathrm{i}$	**2.0.4.1-22100.5-f**	**2.0.4.1-22100.8-f**	**22100.8-f4**
$-2+2\mathrm{i}$	**2.0.4.1-17810.1-b**	**2.0.4.1-17810.8-c**	**17810.1-b3**
$-2+4\mathrm{i}$	**2.0.4.1-82850.3-b**	**2.0.4.1-82850.4-b**	**82850.4-b2**
$-1-6\mathrm{i}$	**2.0.4.1-69745.2-a**	**2.0.4.1-69745.15-a**	**69745.2-a2**
$-1-2\mathrm{i}$	**2.0.4.1-265.1-a**	**2.0.4.1-265.4-a**	**265.4-a2**
$-1-1\mathrm{i}$	**2.0.4.1-1810.2-b**	**2.0.4.1-1810.3-b**	**1810.2-b4**
$-1+1\mathrm{i}$	**2.0.4.1-1810.2-b**	**2.0.4.1-1810.3-b**	**1810.3-b4**
$-1+2\mathrm{i}$	**2.0.4.1-265.1-a**	**2.0.4.1-265.4-a**	**265.1-a2**
$-1+6\mathrm{i}$	**2.0.4.1-69745.2-a**	**2.0.4.1-69745.15-a**	**69745.15-a2**
$0-4\mathrm{i}$	**2.0.4.1-44098.1-b**	**2.0.4.1-44098.4-b**	**44098.4-b2**
$0-3\mathrm{i}$	**2.0.4.1-65700.3-b**	**2.0.4.1-65700.4-b**	**65700.4-b3**
$0-2\mathrm{i}$	**2.0.4.1-650.3-a**	**2.0.4.1-650.4-a**	**650.4-a7**
$0-1\mathrm{i}$	**2.0.4.1-164.1-a**	**2.0.4.1-164.2-a**	**164.2-a1**
$0+1\mathrm{i}$	**2.0.4.1-164.1-a**	**2.0.4.1-164.2-a**	**164.1-a1**

Continued on the following page

$\mathbb{Q}(\sqrt{-1})$, *continued*			
φ	Modular form labels		$\mathcal{E}_F$ label
$0+2\mathrm{i}$	**2.0.4.1-650.3-a**	**2.0.4.1-650.4-a**	**650.3-a7**
$0+3\mathrm{i}$	**2.0.4.1-65700.3-b**	**2.0.4.1-65700.4-b**	**65700.3-b3**
$0+4\mathrm{i}$	**2.0.4.1-44098.1-b**	**2.0.4.1-44098.4-b**	**44098.1-b2**
$1-8\mathrm{i}$	**2.0.4.1-5330.2-b**	**2.0.4.1-5330.7-b**	**5330.7-b4**
$1-4\mathrm{i}$	**2.0.4.1-5780.2-a**	**2.0.4.1-5780.5-b**	**5780.2-a3**
$1-3\mathrm{i}$	**2.0.4.1-71370.4-e**	**2.0.4.1-71370.5-e**	**71370.5-e2**
$1-2\mathrm{i}$	**2.0.4.1-1940.2-a**	**2.0.4.1-1940.3-a**	**1940.2-a3**
$1-1\mathrm{i}$	**2.0.4.1-290.2-a**	**2.0.4.1-290.3-a**	**290.3-a3**
$1+1\mathrm{i}$	**2.0.4.1-290.2-a**	**2.0.4.1-290.3-a**	**290.2-a3**
$1+2\mathrm{i}$	**2.0.4.1-1940.2-a**	**2.0.4.1-1940.3-a**	**1940.3-a3**
$1+3\mathrm{i}$	**2.0.4.1-71370.4-e**	**2.0.4.1-71370.5-e**	**71370.4-e2**
$1+4\mathrm{i}$	**2.0.4.1-5780.2-a**	**2.0.4.1-5780.5-b**	**5780.5-b3**
$1+8\mathrm{i}$	**2.0.4.1-5330.2-b**	**2.0.4.1-5330.7-b**	**5330.2-b4**
$2-2\mathrm{i}$	**2.0.4.1-6130.2-b**	**2.0.4.1-6130.3-b**	**6130.2-b1**
$2-1\mathrm{i}$	**2.0.4.1-3700.3-a**	**2.0.4.1-3700.4-a**	**3700.4-a2**
$2+1\mathrm{i}$	**2.0.4.1-3700.3-a**	**2.0.4.1-3700.4-a**	**3700.3-a2**
$2+2\mathrm{i}$	**2.0.4.1-6130.2-b**	**2.0.4.1-6130.3-b**	**6130.3-b1**
$3-4\mathrm{i}$	**2.0.4.1-49300.6-a**	**2.0.4.1-49300.7-a**	**49300.6-a2**
$3-2\mathrm{i}$	**2.0.4.1-65.2-a**	**2.0.4.1-65.3-a**	**65.3-a2**
$3-1\mathrm{i}$	**2.0.4.1-37850.3-a**	**2.0.4.1-37850.4-a**	**37850.4-a4**
$3+1\mathrm{i}$	**2.0.4.1-37850.3-a**	**2.0.4.1-37850.4-a**	**37850.3-a4**
$3+2\mathrm{i}$	**2.0.4.1-65.2-a**	**2.0.4.1-65.3-a**	**65.2-a2**
$3+4\mathrm{i}$	**2.0.4.1-49300.6-a**	**2.0.4.1-49300.7-a**	**49300.7-a2**
$4-4\mathrm{i}$	**2.0.4.1-25210.1-c**	**2.0.4.1-25210.4-c**	**25210.4-c2**
$4+4\mathrm{i}$	**2.0.4.1-25210.1-c**	**2.0.4.1-25210.4-c**	**25210.1-c2**
$5-4\mathrm{i}$	**2.0.4.1-16564.1-a**	**2.0.4.1-16564.4-a**	**16564.1-a3**
$5+4\mathrm{i}$	**2.0.4.1-16564.1-a**	**2.0.4.1-16564.4-a**	**16564.4-a3**
$7-6\mathrm{i}$	**2.0.4.1-49725.5-c**	**2.0.4.1-49725.8-c**	**49725.8-c4**
$7+6\mathrm{i}$	**2.0.4.1-49725.5-c**	**2.0.4.1-49725.8-c**	**49725.5-c4**
$9-8\mathrm{i}$	**2.0.4.1-52490.3-a**	**2.0.4.1-52490.6-a**	**52490.3-a4**
$9+8\mathrm{i}$	**2.0.4.1-52490.3-a**	**2.0.4.1-52490.6-a**	**52490.6-a4**

$\mathbb{Q}(\sqrt{-2})$			
φ	Modular form labels		$\mathcal{E}_F$ label
$-7-4\sqrt{-2}$	**2.0.8.1-7524.5-c**	**2.0.8.1-7524.8-c**	**7524.5-c3**
$-7+4\sqrt{-2}$	**2.0.8.1-7524.5-c**	**2.0.8.1-7524.8-c**	**7524.8-c3**
$-4-1\sqrt{-2}$	**2.0.8.1-27558.3-d**	**2.0.8.1-27558.4-d**	**27558.4-d3**
$-4+1\sqrt{-2}$	**2.0.8.1-27558.3-d**	**2.0.8.1-27558.4-d**	**27558.3-d3**
$-3-2\sqrt{-2}$	**2.0.8.1-9129.1-a**	**2.0.8.1-9129.8-a**	**9129.8-a3**

Continued on the following page

$\mathbb{Q}(\sqrt{-2})$, *continued*			
φ	Modular form labels		$\mathcal{E}_F$ label
$-3+2\sqrt{-2}$	**2.0.8.1-9129.1-a**	**2.0.8.1-9129.8-a**	**9129.1-a3**
$-2-1\sqrt{-2}$	**2.0.8.1-34518.3-b**	**2.0.8.1-34518.6-b**	**34518.6-b4**
$-2+1\sqrt{-2}$	**2.0.8.1-34518.3-b**	**2.0.8.1-34518.6-b**	**34518.3-b4**
$-1-2\sqrt{-2}$	**2.0.8.1-6732.6-a**	**2.0.8.1-6732.7-a**	**6732.6-a5**
$-1-1\sqrt{-2}$	**2.0.8.1-4716.3-b**	**2.0.8.1-4716.4-b**	**4716.4-b2**
$-1+1\sqrt{-2}$	**2.0.8.1-4716.3-b**	**2.0.8.1-4716.4-b**	**4716.3-b2**
$-1+2\sqrt{-2}$	**2.0.8.1-6732.6-a**	**2.0.8.1-6732.7-a**	**6732.7-a5**
$0-2\sqrt{-2}$	**2.0.8.1-3894.2-a**	**2.0.8.1-3894.7-a**	**3894.7-a3**
$0-1\sqrt{-2}$	**2.0.8.1-978.2-a**	**2.0.8.1-978.3-a**	**978.2-a3**
$0+1\sqrt{-2}$	**2.0.8.1-978.2-a**	**2.0.8.1-978.3-a**	**978.3-a3**
$0+2\sqrt{-2}$	**2.0.8.1-3894.2-a**	**2.0.8.1-3894.7-a**	**3894.2-a3**
$1-8\sqrt{-2}$	**2.0.8.1-42054.1-b**	**2.0.8.1-42054.8-b**	**42054.1-b4**
$1-4\sqrt{-2}$	**2.0.8.1-10956.2-a**	**2.0.8.1-10956.7-a**	**10956.7-a3**
$1-2\sqrt{-2}$	**2.0.8.1-267.2-a**	**2.0.8.1-267.3-a**	**267.2-a2**
$1-1\sqrt{-2}$	**2.0.8.1-1356.1-a**	**2.0.8.1-1356.4-a**	**1356.4-a3**
$1+1\sqrt{-2}$	**2.0.8.1-1356.1-a**	**2.0.8.1-1356.4-a**	**1356.1-a3**
$1+2\sqrt{-2}$	**2.0.8.1-267.2-a**	**2.0.8.1-267.3-a**	**267.3-a2**
$1+4\sqrt{-2}$	**2.0.8.1-10956.2-a**	**2.0.8.1-10956.7-a**	**10956.2-a3**
$1+8\sqrt{-2}$	**2.0.8.1-42054.1-b**	**2.0.8.1-42054.8-b**	**42054.8-b4**
$2-2\sqrt{-2}$	**2.0.8.1-16866.3-d**	**2.0.8.1-16866.4-d**	**16866.4-d1**
$2-1\sqrt{-2}$	**2.0.8.1-8118.6-g**	**2.0.8.1-8118.7-g**	**8118.6-g2**
$2+1\sqrt{-2}$	**2.0.8.1-8118.6-g**	**2.0.8.1-8118.7-g**	**8118.7-g2**
$2+2\sqrt{-2}$	**2.0.8.1-16866.3-d**	**2.0.8.1-16866.4-d**	**16866.3-d1**
$5-2\sqrt{-2}$	**2.0.8.1-31977.9-a**	**2.0.8.1-31977.16-a**	**31977.9-a4**
$5-1\sqrt{-2}$	**2.0.8.1-37764.3-a**	**2.0.8.1-37764.4-a**	**37764.4-a3**
$5+1\sqrt{-2}$	**2.0.8.1-37764.3-a**	**2.0.8.1-37764.4-a**	**37764.3-a3**
$5+2\sqrt{-2}$	**2.0.8.1-31977.9-a**	**2.0.8.1-31977.16-a**	**31977.16-a4**

Appendix F

Monodromy Around Large Complex Structure Points

Upon circling the large complex structure point $\varphi = 0$, the t-coordinate changes by $t \to t + 1$. This can be thought of as a consequence of the transformation $\Pi \to \mathrm{M}\Pi$, of the period vector, with

$$\mathrm{M} \;=\; \begin{pmatrix} 1 & -1 & \frac{1}{6}Y_{111} - Y_{100} & \frac{1}{2}Y_{111} - Y_{110} \\ 0 & 1 & -\frac{1}{2}Y_{111} - Y_{110} & -Y_{111} \\ 0 & 0 & 1 & 0 \\ 0 & 0 & 1 & 1 \end{pmatrix} \;=\; \exp \mathrm{L}\ ,$$

where

$$\mathrm{L} \;=\; \begin{pmatrix} 0 & -1 & -Y_{100} & -Y_{110} \\ 0 & 0 & -Y_{110} & -Y_{111} \\ 0 & 0 & 0 & 0 \\ 0 & 0 & 1 & 0 \end{pmatrix}.$$

Note that $L^4 = 0$ so the exponential is in fact a short finite sum. In these equations, we take the Y_{ijk} to be the minimal Y_{ijk} used previously, and M is understood not to act on these. On the charge vector, the action of the monodromy is

$$Q^{(n)} \stackrel{\mathrm{def}}{=} \mathrm{M}^n \begin{pmatrix} q_0 \\ q \\ p^0 \\ p \end{pmatrix} = \exp(n\mathrm{L}) \begin{pmatrix} q_0 \\ q \\ p^0 \\ p \end{pmatrix} = \begin{pmatrix} \left(\frac{n^3}{6}Y - nY_{100}\right)p^0 + \left(\frac{n^2}{2}Y - nY_{110}\right)p - nq + q_0 \\ -\left(\frac{n^2}{2}Y + nY_{110}\right)p^0 - nYp + q \\ p^0 \\ np^0 + p \end{pmatrix}.$$

The monodromy matrix M is symplectic and the central charge depends on the period and charge vectors only through the symplectic invariant inner product, so the central charge is invariant under the monodromy. It follows that if t is an attractor point corresponding to a charge vector $Q^{(0)}$, then $t + n$ is the coordinate of an attractor point corresponding to the charge vector $Q^{(n)}$. In virtue of this, the entire discussion of the D6 system in §13.2 can be extended to include a restricted set of D4 charges.

F.1 D4-D2-D0 system

The monodromy preserves p^0, and so in particular the condition $p^0 = 0$. In this case the monodromy can be thought of as acting on the charge ratios as

$$\Lambda^{(n)} \;=\; \Lambda^{(0)} + \frac{n^2}{2} Y - n\left(Y_{110} + \Upsilon^{(0)}\right), \qquad \Upsilon^{(n)} \;=\; \Upsilon^{(0)} - nY \;.$$

Since we have in §13.1.2 found an expression for the coordinates x, y of the attractor point in terms of these charges, it is interesting to follow how this transformation gives rise to the coordinate transformation $x \to x+n$, $y \to y$. First note that it follows from the transformation above that the quantities α and $\widetilde{\beta}$ transform so that

$$\widetilde{\beta} \;\to\; \sqrt{\widetilde{\beta}^2 + n^2 + 2n\alpha\widetilde{\beta}}\,, \qquad \alpha\widetilde{\beta} \;\to\; \alpha\widetilde{\beta} + n \;.$$

It follows that $\widetilde{\beta}\sqrt{\alpha^2-1}$ is invariant. Thus the perturbative coordinates transform as

$$x_0 \;=\; \alpha\widetilde{\beta} \;\to\; \alpha\widetilde{\beta} + n \;=\; x_0 + n \;, \qquad y_0 \;=\; 2\widetilde{\beta}\sqrt{\alpha^2-1}\sin\theta \;\to\; y_0 \;.$$

To see that θ is invariant under the monodromy, note that this is required by the definition (13.9), together with the above transformation laws.

The instanton corrections are not expected to modify these transformations and this is indeed the case as $R^x_{\mathfrak{p}}$ and $R^y_{\mathfrak{p}}$ depend on x_0 only via $\cos(2m\pi x_0)$ or $\sin(2m\pi x_0)$ with $m \in \mathbb{Z}$.

F.2 D6-D2-D0 system

A charge vector with $p \;=\; 0$ maps in general to a vector $p \;\neq\; 0$. The charge ratios transform as

$$\Lambda^{(n)} \;=\; \Lambda^{(0)} + \frac{n^3}{6} Y - n(\Upsilon^{(0)} - Y_{100}) \;, \qquad \Upsilon^{(n)} \;=\; \Upsilon^{(0)} - \frac{n^2}{2} Y - nY_{110} \;.$$

Thus, by choosing $\Lambda^{(0)}$ and $\Upsilon^{(0)}$ suitably, we can always have arbitrary values for the first two components. The third component is kept fixed, and the last component is an integer multiple of p^0, the value of the third component. Conversely, given any charge of this form, we can always find a monodromy that transforms it into the form where $p = 0$. So the solutions in §13.2 relate to charge vectors of the form

$$Q \;=\; \begin{pmatrix} q_0 \\ q \\ p^0 \\ p \end{pmatrix}, \qquad \text{with } p^0 \mid p \;\text{ or } p^0 \;=\; 0 \;.$$

Appendix G

The perturbative equations for the D6 system

G.1 The orthogonality equation

The equations (13.14) can also be solved for y_0 as a power series in σ. There are a number of cases that require separate consideration. These, together with the corresponding zeroth-order solutions, are listed in table G.1.

Charge data	x_{00}	y_{00}	**Definition of ν**
$\beta \in \mathbb{R}^+$, $\gamma > 1$	$\beta \cosh \nu$	$\sqrt{3}\beta \sinh \nu$	$\nu = \frac{1}{3} \cosh^{-1} \gamma$
$\beta \in \mathbb{R}^+$, $\gamma < -1$	$-\beta \cosh \nu$	$\sqrt{3}\beta \sinh \nu$	$\nu = \frac{1}{3} \cosh^{-1} -\gamma$
$\beta = \mathrm{i}\mathbb{R}^+$	$\lvert\beta\rvert \sinh \nu$	$\sqrt{3}\lvert\beta\rvert \cosh \nu$	$\nu = \frac{1}{3} \sinh^{-1} \operatorname{Im} \gamma$
$\beta = 0$	$\frac{\nu}{2} \lvert 2\beta^3\gamma\rvert^{1/3}$	$\frac{\sqrt{3}}{2} \lvert 2\beta^3\gamma\rvert^{1/3}$	$\nu = \operatorname{sign} \beta^3\gamma$

Table G.1: *Solutions for x_{00} and y_{00} with $y_{00} > 0$. All the inverse trigonometric functions appearing in the table are understood to have their values in the principal branch. The case $|\gamma| < 1$ does not appear in the table as there are no such solutions with $\operatorname{Im} t_0 > 0$.*

The σ-expansions can be given around these solutions. In this context, let us write $P_n(z)$ for the Jacobi polynomial $P_n^{(\frac{1}{3},-\frac{1}{3})}(z)$.

Additionally, define the quantity

$$\mathrm{T}(k) \;=\; 2\frac{d^k}{dz^k} \sin(z)\bigg|_{z=\frac{2\pi}{3}} \;=\; \begin{cases} \sqrt{3}\,, & k \;=\; 0 \bmod 4 \\ -1\,, & k \;=\; 1 \bmod 4 \\ -\sqrt{3}\,, & k \;=\; 2 \bmod 4 \\ 1\,, & k \;=\; 3 \bmod 4. \end{cases}$$

We show in the next subsection G.1.1 that when β is real

$$\frac{y_0}{\beta} \;=\; \sqrt{3}\sinh\nu + \sum_{n=1}^{\infty} \frac{\mathrm{T}(n)}{6n} \Big[\mathrm{e}^{\nu} P_{n-1}\big(-\coth 3\nu\big) - \mathrm{e}^{-\nu} P_{n-1}\big(\coth 3\nu\big) \Big] \left(\frac{\sigma}{\beta^3 \sinh 3\nu} \right)^n . \qquad \text{(G.1)}$$

In the case where $\beta \in \mathrm{i}\mathbb{R}^+$, there is a similar expression

$$\frac{y_0}{|\beta|} \;=\; \sqrt{3}\cosh\nu + \sum_{n=1}^{\infty} \frac{\mathrm{T}(n)}{6n} \Big[\mathrm{e}^{\nu} P_{n-1}\big(-\tanh 3\nu\big) + \mathrm{e}^{-\nu} P_{n-1}\big(\tanh 3\nu\big) \Big] \left(\frac{\sigma}{|\beta|^3 \cosh 3\nu} \right)^n . \qquad \text{(G.2)}$$

In the β=0 case, we have that

$$t_{00} \;=\; \exp\left[\left(1-\frac{\nu}{3}\right)\frac{\pi\mathrm{i}}{2}\right]\left(\frac{6|\Lambda|}{Y}\right)^{1/3}, \quad t_0 \;=\; t_{00}\left(1+\frac{\mathrm{i}Y\sigma}{3\Lambda}\right)^{1/3},$$

which can be expanded in σ. Picking out the imaginary part, we can write

$$y_0 \;=\; \left(\frac{3|\Lambda|}{4Y}\right)^{1/3}\sum_{n=0}^{\infty}\mathrm{T}(n)\frac{\left(-\frac{1}{3}\right)_n}{n!}\left(-\frac{\sigma Y}{3|\Lambda|}\right)^n.$$

After solving for y_0, the σ-expansions for x_0 can be easily obtained. After separating the equation (13.15) into its real and imaginary parts, one of these will be a quadratic equation for x_0. Precisely which one is quadratic depends on the phase of β. Solving this gives

$$x_0 \;=\; \pm\sqrt{\beta^2+\frac{y_0^3+2\sigma}{3y_0}}\,,$$

where the $\pm$ sign is chosen so that consistency with table G.1 is maintained in the $\sigma\to 0$ limit.

G.1.1 The σ-expansion

The real and imaginary parts of the D6 orthogonality equation (13.15) in the case $\beta\in\mathbb{R}$ are such that, after defining $\widehat{y}=\frac{y_0}{\beta}$, the parameter β disappears from the equation, leaving a pair of equations for x_0 and $\widehat{y}$. Eliminating x_0, one arrives at the single equation

$$\left(3\widehat{y}+4\widehat{y}^3-\widehat{\sigma}\right)^2\left(3\widehat{y}+\widehat{y}^3+2\widehat{\sigma}\right)-27\,\widehat{y}^3\cosh^2 3\nu \;=\; 0\,,$$

Informed by a certain amount of experimentation, we make the following ansatz for $\widehat{y}$:

$$\widehat{y} \;=\; -\sinh 3\nu\,\mathrm{e}^{-2\nu}\sum_{m=0}^{\infty}\mathrm{T}(m)\Psi_m(\mathrm{e}^{-2\nu})\left(-\frac{\widehat{\sigma}\,\mathrm{e}^{3\nu}}{2\sinh^2 3\nu}\right)^m.$$

The function $\Psi_0(z)$ is special, and is found to be $-(1+z+z^2)^{-1}$. For $m\geq 1$, the $\Psi_m(z)$ are polynomials of degree $3m-2$. The first few are

$$\begin{aligned}
\Psi_1(z) &= \tfrac{1}{3}\;(1-z)\;,\\
\Psi_2(z) &= \tfrac{1}{3^2}\;\left(1+2z+2z^3+z^4\right)\;,\\
\Psi_3(z) &= \tfrac{1}{3^4}\;\left(5-14z+35z^3-35z^4+14z^6-5z^7\right)\;,\\
\Psi_4(z) &= \tfrac{1}{3^5}\;\left(10+35z+150z^3+210z^4+210z^6+150z^7+35z^9+10z^{10}\right)\;,\\
\Psi_5(z) &= \tfrac{1}{3^6}\;\left(22-91z+572z^3-1001z^4+1716z^6-1716z^7+1001z^9-572z^{10}+91z^{12}-22z^{13}\right)\;.
\end{aligned}$$

The coefficients are symmetrically distributed and for odd m, the polynomial $\Psi_m(z)$ has a factor of $(1-z)^{2m-1}$. Most importantly for us, the polynomials only contain powers of z that are 0 or 1 mod 3. The Ψ_m are thus naturally divided into two polynomials in z^3.

Recognising a pattern in the coefficients, we see that

$$\Psi_m(z) = \frac{1}{m!}\left[-\left(-\tfrac{1}{3}\right)_m {}_2F_1\left(\begin{matrix}\frac{2}{3}-m,\,1-m\\ \frac{2}{3}\end{matrix};\,z^3\right) + (-1)^m\left(\tfrac{1}{3}\right)_m z\,{}_2F_1\left(\begin{matrix}\frac{4}{3}-m,\,1-m\\ \frac{4}{3}\end{matrix};\,z^3\right)\right]$$

$$= \frac{(1-z^3)^{m-1}}{3\,m!}\left[\left(\tfrac{2}{3}\right)_{m-1} {}_2F_1\left(\begin{matrix}m,\,1-m\\ \frac{2}{3}\end{matrix};-\frac{z^3}{1-z^3}\right) + (-1)^m\left(\tfrac{4}{3}\right)_{m-1} z\,{}_2F_1\left(\begin{matrix}m,\,1-m\\ \frac{4}{3}\end{matrix};-\frac{z^3}{1-z^3}\right)\right].$$

In passing to the second line, we have written this expression in a form where it is easy to recognise that the hypergeometric functions are in fact related to Jacobi polynomials $P_m^{(\frac{1}{3},-\frac{1}{3})}$ as [123]

$$P_n^{(\alpha,\beta)}(z) \;=\; \frac{(\alpha+1)_n}{n!}\,{}_2F_1\left(\begin{matrix}1+\alpha+\beta+n\,,\,-n\\ \alpha+1\end{matrix};\frac{1-z}{2}\right).$$

Writing $z = \mathrm{e}^{-2\nu}$, we arrive at (G.1). The other series (G.2) can be obtained from this.

G.2 The alignment equations

In this section, we solve the quartic equation (13.22),

$$(\widehat{y}^2-1)(\widehat{y}-\widehat{\sigma})^2 + \gamma^2\widehat{y}^2 \;=\; 0 \tag{G.3}$$

in terms of radicals, and also as an expansion around $\sigma = 0$. The highest term in this quartic is $\widehat{y}^4$, and the constant term is $-\widehat{\sigma}^2$, so the product of the four roots of this equation is $-\widehat{\sigma}^2 \le 0$.

We are interested in solutions of (G.3) with a positive imaginary part, and how the number of these solutions varies as a function of $\widehat{\sigma}$. Any quartic polynomial with real coefficients has an associated discriminant D_4, which for the polynomial in (G.3) is

$$D_4 \;=\; 16\,\gamma^2\widehat{\sigma}^2\left(\left(1-\gamma^2-\widehat{\sigma}^2\right)^3 - 27\gamma^2\widehat{\sigma}^2\right).$$

When D_4 is positive, the quartic has either four or no real roots, while when D_4 is negative the quartic has precisely two real solutions.

When $|\gamma| \ge 1$, this discriminant is negative for all $\widehat{\sigma}$, so there are two real solutions to (G.3), and by the earlier observation that the product of the roots is $-\widehat{\sigma}^2$, precisely one of these is positive. This leaves the case $|\gamma| = \cos\phi_{00} < 1$. When $\widehat{\sigma} = 0$, the quartic has four real roots. These are $\pm\sin\phi_{00}$ and 0, the latter with multiplicity two. When $\widehat{\sigma}$ is small but non-vanishing, the solutions $\pm\sin\phi_{00}$ are perturbed slightly and both of the previously vanishing solutions become nonzero.

Since a root can only vanish when $\widehat{\sigma} = 0$, these new nonzero roots cannot change sign as $|\widehat{\sigma}|$ increases. Furthermore, the four roots multiplied together give a negative number. There is always at least one positive and one negative root, so the both newly nonzero roots must have the same sign. To the leading order in $\widehat{\sigma}$, these solutions are

$$\widehat{y} \;=\; \frac{\widehat{\sigma}}{1-\gamma} + \mathcal{O}\left(\widehat{\sigma}^2\right)\;, \qquad \widehat{y} \;=\; \frac{\widehat{\sigma}}{1+\gamma} + \mathcal{O}\left(\widehat{\sigma}^2\right)\;.$$

So, irrespective of the value of ϕ_{00}, the newly nonzero solutions have both the same sign as $\widehat{\sigma}$.

The sign of D_4 is determined by the cubic

$$d(\phi_{00},\xi) \stackrel{\text{def}}{=} \left.\frac{D_4}{16\gamma^2\widehat{\sigma}^2}\right|_{\widehat{\sigma}^2=\xi} = \left(\sin^2\phi_{00}-\xi\right)^3 - 27\cos^2\phi_{00}\,\xi\ .$$

For all $\phi_{00}\in(0,\pi)$, the quantity $d(\phi_{00},\xi)$ is monotonically decreasing as a function of ξ. Such a monotonic cubic has one real root, which is located at

$$\left(1-|\gamma|^{2/3}\right)^3 \stackrel{\text{def}}{=} \Xi(\gamma)^2\ .$$

The sign of D_4 changes when $\widehat{\sigma}^2=\Xi(\gamma)^2$. When $\widehat{\sigma}=\Xi(\gamma)$, the solution flowing from $\sin\phi_{00}$ meets the larger solution that vanishes at $\widehat{\sigma}=0$. For larger $\widehat{\sigma}$, they both become nonreal, and so lose relevance for us. The solution flowing from $\sin\phi_{00}$ remains a solution for every negative value of $\widehat{\sigma}$.

Case	**Topological/charge data**	**Solutions with $y_0>0$**
i	$\lvert\gamma\rvert\geq 1,\quad \widehat{\sigma}=0$	none
ii	$\lvert\gamma\rvert\geq 1,\quad \widehat{\sigma}\neq 0$	y_0^*
iii	$\lvert\gamma\rvert< 1,\quad \widehat{\sigma}\leq 0$	y_0
iv	$\lvert\gamma\rvert< 1,\quad 0<\widehat{\sigma}<\Xi(\gamma)$	$y_0,\ y_0^\pm$
v	$\lvert\gamma\rvert< 1,\quad \widehat{\sigma}=\Xi(\gamma)$	$y_0^\pm$
vi	$\lvert\gamma\rvert< 1,\quad \widehat{\sigma}>\Xi(\gamma)$	y_0^+ or y_0^-

Table G.2: *Solutions to the alignment equations in different cases. The quantities y_0, $y_0^\pm$ and y_0^* are defined in* (G.4), (G.5), *and* (G.6).

We illustrate the cases in table G.2 with plots clarifying the changes in the number of solutions. The locus defined by the second equation in (13.20) is a circle, while the first corresponds to a hyperbola with asymptotes $\widehat{x}=\widehat{\sigma}$ and $\widehat{y}=\gamma$. Note the progression iv→v→vi for increasing positive $\widehat{\sigma}$.

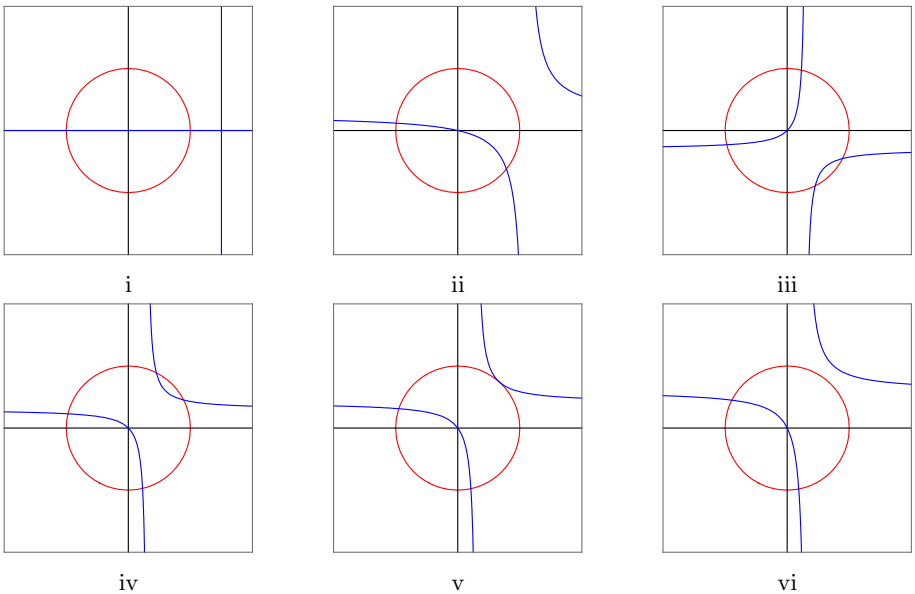


Figure G.1: *Illustrations of the conic intersections. The black lines are the coordinate axes $\widehat{x}=0$ and $\widehat{y}=0$. Our interest is in the solutions with positive $\widehat{y}$, that is, the intersections above the $\widehat{x}$-axis.*

When $\widehat{\sigma} = 0$ and $|\gamma| < 1$, the hyperbola is degenerate and intersects the circle once in the upper half plane. Turning $\widehat{\sigma}$ on will perturb this solution. For a small positive $\widehat{\sigma}$ this perturbed solution is the uppermost point of intersection in the figure iv.

The simplest expression for the root y_0 that becomes y_{00} when $\sigma = 0$ is

$$\frac{2y_0}{\beta} = \widehat{\sigma} + \sqrt{Q_2 + \widehat{\sigma}^2} + \sqrt{2\sin^2\phi_{00} - Q_2 - \frac{2\widehat{\sigma}\left(2 - \sin^2\phi_{00}\right)}{\sqrt{Q_2 + \widehat{\sigma}^2}}}\,, \tag{G.4}$$

where Q_1 and Q_2 are auxiliary quantities with

$$\begin{aligned} Q_1 &= \frac{3}{\sin^2\phi_{00} - \widehat{\sigma}^2}\left(\widehat{\sigma}\cos\phi_{00} + \mathrm{i}\sqrt{\left(\frac{\sin^2\phi_{00} - \widehat{\sigma}^2}{3}\right)^3 - \widehat{\sigma}^2\cos^2\phi_{00}}\right)^{2/3}, \\ Q_2 &= \frac{\sin^2\phi_{00} - \widehat{\sigma}^2}{3}\left(Q_1 + 2 + \frac{1}{Q_1}\right). \end{aligned}$$

The branch of the function $z^{1/3}$ is chosen to be $|z|^{1/3}\mathrm{e}^{\mathrm{i}\arg(z)/3}$, with $-\pi < \arg(z) \le \pi$.

The two additional solutions in the case iv are given by

$$\frac{2y_0^{\pm}}{\beta} = \widehat{\sigma} - \sqrt{Q_2^{\pm} + \widehat{\sigma}^2} + \sqrt{2\sin^2\phi_{00} - Q_2^{\pm} + \frac{2\widehat{\sigma}\left(2 - \sin^2\phi_{00}\right)}{\sqrt{Q_2^{\pm} + \widehat{\sigma}^2}}}\,, \tag{G.5}$$

with

$$\begin{aligned} Q_1^{\pm} &= \frac{3}{\sin^2\phi_{00} - \widehat{\sigma}^2}\left(\pm\widehat{\sigma}\cos\phi_{00} + \mathrm{i}\sqrt{\left|\frac{\sin^2\phi_{00} - \widehat{\sigma}^2}{3}\right|^3 - \widehat{\sigma}^2\cos^2\phi_{00}}\right)^{2/3}, \\ Q_2^{\pm} &= \frac{\sin^2\phi_{00} - \widehat{\sigma}^2}{3}\left(Q_1^{\pm} + 2 + \frac{1}{Q_1^{\pm}}\right). \end{aligned}$$

At the critical value $\widehat{\sigma} = \Xi(\gamma)$ the larger[1] of these becomes equal to solution (G.4), which is the case v in table G.2. For $\widehat{\sigma} > \Xi(\gamma)$ one of these is no longer real and we enter the case vi with the real member of this pair giving the only solution.

In the case ii where $|\gamma| \ge 1$ and $\widehat{\sigma} \ne 0$, there is always a single relevant solution y_0^* given by

$$\frac{2y_0^*}{\beta} = \widehat{\sigma} - \mathrm{sign}(\sigma)\sqrt{Q_2^* + \widehat{\sigma}^2} + \sqrt{\frac{2|\widehat{\sigma}|(2 + \sinh^2\varphi)}{\sqrt{Q_2^* + \widehat{\sigma}^2}} - 2\sinh^2\varphi - Q_2^*}\,, \tag{G.6}$$

where

$$\begin{aligned} \gamma &= \pm\cosh\varphi, \\ Q_1^* &= \frac{3}{\sinh^2\varphi + \widehat{\sigma}^2}\left(-\widehat{\sigma}\cosh\varphi + \sqrt{\left(\frac{\sinh^2\varphi + \widehat{\sigma}^2}{3}\right)^3 + \widehat{\sigma}^2\cosh^2\varphi}\right)^{2/3}, \\ Q_2^* &= \frac{\sinh^2\varphi + \widehat{\sigma}^2}{3}\left(Q_1^* - 2 + \frac{1}{Q_1^*}\right). \end{aligned} \tag{G.7}$$

[1] $y_0^- > y_0^+$ if and only if $\cos\phi_{00} > 0$.

In any nondegenerate case with $\widehat{\sigma} \neq 0$, a value for y_0 singles out one point on the relevant hyperbola in figure G.1, which uniquely specifies the value of x_0:

$$x_0 \;=\; \frac{\beta\gamma y_0}{y_0 - \beta\widehat{\sigma}} \;. \tag{G.8}$$

G.2.1 The σ-expansion

While we ultimately want to solve the equation (G.3) as a power series in $\widehat{\sigma}$, the intermediate calculations are simpler if we begin by writing $\widehat{y}$ as a power series in γ. This approach requires us to work in the region of parameter space where

$$|\widehat{\sigma}| < \left(1 - \gamma^{2/3}\right)^{3/2} .$$

When $|\gamma| < 1$, we can expect to find a series about $\widehat{\sigma} = 0$. If $\gamma = 0$, however, the solution of interest is just $\widehat{y} = 1$, rather than $\widehat{y} = \widehat{\sigma}$.

Our ansatz is, in this case,

$$\widehat{y} \;=\; 1 - \sum_{n=1}^{\infty} \frac{\Phi_n(\widehat{\sigma})}{(1-\widehat{\sigma})^{3n-1}}\, \gamma^{2n} \;. \tag{G.9}$$

The Φ_n turn out to be polynomials. The first few of these are

$$\begin{aligned}
\Phi_1(z) \;&=\; \frac{1}{2} \;, \\
\Phi_2(z) \;&=\; \tfrac{1}{2^3}\;(1+3z) \,, \\
\Phi_3(z) \;&=\; \tfrac{1}{2^4}\;\left(1+8z+5z^2\right) , \\
\Phi_4(z) \;&=\; \tfrac{1}{2^7}\;\left(5+73z+127z^2+35z^3\right) , \\
\Phi_5(z) \;&=\; \tfrac{1}{2^8}\;\left(7+158z+518z^2+398z^3+63z^4\right) , \\
\Phi_6(z) \;&=\; \tfrac{1}{2^{10}}\left(21+667z+3466z^2+5046z^3+2217z^4+231z^5\right) , \\
\Phi_7(z) \;&=\; \tfrac{1}{2^{11}}\left(33+1388z+10355z^2+24040z^3+20015z^4+5756z^5+429z^6\right) , \\
\Phi_8(z) \;&=\; \tfrac{1}{2^{15}}\left(429+22901z+230033z^2+771209z^3+1025575z^4+557983z^5+114139z^6+6435z^7\right) .
\end{aligned}$$

One can proceed either by finding the recurrence relations for the coefficients in these polynomials, or alternatively by seeking a family of differential equations that the Φ_n satisfy. In this way, we find

$$\begin{aligned}
&-z\,(z-1)\left(z^2-1\right)\,\Phi_n'''(z) \\
&+(z-1)\left(1+3(3n-1)z+3(n-2)z^2\right)\Phi_n''(z) \\
&+\left(2-6n-15n(n-1)z-3(n-1)(n-2)z^2\right)\Phi_n'(z) \\
&+n(n-1)\Big(8n-1+(n-2)z\Big)\,\Phi_n(z) \;=\; 0 \;,
\end{aligned} \tag{G.10}$$

with the initial conditions are

$$\Phi_n(0) \;=\; -\frac{\left(-\frac{1}{2}\right)_n}{n!}\;, \qquad \Phi_n'(0) \;=\; 1+\frac{(3n-1)\left(-\frac{1}{2}\right)_n}{n!}\;,$$

$$\Phi_n''(0) \;=\; 2-6n-\frac{\left(2-11n+9n^2+8n^3\right)\left(-\frac{1}{2}\right)_n}{n!}\;.$$

By following the algorithm detailed in [124], one can identify a transformation that brings the equation (G.10) to a form satisfied by the hypergeometric function ${}_3F_2$.

The coefficients in the series (G.9) can be expressed in terms of hypergeometric functions. The result is

$$\widehat{y} \;=\; 1+\sum_{n=1}^{\infty}\left[\frac{\left(-\frac{1}{2}\right)_n}{n!}\,{}_3F_2\left(\begin{matrix}n-\frac{1}{2},\, n,\, n+\frac{1}{2}\\ \frac{1}{2},\;\frac{1}{2}\end{matrix};\;\widehat{\sigma}^2\right)-\widehat{\sigma}\,{}_3F_2\left(\begin{matrix}n,\, n+\frac{1}{2},\, n+1\\ 1,\;\frac{3}{2}\end{matrix};\;\widehat{\sigma}^2\right)\right]\gamma^{2n}\;.$$

The hypergeometric functions in the above series can be expanded as a power series in $\widehat{\sigma}$, yielding a double sum. By interchanging the order of summation and applying identities enjoyed by the Pochhammer symbols, we arrive at the expression

$$\widehat{y}=\sqrt{1-\gamma^2}-\frac{\gamma^2}{2}\sum_{k=1}^{\infty}(k+1)\,{}_3F_2\left(\begin{matrix}\frac{k+1}{2},\,\frac{k+2}{2},\,\frac{k+3}{2}\\ \frac{3}{2},\;2\end{matrix};\;\gamma^2\right)\widehat{\sigma}^k\;.$$

Appendix H

Convergence of Solutions

In this appendix, convergence of the N-expansion appearing in (14.6) is discussed. While we concentrate on the solutions (14.6), we expect that a similar argument can be made to apply to other the solutions found in §13.1 and §13.2 as well.

Let us begin by making a few comments on the asymptotics of the terms in the sum (14.6) as $j \to \infty$. Consider first the individual factors that appear in each summand, $N_{\mathfrak{p}}$, $\boldsymbol{k}_{\boldsymbol{\ell}(\mathfrak{p})-1}$, and $a_{\mathfrak{p}}$: The asymptotics of Gromov-Witten invariants are determined by the radius of convergence of the instanton sum $\mathcal{I}$ in (11.2) (see for example [26, 108–110]). This leads to a formula for the asymptotic growth of N_k^{GW}, which relates the growth of the Gromov-Witten invariants at large k to the coordinate y_{sing} of the singularity closest to the large complex structure point.

$$N_k \simeq N_k^{\mathrm{GW}} \simeq \mathrm{e}^{2\pi k y_{\mathrm{sing}}} \ ,$$

where, by the notation $A \simeq B$, we mean $\log A \sim \log B$, with the asymptotic equality understood in the classical sense. From this, it follows that there is an integer w such that that the quantity

$$\mathrm{e}^{\frac{1}{w}\log N_w} \ = \ N_w^{\frac{1}{w}}$$

is maximal. For $\mathfrak{p}$ a partition of j, this w gives a bound

$$N_{\mathfrak{p}} \ = \ \prod_{k=0}^{\infty} N_k^{\mu_k} \ = \ \prod_{k=0}^{\infty} \left(N_k^{\frac{1}{k}}\right)^{k\mu_k} \leq \prod_{k=0}^{\infty} \left(N_w^{\frac{1}{w}}\right)^{k\mu_k} \ = \ N_w^{\frac{1}{w}\sum_k k\mu_k} \ = \ N_w^{\frac{j}{w}} \ = \ \mathrm{e}^{\frac{j}{w}\log N_w} \ . \qquad \text{(H.1)}$$

The asymptotics of the Bessel functions $\boldsymbol{k}_{\boldsymbol{\ell}(\mathfrak{p})}(2\pi y_0|\mathfrak{p}|)$ can be found by noting that $\boldsymbol{\ell}(\mathfrak{p}) < |\mathfrak{p}|$ so that it is possible to write $|\mathfrak{p}| = \mathfrak{c}\left(\boldsymbol{\ell}(\mathfrak{p}) - \frac{1}{2}\right)$ for some $\mathfrak{c} > 1$, which allows using the asymptotic formula for large order [125]

$$\begin{aligned} \boldsymbol{k}_{\boldsymbol{\ell}(\mathfrak{p})-1}(2\pi y_0|\mathfrak{p}|) \ &= \ \frac{1}{\pi\sqrt{y_0|\mathfrak{p}|}} K_{\boldsymbol{\ell}(\mathfrak{p})-\frac{1}{2}}\left(2\pi y_0 \mathfrak{c}\left(\boldsymbol{\ell}(\mathfrak{p}) - \frac{1}{2}\right)\right) \\ &= \ O\left(\mathrm{e}^{-\sqrt{1+(2\pi y_0\mathfrak{c})^2}\left(\boldsymbol{\ell}(\mathfrak{p})-\frac{1}{2}\right)}\left(\frac{1+\sqrt{1+(2\pi y_0\mathfrak{c})^2}}{(2\pi y_0\mathfrak{c})}\right)^{\boldsymbol{\ell}(\mathfrak{p})-\frac{1}{2}}\right). \end{aligned}$$

If $y_0 > \frac{1}{2\pi}$, then $2\pi y_0 \mathbb{c} > 1$ for any $\mathbb{c} > 1$. This means that we can find constants C_1 and L such that

$$k_{\boldsymbol{\ell}(\mathfrak{p})-1}(2\pi y_0|\mathfrak{p}|) < C_1 \mathrm{e}^{-2\pi y_0 \mathbb{c}\left(\boldsymbol{\ell}(\mathfrak{p})-\frac{1}{2}\right)}(1+\sqrt{2})^{\boldsymbol{\ell}(\mathfrak{p})} \;=\; C_1 \mathrm{e}^{-2\pi y_0|\mathfrak{p}|}(1+\sqrt{2})^{\boldsymbol{\ell}(\mathfrak{p})} \;, \tag{H.2}$$

for $\boldsymbol{\ell}(\mathfrak{p}) > L$. Later, in the following section H.1, we argue that the coefficients $a_{\mathfrak{p}}$ satisfy the bound

$$a_{\mathfrak{p}} \;\leq\; \left(\frac{\mathrm{e}\pi^2}{6\boldsymbol{\ell}(\mathfrak{p})}\right)^{\boldsymbol{\ell}(\mathfrak{p})} \;. \tag{H.3}$$

Denoting the sum appearing in the solutions (14.6) by $S(y_0)$,

$$S(y_0) \;=\; \sum_{j=1}^{\infty} \sum_{\mathfrak{p}\in \mathrm{pt}(j)} a_{\mathfrak{p}} N_{\mathfrak{p}} \left(\frac{j}{2\pi y_0 Y}\right)^{\boldsymbol{\ell}(\mathfrak{p})} \boldsymbol{k}_{\boldsymbol{\ell}(\mathfrak{p})-1}(2\pi j y_0) \;,$$

the bound (H.1) allows us to write

$$S(y_0) \;\leq\; \sum_{j=1}^{\infty} \sum_{\mathfrak{p}\in \mathrm{pt}(j)} a_{\mathfrak{p}} \left(\frac{j}{2\pi y_0 Y}\right)^{\boldsymbol{\ell}(\mathfrak{p})} \boldsymbol{k}_{\boldsymbol{\ell}(\mathfrak{p})-1}(2\pi j y_0)\, \mathrm{e}^{\frac{j}{w}\log N_w} \;.$$

We can break the finite sum over partitions of j into sums over partitions of different length. This gives a further bound

$$S(y_0) \;\leq\; \sum_{j=1}^{\infty} \sum_{l=1}^{j} |\mathrm{pt}_l(j)| \max\left(a_{j,l}\right) \left(\frac{j}{2\pi y_0 Y}\right)^{l} \boldsymbol{k}_{l-1}(2\pi j y_0)\, \mathrm{e}^{\frac{j}{w}\log N_w} \;,$$

where $\max\left(a_{j,l}\right)$ is the maximal value $a_{\mathfrak{p}}$ takes over $\mathrm{pt}_l(j)$, and $|\mathrm{pt}_l(j)|$ is the number of partitions of j of length l. Ramanujan's asymptotic formula for $|\mathrm{pt}(j)|$ tells us that

$$|\mathrm{pt}_l(j)| \;\leq |\mathrm{pt}(j)| \;< \mathrm{e}^{\pi\sqrt{\frac{2}{3}j}} \;,$$

which gives that

$$S(y_0) \;\leq\; \sum_{j=1}^{\infty} \sum_{l=1}^{j} \max\left(a_{j,l}\right) \left(\frac{j}{2\pi y_0 Y}\right)^{l} \boldsymbol{k}_{l-1}(2\pi j y_0) \mathrm{e}^{\frac{j}{w}\log N_w + \pi\sqrt{\frac{2}{3}j}} \;.$$

For $j > L$, the sum over l can be broken into two parts, one from 1 to L and the other from $L+1$ to j. We can then apply the bounds (H.2) and (H.3), allowing us to give another upper bound:

$$S(y_0) \;\leq\; C_2 + \sum_{j=L+1}^{\infty} \left(P(j) + C_1 \sum_{l=L+1}^{j} \left(\frac{\mathrm{e}\pi j(1+\sqrt{2})}{12 y_0 Y l}\right)^{l} \right) \mathrm{e}^{-j\left(2\pi y_0 - \frac{1}{w}\log N_w\right) + \pi\sqrt{\frac{2}{3}j}} \;,$$

where $P(j)$ is a polynomial of degree L in j and C_2 is a constant corresponding to a finite sum over j from 1 to L. To understand the appearance of $P(j)$, recall the relation between $\boldsymbol{k}$ and the polynomials f as in (14.4). The summand in the second sum over l is maximised when

$$l \;=\; j\frac{\pi(1+\sqrt{2})}{12 y_0 Y} \;.$$

At this point the summand takes the value

$$\mathrm{e}^{j\frac{\pi(1+\sqrt{2})}{12 y_0 Y}} \;,$$

giving an upper bound

$$S(y_0) \;\leq\; C_2 + \sum_{j=1}^{\infty} \left(P(j) + C_1 j \mathrm{e}^{j\frac{\pi(1+\sqrt{2})}{12 y_0 Y}} \right) \mathrm{e}^{-j\left(2\pi y_0 - \frac{1}{w}\log N_w\right) + \pi\sqrt{\frac{2}{3}j}} \;.$$

The sum converges when

$$2\pi y_0 - \frac{1}{w}\log N_w - \frac{\pi(1+\sqrt{2})}{12 Y y_0} \;>\; 0 \;,$$

which is a sufficient condition for the N-expansion in (14.6) to converge.

For example, in the case of AESZ34, the above bound is $y_0 > 0.4442$, while the the rank two attractor point near the large complex structure point has $y_0 = \frac{\sqrt{15}}{6} \approx 0.64$.

H.1 Bound for $a_{\mathfrak{p}}$

To finish the proof, we need a bound on $a_{\mathfrak{p}}$, for partitions $\mathfrak{p}$ of a fixed length l. To begin, recall the definition

$$\frac{1}{a_{\mathfrak{p}}} \;=\; \prod_{j=1}^{\infty} \mu_j!\, j^{2\mu_j} \;,$$

where $\mu_j \neq 0$ for only finitely many j. For positive integers n, Stirling's formula gives the bound $n! \geq \sqrt{2\pi} n^{n+1/2} \mathrm{e}^{-n}$. Hence

$$\frac{1}{a_{\mathfrak{p}}} \;\geq\; \prod_j \sqrt{2\pi}\mu_j^{\mu_j+1/2}\mathrm{e}^{-\mu_j}\, j^{2\mu_j} \;=\; \mathrm{e}^{-l} \prod_j \sqrt{2\pi}\mu_j^{\mu_j+1/2}\, j^{2\mu_j} \;,$$

where we have recalled that $\sum_j \mu_j = l$. Because the μ_j are integers, this has a simple bound

$$\frac{1}{a_{\mathfrak{p}}} \;\geq\; \mathrm{e}^{-l} \prod_{j=1}^{|\mathfrak{p}|} \mu_j^{\mu_j}\, j^{2\mu_j} \;,$$

where 0^0 is to be interpreted as 1. On the space $\{\mu_j \geq 0,\, \sum_j \mu_j = l\}$, the above function has a single global minimum. One can determine the minimising μ_j by using a Lagrange multiplier λ:

$$\partial_{\mu_i}\left[\left(\prod_{j=1}^{|\mathfrak{p}|} \mu_j^{\mu_j}\, j^{2\mu_j} \right) - \lambda \sum_{j=1}^{|\mathfrak{p}|} \mu_j \right] \;=\; 0 \;.$$

These relations are solved by $\mu_j = Cj^{-2}$, where C is a constant. Of course, these extremising μ_j are not necessarily integers, but the result suffices for deriving a bound. Taking the logarithm,

$$\log\frac{1}{a_{\mathfrak{p}}} \;\geq\; -l + \sum_{j=1}^{|\mathfrak{p}|} \left(\frac{C}{j^2}\log\frac{C}{j^2} + 2\,\frac{C}{j^2}\log j \right) \;=\; -l + (\log C)\sum_{j=1}^{|\mathfrak{p}|}\frac{C}{j^2} \;=\; -l + l\log C \;,$$

where we recalled the relation $\sum_j Cj^{-2} = l$, which also gives a bound $C > \frac{6l}{\pi^2}$. Therefore

$$\log\frac{1}{a_{\mathfrak{p}}} \;\geq\; -l + l\log\frac{6}{\pi^2} + l\log l \;.$$

And so, as was required,

$$a_{\mathfrak{p}} \;\leq\; \left(\frac{\mathrm{e}\pi^2}{6l}\right)^l \;.$$

Bibliography

[1] P. Candelas, P. Kuusela and J. McGovern, *Attractors with Large Complex Structure for One-Parameter Families of Calabi-Yau Manifolds*, 2104.02718.

[2] P. Candelas, X. de la Ossa, P. Kuusela and J. McGovern, *Mirror Symmetry for Five-Parameter Hulek-Verrill Manifolds*, 2111.02440.

[3] P. Candelas, X. de la Ossa, P. Kuusela and J. McGovern, *Zeta-function for Multiparameter Manifolds*, 2111.02440.

[4] P. Candelas, X. de la Ossa, P. Kuusela and J. McGovern, *Supersymmetric Flux Vacua and their Modularity on $\mathbb{Z}_2$ Symmetric Manifolds*, 2111.02440.

[5] A. J. Wiles, *Modular elliptic curves and Fermat's last theorem*, *Annals Math.* **141** (1995) 443.

[6] R. Taylor and A. Wiles, *Ring-theoretic properties of certain Hecke algebras*, *Ann. of Math. (2)* **141** (1995) 553.

[7] C. Breuil, B. Conrad, F. Diamond and R. Taylor, *On the modularity of elliptic curves over* $\mathbf{Q}$*: wild 3-adic exercises*, *J. Amer. Math. Soc.* **14** (2001) 843.

[8] G. W. Moore, *Arithmetic and attractors*, hep-th/9807087.

[9] G. W. Moore, *Attractors and arithmetic*, hep-th/9807056.

[10] P. Candelas, X. de la Ossa, M. Elmi and D. Van Straten, *A One Parameter Family of Calabi-Yau Manifolds with Attractor Points of Rank Two*, 1912.06146.

[11] S. Kachru, R. Nally and W. Yang, *Flux Modularity, F-Theory, and Rational Models*, 2010.07285.

[12] S. Kachru, R. Nally and W. Yang, *Supersymmetric Flux Compactifications and Calabi-Yau Modularity*, 2001.06022.

[13] P. Candelas, X. De La Ossa and D. Van Straten, *Local Zeta Functions From Calabi-Yau Differential Equations*, 2104.07816.

[14] K. Hulek and H. Verrill, *On modularity of rigid and nonrigid calabi-yau varieties associated to the root lattice a_4*, *Nagoya Math. J.* **179** (2005) 103.

[15] J. M. Maldacena, A. Strominger and E. Witten, *Black hole entropy in M theory*, *JHEP* **12** (1997) 002 [hep-th/9711053].

[16] D. Gaiotto, A. Strominger and X. Yin, *The M5-Brane Elliptic Genus: Modularity and BPS States*, *JHEP* **08** (2007) 070 [hep-th/0607010].

[17] D. Gaiotto and X. Yin, *Examples of M5-Brane Elliptic Genera*, *JHEP* **11** (2007) 004 [hep-th/0702012].

[18] E. Calabi, *On Kähler manifolds with vanishing canonical class*, in *Algebraic geometry and topology. A symposium in honor of S. Lefschetz*, pp. 78–89. Princeton University Press, Princeton, N.J., 1957.

[19] S.-T. Yau, *Calabi's Conjecture and some new results in algebraic geometry*, *Proc. Nat. Acad. Sci.* **74** (1977) 1798.

[20] S.-T. Yau, *On the ricci curvature of a compact kähler manifold and the complex monge-ampére equation, I*, *Commun. Pure Appl. Math.* **31** (1978) 339.

[21] P. Candelas and X. de la Ossa, *Moduli Space of Calabi-Yau Manifolds*, *Nucl. Phys.* **B355** (1991) 455.

[22] R. L. Bryant and P. A. Griffiths, *Some observations on the infinitesimal period relations for regular threefolds with trivial canonical bundle*, in *Arithmetic and geometry, Vol. II*, vol. 36 of *Progr. Math.*, pp. 77–102. Birkhäuser Boston, Boston, MA, 1983.

[23] J. Distler and B. R. Greene, *Some Exact Results on the Superpotential from Calabi-Yau Compactifications*, *Nucl. Phys. B* **309** (1988) 295.

[24] K. Hori, S. Katz, A. Klemm, R. Pandharipande, R. Thomas, C. Vafa et al., *Mirror symmetry*, vol. 1 of *Clay mathematics monographs*. AMS, Providence, USA, 2003.

[25] P. S. Aspinwall and C. A. Lutken, *Geometry of mirror manifolds*, *Nucl. Phys. B* **353** (1991) 427.

[26] P. Candelas, X. C. De La Ossa, P. S. Green and L. Parkes, *A Pair of Calabi-Yau manifolds as an exactly soluble superconformal theory*, *AMS/IP Stud. Adv. Math.* **9** (1998) 31.

[27] S. Hosono, A. Klemm, S. Theisen and S.-T. Yau, *Mirror symmetry, mirror map and applications to complete intersection Calabi-Yau spaces*, *AMS/IP Stud. Adv. Math.* **1** (1996) 545 [hep-th/9406055].

[28] V. Braun, M. Kreuzer, B. A. Ovrut and E. Scheidegger, *Worldsheet Instantons and Torsion Curves, Part B: Mirror Symmetry*, *JHEP* **10** (2007) 023 [0704.0449].

[29] D. A. Cox, J. B. Little and H. K. Schenck, *Toric varieties*, vol. 124 of *Graduate Studies in Mathematics*. American Mathematical Society, Providence, RI, 2011, 10.1090/gsm/124.

[30] W. Fulton, *Introduction to toric varieties*, vol. 131 of *Annals of Mathematics Studies*. Princeton University Press, Princeton, NJ, 1993, 10.1515/9781400882526.

[31] V. Bouchard, *Lectures on complex geometry, Calabi-Yau manifolds and toric geometry*, hep-th/0702063.

[32] C. Closset, *Toric geometry and local Calabi-Yau varieties: An Introduction to toric geometry (for physicists)*, 0901.3695.

[33] V. V. Batyrev, *Dual polyhedra and mirror symmetry for Calabi-Yau hypersurfaces in toric varieties*, *J. Alg. Geom.* **3** (1994) 493 [alg-geom/9310003].

[34] V. V. Batyrev and L. A. Borisov, *On Calabi-Yau complete intersections in toric varieties*, alg-geom/9412017.

[35] L. Borisov, *Towards the mirror symmetry for calabi-yau complete intersections in gorenstein toric fano varieties*, *arXiv preprint alg-geom/9310001* (1993) .

[36] V. Batyrev and B. Nill, *Combinatorial aspects of mirror symmetry*, math/0703456.

[37] V. Batyrev and B. Nill, *Multiples of lattice polytopes without interior lattice points*, *Mosc. Math. J.* **7** (2007) 195.

[38] A. P. Braun, J. Knapp, E. Scheidegger, H. Skarke and N.-O. Walliser, *Palp — a user manual*, *Strings, Gauge Fields, and the Geometry Behind* (2012) 461–550.

[39] A. Weil, *Numbers of solutions of equations in finite fields*, *Bull. Amer. Math. Soc.* **55** (1949) 497.

[40] J. H. Silverman. Springer New York, NY.

[41] The LMFDB Collaboration, "The L-functions and Modular Forms Database." https://www.lmfdb.org/, 2020.

[42] S. Gelbart, *An elementary introduction to the Langlands program*, *Bull. Amer. Math. Soc. (N.S.)* **10** (1984) 177.

[43] E. Frenkel, *Lectures on the Langlands program and conformal field theory*, in *Les Houches School of Physics: Frontiers in Number Theory, Physics and Geometry*, pp. 387–533, 2007, hep-th/0512172, DOI.

[44] F. Q. Gouvêa and N. Yui, *Rigid Calabi-Yau threefolds over $\mathbb{Q}$ are modular*, *Expo. Math.* **29** (2011) 142.

[45] D. Zagier, *Elliptic modular forms and their applications*, in *The 1-2-3 of modular forms*, Universitext, pp. 1–103. Springer, Berlin, 2008. DOI.

[46] J. H. Bruinier, *Hilbert modular forms and their applications*, in *The 1-2-3 of modular forms*, Universitext, pp. 105–179. Springer, Berlin, 2008. DOI.

[47] B. Dwork, *On the rationality of the zeta function of an algebraic variety*, *Amer. J. Math.* **82** (1960) 631.

[48] A. Grothendieck, *Formule de Lefschetz et rationalité des fonctions L*, in *Séminaire Bourbaki, Vol. 9*, pp. Exp. No. 279, 41–55. Soc. Math. France, Paris, 1995.

[49] P. Deligne, *La conjecture de Weil. I*, *Inst. Hautes Études Sci. Publ. Math.* (1974) 273.

[50] P. Deligne, *La conjecture de Weil. II*, *Inst. Hautes Études Sci. Publ. Math.* (1980) 137.

[51] P. Candelas and X. de la Ossa, *The Zeta-Function of a p-Adic Manifold, Dwork Theory for Physicists*, *Commun. Num. Theor. Phys.* **1** (2007) 479 [0705.2056].

[52] N. Koblitz, *p-adic numbers, p-adic analysis, and zeta-functions; 2nd ed.*, Graduate Texts in Mathematics. Springer, New York, 1984, 10.1007/978-1-4612-1112-9.

[53] K. Becker, M. Becker and J. Schwarz, *String theory and M-theory: A modern introduction.* Cambridge University Press, 12, 2006.

[54] S. Ferrara, R. Kallosh and A. Strominger, *N=2 extremal black holes*, *Phys. Rev.* **D52** (1995) R5412 [hep-th/9508072].

[55] S. Ferrara and R. Kallosh, *Supersymmetry and attractors*, *Phys. Rev.* **D54** (1996) 1514 [hep-th/9602136].

[56] E. Cremmer, C. Kounnas, A. Van Proeyen, J. Derendinger, S. Ferrara, B. de Wit et al., *Vector Multiplets Coupled to N=2 Supergravity: SuperHiggs Effect, Flat Potentials and Geometric Structure*, *Nucl. Phys. B* **250** (1985) 385.

[57] D. Z. Freedman and A. Van Proeyen, *Supergravity*. Cambridge Univ. Press, Cambridge, UK, 2012.

[58] A. Strominger, *Macroscopic entropy of N=2 extremal black holes*, *Phys. Lett. B* **383** (1996) 39 [hep-th/9602111].

[59] F. Denef and G. W. Moore, *Split states, entropy enigmas, holes and halos*, *JHEP* **11** (2011) 129 [hep-th/0702146].

[60] F. Denef, *Supergravity flows and D-brane stability*, *JHEP* **08** (2000) 050 [hep-th/0005049].

[61] F. Denef, B. R. Greene and M. Raugas, *Split attractor flows and the spectrum of BPS D-branes on the quintic*, *JHEP* **05** (2001) 012 [hep-th/0101135].

[62] S. Gukov, C. Vafa and E. Witten, *CFT's from Calabi-Yau four folds*, *Nucl. Phys. B* **584** (2000) 69 [hep-th/9906070].

[63] S. B. Giddings, S. Kachru and J. Polchinski, *Hierarchies from fluxes in string compactifications*, *Phys. Rev. D* **66** (2002) 106006 [hep-th/0105097].

[64] F. Denef, *Les Houches Lectures on Constructing String Vacua*, *Les Houches* **87** (2008) 483 [0803.1194].

[65] E. Cremmer, S. Ferrara, C. Kounnas and D. V. Nanopoulos, *Naturally Vanishing Cosmological Constant in N=1 Supergravity*, *Phys. Lett. B* **133** (1983) 61.

[66] J. R. Ellis, A. B. Lahanas, D. V. Nanopoulos and K. Tamvakis, *No-Scale Supersymmetric Standard Model*, *Phys. Lett. B* **134** (1984) 429.

[67] S. Kachru, R. Kallosh, A. Linde and S. P. Trivedi, *de sitter vacua in string theory*, *Physical Review D* **68** (2003) .

[68] C. Vafa, *Evidence for F theory*, *Nucl. Phys. B* **469** (1996) 403 [hep-th/9602022].

[69] T. Weigand, *F-theory*, *PoS* **TASI2017** (2018) 016 [1806.01854].

[70] S. N. Kadir, *The Arithmetic of Calabi-Yau manifolds and mirror symmetry*, other thesis, 9, 2004.

[71] A. Sen, *Orientifold limit of F theory vacua*, *Phys. Rev. D* **55** (1997) R7345 [hep-th/9702165].

[72] K. Bönisch, F. Fischbach, A. Klemm, C. Nega and R. Safari, *Analytic structure of all loop banana integrals*, *JHEP* **05** (2021) 066 [2008.10574].

[73] P. Candelas and R. Davies, *New Calabi-Yau Manifolds with Small Hodge Numbers*, *Fortsch. Phys.* **58** (2010) 383 [0809.4681].

[74] P. Candelas, A. Constantin and C. Mishra, *Hodge Numbers for CICYs with Symmetries of Order Divisible by 4*, *Fortsch. Phys.* **64** (2016) 463 [1511.01103].

[75] H. A. Verrill, *Root lattices and pencils of varieties*, *J. Math. Kyoto Univ.* **36** (1996) 423.

[76] H. Verrill, *Sums of squares of binomial coefficients, with applications to picard-fuchs equations*, *arXiv: Combinatorics* (2004) .

[77] K. Kodaira, *On the structure of compact complex analytic surfaces, i*, *American Journal of Mathematics* **86** (1964) 751.

[78] K. Kodaira, *On the structure of compact complex analytic surfaces, ii*, *American Journal of Mathematics* **88** (1966) 682.

[79] D. A. Cox, J. B. Little and H. K. Schenck, *Toric varieties*, vol. 124 of *Graduate Studies in Mathematics*. American Mathematical Society, Providence, RI, 2011, 10.1090/gsm/124.

[80] G. Almkvist, C. van Enckevort, D. van Straten and W. Zudilin, *Tables of Calabi-Yau equations*, 0507430v2.

[81] D. A. Cox and S. Katz, *Mirror symmetry and algebraic geometry*, vol. 68 of *Mathematical Surveys and Monographs*. American Mathematical Society, Providence, RI, 1999, 10.1090/surv/068.

[82] J. Halverson, H. Jockers, J. M. Lapan and D. R. Morrison, *Perturbative corrections to kähler moduli spaces*, *Communications in Mathematical Physics* **333** (2014) 1563–1584.

[83] P. Candelas, *Yukawa Couplings Between (2,1) Forms*, *Nucl. Phys. B* **298** (1988) 458.

[84] M. Bershadsky, S. Cecotti, H. Ooguri and C. Vafa, *Holomorphic anomalies in topological field theories*, *Nucl. Phys.* **B405** (1993) 279 [hep-th/9302103].

[85] P. Candelas, A. M. Dale, C. A. Lutken and R. Schimmrigk, *Complete Intersection Calabi-Yau Manifolds*, *Nucl. Phys. B* **298** (1988) 493.

[86] J. J. Duistermaat, *Discrete integrable systems*, Springer Monographs in Mathematics. Springer, New York, 2010, 10.1007/978-0-387-72923-7.

[87] A. G. B. Lauder, *Deformation theory and the computation of zeta functions*, *Proc. London Math. Soc. (3)* **88** (2004) 565.

[88] A. G. B. Lauder, *Counting solutions to equations in many variables over finite fields*, *Found. Comput. Math.* **4** (2004) 221.

[89] B. Dwork, *On the zeta function of a hypersurface. II*, *Ann. of Math. (2)* **80** (1964) 227.

[90] A. Thorne, *Zeta functions and modularity of Calabi-Yau manifolds*, Ph.D. thesis, University of Oxford, 2019.

[91] P. Candelas, X. De La Ossa, A. Font, S. H. Katz and D. R. Morrison, *Mirror symmetry for two parameter models. 1.*, *Nucl. Phys. B* **416** (1994) 481 [hep-th/9308083].

[92] G. Faltings, *Finiteness Theorems for Abelian Varieties over Number Fields*, pp. 9–26. Springer New York, New York, NY, 1986.

[93] N. Freitas, B. V. Le Hung and S. Siksek, *Elliptic curves over real quadratic fields are modular*, *Invent. Math.* **201** (2015) 159.

[94] M. Shmakova, *Calabi-Yau black holes*, *Phys. Rev. D* **56** (1997) 540 [hep-th/9612076].

[95] R. Gopakumar and C. Vafa, *M theory and topological strings. 1.*, hep-th/9809187.

[96] R. Gopakumar and C. Vafa, *M theory and topological strings. 2.*, hep-th/9812127.

[97] A. Strominger and C. Vafa, *Microscopic origin of the Bekenstein-Hawking entropy*, *Phys. Lett.* **B379** (1996) 99 [hep-th/9601029].

[98] G. Lopes Cardoso, B. de Wit and T. Mohaupt, *Corrections to macroscopic supersymmetric black hole entropy*, *Phys. Lett. B* **451** (1999) 309 [hep-th/9812082].

[99] G. Lopes Cardoso, B. de Wit and T. Mohaupt, *Deviations from the area law for supersymmetric black holes*, *Fortsch. Phys.* **48** (2000) 49 [hep-th/9904005].

[100] G. Lopes Cardoso, B. de Wit and T. Mohaupt, *Macroscopic entropy formulae and nonholomorphic corrections for supersymmetric black holes*, *Nucl. Phys. B* **567** (2000) 87 [hep-th/9906094].

[101] G. Lopes Cardoso, B. de Wit and T. Mohaupt, *Area law corrections from state counting and supergravity*, *Class. Quant. Grav.* **17** (2000) 1007 [hep-th/9910179].

[102] T. Mohaupt, *Black hole entropy, special geometry and strings*, *Fortsch. Phys.* **49** (2001) 3 [hep-th/0007195].

[103] K. Behrndt, G. Lopes Cardoso, B. de Wit, R. Kallosh, D. Lust and T. Mohaupt, *Classical and quantum N=2 supersymmetric black holes*, *Nucl. Phys. B* **488** (1997) 236 [hep-th/9610105].

[104] K. Behrndt and T. Mohaupt, *Entropy of N=2 black holes and their M-brane description*, *Phys. Rev. D* **56** (1997) 2206 [hep-th/9611140].

[105] K. Behrndt, G. Lopes Cardoso, B. de Wit, D. Lust, T. Mohaupt and W. A. Sabra, *Higher order black hole solutions in N=2 supergravity and Calabi-Yau string backgrounds*, *Phys. Lett. B* **429** (1998) 289 [hep-th/9801081].

[106] A. Sen, *Black Hole Entropy Function, Attractors and Precision Counting of Microstates*, *Gen. Rel. Grav.* **40** (2008) 2249 [0708.1270].

[107] A. Collinucci and T. Wyder, *The Elliptic genus from split flows and Donaldson-Thomas invariants*, *JHEP* **05** (2010) 081 [0810.4301].

[108] M. Bershadsky, S. Cecotti, H. Ooguri and C. Vafa, *Kodaira-Spencer theory of gravity and exact results for quantum string amplitudes*, *Commun. Math. Phys.* **165** (1994) 311 [hep-th/9309140].

[109] A. Klemm and E. Zaslow, *Local mirror symmetry at higher genus*, *AMS/IP Stud. Adv. Math.* **23** (2001) 183 [hep-th/9906046].

[110] R. Couso-Santamaría, R. Schiappa and R. Vaz, *On asymptotics and resurgent structures of enumerative Gromov–Witten invariants*, *Commun. Num. Theor. Phys.* **11** (2017) 707 [1605.07473].

[111] R. P. Stanley, *Enumerative Combinatorics*. Cambridge University Press, Cambridge, 2012.

[112] A. Erdélyi, W. Magnus, F. Oberhettinger and F. G. Tricomi, *Higher transcendental functions. Vol. II*. Robert E. Krieger Publishing Co., Inc., Melbourne, Fla., 1981.

[113] R. Dijkgraaf, E. P. Verlinde and H. L. Verlinde, *Counting dyons in N=4 string theory*, *Nucl. Phys.* **B484** (1997) 543 [hep-th/9607026].

[114] R. Dijkgraaf, G. W. Moore, E. P. Verlinde and H. L. Verlinde, *Elliptic genera of symmetric products and second quantized strings*, *Commun. Math. Phys.* **185** (1997) 197 [hep-th/9608096].

[115] S. Alexandrov, N. Gaddam, J. Manschot and B. Pioline, *Modular bootstrap for D4-D2-D0 indices on compact Calabi-Yau threefolds*, 2204.02207.

[116] J. L. Cardy, *Operator Content of Two-Dimensional Conformally Invariant Theories*, *Nucl. Phys. B* **270** (1986) 186.

[117] F. Denef, *On the correspondence between D-branes and stationary supergravity solutions of type II Calabi-Yau compactifications*, in *Mirror symmetry 4. Proceedings, Conference on Strings, Duality and Geometry: Montreal, Canada, March 22-25, 2000*, 2000, hep-th/0010222.

[118] S. Donaldson and R. Thomas, *Gauge theory in higher dimensions*, in *Conference on Geometric Issues in Foundations of Science in honor of Sir Roger Penrose's 65th Birthday*, pp. 31–47, 6, 1996.

[119] R. Thomas, *Gauge Theory on Calabi-Yau Manifolds*, Ph.D. thesis, University of Oxford, 1997.

[120] H. Rademacher, *A convergent series for the partition function p(n)*, *Proceedings of the National Academy of Sciences* **23** (1937) 78 [https://www.pnas.org/content/23/2/78.full.pdf].

[121] J. Manschot and G. W. Moore, *A Modern Farey Tail*, *Commun. Num. Theor. Phys.* **4** (2010) 103 [0712.0573].

[122] K. Bönisch, A. Klemm, E. Scheidegger and D. Zagier, *D-brane masses at special fibres of hypergeometric families of Calabi-Yau threefolds, modular forms, and periods*, 2203.09426.

[123] A. Erdélyi, W. Magnus, F. Oberhettinger and F. G. Tricomi, *Higher transcendental functions. Vol. III.* Robert E. Krieger Publishing Co., Inc., Melbourne, Fla., 1981.

[124] E. S. Cheb-Terrab and A. D. Roche, *Hypergeometric solutions for third order linear odes*, 0803.3474.

[125] "*NIST Digital Library of Mathematical Functions*." http://dlmf.nist.gov/, Release 1.0.28 of 2020-09-15.